Imperial College London

VWF-dependent platelet 'priming' potentiates novel leukocyte interactions and mediates NETosis under flow

A thesis submitted for the degree of

Doctor of Philosophy in Cardiovascular Science

by

Adela Constantinescu-Bercu, BSc/MPhil

Department of Immunology and Inflammation,

Imperial College London

PhD fully funded by the British Heart Foundation

British Heart Foundation

November 2019

Abstract

Platelet-leukocyte interactions are important in diverse pathophysiological settings from infection to DVT. Previously characterised interactions require robust activation of platelets (e.g. via P-selectin) and/or leukocytes (e.g. via certain β_2-integrins). However, recent studies reveal that platelets captured by von Willebrand factor (VWF) under flow can acquire the ability to bind leukocytes. I hypothesised that, under flow, VWF 'primes' platelets, in turn facilitating an uncharacterised platelet-leukocyte interaction. My aim was to characterise the interaction between VWF-'primed' platelets and leukocytes under flow.

Using microfluidic assays, I demonstrated that, under flow, binding of platelets to the VWF A1 domain causes intracellular Ca^{2+}-release and $\alpha_{IIb}\beta_3$ activation. VWF-'primed' platelets captured neutrophils and T-cells (but not monocytes and B-cells) under low shear. Leukocyte binding was independent of P-selectin and β_2-integrins, but significantly reduced by $\alpha_{IIb}\beta_3$ blockade, and was enhanced in regions of turbulent flow. Bound neutrophils underwent Ca^{2+}-release and formed neutrophil extracellular traps (NETs), in a Ca^{2+}, NADPH-oxidase and shear-dependent manner. The neutrophil receptor was identified as SLC44A2 through differential gene expression analysis using RNA-sequencing data from the Blueprint consortium. Neutrophils and SLC44A2-transfected HEK293T cells bound activated $\alpha_{IIb}\beta_3$, in a manner that was inhibited by blocking the first extracellular loop of SLC44A2. A SNP in *SLC44A2* (rs2288904-G/A, M.A.F.-0.22) encoding the R154Q substitution was recently shown to be protective against DVT. Neutrophils homozygous for *SLC44A2* rs2288904-A and SLC44A2(R154Q)-transfected HEK293T cells exhibited a significant reduction in the ability to bind VWF-'primed' platelets. Platelets from a novel transgenic mouse (*Gp1ba*$^{\Delta sig/\Delta sig}$) exhibit a decreased ability to become 'primed' by VWF and recruit neutrophils under flow.

Taken together, these data reveal a previously unreported interaction between platelets and neutrophils, while providing novel mechanistic insights into platelet-mediated NET formation and into the protective effect of the *SLC44A2* rs2288904-A polymorphism in venous thrombosis.

290 words

Declaration of originality

I, Adela Constantinescu-Bercu, declare that the work presented in this thesis is my own. I confirm that, when information was taken from other sources, this was clearly stated in the thesis and appropriately referenced.

Copyright statement

Acknowledgements

I would like to begin by thanking my main supervisor, Prof. Jim Crawley. Words can hardly describe what a true mentor you have been for me, throughout my entire journey at Imperial College. I first consider myself very lucky to have been assigned to your personal tutor group – you have offered me guidance throughout my BSc years and have put up with hundreds of emails and questions from a young (and probably slightly annoying) student. And, as if this was not enough, you have then been an amazing supervisor, whose work and enthusiasm for science I found truly inspiring throughout my PhD. It has not been an easy journey, but I could not have asked for a better supervisor, who was always there to offer guidance and invaluable advice, for any scientific or life-related problems.

I am equally thankful to my other supervisor, Dr. Isabelle Salles-Crawley. You have been a true role model for me. Thank you for believing in me all these years, so much that you trusted me to continue my journey in this lab, working on a project that I find so inspiring… Thank you for sharing your technical expertise with me, teaching me how to use the flow assays and introducing me into the platelet world, which I find fascinating. I enjoyed so much doing experiments together with you, keeping our fingers crossed that the knock-in mice would have the predicted responses. Thank you for being there every step of the way, offering me both academic and emotional support throughout my years as a PhD student.

I would also like to acknowledge my co-supervisor, Dr. Kevin Woollard. Thank you for all your help and advice throughout these years, and for always being there to answer my questions. I would also like to thank you for always finding challenging questions about the project in our lab meetings, and for providing a different angle to look at my data, from a leukocyte perspective. This project would not have been possible without your support.

I am extremely grateful to the British Heart Foundation for funding my PhD.

I would also like to take the opportunity to thank our collaborators at the University of Cambridge (Dr. Luigi Grassi and Dr. Mattia Frontini) and the University of Toronto (Prof. Heyu Ni and Dr. Miguel Neves) for the help in identifying the neutrophil receptor.

My PhD would not have been the same without my lab colleagues. Thank you to everyone working in the Haemostasis lab and in the Vascular Inflammation lab, for all your help and support in the lab, for kindly donating blood for my experiments and for the wonderful times spent together at conferences, pub nights and Christmas dinners/lunches. To Josefin, thank you for all your nice and encouraging words during times of disappointments. To Mary, thank you for all the fun pub evenings and, of course, eventful conferences and taxi rides in Berlin. A special thank you to Tassos, Dave and Patricia, for all the stress-relief half price pints on “thirsty Thursdays” (or Fridays, or Mondays), and for the lunch breaks filled with thought provoking conversations (educational TV shows etc). To Tassos, it’s been so much fun to organise Christmas lunches together and to learn (or at least try…) to dance Ceilidh at ECTH. To Paru, thank you for all the funny stories you shared with us, during lunches or between experiments. To Patricia, Magda and Adrienn, for all the life-related and thesis-related advice and nice coffee breaks during our PhDs.

I would also like to acknowledge my friends that, despite being all around the world, were there for me throughout my PhD. To Chloé, for being such an amazing friend, being there every step of the way, through what we called a roller-coaster of emotions, sharing my happiness every time I thought I had things figured out and providing pep-talks and half-pints every time things seemed to fall apart. To Nazee, for being there for me from thousands of miles away, through motivational Whatapp calls/Skype and for the amazing surprise of coming to London when I submit this thesis. To Inés, for always reminding me that I can do this and believing in me. To Josca, for sharing this PhD journey – you are next! To Jas, Guillaume and Sandra (i.e. the travelpants club), thank you for all the amazing trips from cold Iceland to warm Alicante and all the wonderful reunions that helped me relax and gain new perspectives on life. Jas, sorry for being such a bad friend during write-up time… To my best friends from home – Mery and Sabina – thank you for always believing in me and being there for me from so far away. It's been so important to know our friendship was so strong to last all these years I have been away. I can't wait for the next stories and adventures together!

And finally, and most importantly, I would like to thank my family.

To Tudor – I don't think you knew what you signed up for during my PhD. Thank you for everything during these past four years, for being so understanding and so supportive throughout this roller-coaster ride. Thank you for listening to the hundreds of practice presentations before conferences (somehow, you probably know more than you wanted to know about VWF and $\alpha_{IIb}\beta_3$…), for sharing my enthusiasm when experiments worked and for picking up the pieces when paper disappointments hit me. And thank you for helping me survive during the write-up times, reminding me to eat and sleep from time to time… You have truly been my rock throughout these years and you're simply the best.

To my sister – thank you for always being there with funny stories and sharing the same passion for science. It means the world to me that we are so close and always there for each other.

To my parents and grandparents – your love and support has made me who I am today. To my dad, for always supporting me, believing in me and seeing the bigger picture and putting things into perspective. And to my mum, for knowing all these years how to be my friend, always listening to me and giving me the best advice and sharing each emotion every step of the way. Mum and dad, thank you for teaching me to dream big and for believing in me to achieve these dreams. You have offered me all I could ever wish for. You are my role models and I could not have achieved anything without you by my side.

Publications arising from this work

Platelet-neutrophil crosstalk: novel roles of $\alpha_{IIb}\beta_3$ and SLC44A2 in flow-dependent NETosis

Adela Constantinescu-Bercu, Isabelle I. Salles-Crawley*, Luigi Grassi, Mattia Frontini, Kevin J Woollard* & James T.B. Crawley*

(Under revision, Elife)

Polyfunctional $CD8^+$ T cells play an active role in primary immune thrombocytopenia (ITP) in adults

Anwar A. Sayed, Amna Malik, Adela Constantinescu-Bercu, Alexander T.H. Cocker, Deena Paul, Camelia Vladescu, Ahmad Khoder, Wayne A. Mitchell, Nesrina Imami, Jim TB Crawley and Nichola Cooper

(Awaiting submission to Blood)

The importance of the GPIbα intracellular tail in VWF- and GPVI-mediated platelet signalling.

Adela Constantinescu-Bercu, Alice Wang, Kevin J Woollard, James TB Crawley and Isabelle I Salles-Crawley$.

(Manuscript in preparation)

Conference presentations

- Oral presentations – British Society for Haemostasis and Thrombosis (BSHT) Annual Meeting, Birmingham, UK (Jan 2020)
- Oral presentation – European Congress for Thrombosis and Haemostasis (ECTH), Glasgow, UK (Oct 2019)
- Oral presentation – XXVII International Society for Thrombosis and Haemostasis (ISTH) Congress, Melbourne, Australia (July 2019)
- Oral presentation – British Society for Haemostasis and Thrombosis (BSHT) Annual Meeting, Coventry, UK (Nov 2018)
- Oral presentation – PhD Away Day, Division of Immunology, Imperial College London (Nov 2018)
- 3-minute thesis presentation – Vascular Networking Event, Imperial College London (July 2018)
- 3-minute thesis presentation – BHF Student Conference, Edinburgh, UK (April 2018)
- 3-minute thesis presentation – Rising Scientist Day, Imperial College London (Feb 2018)
- Oral presentation – British Society for Immunology Congress (BSI), Brighton, UK (Dec 2017)
- Oral presentation – British Society for Haemostasis and Thrombosis (BSHT) Annual Meeting, Coventry, UK (Oct 2017)
- Oral presentation – XXVI International Society for Thrombosis and Haemostasis (ISTH) Congress, Berlin, Germany (July 2017)
- Oral presentation – British Society for Haemostasis and Thrombosis (BSHT) Annual Meeting, Leeds, UK (Nov 2016)
- Oral presentation - BHF Student Conference, Glasgow, UK (April 2016)

Scientific awards during PhD

- Early Career Award – ISTH, Melbourne (2019)
  - Awarded for one of the highest-ranked abstracts submitted to ISTH 2019
- Nominated for the Student Academic Choice Awards – Imperial College London (2019)
  - Nominated for the teaching activities as a Graduate Teaching Assistant
- Scientist in Training Award – BSHT, Coventry (2018)
  - Awarded for the best oral presentation within the Scientist in Training session
- PhD Away Day Award – Imperial College London (2018)
  - Awarded for the best PhD oral presentation within the departmental PhD Away Day
- Young Investigator Award – ISTH, Berlin (2017)
  - Awarded for one of the highest-ranked abstracts submitted to ISTH 2017
- Scientist in Training Award – BSHT, Leeds (2016)
  - Awarded for the best oral presentation within the Scientist in Training session

Certificates during PhD

- Associate Fellowship of the Higher Education Academy (AFHEA, June 2018)
  - For the teaching activities as a Graduate Teaching Assistant within the Faculty of Medicine

Table of contents

Figure list

Table list

Abbreviations

A1* - VWF A1 (Y1271C/C1272R)

a.a. – amino acid

ACD – acid citrate dextrose

ADP – adenine diphosphate

APC – allophycocyanin

BSA – bovine serum albumin

CD – cluster of differentiation

95% CI – 95% confidence interval

CRP – collagen-related peptide

DAMP – damage-associated molecular pattern

$DiOC_6$ – 3,3'-Dihexyloxacarbocyanine Iodide

DPI – diphenyleneiodonium

DVT – deep vein thrombosis

EDTA – ethylenediaminetetraacetic acid

FITC – fluorescein isothiocyanate

FL-VWF – full-length VWF

FPLC – fast protein liquid chromatography

GFP – green fluorescent protein

GP – glycoprotein

GPCR – G-protein coupled receptors

GT – Glanzmann thrombasthenia

GWAS – genome-wide association studies

HEK293T cells – human embryonic kidney 293 cells with SV40 T-antigen

HT – Hepes-Tyrode

IL – interleukin

IP_3 – inositol 1,4,5-triphosphate

ITAM – immunoreceptor tyrosine-based activation motif

ITP – immune thrombocytopaenia

LIBS2 – ligand-induced binding site 2

LPS – lipopolysaccharide

LRR – leucine-rich repeat

MPO - myeloperoxidase

MSD – mechanosensitive domain

mVWF – murine VWF

NADPH – nicotinamide dinucleotide phosphate

NE – neutrophil elastase

NET – neutrophil extracellular trap

NHS – N-hydroxysuccinimide

NK cell – natural killer cell

Nox – NADPH-oxidase

PAD4 – peptidylarginine deaminase 4

PAMP – pathogen-associated molecular pattern

PB – Pacific blue

PBMC – peripheral blood mononuclear cell

PBS – phosphate buffered saline

PE – phycoerythrin

PFB – plasma-free blood

PGE_1 – prostaglandin E_1

PI3-K – phosphoinositide 3-kinase

PIP2 – phosphatidylinositol 4,5-biphosphate

PKC – protein kinase C

PLC – phospholipase C

PMA – phorbol 12-myristate 13-acetate

PMN – polymorphonuclear cells

PRP – platelet-rich plasma

PS – phosphatidylserine

PSGL-1 – P-selectin glycoligand 1

Puro – Puromycin

RBC – red blood cell

RGD – Arginine-Glycine-Aspartic acid

ROS – reactive oxygen species

RT – room temperature

SD – standard deviation

SDS – sodium dodecyl sulphate

SEM – standard error of the mean

TF – tissue factor

TFF – tangential flow filtration

TLR – Toll-like receptor

TRALI – transfusion-related acute lung injury

TTP – thrombotic thrombocytopaenic purpura

TXA_2 – thromboxane A_2

UL-VWF – ultra-large VWF

VWD – Von Willebrand Disease

VWF – Von Willebrand Factor

WB – whole blood

1. Introduction

1.1. Haemostasis

1.1.1. Overview of haemostasis

Haemostasis is a highly regulated mechanism that has evolved to maintain the integrity of the cardiovascular system. The term is derived from the Greek 'haema', meaning 'blood' and 'stasis', meaning 'to stop'. Thus, haemostasis can be defined as the process that prevents excessive bleeding following a vessel injury, through the formation of a haemostatic plug and, eventually, a fibrin clot. However, it is crucial that a fine balance is kept to ensure normal haemostasis as opposed to thrombus formation (thrombosis), which can lead to potentially fatal complications, such as myocardial infarction, deep vein thrombosis (DVT), pulmonary embolism, or stroke. The haemostatic process can be divided into three phases: primary haemostasis (platelet plug formation), secondary haemostasis (coagulation) and fibrinolysis (clot dissolution) [1,2].

1.1.1.1. Primary haemostasis

Upon vessel injury, the first response is vasoconstriction. This is a physiological reflex response, occurring through the contraction of smooth muscle cells lining the blood vessels, to minimise blood flow to the damaged vessel [3]. A haemostatic response is subsequently initiated through the exposure of subendothelial matrix proteins, particularly collagen. This captures von Willebrand factor (VWF), a globular glycoprotein circulating in plasma. Shear forces exerted by the flowing blood cause VWF to unravel and expose binding sites for platelets, namely its A1 domain. This captures platelets at the site of vessel injury via their glycoprotein Ibα (GPIbα) receptor [4] (**Figure 1.1**). The interaction between VWF A1 domain and platelet GPIbα is the focus of this thesis and will be discussed in detail in later sections. Platelets recruited by VWF are brought into close proximity to collagen. This is a potent platelet agonist, that can directly bind platelet via glycoprotein VI (GPVI) and integrin $\alpha_2\beta_1$ [5]. After being recruited to the sites of vessel injury, platelets are also exposed to other agonists, including thrombin, ADP, thromboxane A_2 or serotonin [6]. All these agonists variably activate platelets,

causing them to change their shape, their surface protein expression profile, release their granule contents and, importantly, leading to the activation of a key integrin on the platelet surface, $\alpha_{IIb}\beta_3$ [7]. When activated, $\alpha_{IIb}\beta_3$ can bind to another plasma protein, fibrinogen. In this way, fibrinogen interlinks the platelets, causing them to aggregate and leading to the formation of the primary haemostatic plug [2].

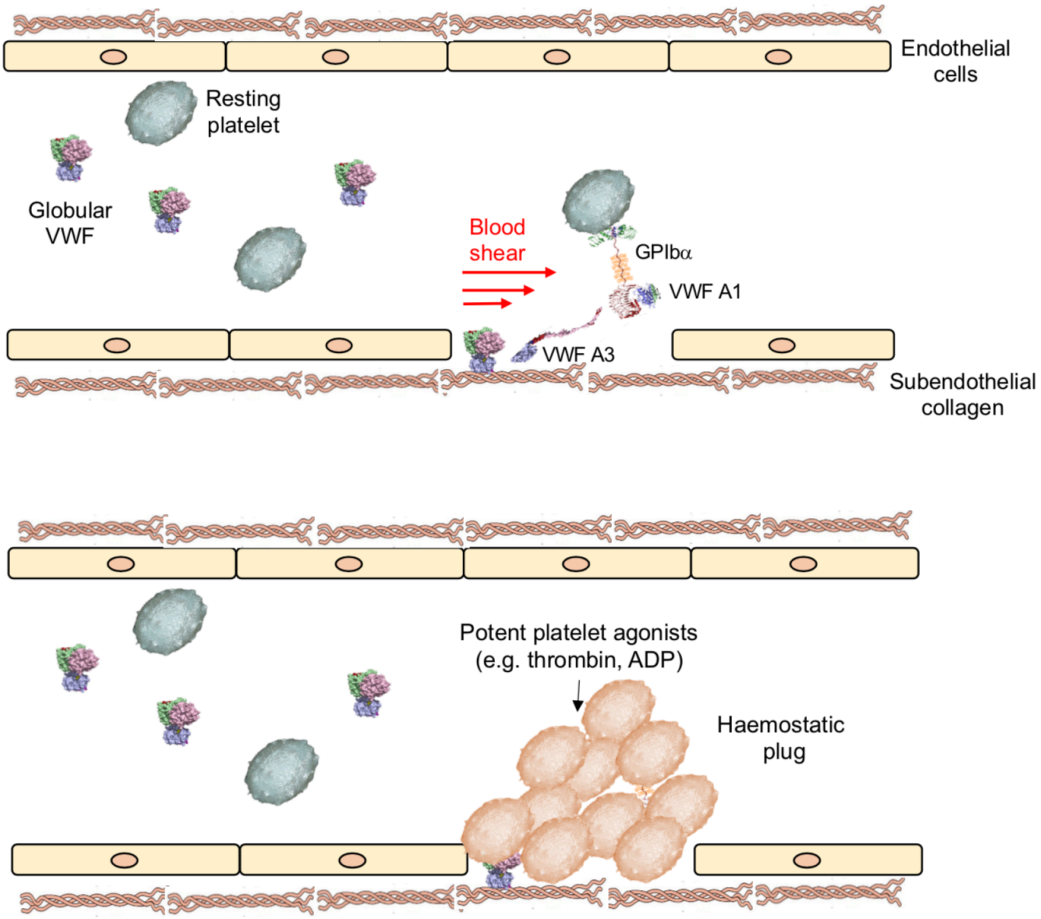

Figure 1.1. The role of VWF in platelet recruitment at the site of vessel damage.

Upon vessel damage, the endothelial cell wall is disrupted, thus subendothelial collagen is exposed. Circulating VWF adopts a globular conformation, with the A3 domain unconcealed. VWF A3 domain binds to the exposed collagen and, subjected to shear forces, VWF unravels. Upon unravelling, VWF exposes its A1 domain, which recruits resting platelets via their GPIbα receptor. Platelets are then exposed to other potent agonists, including collagen, thrombin or ADP and get activated, leading to the haemostatic plug formation.

1.1.1.2. Secondary haemostasis (Coagulation)

Following vessel damage, extravascular/cell surface tissue factor (TF) is exposed. This cellular receptor initiates coagulation – a proteolytic cascade which is based on sequential activation of coagulation factors present in precursor forms in plasma. TF-driven coagulation is known as extrinsic coagulation and generally occurs following vessel damage. However, coagulation can also be initiated intrinsically, through the contact activation pathway. As the name suggests, this is thought to be triggered by the contact between artificial negatively charged surfaces and plasma proteins, such as prekallikrein and high molecular weight kininogen [6,8]. The main events involved in the intrinsic and extrinsic coagulation pathways are summarised in **Figure 1.2**.

The primary role of coagulation is thrombin generation, with the subsequent deposition of fibrin that provides integrity to a haemostatic clot. Apart from cleaving fibrinogen into fibrin, thrombin also has a crucial role in promoting full platelet activation. Indeed, thrombin is considered the most potent platelet agonist [9].

Coagulation is tightly regulated through the actions of three anticoagulant pathways, tissue factor pathway inhibitor (TFPI), antithrombin and activated protein C mediated pathways. TFPI acts upon the initial events in the extrinsic pathway, inhibiting the TF/FVIIa complex. On the other hand, antithrombin and activated protein C mainly act to inhibit thrombin generation in the later stages of coagulation. Together, the anticoagulant pathways serve to spatially and temporally regulate thrombin generation and shut the system down once the haemostatic response is complete [10-12].

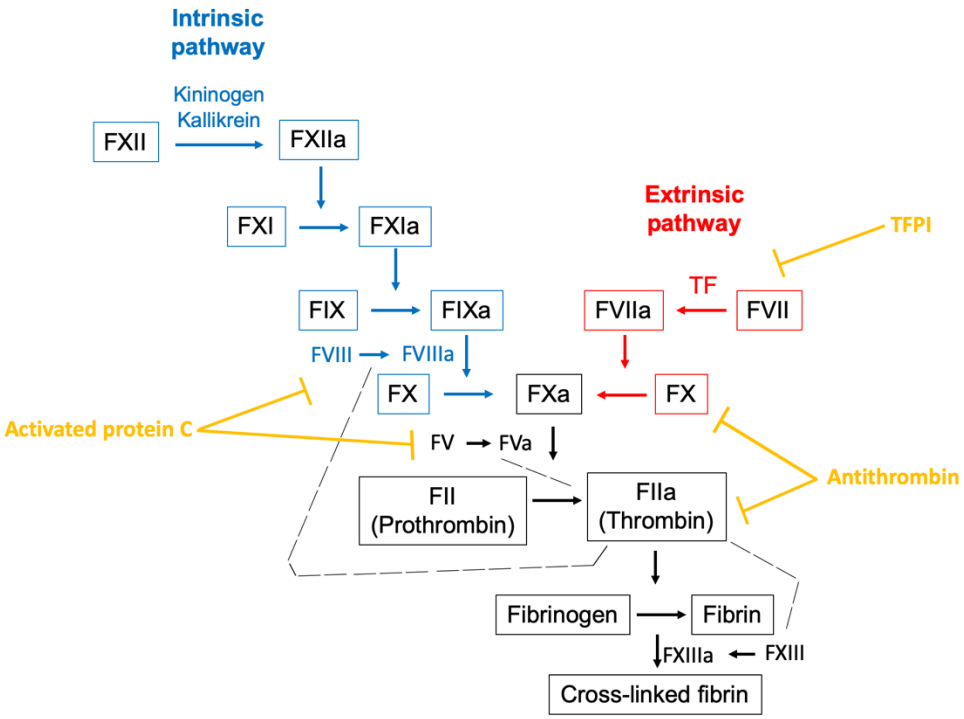

Figure 1.2. Overview of coagulation.

The coagulation cascade is triggered by either negatively charged surfaces and kininogen/kallikrein, which initiate the intrinsic coagulation (blue) or by tissue factor (TF), which initiates the extrinsic pathway (red). Both pathways consist of a series of events leading to activation of various coagulation factors and culminate with the formation of thrombin, which cleaves fibrinogen to fibrin. The three different anticoagulant pathways (TFPI, antithrombin and activated protein C) and their targets are shown in orange.

1.1.1.3. Fibrinolysis

After sealing the site of vessel damage, blood clots are removed through fibrinolysis. Fibrinolysis dissolves the clot when it is no longer required, using a key enzyme – plasmin. Its precursor, plasminogen, is expressed within the liver, in an inactive form. Fibrin acts as a cofactor for tissue plasminogen activator (tPA) and urokinase plasminogen activator (uPA), which cleave plasminogen into plasmin. Plasmin can subsequently cleave fibrin into soluble fibrin degradation products, therefore removing the clot [13].

This thesis focuses on the initial interaction between VWF and platelets that normally occurs as a first step for the normal haemostatic process but could have implications beyond this physiological response.

1.2. Von Willebrand Factor

1.2.1. VWF biosynthesis

The human *VWF* gene is located on the short arm of chromosome 12 (12p13.2) [14] and is 178kb long, consisting of 52 exons [15]. It is transcribed into an 8.9kb *VWF* mRNA [4] and, following translation, a VWF precursor is formed. This is a sequence of 2813 amino acids, comprising of a 22 amino acid signal peptide, a 741 amino acid pro-peptide and 2050 residues that represent the mature VWF subunit [16]. VWF synthesis occurs exclusively within endothelial cells [17,18] and megakaryocytes [16,19-21].

1.2.1.1. VWF post-translational modifications and multimerization

Following translation, VWF undergoes a series of post-translational modifications. These include extensive O-linked and N-linked glycosylation within the endoplasmic reticulum and Golgi apparatus prior to its release or storage [16,22-24].

VWF is initially synthesised as a monomer but undergoes covalent dimerization and subsequent multimerization, these processes being highly important for its function. The dimerization occurs in the endoplasmic reticulum, in a “tail-to-tail” manner, through the formation of disulphide bonds via the C-terminal cysteine knot (CK) domain of monomeric VWF [25]. Multimerization takes place in the Golgi apparatus, and is absolutely dependent on the presence of the VWF pro-peptide domain (D1+D2 domains) [26,27]. In this process, VWF dimers associate in a “head-to-head” manner through the formation of further disulphide bonds in the N-terminal domains. Following multimerization, the pro-peptide domain is proteolytically cleaved by furin although it remains ionically associated with VWF and plays a role in the trafficking and storage of VWF [28].

1.2.1.2. VWF storage and secretion

After multimerization, VWF can be trafficked through three distinct pathways in endothelial cells – the basal pathway, the regulated pathway and the constitutive pathway. Through the basal pathway, VWF gets secreted apically (on the endothelial side facing the vessel lumen) in the absence of a stimulus. In the regulated pathway, VWF is also secreted apically, but this occurs in the presence of an endothelial stimulus (such as histamine). On the other hand, the constitutive pathway leads to the secretion of low-molecular weight VWF through the basolateral side of the endothelial cells (facing the subendothelial matrix) and, in this way, VWF becomes a constituent of the subendothelial matrix [29,30]. VWF undergoing the basal or regulated pathways is packaged and stored in organelles called Weibel-Palade bodies [31,32]. These are endothelial cell-specific, rod-shaped organelles [18,33], which cannot form in the absence of VWF [34]. Conversely, in platelets and megakaryocytes, VWF is stored within α granules [35]. VWF is considered an acute phase protein, therefore its secretion is upregulated in inflammatory conditions [36,37]. Increased release of VWF is also promoted by thrombin (from endothelial cells and platelets), stimulation of β-adrenergic receptors, treatment with DDAVP (1-desamino-8-D-arginine vasopressin), a vasopressin analogue [38,39] and changes in blood pressure [40] (from endothelial cells).

Following secretion, multimeric VWF circulates in plasma at an average concentration of 10μg/ml [39] and has a half-life of approximately 12 hours [16]. However, VWF plasma levels vary appreciably in the normal population with the ABO group being a major determinant of VWF levels. Therefore, individuals with blood group O have 25-35% lower levels of VWF in their plasma compared to non-O blood groups [41,42]. This might be related to the highly glycosylated nature of VWF. Studies showed that VWF contains blood group oligosaccharide structures, which could influence its synthesis, release and clearance, thus explaining the differences in VWF levels [43].

1.2.2. VWF structure

After its secretion into the circulation, VWF circulates in a globular conformation stabilised by weak hydrogen bonds between monomers [44]. In this conformation, most of its functional domains are concealed. However, upon exposure to elevated rheological shear forces, VWF unravels into an extended linear structure [45,46], revealing various domains with distinct roles. VWF domain organisation is depicted in **Figure 1.3**. The importance of the various domains is discussed below.

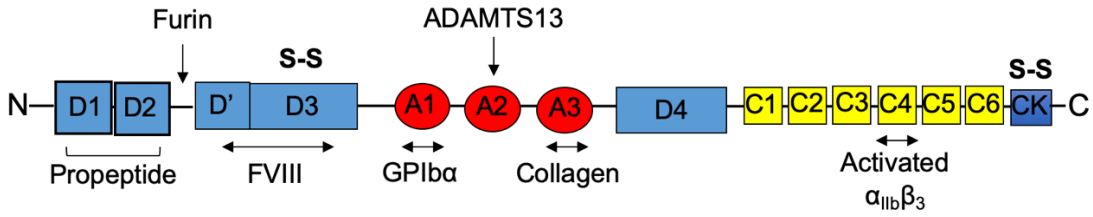

Figure 1.3. VWF structure and main interactions.

VWF has a complex structure. Its propeptide domain (D1+D2) is cleaved by furin prior to VWF release in the circulation. The main VWF interactions described occur between D'D3 and FVIII, A1 and GPIbα, A3 and collagen and C4 and activated $\alpha_{IIb}\beta_3$. Another important domain is the A2 domain, which contains the cleavage site for ADAMTS13.

1.2.2.1. VWF A domains

The crystal structures of the VWF A domains have been resolved and all adopt a characteristic folded conformation [47]. Typically, they have a central hydrophobic β-sheet with 6 β-strands surrounded by 6 α-helices that are amphipathic [48]. As opposed to VWA domains found in other protein structures such as integrins or the complement protein component C2a, VWF A1 and A3 domains do not present a metal ion-dependent site [49], whereas VWF A2 domain contains a Ca^{2+} binding site [50]. The three VWF A domains are VWF A1, VWF A2 and VWF A3, each of which fulfils a different role.

A1 domain

Under physiological conditions, VWF circulates in a globular conformation, where its A1 domain interaction sites are concealed. However, due to elevated shear (e.g. upon vessel damage), VWF unravels, exposing its A1 domain. The crystal structure of the A1 domain fits the VWA domain profile. It has a disulphide bond between Cys1258 and Cys1272, that locks the domain in its functional conformation [51].

The main function of the A1 domain is to capture platelets at sites of vessel damage, initiating the haemostatic process. The A1 domain interacts with resting platelets via the GPIbα receptor. It has also been described that VWF A1 domain can interact with heparin [52,53] and collagen type IV [54] and VI [28], but its primary ligand remains GPIbα.

It was initially thought that this interaction occurs solely for the purpose of recruiting platelets, however, more recent studies have shown that the A1-GPIbα interaction is capable of inducing signalling events within platelets [55]. VWF A1 domain binds to the N-terminal region of GPIbα, within the concave part of its leucine-rich repeat site (**Fig. 1.4**). There are two well-described points of contact between VWF A1 domain and GPIbα. The main point of interaction occurs between the central β-sheet of the A1 domain and the β-switch of GPIbα [56]. The interaction of VWF A1 domain with GPIbα has a low affinity (K_D=2470nM) and is characterised by a 'fast on' and 'fast off' profile [56]. Moreover, the VWF A1-GPIbα interaction can be defined as a 'flex-bond' interaction [49,57] and will be explained in further detail later.

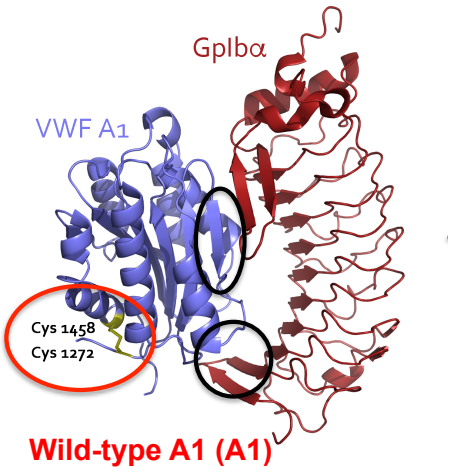

Figure 1.4. Crystal structure of the interaction between VWF A1 domain and GPIbα.

The crystal structure of VWF A1 domain is shown in blue (PDB code 1AUQ), whereas the red structure corresponds to the leucine-rich repeat (LRR) site of GPIbα (PDB code 1GWB). VWF A1 domain binds to GPIbα LRR via its concave region, using two main points of contact highlighted by the black circles. An important characteristic of the VWF A1 domain is the presence of the disulphide bond depicted in yellow and highlighted by the red circle, which is formed between Cys1272 and Cys1458.

The affinity of the A1-GPIbα interaction is increased in certain gain-of-function mutations, either associated with Von Willebrand Disease type 2B (described in **Section 1.2.4.1**) or solely induced *in vitro*. One example explored in this project is the Y1271C/C1272R mutation, which was shown to have a 10-times increase affinity for binding GPIbα (K_D=245nM) due to a shift of the disulphide bond by one amino acid [56].

A2 domain

Like the A1 domain, the A2 domain is folded in a similar manner. However, unlike A1, it gets extended when VWF unravels. Larger VWF multimers more readily unravel upon mechanical shear forces in the circulation [58]. The A2 domain has an essential role in the regulation of VWF multimeric size, as it contains the cleavage site for ADAMTS13. ADAMTS13 cleaves VWF at a single peptide bond site, Tyr^{1605} – Met^{1606}, within the A2 domain, buried within the central β-sheet. Proteolysis leads to a decrease in the multimeric size of VWF, which correlates with a reduced haemostatic function [59]. Upon the unravelling of VWF, the A2 domain itself unfolds,

exposing its ADAMTS13 binding sites [58,60]. The ability of the A2 domain to unfold is believed to be due to the absence of a long-range intradomain disulphide bond that is found within the A1 and A3 domains. Instead, the A2 domain has a vicinal disulphide bond situated close to its C-terminal tail, between Cys^{1669} and Cys^{1670} [61] (**Figure 1.5**). This vicinal disulphide bond forms a plug that stabilises the domain fold, which is also aided by the crucial Ca^{2+} binding site. Under elevated shear, pulling forces upon VWF remove the vicinal Cys-Cys plug and induce unfolding of the A2 domain [50].

Another structural difference between the A2 domain and the other VWA domains is represented by the absence of the α4-helix, which is replaced by a long "α4-less" loop. This loop is thought to hide the ADAMTS13 cleavage site present in the centre of the β-sheet in an hydrophobic core, preventing proteolysis in the folded state [61].

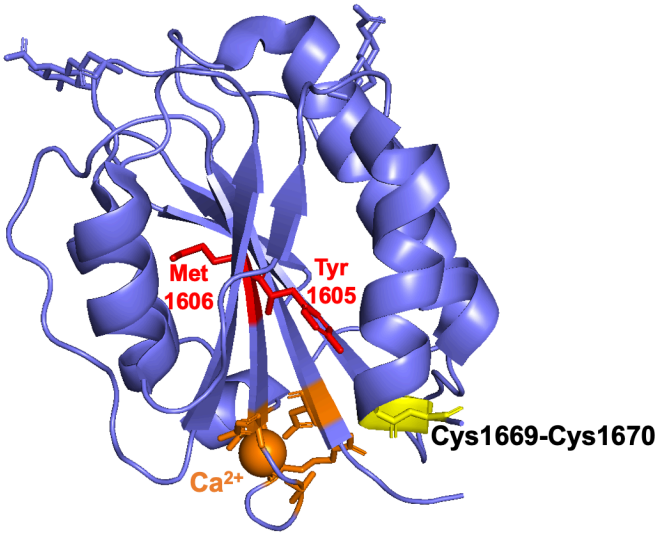

Figure 1.5. Crystal structure of VWF A2 domain.

The cartoon of the crystal structure of VWF A2 domain is shown in blue. Its cleavage site (Tyr^{1605}-Met^{1606}) is shown in red, the Ca^{2+} binding site is shown in orange and the vicinal disulphide bond (Cys^{1669}-Cys^{1670}) is depicted in yellow (PDB code 3ZQK).

A3 domain

VWF A3 domain is the only A domain that has its interaction site constitutively exposed in the globular conformation which VWF adopts within the circulation. The A3 domain is, therefore, the first point of contact in the setting of vessel damage, binding to the exposed subendothelial collagen. Different studies identified collagen type I [28], collagen type III [62] and collagen type VI [63] as being the main subendothelial types of collagen involved in binding VWF A3 domain and aiding the haemostatic process. A3 domain has a similar structure to the A1 domain, having a long-range intradomain disulphide bond and an α4-helix present. As opposed to other collagen-binding domains (such as the α_1, α_2-I or A domain of *Staphylococcus aureus* adhesin), the A3 domain does not have a groove that easily fits with the collagen triple-helix, thus requiring multiple residues to be involved in the interaction [64] (**Figure 1.6**). The affinity of VWF A3 domain for collagen is moderate. If soluble monomeric A3 domain is expressed, it has a significantly reduced ability to bind collagen in solution. The multimeric size of VWF is the determining factor for its affinity for collagen, as VWF multimers with multiple A3 domains have a relatively high affinity to collagen compared to single A3 domain [65].

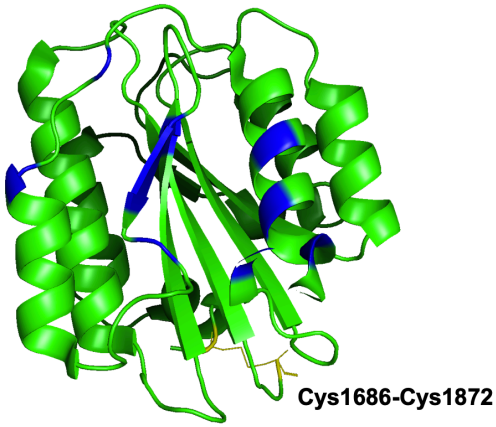

Figure 1.6. Crystal structure of VWF A3 domain.

The cartoon of the crystal structure of VWF A3 domain is shown in green. The binding sites for collagen are depicted in blue and the disulphide bond (Cys^{1686}-Cys^{1872}) is shown in yellow (PDB code 1AO3).

1.2.2.2. VWF D domains

There are four D regions within the structure of VWF, termed D1, D2, D'D3 and the D4 assemblies. The assemblies have a lobular appearance as revealed by electron microscopy and generally consist of a D domain, a cysteine 8 (C8), trypsin-inhibitor-like (TIL) and E module [47] in this order. An exception is represented by the D', which only contains the TIL and E module, and the D4 which does not have an E module, but instead contains a unique segment called D4N, which is linked to its D domain via a disulphide bond [47].

The D1 and D2 assemblies constitute the pro-peptide of VWF, which, as explained earlier, is crucial for the multimerization process and storage in Weibel-Palade bodies [26,27]. The D1-D2 pro-peptide is subsequently cleaved by furin, prior to VWF release in circulation [28].

The roles fulfilled by the D regions in VWF include binding FVIII and thus prolonging its otherwise short plasma half-life (see **Section 1.2.3.2**.). This function is mediated by a high affinity binding site in the D'D3 assembly [66,67]. D'D3 assemblies are also involved in the multimerization process of VWF within the Golgi apparatus [68].

Finally, the D4 assembly appears to be involved in providing additional binding sites to ADAMTS13, perhaps via C-terminal TSP/CUB domains [69], which in turn might induce a conformational change within this protease and helps to conformationally activate it [70].

1.2.2.3. VWF C domains

Together with the D4 assembly, VWF C domains and the CTCK domain form the C-terminal region of VWF. Electron microscopy revealed that this region assembles into an elongated dimeric bouquet within the trans-Golgi and Weibel-Palade bodies, at an acidic pH. The VWF C region forms a stem-like structure in this dimeric bouquet [71] and consists of three VWF C domains by homology (C1, C3 and C5) and three VWC-like domains (C2, C4 and C6). These six tandem domains have an extended conformation, which confers flexibility to the structure of VWF and helps its transition between its globular and extended conformation under shear

stress [47]. A characteristic of the VWF C domains is their rich cysteine content, which either mediate multiple intradomain disulphide bonds, or remain in an unpaired form. The presence of unpaired cysteine residues within the VWF C domains have been shown to be crucial for the secretion of VWF, as mutation of these residues led to VWF retention in the endoplasmic reticulum [72].

One of the most important VWC domains for the purpose of this thesis is the C4 domain. This contains an Arg-Gly-Asp (RGD) sequence, which binds to activated $\alpha_{IIb}\beta_3$ integrin on the platelet surface and stabilises the interaction between VWF and platelets [47,73].

1.2.2.4. CTCK domain

Also found in the C-terminal region of VWF, the C-terminal cysteine knot (CTCK) domain forms the base of the stem-like structure within the dimeric bouquet [47] and is essential for the "tail-to-tail" dimerization process within the endoplasmic reticulum. The CTCK domains from two VWF monomers assemble in anti-parallel dimers via disulphide bonds surrounded by cysteine knots [74]. As a result, the CTCK dimers form a structure highly resistant to haemodynamic forces and reduction of the disulphide bonds [75].

1.2.3. VWF functions

VWF plays a crucial role in haemostasis. Its haemostatic function is fulfilled via two distinct mechanisms. First, VWF is essential for capturing platelets at the sites of vessel injury [76]. Secondly, VWF acts as a carrier molecule for coagulation factor VIII, in this way prolonging its plasma half-life [4,76]. Following multimerization, VWF size ranges between 500kDa and 20,000kDa [77]. VWF multimeric size is directly proportional to its haemostatic function (**Figure 1.7**), i.e. the higher the multimeric size, the more haemostatically active VWF is, for two reasons. Firstly, increased multimeric size translates into the presence of more collagen and platelet binding sites. Secondly, the highest molecular weight VWF molecules are more prone

to unravelling at regions of elevated shear. Therefore, VWF concentration and also multimer size is a risk factor for cardiovascular pathologies, including myocardial infarction, stroke and other thrombotic disorders [78].

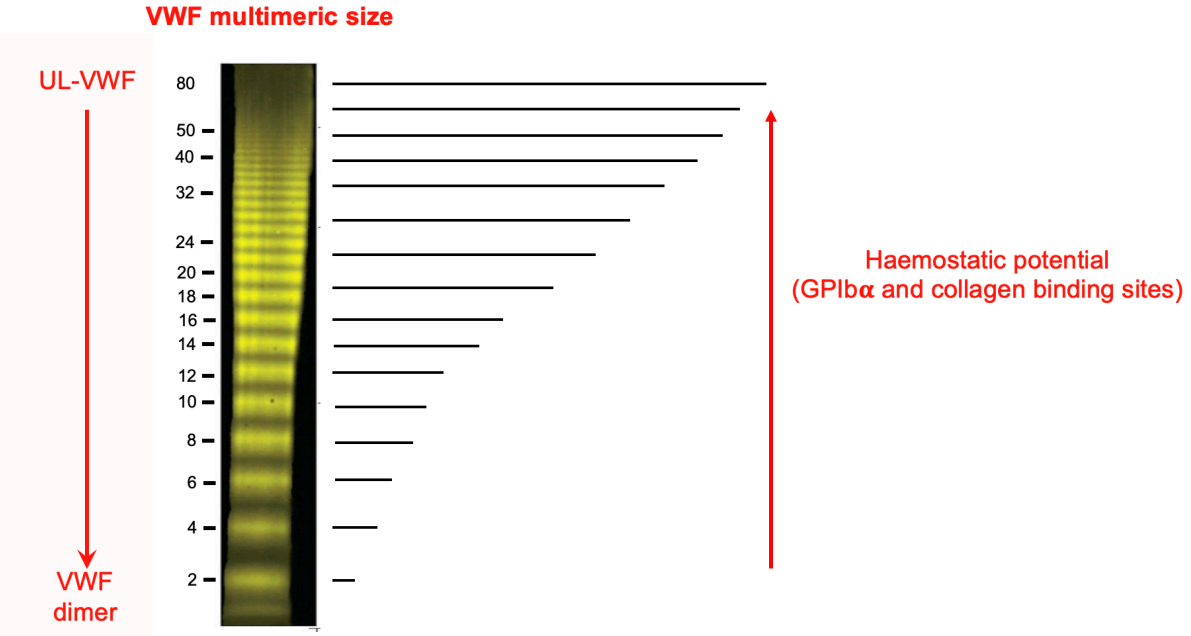

Figure 1.7. VWF multimeric size and its haemostatic potential.

Low resolution agarose gel showing the wide range of VWF multimers present in normal plasma, from ultra-large VWF (top band) to VWF dimers (bottom band) (Adapted from [79], with permission – Appendix 1). VWF haemostatic potential increases proportionally to its multimeric size, as larger multimers present more GPIbα and collagen binding sites and are more prone to unravelling and exposing their functional domains.

1.2.3.1.Mechanics of platelet recruitment

VWF normally circulates in a globular conformation, with most of its functional interaction sites concealed. An exception is the A3 domain. Upon vessel injury, subendothelial collagen gets exposed to which globular VWF binds via its A3 domain [62]. Once tethered, the elevated shear unravels VWF to a linear conformation and exposes its other functional domains. This includes the A1 domain, which, once exposed, is capable of capturing circulating platelets via their GPIbα receptor [56]. This interaction has a 'fast on, fast off' dissociation rate, which causes the platelets to only transiently interact with VWF A1 domain initially. This results in platelet rolling

being observed prior to stable adhesion [80]. Moreover, the interaction between VWF A1 and GPIbα is considered to have a 'flex-bond' nature, transitioning between a low affinity and high affinity state, according to the shear rate it is subjected to. The low affinity state is seen under low shear, during the initial interaction. The high shear forces exerted by the flowing blood over the newly formed VWF A1-GPIbα interaction, were recently shown to induce conformational changes in both the A1 domain and the GPIbα, increasing the affinity of their interaction. This high affinity state has a longer lifetime and an increased force resistance, which can explain the molecular intricacies that help the VWF-platelet interaction withstand high shear environments [57,81,82]. High shear is, therefore, crucial for the VWF A1-GPIbα interaction for two reasons – first, to unravel VWF and expose its platelet binding site, and secondly, to promote a high affinity state interaction between VWF and platelets.

Although initially thought to solely be important for platelet capture, VWF A1 domain was recently shown to initiate signalling events within platelets, without fully activating them [55]. This will be discussed in detail in **Section 1.3.4.1**. Having been recruited to the site of vessel injury via VWF A1 domain, platelets are subsequently subjected to other agonists, such as thrombin, collagen, ADP and thromboxane A_2 [83,84], which promote their full activation and eventually lead to the haemostatic plug formation. The effect of the different agonists upon platelets will be discussed in **Section 1.3.4.2**. Following platelet activation, integrin $\alpha_{IIb}\beta_3$ extends into an active conformation, which can bind to the VWF C4 domain and further stabilise the VWF-platelet interaction [85], or promote platelet aggregation via fibrinogen [86].

Exposure of VWF to shear forces not only reveals its GPIbα binding site, but can also extend the A2 domain, making it available to cleavage by ADAMTS13 [59]. However, at the site of vessel injury, VWF binds collagen via multiple A3 domains, and platelets, via multiple A1 and C4 domains, and is, thus, subjected to limited shear. It is thought, therefore, that ADAMTS13 primarily regulates VWF multimeric size in the layers of the thrombus above the collagen

surface. Here VWF is no longer anchored by collagen, and platelets are more loosely packed, thus ADAMTS13 can act as an important regulator of the size of the platelet plug [87].

1.2.3.2. FVIII carrier

Apart from its crucial function of recruiting platelets to the sites of vessel injury, VWF also contributes to the haemostatic balance by acting as a carrier for FVIII. Plasma levels of VWF directly correlate with plasma levels of FVIII. VWF interacts with FVIII via its D'D3 domains [66], which form high affinity non-covalent bonds with FVIII. Studies show that the main region in FVIII involved in the interaction is represented by its C1 domain, with C2 and A3 domains also aiding by providing additional binding sites [67].

VWF-FVIII interaction acts to stabilise FVIII in circulation, protecting it from otherwise rapid clearance. Different mechanisms have been described to explain the protective role of VWF over FVIII [88-91]. As a result, the VWF-FVIII interaction increases the half-life of FVIII from 2 hours in the absence of VWF, to approximately 12-14 hours when VWF is present [76].

1.2.4. VWF and disease

1.2.4.1. Von Willebrand Disease (VWD)

Von Willebrand Disease (VWD) is considered to be the most prevalent inherited human bleeding disorder, with a reported prevalence of 1 in 1000 people [92]. First described in 1926 by Erik von Willebrand [93], it is a genetic disorder, with an autosomal dominant or recessive transmission, depending on its subtype [14,94]. Rarely, VWD has been reported to be acquired, and is referred to as acquired von Willebrand syndrome [95,96].

Inherited VWD is caused by either a quantitative or qualitative defect in VWF. Based on the nature of the cause, VWD is classified in three types: VWD type 1, which is a partial quantitative defect, VWD type 2, which is a qualitative defect and type 3, characterised by virtually a total deficiency of VWF and considered the most serious form of the disease [93].

VWF type 1 is a quantitative disorder and is the most common form of the disease, accounting for 70-80% of the VWD cases [93]. The main cause of VWD type 1 is missense mutations in the *VWF* gene [97], which leads to disruption of transcription, translation, trafficking, storage and/or secretion of VWF. As a result, VWF plasma levels in patients with type 1 VWD vary between 30IU/dl to 5IU/dl (compared to 50-200IU/dl normal range), with symptoms ranging from mild to severe respectively, usually depending on the VWF levels [93].

Type 2 VWD is caused by a range of different qualitative defects in VWF. Based on the type of defect, this disease type is further subcategorised in four subclasses: type 2A, type 2B, type 2M and type 2N. Type 2A VWD is characterised by a defect in platelet adhesion due to a decrease in high-molecular weight VWF multimers present in plasma. This is caused primarily by a higher susceptibility of VWF to cleavage by ADAMTS13, as type 2A is considered to mainly be caused by mutations within the VWF A2 domain that destabilise its conformation leading to enhanced exposure to ADAMTS13 [98]. Type 2B is considered to be caused by 'gain-of-function' mutations that increase VWF affinity for GPIbα on the surface of resting platelets, but, in turn, this increases VWF clearance. It is likely that most of these mutations reduce the ability of globular VWF to conceal the interaction site of the A1 domain, leading to spontaneous platelet binding and clearance, together with increased unravelling of the A2 domain and subsequent proteolysis [99]. Type 2M is similar to type 2A, given that in both cases VWF exhibits a decreased ability to bind platelets. However, in type 2M this is not linked to the deficiency of high-molecular weight multimers but rather disruption of the GPIbα binding site. Finally, type 2N is characterised by a reduced affinity of VWF for FVIII, caused by mutations associated with the D'D3 region of VWF [94]. This produces VWF with normal platelet tethering function, but reduced FVIII levels due to diminished protein carrier function.

Type 3 VWD is the rarest form of VWD but also the most severe, as patients present with levels below 5IU/dl of plasma VWF and, as a result, suffer from severe bleeding tendencies. Given the importance of VWF in increasing the plasma half-life of FVIII, patients suffering from type 3 VWD also present low levels of FVIII (<10IU/dl) that further promote the bleeding

phenotype [100]. Type 3 VWD is inherited in an autosomal recessive way and is mainly caused by non-sense or frameshift mutations [94].

Acquired von Willebrand syndrome (AVWS) is often misdiagnosed as VWD as it presents with similar clinical profile. However, AVWS is not caused by mutations of the *VWF* gene but can be associated with different causes. VWF deficiency in AVWS has been shown to be triggered by autoimmunity, through antibody-mediated clearance, absorption to surfaces of transformed cells or increased proteolysis due to shear stress increase. In most cases, AVWS develops on the basis of pre-existing cardiovascular, lymphoproliferative, myeloproliferative or other autoimmune disorders [95].

As both inherited and acquired VWD are defined by a deficiency in either VWF levels or function, patients mainly present with bleeding tendencies. However, most symptomatic patients suffer from type 3 VWD, where VWF is virtually absent. These patients can present with mucosal bleeding, menorrhagia, gastrointestinal bleeding, muscle haematomas, post-operative bleeding, gingival bleeding, epistaxis and easy bruising [100].

1.2.4.2. Thrombotic thrombocytopenic purpura (TTP)

In contrast to VWF deficiency, which causes bleeding problems, increased levels of VWF are associated with increased risk of myocardial infarction and stroke [78,101-104]. In addition to quantitative increases, elevated VWF multimeric size is associated with thrombotic thrombocytopenic purpura (TTP).

TTP is caused by congenital (5% cases) or acquired (95% cases) ADAMTS13 deficiency. ADAMTS13 is the protease responsible for cleaving VWF at its A2 domain site. Therefore, ADAMTS13 plays a crucial role in regulating the multimeric size of VWF [59]. Severe deficiency of ADAMTS13 level (<5%) or function results in the abnormal presence of ultra-large VWF (UL-VWF) that can lead to the spontaneous formation of thrombi within the microvasculature. Patients suffering from TTP present with a specific clinical pentad, including microangiopathic

haemolytic anaemia, fever, renal failure, thrombocytopaenia and neurological complications. TTP is a rare disorder, with an incidence of approximately 6/1,000,000 reported in the UK [105]. However, if left untreated, TTP has a very high mortality rate of 90%. Current treatment for acquired TTP is primarily based on plasma exchange to provide a source of ADAMTS13 and help reduce autoantibodies titre and UL-VWF [106], whereas for inherited TTP the current main therapeutic strategy is plasma infusion to provide a source of ADAMTS13 [106]. Research is underway to identify more specific therapeutic targets by treating causality rather than effect.

1.3. Platelets

1.3.1. Overview of platelets

Platelets are small, anucleate blood cells, with a diameter of approximately 2-4μm [107]. The process through which they are generated is called thrombopoiesis and mainly occurs in the bone marrow. Briefly, haematopoietic stem cells differentiate into polyploid megakaryocytes, which are the platelet precursors [108]. Megakaryocytes reside predominantly in the bone marrow, although a recent study has also identified a population of megakaryocytes in mouse lungs [109]. Platelet production is physiologically stimulated via thrombopoietin when the platelet count is low [110], or via chemokines such as interleukin 6 (IL-6) which increase thrombopoietin production in the liver, under inflammatory conditions [111]. During platelet production, megakaryocytes are thought to extend cytoplasmic protrusions consisting of proplatelets within the bone marrow sinusoids. Current understanding suggests that, when subjected to the shear exerted by the flowing blood, these megakaryocytic protrusions release proplatelets within the circulation [108]. Following release, platelets have a life span of 7-10 days in human blood [112], or 4-5 days in mouse blood [113], being subsequently cleared within the liver or spleen. Several mechanisms have been described to understand platelet clearance, including senescence induced degradation or apoptosis, seclusion in the spleen, deposition at the vascular wall or immune-mediated clearance [114-117].

The main role of platelets has for many years been considered to be in the haemostatic process. Normal platelet count within the human blood is considered to be between 150,000-450,000/μl. However, it appears that only about 20-30% of platelets are required for normal haemostasis to take place [118-120], although more are necessary to protect against trauma or childbirth-associated bleeding. This suggests that alternative processes require platelets as well for such a high platelet count to have been preserved through evolution. Indeed, there is increasing evidence to also classify platelets as immune cells, through more recent roles being

identified within the settings of infection or inflammation [121-123]. Platelet roles beyond haemostasis will be discussed in detail in **Section 1.3.6**.

1.3.2. Platelet receptors

Despite their size and being anucleated, platelets fulfil a crucial function in haemostasis (and beyond), due to their complex structure. Platelet plasma membrane contains a variety of important receptors and ligands, including glycoproteins and integrins. The most functionally important glycoproteins for haemostasis include the GPIb-V-IX complex (consisting of GPIbα, GPIbβ, GPV and GPIX), which mediates platelet capture by VWF [124] and GPVI, which binds to collagen and is specific to platelets and megakaryocytes [125]. There are six different integrins present on the platelets surface, namely $\alpha_{IIb}\beta_3$ (also known as GPIIbIIIa), $\alpha_V\beta_3$, $\alpha_2\beta_1$, $\alpha_5\beta_1$, $\alpha_6\beta_1$ and $\alpha_L\beta_2$, although the latter appears to only be expressed on mouse platelets [126,127]. This section focuses on the GPIb-V-IX complex and the $\alpha_{IIb}\beta_3$ integrin.

1.3.2.1. GPIb-V-IX complex

The glycoprotein GPIb-V-IX complex is the second most abundant complex on the platelet surface, each platelet having 25,000-35,000 copies [128]. It is exclusively expressed on platelets and megakaryocytes and is formed of four different subunits: GPIbα, GPIbβ, GPIX and GPV in a 1:2:1:1 stoichiometry. GPIbα associates with the two GPIbβ subunits via disulphide bonds, forming the GPIb part of the complex [129]. This subsequently forms strong non-covalent bonds with GPIX and weaker bonds with GPV, possibly via their transmembrane domains. All subunits are individually encoded by different genes – *GPIBA* (chromosome 17p12), *GPIBB* (22q11.2), *GP9* (3q21) and *GP5* (3q29) [130-133], but they are highly dependent on their association in a complex for successful expression on the plasma membrane. It has however been shown that GPIb complex expression on the platelet surface is more dependent of GPIX than of GPV [131,134,135]. Indeed, GPV association to the GPIb-IX complex and its relevance are not fully understood [131].

All four subunits of the GPIb-V-IX complex are type I transmembrane proteins, with a large extracellular domain containing a leucine-rich repeats region, a single-span transmembrane helix, and a short intracellular domain at their C-terminal tail. The largest subunit is GPIbα, which is approximately 120-140kDa, followed by the GPV (85kDa), GPIbβ (24kDa) and finally, GPIX (20kDa) [136]. The main function of this complex is facilitating platelet recruitment at the sites of vessel injury, by binding to the VWF A1 domain. Other known ligands for this complex are thrombin and the Mac-1 integrin (also known as $\alpha_M\beta_2$ or CD11b/CD18). Evidence also suggests that GPIb-V-IX complex can bind coagulation factors XI and XII, P-selectin and high molecular weight kininogen [137-141]. The receptor function of this complex is fulfilled predominantly by GPIbα [124].

1.3.2.1.1. Structure – GPIbα

Similar to the other subunits of the GPIb-V-IX complex, GPIbα is a type I transmembrane protein with a large N-terminal extracellular domain, a transmembrane helix and a short intracellular tail. Its structure is summarised in **Figure 1.8**. GPIbα extracellular domain contains a leucine-rich repeat site, with seven leucine-rich repeats (LRRs), a highly glycosylated macro-glycopeptide region and, importantly, a folded juxtamembrane stalk [124]. The LRR region is known as the ligand-binding domain and can bind VWF A1 domain and the Mac-1 integrin via its concave region [142], whereas the thrombin binding site resides right after the LRR, in a highly acidic residue-rich region, with sulphated tyrosines [136]. The initial binding sites for VWF A1 domain include β-switch around the LRR 5-8 of GPIbα and the β-finger around LRR1 of GPIbα. It was proposed that there is a third point of contact between VWF A1 domain and the central LRRs (2-4) of GPIbα that appears as a result of a shear forces exerted to this interaction. As mentioned earlier, high shear forces can induce a conformational change in both the A1 domain, and in GPIbα, in which the β-switch changes from a loop to a hairpin structure, being responsible for the 'flex-bond' nature of this interaction [81].

The macroglycopeptide site is also known as the variable region, having 13 O-glycosylated tandem repeats. One of the most important regions to consider for the purpose of this thesis is the juxtamembrane stalk, which consists of 40-50 amino acids, and adopts a folded conformation. This region is thought to unfold under shear forces of 5-20pN following VWF A1 domain binding to GPIbα [143] and extend to approximately 25nm. For this reason, the juxtamembrane stalk is considered a mechano-sensitive domain (MSD) [143,144].

GPIbα has a single transmembrane domain. This is the most conserved region of GPIbα and is represented by a short hetero-tetrameric α helix consisting of 25 amino acids. This domain is responsible for the formation of disulphide bonds with the two vicinal subunits of GPIbβ, via Cys484/485 and Cys122 [145].

The intracellular domain of GPIbα is the longest of the different subunits of GPIb-V-IX, comprising of 97 amino acid residues in human (Ser513-Leu610) [124]. In human platelets, three serine residues (Ser587, Ser590, Ser609) are seemingly phosphorylated [146-148]. The cytoplasmic domain of GPIbα contains binding sites for filamin A (residues 535-568) [149-151], 14-3-3ζ and other 14-3-3 isoforms [152,153] and phosphoinositide 3-kinase (PI3-kinase) (residues 580-610) [124,154].

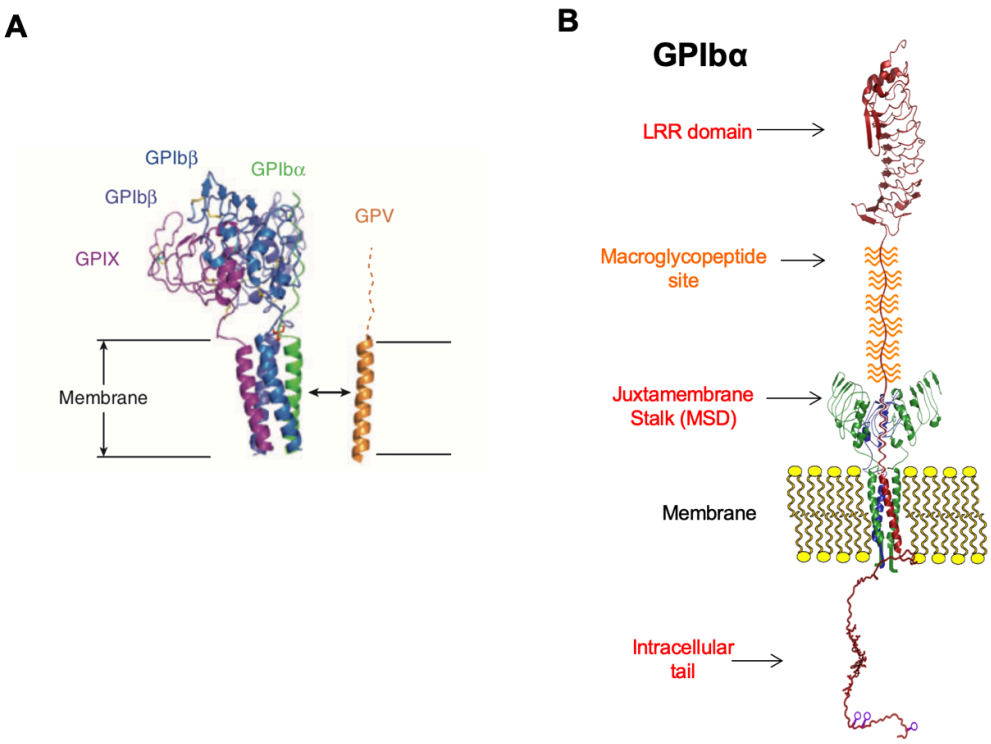

Figure 1.8. Structure of the GPIb-IX complex.

A) *Crystal structure of the GPIb-IX complex, illustrating the links between GPIbα, the two GPIbβ, GPIX and GPV subunits. Adapted from [124], PDB codes 1GWB, 3REZ* ***B)*** *Crystal structure of GPIbα, illustrating its extracellular domain consisting of a leucine-rich repeat (LRR), macroglycopeptide site and a folded juxtamembrane stalk (MSD), a short transmembrane domain and an intracellular tail that is constitutively phosphorylated. Adapted from [124].*

1.3.2.1.2. Disorders associated with the GPIb-V-IX complex

The lack or severe deficiency of the GPIb-V-IX complex is associated with the Bernard-Soulier syndrome (BSS). Also known as Hemorrhagiparous thrombocytic dystrophy, BSS is a rare genetic bleeding disorder first reported in 1948, with an estimated prevalence of 1/1,000,000. It is mainly inherited in an autosomal recessive manner, although some mutations have been shown to have an autosomal dominant pattern. Mutations associated with BSS have been identified within the genes encoding GPIbα, GPIbβ and GPIX, but there are no reports of mutations within the gene coding for GPV [155].

Patients suffering from BSS present with bleeding tendencies, including gingival and gastrointestinal bleeding, menorrhagia, purpura and epistaxis. Phenotypic markers of BSS

include a significant increase in platelet size (from 1-2μm to 4-10μm) [155] and thrombocytopenia [156,157]. Changes in platelet size are also associated with markedly reduced platelet counts and lack of VWF binding, all of which contribute to the bleeding phenotype these patients present with.

1.3.2.1.3. Function of the GPIb-V-IX complex

Being the second most abundant protein complex on the platelet surface, the GPIb-V-IX complex fulfils several different roles. These include platelet capture to sites of vessel injury, maintaining platelet integrity, as well as mediating signalling events within the platelets, all these functions being orchestrated by GPIbα.

GPIbα is important for maintaining the platelet integrity due to its filamin binding site within its cytoplasmic tail (residues 535-568). Through this molecular interaction, GPIbα anchors the actin cytoskeleton and ensures normal platelet formation. As a consequence, if the filamin binding site is disrupted, both in *GpIbα*$^{-/-}$ mice and in individuals suffering from Bernard-Soulier syndrome, the platelet size is markedly increased [149-151,157].

However, the main function achieved by GPIbα is represented by its binding to VWF A1 domain and mediating platelet recruitment at the sites of vessel damage at high shear. As mentioned earlier, upon vessel injury, subendothelial collagen is exposed, capturing VWF via its A3 domain [62]. Downstream events include unravelling of VWF with the associated exposure of the A1 domain interaction sites, following which platelets bind via GPIbα via its extracellular LRR site, and haemostatic plug formation is thus initiated [56]. It was originally thought that the VWF A1-GPIbα interaction solely occurs for the purpose of platelet recruitment. However, more recent studies have shown that this interaction is capable of inducing signalling events within platelets [55] through the ability of the intracellular tail of GPIbα to bind 14-3-3ξ and other 14-3-3 isoforms, as well as PI3-K [124,152-154]. The signalling events triggered by the VWF A1-GPIbα axis will be reviewed in further detail in **Section 1.3.4.1**.

1.3.2.2. $\alpha_{IIb}\beta_3$/GPIIbIIIa

Integrin $\alpha_{IIb}\beta_3$ (also known as GPIIbIIIa or CD41/CD61) is the most abundant protein on the platelet surface (80,000 copies per platelet) [158]. An additional $\alpha_{IIb}\beta_3$ pool is present intracellularly, within the granule membranes, and translocates to the platelet surface during platelet stimulation [159]. $\alpha_{IIb}\beta_3$ is specific to megakaryocytes and platelets [160] and is recognised for its crucial role in haemostasis.

1.3.2.2.1. Structure – active vs inactive conformations

Similar to all other platelet integrins, $\alpha_{IIb}\beta_3$ is a heterodimeric protein, with one α and one β subunit non-covalently linked. Each subunit has a large extracellular ectodomain, a single transmembrane-spanning helix and a short cytoplasmic tail consisting of 20-60 amino acids [161]. The α_{IIb} and β_3 subunits are encoded by the *ITGA2B* and *ITGB3* genes respectively, located on chromosome 17q21.31 and 17q21.32 [162]. After translation, α_{IIb} and β_3 subunit precursors associate in megakaryocytes within the endoplasmic reticulum [163] and undergo subsequent post-translational modifications within the Golgi apparatus [164].

The structure of $\alpha_{IIb}\beta_3$ has been predicted based on its homology with the $\alpha_V\beta_3$ integrin. Electron microscopy showed that the α and β subunits association led to the formation of a large globular head domain (8 by 12nm) containing the ligand-binding site, followed by a long rigid stalk with two flexible tails (18nm length), consisting of the transmembrane domain and short intracellular tail [165,166]. The crystal structure of the extracellular domain of α_v, which is thought to be 50% homologous to α_{IIb} was shown to be folded into a β-propeller conformation, followed by a “thigh” and two “calf” domains. In unstimulated platelets, this subunit is found in a bent conformation, with a “knee” region forming between the “thigh” and first “calf” domains. The β_3 subunit has a βA domain, which associates with the α_v head and contains three metal ion site motifs – the metal ion-dependent adhesion site (MIDAS, where Mn^{2+} and Ca^{2+} were shown to bind), the adjacent site (ADMIDAS) and the ligand-induced metal-binding site (LIMBS). In addition, the β_3 subunit contains a PSI (plexin, semaphorin, integrin) site, four EGF

(epidermal growth factor-like) tandem repeats and a βTD domain [167-169]. The crystal structure of $\alpha_V\beta_3$ is illustrated in **Figure 1.9**.

An important characteristic of $\alpha_{IIb}\beta_3$ and $\alpha_V\beta_3$, but also seen in the $\alpha_5\beta_1$ integrin is the presence of an RGD-binding groove (Arg-Gly-Asp), through which these integrins can bind to different ligands containing this sequence. As revealed by the crystal structure of $\alpha_V\beta_3$, this region is located between the β-propeller and the βA domains, being unavailable for binding in the inactive bent conformation [170]. When $\alpha_{IIb}\beta_3$ headpiece was co-crystallised with a ligand, the extracellular part of the integrin adopted an open conformation, in which the RGD binding site was exposed [171].

The transmembrane domain of $\alpha_{IIb}\beta_3$ is predicted to have an α-helical coiled-coil structure formed through the association of the α and β subunits [165].

Together with the transmembrane domains, the intracellular tails of the α_{IIb} and β_3 are thought to be crucial determinants of the integrin affinity state. The current model of $\alpha_{IIb}\beta_3$ activation involves a “switchblade” mechanism through which the separation of the cytoplasmic tails of the two subunits is thought to promote the extension of the knee-bent inactive conformation into an open, active conformation of the extracellular domain of $\alpha_{IIb}\beta_3$ [171]. This is available to bind various ligands and establish important interactions.

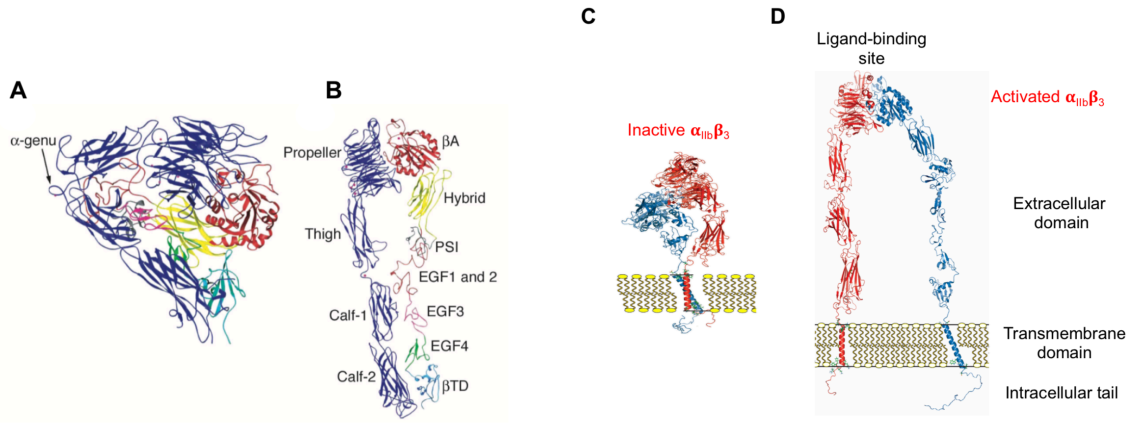

Figure 1.9. Structure of $\alpha_v\beta_3$ / $\alpha_{IIb}\beta_3$.

A) *Inactive bent conformation of $\alpha_v\beta_3$, with the α-genu region indicated.* ***B)*** *Active extended conformation of $\alpha_v\beta_3$, with the main domains indicated – the propeller head, thigh, calf 1 and calf 2 within the α_v subunit, and the βA domain, the hybrid, PSI, four EGF and βTD domains within the β_3 subunit. A and B are adapted from [160], PDB code 4G1M.* ***C)*** *Inactive bent conformation of $\alpha_{IIb}\beta_3$. The α_{IIb} subunit is red and the β_3 subunit is blue.* ***D)*** *Active conformation of $\alpha_{IIb}\beta_3$, indicating its now-exposed ligand-binding site within the extracellular domain. Adapted from [172].*

1.3.2.2.2. Disorders associated with $\alpha_{IIb}\beta_3$

The discovery of $\alpha_{IIb}\beta_3$ was in part due to studies done on the disease associated with its deficiency. First described in 1918, Glanzmann thrombasthenia (GT) is an autosomal recessive disease, with an estimated incidence of 1/1,000,000 [173] and is caused by mutations in either *ITGA2B* or *ITGB3* genes encoding for the α_{IIb} and β_3 subunits respectively [162]. A large number of mutations associated with GT have been reported to date in both *ITGA2B* (255 mutations) or *ITGB3* (164 mutations) [173]. Patients with mutations in the *ITGA2B* gene only present with defects in $\alpha_{IIb}\beta_3$, whereas mutations in *ITGB3* have been associated with defects in both $\alpha_{IIb}\beta_3$ and $\alpha_v\beta_3$. However, due to the low copy number of $\alpha_v\beta_3$ under normal circumstances, these patients do not present with a more severe platelet phenotype [174]. GT is characterised by lack of platelet aggregation in response to platelet agonists and consequent bleeding tendencies in patients suffering from this disease. There are three types of GT according to the level and functionality of $\alpha_{IIb}\beta_3$. Type I and II are caused by a quantitative defect, while type III is due to a qualitative problem. Type I GT patients have less than 5%

levels of $\alpha_{IIb}\beta_3$ on their platelet surface, type II present 5-15% levels of $\alpha_{IIb}\beta_3$, whereas in type III GT platelets have normal levels of the integrin, but its function is disrupted [175]. Mouse models of GT were obtained by knocking out the β_3 subunit. These mice exhibited reduced survival due to severe bleeding problems [176]. The bleeding problems associated with $\alpha_{IIb}\beta_3$ further underline the importance of this integrin for haemostasis.

1.3.2.2.3. $\alpha_{IIb}\beta_3$ ligands and interactions

$\alpha_{IIb}\beta_3$ helps platelets fulfil various functions, including platelet aggregation and spreading, thrombus formation and clot retraction [2,177,178], through its ability to bind to various ligands. Its main ligands are fibrinogen [179], VWF (C4 domain) [47,73], fibronectin [180], vitronectin [181], fibrin [182] and thrombospondin [183].

The major ligand binding to $\alpha_{IIb}\beta_3$ is fibrinogen. Fibrinogen is an abundant hetero-hexameric ($A\alpha$ $B\beta$ γ_2) plasma glycoprotein with a molecular weight of approximately 340kDa and plays a crucial role in haemostasis. It is mainly synthesised by hepatocytes and its structure comprises of pairs of Aα, Bβ and γ polypeptide chains, which fold into nodular domains [184]. Fibrinogen binds to activated $\alpha_{IIb}\beta_3$ via its α chain, which contains an RGD sequence. Through binding to this integrin, fibrinogen interlinks activated platelets and causes them to aggregate, leading to the formation of the haemostatic plug [86]. Fibrinogen circulates freely in plasma, at a high concentration of 2-5mg/ml, which can increase in inflammatory conditions, as it is an acute phase protein [184]. Fibrinogen is also stored within platelet α granules (3% of the total circulating fibrinogen pool), being released following platelet activation [185].

However, ligand binding to $\alpha_{IIb}\beta_3$ is not only dependent upon ligand availability, but also on the affinity state of the integrin. As mentioned in the previous section, $\alpha_{IIb}\beta_3$ primarily binds to its ligands through its RGD-binding groove, which is only available for binding in the activated, high-affinity state of the integrin. In fact, $\alpha_{IIb}\beta_3$ is involved in a bidirectional signalling that permits its transition from the low-affinity state, to an intermediate-affinity state and, eventually,

to the high-affinity activated state. These can be categorised as “inside-out” and “outside-in” signalling events [186,187], and will be discussed in detail in **Section 1.3.4.2.3**.

1.3.3. Platelet ultrastructure – Platelet granules

The complex platelet structure is not only limited to the platelet surface, but also includes their cytoplasmic content. Within their cytoplasm, platelets have important secretory granules, which contain various proteins/molecules crucial to their function. Based on their content and density, platelet granules are categorised into α, dense/δ granules and lysosomes [188,189]. More recently, another type of granules has been described – T granules [190]. This section focuses on α and dense granules, as their contents are key to platelet function in haemostasis.

1.3.3.1. α granules

α granules are the most abundant type of granules found in platelets, constituting approximately 10% of the platelet volume. There are about 50-80 α granules within a platelet, with a total membrane surface area of approximately 14μm^2. During platelet activation, degranulation occurs and α granules fuse with the platelet plasma membrane to release their contents. Through this process, α granules allow platelets to increase their surface area 2-4 times during spreading [191].

α granules form within megakaryocytes, being derived from multivesicular bodies that form from the trans-Golgi network [192]. They are passed to platelets during megakaryocytopoiesis and continue to develop within the circulating platelets [193].

Through their contents, α granules are important for haemostasis, angiogenesis, antimicrobial and inflammatory responses. A proteomic analysis revealed that there are more than 284 different proteins within α granules [194]. Amongst the most abundant proteins are fibrinogen, VWF, albumin, IgG, coagulation factors (factor V), thrombospondin, platelet-derived growth factor TGFβ, α_2-macroglobulin, α_2-antiplasmin and platelet chemokines (platelet factor 4/CXCL4) [195]. Importantly, the membranes of the α granules were reported to represent a pool

of $\alpha_{IIb}\beta_3$ and another important platelet receptor, P-selectin [196]. Soluble proteins such as platelet factor 4 are thought to be packaged into vesicles within the trans-Golgi network and then incorporated into α granules as cargo, whereas plasma proteins (fibrinogen, factor V) were shown to be taken up by α granules through endocytosis or pinocytosis. For example, fibrinogen is reported to be internalised in α granules through a clathrin-dependent process, following binding to its receptor, activated $\alpha_{IIb}\beta_3$ [191].

Problems in the formation of α granules have been analysed both in humans and mice. The absence of α granules and their cargo in humans has been associated with the Gray platelet syndrome [197] or arthrogryposis, renal dysfunction and cholestasis syndrome [198]. The latter is not restricted to platelet defects and has a low survival rate [199]. The Gray platelet syndrome is a rare genetic platelet disorder, with an autosomal recessive inheritance, although there are reports of sporadic cases of autosomal dominance or X-linked transmission [200]. For many years, the gene responsible for this disease remained unknown. However, exome sequencing studies in 2011 identified *NBEAL2* mutations to be responsible for this disorder [201-203]. Patients suffering from Gray platelet syndrome mainly present with bleeding diatheses, but complications can include thrombocytopenia and myelofibrosis, as the absence of α granules can cause defects in normal megakaryocyte development [191,204].

1.3.3.2. Dense granules

Unlike α granules, dense granules are much less abundant within platelets, each platelet containing only about 3-8 dense granules. The biogenesis of dense granules is not well understood, but they are thought to form during early megakaryocyte maturation, originating from the endolysosome, and thus being considered lysosome-related organelles [205,206].

Compared to α granules, dense granules store appreciably fewer molecules [207]. Their contents include serotonin, calcium, magnesium, potassium, pyrophosphate, polyphosphate, ATP and ADP [207,208]. Following release of dense granules, serotonin and ADP act as secondary platelet agonists and mediate autocrine or paracrine responses [209]. On the other hand,

polyphosphates have recently been identified as modulators of coagulation, due to their anionic nature that can trigger the contact activation pathway [210].

Defects in dense granule formation are linked to the Hermansky-Pudlak and Chediak-Higashi syndromes. These are inherited platelet disorders, with autosomal recessive transmission. Problems with dense granules are also thought to be linked to defects in other lysosome-related organelles, such as the melanosome. Therefore, patients suffering from Hermansky-Pudlak or Chediak-Higashi syndromes not only present with bleeding tendencies, but also have pigmentation problems, known as oculocutaneous albinism [211-213].

1.3.4. Overview of platelet signalling

To fulfil most of their functions, platelets need to undergo intricate signalling events which are outlined below. Platelets respond to a variety of different agonists in an agonist type and concentration dependent manner. They thus exhibit a 'tunable' response, which is dictated by their spatial and temporal availability within the haemostatic plug.

1.3.4.1. VWF A1-GPIbα dependent signalling

The first step in the haemostatic process is platelet capture to sites of vessel injury via their interaction with the VWF A1 domain. Platelets interact with VWF A1 domain via GPIbα [56]. Although it was initially thought that this interaction occurs solely to recruit platelets, more recent studies have revealed that the A1-GPIbα interaction is capable of inducing signalling events within platelets. Importantly, VWF A1-mediated signalling is absolutely dependent on the presence of shear [55,214].

Following their initial interaction, the A1 and GPIbα are subjected to shear that they can withstand due to the 'flex bond' nature of their interaction [57,80,81]. Thus, under shear conditions, VWF A1 and GPIbα undergo conformational changes that lead to a higher affinity interaction [57]. As depicted in **Figure 1.10**, GPIbα has a juxtamembrane stalk (Ala^{417}-Phe^{483}), which is folded, but that lacks disulphide bonds to secure structural integrity. Zhang *el al.* proposed

that rheological forces applied on the tethered platelet leads to the unfolding of the juxtamembrane stalk. For this reason, the juxtamembrane stalk is considered a mechanosensitive domain (MSD). This is thought to cause a conformational change, which translates the mechanical stimulus into a biochemical signal transduced by the intracellular domain of GPIbα [143,144]. The intracellular tail of GPIbα has the ability to associate with 14-3-3ζ and other 14-3-3 isoforms [147,148,152-154,215,216] and also with the p85 subunit of PI3 kinase through its last 30 amino acids (a.a. 580-610). The p85 subunit can recruit the p110 catalytic subunit of PI3 kinase and initiate signalling events through the phosphorylation of the PI3 kinase [217,218]. Evidence also suggests an involvement of Src kinase in VWF A1-dependent signalling. These different signalling pathways are thought to activate Akt, phospholipase Cγ2 (PLCγ2) and subsequently protein kinase C (PKC), and lead to Ca^{2+} release from intracellular stores [218-220]. Given the multimeric nature of VWF and the high number of copies of GPIbα on the platelet surface, it is thought that GPIbα clustering may also play a role in VWF-mediated platelet signalling, by aiding downstream Syk phosphorylation [221]. The events involved in the A1-dependent signalling cascade are not fully understood, but they are known to culminate with the activation of the $\alpha_{IIb}\beta_3$ integrin [55]. There are studies that report modest α granule release with consequent P-selectin exposure, but it is widely accepted that the amount of P-selectin is minimal compared to that induced by potent platelet agonists, such as thrombin or collagen [222,223]. However, the systems used to analyse the VWF A1-GPIbα interaction require further investigation, as they often use static conditions or the addition of Botrocetin/Ristocetin, which do not reflect the physiological conditions under which this interaction takes place [218,223].

VWF-mediated platelet signalling is frequently considered redundant in the setting of haemostasis, as it only transduces a mild signal. At sites of vessel damage, other appreciably more potent platelet agonists are present and initiate more robust signalling events [224]. Understanding the importance of A1-GPIbα signalling was a focus of this thesis and will be discussed in further detail later.

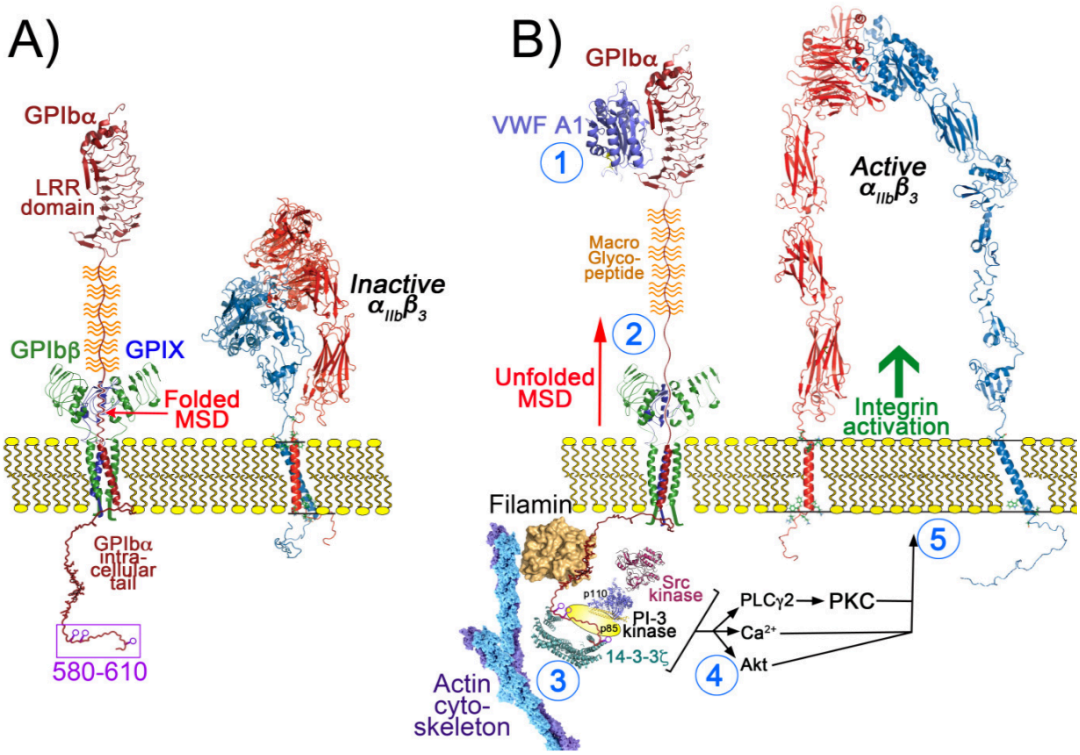

Figure 1.10. Overview of VWF A1-GPIbα signalling.

A) Schematic representation of the main receptors on the resting platelet membrane – GPIb-IX complex, consisting of GPIbα, GPIβ, GPIX and GPV (not shown) and $\alpha_{IIb}\beta_3$ integrin in its inactive conformation. Residues 580-610 from the intracellular tail of GPIbα are highlighted because they are involved in signalling events. B) Schematic representation of the GPIbα-mediated platelet signalling: 1. VWF A1 domain binds to GPIbα at its leucine-rich repeat site (LRR); 2. The juxtamembrane stalk (MSD) unfolds due to the presence of shear, leading to a conformational change in the intracellular tail of GPIbα; 3. GPIbα intracellular tail binds to filamin, 14-3-3ζ and the p85 subunit of PI3-kinase; 4. These lead to signalling events, including Src kinase activation, PLCγ2 activation, release of intracellular Ca^{2+} and, finally, 5. result in the activation of $\alpha_{IIb}\beta_3$.

1.3.4.2. Platelet activation

After being recruited to sites of endothelial injury via VWF, platelets are subjected to a variety of other potent stimuli that fully activate them. The major changes observed following platelet activation include integrin activation, degranulation resulting in presentation of new cell surface proteins (e.g. P-selectin, CD40 ligand), shape change and exposure of phosphatidylserine on the outer phospholipid layer of the platelet membrane. Platelet activation is induced by different agonists, which include subendothelial collagen exposed following vessel damage, and soluble agonists released from platelets or damaged cells (i.e. ADP, serotonin, thromboxane A2) or resulting from the coagulation cascade (i.e. thrombin)

[225]. Platelets within a haemostatic plug/thrombus present different activation levels (**Figure 1.11**) depending on agonist type and availability, thus exerting a 'tunable' activation response.

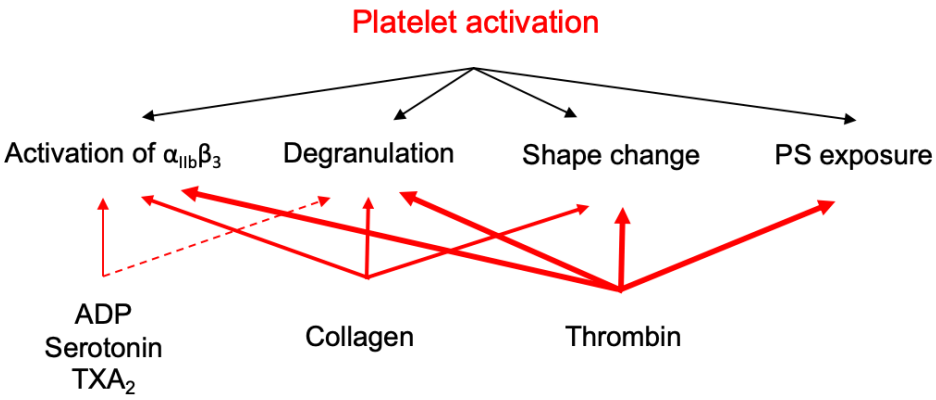

Figure 1.11. Schematic representation of platelet agonists and their impact upon platelets.

Different platelet agonists induce different responses within platelets. ADP, serotonin and TXA_2 are weak platelet agonists and mainly induce the activation of $\alpha_{IIb}\beta_3$ with minimal degranulation, as opposed to collagen, which induces appreciably more degranulation and shape change. Thrombin, the most potent platelet agonist, induces activation of $\alpha_{IIb}\beta_3$, degranulation, exposure of phosphatidylserine (PS) and shape change.

1.3.4.2.1. Collagen-mediated signalling

After recruitment to sites of vessel injury via collagen-bound VWF, platelets can bind to collagen directly, via $\alpha_2\beta_1$ and glycoprotein (GP) VI [5]. Being a potent platelet agonist, collagen is known to induce degranulation, activation of $\alpha_{IIb}\beta_3$ and synthesis of thromboxane A_2 (TXA_2) [7].

While $\alpha_2\beta_1$ is essential for platelet binding, collagen primarily induces signalling events within platelets through GPVI. GPVI belongs to the immunoglobulin superfamily, being non-covalently associated with the immunoreceptor tyrosine-based activation motif (ITAM) FcRγ [226]. Studies suggest that collagen binding to platelets induces clustering of GPVI, which results in the phosphorylation of FcRγ by Src family kinases Lyn and Fyn, associated with the intracellular domain of GPVI [227,228]. This, in turn, is thought to phosphorylate the Syk tyrosine kinase, which is central to the downstream signalling cascade. Syk is thought to lead to the

formation of a signalosome that consists of a scaffold of intracellular adapter proteins, such as LAT, SLP-76 or Gads, which drive the activation of PLCγ2, subsequently leading to PKC activation and intracellular Ca^{2+} release [7] (**Figure 1.12**).

As collagen is a subendothelial protein, it might be considered that only the first layers of platelets recruited to sites of vessel injury will be exposed to this agonist and undergo GPVI-mediated signalling. However, studies identified GPVI as being a fibrin receptor, as well as a collagen receptor, suggesting that fibrin can induce similar signalling involving tyrosine phosphorylation via the GPVI axis. GPVI-mediated signalling could therefore be important for platelets within the outer layers of a thrombus as well [229].

1.3.4.2.2. Soluble agonists-mediated signalling

Soluble agonists including thrombin, ADP, serotonin and thromboxane A_2 induce signalling events through G-protein coupled receptors (GPCRs). GPCRs are receptors with seven transmembrane domains and, as the name suggests, signal through G proteins [84]. These are heterotrimeric proteins, with three subunits that associate in an $\alpha/\beta/\gamma$ complex. G proteins are categorised in four subtypes: Gq/G11, G12/13, Gi/Go/Gz and Gs. The main subtypes associated with the platelet GPCRs are Gq, G12/13 and Gi, involved in platelet activation [230]. Conversely, signalling via Gs occurs as a regulatory mechanism for platelet activation and is mediated by molecules such as prostacyclin (PGI_2), prostaglandin D_2 (PDG_2) or adenosine. These act by increasing the levels of cyclic adenosine monophosphate (cAMP) within the platelets, through promoting their generation via adenylyl cyclase [231]. Increased levels of cAMP have inhibitory effects against platelets. Therefore, signalling through Gs ensures the limitation of platelet activation [232,233]. This is also aided by nitric oxide, which, following release from endothelial cells can diffuse through the platelet membrane and stimulate guanylyl cyclase, increasing the levels of cyclic guanosine monophosphate (cGMP), which also has inhibitory effects against platelets [231].

Thrombin

The most potent platelet agonist is thrombin. Thrombin is generated locally through the coagulation cascade and is essential for the formation of the fibrin clot. Thrombin has multiple platelet receptors, including the protease-activated receptors PAR1 and PAR4 (coupled to Gq, G12/13 and possibly Gi) in human [234], or PAR3 and PAR4 in mice [235], but has also been reported to have the ability to bind GPIbα both in human and mice. It is thought that thrombin first binds to GPIbα, which then allows it to cleave a part of PAR1 and PAR4 extracellular domain. The cleavage product folds onto the central region of the receptor and act as a ligand to initiate signalling [236,237]. Interestingly, a recent study by Estevez *et al.* suggests that GPIbα signalling synergises with PAR signalling in mediating thrombin responses within platelets. This common signalling pathway was shown to involve 14-3-3, Rac1 and LIMK1 [238]. Moreover, amongst the important signalling pathways induced by PAR1 and PAR4 is the activation of the Rho/Rho-kinase pathway by G12/13. This results in myosin light chain phosphorylation, actin cytoskeleton rearrangement and, therefore, mediates platelet shape change from a discoid into a stellar shape, with filopodia extensions [239,240] (**Figure 1.12**).

The first layer of platelets, exposed to both collagen and thrombin, are known as procoagulant platelets and are highly activated. These platelets present phosphatidylserine on their surface and release soluble agonists (such as ADP, thromboxane A_2 and serotonin) that diffuse through the higher layers of the haemostatic plug, inducing platelet signalling within the shell region [241].

ADP, thromboxane A_2 and serotonin

ADP is released from damaged cells, such as endothelial cells during vessel injury, or from platelet dense granules during platelet activation. After release, ADP can bind to its platelet receptors P_2Y_1 (coupled to Gq) and P_2Y_{12} (coupled to Gi), and initiate signalling [242,243]. This happens in a molecule concentration dependent manner – platelets are exposed to a concentration gradient, as ADP gets carried away by the flowing blood once it is released.

Similar to ADP, serotonin is also released from dense granules upon platelet stimulation and acts as an autocrine or paracrine signalling molecule. It can induce signalling through binding to its receptor 5HT2a [84]. Thromboxane A_2 (TXA_2) is synthesised from arachidonic acid as a result of the increase in Ca^{2+} levels during platelet activation. Upon release, it can bind to the platelet receptor TP (coupled to Gq and G13) and further support platelet activation, signalling through PLCβ [244].

Similar to collagen and VWF, soluble agonists initiate different signalling pathways, however these all converge into the activation of PLCβ2, which catalyses the hydrolysis of the phosphatidylinositol biphosphate (PIP2) into diacylglycerol (DAG) and inositol 1,4,5-triphosphate (IP_3). DAG can then activate protein kinase C (PKC), whereas IP_3 triggers the release of Ca^{2+} from the platelet intracellular stores [245,246]. Depending on agonist concentration, these events have the potential to culminate with the release of α and dense granule contents, exposure of phosphatidylserine, shape change and, importantly, activation of $\alpha_{IIb}\beta_3$ [246]. The activation of $\alpha_{IIb}\beta_3$ through this mechanism, is known as 'inside-out' signalling [187] (**Figure 1.12**).

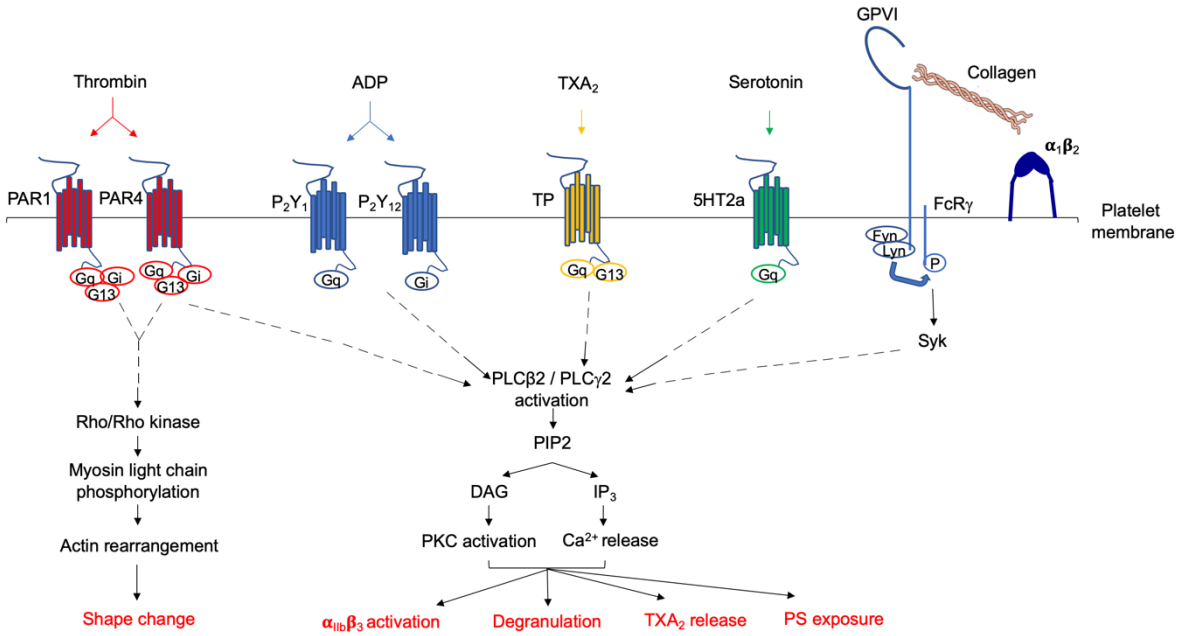

Figure 1.12. Overview of GPCR and GPVI-mediated platelet signalling.

Schematic representation of the main signalling events occurring after platelet stimulation with thrombin, ADP, TXA_2, serotonin and collagen. Initial signalling events differ, but all pathways converge with the PLCβ2/PLCγ2 activation, which catalyses the hydrolysis of PIP2 into DAG and IP_3. DAG then activates PKC, whereas IP_3 induces Ca^{2+} release. Thrombin also activates the Rho/Rho kinase pathway, which phosphorylates the myosin light chain, leading to actin rearrangement. All these events result in the full activation of the platelets, leading to their shape change, activation of $\alpha_{IIb}\beta_3$, degranulation, TXA_2 release and exposure of PS.

1.3.4.2.3. $\alpha_{IIb}\beta_3$-mediated 'inside-out' and 'outside-in' signalling

For a ligand to bind to $\alpha_{IIb}\beta_3$, 'inside-out' signalling events are required to activate the integrin. Studies using NMR spectroscopy revealed that the intracellular tail of the β_3 subunit plays a crucial role in the 'inside-out' signalling through its ability to bind talin [187] and kindlins [247], which are thought to aid talin binding to β_3 [248]. Talin is an anti-parallel homodimer with a molecular weight of approximately 280kDa. It has a large C-terminal rod domain and a small N-terminal domain called FERM (4.1. ezrin, radixin, moesin), which was shown to have the ability to engage with the cytoplasmic tails of β integrins and modulate their activation [249]. According to Vinogradova *et al.*, when platelets are in a resting state, the cytoplasmic tails of the α_{IIb} and β_3 subunits interact with each other. Upon platelet stimulation, talin undergoes a conformational change that allows its FERM domain to bind to the intracellular tail of the β_3 subunit, causing

it to dissociate from the α_{IIb} tail and extend the extracellular domain of the integrin into an open conformation [187]. This conformational change exposes the RGD-binding site of $\alpha_{IIb}\beta_3$, eventually promoting the binding of available ligands.

Ligand binding to activated $\alpha_{IIb}\beta_3$, in turn, leads to "outside-in" signalling taking place, causing further stimulation of the platelets and presentation of the additional pool of $\alpha_{IIb}\beta_3$ from the α granule membranes. 'Outside-in' signalling involves a cascade of events. Initial events involve tyrosine phosphorylation of Src family kinases, including c-Src, Lyn and Fyn and also of Syk kinase [224,250,251]. These phosphorylate proteins downstream, notably FAK (focal adhesion kinase), ADAP (adhesion- and degranulation-promoting adaptor protein) and PLCγ2 (phospholipase Cγ2) [252-254]. As mentioned earlier, phosphorylation of PLCγ2 catalyses the formation of DAG and IP_3, leading to the activation of protein kinase C (PKC) and release of intracellular calcium [254]. Src and Syk kinases are thought to associate with the β_3 tail of $\alpha_{IIb}\beta_3$ [251], whereas the cytoplasmic tail of α_{IIb} was shown to bind to calcium- and integrin-binding protein 1 (CIB1), which also plays a role in the downstream phosphorylation of FAK [255]. FAK substrates include α-actinin and was thus shown to be a key factor in platelet spreading, through cytoskeletal engaging [252]. "Outside-in" signalling events have been shown to be essential for the full platelet activation, aiding platelet spreading, thrombus formation and fibrin clot retraction [186]. 'Inside-out' and 'outside-in' signalling events are summarised in **Figure 1.13**.

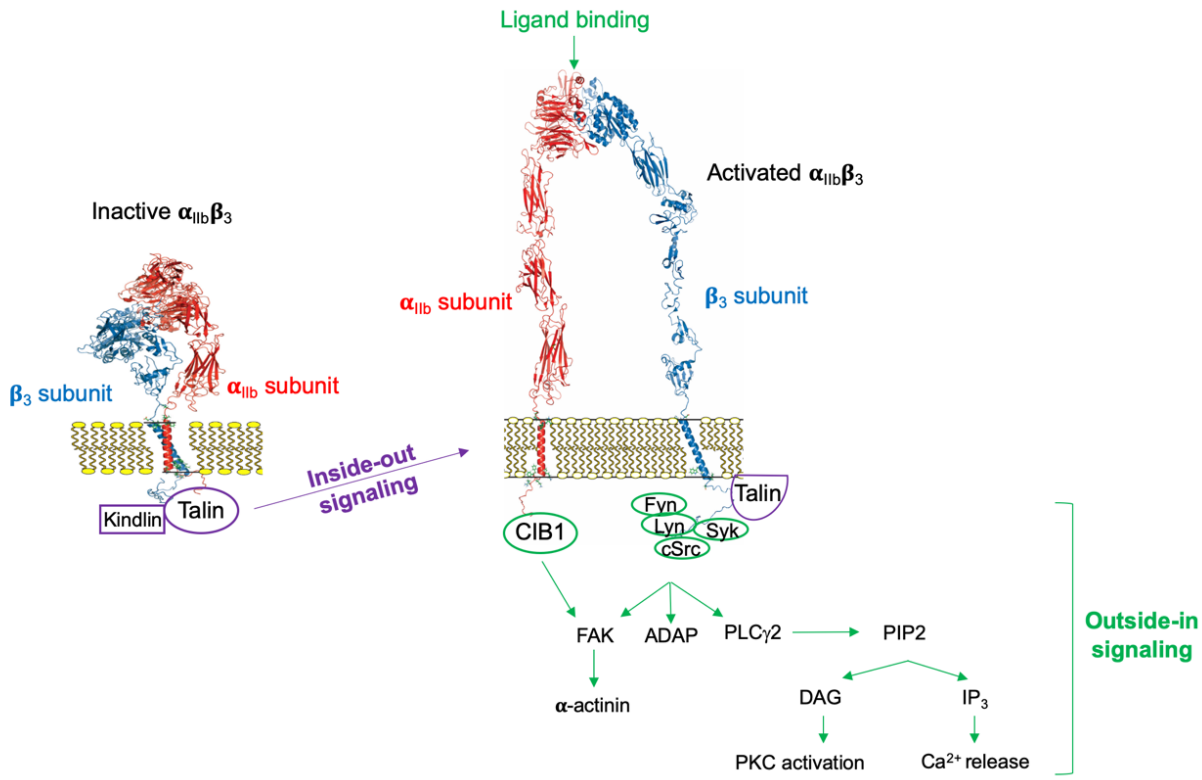

Figure 1.13. 'Inside-out' and 'outside-in' signalling.

$\alpha_{IIb}\beta_3$ mediates 'inside-out' signalling (purple), mainly through its ability to bind talin and kindlin. Talin can undergo a conformational change which interrupts the interaction between the intracellular tails of α_{IIb} and β_3 subunits, leading to the activation of $\alpha_{IIb}\beta_3$. Ligands can then bind to $\alpha_{IIb}\beta_3$ and induce 'outside-in' signalling (green), via CIB1, Src kinases (Lyn, Fyn, cSrc) and Syk. These phosphorylate FAK, ADAP and PLCγ2, which induce cytoskeletal rearrangements (via α-actinin), PKC activation and Ca^{2+} release.

All platelet signalling events are crucial for their roles in haemostasis and beyond. Depending on the type of agonists and the concentration they are exposed to, platelets undergo different phenotypic changes, reaching different activation states. Therefore, platelets have a 'tunable' response, which is best demonstrated by the modern understanding of thrombus architecture.

1.3.5. Thrombus architecture

Classical understanding of thrombus architecture defined it as a structure consisting of fully activated platelets, that underwent shape change and present otherwise intracellularly stored proteins on their surface (i.e. P-selectin, CD40 ligand). However, more recent studies shed light on a different thrombus structure, consisting of a core and a shell region (**Figure 1.14**) [256-260]. The core region was shown to form in the close proximity of the vessel injury site and consist of tightly packed fully activated platelets, with high levels of P-selectin, whereas the shell is represented by loosely adherent platelets, which maintain a discoid initial shape and do not present P-selectin on their surface [256]. The working hypothesis is that the higher platelet density within the core region leads to a slow molecular transport of soluble agonists towards the shell. Larger agonists, such as thrombin, are thought to be restricted to the core region, whereas smaller but also weaker agonists, such as ADP and thromboxane A_2 can reach the shell region [256,257]. Interestingly, studies show that the platelet presence in the external layers of the thrombus is dependent on the VWF A1-GPIbα interaction [261].

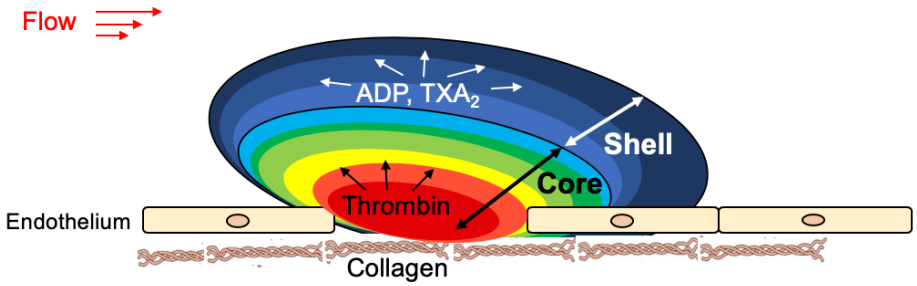

Figure 1.14. Thrombus structure.

Recent understanding of the thrombus structure suggests if consists of a core and a shell region. The core region contains tightly packed fully activated platelets, that are in close proximity to the vessel injury and have access to thrombin. The shell region consists of the outer thrombus levels, where platelets are loosely packed and are stimulated mainly by small soluble agonists, such as ADP and TXA_2.

1.3.6. Platelets beyond haemostasis – Platelets as immune cells

Platelets have classically been recognised for their key role in haemostasis. However, more recent work unravelled crucial platelet roles beyond haemostasis, most notably within the setting of inflammation and infection. This is not only due to the fact that the platelet granules contain numerous inflammatory mediators and cytokines (such as PF4, CCL5), but also due to the presence of receptors associated with infection and inflammation, such as TLR4, TLR2 or TLR7 [262-264]. For this reason, platelets are currently also considered immune cells [122,123,265]. This section focuses on the platelet roles beyond haemostasis.

1.3.6.1. Platelets in inflammation

Platelets have been described to be involved in various inflammatory conditions, including atherosclerosis [266], stroke [267], rheumatoid arthritis [268,269], multiple sclerosis [270] and deep vein thrombosis [271,272].

1.3.6.1.1. Platelets in atherosclerosis

Platelets have been related to the pathology of atherosclerosis. Atherosclerosis is a chronic inflammatory disorder, with severe cardiovascular complications. These include myocardial infarction that occurs following the rupture of the atherosclerotic plaque. Platelets have been shown to have a crucial role both in the initiation and progression of atherogenesis and in the aftermath of the plaque rupture [266,273]. Platelets mediate the inflammatory pathogenesis of atherosclerosis through release of chemokines, such as platelet factor 4 (PF4 or CXCL4) or RANTES (CCL5), from their granules [274]. This is thought to be triggered by the presence of oxidised LDL (oxLDL) at the atherosclerotic plaque site, which can stimulate platelets via TLR4 and cause degranulation [275]. Moreover, platelets adhere to the inflamed endothelium and are subsequently thought to play a crucial role in recruiting monocytes, facilitating, in this way, their transmigration in the vessel wall, where they transform into macrophages and, eventually, into foam cells [273].

1.3.6.1.2. Platelets in deep vein thrombosis

Although considered to mainly play a role in arterial thrombotic disorders, platelets have more recently been shown to be a key factor in the initiation events of deep vein thrombosis (DVT) [271,272]. DVT is a leading cause of cardiovascular morbidity and mortality worldwide and is identified as an inflammatory disorder [276]. Compared to other cardiovascular diseases, the incidence of DVT and its associated complications, such as pulmonary embolism, continues to increase [277]. As DVT occurs in the absence of overt vessel damage, the underlying mechanisms leading to this inflammatory thrombotic disorder are not fully understood. Platelets have recently been identified to be involved in DVT, through their ability to recruit neutrophils and monocytes [272]. Interestingly, both *Vwf*$^{-/-}$ and *GpIb*$\alpha^{-/-}$ mice were shown to be protected against DVT, although the reasons for this protective phenotype have not been fully unveiled [271,272].

1.3.6.2. Platelets in infection

Platelets are amongst the first cells to be recruited at sites of vessel injury. This is thought to not only occur for the purpose of stopping excessive bleeding, but also for preventing pathogens from entering and disseminating in the vasculature. In this situation, platelets are the first line of host defence. Moreover, it recently became apparent that platelets continuously scan the vascular wall, particularly within the liver sinusoids. Within the hepatic vasculature, platelets were shown to interact with Kupffer cells, in a VWF and GPIbα-dependent manner [278].

When encountering pathogens, platelets act as immune cells through two main mechanisms: 1) their ability to directly bind bacteria and viruses and 2) their ability to release antimicrobial molecules [122,263].

Platelets can directly interact with bacteria and viruses through Toll-like receptors (TLRs). TLRs are receptors that have the ability to recognise pathogen-associated molecular patterns

(PAMPs). These are represented by components specific to bacterial cells walls (i.e. lipopolysaccharides – LPS, peptidoglycan, teichoic acid), or viral-specific markers (i.e. double stranded RNA or unmethylated CpG islands) [279]. Platelets express TLRs on their surface. Among the best characterised platelets TLRs are TLR2 and TLR4, which aid bacterial recognition, and TLR7, which helps in viral recognition [280].

Platelet engagement of TLR2 by bacteria such as *Streptococcus pneumoniae* stimulates platelets via PI3-kinase pathway and promote platelet aggregation and neutrophil recruitment at sites of infection [264]. Similarly, engagement of platelet TLR4 via LPS stimulation or *Escherichia coli* was associated with thrombocytopenia, platelet aggregation and cytokine release and subsequent interactions with neutrophils [262,281]. Through their direct interactions with bacteria and ability to form aggregates at sites of infection, platelets are thought to aid bacterial sequestration and promote bacterial clearance through recruitment of neutrophils and inducing neutrophil extracellular trap (NET) release [282].

Platelets were also shown to be able to release antimicrobial molecules, that further demonstrate their immune function. Amongst these are kinocidins, thrombocidins or defensins [283-285].

An additional mechanism through which platelets contribute to inflammation and infection is dependent upon their ability to interact with leukocytes. Platelet-leukocyte interactions have been the focus of this thesis and will be discussed in detail in **Section 1.5**.

1.4. Leukocytes

1.4.1. Overview of leukocytes

Leukocytes are nucleated cells and their normal blood levels range between 4,000 to 10,000/mm^3 [286]. Apart from blood, leukocytes can also be found within the lymphatic system, and can additionally migrate to tissues, towards sites of infection. Through this mechanism, and many others, leukocytes fulfil their functions – protecting against and fighting off infections. Therefore, leukocytes (particularly myeloid and lymphoid cells) can be defined as immune cells, representing the major constituents of the innate and adaptive immune system respectively.

Leukocytes are formed in the bone marrow, through a process called haematopoiesis. Although initially arising from the common pluripotent haematopoietic stem cell, different downstream lineages result in the production of various leukocyte subtypes, that differ in morphology and function. A schematic representation of the haematopoietic tree is illustrated in **Figure 1.15**. Briefly, the pluripotent haematopoietic stem cell gives rise to a common myeloid progenitor and a common lymphoid progenitor. The common myeloid progenitor leads to the formation of the megakaryocyte-erythrocyte progenitor (MEP) and the granulocyte-monocyte progenitor (GMP). MEP develops into erythroblasts, which give rise to erythrocytes/red blood cells, and megakaryocytes which further develop into platelets. GMP, as the name suggests, can progress into different leukocyte types, including granulocytes (basophils, eosinophils, neutrophils) or monocytes. On the other hand, the common lymphoid progenitor can give rise to another type of leukocytes, named lymphocytes (B cells, T cells and natural killer cells (NK cells)) [287].

The different types of leukocytes formed through haematopoiesis further fall under two main categories: peripheral blood mononuclear cells, comprising of monocytes and lymphocytes, and granulocytes/polymorphonuclear cells, including neutrophils, eosinophils and basophils.

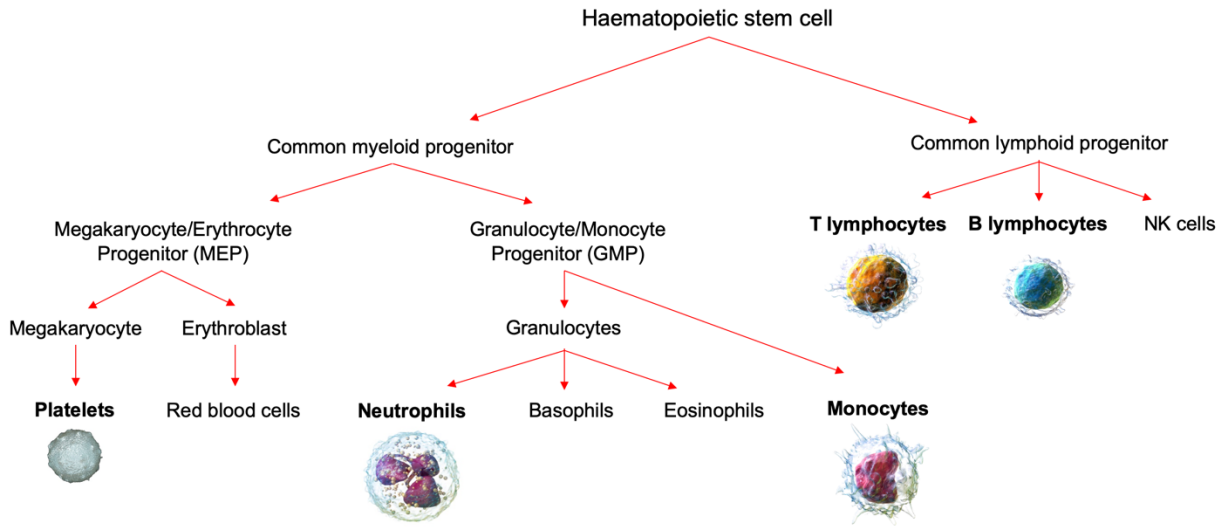

Figure 1.15. Haematopoietic tree.

Schematic representation of the haematopoiesis process, in which the initial pluripotent haematopoietic stem cells gives rise to two lineages – the common myeloid progenitor lineage and the common lymphoid progenitor lineage. The common myeloid progenitor eventually results into the formation of platelets, red blood cells, granulocytes (neutrophils, basophils and eosinophils) and monocytes. On the other hand, the common lymphoid progenitor gives rise to T lymphocytes, B lymphocytes and NK cells. Platelets, as well as the main leukocyte subtypes discussed in this section are highlighted in bold and their morphology is illustrated.

1.4.2. Peripheral blood mononuclear cells

Peripheral blood mononuclear cells (PBMCs) are leukocytes that contain a limited number of granules in their cytoplasm and have a single, non-lobulated nucleus. These represent monocytes and lymphocytes (T cells, B cells and NK cells).

1.4.2.1. Monocytes

Monocytes are primarily involved in the innate immune responses. They have a large, kidney-shaped nucleus and are the main type of phagocytic cell found in the blood [288]. There are at least three subtypes of monocytes in humans, based on the markers expressed on their surface – classical (85%, $CD14^{++}/CD16^{-}$), intermediate (5-10%, $CD14^{+}/CD16^{+}$) and non-classical (5-10%, $CD14^{-}/CD16^{++}$) monocytes [289,290], which are equivalent to two subtypes of monocytes in mice – classical ($Ly6C^{high}$) and non-classical ($Ly6C^{low}$) [291]. Recent single cell RNA sequencing data has shown that there may be more than 2-3 subsets of monocytes

circulating in the blood of mice and humans respectively [292]. Validation of this observation is currently underway.

Monocytes are recruited at sites of infection, promoting inflammation or aiding tissue repair. They are the main type of phagocytes within the immune system, their involvement in the innate immune response being based to their phagocytic function [288]. After migrating into tissues, at sites of inflammation, monocytes are known to progress into macrophages [289]. Macrophages can be found in almost all tissues, being able to recognise and engulf microorganisms. Some tissues present with a population of resident macrophages, namely Kupffer cells in the liver [293], microglia in the nervous system and Langerhans cells in the skin [294]. Macrophages can phagocytose pathogens and then present antigens on their surface, being classified as antigen-presenting cells. In this way, macrophages facilitate pathogen recognition by lymphocytes and contribute to the adaptive immune response as well [288].

1.4.2.2. Lymphocytes

Lymphocytes are more abundant than monocytes, constituting approximately 20-45% of the total leukocyte population [286], but are smaller in size, with a diameter of 8-10μm. There are three main types of lymphocytes, including T cells, B cells and NK cells. T cells and B cells are the leading constituents of the adaptive immune response, whereas NK cells are important in innate immunity [295].

T cells

Similar to the other blood cell types, T cells originate in the bone marrow, but they subsequently undergo a maturation process within the thymus. During the maturation process, T cells develop into two major subtypes – T helper cells (CD4+) and cytotoxic T cells (CD8+). Based on their cytokine profile, T helper cells are further divided in different sub-categories, including Th1, Th2, Th9, Th17, Th22 and Treg (regulatory T cells). The different T helper cells contribute to the adaptive immune system by releasing cell-specific pro- or anti-inflammatory

cytokines, such as interferon γ (IFN-γ), interleukins (e.g. IL-4, IL-10, IL-21), TNF, or TGF-β. These help in either promoting or suppressing immune responses [296].

CD8+ cytotoxic T cells contribute to the adaptive immunity by directly targeting and destroying infected cells. Studies also show that CD8+ can also target and destroy malignant cells. Cytotoxic T cells recognise infected cells as these present antigens on their major histocompatibility complex (MHC), which is present on all nucleated cells. Cytotoxic T cells mainly act on virally infected cells via three different mechanisms. First of all, they can release TNF-α and IFN-γ, which have anti-viral properties. Secondly, they release the contents of cytotoxic granules, including perforin and granzymes, which can enter the infected cells and supress the viral protein synthesis. Finally, cytotoxic T cells are also known to induce the apoptosis of the infected cells via Fas/Fas ligand interaction, which triggers the caspase cascade, a well-characterised apoptotic pathway. The type of adaptive immunity mediated by T cells is known as cellular adaptive immunity [297,298].

B cells

B cells contribute to the adaptive humoral immune response. Upon antigen encounter, B cells can transform into plasma cells, which are crucial for the production of immunoglobulins or antibodies. Thus, as opposed to T cells that induce cellular responses, B cells mediate humoral adaptive immunity. Antibodies can be defined as Y-shaped glycoproteins, that recognise a specific antigen. Their structure consists of two light chains and two heavy chains, linked via disulphide bonds, and contain a variable region and a constant region. Antibodies bound to antigens can aid phagocytosis by macrophages or NK cells, as well as by blocking pathogens from binding to their host cells [299].

NK cells

Natural killer (NK) cells are a subtype of lymphocytes with a crucial role in innate immunity. Unlike other immune cells, NK cells do not need to be primed or activated in order to destroy

tumour cells or virally-infected cells [300]. When in contact with an infected or malignant cell, NK cells are known to release cytokines, including IFN-γ and TNF-α and also cytotoxic granules containing perforin and granzymes, which ultimately promote the apoptosis of infected cells [300,301]. Due to their ability to recognise and target malignant cells, NK cells are currently analysed as a potential immunotherapeutic strategy for cancer [302].

1.4.3. Granulocytes/Polymorphonuclear cells

Granulocytes/polymorphonuclear cells (PMNs), as their name suggests, have lobular nuclei (generally 3-5 nuclear lobes) and a high granule content. They have a diameter of approximately 12-15μm and are the most abundant type of leukocytes, representing more than 50% of the total leukocyte population in humans. Granulocytes are further divided in three subtypes, represented by neutrophils, basophils and eosinophils [303-305].

Basophils and eosinophils

Basophils and eosinophils only constitute approximately 5% of the leukocyte population [286]. Eosinophils are known to be involved in parasitic infections, as well as in allergic asthma [305,306]. Basophils fulfil a significant role in allergic reactions, as well as in filarial worm and tick infections. They become activated after binding to pathogen-associated molecular patterns (PAMPs) or, importantly, to IgE, the major immunoglobulin involved in allergies. During activation, basophils release the contents of their granules, including histamine, which triggers allergic reactions [303].

Neutrophils

Neutrophils are the most abundant type of leukocytes, constituting approximately 50-80% of the circulating leukocytes. Their distinctive morphology includes a multilobular nucleus (2-5 lobuli), and a high granular content [304]. Similar to the other blood cell types, neutrophils are formed within the bone marrow, as a result of granulocyte colony-stimulating factor (G-CSF) stimulation. It has been shown that the bone marrow of a healthy individual generates

approximately 1-2 x 10^{11} neutrophils per day, which can increase further to 10^{12}, following bacterial infections. Once released in the circulation, neutrophils have a relatively short life-span of approximately 8-12 hours within the circulation, and 1-2 days within tissues [304,307]. Neutrophils have been identified as the first line of defence against infections caused by bacteria, fungi and protozoa. Neutrophils are involved in both innate and adaptive immunity [308]. The latter is mainly regulated through their ability to interact with other immune cells, such as macrophages, dendritic cells or lymphocytes [309]. The crucial role neutrophils fulfil in innate immunity is discussed below.

1.4.4. Neutrophil function in innate immunity

Neutrophils have been recognised for their crucial role in innate immunity, as they are the first cells recruited to sites of infection. As a result, both neutropenia and loss of neutrophil function have been linked to severe, life-threatening bacterial infections [310,311]. Like all leukocytes, neutrophil recruitment to sites of infection is a multistep process. Neutrophils first roll on the activated endothelium before becoming strongly attached. Recent studies suggest that platelets have a major contribution to neutrophil recruitment at sites of extravasation. Subsequently, neutrophils can spread and transmigrate into the infected tissue, where they become activated [312].

Once recruited to the site of infection, neutrophils identify the pathogen through pathogen recognition receptors (PRRs). PRRs recognise pathogen-associated molecular patterns (PAMPs) (e.g. LPS, teichoic acid, double-stranded RNA) or damage-associated molecular patterns (DAMPs) (e.g. mitochondrial DNA, high-mobility group protein B1), enabling neutrophils to distinguish both pathogens and infected/damaged cells. Amongst the most important PRRs are Dectin-1 (involved in fungi infections), TREM-1 (involved in bacterial and fungi infections) and TLRs (well-characterised in bacterial infections) [309]. Apart from PRRs, neutrophils also express opsonic receptors, including Fc receptors (FcγRIIA, FcγRIIIB, FcγRI), through which they can identify immune complexes [313].

After recognising the pathogen, there are different ways in which neutrophils promote pathogen clearance, including phagocytosis, release of their granule contents, production of reactive oxygen species (ROS) and release of neutrophil extracellular traps (NETs) [304]. This section describes the different mechanisms involved in pathogen clearance, with a focus on NET formation.

1.4.4.1. Phagocytosis

After recognising a pathogen, neutrophils are known to engulf it through phagocytosis. This is a very rapid process, that can take place within seconds [314] and results in the uptake of the pathogen in a specific vacuole. This can subsequently fuse with neutrophil granules, forming the phagosome. Amongst neutrophil granular contents that can promote direct mechanisms to destroy the pathogen are hydrolytic enzymes and NADPH oxidase [315].

1.4.4.2. Degranulation and ROS production

Neutrophil granules have antimicrobial properties through their contents. Apart from fusing with the phagocytic vacuole to contribute to the process of phagocytosis, neutrophil granules can also fuse with their plasma membrane, being released extracellularly where they can act directly upon pathogens or infected cells. Simultaneously, neutrophil NADPH oxidase gets activated, promoting the generation of reactive oxygen species (ROS) [304].

Neutrophil granules can be divided into three categories: azurophilic/primary granules, specific granules and gelatinase granules. The predominant granule protein is represented by myeloperoxidase (MPO) and is found within the azurophilic granules. Its main action is to catalyse the reaction of hydrogen peroxide with chloride, resulting in the formation of hypochlorous acid. This, in turn, acts as a bactericidal oxidant and, therefore, contributes to ROS production. Alongside MPO, azurophilic proteins contain a series of neutrophil serine proteases, including cathepsin G, neutrophil elastase (NE), proteinase 3 or neutrophil serine protease 4. These were shown to have the ability to directly induce bacterial death by

destroying their membrane integrity, or cleave other crucial proteins involved in the pathogen virulence. Other important proteins within neutrophil granules are cationic peptides, such as α-defensin, also present within azurophilic granules and cathelicidins (such as LL-37) present in specific granules, which contribute to pathogen clearance through formation of pores in their membranes and subsequent inhibition of pathogen DNA, RNA and protein synthesis. The specific granules also importantly contain lactoferrin, which prevents pathogen binding to their target cells, and calprotectin, which inhibits bacterial growth [316,317].

Granule contents are also released during the formation of neutrophil extracellular traps, which are the focus of the next sub-section.

1.4.4.3. Neutrophil extracellular trap (NET) formation

Neutrophil extracellular traps (NETs) were first observed in 2004 by Zychlinsky *et al.* and can be defined as mesh-like structures consisting of chromatin fibres (15-17nm in diameter), histones and granule cytotoxic proteins through which neutrophils can "trap" and destroy pathogenic microorganisms [318,319]. Studies have since classified the release of NETs as both a novel mechanism of programmed cell death and a pathogen clearance mechanism from intact neutrophils [320]. Other types of immune cells, such as eosinophils and mast cells have been indicated to release extracellular traps, but NETs have been best characterised so far [321,322].

Different pathogens are thought to induce NET release, including a variety of bacteria, protozoa and fungi [318,323,324]. Additionally, there are different chemical triggers described, including pro-inflammatory cytokines (such as TNFα or IL-8), PAMPs (such as LPS) or reactive oxygen species (ROS). More recently, platelets have also been identified as potential mediators of NET formation (NETosis) via different mechanisms [282,325]. In experimental settings, phorbol 12-myristate 13-acetate (PMA) is the most commonly used NET stimulus. Classical NETosis is considered to be a slow process, occurring over the course of 2-4 hours

following pathogen encounter [318-320]. In contrast, LPS-stimulated platelets were recently shown to induce NET release within minutes, although the underlying molecular mechanism is not fully understood [282].

For a long time, NETosis has been considered to be a process that always results in the neutrophil death. However, more recently, studies revealed that NETosis could also be a vital process, following which neutrophils can retain their phagocytic and chemotactic function [326,327]. Therefore, two pathways have been proposed to explain the process of NETosis: lytic/'suicidal' NETosis and non-lytic/vital NETosis (**Figure 1.16**). Lytic NETosis has been well-characterised and is thought to occur via the NADPH oxidase (Nox)-dependent pathway, being triggered by the main characterised chemical stimuli, such as PMA. Due to the involvement of NADPH oxidase, the formation of reactive oxygen species is a crucial step for lytic NETosis. On the other hand, vital NETosis is thought to occur through a Nox-independent mechanism. In this situation, the cell does not become lysed, but the NETs are thought to be extruded via vesicles that leave the cell membrane intact. Studies suggest that vital NETosis is a more rapid response, taking place within 1-2 hours following stimulation by direct contact with the pathogen (such as *Staphylococcus aureus*) or via interactions with TLR4-stimulated platelets [327-329].

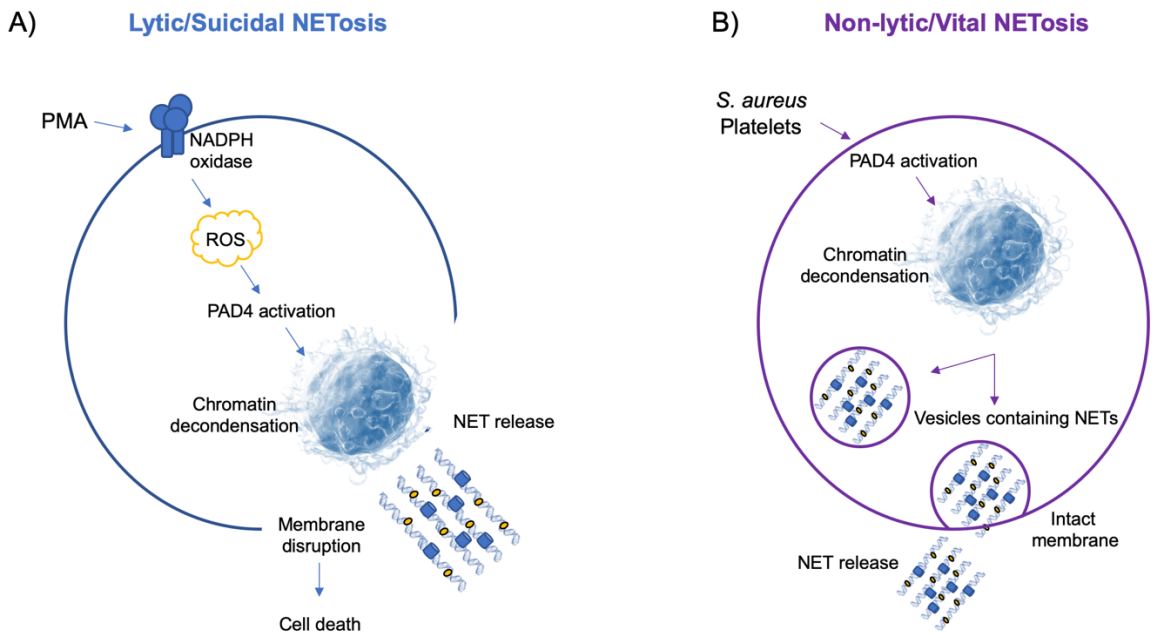

Figure 1.16. Overview of lytic/suicidal vs. vital NETosis.

A) Lytic/Suicidal NETosis is thought to be NADPH oxidase-dependent, being initiated by PMA mainly, but also by antibodies or cholesterol crystals. NADPH oxidase leads to ROS production and subsequent PAD4 activation. This causes chromatin decondensation. Granule proteins, such as myeloperoxidase (MPO) and neutrophil elastase (NE) are translocated to the nucleus. NETs are released through the neutrophil membrane disruption, resulting in neutrophil death. B) Vital NETosis is NADPH oxidase-independent and is initiated via direct interaction with bacteria (S. aureus, E. coli), DAMPs or TLR4-stimulated platelets. PAD4 activation and chromatin decondensation, together with MPO and NE translocation to the nucleus occur in vital NETosis as well. The main difference compared to lytic NETosis is represented by the fact that NETs are released via vesicles, while the neutrophil membrane remains intact. These neutrophils are thought to retain their phagocytic and chemotactic functions [326,329].

Both Nox-dependent and Nox-independent NETosis pathways converge within the nucleus, where they initiate chromatin decondensation. This process is dependent on histone deamination, which relies on the ability of peptidylarginine deiminase 4 (PAD4) to convert arginine side chains to citrullines [330,331]. This disassembles the tightly packed DNA-histone chromatin structure, allowing it to decondense and resulting in the nucleus losing its well-defined lobular morphology after about 60 minutes from stimulation (**Figure 1.17**) [320]. Finally, during expulsion from the cells, chromatin binds to granular contents, including MPO, NE, lactoferrin, LL-37 or S100A. These, together with citrullinated histones, represent specific hallmarks for NETosis and have important antimicrobial properties, as described above [332].

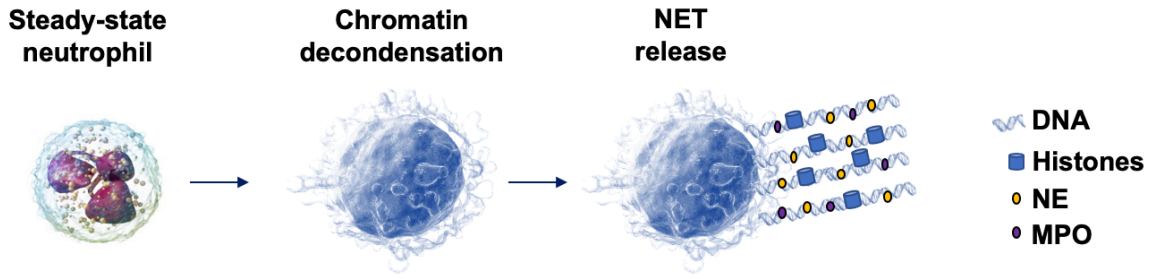

Figure 1.17. Overview of NETosis.

The steady-state neutrophil presents an intact, multi-lobulated nucleus and multiple granules within its cytoplasm. The first step towards the formation of NETs is represented by chromatin decondensation, with subsequent cell size increase. Finally, DNA is extruded from the neutrophils, together with granular content, including histones, myeloperoxidase (MPO) and neutrophil elastase (NE), which constitute the NET.

1.4.4.3.1. NETs – Double-edged swords

Despite their beneficial effects in clearing pathogens and being a part of the innate immune system, excessive intravascular NETosis has been shown to be detrimental in many respects. For this reason, NETs are considered double-edged swords [319], as a balance must be maintained to ensure that, while they fulfil their positive effects, they are prevented from causing more harm than good. This balance is partly regulated by DNases that clear NETs [333].

Excessive NETosis has been associated with various pathological conditions, varying from autoimmune disorders (vasculitis, systemic lupus erythematosus, psoriasis) [321,334-336], pre-eclampsia [337], sepsis [282] and, importantly, thrombosis [331,338-340].

Intravascular NETs are highly pro-thrombotic. Evidence suggests that NETs provide a scaffold for the forming thrombus, being able to bind platelets and sequester red blood cells, thus leading to the increase in the thrombus size and aiding thrombus stability. Moreover, NETs have the ability to bind plasma proteins, such as VWF, fibrinogen and fibronectin [338]. NETs are negatively charged and, as such, can bind and activate FXII, thus initiating the intrinsic

coagulation cascade [272]. Therefore, NETs aid the thrombotic process through a variety of mechanisms.

There is increasing evidence to suggest that NETs promote the development of deep vein thrombosis [340]. Indeed, treatment with DNase I prevented thrombus formation in mouse DVT models and prevented further thrombus growth if administered after the thrombus formed, confirming the involvement of NETs in the development of this disease. Neutrophil involvement in DVT has been established not only through the link between NETs and DVT, but also through studies that shown that neutrophil depletion is protective against DVT. The contribution of neutrophils to DVT is also thought to be mediated through their ability to bind platelets [272,338]. The importance of platelet-leukocyte interactions is further discussed in the following section.

1.5. Platelet-leukocyte interactions

Platelets fulfil many roles beyond haemostasis and have more recently been recognised as immune cells. However, to contribute in immune settings, such as inflammation and infection, platelets invariably need to interact with leukocytes or modify leukocyte function [122,123,265,284,341]. Various platelet-leukocyte interactions have been characterised previously and are discussed in this section.

1.5.1. Characterised platelet-leukocyte interactions

Resting platelets do not interact with resting leukocytes. For this reason, platelet-leukocyte interactions generally require either the platelet or the leukocyte, or both cell types, to be activated.

The main previously characterised platelet-leukocyte interactions require platelets to undergo degranulation. Through this process, platelets present important leukocyte receptors on their surface, namely P-selectin and CD40 ligand (CD40L). P-selectin is a transmembrane glycoprotein found both on platelets and endothelial cells. It is constitutively presented on the endothelium in low amounts and also stored within Weibel-Palade bodies together with VWF, being rapidly exposed upon endothelial activation [342]. Platelet P-selectin is often viewed as a specific marker for platelet activation. Similarly, CD40L is presented onto the platelet surface following robust activation and degranulation. P-selectin and CD40L can then interact with their respective receptors constitutively expressed on the surface of leukocytes, P-selectin glycoligand-1 (PSGL-1) and CD40 [343-346].

Leukocyte activation occurs during an acute infectious or inflammatory event, as a response to various signals that stimulate the host immune system. Moreover, the P-selectin-PSGL-1 interaction can trigger signalling events within the leukocyte, leading to the activation of leukocyte Mac-1 integrin (i.e. Mac-1, also termed CD11b/CD18 or $\alpha_M\beta_2$) [347], which can stabilise the platelet-leukocyte interactions directly, via GPIbα, or indirectly, via fibrinogen that binds to

the activated $\alpha_{IIb}\beta_3$ [141,348]. Studies also report another integrin on the leukocyte surface, LFA-1 (also termed CD11a/CD18 or $\alpha_L\beta_2$) to be able to mediate interactions with platelets via ICAM-2 [349]. The main previously characterized platelet-leukocyte interactions are summarized in **Figure 1.18**.

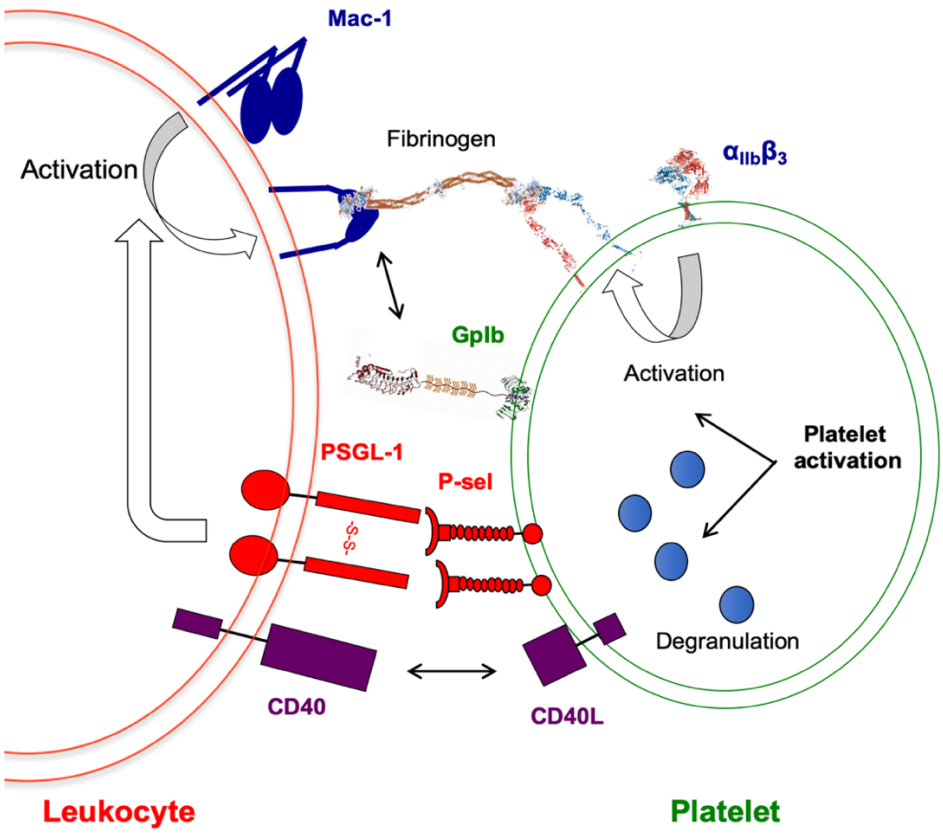

Figure 1.18. Characterised platelet-leukocyte interactions.

Previously characterised platelet-leukocyte interactions require either the platelet or the leukocyte, or both, to be fully activated. The main interactions are mediated via P-selecin-PSGL-1 axis and CD40L-CD40. P-selectin-PSGL-1 can induce the activation of the Mac-1 integrin on the surface of leukocytes, which can further stabilise the interactions by binding to GPIbα or to fibrinogen, which binds to activated $\alpha_{IIb}\beta_3$.

1.5.2. Importance of platelet-leukocyte interactions

The importance of platelet-leukocyte interactions has been increasingly recognised. Physiologically, these interactions have been shown to contribute to the normal haemostatic response,[350] as well as being involved in innate immunity. From a pathological perspective, the presence of platelet-leukocyte aggregates in the vasculature has been associated with an increased severity of certain inflammatory and infectious diseases [271,312,346,351]. The importance of platelet-leukocyte interactions is summarised in **Figure 1.19**.

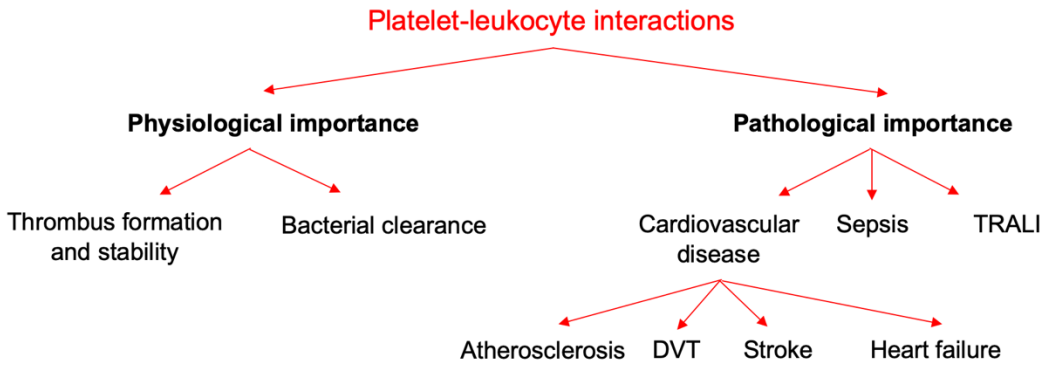

Figure 1.19. Importance of platelet-leukocyte interactions.

Schematic representation summarising the main physiological and pathological conditions in which platelet-leukocyte interactions are involved.

1.5.2.1. Physiological importance

From a physiological perspective, platelet-leukocyte interactions contribute to thrombus formation and stability, as well as to the innate immune system.

1.5.2.1.1. Platelet-leukocyte interactions in haemostasis

Leukocyte involvement in the setting of haemostasis has been recognised for a long time. The first observation of leukocytes being present within a thrombus dates back to the original platelet study published by Bizzozero in 1882 [352]. Since then, the role of leukocytes in thrombus formation and stability has been well characterised. Studies indicate that the main leukocytes involved in haemostasis are represented by monocytes and neutrophils.

Neutrophils appear to be recruited at the site of vessel injury even prior to platelets, in an activated endothelial cell-dependent manner. On the other hand, monocytes are observed 3-5 minutes following vessel damage [350]. Leukocyte recruitment at the site of thrombus formation was also shown to be mediated via P-selectin expressed by activated platelets [346,353], although it is not clear how leukocytes are interacting with the platelets in the shell of the thrombus, as these platelets do not express P-selectin [256]. Recruited by endothelial cells and platelets, leukocytes are a major contributor to the normal haemostatic process by promoting fibrin deposition at the sites of vessel injury and, thus, stabilising the clot [353]. It was recently shown that neutrophils represent the main blood-borne tissue factor source at the site of vessel injury, thus being a key factor in the continued initiation of the extrinsic coagulation cascade [350].

1.5.2.1.2. Platelet-leukocyte interactions in innate immunity – Platelets as mediators of NETosis

Aside from their physiological role in haemostasis, platelet-leukocyte interactions have been recognised for their importance within the innate immune system. Thus, platelet-monocyte aggregates play a key role in infections with *Leichmania major* whereas platelet-neutrophil aggregates have been reported in cases of *Staphylococcus aureus* and *Escherichia coli* infections [354,355].

Platelets help leukocytes fulfil their immune functions in different ways. First of all, leukocytes need to migrate outside the vasculature towards sites of infection to initiate an effective rapid immune response. Recent studies identified platelets as playing a key role in guiding leukocytes towards their sites of extravasation, in interactions mediated mainly via CD40L-CD40 and P-selectin-PSGL-1 [356]. Secondly, platelets interacting with neutrophils have the ability to promote NETosis and, in this way, contribute to bacterial clearance. Platelets can modulate NET formation either through direct interactions with neutrophils, or via released chemokines (i.e. platelet factor 4, RANTES, thromboxane A2 or high mobility group box 1) [357]. Studies show that, in some settings, platelets can induce NET release in a P-selectin-dependent manner [358], although more recent research focussing on mechanisms mediating

bacterial clearance within the liver sinusoids revealed that platelets can also bind neutrophils and initiate NETosis via an yet unknown platelet receptor [359]. Finally, platelets stimulated via their TLR4 receptor were also shown to be able to interact with neutrophils and induce NETosis, despite the absence of P-selectin from their surface [282]. These studies suggest that there might be crucial additional interactions between platelets and leukocyte that are yet to be characterised.

1.5.2.2. Pathological importance

Studies suggest that platelet-leukocyte interactions play a key role in cardiovascular conditions, such as atherothrombosis, atherosclerosis, stroke or deep vein thrombosis (DVT) [272,344,360]. There are also reports of higher number of circulating platelet-leukocyte aggregates in sepsis [361] and transfusion-related acute lung injury (TRALI) [362], or in chronic conditions including diabetes [363] and heart failure [364].

Monocytes and neutrophils are the major leukocyte subsets involved in platelet interactions. Platelet-monocyte aggregates are a major marker for atherosclerosis and heart failure [351,364], whereas platelet-neutrophil interactions are an important determinant in sepsis and TRALI [361,362]. Platelets, neutrophils and monocytes are involved in the pathogenicity of DVT in mice [272], although precisely how this is mediated is not fully understood. As suggested by von Brühl *et al.* (2012), monocytes promote the thrombotic state by being an important source of intravascular tissue factor, whereas neutrophils contribute by the release of neutrophil extracellular traps (NETs), which are highly pro-thrombotic and can initiate the intrinsic coagulation cascade via FXII [272]. Interestingly, leukocyte recruitment to sites of thrombus formation were markedly reduced in the absence of VWF (*Vwf*$^{-/-}$ mice) [271] or in mice lacking the extracellular domain of GPIbα (*IL4-R/Ibα* mice) [272], suggesting a role for the VWF-GPIbα interaction in DVT.

Venous thromboembolism (a term describing DVT and its major complication, pulmonary embolism) is a major cause of morbidity and mortality worldwide [276,277]. Recent Genome Wide Association Studies (GWAS) identified two new susceptibility loci for VTE – *TSPAN15* and *SLC44A2,* both of which have no known links with thrombosis/coagulation and could, therefore, provide new mechanistic insights into the pathogenesis of DVT and potential novel therapeutic targets against this condition [365-367].

SLC44A2

Also known as choline transporter-like protein-2 (CTL-2) or human neutrophil antigen-3 (HNA-3), SLC44A2 is transmembrane protein with 10 membrane-spanning domains [368]. It is highly expressed in neutrophils and, in lower levels, in endothelial cells and platelets (http://immprot.org). Given its homology with choline-transporter protein 1 (CTL1), SLC44A2 is speculated to have a transporter function, aiding the transport of choline, but this has not been demonstrated [369]. In fact, the cellular function of SLC44A2 is not well-defined. It has been associated with hair cell loss, spiral ganglion degeneration and hearing loss in mice [370], and with Meniere's disease and transfusion related acute lung injury (TRALI) in humans [368,371].

SLC44A2 became a focus of haemostatic research when GWAS studies identified a polymorphism in its encoding gene (*rs2288904-G/A*), which is linked to protection against VTE [365,367,372]. This mutation affects the first and longest extracellular loop of SLC44A2, but its effect has not previously been investigated. This thesis uncovers a potential new role for SLC44A2, which could provide a mechanistic link between this candidate and DVT.

Given the implication of platelet-leukocyte interactions in a wide range of chronic and acute pathological conditions, it is crucial to understand and identify all the receptors and ligands involved.

1.6. Hypothesis and aims

Hypothesis

The ability of VWF A1 domain to induce modest signalling within platelets has been widely accepted, although its role was not fully elucidated. A recent study showed that platelets bound to von Willebrand Factor (VWF) are able to capture leukocytes under flow, in the absence of any potent platelet agonists [85]. I hypothesised that VWF A1 'primes' platelets under flow, enabling them to form novel interactions with leukocytes, while modulating their effector function.

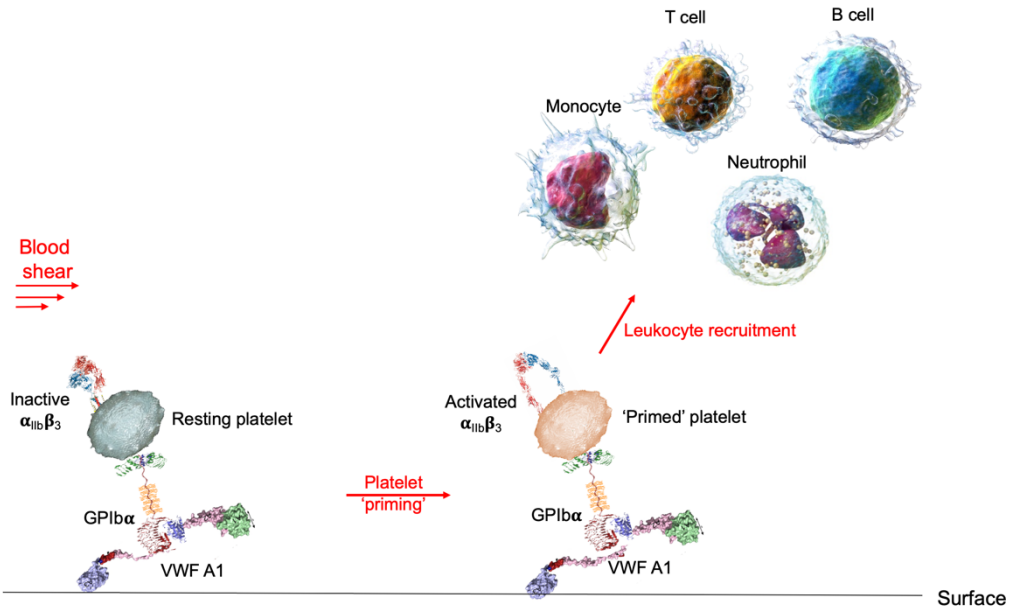

Figure 1.20. Summary of PhD hypothesis.

Globular VWF does not interact with resting platelets. However, when VWF binds to a surface or gets tangled, it can unravel and capture platelets via the A1-GPIbα interaction. I hypothesised that this can 'prime' the platelets and lead to novel interactions with leukocytes under flow.

Aims

To test this hypothesis, my PhD was developed around seven aims:

Aim 1: Express and purify recombinant VWF A1 domain and A1* (Y1271C/C1272R)

Aim 2: Characterise the VWF A1-GPIbα interaction under flow

Aim 3: Identify the platelet receptor interacting with leukocytes under flow

Aim 4: Identify the leukocyte subset interacting with the VWF-'primed' platelets

Aim 5: Analyse the impact of VWF-'primed' platelet-leukocyte interactions on leukocyte effector function

Aim 6: Identify the leukocyte receptor interacting with the VWF-'primed' platelets

Aim 7: Investigate the *in vivo* pathophysiological importance of the 'primed' platelet-leukocyte interaction

Chapters

These aims were addressed as part of five Results Chapters:

Chapter 1 – VWF A1-dependent platelet 'priming' (aims 1 and 2)

Chapter 2 – Characterising the 'primed' platelet-leukocyte interaction (aims 3 and 4)

Chapter 3 – 'Primed'-platelet leukocyte interaction effect upon neutrophil phenotype (aim 5)

Chapter 4 – Identifying the leukocyte receptor interacting with the 'primed' platelets (aim 6)

Chapter 5 – Characterisation of VWF A1-GPIbα mediated signalling *in vivo* (aim 7)

2. Materials and Methods

Materials

Antibodies flow assay	Target	Company	Fluorophore	Dilution
CD14	Monocytes	BioLegend	FITC, APC, PB	1:20, 1:10
CD3	T cells	BioLegend	APC	1:20
CD19	B cells	BioLegend	APC	1:20
CD16	Neutrophils, non-classical monocytes	Biosciences	FITC, APC	1:20
Citrullinated H3	Neutrophil extracellular traps (NETs)	Abcam	-	10μg/ml
2° antibody	Citrullinated H3 antibody	Abcam	Alexa647	1:500

Table 2.1. Antibodies used in flow assays.

Antibodies Western Blotting	Target	Company	Dilution
Anti-VWF-HRP	VWF	Dako	1:200
Anti-His-HRP	VWF A1-His VWF A1*-His	Abcam	1:50,000
Anti-SLC44A2#2	SLC44A2	LS Bio	20μg/ml

Table 2.2. Antibodies used in Western blotting.

Antibodies FACS	Target	Company	Fluorophore	Dilution
CD14	Monocytes	BioLegend	FITC, APC, PB	1:50
CD3	T cells	BioLegend	APC	1:50
CD19	B cells	BioLegend	APC	1:50
CD16	Neutrophils, non-classical monocytes	Biosciences	FITC, APC	1:50
PAC-1	Activated $\alpha_{IIb}\beta_3$	BD Biosciences	FITC	1:20
CD41	$\alpha_{IIb}\beta_3$	Immunotools	PE	1:20
X-488	GPIbβ	Emfret Analytics	Alexa488	1:15
CD62	P-selectin	BD Biosciences	PE	1:20
Anti-SLC44A2	SLC44A2	Abcam	-	1:25
2° antibody	Anti-SLC44A2	Abcam	Alexa488	1:100
2° antibody	Anti-SLC44A2	Abcam	Alexa647	1:100
Anti-IgG	IgG	ImmunoTools	APC	1:50

Table 2.3. Antibodies used in FACS.

Inhibitor	Target	Company	Concentration
Eptifibatide	Activated $\alpha_{IIb}\beta_3$	Sigma	9μM
GR144053	Activated $\alpha_{IIb}\beta_3$	Tocris	10μM
CD62, AK4 clone	P-selectin	BioLegend	50μg/ml
anti-β2	β2 integrin	R&D Systems	20μg/ml
TMB-8	Intracellular Ca^{2+} stores Protein kinase C	Sigma	20μM
U73122	Phospholipase C	Sigma	2μM
DPI	NADPH oxidase	Sigma	30μM
PP2	Src kinase	Tocris	20μM
anti-SLC44A2#1	SLC44A2	Abcam	0.1-20μg/ml
anti-SLC44A2#2	SLC44A2	LS Bio	20μg/ml

Table 2.4. Inhibitors used for flow assays.

Buffers

10x HEPES/Tyrode (HT) Buffer – pH 7.35

1.37 M NaCl

20 mM KCl

3 mM NaH_2PO_4

10 mM $MgCl_2$

55 mM Glucose

50 mM Hepes

120 mM $NaHCO_3$

Buffer A

50mM Tris (pH 7.4)

300mM NaCl

5x Acid Citrate Dextrose (ACD) – pH 4.5

425 mM Na_3Citrate

325 mM Citric Acid

555 mM D(+) Glucose

Buffer X

20mM Hepes

150mM NaCl

1mM $MnCl_2$

0.1mM $CaCl_2$

Methods

Overview of experimental design – Part I

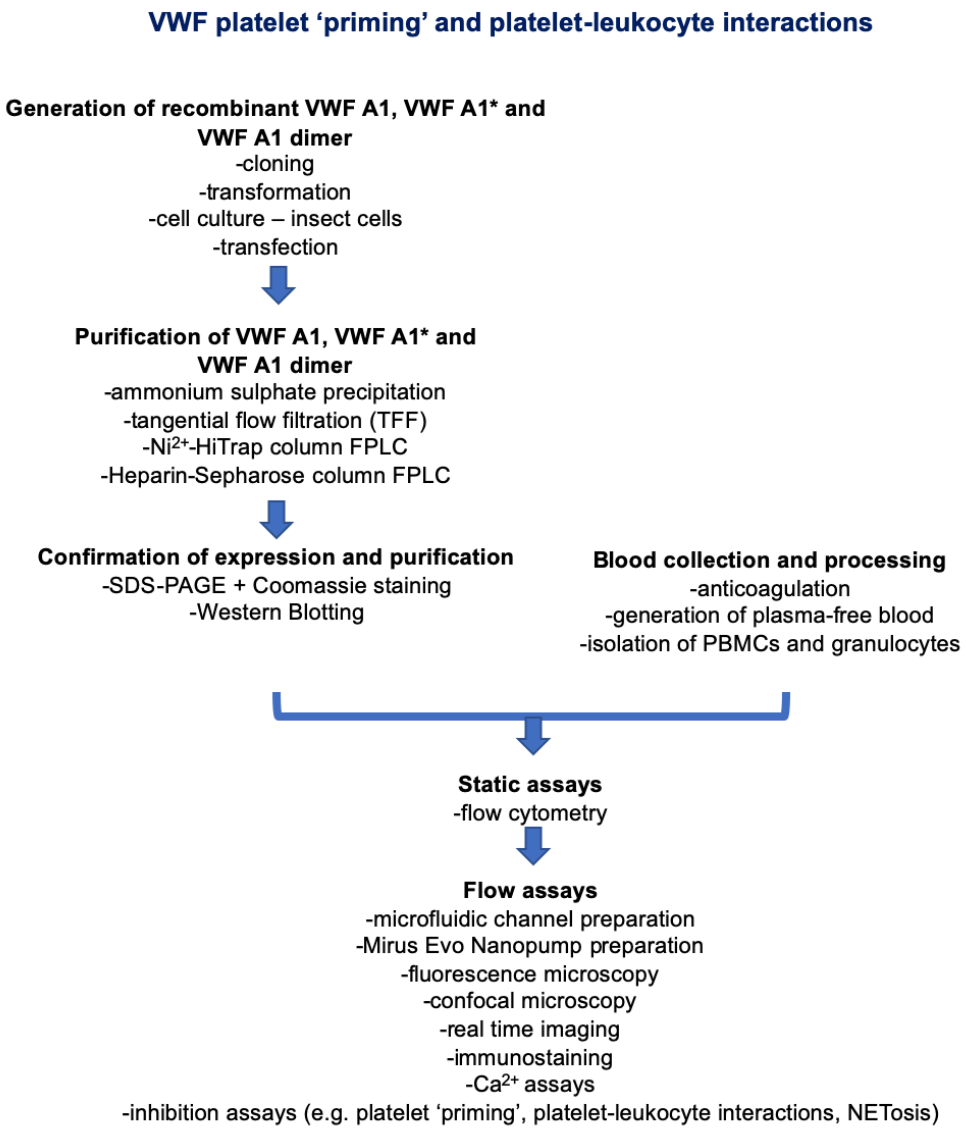

In order for the specific interaction between resting platelets and VWF to be assessed, recombinant A1 domain, together with a variant of the A1 domain, termed A1* (Y1271C/C1272R) were expressed in insect cells and purified using a two-step chromatographic approach. Expression of A1 and A1* was confirmed using SDS-PAGE followed by Coomassie staining and Western Blotting. Purified proteins were used in static flow cytometry assays or coated onto microchannels for flow assays to be performed using whole blood, plasma-free blood or isolated leukocyte subsets.

2.1. Generation of recombinant VWF A1 and VWF A1* (Y1271C/C1272R)

2.1.1. Cloning into pMT-puro vector

The coding sequence of VWF A1 domain (Glu1264 to Leu1469) was obtained by Prof. Jim Crawley and cloned into a pMT BiP-puro vector, containing a V5 and polyhistidine tag. The vector (**Figure 2.1**) contains a metallothionein (MT) promoter, which allows an inducible expression of the gene of interest in insect cells. This expression can be induced by copper sulphate ($CuSO_4$). Apart from the MT promoter, the vector contains a BiP insect cell signal peptide that enables entrance into the secretory pathway and is cleaved off prior to secretion. The vector also contains a Puromycin resistance gene (Puro), which allows for the selection of successfully transfected insect cells, and an Ampicillin resistance gene (Amp), which facilitates the selection of the successfully transformed *E.coli*. The vector also contains a V5 and a polyhistidine (6 x His) tag that assists the further recognition and allow purification of the protein of interest and assist with purity assessment using anti-V5 and anti-His antibodies in Western blots.

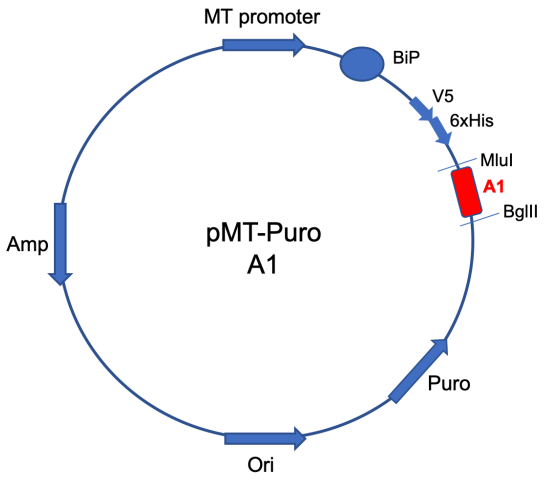

Figure 2.1. pMT-puro vector.

Representation of the vector used for expressing the A1 domain, depicting its relevant sites. These include the MT promoter that is responsible for the inducible nature of the vector, the BiP signal peptide responsible for the secretion, the Ampicillin (Amp) and Puromycin (Puro) resistance genes and the cloned A1 domain, linked to a V5 and 6 x His tag. The A1 also had restriction enzyme sites – BglII site at its 5' end and MluI at its 3' end.

The Y1271C/C1272R mutant A1 (A1*) domain was generated by PCR amplification of the wild-type A1, using a forward primer containing the mutation. The forward primer also contained a BglII site, whereas the reverse primer contained a MluI site (**Table 2.5**). Therefore, the PCR product contained a BglII site at the 5' end and a MluI site at the 3' end. To prepare it for cloning into the pMT-puro vector, the construct was digested with BglII and MluI at 37°C for 1 hour, leading to the formation of sticky ends, and purified using the Qiagen Gel Extraction kit, according to the manufacturer's instructions.

The wild-type A1 domain gene was excised from the vector by digestion with BglII and MluI restriction enzymes for 3 hours, at 37°C. The products were run on a 1% agarose gel and the band corresponding to the cut vector was purified using the Qiagen Gel Extraction kit, according to the manufacturer's instructions.

A1* was then ligated into the cut pMT-puro vector using the QuickLigase kit (NEB). The vector (10ng) was incubated with the insert (A1*, 30ng), enzyme and QuickLigase Buffer, at RT for 30 minutes. Negative controls were set for the sample by preparing the same master mix without the inserts.

Forward primer	CGTTGCACGATTTCTGCCGCAGCAGGCTACTGG
Reverse primer	CCAGTAGCCTGCTGCGGCAGAAATCGTGCAACG

Table 2.5. Primers for generation of A1* (Y1271C/C1272R)

2.1.2. Transformation into E.coli (NEB Turbo C2984)

Ligated DNA were transformed in the highly competent *E.coli* (NEB Turbo). For this, 1µl ligation reaction (2ng) was added to 50µl cells. Cells were incubated on ice for 30 minutes and then heat-shocked at 42°C for 30 seconds. After incubating them on ice for another 5 minutes, 500µl SOC medium were added to the cells and these were incubated for one hour, at 37°C

and with shaking (230 rpm). Following this, 150µl of the culture was plated on a LB agar (Invitrogen) plate supplemented with 100µg/ml Ampicillin and incubated at 37°C overnight.

To screen for correct clones, single colonies were inoculated into 5ml LB Broth (Invitrogen) supplemented with 100µg/ml Ampicillin and incubated at 37°C overnight with shaking. Glycerol stocks were prepared by adding 300µl 50% glycerol to 700µl of the culture and these were stored at -80°C. The remaining samples were miniprepped using the Qiagen Miniprep kit, according to the manufacturer's instructions. Plasmids were sequenced to verify mutations and successful cloning.

Clones that were correctly verified by sequencing were maxiprepped using the Qiagen Maxiprep kit, according to the manufacturer's instructions, in order to generate large quantities (300µg - 500µg) of plasmid for transfections.
DNA from the Maxiprep was quantified using the NanoDrop2000 technology. Absorbance was read at 280nm + 260nm.

2.1.3. Cell culture of Drosophila S2 insect cells

Drosophila S2 cells were cultured in Schneider's Drosophila medium supplemented with 10% heat-inactivated fetal bovine serum (FBS) and 50µg/ml Penicillin and 50U/ml Streptomycin. Cells were cultured under sterile conditions at 28°C, in the absence of CO_2 and light. Cells were initially cultured in 6-well plates, followed by T75 flasks and T175 flasks, as semi-adherent monolayers, and, eventually, the cultures were scaled up and grown in suspension in conical 2L flasks, under shaking conditions, in the absence of CO_2 and light.

2.1.4. Transfection of S2 insect cells

pMT-A1 and pMT-A1* vectors (19µg) were both transfected into S2 cells using the calcium phosphate method. The transfection mix was obtained by mixing 300µl solution A (2M $CaCl_2$, 19µg vector in sterile water) with 300µl solution B (2x Hepes buffered saline – 50mM Hepes, 1.5mM Na_2HPO_4, 280mM NaCl, pH 7.1) and incubating the resulting solution at RT for 30

minutes. The transfection mix was added dropwise to 6-well plates containing $3x10^6$ cells/well. Cells were incubated at 28°C overnight. The calcium phosphate solution was removed the next day and cells were washed twice with complete Schneider's Drosophila medium. Cells were reseeded into the same plate using complete medium and incubated at 28°C for two days.

2.1.5. Selection of stably transfected S2 insect cells

72 hours post-transfection, cells were resuspended in complete Schneider's Drosophila medium supplemented with 10µg/ml Puromycin to select stably transfected cells. The medium was replaced every 4-5 days (leaving 30% of the old media in the wells), until resistant cells started to grow. This process took approximately three weeks. Following that, the resistant cells were transferred into new plates containing the selective medium and scaled up to 1L. The complete medium was supplemented with 0.1% Pluronic F68 for growing cells in suspension.

2.1.6. Expression of VWF A1 and VWF A1*

For expression, stably transfected cells were transferred to 2L conical flasks and grown until the cells reached a yield of approximately $2x10^6$ cells/ml. Following this, the expression was induced by $CuSO_4$ (500µM). Subsequent to adding the $CuSO_4$, the cells were incubated in the shaker at 28°C, 110 rpm for 5-7 days.

2.2. Purification of recombinant VWF A1 and VWF A1* (Y1271C/C1272R)

Media was harvested and centrifuged at 4000xg for 10 minutes, at RT, to pellet the cells. The supernatant was then filtered before further steps could be performed.

2.2.1. Ammonium sulphate precipitation

Due to the presence of 10% FBS in the conditioned media, media was initially concentrated using ammonium sulphate precipitation. Ammonium sulphate (300g) was slowly added to 1L of harvested media and left stirring at 4°C until dissolved. The solution was centrifuged at 12,000xg for 20 minutes. Pellets were washed in 20mM Tris, 500mM NaCl (pH 7.8) to remove the $CuSO_4$, and resuspended in 20ml of 20mM Tris, 500mM NaCl (pH 7.8).

2.2.2. Tangential flow filtration

Further concentration of the collected media was achieved by tangential flow filtration using a 10kDa cut-off membrane. Concentrated media was dialysed in 20mM Tris (pH 7.8) 500mM NaCl.

2.2.3. Ni^{2+}-HiTrap column FPLC

Concentrated and dialysed conditioned media from VWF A1 and A1* transfected cells was loaded onto a Ni^{2+}-HiTrap column. The presence of a His tag on both A1 and A1* recombinant proteins facilitated binding to the columns. The columns were washed with 20mM Tris (pH 7.8), 500mM NaCl, 20mM Imidazole. Proteins were eluted with 20mM Tris (pH 7.8), 500mM NaCl, 300mM Imidazole. The elution sample was dialysed in 20mM Tris (pH 7.8), 100mM NaCl.

2.2.4. Heparin-Sepharose column FPLC

Due to the affinity of the VWF A1 domain for heparin [53], heparin-Sepharose columns were used to further purify the VWF A1 and A1*. Columns were washed with 300mM NaCl. Bound A1 and A1* were eluted with 600mM NaCl and dialysed into phosphate-buffered saline (PBS).

Proteins were quantified by NanoDrop with absorbance read at 280nm. A1 and A1* concentrations were estimated using their extinction coefficient and the approximation of the percentage purity assessed by SDS-PAGE.

2.2.5. SDS-PAGE

Samples were incubated with Bolt 4x LDS Sample Buffer, in the presence or absence of 5% β-mercaptoethanol, at 95°C, for 5 minutes. Thereafter, samples were loaded on a Bolt 4-12% Bis-Tris Plus gel and run at 200V for 30 minutes, using 1x Bolt MES running buffer.

2.2.6. Coomassie straining

The SDS-PAGE gel was washed three times with MQ water, then stained using Imperial^{TM} Protein Stain for 1 hour and then left in MQ water overnight to destain. Purity of the proteins was estimated to be approximately 50% after Ni^{2+} column FPLC and 80% after Heparin Sepharose FPLC.

2.2.7. Western blotting

To detect specific proteins of interest and confirm their purity, SDS-PAGE was performed, followed by Western Blotting. Proteins from the SDS-PAGE gel were transferred to a nitrocellulose membrane (20V, 1 hour). The membrane was blocked for one hour in 4% milk 1% BSA / PBS and then incubated for one hour with either anti-His HRP antibody (1:50,000) or anti-VWF HRP antibody (1:200). Antibody binding was detected with the Immobilon Western Chemilluminescent HRP Substrate (Millipore) according to manufacturer's instructions and revealed using a ChemiDoc Imager (Bio-Rad).

2.3. Blood collection and processing

After VWF A1 and VWF A1* were expressed and purified, their effect on platelet phenotype and ability to mediate platelet-leukocyte interactions was analysed. Experiments were performed using blood donated by healthy human volunteers who had not taken any antiplatelet agents on the day of the experiment. Informed consent was provided by all human volunteers prior to collection. The study was approved through Ethical Approvals - REC reference: 14/LO/0662 IRAS project ID: 136562, followed by ICREC ref 19IC5523.

2.3.1. Anticoagulation methods during blood collection

Fresh blood was collected immediately prior to each experiment from healthy human volunteers. Blood was collected in 40μM PPACK (Calbiochem, for whole blood experiments), 3.13% citrate (1/10ml for leukocyte isolation) or 1x acid citrate dextrose (ACD) (1.5/10ml for plasma-free blood preparation), using a 21-gauge needle through venepuncture. For whole blood experiments, blood was supplemented with a further 10μM PPACK one hour following collection, as necessary.

2.3.2. Generation of plasma-free blood

For plasma-free blood generation, blood collected in 1x ACD was centrifuged for 10min, at 150xg, with no brake at RT to allow density-gradient separation of the platelet-rich plasma from the red blood cells and leukocytes. Thereafter, platelets were washed separately, whereas red blood cells and leukocytes were washed together, as detailed below.

2.3.2.1. Platelet washing

Platelet-rich plasma (PRP) obtained in the initial step was centrifuged for 10min, at 1500xg, with no brake at RT and the platelets were then washed in 1x HT buffer supplemented with 0.35% BSA, 75mU Apyrase (Sigma) and 100nM prostaglandin E1 (PGE1) (Sigma) twice.

Platelets were finally resuspended in 1x HT supplemented with 0.35% BSA, to a volume corresponding to the initial volume of PRP.

2.3.2.2. Red blood cell and leukocyte washing

RBCs and leukocytes were washed twice in an equal volume of PBS by centrifugation at 650xg for 10 min at RT. Thereafter, cells were resuspended in 1x HT buffer supplemented with 0.35% BSA to a volume corresponding to the initial volume of blood remaining after PRP removal.

Finally, plasma-free blood was reconstituted by adding the washed platelets to the washed red blood cells and leukocytes.

10%, 25% and 50% plasma were added back to the plasma-free blood for the plasma titration experiments. Purified fibrinogen (Haematologic Technologies Inc.) was added to plasma-free blood in separate experiments at a concentration of 1.3mg/ml, equivalent to 50% of its physiological concentration.

2.3.3. Isolation of peripheral blood mononuclear cells and granulocytes/ polymorphonuclear cells

2.3.3.1. Lymphoprep method

Blood (10ml) was collected in 3.13% citrate and diluted 1:2 in PBS supplemented with 1% fetal bovine serum (FBS). Diluted blood was slowly added to an equal volume of Lymphoprep (STEMCELL Technologies) and centrifuged at 800xg for 20 min at RT, without brake, to allow density gradient separation. The ‘buffy coat’ consisting of PBMCs was transferred to a new tube and washed in PBS twice, by centrifugation at 300xg for 10 min at 4°C, without brake. The PBMC pellet was eventually resuspended in PBS, to the initial volume. All steps were performed under sterile conditions.

2.3.3.2. Histopaque method

Granulocytes and PBMCs were separated according to their densities. Blood collected in 3.13% citrate was layered onto Histopaque1077 and Histopaque1119 (ratio 2:1:1) under sterile conditions and centrifuged for 30 min, at 700xg, RT, with no brake. PBMCs (present at the interface of plasma and Histopaque1077) and granulocytes (interface between Histopaque1077 and Histopaque1119) were transferred to new tubes and washed with filtered 1x HT buffer by 10 min centrifugation at 500xg, 4°C, with no brake and finally resuspended in 1x HT buffer, to their initial volume.

As the granulocytes layer was in close proximity to the red blood cells (RBCs), a further step was employed during the granulocyte isolation, to lyse the RBCs. Washed granulocytes were resuspended in 1ml 1x HT buffer and incubated with 14ml 1x RBC lysis buffer for 10min, at 4°C. Following this, granulocytes were washed with 1x HT buffer and finally resuspended in 1x HT buffer to their initial volume. All steps were performed under sterile conditions to ensure minimal leukocyte activation.

2.4. Static assays – Flow cytometry

To analyse the effect of the VWF A1 upon platelet phenotype, static assays using flow cytometry were first performed.

PRP (20µl) was incubated for 20 minutes, at RT, with A1 (2µM), Ristocetin (1mg/ml), PBS or negative control represented by an FPLC wash fraction, to ensure that any effects observed are not due to contaminants present in the purified material. After the incubation, samples were diluted 1/10 in 1x HT-BSA buffer and incubated in the presence or absence of adenosine diphosphate (ADP, 5µM) at RT for 10 minutes.

Two different antibodies were used to detect different platelet activation markers. PAC1-FITC (fluorescein-isothiocyanate) was used to detect the activated form of $\alpha_{IIb}\beta_3$ and CD62-PE (phycoerythrin) was used to detect the expression of P-selectin. Each antibody was added to

the samples (1/10 dilution) and, after 15 minutes incubation at RT, these were diluted in PBS and analysed using flow cytometry.

2.5. Flow assays

2.5.1. Microfluidic channel preparation

After analysing the effect of VWF A1 upon platelet phenotype in static assays, flow experiments were performed. Flow assays were used in order to better reflect the physiological conditions present in the vasculature *ex vivo*. Microfluidic biochips (Cellix) were coated with various proteins of interest prior to the flow assays. Different types of biochips were used depending on the proteins to be coated, with their respective protocols presented below.

2.5.1.1. Cellix VenaFluo8+ microchannels

VenaFluoro8+ microchips (Cellix) were coated with the protein of interest: FL-VWF (purified from Haemate P using gel filtration, 2μM in PBS), LIBS2 (Millipore, 0.5-2μM in PBS), BSA (Sigma, 0.25mg/ml in PBS), collagen (Nycomed, 100μg/ml in PBS) by incubating overnight at 4°C in a humidified chamber. Coated channels were blocked for 1 hour with 1x Hepes-Tyrode (HT) buffer supplemented with 1% bovine serum albumin (BSA) and then washed with 1x HT buffer prior to the flow experiments.

After blocking, channels coated with LIBS2 were further incubated with purified $\alpha_{IIb}\beta_3$ (2.6μM, Enzyme Research Laboratories) for 30 min, at RT. Finally, channels were washed with 1x HT buffer.

2.5.1.2. Cellix PEGylated microchannels

Given the presence of a His tag within the structure of VWF A1 and A1*, NTA PEGylated microchips (Cellix) were used. This approach helped to ensure the correct orientation of the VWF A1/A1*, with the platelet interaction sites available for binding.

2.5.1.2.1.1. Cu^{2+}/Ni^{2+} coating

Microchannels were purchased with Cu^{2+} layered onto the PEGylated surface. These were incubated with the VWF A1 or A1* (3.75μM, in the presence of 10% glycerol) or PilC (4μM, negative ctrl, in the presence of 10% glycerol) for 20 min, at RT, to allow the A1/A1*/PilC to attach via their His tags. The unbound proteins were then removed by washing with Buffer A (see Buffers, p. 88).

To improve the A1/A1* attachment, channels were also stripped of the Cu^{2+} layer using 50mM EDTA. Channels were then washed with Buffer A for 5 min and then incubated with $NiSO_4$ for 5 min at RT to allow Ni^{2+} layering onto the PEGylated surface and then washed to remove the unbound Ni^{2+}. Channels were then incubated with the A1 or A1* (3.75μM, in the presence of 10% glycerol) for 20 min, at RT and finally washed again with Buffer A prior to flow assays. As a negative control, channels were coated with 4-40μM PilC-His using the same conditions as above.

2.5.1.2.1.2. Co^{2+} coating

To improve protein coating stability, Co^{2+} was used [373]. Channels were stripped using 50mM EDTA and Co^{2+} was bound to the channels by incubating the channels with $CoSO_4$ (100mM) for 5 min, at RT. Thereafter, channels were washed Buffer A. A1 or A1* (3.75μM, in the presence of 10% glycerol) were then incubated at room temperature (RT) for 20 min, in a humidified chamber. Channels were then incubated with H_2O_2 (10mM) for 30 min at RT to oxidise Co^{2+} to Co^{3+} and stabilize the A1/A1* coating. Finally, channels were washed with Buffer A.

2.5.1.3. Cellix NHS microchannels

Prior to coating, $\alpha_{IIb}\beta_3$ was dialysed three times in Buffer X (see Buffers, p. 88).

NHS microchips (Cellix) were coated with either 2.6µM purified $\alpha_{IIb}\beta_3$ (Enzyme Research Laboratories), 0.25mg/ml BSA or 0.25mg/ml antibodies against PECAM-1 (BioLegends) or CD16 (Biosciences) by incubation for 20 min at RT, in a humidified chamber. Channels were washed 3x with Buffer X. Channels were subsequently incubated with Deactivating Buffer (Cellix) for 30 min at RT, in a humidified chamber and finally washed with Buffer X.

2.5.1.4. Cellix Delta Y1 and Y2 channels

In an attempt to better mirror the vasculature *ex vivo*, bifurcated channels Delta Y1 and Y2 were coated with the protein of interest (FL-VWF 2µM in PBS) by incubating overnight at 4°C in a humidified chamber. Coated channels were blocked for 1 hour with 1x Hepes-Tyrode (HT) buffer supplemented with 1% BSA and then washed with 1x HT buffer prior to the flow experiments.

2.5.2. Mirus Evo Nanopump

2.5.2.1. Pump preparation

A Mirus Evo Nanopump (Cellix) was used to perform experiments under flow conditions. Prior to each flow assay, the pump was washed 1x with 70% filtered ethanol, 3x with filtered H_2O and 2x with filtered 1xHT buffer. At the end of each experiment, the pump and all its associated tubing were cleaned by washing 2x with filtered H_2O, 2x with filtered 70% ethanol and finally dried by 2x runs with air.

2.5.2.2. Shear rates used

The pump was operated by the VenaFlux2.3 software (Cellix). Protocols were generated taking into consideration the geometry of the microchannels and the viscosity of the blood/buffer to be passed through. Blood viscosity was considered 0.045 dyne*s/cm^2 and buffer viscosity was considered 0.01 dyne*s/cm^2.

For platelet capture and 'priming', blood was perfused for 3.5min at high shear (1000s^{-1}). Subsequently, shear was reduced to 50s^{-1} to observe platelet-leukocyte interactions. Shear rates and flow rates respectively were calculated using the formula below and were dependent on channel geometry. The geometry of the different types of channels used is summarised in **Table 2.6**.

$$\textbf{Shear Stress: } \tau = \frac{6Q\mu}{bh^2}$$

$$\textbf{Flow Rate: } Q = \frac{\tau bh^2}{6\mu}$$

μ – viscosity
b – width
h – height
Q – flow rate
τ – shear stress

	Cellix VenaFluoro8+ microchannels	Cellix PEGylated microchannels	Cellix NHS microchannels	Cellix Delta Y1 microchannels
Channel width (cm) (b)	0.04	0.08	0.08	0.008
Channel height (cm) (h)	0.01	0.01	0.01	0.012
Channel length (cm)	2	2	2	2

Table 2.6. Microfluidic channel geometries.

2.5.3. Real-time imaging

Platelet and leukocyte attachment to the proteins of interest was monitored in real-time by fluorescence microscopy (Zeiss), using an inverted CCD camera operated by the SlideBook^{TM}5.0 software.

For the purpose of dual colour visualisation in real time and at a higher resolution, the Mirus Evo Nanopump was coupled to a SP5 Leica confocal microscope. When using the confocal microscope, flow assays were performed in a temperature-controlled chamber at 37°C.

2.5.3.1. Whole blood, plasma-free blood and isolated leukocyte staining

Whole blood, plasma-free blood and isolated leukocytes were labelled with $DiOC_6$ (2.5µM), staining the endoplasmic reticulum and/or Hoechst dye (8µM) to visualise nuclear DNA. Antibodies specific to the different types of leukocytes were also added to isolated leukocytes, i.e. CD14 (BioLegend, 1:20, 1:10) conjugated to allophycocyanin (APC), Pacific blue (PB) or FITC to identify monocytes, CD16-APC (eBiosciences, 1:20) for neutrophils, CD3-APC (BioLegend, 1:20) for T cells or CD19-APC (BioLegend, 1:20) for B cells.

Antibodies flow assay	Target	Company	Fluorophore	Dilution
CD14	Monocytes	BioLegend	FITC, APC, PB	1:20, 1:10
CD3	T cells	BioLegend	APC	1:20
CD19	B cells	BioLegend	APC	1:20
CD16	Neutrophils, non-classical monocytes	eBiosciences	FITC, APC	1:20

Table 2.7. Leukocyte subset-specific markers

2.5.3.2. Analysis of platelet phenotype under flow

Similar to the static assays, two markers were assessed under flow – activation of integrin $\alpha_{IIb}\beta_3$ and exposure of P-selectin.

The activation of $\alpha_{IIb}\beta_3$ was investigated by analysing the ability of platelets to bind fibrinogen, the main ligand of $\alpha_{IIb}\beta_3$. Plasma-free blood was perfused at $1000s^{-1}$ for 3.5 minutes, through channels coated with VWF, collagen (positive control) or anti-PECAM-1 (negative control). Thereafter, channels were washed with 1x HT buffer and fluorescent fibrinogen (Alexa647, Thermo Fisher Scientific 1.3mg/ml in 1x HT) was perfused through these channels at $50s^{-1}$ for 5 minutes. Channels were washed with 1x HT and fluorescent fibrinogen binding was monitored using confocal microscopy.

To investigate whether platelets bound by VWF present P-selectin on their surface, plasma-free blood was perfused through channels coated with VWF, collagen or anti-PECAM-1 and then washed using the conditions described above. Subsequently, an antibody staining for P-selectin-APC (Biosciences, 50 µg/ml in 1x HT) was perfused through these channels at $50s^{-1}$ for 5 minutes and incubated under static conditions for another 5 minutes. Channels were washed and P-selectin staining was assessed via confocal microscopy.

2.5.3.3. Platelet Ca^{2+} assays

To monitor intracellular Ca^{2+} release, PRP was incubated with 5µM Fluo-4 AM (Thermo Fisher Scientific) for 30 min at 37°C, washed and added back to the RBC and leukocyte preparation to obtain plasma-free blood. Plasma-free blood was recalcified, i.e. supplemented with 1mM $CaCl_2$ prior to the flow experiments.

2.5.3.4. Neutrophil Ca^{2+} assays

To monitor intracellular Ca^{2+} release, isolated granulocytes were incubated with 5μM Fluo-4 AM (Thermo Fisher Scientific) for 30 min at 37°C and then washed. The granulocyte suspension was recalcified, i.e. supplemented with 1.5mM $CaCl_2$ prior to the flow experiments and left to equilibrate for 30 min at 37°C.

2.5.3.5. Neutrophil extracellular traps (NETs) release imaging

To visualize NETosis, neutrophils were labelled with 8μM Hoechst dye (cell permeable DNA dye) and 1μM Sytox Green (cell impermeable DNA dye) and perfused on either activated $\alpha_{IIb}\beta_3$-coated channels or on VWF or A1*-'primed' platelets. Neutrophils were perfused at low shear ($50s^{-1}$) for 10 minutes, in the presence of $CaCl_2$ (1mM) and $MnCl_2$ (0.1mM), and then monitored under static conditions for 2 hours using confocal microscopy. These assays were performed in a temperature-controlled chamber at 37°C.

To confirm the presence of NETs, neutrophils captured by activated $\alpha_{IIb}\beta_3$ were fixed after 2 hours of attachment using 4% paraformaldehyde. Following that, to identify neutrophils at different stages of NETosis, fixed neutrophils were permeabilised with 0.1% Triton X-100 and blocked with 3% BSA in PBS. Thereafter, fixed neutrophils were incubated with a rabbit polyclonal anti-citrullinated H3 (Abcam, 10μg/ml) overnight at 4°C, as previously described [331]. The next day, neutrophils were incubated with a goat anti-rabbit secondary antibody conjugated with Alexa647 (Abcam, 1:500) and with the Hoechst dye (8μM) for 2 hours at RT, washed and then visualised using confocal microscopy.

2.5.4. Inhibition assays

2.5.4.1. Inhibition of platelet aggregation and leukocyte binding

Whole blood or plasma-free blood were pre-incubated with Eptifibatide (Sigma, 2.4μM) or GR144053 (Tocris, 10μM) for 10 minutes prior to perfusion through channels coated with VWF, A1 or A1* in order to investigate the role of integrin $\alpha_{IIb}\beta_3$ in platelet aggregation and leukocyte binding.

In separate experiments, whole blood or plasma-free blood were pre-incubated with an antibody blocking P-selectin (Biosciences, AK4 clone, 50 μg/ml), an anti-β_2 integrin antibody (R&D Systems, 20 μg/ml), anti-SLC44A2#1 (Abcam, 0.1-20 μg/ml) or anti-SLC44A2#2 (LS Bio, 20 μg/ml) for 20 minutes prior to perfusion through channels coated with VWF or A1* to investigate the role of P-selectin, activated β_2 integrins and SLC44A2 upon platelet-leukocyte interactions. As a control, blood was incubated with a polyclonal rabbit IgG (Abcam, 20 μg/ml).

Isolated granulocytes were also incubated with the anti-β_2 integrin antibody or with the anti-SLC44A2#1 and #2 prior to being perfused on activated $\alpha_{IIb}\beta_3$-coated channels. As a control, isolated granulocytes were incubated with a polyclonal rabbit IgG.

2.5.4.2. NET inhibitors

Isolated granulocytes were preincubated with 20μM TMB-8 (Ca^{2+} antagonist and protein kinase C inhibitor; Sigma), 20μM PP2 (Src kinase inhibitor; Tocris) or 2μM U73122 (phospholipase C inhibitor; Sigma) for 15 minutes, or 30μM DPI (NADPH oxidase inhibitor; Sigma) for 30 minutes at 37°C prior to NETosis inhibition assays (**Table 2.8**). In some experiments, neutrophils were captured on microchannels coated with anti-CD16 and stimulated with 160nM phorbol 12-myristate 13-acetate (PMA) prior to analysis of NETosis in the presence and absence of inhibitors. These assays were performed in the presence of $CaCl_2$ (1mM) and $MnCl_2$ (0.1mM).

Inhibitor	Target	Company	Concentration
TMB-8	Intracellular Ca^{2+} stores Protein kinase C	Sigma	20μM
U73122	Phospholipase C	Sigma	2μM
DPI	NADPH oxidase	Sigma	30μM
PP2	Src kinase	Tocris	20μM

Table 2.8. NET inhibitors

2.6. Quantification

Quantification of platelet rolling, aggregation and intracellular Ca^{2+} release was performed using the SlideBook 5.0 software (3i). The number of platelet-leukocyte interactions was manually quantified and expressed as a function of number of leukocytes rolling/attaching per minute, over a period of 13 minutes. NETosis was quantified by determining the proportion of neutrophils attached to the channels that had signs of chromatin decondensation/Sytox Green staining after 2 hours, using the confocal microscope.

Overview of experimental design – Part II

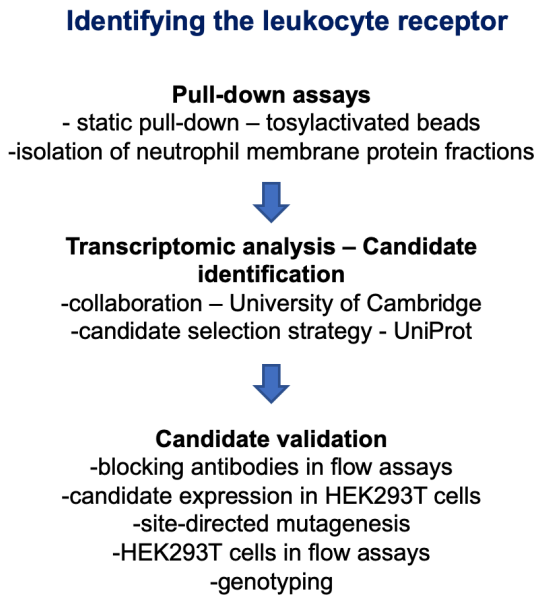

2.7. Identifying the leukocyte receptor

For the identification of the leukocyte receptor, different strategies were employed, including pull-down assays, transcriptomic and proteomic analysis. Candidate validation was ultimately performed through various assays detailed below.

2.7.1. Pull-down assays

2.7.1.1. Capture of $\alpha_{IIb}\beta_3$ on tosylactivated beads

The first step undertaken to identify the leukocyte receptor was represented by pull-down assays using M-280 tosylactivated dynabeads (Invitrogen, 14203).

$\alpha_{IIb}\beta_3$ was first desalted in PBS/Buffer B (**Table 2.9**) using the 7kDa Zeba columns according to the manufacturer's instructions. M-280 tosylactivated dynabeads (Invitrogen, 14203) were resuspended by vortexing for 30s and transferred to a 1.5ml tube (165µl, i.e. 5mg beads). The tube was placed against a magnet for 1 min and the beads storage solution was removed. The tube was removed from the magnet and beads were resuspended in Buffer B. The tube was placed against the magnet for 1 min and supernatant was removed. Washed beads were

resuspended in the initial volume (165µl) of Buffer B and transferred to a new 1.5ml tube. The buffer was removed and beads were resuspended with 100µg $\alpha_{IIb}\beta_3$. Buffer B was added to a total of 150µl and the beads and ligand were mixed thoroughly by vortexing. Buffer C (100µl, **Table 2.9**) was added to the mixture and this was placed on a rotor for 12-18hrs at 37°C to allow coupling of $\alpha_{IIb}\beta_3$ to the beads. The tube was placed against a magnet for 2 min. The supernatant was then removed from the tube and kept separately to analyse the amount of ligand not bound to the beads. Beads were washed with Buffer D (1ml) at 37°C for 1hr. The tube was again placed against a magnet for 2 min and Buffer D was replaced with Buffer E (1ml) and vortexed for 5-10sec. This washing step in Buffer E was repeated twice to wash the beads and supernatants were kept to analyse the stability of $\alpha_{IIb}\beta_3$ coupled to the beads. Eventually, beads were resuspended in 240µl Buffer E, to a final bead concentration of 20mg/ml and a final ligand $\alpha_{IIb}\beta_3$ concentration of 420µg/ml. Beads were kept at -20°C until use.

A second approach to couple $\alpha_{IIb}\beta_3$ on the beads was made by first coupling the LIBS2 antibody to the beads as described above and then adding $\alpha_{IIb}\beta_3$ to ensure the activated state of the integrin.

Finally, the third approach included incubating $\alpha_{IIb}\beta_3$ and LIBS2 in solution before adding the complex onto the beads.

The presence of $\alpha_{IIb}\beta_3$ on the beads was confirmed using flow cytometry using a CD41-PE antibody (Immunotools) and NanoDrop readings comparing the stock solution of $\alpha_{IIb}\beta_3$ and the supernatant from the initial coupling step. The activated state of $\alpha_{IIb}\beta_3$ on the beads was assessed using the PAC-1 antibody in flow cytometry.

Buffer	Composition
Buffer B	0.1M borate buffer, pH 9.5
Buffer C	3M ammonium sulphate in Buffer B
Buffer D	PBS (pH 7.4) with 0.5% BSA
Buffer E	PBS (pH 7.4) with 0.1% BSA

Table 2.9. Buffers for tosylactivated beads coating

2.7.1.2. Control pull-down experiments

Control pull-down experiments were carried out using fibrinogen, the main ligand for $\alpha_{IIb}\beta_3$.

Beads coupled with activated $\alpha_{IIb}\beta_3$ (25µl, equivalent of 0.5mg beads, 10µg $\alpha_{IIb}\beta_3$) were transferred to a new 1.5ml tube. Fibrinogen (25µl) diluted in Buffer E (200µg/ml) was added to the coupled beads in the presence or absence of GR144053 (10µM) and incubated at RT on a rotor, for 20-30min. The tube was placed against a magnet for 2 min and the supernatant was removed and kept to determine the amount of unbound fibrinogen. Beads were then washed twice in 500µl Buffer E and finally resuspended in 50µl Bolt LB Buffer with 5% β-mercaptoethanol. Samples were loaded onto a Bolt 4-12% Bis-Tris gel, using 100µg/ml fibrinogen as a positive control.

Western blotting was then carried on using a rabbit polyclonal anti-fibrinogen antibody (Santa Cruz, 1/1000) overnight at 4°C followed by a secondary goat anti-rabbit antibody-HRP (1:2000) for 1hr, at RT.

2.7.2. Preparation of neutrophil membrane protein fraction

Neutrophils from 20ml of blood were isolated as described in **Section 2.3.3.2** and resuspended to 10^6 cells/ml. Neutrophil membrane proteins were then extracted using the Mem-Per™ Plus Membrane Protein Extraction Kit (Thermo Scientific) according to Protocol 2: Suspension Mammalian Cells. To ensure a high protein concentration, the permeabilization

and solubilisation buffers were supplemented with Protease Inhibitors (Sigma P8849, 1:100), containing AEBSF, Bestatin, E-64, Pepstatin A and Phosphoramidon. Briefly, tubes containing $5x10^6$ cells were centrifuged at 300xg for 5 min and cells were resuspended in 3ml Cell Wash Solution. Tubes were centrifuged again at 300xg for 5 min and cells were resuspended in 1.5ml Cell Wash Solution and transferred to 1.5ml tubes. Following another centrifugation step, the pellets were resuspended in 0.75ml Permeabilisation Buffer supplemented with Protease Inhibitors, briefly vortexed and incubated for 10 min, at 4°C with constant mixing. Permeabilised cells were centrifuged at 16,000xg for 10 min to remove the cytosolic proteins. Pellets consisting of membrane proteins were subsequently resuspended in 0.5ml Solubilisation Buffer supplemented with Protease Inhibitors and incubated at 4°C for 30 min, with constant mixing. Finally, tubes were centrifuged at 16,000xg for 15 min, at 4°C and the supernatant containing solubilised membrane and membrane-associated proteins was transferred to a new tube. Membrane protein fractions were quantified using NanoDrop 2000 (60μg/ml) and stored at -80°C for further use.

2.7.2.1. Competition assays using neutrophil membrane protein fraction

The membrane fraction was first desalted in PBS using the 7kDa Zeba columns according to the manufacturer's instructions.

To confirm the presence of the unknown leukocyte receptor within the neutrophil membrane protein fraction, competition flow assays were carried out. Specifically, isolated neutrophils were diluted 1:2 with either PBS or the membrane protein fraction before being perfused over $\alpha_{IIb}\beta_3$-coated microchannels. Similar experiments were performed using plasma-free blood on VWF or anti-PECAM-1 coated channels.

2.7.3. Transcriptome analysis – Candidate identification

Transcriptomic analysis was performed by Dr. Mattia Frontini and Dr. Luigi Grassi, from the University of Cambridge. They analysed RNA sequencing data from the BLUEPRINT

consortium [374], and performed differential expression analyses between mature neutrophils (n=7) vs. monocytes (n=5) and αβ T cells (n=8) vs. monocytes (n=5). The effective log2(FPKM+1) data was displayed in a heatmap that we were provided with.

The heatmap consisted of 93 candidates ordered according to the mean expression RNA level in neutrophils. Candidates were further scrutinised using the UniProt database, using different exclusion criteria: the presence within the intracellular organelle membranes, the presence of a short extracellular domain (<30a.a.) and the proteomic levels higher in monocytes compared to neutrophils (https://immprot.org). Based on this analysis and its recent association with DVT and stroke [365,372], SLC44A2 was selected for further validation.

2.8. Candidate validation

2.8.1. Blocking SLC44A2 in flow assays

Whole blood or plasma-free blood were pre-incubated with antibodies against either the first (anti-SLC44A2#2, LS Bio, LS-C750149, 20μg/ml) or second extracellular loop (anti-SLC44A2#1, Abcam, Ab177877, 0.1-20μg/ml) of SLC44A2, or a control rabbit IgG (Abcam, 20μg/ml) for 20 min prior to being perfused on channels coated with A1* or FL-VWF. Isolated granulocytes were also incubated with these antibodies prior to being perfused through channels coated with activated $\alpha_{IIb}\beta_3$. Platelet-leukocyte interactions were monitored in real-time, using fluorescence microscopy as described in **Section 2.5.3**.

2.8.2. Expression of SLC44A2 in HEK293T cells

2.8.2.1. Vector amplification

A GFP-tagged pCMV6-Entry Vector containing the cDNA for *SLC44A2* was purchased from OriGene and resuspended in H_2O to a final concentration of 1μg/ml. Using the primers acquired together with the vector, the cDNA was amplified using the conditions in **Table 2.12** (SLC44A2 amplification column).

2.8.2.2. Transformation into *E.coli* (Top10 Competent Cells)

The amplified vector was transformed in the highly competent *E.coli* (Top10 Competent Cells). These were transformed, miniprepped and maxiprepped as described in **Section 2.1.2**. DNA from the Maxipreps was quantified using the NanoDrop2000 technology. Absorbance was read at 280 + 260nm.

2.8.2.3. Cell culture

HEK293T cells stored in liquid nitrogen were thawed and seeded in T175 flasks. Cells were cultured as adherent layers, in the humidified incubators at 37°C, 5% CO_2, in complete media consisting of minimum essential media (MEM Sigma, M2279) supplemented with 10% FBS, 1U/ml Penicillin 0.1mg/ml Streptomycin, 1% non-essential amino acids (Sigma, M7145) and 2mM L-Glutamine (G7513). When confluent, cells were split 1:4. For this, cells were washed twice in PBS and detached through trypsinization using 2ml TrypLE™ Express (Thermo Fisher) per flask. Once cells detached, trypsinization was stopped by addition of 10ml complete media.

2.8.2.4. Transient transfection

Cells were split and seeded in 6-well plates 24 hours prior to transfection. On the day of transfection, Lipofectamine 2000 was diluted in Opti-MEM (Thermo Fisher), alongside with DNA (3µg/well) diluted in Opti-MEM. The diluted DNA was added to the diluted Lipofectamine 2000 drop-wise, and incubated at RT for 5 min. Following that, 300µl mixture was added to each well. For control wells, 300µl Opti-MEM alone were added.

Cells were harvested 24 hours post-transfection. For this, cells were washed twice with PBS and then detached using 40µl TrypLE™ Express. To stop the trypsin reaction, cells were resuspended in 2ml of complete media and transferred to 15ml falcon tubes. These were placed onto an orbital shaker and incubated at RT for one hour prior to being centrifuged at 150g, 10min at RT. Eventually, cells were resuspended in 2ml Opti-MEM and used for

downstream experiments. Harvested cells were counted using Trypan Blue to assess the number of cells and their viability prior to downstream experiments. Due to the presence of the GFP tag within the vector, transfection efficiency could be visually observed using fluorescence microscopy and quantified using flow cytometry.

2.8.2.5. Primer design

Primers were designed for site-directed mutagenesis and their sequences are provided in the table below (**Table 2.10**).

R154Q Primers	
Forward	5′GTG GCT GAG GTG CTT **CAA** GAT GGT GAC TGC CCT 3′
Reverse	5′AGG GCA GTC ACC ATC TTG AAG CAC CTC AGC CAC 3′

Table 2.10. Primers for site-directed mutagenesis of SLC44A2

2.8.2.6. Site-directed mutagenesis

SLC44A2 vectors were amplified using the R154Q primers and the conditions summarised in **Table 2.12** (Site-directed mutagenesis column). Following amplification, the PCR reactions were treated with DpnI for 1hr, at 37°C and transformed in Top10 Competent Cells as described in **Section 2.1.2** and then miniprepped using the Qiagen Kit. Minipreps then sequenced using the sequencing primers described in **Table 2.11** and further used for transfection, given the high yield of DNA as determined by NanoDrop2000.

Sequencing Primers	
Forward	5′ ACCTCACGTACCTGAATG 3′
Reverse	5′AGCCATGCCCATCCTCATAG 3′

Table 2.11. Sequencing primers for SLC44A2.

PCR step	*SLC44A2* amplification	Site-directed mutagenesis	*SLC44A2* screening
Initial denaturing	95°C-1min	95°C-2min	95°C-30s
No. of cycles	15 cycles	24 cycles	30 cycles
Denaturing	95°C-10s	95°C-20s	95°C-20s
Annealing	56°C-20s	58°C-12s	47°C-30s
Extension	72°C-4min	70°C-3min	68°C-25s
Final extension	72°C-10min	70°C-10min	68°C-5min
Ending stage	4°C-∞	4°C-∞	4°C-∞

Table 2.12. PCR cycle conditions for SLC44A2 amplification, site-directed mutagenesis and sequencing

Reaction mix	*SLC44A2* amplification	*SLC44A2* screening
Taq MMix	12.5ul	25ul
Forward primer	0.6ul	1ul
Reverse primer	0.6ul	1ul
DNA	2ul	10ul
H_2O	to 25ul	to 50ul

Table 2.13. PCR reaction mixes for SLC44A2 amplification and screening

Reaction mix	Site-directed mutagenesis
KOD buffer	5ul
dNTPs	5ul
Forward primer	1.5ul
Reverse primer	1.5ul
$MgSO_4$	3ul
Template	1ul
H_2O	to 50ul

Table 2.14. PCR reaction mixes for SLC44A2 site-directed mutagenesis

2.8.2.7. Flow assays

Microchannels were coated with FL-VWF or LIBS2 antibody-$\alpha_{IIb}\beta_3$ as described in **Section 2.5.1**.

Plasma-free blood was generated as described in **Section 2.3.2** and perfused over the FL-VWF coated channels at high shear for 3.5 min to obtain a carpet of 'primed' platelets. Platelet coverage could be observed in bright field, as blood was not labelled. Channels were subsequently washed with 1x HT buffer to remove the blood and harvested HEK293T cells were then perfused over the carpet of platelets at low shear ($25s^{-1}$) for 10 min.

In separate experiments, harvested HEK293T cells were also perfused on FL-VWF channels in the absence of platelets for 30 min at $25s^{-1}$ to confirm that they are not directly binding to VWF. Harvested HEK293T cells were perfused on LIBS2 antibody-$\alpha_{IIb}\beta_3$ at $25s^{-1}$ for 10 min.

Quantification was achieved by counting the cells attached after 10 min across the whole channel and then expressing this as the number of cells/field of view.

2.8.3. Flow cytometry – Confirming the expression of SLC44A2 in neutrophils

The expression of SLC44A2 in neutrophils was analysed using flow cytometry.

Granulocytes were isolated as described in **Section 2.3.3.2** from 20ml blood and finally resuspended in 1ml of 1x HT buffer. Resuspended cells (100µl) were then incubated with CD16-APC and/or anti-SLC44A2#2 for 15 min, at RT. Samples incubated with the anti-SLC44A2#2 were first incubated with this antibody for 30 min at RT, washed, and subsequently incubated with the secondary antibody conjugated to Alexa647 for 15 min, at RT.

2.8.3.1. Antibody labelling

To avoid the unspecific binding of the Alexa647-conjugated secondary antibody, the anti-SLC44A2#2 antibody was also labelled using the DyLight 650 Antibody Labelling Kit (84535, Thermo Scientific). The antibody (100µg) was first desalted using the 7kDa Zeba columns. The columns were equilibrated in PBS + Borate buffer (0.05M) and the antibody was then passed through the columns to remove the 2% sucrose and 0.09% sodium azide. The degree of labelling was calculated using the formulas below. The A280 and A_{max} were determined using the 'Proteins and Labels' protocol within the NanoDrop 2000, where the correction factor for the DyLight 650 was 0.037.

$$\text{Moles dye per mole protein} = \frac{A_{max} \text{ of the labeled protein} \times \text{dilution factor}}{\varepsilon_{dye} \times \text{protein concentration (M)}}$$

ε_{dye} = dye (fluorophore) molar extinction coefficient

$$\text{Protein concentration (M)} = \frac{[A_{280} - (A_{max} \times CF)]}{\varepsilon_{protein}} \times \text{dilution factor}$$

$\varepsilon_{protein}$ = protein molar extinction coefficient (e.g., the molar extinction coefficient of IgG is ~210,000 M^{-1} cm^{-1})

$$CF = \text{Correction factor} = \frac{A_{280} \text{ of the dye}}{A_{max} \text{ of the dye}}$$

2.8.4. Western Blotting

Protein levels of SLC44A2 were also tested by Western Blotting using lysates from isolated human neutrophils.

Neutrophils were isolated as presented in **Section 2.3.3.2** and resuspended in radioimmunoprecipitation buffer (RIPA buffer, Sigma) supplemented with protease and phosphatase inhibitors (Roche) for lysis. Lysates were kept at -20°C until use.

The protein concentration of the lysate was quantified using the Pierce BCA Protein Assay Kit (Thermo Fisher) following the manufacturer's instructions. Following quantification, 20µg of

each lysate was loaded on a 4-12% Bis-Tris gel and run for 30min at 200V and then transferred to a nitrocellulose membrane. The membrane was blocked with 3% BSA/TBS and incubated with the anti-SLC44A2#2 (1:500) overnight at 4°C. Following that, the membrane was incubated with a goat anti-rabbit IgG-HRP (1:5000) and bands revealed with the Immobilon Western Chemiilluminescent HRP Substrate (Millipore).

2.9. Genotyping

Genotyping was performed to identify individuals homozygous for *SLC44A2 rs2288904-A* SNP that encodes for the R154Q variant of SLC44A2. A small amount of blood (25μl) was collected through pin prick from 37 volunteers who had provided written informed consent for this study.

Genomic DNA was then extracted using the PureLink® Genomic DNA kit (Invitrogen), according to the manufacturer's instructions. Briefly, collected blood diluted in PBS and supplemented with Proteinase K and RNase A was incubated with an equal volume of PureLink® Genomic Lysis/Binding Buffer at 55°C for 10 min with constant mixing. 100% ethanol was then added, and the mixed sample was transferred to a spin column. DNA binding was performed by spinning the columns at 10,000xg, 1min, at RT. The columns were then washed with Wash Buffer 1 and Wash Buffer 2. Columns were dried and, finally, a two-step elution (25μl each) was performed. The DNA yield was quantified using the NanoDrop Nucleic Acid read-out (260nm).

After extraction, gDNA was subjected to PCR using the primers designed for sequencing (**Table 2.11**). The optimal PCR conditions are summarised in **Table 2.11** (*SLC44A2* screening).Following PCR, samples were run on 1% agarose gel in 0.5% TBE buffer for 30min at 100V and bands corresponding to the appropriate size (410bp) were excised and purified using the Qiagen Gel Extraction kit, according to the manufacturer's instructions.Purified DNA was quantified using Nanodrop and sent to sequencing using the forward sequencing primer.

Overview of experimental design – Part III

Investigating the importance of VWF A1-GPIbα interaction

***GPIbα knock-in* mice characterization**
-platelet counts
-platelet aggregometry
-platelet spreading
-flow assays

2.10. Characterisation of novel *GpIbα knock-in mice (GpIbα$^{\Delta sig\Delta sig}$)*

Based on my results, a *GpIbα knock-in* mouse (*GpIbα$^{\Delta sig/\Delta sig}$*) was generated by CRISPR/Cas9 technology by Dr. Isabelle Salles-Crawley and Prof. Jim Crawley, where VWF-mediated platelet capture was intact but signalling events downstream the VWF-GPIbα were abolished. For this, the last 24 amino acids from the intracellular tail of GPIbα were deleted. Experiments described below were performed to characterise the platelet function in these mice.

2.10.1. Full blood counts and platelet counts

Mouse blood was collected by Dr. Isabelle Salles-Crawley retro-orbitally in 3.8% citrate, after mice were anaesthetised using a combination of Ketamine and Medetomidine. Blood was diluted 1:40 in 1x HT buffer for whole blood counts or 1:2 in 1x HT supplemented with 0.35% BSA for platelet washing. Whole blood samples were analysed for full blood counts within the Pathology Laboratory at Hammersmith Hospital.

Mouse platelets were washed as previously described. Blood diluted in 1x HT-BSA was centrifuged at 150xg, 10 min, at RT, without break. Platelet-rich plasma (PRP) was transferred to a new tube and diluted 1:2 in 1x HT-BSA, supplemented with 10% 1x ACD, 20mU Apyrase (Sigma) and 1μM prostaglandin E1 (PGE1) (Sigma). Diluted PRP was centrifuged at 1000xg, 10 min, at RT. Platelets were subsequently resuspended and washed twice with 1x HT-BSA supplemented with Apyrase and PGE1 before being resuspended in 100μl 1x HT. An aliquot of 10μl was removed and diluted 1:4 in 1x HT buffer for platelet counting using flow cytometry.

Diluted whole blood or washed platelets (40µl) were incubated with 2µl X-488 (anti-GPIbβ, Emfret) for 15 min, at RT. Following incubation, 1ml of filtered PBS was added, together with 50µl precission count beads (BioLegend). Flow cytometry was then performed using BD Fortessa, counting a fixed number of beads (500 events).

The number of platelets was then determined using the following formula and platelet count was adjusted with the dilution factor accounting for the anti-coagulant.

$$(A/B) \text{ X } (C/D) = \text{cells}/\mu l$$

A # events in TEST sample; B # events in ACFP particles; C # of particles in the lot; D Volume of TEST sample (40µl)

2.10.2. Platelet aggregometry

Washed platelets counted as described in **Section 2.10.1.** were resuspended to a final concentration of 300,000 platelets/µl using 1x HT-BSA.

Platelet aggregation was assessed using the Chronolog 700. To minimise the amount of blood collected from the mice, inserts were attached to the cuvettes used in aggregometry. Washed platelets (200µl) isolated from *GpIbα*$^{+/+}$ or *GpIbα*$^{\Delta sig/\Delta sig}$ mice were transferred to these cuvettes with inserts and stir bars and supplemented with 70µg/ml fibrinogen, 1mM $CaCl_2$ and the agonist to be tested (**Table 2.15**). HT-BSA was then added to a final volume of 250µl. As platelet-poor plasma (PPP) control, cuvettes with 250µl HT-BSA were used. Platelet aggregation was monitored over 6 min.

Agonists	Stock	Volume	[Final]	Buffer
ADP	0.1 mM*	2.5µl	1µM	41.5µl
	1mM	1.25 µl	5 µM	42.8 µl
	1 mM	2.5µl	10µM	41.5 µl
CRP	0.03mg/ml**	8.3µl	1 µg/ml	35.7 µl
	0.3mg/ml*	0.8µl	3µg/ml	43.2 µl
	0.3mg/ml*	8.3µl	10µg/ml	35.7 µl
Thrombin	1U/ml*	2.5 µl	0.01U/ml	41.5 µl
	1U/ml*	5 µl	0.02U/ml	39 µl
	10U/ml	1.25 µl	0.05U/ml	42.8 µl

Table 2.15. Agonists used in aggregometry for platelet stimulation.

2.10.3. Platelet spreading

Coverslips were cleaned with 100% ethanol and left to dry. Following that, coverslips were placed in 12-well plates and coated with 50µl/coverslip fibrinogen (200µg/ml), CRP (100µg/ml), murine VWF (10µg/ml) or BSA (0.5mg/ml) for 2hrs, at RT or overnight at 4°C. Coverslips were then blocked with PBS-BSA (5mg/ml) for 1hr, at RT. Following that, some of the fibrinogen-coated coverslips were incubated with 1U/ml thrombin for 15 min, at RT, to promote fibrinogen conversion to fibrin. The thrombin effect was neutralised by addition of excess hirudin (Refludan, 100µg/ml) for 5 min, at RT. Coverslips were washed 2x with PBS and then blocked with PBS-BSA (5mg/ml) for 1hr, at RT.

Washed WT or KI mouse platelets were added to the coverslips (150µl/coverslip, 25,000 platelets/µl) in the presence or absence of thrombin (1U/ml) or Botrocetin (2µg/ml) and allowed to adhere for 30 min – 1hr, at RT. In experiments using Botrocetin, additional coverslips were first incubated with GR144054 (20µg/ml) for 10 minutes to inhibit $\alpha_{IIb}\beta_3$ outside-in signalling.

Unbound platelets were removed by washing 2x with PBS. Coverslips were afterwards fixed with 10% formalin (1/10V of Formaldehyde 37% stock) for 10 min, at RT and then washed 2x

with PBS. NH_4Cl-PBS (50mM) was used to quench the coverslips for 10 min, at RT or overnight at 4°C. Platelets were then permeabilised by incubation with 0.1% Triton-PBS for 2 minutes. Coverslips were washed with PBS and stained with Phalloidin-Alexa488 (2U/ml) for 1.5hrs, at RT. Finally, coverslips were washed with PBS-BSA, PBS and water and mounted onto slides using ProLong (with DAPI staining) or VectaShield mounting media (20µl/coverslip). Spread platelets were visualised using the fluorescent microscope (40x objective) for quantification purposes – 3 fields of view/coverslip, and using the confocal microscope (63x objective, z-stack, oil immersion) for imaging purposes.

2.10.4. Flow assays

To investigate whether platelets from *GPIbα$^{\Delta sig/\Delta sig}$* mice exhibit a reduction in the VWF A1-GPIbα-mediated signalling and subsequent leukocyte recruitment, flow experiments were performed. Microchannels were coated with human VWF A1* as detailed in **Section 2.5.1.2**. Additionally, for a more physiologically relevant murine system, microchannels were coated with murine VWF (mVWF, kindly provided by Dr. Vanhoorelbeke from KU Leuven; concentration used 36.75µg/ml).

Blood was collected from wild-type or knock-in mice by Dr. Salles-Crawley in 3.8% citrate and labelled with X-488 anti-GPIbβ (Emfret Analytics, 1:15). Thereafter, whole blood or recalcified plasma-free blood was perfused through A1* or mVWF-coated channels at defined shear rates ($1000s^{-1}$ to $3000s^{-1}$) for 3.5 minutes and monitored in real-time. After platelets were captured, channels were washed with 1x HT buffer supplemented with 2mM $CaCl_2$. Quantification was performed using SlideBook 5.0 software (3i), to analyse platelet coverage over blood perfusion at high shear.

To investigate leukocyte binding to mouse platelets, blood was collected by Dr. Salles-Crawley and red blood cells (RBCs) were subsequently lysed. For this, blood was incubated with 10ml 1x RBC lysis buffer (BioLegend), for 10 minutes, in the dark, at RT. Thereafter, lysed blood was centrifuged for 5 minutes, at 350xg. The pellet was washed in 1x HT-BSA and finally

resuspended in a volume corresponding to the initial volume of blood. Lysed blood was incubated with a Ly6G-PE antibody (BD Pharmingen, 1:15), which specifically labels mouse neutrophils, and then perfused over the carpet of platelets captured at $50s^{-1}$ for 10 minutes. In separate experiments, lysed blood was pre-incubated with GR144053 (10μM) or with an anti-β_2 antibody prior to perfusion over the platelet carpet to investigate the role of $\alpha_{IIb}\beta_3$ and Mac-1/LFA-1 in neutrophil capture.

Neutrophil binding was monitored in real-time and the number of neutrophils bound was quantified throughout the entire channel and expressed as number of neutrophils/field of view.

2.11. Statistical analysis

Statistical analysis was performed using GraphPad Prism 6.0 software. Data was analysed using unpaired Student's t-tests, One-way ANOVA, or Mann-Whitney test, as appropriate and as detailed in the figure legends. Data was plotted as mean ± standard deviation (SD) / standard error of the mean (SEM) for normally distributed data, or as median ± 95% confidence intervals (CI) for data that was not normally distributed, according to the Pearson D'Agostino normality test. n numbers, as well as p-values are provided within the figure legends. P-values < 0.05 were considered significant.

Results

3. Chapter 1 – VWF A1-dependent platelet ‘priming’

3.1. Introduction

Platelets respond to a variety of different agonists, in a concentration and agonist type-dependent manner. Thus, platelets have a 'tunable' response. In support of this is the current understanding of the thrombus architecture. Contrary to the classical thrombus structure consisting of equally activated platelets, the current model proposes that a thrombus/haemostatic plug is organised within a core and shell region (**Figure 1.12**) [256-260]. The core of the thrombus is found in close proximity to the vessel injury and consists of tightly packed platelets that have been exposed to thrombin and are, therefore, fully activated. These platelets express activated $\alpha_{IIb}\beta_3$ on their surface, as well as high levels of P-selectin following degranulation [256]. The first layer of platelets recruited to the site of vessel injury is also exposed to collagen, another potent platelet agonist. These platelets present phosphatidylserine on their surface and are known as procoagulant platelets. In contrast, platelets from the shell region are more loosely packed and do not present P-selectin on their surface. They are thought to only be exposed to weaker agonists, namely ADP and thromboxane A2, which impart a reduced level of platelet stimulation, with $\alpha_{IIb}\beta_3$ activation, but reduced/concentration-dependent P-selectin exposure and limited exposure of phosphatidylserine (PS) positive surfaces [256-258].

VWF is well recognised for its crucial role in haemostasis, fulfilled by recruiting platelets at sites of vessel injury, through its A1 domain, which binds to GPIbα. It has become apparent that platelet presence in the shell region of the thrombus is dependent on their interaction with VWF [261]. Previous work suggests that VWF itself also acts as a platelet agonist, by inducing signalling events within platelets [55,215,216,220,375]. These signalling events are yet to be fully understood, as there is a gap in literature with respect to the best way to study the VWF A1-GPIbα interaction *ex vivo* in a manner that most accurately reflects what occurs within the vasculature. Previous studies generally use static assays, as well as Botrocetin/Ristocetin to induce the VWF A1-GPIbα interaction, both of which are not physiological. A recent study by

Zhang *et al.* proposes that the A1-dependent platelet signalling is absolutely dependent on the presence of shear [144]. It is, therefore, essential for this interaction to be investigated under flow. For this reason, the first aim of my PhD was to establish a flow system to analyse the A1-GPIbα interaction effect upon platelets.

The implications of the A1-dependent platelet signalling have long been overlooked due to the apparent redundancy in the setting of haemostasis, where more potent agonists, such as thrombin, collagen, ADP or thromboxane A2, are present and can, themselves, initiate a platelet response. However, in addition to the ability of VWF to induce platelet signalling, a recent study has shown that VWF-captured platelets are also able to recruit leukocytes *in vitro* [85]. This was perhaps not unexpected as previously characterised interactions between platelets and leukocytes require the platelets to be fully activated [344,346]. Therefore, the results presented within this chapter were intended to lay the ground work for the major aim of this thesis, which ultimately is understanding the contribution of VWF-dependent platelet signalling in the recruitment of leukocytes under flow.

The results in this chapter include the generation and purification of VWF A1 domain and a variant of the A1 (A1*) and the investigation of their effects upon platelets under static and flow conditions. The effects were explored by analysing Ca^{2+} signalling, $\alpha_{IIb}\beta_3$ activation and degranulation.

3.2. Results

3.2.1. Generation and purification of recombinant VWF A1 and A1* (Y1271C/C1272R)

VWF interacts with platelets via its A1 domain, which binds to GPIbα, and also via the C4 domain, which binds to activated $\alpha_{IIb}\beta_3$ [47]. The first milestone of this project was to express and purify recombinant human VWF A1 domain, to specifically study the A1-GPIbα interaction. However, as the A1-GPIbα interaction is characterised by a 'fast on' and 'fast off' profile and has low affinity (K_D=2470nM), I also aimed to generate, express and purify a mutant variant of the A1 domain, termed A1* (Y1271C/C1272R), which has a 10-fold increase in the affinity for GPIbα (K_D=245nM) [56].

VWF A1 and VWF A1* were expressed in insect cells and purified to homogeneity using a two-step FPLC method. Conditioned media collected from insect cells and concentrated using ammonium sulphate precipitation and TFF, was first loaded onto a Ni^{2+}-HiTrap column, capturing the A1/A1* via their 6xHis tags. Both proteins were eluted with 300mM Imidazole. The presence of A1/A1* in the elution samples was confirmed by Coomassie staining, as illustrated in **Figure 3.1(A)**, where bands corresponding to the predicted size of VWF A1 domain (27kDa) can be observed. The elution samples were run on an SDS-PAGE gel under both non-reducing and reducing conditions to ensure the correct folding of the proteins. As suggested by the shift in the bands under reducing conditions, both the A1 and A1* had the single disulphide bond formed. This was required for the correct folding of this domain.

In the second purification step, the elution samples from the Ni^{2+} column FPLC were dialysed in 20mM Tris (pH 7.8), 100mM NaCl and loaded onto a Heparin-Sepharose column, as VWF A1 domain can directly bind to heparin [52,53]. Proteins were eluted with 600mM NaCl and bands corresponding to the predicted size of VWF A1 (27kDa) can be observed in the respective Coomassie staining (**Figure 3.1(B)**).

The expression of VWF A1 and A1* was confirmed by Western Blotting using either an anti-VWF or an anti-His antibody (**Figure 3.1(C)**). Protein concentrations were subsequently determined using NanoDrop at the absorbance of 280nm and estimated according to their extinction coefficient to be approximately 14μM for VWF A1 and 9μM for VWF A1*.

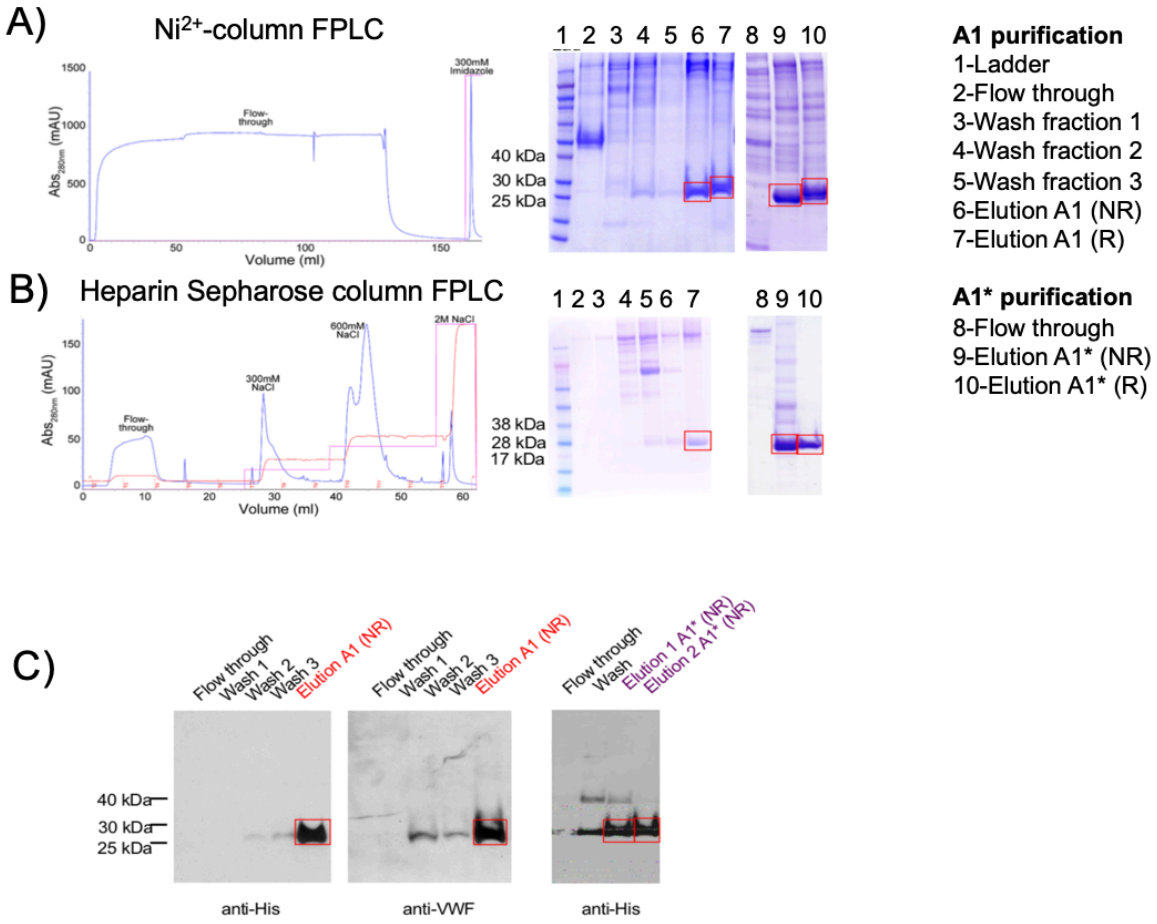

Figure 3.1. Purification of VWF A1 and A1*.

A) Chromatogram and Coomassie stain following HiTrap Ni^{2+}-column FPLC. Flow-through was collected first and then VWF A1 and A1 were eluted with 300mM Imidazole. Elution fractions were run under both non-reducing (NR) and reducing (R) conditions. B) Chromatogram and Coomassie stain following heparin-column FPLC. Elution fractions presented in A) were further purified using a heparin-Sepharose column. Flow-through was collected first and columns were washed with 300mM NaCl. The new elution fractions were collected using 600mM NaCl and, finally, the column was stripped with 2M NaCl. C) Western blot confirming the presence of VWF A1 and A1* in the elution fractions, detected with anti-His and anti-VWF antibodies.*

3.2.2. Effect of VWF A1 on platelets in static assays (FACS)

As it has previously been shown that the VWF A1-GPIbα interaction can induce signalling events within platelets, I investigated the effect of VWF A1 domain upon platelet phenotype. In the first instance, the A1-GPIbα interaction was assessed under static conditions, using FACS. Two platelet activation markers were analysed, namely $\alpha_{IIb}\beta_3$ (using a PAC1-FITC antibody) and P-selectin (using a CD62-PE antibody). These markers were analysed under resting conditions (in the absence of any agonists) or in the presence of ADP (5μM). As negative controls, platelet-rich plasma (PRP) was incubated either with PBS or with an FPLC wash fraction collected during the Heparin column FPLC, to ensure that the observed effects are not due to contaminants present in the purified material. As a positive control, PRP was incubated with Ristocetin, which is known to have the ability to unravel plasma VWF and promote its interaction with GPIbα [376].

When incubated with the A1 and Ristocetin, platelets presented a trend towards an increase in the level of activated $\alpha_{IIb}\beta_3$ on their surface, as seen by a shift in the histograms to the right (**Figure 3.2**), both in the presence and absence of ADP. On the other hand, P-selectin expression levels were similar across all conditions used, as depicted by the overlap in the histograms, suggesting that A1 and Ristocetin are not potent platelet agonists that can induce degranulation.

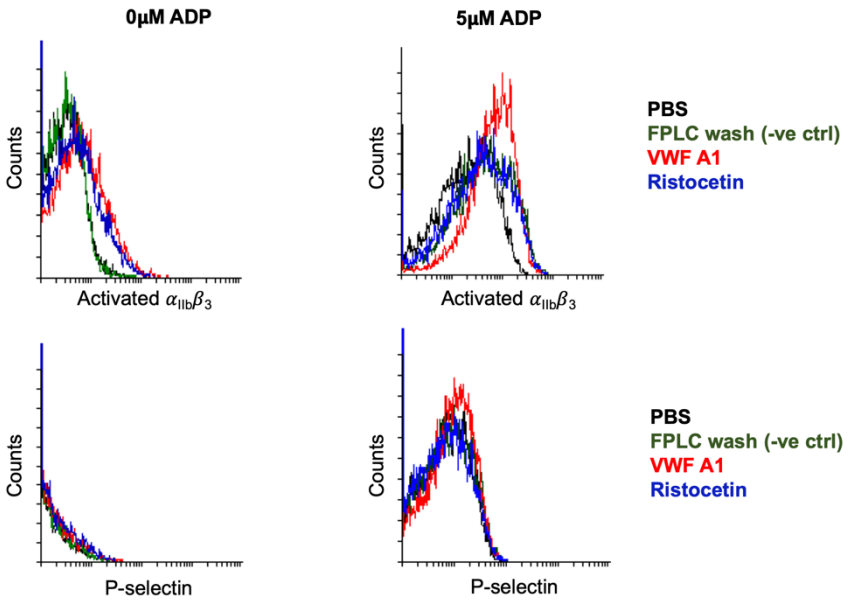

Figure 3.2. The effect of the A1-GPIbα interaction under static conditions.

Histograms analysing the expression of activated $\alpha_{IIb}\beta_3$ (top panels) and P-selectin (bottom panels) when platelets were incubated with PBS (black), an FPLC wash fraction (green), A1 (red) or Ristocetin (blue). The $\alpha_{IIb}\beta_3$ and P-selectin markers were assessed in the absence of ADP (left panels) and in the presence of 5µM ADP (right panels). Representative of n=3.

3.2.3. Effect of VWF A1/A1* on platelets in flow assays

Static assays do not reflect the physiological conditions under which platelets interact with VWF A1 domain, because, in the vasculature, this interaction occurs under flow and platelets are exposed to multiple A1 domains, as VWF is a multimeric molecule [16,45]. Moreover, a recent study by Zhang *et al.* suggests that, after interacting with VWF via the A1 domain, GPIbα needs to be subjected to shear, which unfolds its juxtamembrane stalk or mechanosensitive domain (MSD) and, thus, induces signalling events within platelets [144]. For this reason, the following experiments presented in this thesis were performed under flow.

To explore the effect of the A1-GPIbα interaction under flow, I set up a microfluidic system, in which microchannels were coated with the proteins of interest (i.e. A1, A1* or full-length VWF) and connected to a Mirus Evo Nanopump. Fluorescently-labelled whole blood, plasma-free

blood, or isolated cells were then perfused through these channels at physiological shear rates, in an attempt to accurately recreate physiological flow conditions *ex vivo*.

3.2.3.1. Optimising the capture of A1/A1* and FL-VWF onto microchannels

Different conditions used in flow assays required optimisation, including the types of microchannels to be used (depending on the nature of the protein to be immobilised), the concentration of proteins to be coated, and the shear rate used for perfusion of blood or cells.

During initial experiments, VenaFluoro8+ Cellix microchannels were used, onto which proteins were directly adsorbed overnight. Different concentrations of A1 and A1* were used, as well as a positive control represented by full-length VWF (FL-VWF, 2μM). Whole blood labelled with $DiOC_6$ was perfused through these channels at shear rates varying from high arterial shear ($1500s^{-1}$) to low venous shear ($50s^{-1}$). Channels coated with FL-VWF captured platelets in a time-dependent manner (**Figure 3.3i-iii**), with optimal platelet binding occurring at $1000s^{-1}$. Lower shear rates ($800s^{-1}$, $500s^{-1}$, $100s^{-1}$, $50s^{-1}$) still resulted in platelet binding although the platelet coverage was reduced across the channels (data not shown). Using a higher shear of $1500s^{-1}$ led to a similar platelet coverage as the one obtained when using $1000s^{-1}$. Channels directly coated with A1 and A1* failed to recruit platelets under flow at any shear (data not shown). A potential reason for this is that adsorption of the isolated A1 blocks the GPIbα binding site, which spans an appreciable surface of the A1 domain.

A recent study by Tischer *et al.* used Cu^{2+} biochips to capture the A1 domain [99]. These microchannels have a PEGylated surface which can bind cations, such as Cu^{2+}, Ni^{2+} or Co^{2+}, that can, in turn, bind 6x His-tagged proteins. Capturing the A1 domain via its His tag enables the whole A1 domain to be presented for interaction. Therefore, I used these channels to capture the A1/A1* via their His tags, which led to a uniform and consistent platelet capture (**Figure 3.3iv-ix**). The concentration of A1 was titrated (14μM, 8μM, 5μM and 3.75μM) and no differences were observed between these concentrations, probably as they saturated the

channels. However, platelet recruitment was decreased with lower concentrations (data not shown). Therefore, I chose the concentration of 3.75μM for the A1 domain based on the titration, and the same concentration for the A1* to be able to directly compare the two conditions. As illustrated in **Figure 3.3**, there was a time-dependent increase in the platelet capture by A1/A1* and FL-VWF coated channels. Channels coated with BSA or with another His-tagged protein (PilC) failed to capture platelets under flow (**Figure 3.3x-xii**), confirming the dependency on VWF A1 domain.

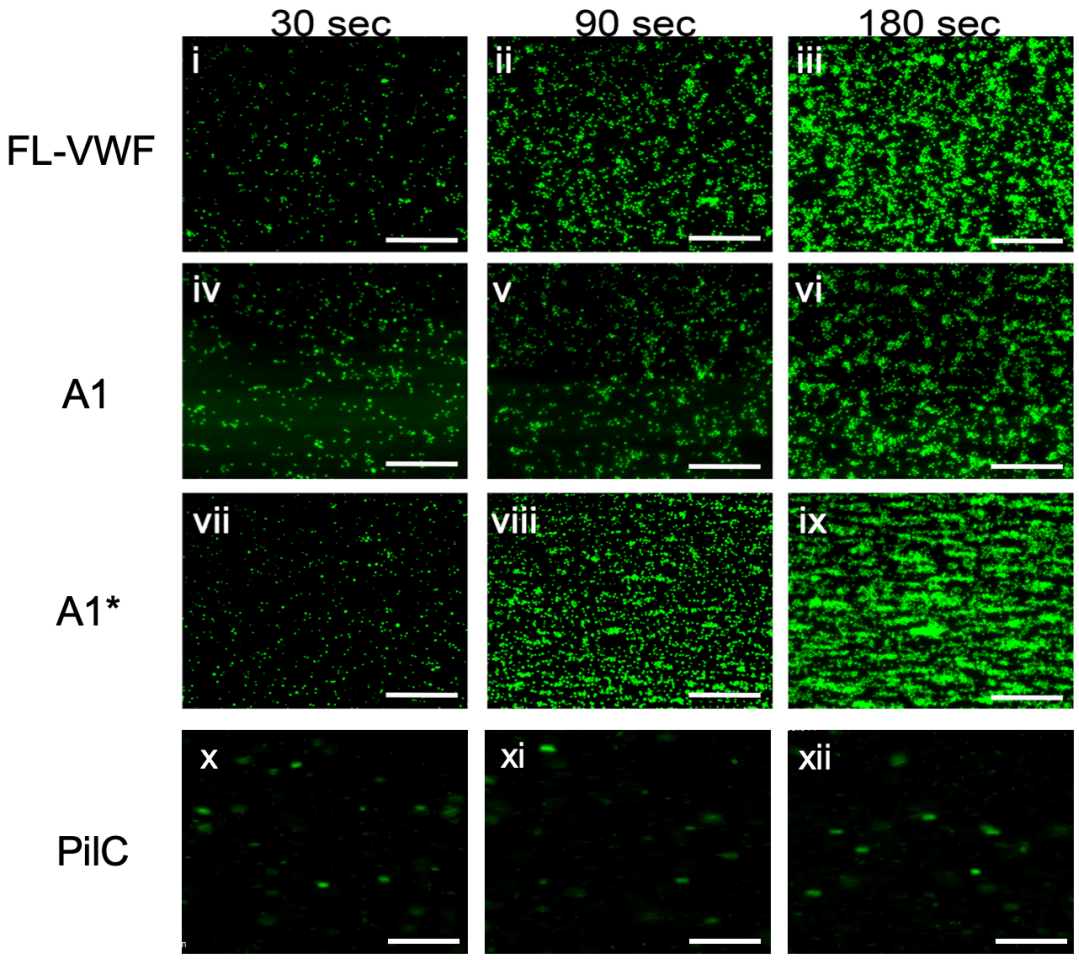

Figure 3.3. Platelet rolling and attachment to VWF under flow.

Microchannels were coated with either full-length VWF (FL-VWF; i-iii), VWF A1 (iv-vi), A1 (vii-ix) or a negative control, PilC (x-xii). Whole blood labelled with $DiOC_6$ was perfused at $1000s^{-1}$. Representative images (n=3) of platelet coverage after 30, 90 and 180 seconds are shown. Scale bar=50μm*

3.2.3.2. Platelet rolling

An important observation made during blood perfusion through microchannels coated with A1 and A1* was that platelets appeared to roll rapidly on the recombinant A1 domain before binding, whereas they rolled less before stably attaching to A1*. This is illustrated in **Figure 3.4(A)** and in **Movie 1** where platelets were tracked and the distance they travelled during the first 30 seconds is shown by their respective multicoloured lines. Platelet rolling was quantified by analysing the average velocity of platelets during the first 30 seconds of perfusion through channels coated with A1, A1* or FL-VWF. As predicted, there was a significant increase in the platelet velocity on channels coated with A1 as opposed to channels coated with A1* ($p<0.0001$) (**Figure 3.4(B)**). Platelets rolled on A1 with a median speed of 1.76μms^{-1}, whereas their median velocity on A1* was 0.23μms^{-1}. This finding is consistent with the 10-fold higher affinity of A1* for GPIbα [56]. As expected, platelets rolled on FL-VWF in the first few seconds of perfusion, with stable attachment following at later timepoints due to the multimeric nature of VWF. For this reason, most of the remaining experiments presented in this thesis used channels coated with A1* or FL-VWF as representative for all conditions.

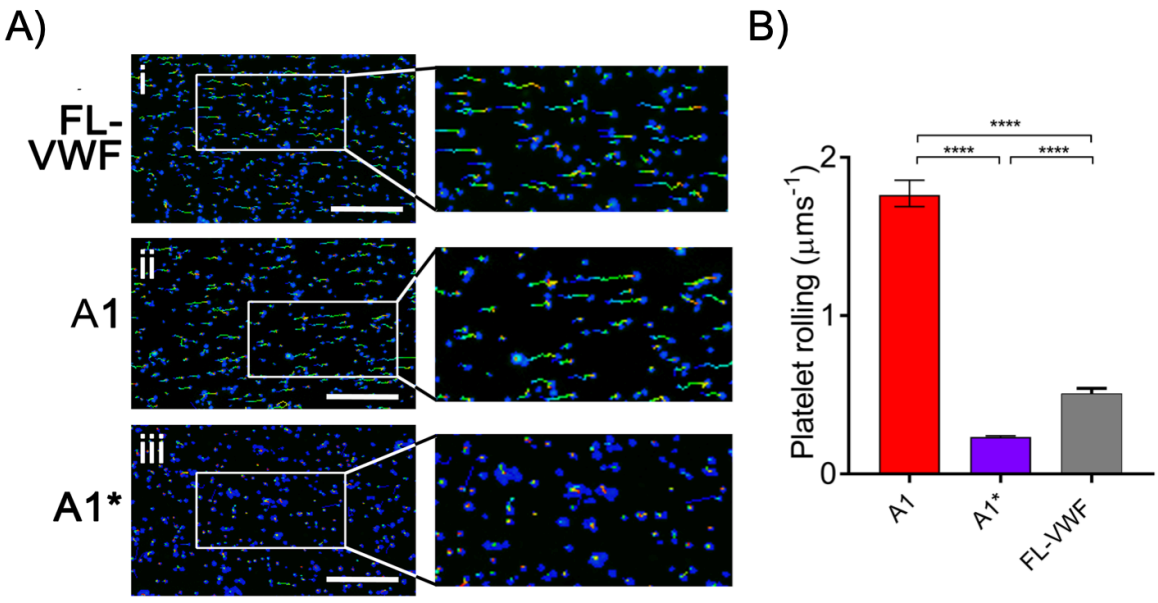

Figure 3.4. Platelet rolling under flow.

A. Whole blood was perfused at 1000s^{-1} through channels coated with FL-VWF, A1 or A1. Bound platelets (blue) were tracked, with the multi-coloured lines representing the distance travelled in the first 30 seconds of perfusion. Images representative of n=3; Scale bar=50μm. B. Platelet rolling velocity on channels coated with A1, A1* and FL-VWF. Data plotted are median ±95% CI. n=3562 platelets from 3 different experiments (A1), n=4047 platelets from 3 different experiments (A1*), n=3538 platelets from 3 different experiments (FL-VWF). Data were analysed using the Mann-Whitney test; **** p<0.001.*

3.2.3.3. Intracellular Ca^{2+} release

The A1-GPIbα interaction can induce signalling within platelets in the absence of other platelet agonists [55,144,146,216,220,375]. Intracellular Ca^{2+} is known to be crucial for platelet signalling, and is involved in the A1-GPIbα signalling axis [245]. Therefore, to investigate whether in the flow system I established, the recombinant A1/A1* domain induced signalling events within platelets, I performed Ca^{2+} assays. As part of these experiments, platelets were pre-loaded with a Ca^{2+} sensitive permeable dye (Fluo-4 AM) and added back to plasma-free blood prior to being perfused through channels coated with A1/A1* or FL-VWF. As a negative control, channels were coated with an anti-PECAM-1 antibody, that can capture platelets but is not known to induce signalling. During flow assays, transient increases in fluorescence could be observed in platelets subsequent to platelet attachment to A1/A1* or FL-VWF (**Figure 3.5** and **Movie 2**), but not when platelets were captured via the anti-PECAM-1 antibody (data not shown). These transient spikes in fluorescence correspond to Ca^{2+} being repeatedly released from platelet intracellular stores. These repeated cycles of release continued throughout the 5 minutes of perfusion at high shear.

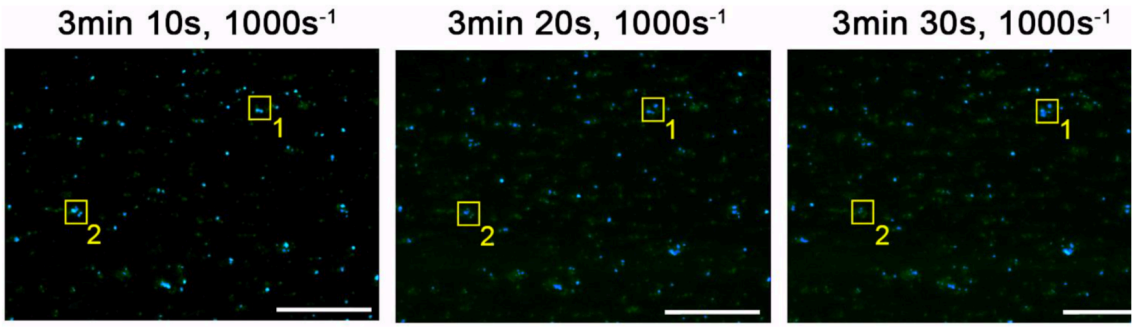

Figure 3.5. The effect of the A1-GPIbα interaction on platelet Ca^{2+} release.

Images were captured after 3min 10s, 3min 20 s and 3min 30s of flowing plasma-free blood containing platelets pre-loaded with Fluo-4 AM over channels coated with A1. The fluorescence (bright blue) corresponds to the platelet intracellular Ca^{2+} release, following platelet capture to A1*. Box 1 shows an increase in fluorescence over time, corresponding to Ca^{2+} being released, whereas box 2 illustrates an example of Ca^{2+} release ending, as suggested by the decrease in fluorescence over time. Images representative of n=3 on channels coated with A1* or FL-VWF. Scale bar = 100μm*

3.2.3.4. Under flow, VWF-GPIbα signalling induces activation of $\alpha_{IIb}\beta_3$

During perfusion of whole blood at high shear, individual platelets could be distinguished attaching to the surface. Over time, these started to aggregate into clumps (after approximately 3 min) (**Figure 3.6(Ai)**). This occurred irrespective of the anticoagulant used (PPACK or citrate). Aggregation could occur via fibrinogen, a protein which is abundantly present in the plasma and responsible for interlinking the platelets via activated $\alpha_{IIb}\beta_3$ as part of the normal haemostatic response [86]. To investigate the role of fibrinogen in platelet aggregation within these settings, the same experiments were performed in plasma-free blood, i.e. in the absence of soluble fibrinogen. After 3.5 min of perfusing plasma-free blood, individual platelets could still be distinguished (**Figure 3.6(Aii)**), and aggregation was markedly reduced with uniformly spread monolayers of platelets observed.

The main fibrinogen receptor on the platelet surface is activated integrin $\alpha_{IIb}\beta_3$ [86,160]. Based on these flow and previously presented static assays results, and on previous studies [55], I hypothesised that, following the A1-GPIbα interaction, $\alpha_{IIb}\beta_3$ becomes activated and can therefore bind fibrinogen, leading to platelet aggregate formation. This contention was

investigated by pre-incubating whole blood with two different $\alpha_{IIb}\beta_3$ inhibitors – Eptifibatide (9μM) and GR144053 (10μM) prior to perfusion through channels coated with A1/A1* or FL-VWF. As presented in **Figure 3.6(Aiii,iv)**, aggregation was abolished in the presence of these inhibitors, confirming that $\alpha_{IIb}\beta_3$ is activated following the A1-GPIbα interaction. Aggregation was quantified in all these conditions by analysing the number of platelet aggregates over time and the area under curve (AUC) and the analysis is shown in **Figure 3.6(B-E)**. Aggregation was significantly reduced in plasma-free blood or in the presence of $\alpha_{IIb}\beta_3$ inhibitors, in channels coated with either A1* or FL-VWF.

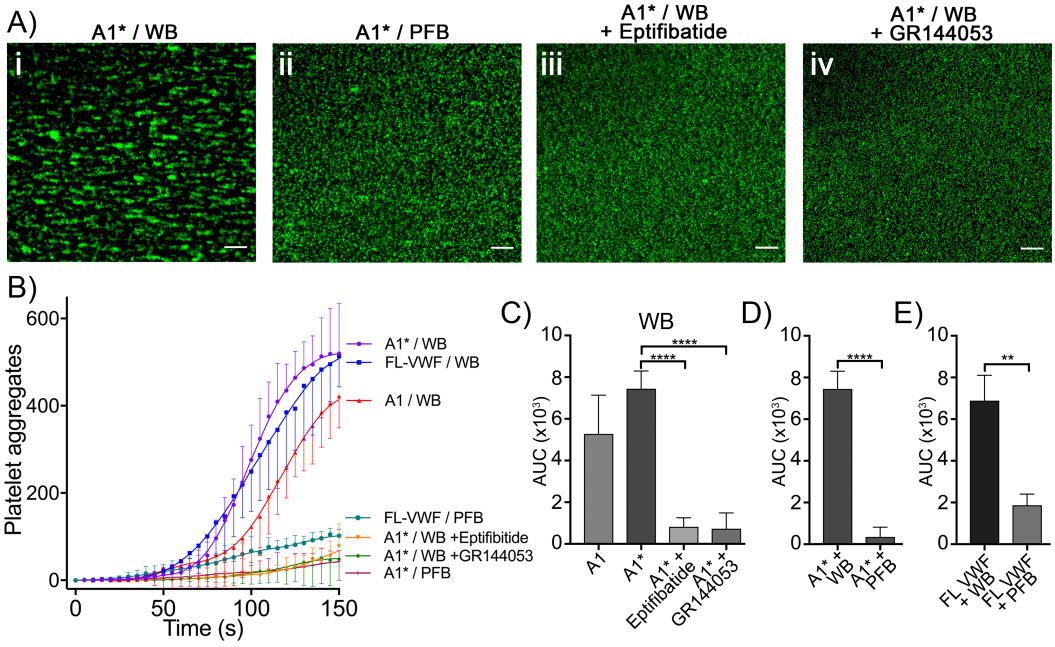

Figure 3.6. Platelet binding to VWF under flow induces $\alpha_{IIb}\beta_3$-dependent aggregation.

A) Vena8 microchannels were coated with A1 via its 6xHis tag. i) Whole blood (WB) or ii) plasma-free blood (PFB), iii) WB containing Eptifibatide (9μM) or iv) WB containing GR144053 (10μM) were perfused through channels at 1000s^{-1}. Representative images acquired after 3 minutes. Scale bar=50μm. B) Graph measuring platelet aggregation over time in WB perfused through channels coated with A1 (red, n=3), A1* (purple, n=4) and FL-VWF (blue, n=3), WB pre-incubated with Eptifibatide (orange, n=3) or GR144053 (green, n=4) over channels coated with A1* and PFB over channels coated with A1* (magenta, n=3) or FL-VWF (teal, n=3). Data plotted are mean ±SD. C) Bar chart comparing area under the curve (AUC) of WB perfused on A1 or A1*, in the presence and absence of $\alpha_{IIb}\beta_3$ inhibitors. D) Bar chart comparing AUC of WB vs. PFB perfused over A1*. E) Bar chart comparing AUC of WB vs. PFB perfused over FL-VWF. Data presented are mean ±SD, n=3 or 4 as indicated. Data were analysed using unpaired, two-tailed Student's t test; **** p<0.0001, ** p<0.01.*

To ascertain whether the reduction in aggregation was due to the lack of fibrinogen or inhibition of $\alpha_{IIb}\beta_3$ and not by a difference in platelet capture, the surface coverage was quantified for all experimental conditions. As seen in **Figure 3.7**, although there were some variations in the platelet coverage across the different conditions, these were not correlated with the corresponding number of aggregates.

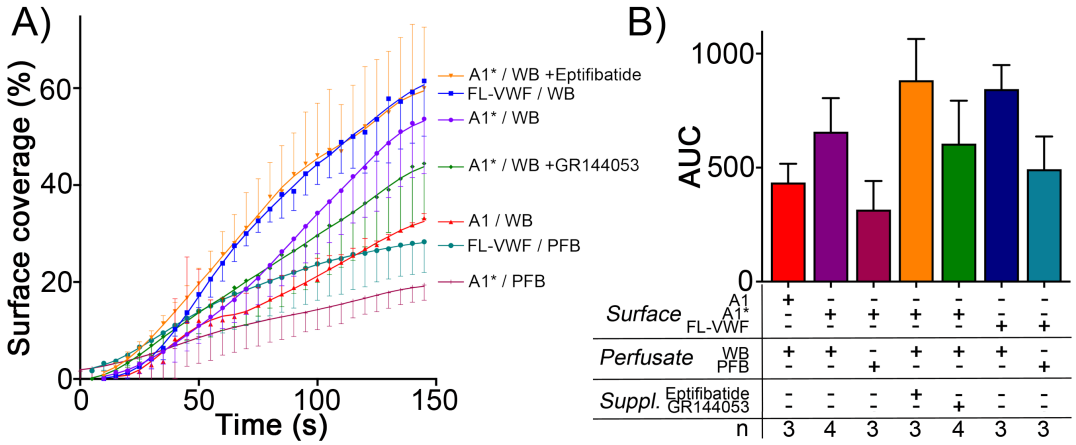

Figure 3.7. Platelet coverage.

A) Graph showing the surface coverage over time of microchannels coated with FL-VWF, VWF A1 or VWF A1 by platelets in either whole blood (WB) or plasma-free blood (PFB), in the presence or absence of $\alpha_{IIb}\beta_3$ inhibitors at a shear rate of 1000s^{-1}. B) Bar chart of the area under the curve (AUC) of conditions analysed in A). Data presented are mean ±SD, n=3 or 4 as indicated.*

The activation of the platelet integrin $\alpha_{IIb}\beta_3$ in response to A1-GPIbα signalling was further examined using confocal microscopy. In these experiments, plasma-free blood was perfused at 1000s^{-1} for 3.5 minutes over channels coated with FL-VWF, collagen (positive control) or anti-PECAM-1 (negative control). Thereafter, channels were washed, and fluorescent fibrinogen-Alexa647 was perfused over the captured platelets at 50s^{-1}. As shown in **Figure 3.8**, platelets captured by collagen, a potent platelet activator, bound fluorescent fibrinogen efficiently and also assembled into microthrombi/aggregates. Platelets captured by FL-VWF also bound fluorescent fibrinogen. They were seen as individual platelets (rather than aggregates), as the assay was performed using plasma-free blood. In contrast, platelets

captured by the anti-PECAM-1 antibody failed to bind fluorescent fibrinogen. These data confirm that VWF-dependent signalling lead to fibrinogen binding, and therefore demonstrate that $\alpha_{IIb}\beta_3$ is in its open active conformation.

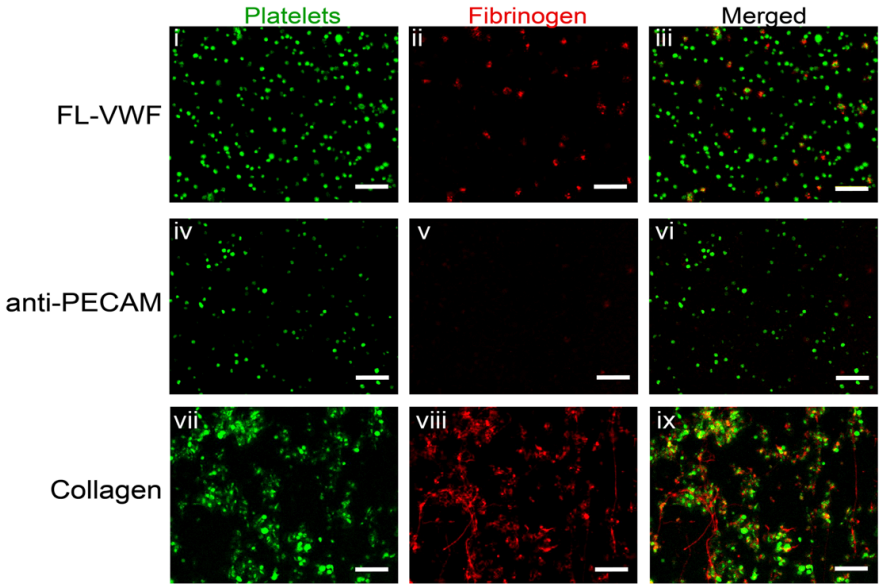

Figure 3.8. **Confirmation of $\alpha_{IIb}\beta_3$ activation following A1-dependent platelet 'priming'.**

Representative images (n=3) depicting platelets ($DiOC_6$, green) captured from plasma-free blood at $1000s^{-1}$ for 3.5 minutes onto microchannel surfaces coated with either FL-VWF (i-iii), anti-PECAM (iv-vi) or collagen (vii-ix). Plasma-free blood was supplemented with fibrinogen-Alexa647 (red). Merged images show fluorescent fibrinogen attached to the platelets captured by FL-VWF and collagen, but not by platelets captured by anti-PECAM-1. Images representative of n=3. Scale bar=20μm.

3.2.3.5. Under flow VWF-GPIbα signalling induces minimal platelet degranulation

Under flow, the A1-GPIbα interaction can induce intracellular platelet Ca^{2+} release and activation of $\alpha_{IIb}\beta_3$ on the platelet surface. To investigate whether VWF A1-GPIbα signalling can lead to full platelet activation, with degranulation, several approaches were adopted.

One of the main platelet activation markers is P-selectin, which in resting platelets is stored in the platelet α granules [196]. Degranulation results in presentation of P-selectin on the platelet

surface. To test whether P-selectin is presented onto the platelet surface, platelets captured by FL-VWF, collagen or anti-PECAM-1 were incubated with an anti-P-selectin antibody conjugated to APC and visualised using confocal microscopy. As illustrated in **Figure 3.9**, platelets captured by collagen exhibited strong expression of P-selectin on their surface, whereas platelets bound to VWF had little/no P-selectin staining, indicative of minimal release of the α granules. Further experiments confirming the minimal P-selectin exposure will be presented in the **Section 4.2.2.3**.

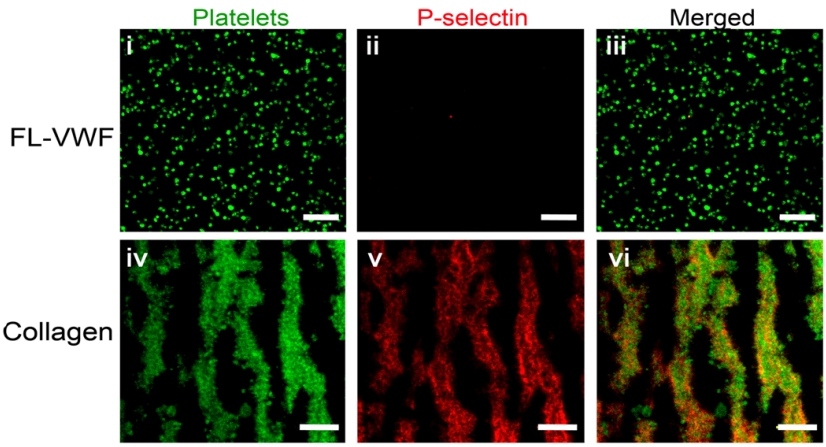

Figure 3.9. **Minimal P-selectin exposure following the A1-GPIbα interaction.**

Representative images (n=3) depicting platelets ($DiOC_6$, green) captured from whole blood at $1000s^{-1}$ for 3.5 minutes onto microchannel surfaces coated with either FL-VWF (i-iii) or collagen (iv-vi). Blood was supplemented with anti-P-selectin-APC (red). Merged images show the presence of P-selectin on the surface of platelets captured by collagen, but very little/no P-selectin on platelets captured FL-VWF. Scale bar=20μm.

In separate experiments, whole blood was pre-incubated with Apyrase. Apyrase acts as a platelet activation antagonist by degrading the ADP secreted from the dense granules and thus preventing secondary signals via the activation of the P_2Y_1 and P_2Y_{12} receptors [242,243]. Using this approach, there was no difference in the level of aggregation over VWF-coated surfaces either in the presence or absence of Apyrase (**Figure 3.10**). This indirectly suggests that there is no dense granule release or at least demonstrates that there is no effect/dependency of secondary messenger to induce aggregation.

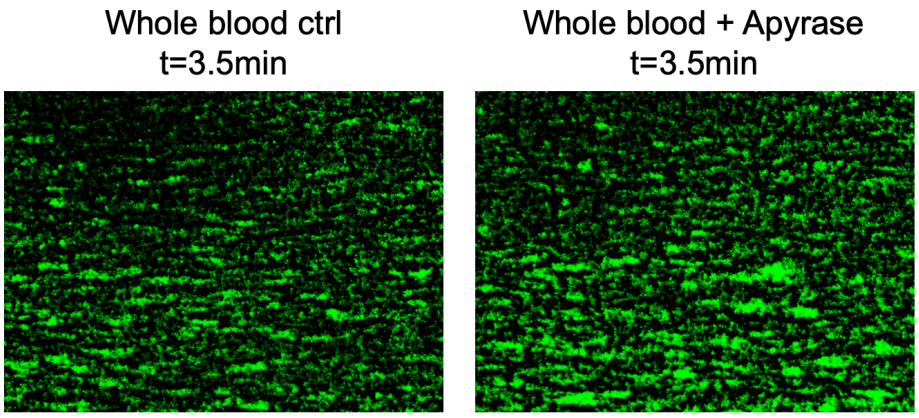

Figure 3.10. Platelet aggregation on VWF A1* is independent of ADP.

Microchannels were coated with A1 via its 6xHis tag. Whole blood was perfused through channels at 1000s^{-1}, in the presence or absence of Apyrase. Images acquired after 3.5 minutes. Representative of n=3.*

3.3. Discussion

The purpose of this chapter was to investigate the effect of the VWF A1 domain-GPIbα interaction upon platelet physiology. Through GPIbα, VWF A1 is known to induce signalling events within platelets [55,220,375], but these are yet to be fully characterised and their importance remains unclear.

To specifically study the A1-GPIbα interaction, I first expressed and purified recombinant VWF A1 domain and a variant of the A1, termed A1*. This variant, Y1271C/C1272R, causes a shift in the long-range disulphide bond within the A1 domain by one amino acid and induces a conformational change in the β-sheet placed at the surface of interaction between the A1 domain and GPIbα. Blenner *et al.* studied this mutation and showed that it was associated with a 10-fold increase in the affinity of VWF for GPIbα [56].

VWF is a multimeric protein, with multiple A1 domains being able to interact with a single platelet at sites of vessel injury. Therefore, using the higher affinity mutant A1 domain could, perhaps, more closely reflect the interaction that occurs *in vivo*. An A1 domain dimer was also

expressed and purified, but, due to a lower yield, this was only used in preliminary experimental settings and is not a focus for this thesis.

VWF A1 and A1* were cloned into a pMT-Puro vector, containing a 6x polyhistidine (His) tag and a V5 tag. They were subsequently expressed in insect cells, which ensured correct formation of the essential disulphide bond in the A1 domain. Given the presence of a His tag, proteins were initially purified using a Ni^{2+}-HiTrap column FPLC. To improve protein purity, a second purification step was performed, consisting of a Heparin-Sepharose column FPLC, as VWF A1 was previously shown to have the ability to bind heparin [52,53].

After purification, I investigated the contribution of these proteins to platelet activation using static assays. For these, flow cytometry was used to analyse the effect of A1 on platelet expression of activated $\alpha_{IIb}\beta_3$ and P-selectin, in the presence or absence of a known platelet agonist, ADP. Incubating platelets with the A1 domain led to a very modest increase in the expression of activated $\alpha_{IIb}\beta_3$ on the platelet surface, even in the absence of ADP. This increase, although modest, is in line with existing literature reporting that the A1-GPIbα interaction on its own is capable of inducing $\alpha_{IIb}\beta_3$ activation [55]. A similar increase was observed when platelet-rich plasma was incubated with Ristocetin, which is known to promote the the A1-GPIbα binding [376]. Neither VWF A1, nor Ristocetin appeared to augment P-selectin exposure under these conditions. These results are the first line of evidence to suggest that the VWF A1 is not a potent platelet activator like thrombin or collagen, as it does not appear to induce degranulation and subsequent P-selectin exposure.

However, analysing the effects of VWF A1 on platelets using flow cytometry had a major limitation associated with the experiments being performed under static conditions. Apart from not reflecting the physiological environment of the vasculature, where the A1-GPIbα interaction would normally occur, these experiments are not in line with recent findings outlining the importance of shear for VWF-dependent platelet signalling. Zhang *et al.* proposed a mechanism through which the A1-GPIbα interaction can lead to platelet signalling. As

mentioned in the introduction (**Section 1.3.4.1**), the A1 domain binds to the leucine-rich repeat site of the GPIbα. Under flow, this is thought to exert pulling forces on the juxtamembrane stalk of GPIbα, which, in turn, elongates and acts as a mechanosensitive domain. This presumably leads to a conformational change in the intracellular tail of GPIbα and, thus, converts the mechanical stimulus into a biochemical signal [144]. For this reason, I established a flow system to more accurately determine the effect of the A1-GPIbα interaction on the platelet phenotype.

For this, microfluidic channels were connected to a Mirus Evo Nanopump, and fluorescently labelled blood was perfused through these channels at various shear rates. In initial experiments, blood was collected in 3.13% citrate from healthy volunteers and used within two hours of collection to minimise platelet activation. Platelet capture was monitored in real-time using fluorescent microscopy, by labelling blood with $DiOC_6$.

The proteins of interest (A1/A1* or FL-VWF) were initially adsorbed directly on Vena Fluoro8+ microchannels. Optimal platelet capture on full-length VWF (FL-VWF) was seen to occur at $1000s^{-1}$, which corresponds to physiological arterial shear rates. However, direct adsorption of A1 and A1* was associated with poor platelet recruitment, irrespective of the density of A1/A1* coated on the channels. This may be due to steric hindrance, as the high surface of interaction required between the VWF A1 and GPIbα could be obstructed during direct immobilisation. Other studies reported using PEGylated channels with Cu^{2+} bound to the surface to capture the A1 domain [99]. I therefore started using these channels coated with either Cu^{2+} or Ni^{2+} and capturing the A1/A1* via their His tags in an orientation specific manner. This ensured that the surface of interaction with GPIbα is available for binding and, as expected, resulted in a good and uniform platelet recruitment. There was a limitation associated with variability between channels and platelet detachment occurring at later time points in some channels. To address this issue, I started coating the channels with Co^{2+} and, following A1/A1* capture, using H_2O_2 to oxidise Co^{2+} to Co^{3+} as this improves protein coating stability by

increasing the affinity of capture [373]. Platelet capture was similar in all conditions, however, platelets rolled on channels coated with A1, whereas they more stably attached to A1*, having a significantly lower velocity on A1* than on A1. This result is not unforeseen, as A1* has a higher affinity for GPIbα [56]. Platelets captured by FL-VWF had a similar velocity to A1 initially, but platelets eventually stably attached, suggesting that coating channels with A1* might more accurately represent the physiological conditions at later timepoints. This could be either due to the multimeric nature of VWF and/or to the potential activation of platelet integrin $\alpha_{IIb}\beta_3$, which could stabilise the interaction by binding to the C4 domain of VWF.

When whole blood was perfused through the channels, individual platelets could initially be distinguished, but these aggregated into clumps as time progressed. Of note, platelets did not form large 3D aggregates, but instead aggregated in thin monolayers. This effect was observed in channels coated with A1/A1* and FL-VWF, to similar extents. A possible reason behind this could be the initial use of citrate as an anticoagulant. Being a Ca^{2+} chelator, it is possible that citrate impairs the normal activity of certain enzymes and integrins present in the blood. One of the enzymes requiring Ca^{2+} for optimal activity is ADAMTS13. ADAMTS13 is a metalloprotease that is responsible for regulating the VWF multimeric size [59]. I hypothesized that a disruption in the normal activity of ADAMTS13 could lead to a higher level of VWF multimers that could interlink the platelets, augmenting aggregation. However, using another anticoagulant, PPACK, a serine protease inhibitor, did not influence the formation of aggregates. Importantly, heparin was not chosen as an anticoagulant, due to its ability to bind to VWF A1 domain [52,53], which may have impaired platelet binding.

While the change of anticoagulant did not have an impact upon platelet aggregation, this was not the case when experiments were performed in the presence of Eptifibatide or GR144053. Indeed, supplementing blood with either greatly reduced aggregate formation. Eptifibatide and GR144053 are peptide mimetics known to inhibit the activated form of $\alpha_{IIb}\beta_3$ [377,378]. By doing so, these inhibitors block the binding of the primary $\alpha_{IIb}\beta_3$ ligand, fibrinogen. Fibrinogen is a

hetero-hexameric protein, circulating in a high concentration within plasma. It binds to activated $\alpha_{IIb}\beta_3$ via its RGD site and, in doing so, it interlinks the platelets, causing them to aggregate [86]. Therefore, another way to test whether aggregation is dependent on the activation of $\alpha_{IIb}\beta_3$ was to deplete fibrinogen from blood prior to the flow assays. This was achieved by washing platelets, leukocytes and red blood cells and resuspending them in buffer to remove the fibrinogen-containing plasma. As expected, the aggregation was abolished in the absence of plasma. Importantly, under flow, washed platelets alone do not bind to either A1/A1* or FL-VWF due to the lack of red blood cells, which normally exert a margination effect, pushing platelets towards the vessel/channel edges, where they can interact with VWF.

My results clearly show that, following the A1-GPIbα interaction, integrin $\alpha_{IIb}\beta_3$ becomes activated, through four main lines of evidence:

1) Aggregation of platelets on VWF/A1-coated surfaces
2) Lack of platelet aggregation when fibrinogen is removed from blood (in plasma-free conditions) in flow assays
3) Inhibition of aggregation when blood is pre-incubated with $\alpha_{IIb}\beta_3$ inhibitors
4) Binding of fluorescent fibrinogen to VWF-captured platelets

Furthermore, when pre-incubated with Eptifibatide or GR144053, platelets exhibited prolonged rolling on FL-VWF (data not shown), which could be attributed to the inability of these platelets to bind to VWF C4 domain via activated $\alpha_{IIb}\beta_3$ and stabilise their initial interaction with VWF via its A1 domain.

As reported previously in the literature, VWF-dependent $\alpha_{IIb}\beta_3$ activation is preceded by release of intracellular Ca^{2+} stores [219,220,224]. Pre-loading platelets with a Ca^{2+}-sensitive fluorophore prior to perfusing them through the channels was associated with spikes in fluorescence corresponding to transient Ca^{2+} release from intracellular stores following platelet interaction with A1/A1* or FL-VWF. Importantly, platelets captured by an anti-PECAM-1

antibody failed to exhibit intraplatelet Ca^{2+} release and also did not bind fluorescent fibrinogen, confirming that these effects are dependent on platelets interacting with the A1 domain, and not induced simply by platelet immobilisation to a surface.

Finally, I investigated whether the VWF A1-GPIbα interaction induces platelet degranulation. However, my results show no clear evidence of P-selectin exposure, which translates into a lack of α granule release. Although there are other reports suggesting a modest α granule release as a result of the VWF A1-GPIbα interaction, these studies were commonly performed in the presence of Botrocetin/Ristocetin, which are not present under physiological conditions. It is, therefore, generally acknowledged that, when compared to other platelet agonists, P-selectin exposure is very low [222,223], thus my results are supported by the literature. In line with no P-selectin exposure, my results also show no clear evidence of platelets releasing ADP, which indirectly demonstrates a lack of dense granule release as well.

Based on the results discussed in this section, I concluded that platelets captured by VWF or the isolated A1 domain, under flow, undergo Ca^{2+} release with subsequent activation of $\alpha_{IIb}\beta_3$, but minimal degranulation. These data are in line with existing literature [214] but provide novel tools to specifically study the VWF A1-GPIbα under flow, using experimental settings that can better mirror the physiological conditions *ex vivo*. These results also reflect the current understanding of platelets having a 'tunable' response, by undergoing different degrees of activation depending on the agonist type and concentration. As VWF-captured platelets express activated $\alpha_{IIb}\beta_3$ but no P-selectin, they are not fully activated. Consequently, throughout this thesis, the term **'primed' platelets** was used to describe the phenotype of VWF-captured platelets.

One of the main challenges that remains is understanding the importance of VWF-dependent platelet 'priming'. As mentioned in the introduction, VWF-induced platelet signalling might be considered redundant in the setting of haemostasis, due to the more potent platelet agonists, such as thrombin or collagen, being present and able to fully activate the platelets. However,

considering that highly activated platelets are restricted to the core region of a forming thrombus, VWF-platelet 'priming' might play a role into the formation of the thrombus shell, where platelets are loosely packed and present activated $\alpha_{IIb}\beta_3$ but no P-selectin on their surface [256]. In fact, studies show that platelet accumulation on the outer layers of the thrombus is dependent on VWF [261].

Moreover, platelets have recently been classified as immune cells, due to the roles they fulfil in the settings of infection and inflammation. Their functions beyond haemostasis are not fully understood and generally require platelets to interact with other cells and molecules, particularly with leukocytes [122,123,265]. It has recently been shown that VWF-captured platelets are able to recruit leukocytes under flow, in the absence of any other platelet agonists, via an yet unknown mechanism [85]. Therefore, I hypothesise that VWF-dependent platelet 'priming' may be important for the platelet roles beyond haemostasis, by leading to novel platelet-leukocyte interactions under flow. The ability of VWF-'primed' platelets to interact with leukocytes will be explored in the following chapters.

4. Chapter 2 – Characterising the ‘primed’ platelet-leukocyte interaction

4.1. Introduction

Platelet-leukocyte interactions are increasingly recognised for their role in different pathophysiological conditions, including infections and a variety of cardiovascular disorders, such as atherosclerosis, atherothrombosis, stroke and deep vein thrombosis [272,344,364]. Previously characterised interactions between platelets and leukocytes have been identified in settings in which either the platelet and/or the leukocyte is/are fully activated. It is widely accepted that platelets require activation/degranulation to interact with leukocytes. This process facilitates presentation of the receptors that mediate the best characterised platelet-leukocyte interactions, namely P-selectin (which binds to P-selectin glycoligand 1 (PSGL-1) on the surface of leukocytes), and platelet CD40 ligand (CD40L) (which binds to leukocyte CD40) [343,345,346]. The P-selectin-PSGL-1 interaction also induces signalling within leukocytes, that can lead to the activation of integrin Mac-1 [347]. In its activated form, this integrin can further stabilise the interaction with platelets by binding directly to GPIbα or to fibrinogen, which, in turn, binds activated $\alpha_{IIb}\beta_3$ on platelets [141,348].

However, it appears that these are not the only existing platelet-leukocyte interactions. A recent study showed that platelets bound to VWF strings from endothelial cells are able to capture leukocytes under flow [85] (primarily neutrophils – José López personal communication). In this setting, the platelets were not exposed to any known potent platelet agonists such as collagen, thrombin, ADP or thromboxane A_2. Therefore, this platelet-leukocyte interaction likely occurs via a mechanism that is not dependent on degranulation, being solely dependent on prior platelet binding to VWF.

As presented in the previous chapter, VWF can induce signalling within platelets under flow, including intracellular Ca^{2+} release and activation of $\alpha_{IIb}\beta_3$. This does not lead to appreciable P-selectin exposure. Due to this, these platelets are considered 'primed', as opposed to activated. Based on these results and the study by Zheng *et al.* [85], I hypothesised that VWF-'primed' platelets acquire the ability to bind leukocytes via an interaction that is independent

of P-selectin/CD40L on platelets or Mac-1/LFA-1 on leukocytes. This chapter aims to characterise this platelet-leukocyte interaction by setting up a flow system in which this can be observed and investigated in real-time, under flow.

In this chapter, I present the optimisation of conditions for the analysis of VWF-'primed' platelet-leukocyte interactions, the identification of the platelet receptor and of the leukocyte subsets involved.

4.2. Results

4.2.1. Optimising the conditions required for platelet-leukocyte interactions

Having optimised the flow assay using linear microfluidic channels to enable analysis of VWF-dependent platelet 'priming', I aimed to modify these to explore the interactions between 'primed' platelets and leukocytes. As in the previous chapter, the optimal shear rate for platelet capture to VWF was $1000s^{-1}$ which corresponds to arterial shear, although platelet capture still occurs at lower shear rates. However, at this high shear rate, we did not observe leukocytes interacting with the 'primed' platelets. Therefore, I first flowed blood at $1000s^{-1}$ for 3.5 minutes to capture and 'prime' the platelets. Thereafter, shear was gradually reduced to enable potential leukocyte binding to occur. No leukocytes could be observed at $800s^{-1}$, $500s^{-1}$ or $100s^{-1}$. However, at $50s^{-1}$, leukocytes could be seen rolling over the 'primed' platelets, as illustrated in **Figure 4.1(A)**. Leukocytes (also labelled with $DiOC_6$) were pseudo-coloured in red for visualisation purposes and the number of platelet-leukocyte interactions were quantified as a function of number of leukocytes rolling per minute.

Leukocytes did not bind directly to VWF or A1* in the absence of platelets (data not shown). Moreover, platelets that were captured by an anti-PECAM-1 antibody as opposed to VWF could not recruit leukocytes under the same conditions, confirming the dependency on platelets first being 'primed' by VWF (**Figure 4.1(B)**).

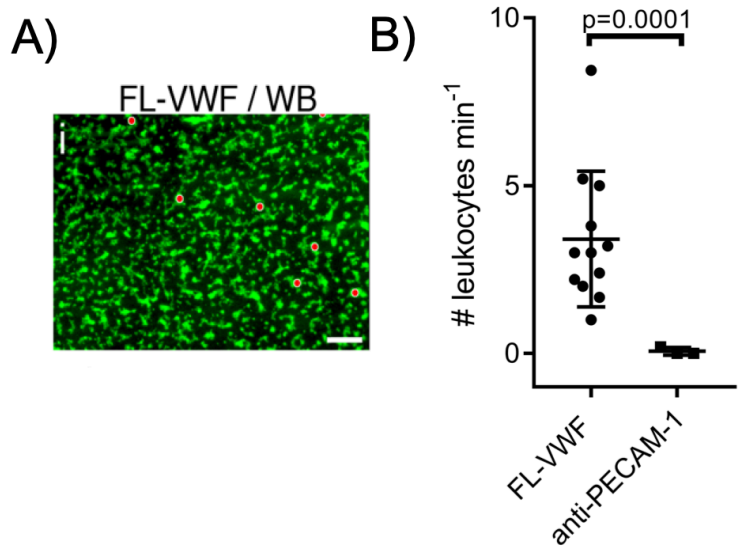

Figure 4.1 Optimisation of the conditions required to observe platelet-leukocyte interactions under flow.

A. Representative image (n=12) depicting platelets ($DiOC_6$, green) captured from whole blood at $1000s^{-1}$ for 3.5 minutes onto microchannel surfaces coated with FL-VWF. Platelets are seen to interact with leukocytes (pseudo-coloured in red for visualisation purposes) at $50s^{-1}$. Scale bar=20μm. B. Graph comparing the number of leukocytes rolling per minute over platelets captured by FL-VWF or anti-PECAM-1. n=12 for FL-VWF and n=3 for anti-PECAM-1. Data were analysed using the unpaired two-tailed Student's t-test. p=0.0001.

4.2.2. Identifying the platelet receptor involved in leukocyte recruitment

As defined in the previous chapter, VWF-'primed' platelets present activated $\alpha_{IIb}\beta_3$ on their surface, but there is no evidence to suggest appreciable amounts of P-selectin also being present. I therefore hypothesised that leukocytes interact with VWF-'primed' platelets in an activated $\alpha_{IIb}\beta_3$-dependent, P-selectin independent manner. The roles of $\alpha_{IIb}\beta_3$, 'outside-in' signalling and P-selectin were evaluated and are presented below.

4.2.2.1. Evaluating the role of 'outside-in' signalling in leukocyte recruitment

VWF-'primed' platelets present activated $\alpha_{IIb}\beta_3$ on their surface, which can bind fibrinogen as suggested by **Figure 4.2**. It is known that fibrinogen binding can initiate 'outside-in' signalling events within platelets, resulting in the further stimulation of platelets [224]. I therefore hypothesised that the 'primed' platelet-leukocyte interactions may be dependent on the consequences of 'outside-in' signalling. To investigate this, I performed experiments under the same conditions (3.5min at $1000s^{-1}$, followed by $50s^{-1}$) using plasma-free blood, as opposed to whole blood, to create fibrinogen-depleted conditions and therefore to minimise the outside-in signalling through activated $\alpha_{IIb}\beta_3$. Surprisingly, as illustrated in **Figure 4.2**, **Figure 4.3(C)** and in **Movie 3**, there was a significant increase (≈2-3-fold) in the number of leukocytes interacting with the 'primed' platelets, suggesting not only that 'outside-in' signalling is not required for leukocyte binding, but also that leukocytes might be competing with a plasma component (such as fibrinogen) to bind the 'primed' platelets.

To further test this contention, I titrated plasma back into plasma-free blood prior to perfusion through FL-VWF or A1*-coated microchannels. As shown by **Figure 4.2**, there was a gradual decrease in the number of platelet-leukocyte interactions with increasing plasma concentrations (0%, 25%, 50%, 100%). Furthermore, adding fibrinogen back into plasma-free blood at a concentration equivalent with 50% of its physiological concentration was associated with a decrease in platelet-leukocyte interactions similar to the effect seen when adding 50% plasma. These data suggest that leukocytes compete with fibrinogen to bind the 'primed' platelets. However, it is important to note that, at normal physiological concentrations of fibrinogen, leukocyte binding is still evident, as these are still seen to interact with the 'primed' platelets.

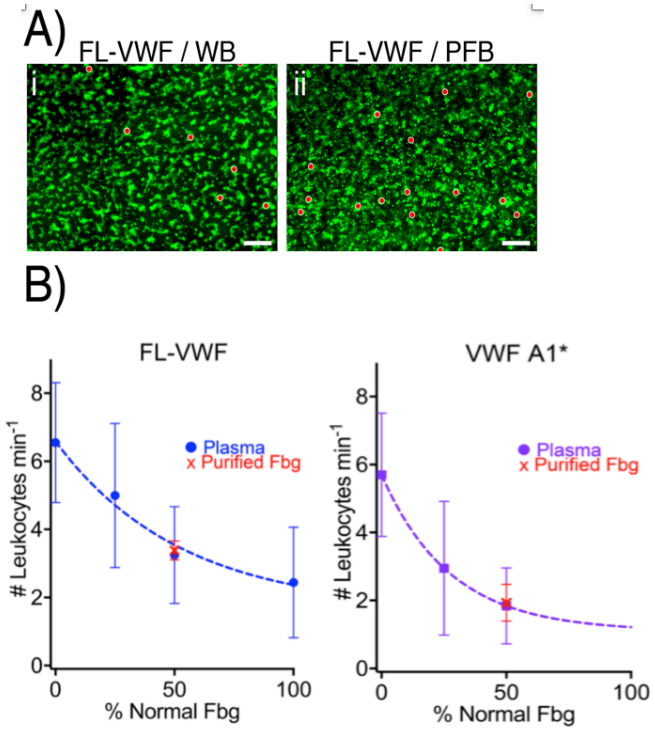

Figure 4.2 Leukocytes compete with plasma in binding 'primed' platelets.

A) Representative images depicting platelets ($DiOC_6$, green) interacting with leukocytes (pseudo-coloured in red). B) Graphs showing a gradual decrease in the number of leukocytes interacting with the platelets captured by FL-VWF (left panel) or A1 (right panel), with increasing plasma concentration. Addition of fibrinogen to 50% of its physiological concentration is highlighted in red. n=3; Data plotted are mean ±SD.*

4.2.2.2. Evaluating the role of activated $\alpha_{IIb}\beta_3$

As leukocytes appeared to compete with fibrinogen for platelet binding, I hypothesised that leukocytes might directly bind to the main fibrinogen receptor on platelets, activated $\alpha_{IIb}\beta_3$. To test this, I incubated both whole blood and plasma-free blood with either Eptifibatide or GR144053, the two RGD peptide mimetics known to inhibit the activated form of $\alpha_{IIb}\beta_3$ prior to perfusion through A1* or FL-VWF-coated channels. As illustrated in **Figure 4.3** and **Movie 3**, both inhibitors significantly reduced the number of platelet-leukocyte interactions, suggesting that the leukocyte interactions do indeed depend upon binding to activated $\alpha_{IIb}\beta_3$.

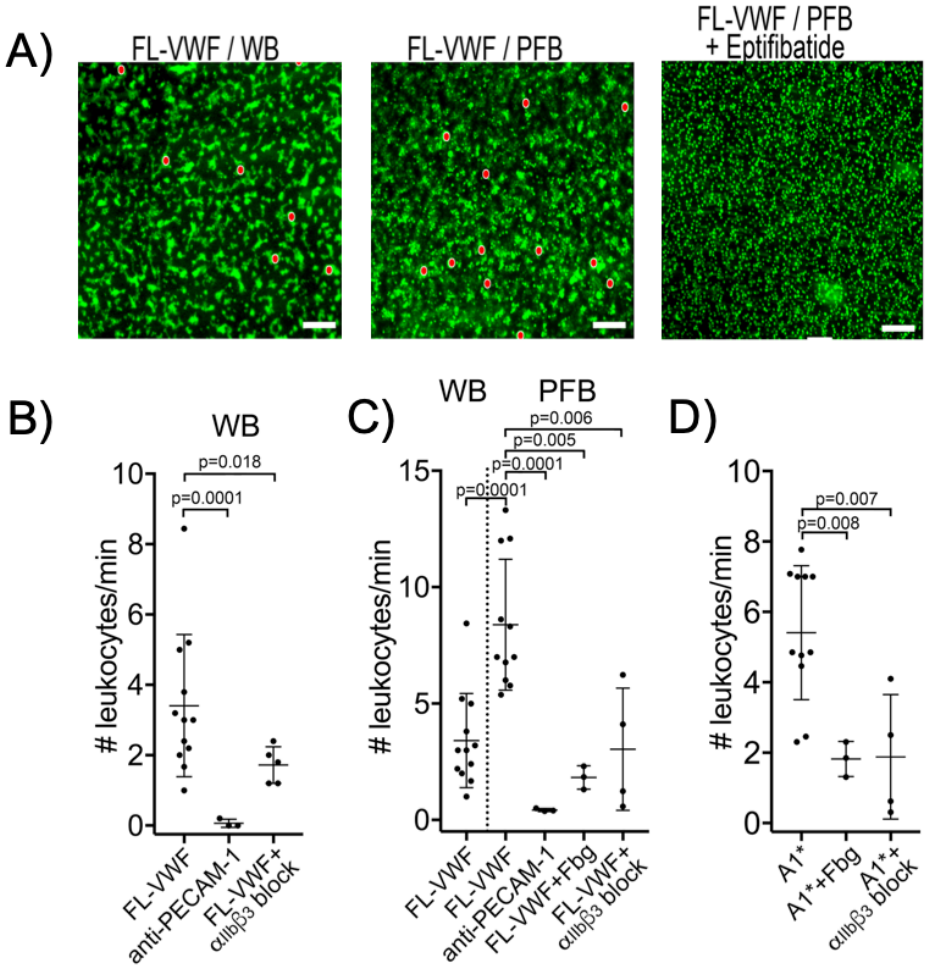

Figure 4.3 Leukocytes interact with 'primed' platelets in an activated $\alpha_{IIb}\beta_3$-dependent manner.

A) Representative images depicting platelets ($DiOC_6$, green) interacting with leukocytes (pseudo-coloured in red). B) Graph of the number of leukocytes/minute in WB interacting with platelets bound to FL-VWF in the absence (n=12) or presence of eptifibatide/GR144053 (n=5) or binding to platelets bound to anti-PECAM-1 antibody (n=3). C) Graph of the number of leukocytes/minute in WB or PFB interacting with platelets bound to FL-VWF in the absence (n=12) or presence of 1.3mg/ml fibrinogen (n=3) or eptifibatide/GR144053 (n=4), or binding to platelets bound to anti-PECAM-1 antibody (n=3). D) Graph of the number of leukocytes/minute in PFB interacting with platelets bound to A1 in the absence (n=11) or presence of fibrinogen (n=3) or eptifibatide/GR144053 (n=4).*

To further investigate whether leukocytes directly bind to activated $\alpha_{IIb}\beta_3$, I coated microchannels directly with the integrin (purified from platelets and commercially available). Two different approaches were used for capturing this integrin to the channel surface and activating it.

First, NHS microchannels were used, which covalently capture proteins by free amine groups. Purified $\alpha_{IIb}\beta_3$ was commercially available and was first dialysed to remove Tris from its storage solution and then captured on the NHS channels as stated in **Methods Section 2.5.1.3**. The concentration of $\alpha_{IIb}\beta_3$ coated onto the channels was titrated (data not shown) and the optimal concentration was established at 2.6μM. Coated $\alpha_{IIb}\beta_3$ was activated by incubating with $MnCl_2$ and $CaCl_2$ as previously reported [171].

The second approach was to coat channels with an anti-β_3 antibody (LIBS2) and then incubate them with $\alpha_{IIb}\beta_3$. LIBS2 is known to be able to induce a conformational change in the $\alpha_{IIb}\beta_3$ structure that mimics its activated state [379].

Channels coated with $\alpha_{IIb}\beta_3$ activated in these two ways were subsequently used in flow assays. Isolated PMBCs or granulocytes were perfused through these channels at $50s^{-1}$ for 15 minutes and monitored in real-time. As illustrated in **Figure 4.4**, cells from both PBMCs and granulocyte preparations bound to these channels. If cells were preincubated with Eptifibatide or GR144053, or with a concentration of fibrinogen equivalent to 50% of its physiological concentration, the number of leukocytes binding was significantly reduced by 70%. Neutrophils did not bind to channels coated with the LIBS2 antibody in the absence of $\alpha_{IIb}\beta_3$ (**Figure 4.4(C)**).

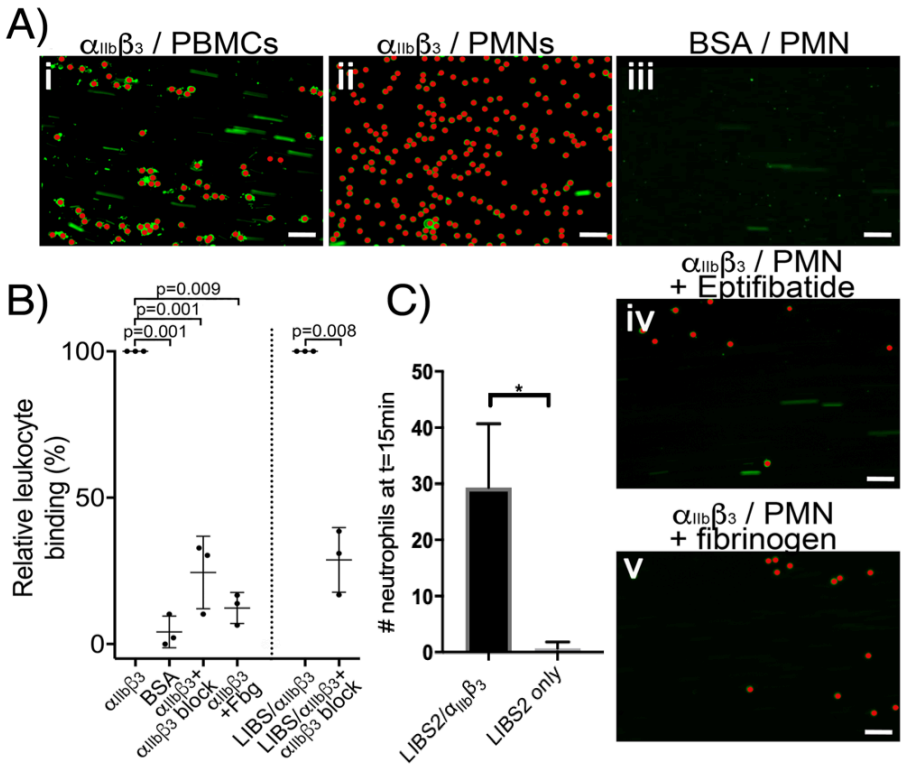

Figure 4.4 Leukocytes interact with activated $\alpha_{IIb}\beta_3$.

A) *Peripheral blood mononuclear cells (PBMCs) (i) or polymorphonuclear cells (PMNs) (ii-v) labelled with $DiOC_6$ were perfused through channels coated with $\alpha_{lib}\beta_3$ in the presence and absence of eptifibatide (iv) or 1.3mg/ml purified fibrinogen (v). Bound leukocytes were pseudo-coloured red to aid visualization. Scale bar=50μm.* ***B)*** *Graphical representation of relative leukocyte binding to $\alpha_{lib}\beta_3$ activated via Mn^{2+} or via incubation with LIBS2, in the presence and absence of eptifibatide or 1.3mg/ml purified fibrinogen, or to BSA after 15 minutes of leukocyte perfusion (n=3).* ***C)*** *Graphical representation of the number of neutrophils bound to channels coated with $\alpha_{lib}\beta_3$ activated with LIBS2 or channels coated with LIBS2 alone after 10 minutes of perfusion at $50s^{-1}$. n=3; Data plotted are mean ±SD. Data were analysed using unpaired, two-tailed Student's t test.*

Additional experiments demonstrating the ability of leukocytes to bind activated $\alpha_{lib}\beta_3$ were performed using anti-PECAM-1 coated channels. Platelets captured by anti-PECAM-1 antibody were unable to recruit leukocytes at low shear as previously shown, but acquired the ability to do so after being incubated with the LIBS2 antibody, which activated $\alpha_{lib}\beta_3$ (**Figure 4.5**). The interactions acquired following LIBS2 incubation were reduced in the presence of Eptifibatide, confirming their dependency on activated $\alpha_{lib}\beta_3$.

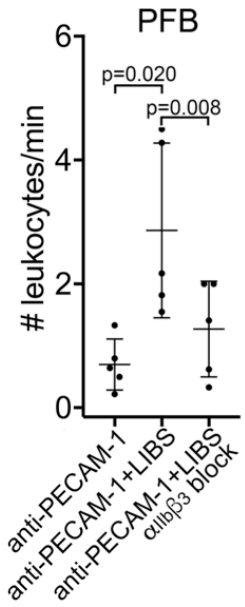

Figure 4.5 Leukocytes interact with $\alpha_{IIb}\beta_3$ activated by LIBS2.

Platelets were captured by an anti-PECAM-1 antibody and incubated with LIBS2 to induce $\alpha_{IIb}\beta_3$ activation. Thereafter, leukocytes were perfused at low shear and binding was quantified as number of leukocytes rolling per minute, in the presence or absence of LIBS2, with or without an $\alpha_{IIb}\beta_3$ blocker. Data were analysed using unpaired, two-tailed Student's t test. n=3; Data plotted are mean ±SD.

The ability of LIBS2 to activate $\alpha_{IIb}\beta_3$ on the anti-PECAM-1-captured platelets was confirmed by confocal microscopy, in images showing that fluorescent fibrinogen binds platelets incubated with the LIBS2 antibody, in a manner that can be inhibited by GR144053, as shown below (**Figure 4.6**).

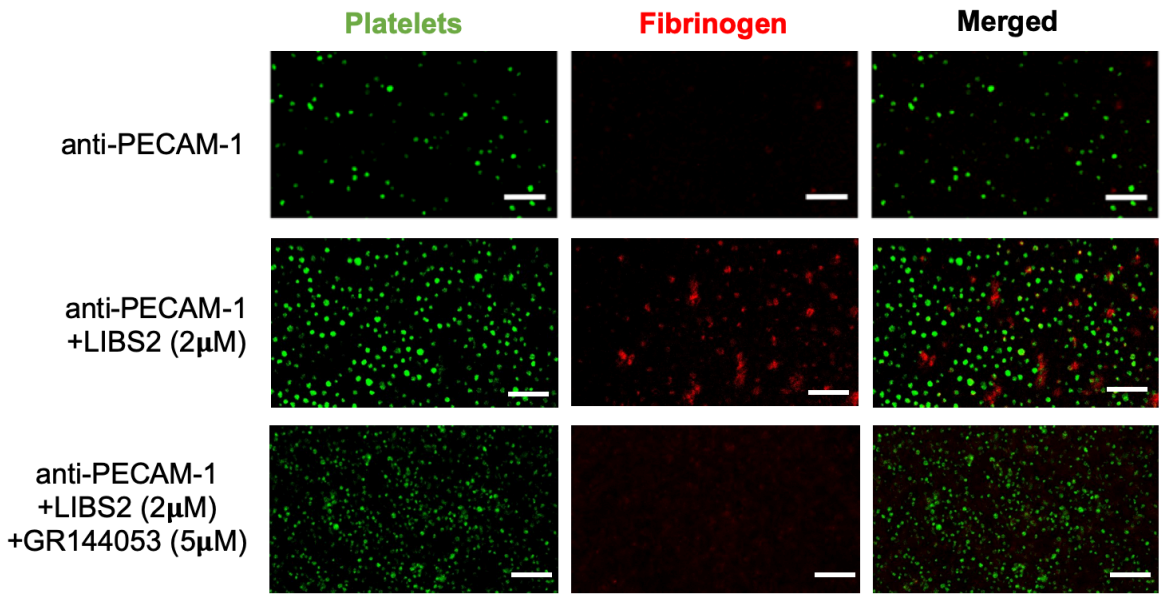

Figure 4.6 Confirmation of $\alpha_{IIb}\beta_3$ activation following platelet incubation with anti-LIBS2.

Representative images (n=3) depicting platelets ($DiOC_6$, green) captured from plasma-free blood at $1000s^{-1}$ for 3.5 minutes onto microchannel surfaces coated with anti-PECAM-1. Plasma-free blood was supplemented with fibrinogen-Alexa647 (red). Merged images show fluorescent fibrinogen attached to the platelets captured by anti-PECAM-1 only in the presence of anti-LIBS2, and not when adding GR144053. Scale bar=20μm.

4.2.2.3. Evaluating the role of P-selectin

As the best characterised interaction between platelets and leukocytes occurs via the P-selectin-PSGL-1 axis,[346] I performed experiments in the presence of a P-selectin blocker. As illustrated in **Figure 4.7(A-B)**, there was no reduction in the number of leukocytes interacting with VWF-'primed' platelets in the presence of the P-selectin blocker, in either whole blood or plasma-free blood conditions.

However, although the P-selectin blocker had no impact upon the number of leukocyte interactions with VWF-'primed' platelets, there was an increase in the leukocyte rolling velocity in the presence of the P-selectin blocker (**Figure 4.7(C)** and **Movie 3**), suggesting that, although P-selectin may not be required for the initial interaction with leukocytes, it may play a role in stabilising the platelet-leukocyte interactions in these conditions.

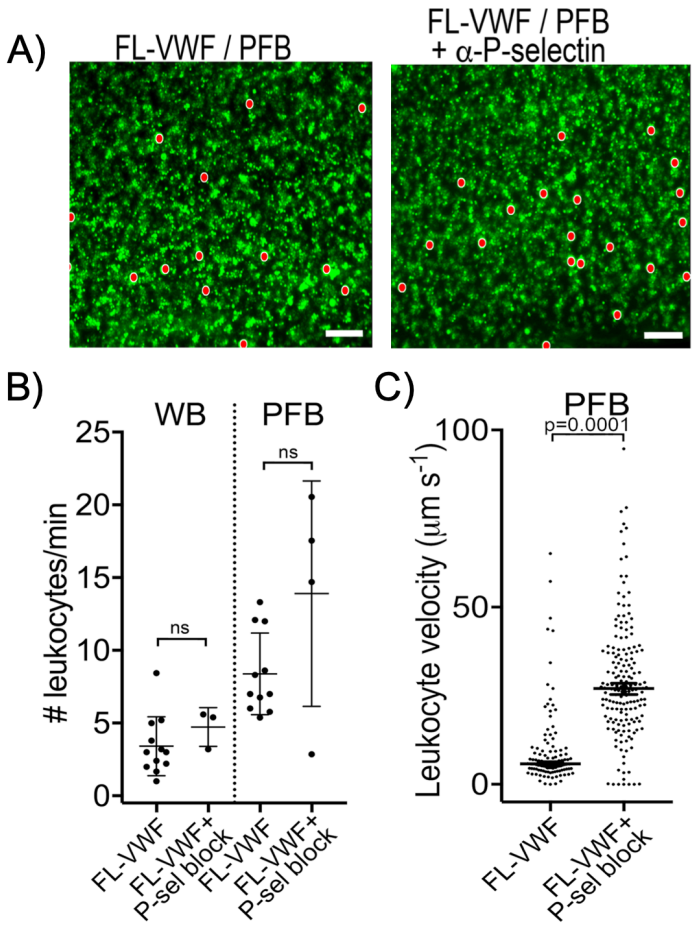

Figure 4.7 Leukocytes interact with VWF-'primed' platelets independently of P-selectin.

A) Representative images depicting platelets (green) captured by FL-VWF, interacting with leukocytes (pseudo-coloured in red) in plasma-free blood conditions. B) Graphical representation of the number of leukocytes rolling per minute on platelets from whole blood or plasma-free blood, in the presence or absence of a P-selectin blocker. C) Graphical representation of the leukocyte velocity when rolling on VWF-'primed' platelets, in the presence or absence of a P-selectin blocker. n=121 and 178 leukocytes respectively, from 4 different experiments. Data plotted are mean ±SD. Data were analysed using unpaired, two-tailed Student's t test.

To test the ability of the P-selectin blocker to efficiently inhibit P-selectin, channels were coated with collagen, a potent platelet agonist that is known for inducing platelet degranulation and P-selectin exposure. Using the P-selectin blocker under these conditions led to a significant reduction in the number of leukocytes binding to platelets compared to the control, confirming the efficacy of the P-selectin blocker (**Figure 4.8**). However, it is important to note that this did not completely block leukocyte interactions.

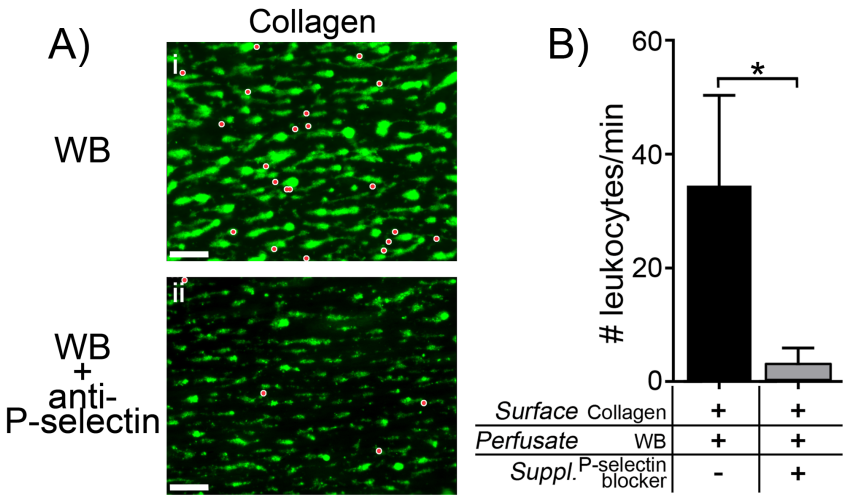

Figure 4.8 Antibody-mediated blockade of P-selectin diminishes leukocyte binding to collagen captured platelets.

A) Whole blood (WB), labelled with $DiOC_6$ was perfused over collagen microchannels at $1000s^{-1}$ for 3.5 minutes. Thereafter, the shear rate was reduced to $50s^{-1}$ to monitor leukocyte interactions. (i) Representative image (n=3) shown after 5 minutes platelets (green) and leukocytes (pseudo-colored red). (ii) as in (i) except WB was supplemented with a blocking anti-P-selectin antibody (AK-4 clone). Scale bar=50μm. B) Graphical representation of the mean number of leukocytes binding per minute. Data were analysed using the unpaired, two-tailed Student's t test, $p<0.05$ (*). Data plotted are mean ±SD.

4.2.3. Identifying the leukocyte subset

Having identified activated $\alpha_{IIb}\beta_3$ as the platelet receptor capable of recruiting leukocytes under flow, I endeavoured to identify the leukocyte subset(s) involved in the interaction, as cells from both PBMCs and granulocytes bound these platelets or activated $\alpha_{IIb}\beta_3$ (**Figure 4.4(A)**). Initially, whole blood was pre-incubated with subset-specific antibodies and flow assays were monitored in real-time using fluorescent microscopy. However, fluorescent detection of leukocytes was poor, possibly due to the low sensitivity of the widefield fluorescent microscope. Therefore, experiments were repeated using confocal microscopy in an attempt to improve fluorophore detection. A similar issue was initially encountered, potentially due to the abundance of the red blood cells in whole blood and plasma-free blood that may quench the fluorescent signal. Therefore, the experimental setup was changed to avoid using the subset-specific antibodies in the presence of red blood cells. Whole blood or plasma-free blood was perfused through channels coated with VWF or VWF A1* at high shear for 3.5min

to first capture a layer of platelets, and channels were then washed with 1x HT to remove the red blood cells. Following that, isolated PBMCs or granulocytes incubated with subset-specific antibodies were perfused through these channels at low shear for 10 minutes. In separate experiments, PBMCs and granulocytes were also perfused through channels coated with activated $\alpha_{IIb}\beta_3$ as before. PBMCs were pre-incubated with anti-CD14 to identify classical monocytes, anti-CD3 to identify T cells, anti-CD19 to identify B cells and anti-CD16 to identify non-classical monocytes. Granulocytes were labelled with an anti-CD16 antibody that stained neutrophils. All isolated leukocytes were also pre-incubated with Hoechst dye, to visualise their nuclei.

PBMCs stained with anti-CD14 (monocytes) did not bind VWF-'primed' platelets or activated $\alpha_{IIb}\beta_3$. Importantly, successful staining of the monocytes with anti-CD14 conjugated to four different fluorophores (APC, FITC, PB and PE) was observed when the flow was stopped, confirming antibody binding. Similarly, PBMCs stained with CD19-APC or CD16-APC could be observed under static conditions but failed to bind under flow (data not shown). These data suggest that neither monocytes (either classical or non-classical) nor B cells interact with $\alpha_{IIb}\beta_3$. However, PBMCs stained with anti-CD3-APC were seen to bind to both VWF-'primed' platelets and to activated $\alpha_{IIb}\beta_3$ (**Figure 4.9(A-B)**), indicating that T cells represent a subset of leukocytes in PBMCs interacting with the 'primed' platelets. Similarly, granulocytes stained with anti-CD16-APC or anti-CD16-FITC also interacted with both VWF-'primed' platelets and activated $\alpha_{IIb}\beta_3$ (**Figure 4.9(C-D)**). Given the lobular structure of the nuclei as indicated by the Hoechst staining, and their positivity for CD16, it can be deduced that neutrophils also interact with activated $\alpha_{IIb}\beta_3$.

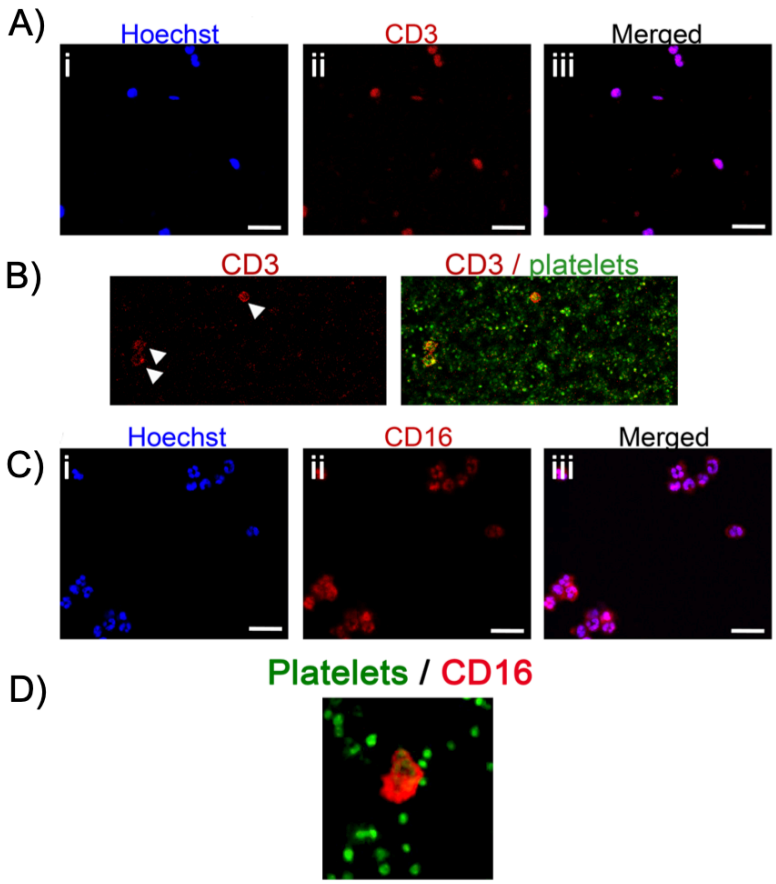

Figure 4.9 T cells and neutrophils interact with activated $\alpha_{IIb}\beta_3$.

A) *PBMCs stained with Hoechst dye (i - blue), anti-CD3 (ii - red) and merged (iii).* ***B)*** *PBMCs stained with anti-CD3 (red) perfused over VWF-captured platelets (green).* ***C)*** *PMNs stained with Hoechst dye (i - blue), anti-CD16 (ii - red) and merged (iii).* ***D)*** *Images depicting a neutrophil stained with anti-CD16 (red) bound to 'primed' platelets stained with DiOC6 (green). Representative of n=4. Scale bar=20μm.*

4.3. Discussion

The aim of this chapter was to investigate the interaction between VWF-'primed' platelets and leukocytes under flow, the conditions under which these interactions occur, the platelet receptor and the subset of leukocytes involved. The rationale for investigating a potential VWF-'primed' platelet-leukocyte interaction was based on a study published in 2015, which revealed that, under flow, platelets captured by VWF can subsequently recruit leukocytes *in vitro* [85]. As concluded from Results Chapter 1 of this thesis, VWF induces signalling events within platelets, without fully activating them. My results show that VWF 'primes' platelets, leading to Ca^{2+} release and activation of integrin $\alpha_{IIb}\beta_3$, but provide no evidence of appreciable degranulation and subsequent P-selectin exposure, distinguishing 'primed' platelets from activated platelets. As previously characterised platelet-leukocyte interactions require platelets to have undergone degranulation [344-346], I hypothesised that VWF-'primed' platelets are able to recruit leukocytes via a previously uncharacterised interaction.

To test this contention, I first optimised the conditions required to observe platelet-leukocyte interactions under flow. At high shear, leukocytes did not interact with 'primed' platelets. However, under these conditions, collagen-captured platelets were also unable to recruit leukocytes, despite being fully activated (data not shown). This is not surprising considering that linear channels were used, with laminar, constant shear, and, possibly due to their size, leukocytes cannot withstand the forces to bind platelets. Previous literature analysing platelet-leukocyte interactions under flow *in vitro* is in line with these findings, using venous shear rates to observe these. Although some studies performed *in vivo* show leukocytes being recruited on arterial thrombi after 4/5 min at high shear [350], it is possible that the presence of endothelium, as well as the absence of an anticoagulant play an important role under these conditions compared to experiments done *in vitro*. Therefore, after capturing and 'priming' the platelets at $1000s^{-1}$ for 3.5 minutes, I reduced the shear rate to $50s^{-1}$, at which point leukocytes could be seen to roll over the carpet of VWF-'primed' platelets. However, flowing the blood at

high shear first followed by low shear is not physiological and does not reflect the distorted and branched vasculature, in which there is a constant interplay between laminar and disturbed or even turbulent flow, which can be generated around bifurcations or venous valves. In an attempt to mimic these conditions better, I used channels with varying geometries, presenting bifurcations (**Figure 4.10**) and coated these with VWF. Instead of perfusing blood at high shear followed by low shear, a shear rate of $50s^{-1}$ was used throughout the experiment. However, blood was drawn through three different channel inlets, in an attempt to generate slightly disturbed flow at the bifurcation site. Under these conditions, there was a uniform platelet coverage with subsequent aggregation across the channel. Leukocytes were seen to roll over these platelets and to bind, in a manner that could be inhibited by Eptifibatide, which is in line with my findings from linear channels. The number of aggregates and rolling leukocytes was greatly enhanced at bifurcation sites and, importantly, the aggregates developed around the bound leukocytes. These results imply that VWF can 'prime' platelets and mediate leukocyte recruitment under venous shear as well. This is in contrast with the classical understanding of VWF, which limits its function to arterial shear settings. This is primarily due to the use of uniform linear channels. The importance of VWF-platelet binding at venous shear is highlighted by more recent studies that identify VWF as a key player in the development of experimental DVT [271,272]. Future experiments aiming to investigate this further may be achieved using microchannels that more closely mirror the venous system. Custom-made channels mimicking venous valves were developed in collaboration with the Bioengineering Department at Imperial College London. I performed preliminary experiments using these channels and results suggest higher platelet-dependent leukocyte accumulation around valves (data not shown), but these assays, together with the channel geometries and valve mobility require further optimisation.

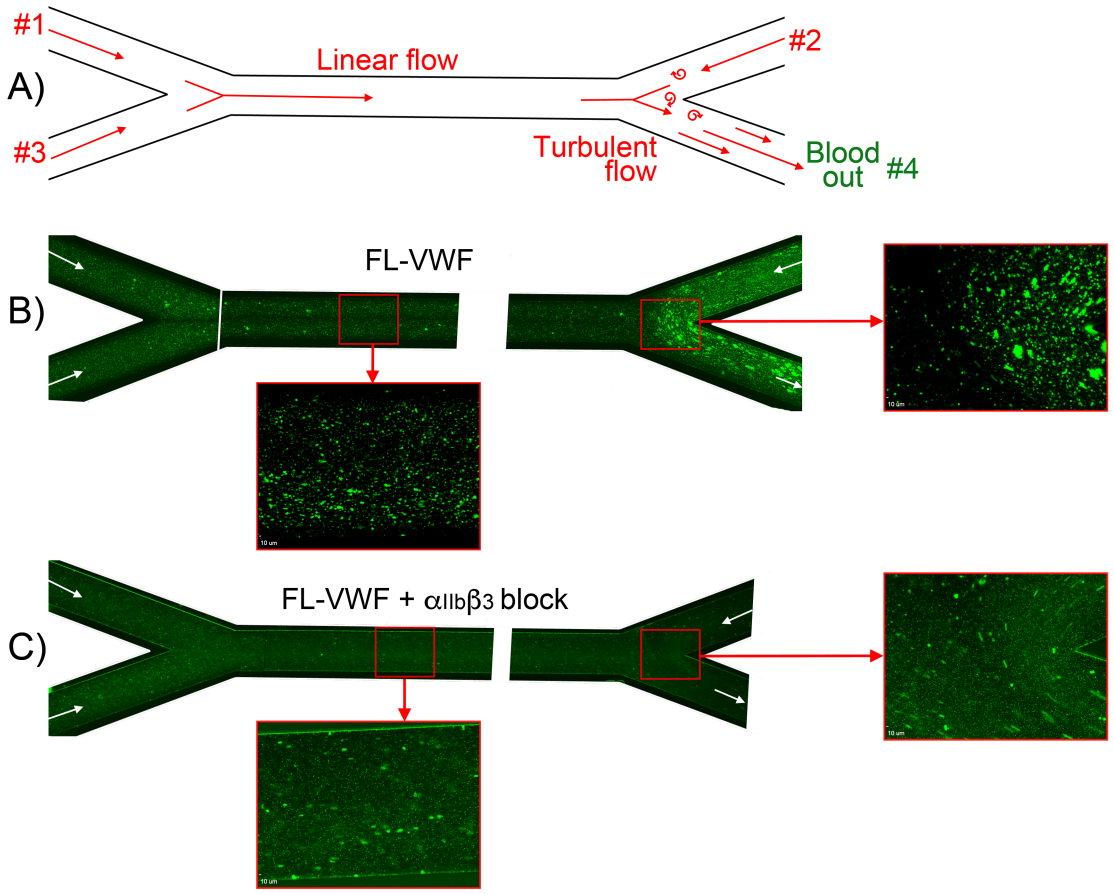

Figure 4.10 Analysis of platelet binding to FL-VWF under low/turbulent flow and subsequent leukocyte recruitment.

A) Schematic representation of blood flow through bifurcated channels. Blood is drawn through inlets #1, #2 and #3, and out through outlet #4. For much of the channels, the flow is linear, with particular exception to the bifurcation site on the right where turbulent flow exists due to convergence of flows. B) Channels were coated with FL-VWF and whole blood labelled with DiOC6 was perfused through channels as in A), and as denoted by arrows, at an exit shear rate of $50s^{-1}$. At this low shear rate, platelets can be seen binding to the channel surface to which leukocytes (larger cells also stained in green) also bind. Although this is evident in the linear part of the channel (inset), at the site of most turbulent flow increased platelet and leukocyte binding was observed. C) As in B) except GR144053 was added to block $\alpha_{IIb}\beta_3$. Blocking $\alpha_{IIb}\beta_3$ inhibited the majority of leukocyte binding to platelets (the majority of those observed are in transit). However, in the absence of leukocyte binding the binding of platelets to the VWF surface under low flow can be more clearly observed in both the linear and turbulent flow areas.

Platelets captured by an anti-PECAM-1 antibody, which binds but does not induce signalling/'priming' within platelets, were unable to recruit leukocytes under the same conditions, confirming the dependency of leukocyte binding on prior VWF-dependent 'priming' of the platelets. Moreover, isolated leukocytes perfused through VWF or A1*-coated channels

in the absence of platelets failed to bind, confirming that the interaction occurs between platelets and leukocytes rather than between VWF/A1* and leukocytes.

Given the presence of activated $\alpha_{IIb}\beta_3$ on VWF-'primed' platelets, I hypothesised that 'outside-in' signalling induced by fibrinogen binding is responsible for the subsequent platelet-leukocyte interactions. Unexpectedly, performing the same experiments using plasma-free blood revealed a significant increase in the number of leukocytes interacting with the 'primed' platelets. This decreased gradually with the addition of increasing concentrations of plasma or fibrinogen back, suggesting that leukocytes compete with fibrinogen to bind the 'primed' platelets. This result provides further evidence that VWF-'primed' platelets interact with leukocytes through a previously uncharacterised mechanism. Previous studies identified fibrinogen as being a bridging protein between activated platelets and activated leukocytes. Specifically, fibrinogen has been shown to have the ability to bind both activated $\alpha_{IIb}\beta_3$ on the platelet surface and activated Mac-1 on the leukocyte surface [184,349]. If this were to be the case between VWF-'primed' platelets and leukocytes, a decrease in the number of interactions would be expected when depleting fibrinogen. The competition between leukocytes and fibrinogen to bind the 'primed' platelets led to the hypothesis that leukocytes directly bind the main platelet receptor for fibrinogen - activated $\alpha_{IIb}\beta_3$.

This hypothesis is supported by different lines of evidence presented in this chapter. First, pre-incubating whole blood and plasma-free blood with Eptifibatide or GR144053, two inhibitors of activated $\alpha_{IIb}\beta_3$, induced a significant decrease in the number of platelet-leukocyte interactions. Secondly, channels coated directly with activated $\alpha_{IIb}\beta_3$ bound isolated leukocytes in a manner that could be inhibited by $\alpha_{IIb}\beta_3$ inhibitors or by addition of fibrinogen. Furthermore, platelets captured by an anti-PECAM-1 antibody and incubated with LIBS2, an antibody that induces a conformational change in $\alpha_{IIb}\beta_3$ and activates it, acquired the ability to recruit leukocytes under flow. The fact that leukocytes compete with fibrinogen and that their

binding can be blocked by Eptifibatide or GR144053 provide scope to assume that leukocytes interact with activated $\alpha_{IIb}\beta_3$ in a manner that is dependent on its RGD-binding groove.

$\alpha_{IIb}\beta_3$ is a heterodimeric protein, with the α_{IIb} and β_3 subunits non-covalently linked. The two subunits are encoded by the *ITGA2B* and *ITGB3* genes, respectively. Mutations in either of these genes result in qualitative or quantitative defects with this integrin, all known as Glanzmann's thrombasthenia (GT) [173,174]. To further test the contention that leukocytes directly interact with $\alpha_{IIb}\beta_3$, I also performed experiments using blood donated by three patients suffering from GT (data not shown). However, the data obtained was rather inconclusive. Interestingly, despite our hypothesis that VWF-captured platelets from GT patients would be unable to recruit leukocytes due to the lack of $\alpha_{IIb}\beta_3$, there was a high number of leukocytes seen to interact with these platelets. However, a recent clinical study suggests that platelets from GT patients more readily express P-selectin on their surface in response to Ristocetin [380]. Ristocetin is known for unravelling VWF and aiding platelet binding via its A1 domain. Therefore, it could be hypothesised that GT platelets develop a compensatory mechanism for their lack of $\alpha_{IIb}\beta_3$ and, therefore, more easily degranulate and can interact with leukocytes in a P-selectin-dependent manner. Further experiments pre-incubating blood from GT patients with a P-selectin blocker should be performed to test this theory. This is, however, technically challenging given the small number of GT patients and the necessity to perform the experiments immediately after collecting blood.

Experiments using a blocking anti-P-selectin antibody were performed using blood collected from healthy human volunteers. Incubating platelets captured by VWF from either whole blood or plasma-free blood with a P-selectin blocker did not result in significant changes in the number of 'primed' platelet-leukocyte interactions. This opposed the results obtained when platelets captured by collagen were incubated with the P-selectin blocker. Collagen is a known potent platelets agonist that induces P-selectin exposure [5]. Under these conditions, the number of leukocytes binding was severely reduced. Interestingly, despite the high

concentration of the anti-P-selectin blocking antibody, leukocyte binding was not completely abolished, suggesting potential for additional interactions. Collagen-captured platelets undergo not only degranulation, but also activation of $\alpha_{IIb}\beta_3$. Therefore, the remaining platelet-leukocyte interactions could be mediated via activated $\alpha_{IIb}\beta_3$. Further experiments using Eptifibatide in conjunction with the P-selectin blocker were performed, in an attempt to analyse whether there is a synergistic effect in blocking the interaction between activated platelets and leukocytes under flow. However, although the number of leukocytes binding seemed to be reduced further with the addition of Eptifibatide, the data remained inconclusive due to variability between channels. Additional experiments titrating the concentrations of both Eptifibatide and the P-selectin blocker should be performed to assess this.

Despite the lack of effect upon the number of platelet-leukocyte interactions, the blockade of P-selectin induced an increase in leukocyte rolling velocity. This suggests that, although the levels of P-selectin on VWF-'primed' platelets are too low to facilitate leukocyte recruitment, they might augment leukocyte stable adhesion following their initial interaction with activated $\alpha_{IIb}\beta_3$. P-selectin is also expressed on endothelial cells, following release of Weibel-Palade bodies and is known to bind circulating leukocytes and promote their extravasation [381]. However, this interaction likely requires additional receptors/molecules to be present, otherwise leukocytes would constantly bind to the endothelium and extravasate.

After establishing that leukocytes interact with activated $\alpha_{IIb}\beta_3$, I aimed to identify the leukocyte subset involved. Previous studies identify monocytes and neutrophils as the major subsets that have the ability to bind platelets. Platelet-monocyte aggregates are recognised as a marker for atherosclerosis, heart failure and also infections [354,364,382]. Similarly, platelet-neutrophil interactions have been shown to play key roles in the setting of infection and inflammation, particularly in DVT [312,353,356]. Through their interactions with leukocytes, platelets have recently been classified as immune cells, for their key contribution to the settings of infection and inflammation [122,123,265].

Contrary to previous literature that identified monocytes and neutrophils as being the main types of leukocytes interacting with platelets, my results reveal that neutrophils and T cells interact with the 'primed' platelets and bind to activated $\alpha_{IIb}\beta_3$, whereas monocytes and B cells do not. Whereas the role of platelet-neutrophil interactions has been well established, there are few studies investigating the cross-talk between platelets and T cells. Recent work identified interactions between platelets and T cells in the setting of hepatic viral infections. In this case, CD8+ cytotoxic T cells were the major T cell subtype binding to platelet aggregates. [383]. I endeavoured to determine whether CD8+ T cells were the T cell subtype involved in the interaction with VWF-'primed' platelets. Experiments were performed using confocal microscopy for real-time imaging of CD4+ (helper T cells), CD8+ (cytotoxic T cells) or CD56+ (NK T cells) perfused on activated $\alpha_{IIb}\beta_3$-coated channels. Although experiments require further optimisation, it appeared that the majority of T cells binding to activated $\alpha_{IIb}\beta_3$ were represented by CD4+ T cells, with CD8+ T cells also being able to bind.

Several lines of evidence presented in this chapter support the hypothesis that the interaction between VWF-'primed' platelets and neutrophils/T cells occurs via a novel mechanism, that perhaps involves an unknown leukocyte receptor:

1. Leukocytes directly bind to activated $\alpha_{IIb}\beta_3$ both on VWF-'primed' platelets and on channels directly coated with activated $\alpha_{IIb}\beta_3$, in the absence of any other platelet receptor or chemokines.

2. Leukocytes compete with fibrinogen to bind the 'primed' platelets, excluding a bridging role for fibrinogen via the activated $\alpha_{IIb}\beta_3$-activated Mac-1 axis.

3. P-selectin blockade does not influence the number of platelet-leukocyte interactions, excluding a role for the P-selectin-PSGL-1 axis in the initial binding of leukocytes.

4. Leukocyte subset specificity (neutrophils and T cells, as opposed to monocytes and B cells) suggest a subset-specific receptor; the expression levels of PSGL-1 (the main P-selectin

receptor), CD40 and integrins such as Mac-1 and LFA-1 do not appreciably vary across the different leukocyte subtypes [343].

Increasing evidence that platelet-leukocyte interactions can also occur independently of P-selectin via yet unknown mechanisms is also presented by recent literature. Guidotti *et al* investigated the interactions between hepatic intrasinusoidal platelet aggregates and T cells in a viral infection model and revealed that these happen independently of both P-selectin and CD40L [383]. Moreover, murine models of infection or ischemia-reperfusion injury demonstrate that neutrophil recruitment and extravasation are dependent on VWF, GPIbα and platelets, but independent of P-selectin [384,385] and refer to an "unknown" receptor on the platelet surface [359]. There is, therefore, scope to believe that there is an important platelet-leukocyte interaction yet to be uncovered and understood. The next chapter focuses on further understanding the implications of this novel interaction by investigating the effect of VWF-'primed' platelets on leukocyte phenotype.

5. Chapter 3 – Investigating the ability of VWF-'primed' platelets to modulate neutrophil phenotype and induce NETosis

5.1. Introduction

Results presented in **Chapters 1 and 2** led me to propose that VWF-bound platelets become 'primed' rather than activated. I also demonstrated that neutrophils and T cells directly bind to activated $\alpha_{IIb}\beta_3$. However, to understand the physiological significance of this interaction and further characterise it, it was important to establish whether VWF-'primed' platelets are involved solely in the recruitment of leukocytes, or whether they are able to also transduce a signal within them. I focussed on identifying the effect of VWF-'primed' platelets on neutrophil phenotype.

Platelet-neutrophil interactions have been defined in a variety of pathophysiological settings. Neutrophils fulfil a crucial role in the innate immune response [308,318], but, more recently, it has emerged that this neutrophil function is further aided through interactions with platelets. This finding has led to the further classification of platelets as immune cells [122,265]. However, apart from their beneficial role in bacterial clearance, platelet-neutrophil interactions have also been identified as markers for different cardiovascular pathologies, particularly atherosclerosis, stroke or DVT [123,271-273,312,360].

As innate immune cells [308], neutrophils are generally the first cells recruited to sites of infection, where they recognise a wide variety of pathogens, including bacteria, fungi and protozoa [318,323,324]. Given their role in immunity, neutropenia and loss of neutrophil function have both been associated with risks of severe, life-threatening bacterial infections [310,311]. After recognising the infectious agent, neutrophils employ different mechanisms to clear pathogens. These include phagocytosis, release of toxic granule contents, production of reactive oxygen species and, importantly for the purpose of this thesis, release of NETs [304,315,316,318].

First described in 2004, NETs represent extracellular mesh-like structures consisting of DNA and toxic granule contents that can entrap and kill microorganisms [318]. The release of NETs, termed NETosis, has initially been described as a 'suicidal' process, given that the extrusion of NETs was thought to exclusively occur as a result of plasma membrane disruption.

However, more recent work has introduced the concept of 'vital' NETosis, in which neutrophils release NETs through vesicles, maintaining their plasma membrane intact and, in this way, preserving their phagocytic and chemotactic functions following NETosis [320,326,327].

Despite their well-established beneficial role in clearing pathogens and contributing to innate immune responses, NETs have been defined as 'double-edged swords' [319]. The reason for this is represented by the involvement of NETs in various pathological conditions, such as autoimmune disorders, pre-eclampsia, sepsis and DVT [321,334-338,386]. This is because NETs do not only trap pathogens and exhibit cytotoxic effects on invading cells but can also be cytotoxic to host cells and are highly thrombogenic within the vasculature.

The involvement of neutrophils in the development of DVT has been demonstrated in various studies showing that depletion of neutrophils has a thrombo-protective effect. Neutrophil contribution to DVT is mainly attributed to the release of NETs. Intravascular NETs are known to be highly thrombogenic, aiding thrombus formation and stability by sequestering red blood cells and platelets, binding plasma proteins and initiating the intrinsic coagulation cascade. Consistent with this, treatment with DNase I, which degrades NETs, appreciably diminishes thrombus formation in experimental DVT models [272]. However, although it is widely accepted that neutrophils contribute to DVT through NETs, it remains unclear what drives NETosis in the first place, considering that DVT generally occurs in the absence of any pathogens that would activate neutrophils and trigger this process. Recent studies identify platelets as mediators of NETosis, through their interactions with neutrophils within the vasculature [272,362].

Indeed, the ability of platelets to induce NETosis has attracted an increasing research interest recently. The contribution of platelets to NET release is thought to be highly dependent on their granule release, with subsequent roles for HMGB2, PF4, RANTES to the process of NETosis described [387,388]. However, initial events responsible for platelet-mediated NETosis are unclear. It was initially reported that platelet-induced NET release is dependent on prior P-selectin exposure by platelets [325], but more recent studies show that LPS-stimulated

platelets can also lead to NET formation independently of P-selectin [282,389]. Moreover, within liver sinusoids, platelets were shown to promote NETosis via an “unknown” receptor that is not P-selectin [359].

In light of these findings and the results presented in **Chapter 2**, I hypothesised that the interaction between activated $\alpha_{IIb}\beta_3$ on VWF-‘primed’ platelets and neutrophils leads to phenotypic changes within neutrophils, culminating with NETosis. Chapter 3 explores this hypothesis in an attempt to provide further mechanistic insights into platelet-mediated NET formation and outline the importance of this interaction.

5.2. Results

5.2.1. VWF-‘primed’ platelets induce phenotypic changes within neutrophils

After identifying a novel interaction between VWF-‘primed’ platelets and neutrophils, I aimed to investigate the pathophysiological importance of these findings by exploring the neutrophil phenotype following their interaction with the ‘primed’ platelets. As illustrated in **Figure 5.1** and in **Movie 4**, after binding to the VWF-‘primed’ platelets, neutrophils appear to be patrolling and trying to spread, extending pseudopodia. Importantly, if neutrophils are directly captured by activated $\alpha_{IIb}\beta_3$ they undergo similar phenotypic changes, including migration against flow (**Movie 4**). As this occurs in the absence of other platelet receptors or chemokines, it can be hypothesised that $\alpha_{IIb}\beta_3$ can itself induce signalling within neutrophils.

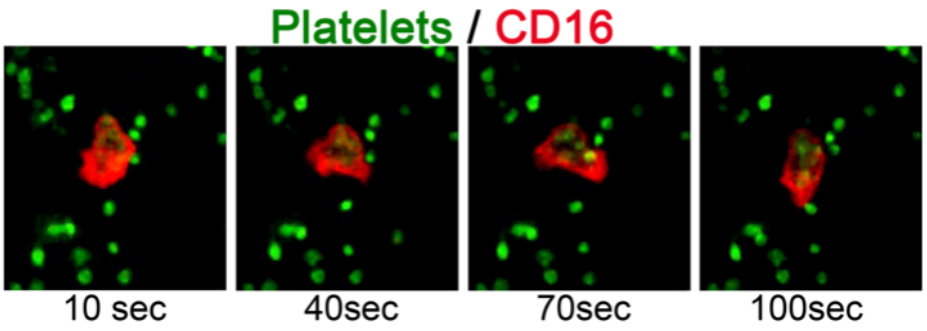

Figure 5.1 VWF-'primed' platelets induce phenotypic changes in neutrophils binding.

Images depicting a neutrophil stained with anti-CD16-APC (red) 'scanning' the 'primed' platelets stained with $DiOC_6$ (green). Images were taken 10, 40, 70 and 100 seconds after neutrophil attachment and show the movement of the bound neutrophil. Representative of n=15.

5.2.2. VWF-'primed' platelets induce Ca^{2+} signalling within neutrophils

To investigate the phenotypic changes that neutrophils undergo following their interaction with VWF-'primed' platelets and activated $\alpha_{IIb}\beta_3$ further, I performed Ca^{2+} assays under flow. Neutrophils were pre-loaded with Fluo-4 AM prior to being perfused over VWF-'primed' platelets or activated $\alpha_{IIb}\beta_3$ at low shear. As a control, neutrophils were perfused over channels coated with an anti-CD16 antibody. Neutrophils were monitored for 10 minutes after binding.

As shown in **Figure 5.2** and **Movie 5**, neutrophils captured by VWF-'primed' platelets or activated $\alpha_{IIb}\beta_3$ undergo intracellular Ca^{2+} signalling, which reaches a maximum after 200-300 seconds. There was no significant difference between the time required for this event to occur in the two conditions (**Figure 5.2(C)**). In contrast, neutrophils captured by anti-CD16 did not exhibit any change in fluorescence, indicating that these do not undergo Ca^{2+} signalling (**Figure 5.2(B)**). This provides real-time evidence of the activation of intra-neutrophil signalling pathways following interaction with activated $\alpha_{IIb}\beta_3$ on platelets.

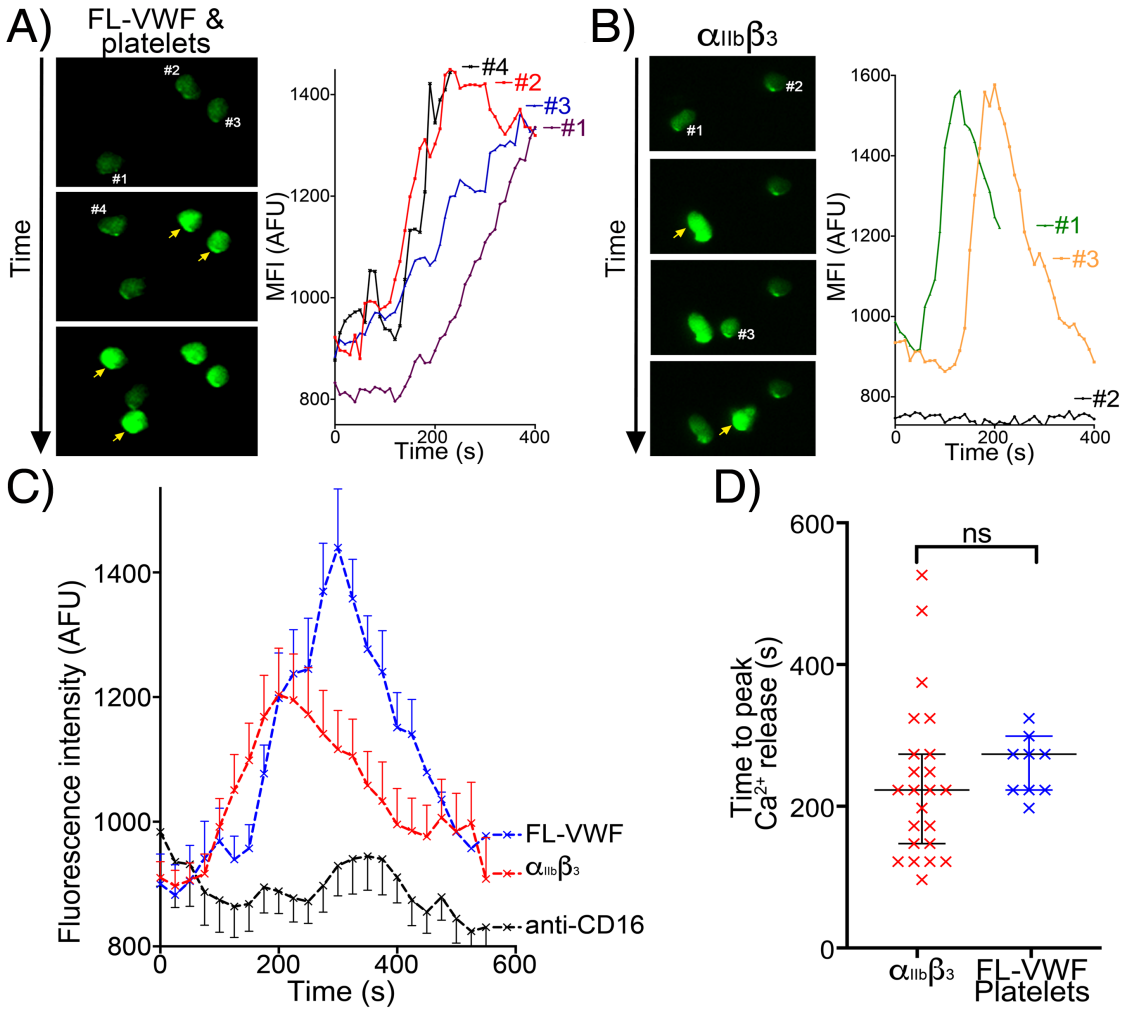

Figure 5.2 Binding to $\alpha_{IIb}\beta_3$ induces intracellular Ca^{2+} signalling in neutrophils.

A) Representative images of neutrophils pre-loaded with Fluo-4 AM bound to VWF-'primed' platelets captured (Movie 5). Neutrophils are numbered #1-#4. The yellow arrow highlights a frame in which the fluorescence has increased in the attached neutrophil. For each neutrophil shown, intracellular Ca^{2+} release is quantified by measurement of cellular mean fluorescent intensity (MFI) over time. B) As in A) except neutrophils were perfused over activated $\alpha_{IIb}\beta_3$. MFI increased for neutrophils #1 and #3, but not for neutrophil #2. C) Graph depicting the change in MFI as a function of time after neutrophil attachment to microchannels coated with activated $\alpha_{IIb}\beta_3$ (n=24 neutrophils from 3 different experiments), VWF-'primed' platelets (n=9 neutrophils from 1 experiment) or anti-CD16 (n=13 neutrophils from 2 different experiments). Data plotted are mean ±SEM. D) Dot plot presenting the time between neutrophil attachment and maximum MFI of neutrophils binding to purified $\alpha_{IIb}\beta_3$ (red), or VWF-'primed' platelets (blue). Data plotted are median ±95% confidence interval. Data were analysed using the Mann-Whitney test.

5.2.3. Activated $\alpha_{IIb}\beta_3$ induces the release of neutrophil extracellular traps (NETs)

Neutrophils fulfil their immune function through various means. One important mechanism leading to pathogen clearance is represented by NET release. Platelets have recently been classified as immune cells and evidence suggests that they can act as mediators of NETosis [318,323,324]. However, despite increased interest in platelet-augmented NETosis, the mechanism driving this remains unclear [282,325]. Considering the ability of activated $\alpha_{IIb}\beta_3$ to induce phenotypic changes and Ca^{2+} release after binding neutrophils, I hypothesised that this would lead to NETosis.

To assess this, I isolated neutrophils and perfused them through channels directly coated with activated $\alpha_{IIb}\beta_3$, at low shear. Neutrophils were labelled with Hoechst (staining the intracellular DNA) and Sytox Green (a cell-impermeant DNA stain) and perfused through channels at $50s^{-1}$ for 10 minutes. Thereafter, unbound neutrophils were removed by washing with 1x HT buffer supplemented with $CaCl_2$, $MnCl_2$ and Sytox Green. Flow was then stopped to improve imaging of neutrophils, and they were monitored in real-time using confocal microscopy. The experiments were carried out at 37°C to better reflect physiological conditions.

As depicted by **Figure 5.3**, at the 30 minutes, neutrophil nuclei had a clear, well-defined lobular structure. After 75 minutes, neutrophil nuclei increased in size and, after 85 minutes, lost their well-defined shape. This is indicative of chromatin decondensation, which precedes NET formation [320]. Indeed, a few minutes later, positive Sytox Green fluorescence was observed, suggesting increased cell permeability and/or extrusion of DNA extracellularly (**Figure 5.3**).

As a negative control, neutrophils captured by anti-CD16 under the same conditions did not exhibit any change in nuclear shape or increased cell permeability, remaining negative for Sytox Green after 95 minutes (**Figure 5.3**, **Movie 6**). Monitoring these neutrophils further did not reveal any changes, even after 180 minutes (data not shown).

Experiments were also performed using plasma-free blood with neutrophils bound to VWF-'primed' platelets, or VWF A1*-'primed' platelets. These neutrophils exhibited similar changes within their nuclei and were positively stained for Sytox Green after 90 minutes (data not shown).

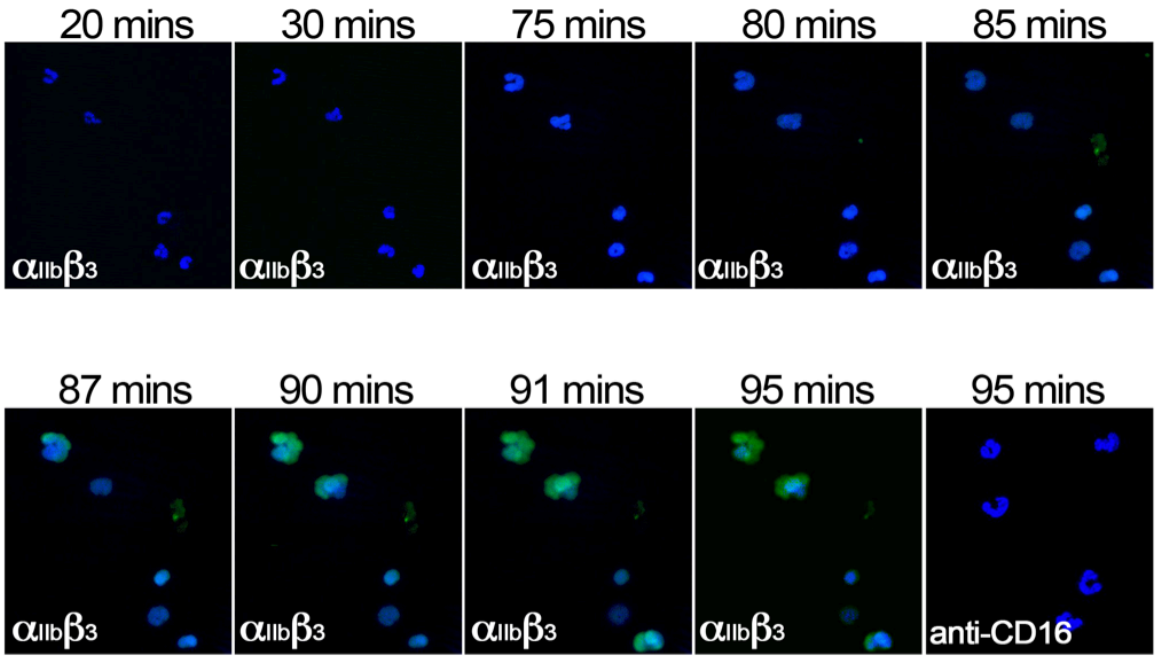

Figure 5.3 Binding of neutrophils to $\alpha_{IIb}\beta_3$ under flow induces NETosis.

Isolated PMNs labelled with Hoechst (blue) and cell-impermeable Sytox Green were perfused over $\alpha_{IIb}\beta_3$-coated microchannels, or anti-CD16, (-ve ctrl) at 50s^{-1} for 10 minutes and then monitored under static conditions for 2 hours. Representative composite images after 20, 30, 75, 80, 85, 87, 90, 91 and 95 minutes of attachment. Neutrophils bound to $\alpha_{IIb}\beta_3$ exhibited nuclear decondensation and increased cell permeability that precedes NETosis after about 85 minutes. Sytox Green staining appears shortly after, indicative of increased cell permeability and/or DNA becoming extracellular (see Movie 6). Neutrophils bound to surfaces using an anti-CD16 antibody did not exhibit signs of NETosis or did so very rarely.

Despite chromatin decondensation and Sytox Green staining observed, the ability of activated $\alpha_{IIb}\beta_3$ to induce NETosis needed to be validated, as Sytox Green is not a specific marker for NETs. For this reason, neutrophils were perfused over channels coated with activated $\alpha_{IIb}\beta_3$ and, after two hours, they were fixed as detailed in **Methods Section 2.5.3.5** and incubated with an antibody against citrullinated histone H3 overnight. The next day, channels were washed, blocked, and stained with a secondary antibody conjugated to Alexa647 (**Figure 5.4**).

As histone citrullination occurs prior to NET release [320], neutrophils were also permeabilised to identify the cells in the process of NETosis. Quantification of NETosis is detailed in the next sub-section. As depicted in **Figure 5.4**, staining with anti-citrullinated H3 antibody confirmed that $\alpha_{IIb}\beta_3$ can induce NETosis.

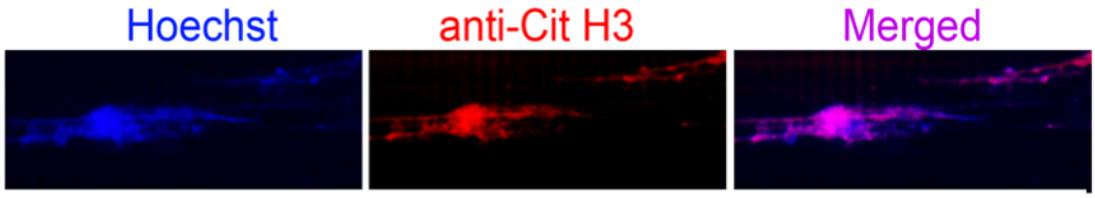

Figure 5.4 Binding of neutrophils to $\alpha_{IIb}\beta_3$ under flow induces NETosis.

Isolated PMNs were perfused over $\alpha_{IIb}\beta_3$-coated microchannels at 50s^{-1} for 10 minutes and then left under static conditions for 2 hours. Attached neutrophils were thereafter stained with an anti-citrullinated H3 antibody overnight and then stained with a secondary antibody conjugated to Alexa-647 and with the Hoechst dye. Representative composite images of NETs positively stained for DNA (Hoechst staining) and citrullinated H3 (anti-Cit H3).

5.2.4. Activated $\alpha_{IIb}\beta_3$-induced NETosis is shear-dependent

After confirming that neutrophils captured by activated $\alpha_{IIb}\beta_3$ do indeed undergo NETosis, I used Sytox Green staining to quantify NETosis. Quantification was achieved by manually counting the neutrophils in the process of NETosis (chromatin decondensation and Sytox green positive stain) after 2 hours, throughout the whole channel, and expressing this as a percentage of the total number of neutrophils bound. On activated $\alpha_{IIb}\beta_3$, 69%±14% of neutrophils throughout the entire channel formed NETs after 2 hours, whereas only 8%±8% of neutrophils underwent NETosis when bound to anti-CD16 (**Figure 5.5**). Interestingly, if no shear was applied in the first 10 minutes and neutrophils were left to bind to activated $\alpha_{IIb}\beta_3$ under static conditions, there was a significant decrease in the number of NETs by approximately 60%, suggesting that $\alpha_{IIb}\beta_3$-induced NETosis is shear-dependent and, therefore, occurs through a mechano-sensitive mechanism.

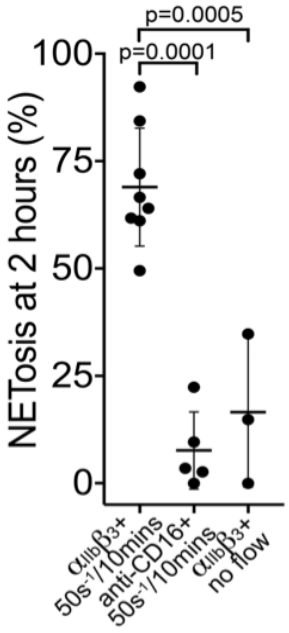

Figure 5.5 $\alpha_{IIb}\beta_3$-induced NETosis is dependent on the presence of shear.

Isolated neutrophils were perfused over $\alpha_{IIb}\beta_3$ (n=8) or anti-CD16-coated (n=5) microchannels at $50s^{-1}$ for 10 minutes and then left under static conditions for 2 hours. In separate $\alpha_{IIb}\beta_3$-coated channels (n=3), neutrophils were left to attach under static conditions. The graph shows the mean % of neutrophils ±SD in the entire microchannel that formed NETs after 2 hours of attachment to $\alpha_{IIb}\beta_3$ or anti-CD16. Data plotted is mean ±SD. Data were analysed using unpaired, two-tailed Student's t-test.

5.2.5. Activated $\alpha_{IIb}\beta_3$-induced NETosis is dependent on intracellular Ca^{2+} release and NADPH oxidase

After establishing the importance of shear for $\alpha_{IIb}\beta_3$-induced NET release, I endeavoured to investigate the pathway(s) responsible for NETosis using a variety of inhibitors. Given the observation presented in an earlier section that neutrophils captured by activated $\alpha_{IIb}\beta_3$ and VWF-'primed' platelets undergo intracellular Ca^{2+} release, I investigated whether NETosis is dependent on these early events. To test this, I pre-incubated neutrophils with TMB-8, an intracellular Ca^{2+} antagonist, for 30 minutes prior to their perfusion through activated $\alpha_{IIb}\beta_3$-coated channels. As indicated by **Figure 5.6(A)**, TMB-8 significantly reduced $\alpha_{IIb}\beta_3$-induced NETosis to 17%±9%, suggesting its dependency on intracellular Ca^{2+}.

Studies report that NETosis can occur via two different pathways, based on the involvement of NADPH oxidase (Nox), i.e. it can be Nox-dependent (also known as suicidal/lytic NETosis) or Nox-independent (also known as vital/non-lytic NETosis) [327,328]. To identify the pathway responsible for $\alpha_{IIb}\beta_3$-induced NETosis, I pre-incubated neutrophils with DPI, a well-established Nox inhibitor, for 30 minutes prior to their perfusion through $\alpha_{IIb}\beta_3$-coated channels. Similar to TMB-8, the addition of DPI led to a significant reduction in the number of neutrophils forming NETs after 2 hours (25%±10%) (**Figure 5.6(A)**), suggesting that $\alpha_{IIb}\beta_3$-induced NETosis is Nox-dependent.

One of the most well-described non-physiological NET inducers *in vitro* is PMA [318,390]. Incubating neutrophils captured by anti-CD16 with PMA resulted in 100%±0.5% neutrophils releasing NETs after 2 hours. Similar to $\alpha_{IIb}\beta_3$-induced NETosis, PMA-induced NETosis was significantly inhibited by DPI (16%±13%) (**Figure 5.6(B)**). In contrast, the addition of TMB-8 to neutrophils prior to their stimulation with PMA did not lead to a significant decrease in the number of neutrophils forming NETs after 2 hours (90%±9%) (**Figure 5.6(B)**). These results suggest that $\alpha_{IIb}\beta_3$-induced NETosis and PMA-induced NETosis share some mechanistic similarities but differ in their dependency to Ca^{2+} release.

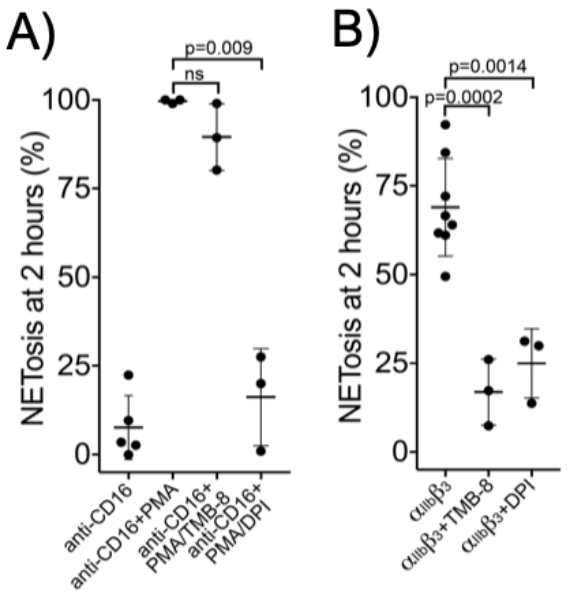

Figure 5.6 $\alpha_{IIb}\beta_3$-induced NETosis is dependent on NADPH oxidase and Ca^{2+} release.

A) Graph showing the % of neutrophils attached to anti-CD16 that formed NETs after 2 hours, in the presence and absence of PMA and two different inhibitors – TMB-8 and DPI. B) Graph showing the % of neutrophils attached to activated $\alpha_{IIb}\beta_3$ after 2 hours, in the presence or absence of TMB-8 and DPI. n≥3; Data plotted is mean±SD. Data were analysed using unpaired, two-tailed Student's t-test.

5.3. Discussion

The aim of this chapter was to investigate the impact of activated $\alpha_{IIb}\beta_3$ on the neutrophil phenotype. For this, I analysed the ability of $\alpha_{IIb}\beta_3$ to induce neutrophil polarisation, Ca^{2+} signalling and, ultimately, NET release.

The fact that neutrophils receive polarisation signals through interactions with platelets has been established. Upon activation, platelets can release chemokines, such as HMGB2, CXC, RANTES that, upon neutrophil binding, can modify their shape and behaviour [387,388]. The capacity of VWF-'primed' platelets to influence neutrophil phenotype was, initially, analysed using confocal microscopy. High-resolution imaging revealed that neutrophils bound to VWF-'primed' platelets appear to scan their surroundings, emitting pseudopodia and, eventually, spreading. All these observations indicate that VWF-'primed' platelets can induce signalling within neutrophils. Further experiments aim to establish whether VWF-captured platelets

release chemokines that modulate neutrophil phenotype. However, given the low number of platelets captured to the microchannels and the dependency on flow to 'prime' the platelets, this would be technically difficult to study. The importance of shear for VWF-GPIbα-dependent signalling would prevent the investigation of this using an established static approach such as an ELISA. An alternative method would be the use of chemokine inhibitors in flow assays to investigate whether they have an effect. However, given the minimal degranulation demonstrated in the previous chapter, it is unlikely that platelets release any chemokines. However, this was indirectly assessed by analysing the neutrophil behaviour following their direct binding to microchannels coated with activated $\alpha_{IIb}\beta_3$. In this case, neutrophils were only exposed to this platelet integrin, in the absence of any other platelet receptors, soluble agonists and/or chemokines. As observed in **Movie 4**, these neutrophils behaved similarly to those bound to VWF-'primed' platelets. They were seen to scan, spread and, additionally, some could be observed migrating against flow. These results suggest, for the first time, that neutrophils not only bind directly to activated $\alpha_{IIb}\beta_3$, but that they can also undergo signalling in response to this interaction.

To investigate this further, I performed Ca^{2+} assays. Neutrophils were pre-loaded with a Ca^{2+}-sensitive fluorophore (Fluo-4 AM) prior to being perfused through microchannels at low shear. After 200-300 seconds following binding, neutrophils captured by activated $\alpha_{IIb}\beta_3$ or VWF-'primed' platelets exhibited an increase in fluorescence, corresponding to intracellular Ca^{2+} signalling. Monitoring these neutrophils for a longer period of time did not reveal any further or repeated fluorescence spikes. Therefore, in contrast to platelets bound to VWF, which undergo repeated transient Ca^{2+} release (**Movie 2, Chapter 1**), neutrophils undergo a single Ca^{2+} release spike. Importantly, to confirm that neutrophil Ca^{2+} signalling was dependent on activated $\alpha_{IIb}\beta_3$, anti-CD16-coated channels were used as a control. As predicted, neutrophils captured by this antibody did not exhibit Ca^{2+} signalling. Future experiments aim to investigate whether $\alpha_{IIb}\beta_3$ can also cause signalling within T cells. Additional experiments also aim to explore whether neutrophils and T cells release any cytokines in response to $\alpha_{IIb}\beta_3$ binding,

although this presents limitations due to the limited number of neutrophils attaching and the difficulty of collecting the supernatant containing these cytokines from the microchannels.

Finally, I aimed to explore whether $\alpha_{IIb}\beta_3$ can trigger the release of NETs from bound neutrophils. Defining platelets as mediators of NETosis has been a topic of recent scientific interest. Evidence is controversial with regards to the involvement of already characterised platelet-neutrophil interactions in platelet-mediated NETosis, as some studies suggest this process is P-selectin dependent, whereas others show P-selectin does not play a role [282,325]. Moreover, a recent study suggests that, in a model of hepatic infection, platelets aid bacterial clearance by binding to neutrophils via an "unknown" receptor and inducing NETosis [359]. All this evidence provided scope to hypothesise that activated $\alpha_{IIb}\beta_3$ may induce NETosis.

To investigate this, neutrophils captured by activated $\alpha_{IIb}\beta_3$ were monitored for two hours. Prior to DNA being extruded from the cells, chromatin decondensation needs to occur. This is dependent on the activity of peptidylarginine deiminase 4 (PAD4), that converts arginine side chains to citrullines, loosening the link between histones H3 and H4 and nuclear DNA [391]. Within our experimental setup, chromatin decondensation could be observed after 85 minutes of neutrophil attachment to activated $\alpha_{IIb}\beta_3$. This immediately preceded the appearance of Sytox Green fluorescence, after 87 minutes. However, this could be indicative of either extracellular DNA presence, or increased cell permeability. The presence of NETs was validated using an antibody against citrullinated histone H3, which is a specific marker for NETosis. Future experiments aim to use other NET-specific markers, such as myeloperoxidase or neutrophil elastase. However, there is no consensus yet regarding the precise definition of a NET or how to quantify it [392].

After establishing the ability of $\alpha_{IIb}\beta_3$ to induce NETosis, I aimed to explore the pathway preceding it. NET release has recently been divided into two pathways: lytic (suicidal, NADPH oxidase-dependent) and non-lytic (vital, NADPH oxidase-independent) NETosis [328,329]. However, literature reveals that only about 25% of neutrophils release vital NETs [327]. I

therefore hypothesised that $\alpha_{IIb}\beta_3$ drives lytic NETosis. To test this, I used a NADPH oxidase (Nox) inhibitor, DPI, which led to a significant reduction in the number of neutrophils forming NETs after 2 hours. DPI also inhibited PMA-induced NET release, suggesting that $\alpha_{IIb}\beta_3$ triggers NETosis in a PMA-similar manner.

Given the earlier observation that neutrophils bound to $\alpha_{IIb}\beta_3$ or VWF-'primed' platelets undergo Ca^{2+} release, I also endeavoured to investigate whether NET formation is dependent on these early events. Incubating neutrophils with TMB-8, an intracellular Ca^{2+} antagonist, resulted in a significant decrease in the number $\alpha_{IIb}\beta_3$-triggered NETs. However, as opposed to DPI, TMB-8 only inhibited $\alpha_{IIb}\beta_3$-induced NETosis and not PMA-induced NETosis. This suggests that, although sharing some similarities with PMA-driven NET formation, $\alpha_{IIb}\beta_3$ induces a distinct signalling pathway within neutrophils. Interestingly, Douda *et al.* showed that Ca^{2+} release is an essential step for Nox-independent NETosis. Their study suggests that Nox-independent NETosis occurs in a manner that is dependent on Ca^{2+}-activated small conductance K^+ channel (SK3) and mitochondrial ROS formation. Moreover, they suggest that this NET pathway occurs within 1-2 hours following stimulation with ionomycin or A23187 [393]. $\alpha_{IIb}\beta_3$-induced NETosis appears to combine these two mechanisms, being dependent on both NADPH oxidase activity and Ca^{2+}, but further experiments analysing the signalling events occurring should be performed to ascertain whether one pathway is responsible or whether there is another, yet uncharacterised pathway involved. Additional experiments aimed to investigate the involvement of Src kinases or phospholipase C in $\alpha_{IIb}\beta_3$-induced NETosis. Preliminary data was obtained using PP2 (a Src kinase inhibitor) and U73122 (a phospholipase C inhibitor), but no difference was observed compared to the control (data not shown). These experiments should be repeated using other NET stimulants as controls, to validate the concentration and efficiency of these inhibitors.

NETosis is a crucial mechanism involved in innate immunity, given the ability of NETs to entrap and eliminate pathogens [318]. However, experimental settings using stimulants such as PMA,

LPS, bacteria, suggest a timeline for NETosis of 3-8 hours following stimulation [320,390]. Physiologically, this could be considered a profoundly delayed response after exposure to pathogens. Interestingly, recent studies show that platelets stimulated with thrombin and incubated with neutrophils under static conditions can induce NETosis more rapidly, in a P-selectin dependent manner [325]. Moreover, other studies suggest that platelets stimulated with LPS via TLR4 and perfused over bound neutrophils can induce NET release within minutes, in a P-selectin independent manner [282]. My results are in line with these recent findings, showing that $\alpha_{IIb}\beta_3$-mediated NETosis occurs more rapidly than other *in vitro* NET assays, within 1.5 hours from neutrophil attachment. Moreover, despite previous studies reporting that PMA-induced NETosis requires 3-8 hours following stimulation, we observed that 100% neutrophils captured by anti-CD16 and stimulated by PMA formed NETs after 2 hours. The only difference present in these assays compared to other published NETosis *in vitro* studies, is the presence of flow.

Indeed, recent research recognises the importance of shear in the release of NETs. Yu *et al.* showed that shear upregulation results in NET release from physically entrapped neutrophils [394]. Based on this, I hypothesised that shear may act as a secondary signal in $\alpha_{IIb}\beta_3$-induced NETosis. In support of this, if neutrophils were left to attach on $\alpha_{IIb}\beta_3$ in the absence of flow, there was a significant reduction in the number of NETs formed after two hours. It appears, therefore, that the first 10 minutes of low shear are essential in driving $\alpha_{IIb}\beta_3$-induced NETosis, suggesting that this occurs in a mechanosensitive manner. Maintaining the shear for longer than 10 minutes did not lead to earlier NET formation, nor did it cause a higher proportion of neutrophils to release NETs (data not shown). Considering that Ca^{2+} release occurs within the first 5 minutes of neutrophil attachment to activated $\alpha_{IIb}\beta_3$, shear might be important for the early events leading to NET release. Moreover, in our experimental setting, increasing the shear from $50s^{-1}$ to $1000s^{-1}$ after 10 minutes of attachment mainly led to neutrophil detachment, but did not trigger earlier NETosis in neutrophils that did not detach. If, however, flow was restarted after Sytox Green confirmed the increased cell permeability or DNA

release, NETs were seen to extend in mesh-like structures rather than being confined to the surroundings of individual neutrophils.

Neutrophils captured by VWF-'primed' or A1*-'primed' platelets could also release NETs after 90 minutes. However, in linear channels, neutrophils mainly roll on VWF-'primed' platelets, and only a limited proportion is able to stably attach to these platelets and be monitored for prolonged periods of time to investigate the possibility of NET release. To circumvent this issue, bifurcated channels should be used as presented in Chapter 2. Preliminary data suggests a significant number of neutrophils attach to VWF-'primed' platelets in areas with disturbed flow patterns, at bifurcation sites. As observed through fluorescence microscopy, these neutrophils stably attached and were seen to spread soon after binding to the VWF-'primed' platelets. Future experiments aim to investigate whether this observed effect translates into more rapid NET release at sites of disturbed flow.

Platelet-induced NET release is thought to be both a physiological and a pathological process, as it aids bacterial clearance, playing a role in the innate immune response [318,324,330,355], while also being highly pro-thrombotic, being involved in the development of DVT [339,340]. In DVT, the thrombus generally forms despite lack of vessel damage, over an intact endothelium. The nidus for thrombus formation in DVT is mainly represented by areas of turbulence that, in the venous system, are present at branch sites or around venous valves [395]. NETs have been linked to the development of DVT through their thrombogenic nature [338,340], however, the mechanism driving NETosis in the absence of overt vessel damage or pathogenic microorganisms is currently not understood. This is further explored in the **Final Discussion**.

The results presented in Chapter 3 provide further mechanistic insights for platelet-induced NET release and suggest a role for activated $\alpha_{IIb}\beta_3$ in NET production, independently of other stimuli. However, the pathophysiological relevance of this remains unclear in the absence of the neutrophil receptor. The next chapter aims to identify the neutrophil receptor involved in this interaction.

6. Chapter 4 – Identifying the leukocyte receptor interacting with VWF-'primed' platelets

6.1. Introduction

The ability of platelets to induce NETosis has attracted an increasing research interest recently. However, the precise mechanisms responsible for platelet-mediated NETosis are unclear, as well as the interaction preceding it. Some studies report that platelet-induced NET release is dependent on P-selectin [325], whereas others show that LPS-stimulated platelets can also lead to NET formation independently of P-selectin [282]. Moreover, within liver sinusoids, platelets were shown to promote NETosis via an "unknown" receptor [359]. In line with this, my results identified a novel interaction that triggers NETosis via activated $\alpha_{IIb}\beta_3$. All these findings provide scope to further investigate and characterise the novel interaction between VWF-'primed' platelets and neutrophils.

Understanding this interaction, as well as demonstrating its novelty relies on identifying the leukocyte counter-receptor. Although it could be a reasonable assumption that neutrophils and T cells interact with activated $\alpha_{IIb}\beta_3$ via the same counter-receptor, this may not be the case. Given the clear impact upon the neutrophil phenotype demonstrated in **Chapter 3**, this chapter focuses on identifying the neutrophil receptor involved, with scope to subsequently validate this in future T cell experiments.

As mentioned in **Chapter 2**, platelet-neutrophils interactions have been well-characterised in the settings in which either the platelet or the neutrophil, or both cells are fully activated. The previously identified neutrophil receptors binding to platelets include P-selectin glycoligand-1 (PSGL-1), CD40, which are constitutively expressed onto the neutrophil surface, and activated Mac-1 (also termed CD11b/CD18 or $\alpha_M\beta_2$) and LFA-1 (also termed CD11c/CD18 or $\alpha_L\beta_2$), which require activation or clustering prior to binding to platelets [141,343-345,349,396]. As the results presented so far reveal that VWF-bound platelets are 'primed' instead of activated, a role for PSGL-1 and CD40 should be excluded from the potential neutrophil receptors involved, due to the lack of P-selectin and CD40L as counter-receptors on the platelet surface. Moreover, there is no indication that neutrophils have been activated prior to the flow assays, suggesting

that activated Mac-1 or LFA-1 are unlikely to form interactions with platelets under these conditions. The involvement of these receptors would also fail to explain the cell specificity of the leukocyte recruitment. All these data imply that there is a novel receptor on neutrophils (and T cells) that interacts with activated $\alpha_{IIb}\beta_3$ and leads to NET formation. This chapter aims to identify this receptor using different strategies, including blocking assays, pull-down experiments, together with extensive transcriptomic and proteomic analyses.

6.2. Results

6.2.1. Evaluating the role of leukocyte β_2 integrins in platelet binding

After excluding a role of P-selectin-PSGL-1 and, indirectly, of CD40L-CD40 in the VWF-'primed' platelet-leukocyte interactions (**Chapter 2**), I endeavoured to investigate whether the leukocyte β_2 integrins (Mac-1 and LFA-1) are involved in this interaction. Despite indirect evidence presented in the previous chapter that these integrins do not play a role in the distinct interaction observed, I performed flow assays using an antibody that blocks β_2 integrins, by binding to the CD18 subunit. As shown in **Figure 6.1(A-B)**, pre-incubating plasma-free blood with the anti-β_2 antibody prior to perfusion through VWF-coated channels did not lead to any changes in the number of platelet-leukocyte interactions under flow. Moreover, isolated neutrophils were pre-incubated with this blocking antibody before being perfused through channels coated with activated $\alpha_{IIb}\beta_3$ (**Figure 6.1(C-D)**). There was no difference in the number of neutrophils binding to the activated $\alpha_{IIb}\beta_3$, supporting the contention that Mac-1 and LFA-1 are not the receptors involved in this novel interaction.

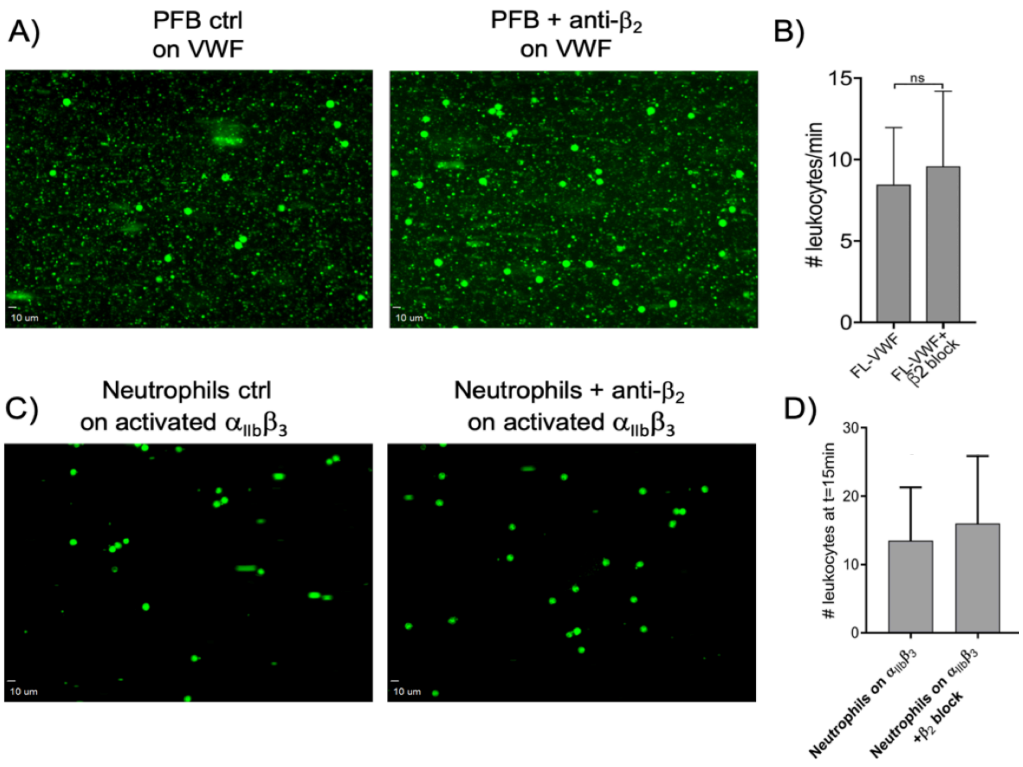

Figure 6.1 VWF-'primed' platelet-leukocyte interactions occur independently of β_2 integrins.

A) Representative micrographs (n=3) of plasma-free blood perfused over VWF-coated channels at high shear, followed by low shear, in the absence or presence of an anti-β_2 antibody. B) Graph quantifying the number of leukocytes rolling over VWF-'primed' platelets in the presence or absence of the anti-β_2 antibody. Data plotted are mean ±SD; n=3. Data were analysed using an unpaired, two-tailed Student's t-test. C) Representative micrographs (n=2) of isolated neutrophils perfused over activated $\alpha_{IIb}\beta_3$-coated channels in the absence or presence of an anti-β_2 antibody. D) Graph quantifying the number of neutrophils attached to activated $\alpha_{IIb}\beta_3$ in the presence or absence of the anti-β_2 antibody after 15 min of perfusion at 50s^{-1}. Data plotted are mean ±SD; n=2.

6.2.2. Pull-down experiments

After establishing that neutrophils and T cells interact with activated $\alpha_{IIb}\beta_3$ via an uncharacterised receptor, I first aimed to perform pull-down assays, using tosylactivated magnetic beads coated with activated $\alpha_{IIb}\beta_3$. Various approaches were employed to ensure the coupling of $\alpha_{IIb}\beta_3$ and its activated state on the beads (see **Methods Section 2.7.1.1**). Beads were initially coated through direct coupling of the purified integrin. The coupling was performed in the presence of $MnCl_2$ and $CaCl_2$ to ensure that $\alpha_{IIb}\beta_3$ was in its activated form

as in previously presented flow assays. However, through this approach $\alpha_{IIb}\beta_3$ was not efficiently captured onto the beads (data not shown). To address this issue, I coupled the beads with the anti-LIBS2 antibody and, thereafter, incubated them with $\alpha_{IIb}\beta_3$. This approach led to successful capture of $\alpha_{IIb}\beta_3$ on the beads, however, its activation was inefficient (data not shown). The coupling and activation of $\alpha_{IIb}\beta_3$ on tosylactivated beads therefore required further optimisation prior to pull-down assays.

However, during the period of optimisation, a group at the University of Toronto led by Prof. Heyu Ni published a study using magnetic beads coated with activated $\alpha_{IIb}\beta_3$ [397]. We therefore established a collaboration with Prof. Heyu Ni, through which I would isolate proteins from neutrophil membranes and send them to his laboratory for subsequent pull-down assays. For this, I isolated the membrane proteins from purified neutrophils according to the methodology detailed in **Section 2.7.2**. A total of 850µl containing 60µg/ml neutrophil membrane proteins was obtained from $1x10^7$ neutrophils.

Prior to sending the sample to the University of Toronto, I endeavoured to confirm the presence of the neutrophil receptor within the isolated neutrophil membrane proteins. For this, I performed flow assays where isolated neutrophils were incubated with the membrane protein fraction prior to perfusion over channels coated with activated $\alpha_{IIb}\beta_3$ to investigate whether this competes with neutrophils to bind activated $\alpha_{IIb}\beta_3$. As illustrated in **Figure 6.2**, in the presence of membrane fraction, neutrophil binding to activated $\alpha_{IIb}\beta_3$ was completely inhibited.

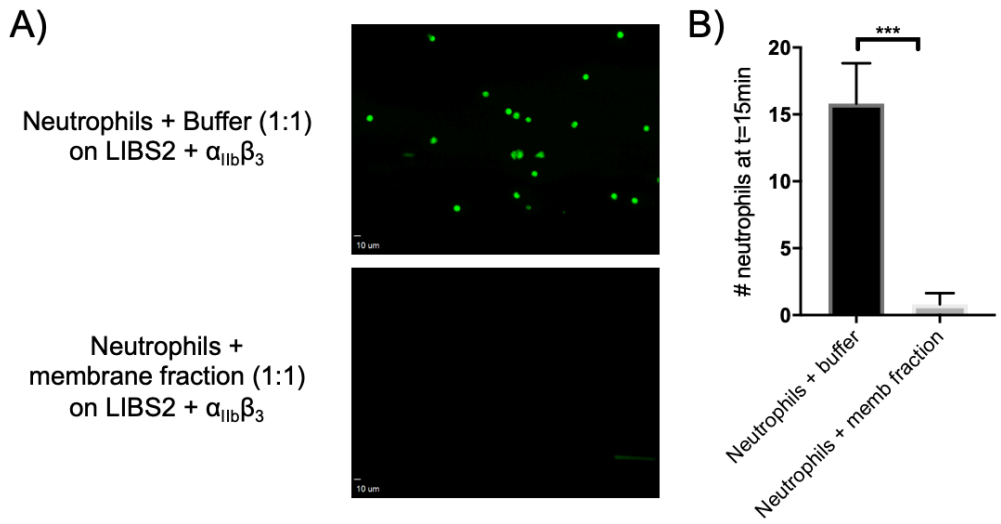

Figure 6.2 Purified neutrophils compete with isolated neutrophil membrane fractions to bind activated $\alpha_{IIb}\beta_3$.

*A) Representative images (n=3) of neutrophils bound to LIBS2/$\alpha_{IIb}\beta_3$-coated channels, in the presence of neutrophil membrane fraction or the buffer this was collected in, after 10 minutes of perfusion at 50s^{-1}. B) Graph quantifying the number of neutrophils bound to LIBS2/$\alpha_{IIb}\beta_3$-coated channels as in A). n=3; Data plotted are mean ±SD. Data were analysed using an unpaired, two-tailed Student's t-test. *** p<0.001.*

After confirming the presence of the neutrophil receptor within the membrane fraction sample, this was sent to the University of Toronto for pull-down experiments. A list of 265 proteins was provided. However, the majority of these proteins were intracellular proteins, particularly actin filament fragments from the cytoskeleton. Some membrane proteins (50) were pulled down although further optimisation and controls were necessary to employ this approach in a meaningful manner. However, one of the membrane proteins that was pulled down was represented by SLC44A2, the importance of which will become clear later in this chapter.

6.2.3. Transcriptomic analysis

Given the issues encountered during the pull-down assays (i.e. the coupling of $\alpha_{IIb}\beta_3$ and ensuring its activated state, the presence of intracellular protein contaminants in the isolated membrane proteins and the need for disrupting the neutrophil membranes), a different approach was used to identify the leukocyte receptor involved. This approach was based on the specificity of the interaction between VWF-'primed' platelets with neutrophils and T cells and not with monocytes and B cells. Therefore, we established a collaboration with Dr. Luigi Grassi and Dr. Mattia Frontini from the University of Cambridge. They provided us with RNA sequencing data (Blueprint consortium) from different human leukocyte populations, selecting genes that are expressed at higher levels in neutrophils (and T cells) compared to monocytes. RNA sequencing data was obtained from seven human neutrophil samples, eight CD4-positive $\alpha\beta$ T cell samples and five monocyte samples, all isolated from venous blood. Differential expression analysis was performed between neutrophils and monocytes and CD4-positive $\alpha\beta$ T cells and monocytes. The intersection of the upregulated genes from these two independent comparisons led to the identification of 598 genes, of which 93 genes encoded for transmembrane proteins.

Following that, we were provided with a heatmap that arranged the 93 candidates according to their level of expression in neutrophils. Within the heatmap, one sample of regulatory T cells (Treg) and one sample of B cells are also included, but these were not used in the differential expression analysis. To reduce the number of candidates, three different exclusion criteria were applied, and the candidates excluded for each are indicated in **Figure 6.3**. Of the total 93 candidates, 33 genes were excluded as the proteins they encoded were primarily associated with intracellular organelle membranes rather than the plasma membrane and, thus, were unlikely to induce interactions with platelets. Subsequently, 16 candidates were excluded due to the presence of a short extracellular domain (<30 amino acids), which may be less likely capable of mediating a highly specific interaction with activated $\alpha_{IIb}\beta_3$. Finally, I

analysed proteomic data using the ImmProt database (http://immprot.org), to check whether the remaining candidates were indeed preferentially expressed in neutrophils compared to monocytes at the protein levels. This strategy removed an additional 14 candidates, resulting in 30 possible candidates remaining. Inspection of this list may facilitate further selection based on known roles, enzymatic function and expression levels.

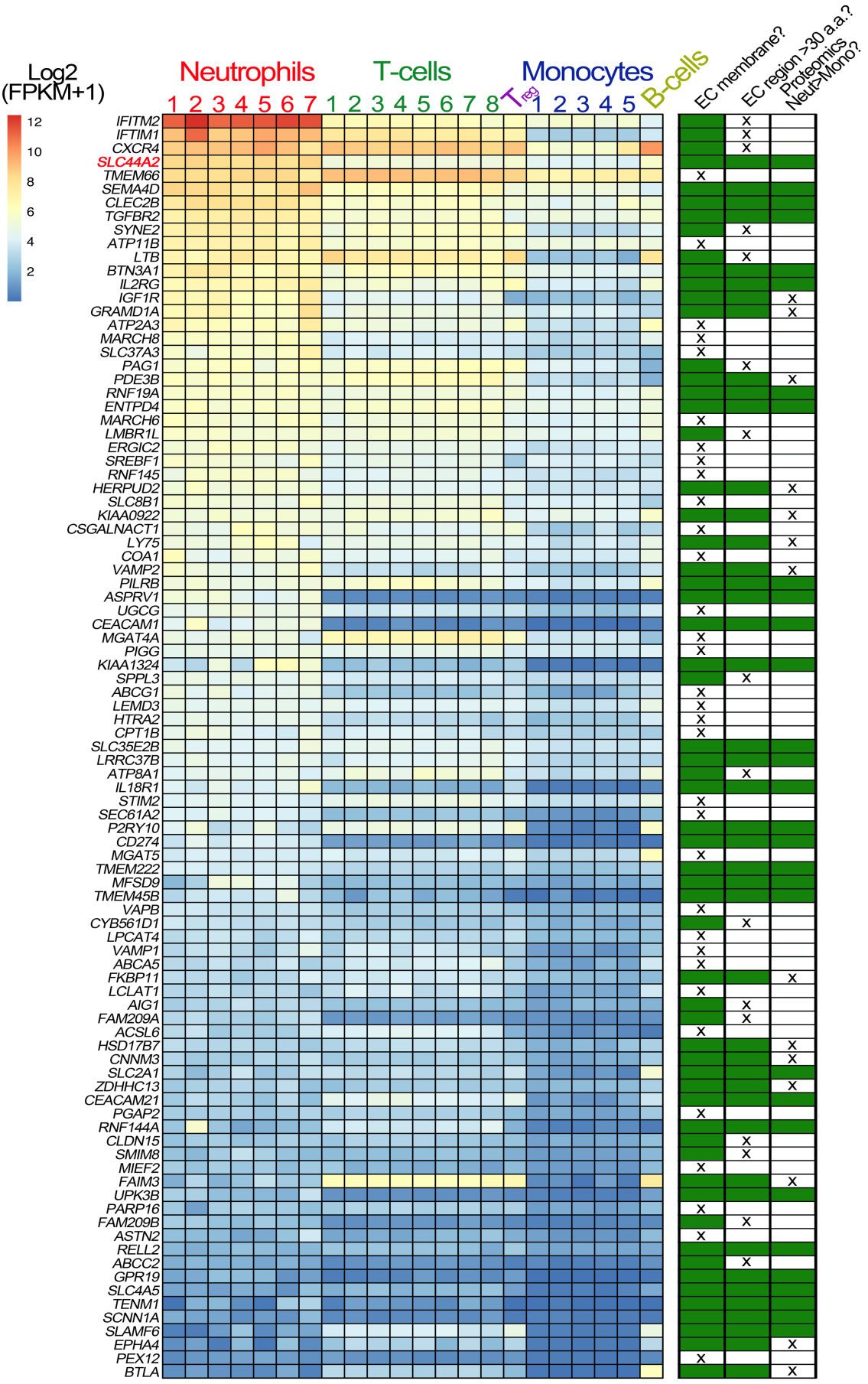
Log2
(FPKM+1)
12
10
8
6
4
2
Neutrophils
1 2 3 4 5 6 7
T-cells
1 2 3 4 5 6 7 8
Treg
Monocytes
1 2 3 4 5
B-cells
EC membrane?
EC region >30 a.a.?
Proteomics
Neut>Mono?
IFITM2
IFTIM1
CXCR4
SLC44A2
TMEM66
SEMA4D
CLEC2B
TGFBR2
SYNE2
ATP11B
LTB
BTN3A1
IL2RG
IGF1R
GRAMD1A
ATP2A3
MARCH8
SLC37A3
PAG1
PDE3B
RNF19A
ENTPD4
MARCH6
LMBR1L
ERGIC2
SREBF1
RNF145
HERPUD2
SLC8B1
KIAA0922
CSGALNACT1
LY75
COA1
VAMP2
PILRB
ASPRV1
UGCG
CEACAM1
MGAT4A
PIGG
KIAA1324
SPPL3
ABCG1
LEMD3
HTRA2
CPT1B
SLC35E2B
LRRC37B
ATP8A1
IL18R1
STIM2
SEC61A2
P2RY10
CD274
MGAT5
TMEM222
MFSD9
TMEM45B
VAPB
CYB561D1
LPCAT4
VAMP1
ABCA5
FKBP11
LCLAT1
AIG1
FAM209A
ACSL6
HSD17B7
CNNM3
SLC2A1
ZDHHC13
CEACAM21
PGAP2
RNF144A
CLDN15
SMIM8
MIEF2
FAIM3
UPK3B
PARP16
FAM209B
ASTN2
RELL2
ABCC2
GPR19
SLC4A5
TENM1
SCNN1A
SLAMF6
EPHA4
PEX12
BTLA

Figure 6.3 Transcriptomic profiling of human leukocytes.

RNA sequencing data from different leukocytes were obtained from the BLUEPRINT consortium [374]. Differential gene expression analyses were performed: mature neutrophils (n=7) vs monocytes (n=5) and CD4-positive/$\alpha\beta$ T cells (n=8) vs monocytes (n=5). Regulatory T cells (T_{reg}, n=1) and native B cells (n=1), are included in the heatmap, for comparison but were not used in differential gene expression analysis due to the low number of biological replicates. Differential expression analysis first selected genes that were expressed significantly higher in neutrophils than in monocytes, and also those that were significantly higher in CD4-positive/$\alpha\beta$ T cells than in monocytes. Their intersection identified 750 genes (598 of which protein coding). From these 598 genes, 93 genes were selected, that contained the Uniprot annotation of "INTRAMEMBRANE DOMAIN" or "TRANSMEM DOMAIN". The effective log2(FPKM+1) data are presented in the heatmap of the 93 genes, with the rows ordered according to the mean neutrophil expression levels. Next to the heatmap is a table highlighting the subsequent selection criteria used to further narrow the search for candidate receptors for $\alpha_{IIb}\beta_3$. The first round of selection involved discarding those transmembrane proteins that are not present on the extracellular membrane, or primarily associated with intracellular membranes. The second selection criterion was to discard those proteins that had extracellular regions of <30 amino acids that might be less likely capable of mediating specific ligand binding. Finally, analysis of proteomic data from the ImmProt (http://immprot.org) resource was used to verify higher levels of protein of each selected gene in neutrophils than in monocytes.

6.2.4. SLC44A2

From the remaining 30 candidates, *SLC44A2* gene was selected as the first and major candidate for subsequent validation, given recent studies that identified it as a risk locus for deep vein thrombosis and stroke [365-367] and also its position within the heatmap and identified through preliminary pull-down experiments.

6.2.4.1. Confirmation of expression in neutrophils

I first endeavoured to confirm the expression of SLC44A2 in neutrophils. Initially, flow cytometry was performed on purified neutrophils. As illustrated by **Figure 6.4(A)**, 68% of cells were double positive for CD16 (a granulocyte-specific marker) and SLC44A2, suggesting that the majority of the granulocyte population expresses SLC44A2 on the cell surface. The fact that not all neutrophils were stained positively for SLC44A2 could be attributed to antibody specificity or the presence of different neutrophil populations within the blood. Investigating different neutrophil subsets enriched in SLC44A2 would be a good future avenue to explore in future experiments.

Expression of SLC44A2 in neutrophils was also confirmed using Western blotting. As shown in **Figure 6.4(B)**, a band corresponding to the predicted molecular weight of SLC44A2 (80kDa) was identified under both non-reducing and reducing conditions in neutrophil lysates. A second band, of around 65kDa can be observed on the blot, that represents the nascent/non-glycosylated SLC44A2.

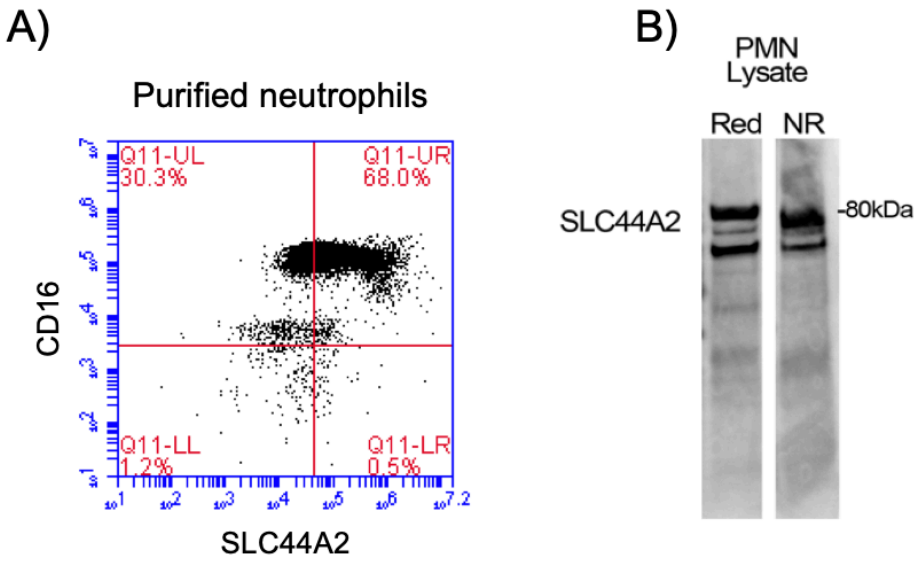

Figure 6.4 Confirmation of SLC44A2 expression in neutrophils.

A) *Dot plot analysing isolated neutrophils labelled with an anti-CD16-APC and an anti-SLC44A2#2 with a secondary antibody conjugated to Alexa488.* ***B)*** *Isolated neutrophil lysates were analysed by Western blotting under reducing and non-reducing conditions using the anti-SLC44A2#2 antibody. In both lanes, two bands corresponding to glycosylated (~80kDa) and nascent, non-glycosylated (~65kDa) SLC44A2 were detected.*

As mentioned earlier, to confirm that SLC44A2 was preferentially expressed in neutrophils compared to monocytes, I analysed proteomic data from the ImmProt database (http://immprot.org). This is based on high-resolution mass-spectrometry proteomics performed on human haematopoietic cell populations in either steady or activated states [398]. To analyse the comparative levels of the SLC44A2 protein in neutrophils and monocytes, I performed a pair-wise comparison displayed as a volcano plot. The expression levels were analysed statistically using a two-tailed Student's t-test with Welch's correction, and proteins with a significantly different level of expression are shown as red dots in the plot. As illustrated

in **Figure 6.5**, SLC44A2 is expressed in significantly higher levels in neutrophils compared to monocytes, which corroborates the RNA sequencing data from the BLUEPRINT consortium [374].

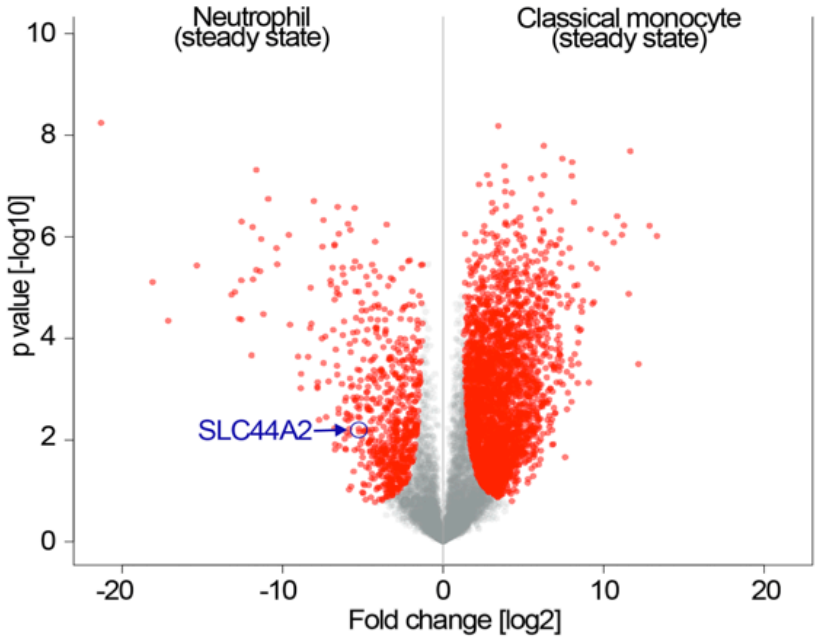

Figure 6.5 Comparative analysis of the SLC44A2 protein levels in neutrophils vs. monocytes.

Preferential expression of SLC44A2 in neutrophils over monocytes was ascertained through analysis of proteomic data from ImmProt (http://immprot.org), which is based on high-resolution mass-spectrometry proteomics performed on human hematopoietic cell populations in either steady or activated states [398]. A pair-wise comparison between neutrophils (steady-state) and classical monocytes (steady state) is displayed as a volcano plot. Protein expression levels were compared using two-tailed Student's t-test with Welch's correction (S0=1, FDR<5%), and proteins with a significantly different expression level are shown in red on the plot. The point corresponding to SLC44A2 is highlighted revealing preferential expression in neutrophils.

6.2.4.2. Blocking SLC44A2 in flow assays

After confirming the preferential expression of SLC44A2 in neutrophils compared to monocytes, I aimed to investigate the effect of blocking SLC44A2 on neutrophils in the ability to interact with 'primed' platelets and activated $\alpha_{IIb}\beta_3$ in flow assays. SLC44A2 is a multi-span membrane protein. Its structure consists of 10 membrane-spanning domains, with its N-

terminal and C-terminal regions present intracellularly. The 10 membrane-spanning domains are interconnected by five extracellular loops and four intracellular loops. Two antibodies raised against the first two extracellular loops of SLC44A2 (anti-SLC44A2#1 and #2) were commercially available and investigated in flow experiments.

The role of SLC44A2 in flow assays was first explored using plasma-free blood perfused over VWF-coated channels. As in previous experiments, plasma-free blood was first perfused at $1000s^{-1}$ for 3.5min to capture and 'prime' the platelets, following which the shear was reduced to $50s^{-1}$ to observe leukocyte interactions. Plasma-free blood was perfused in the absence and presence of two different anti-SLC44A2 antibodies (anti-SLC44A2#1 and #2). As seen in the graphical representation below (**Figure 6.6**), there was a significant decrease in the number of 'primed' platelet-leukocyte interactions in the presence of both antibodies, although the anti-SLC44A2#2 almost completely abolished the interactions, suggesting that it more effectively blocks SLC44A2. This may suggest that the first and largest extracellular loop of SLC44A2 is involved in the interaction with activated $\alpha_{IIb}\beta_3$. As a control, plasma-free blood was incubated with a rabbit IgG to ensure that the reducing effect seen with the anti-SLC44A2 antibodies is specific to blocking this receptor. As seen in **Figure 6.6**, pre-incubating plasma-free blood with the control IgG did not impact upon the platelet-leukocyte interactions.

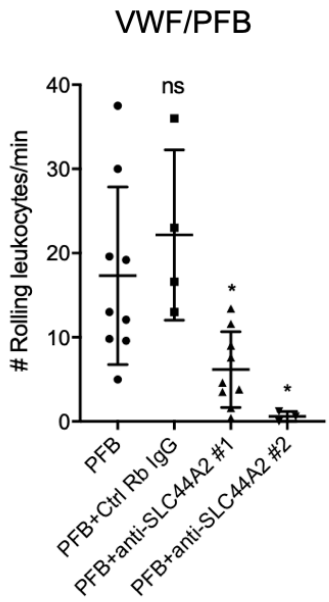

Figure 6.6 VWF-'primed' platelet-leukocyte interactions are reduced when SLC44A2 is blocked.

*Graphical representation of the number of neutrophils rolling per minute on VWF-'primed' platelets. Plasma-free blood was perfused through VWF-coated microchannels at 1000s^{-1} for 3.5mins, followed by 50s^{-1} for 10 minutes. Perfusion at low shear was done in the absence (n=8) or presence of a control rabbit IgG (n=4), or two antibodies against SLC44A2 – anti-SLC44A2#1 (n=9) and anti-SLC44A2#2 (n=3). Data plotted are mean ±SD. Data were analysed using One-Way ANOVA with multiple comparisons; ns-non-significant, * p<0.05.*

The ability of SLC44A2 to bind activated $\alpha_{IIb}\beta_3$ was further investigated in experiments in which isolated neutrophils were perfused over channels coated with activated $\alpha_{IIb}\beta_3$ at low shear, in the presence of anti-SLC44A2#1 and #2, or in the presence of the control rabbit IgG. The concentration of anti-SLC44A2#1 was titrated (**Figure 6.7**) and increasing concentrations (0.1μg/ml, 1μg/ml, 5μg/ml, 10μg/ml and 20μg/ml) of the antibody were correlated with a gradual decrease in the number of neutrophils bound to activated $\alpha_{IIb}\beta_3$. The results were quantified using the relative neutrophil binding compared to the control (purified neutrophils in the absence of antibodies/control IgG). The highest concentration of anti-SLC44A2#1 (20μg/ml) reduced the number of neutrophils binding to activated $\alpha_{IIb}\beta_3$ by approximately 90%, whereas the same concentration of anti-SLC44A2#2 almost completely abolished the binding (**Figure 6.7**). Again, this supports the contention that neutrophils interact with activated $\alpha_{IIb}\beta_3$ via the first extracellular loop of SLC44A2.

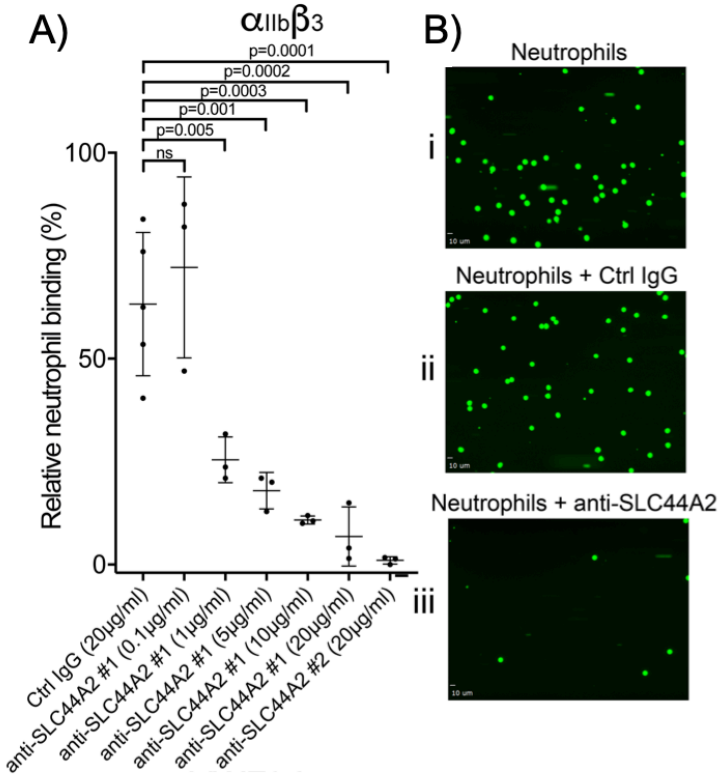

Figure 6.7 Neutrophil binding to activated $\alpha_{IIb}\beta_3$ is inhibited when SLC44A2 is blocked.

A) Graphical representation of relative neutrophil binding after 15 minutes of leukocyte perfusion to activated $\alpha_{IIb}\beta_3$ captured and activated by LIBS2/anti-β_3 activating antibody in the presence and absence of increasing concentrations of anti-SLC44A2#1 or #2 antibodies. Data plotted are mean ±SD. Data were analysed using One-Way ANOVA with multiple comparisons. B) Representative micrographs of neutrophils bound to activated $\alpha_{IIb}\beta_3$ i) in the absence of antibody, ii) in the presence of control IgG and iii) in the presence of anti-SLC44A2#1.

6.2.4.3. HEK293T cell expression of SLC44A2

My data supported the contention that SLC44A2 on neutrophils directly interacts with activated $\alpha_{IIb}\beta_3$. Therefore, I aimed to confirm this by expressing *SLC44A2* in HEK293T cells and exploring whether these transfected cells acquire the ability to interact with activated $\alpha_{IIb}\beta_3$.

HEK293T cells were transfected with an expression vector for human SLC44A2 fused to eGFP at the intracellular C-terminus tail. Transfection efficiency was determined by fluorescence microscopy (**Figure 6.8**) and quantified by flow cytometry, which revealed that

75% of the cells were successfully transfected (data not shown). Investigating the transfection efficiency via microscopy was preferred so that cells can be used in other assays.

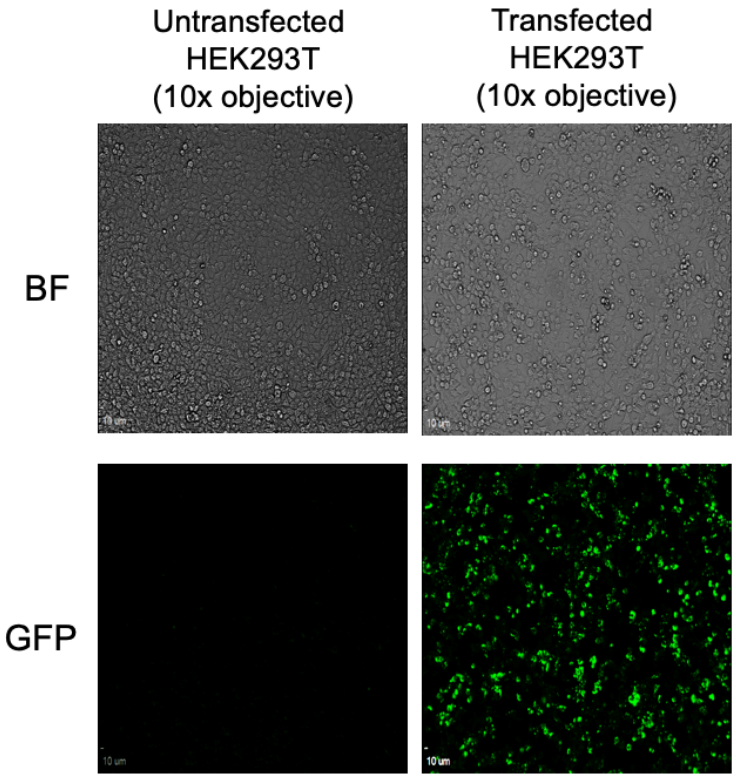

Figure 6.8 Transfection efficiency of HEK293T cells with SLC44A2-eGFP.

Representative micrographs (n=6) of HEK293T cells untransfected vs. transfected with SLC44A2-eGFP after 24 hours, under brightfield and GFP.

After confirming the successful transfection of HEK293T cells 24 hours post-transfection, cells were harvested from the 6-well plates and used in flow assays. Initially, cells were perfused over VWF-'primed' platelets at $50s^{-1}$. However, at this shear rate, cells were seen to briefly interact with platelets, but their interaction could not withstand the flow. To address this issue, I further decreased the shear rate to $25s^{-1}$ when flowing HEK293T cells through these channels. At this shear rate, SLC44A2-transfected cells were seen to roll on and bind to the VWF-'primed' platelets. Importantly, untransfected cells did not interact with the 'primed' platelets at the same shear rate (data not shown). Moreover, perfusing SLC44A2-transfected HEK293T cells through channels coated with VWF, in the absence of platelets, at $25s^{-1}$ for 30

minutes, did not result in any cell binding, confirming that SLC44A2-transfected cells indeed interact with platelets and not with VWF alone. When SLC44A2-transfected cells were pre-incubated with the anti-SLC44A2#1 and when VWF-'primed' platelets were pre-incubated with GR144053, the number of interactions between 'primed' platelets and SLC44A2-transfected HEK293T cells were severely diminished (**Figure 6.9(A-B)**).

Similar results were obtained when perfusing SLC44A2-transfected HEK293T cells through channels directly coated with activated $\alpha_{IIb}\beta_3$. Once again, untransfected HEK293T cells did not bind to these channels, whereas SLC44A2-transfected cells bound to immobilised $\alpha_{IIb}\beta_3$. Pre-incubating these cells with anti-SLC44A2#1 or with GR144053 resulted in a 3-fold and 10-fold decrease, respectively. Pre-incubating the cells with a control rabbit IgG did not result in any changes in the number of cells bound to activated $\alpha_{IIb}\beta_3$ (**Figure 6.9(C)**).

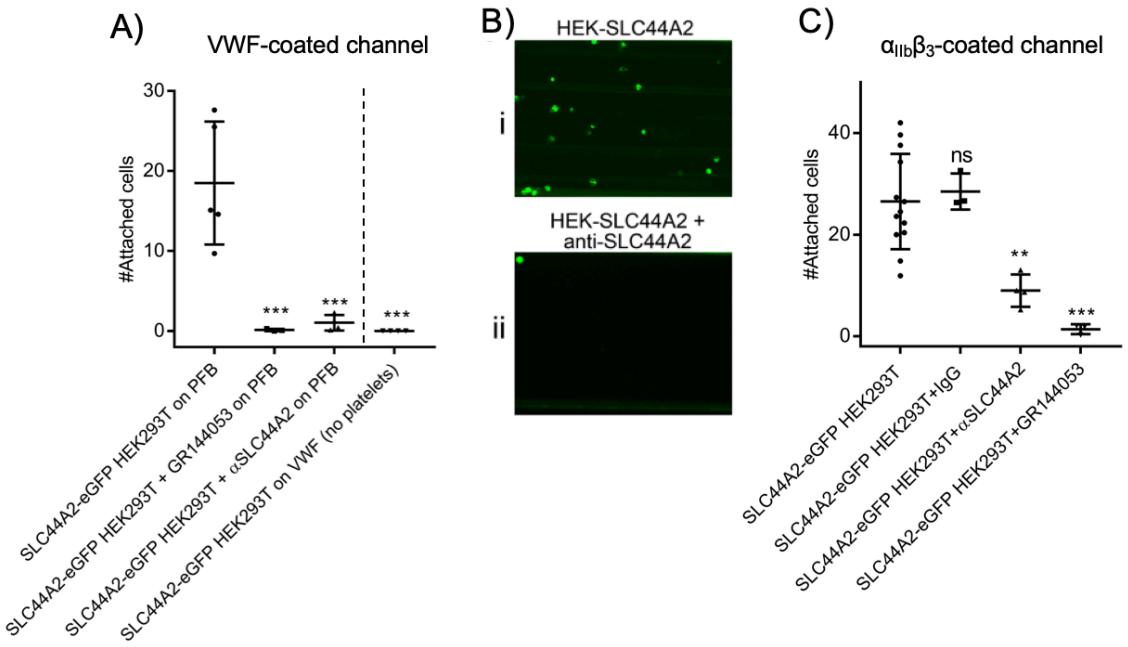

Figure 6.9 HEK293T cells transfected with SLC44A2-eGFP bind to activated $\alpha_{IIb}\beta_3$ under flow.

*A) Graphical representation of the number of HEK293T cells transfected with SLC44A2-eGFP expression vectors interacting with VWF-'primed' platelets. Plasma-free blood was first perfused at 1000s^{-1} for 3.5 mins to capture and 'prime' the platelets, and transfected HEK293T cells were subsequently perfused at 25s^{-1} for 10 mins, in the presence and absence of GR144053 or anti-SLC44A2#1 antibody. HEK293T cells transfected with SLC44A2-eGFP were also perfused over VWF in the absence of platelets, for 30 mins at 25s^{-1}. Data presented are the mean number of bound cells per field of view. Data were analysed using One-Way ANOVA with multiple comparisons. B) Representative micrographs of transfected HEK293T cells attached to VWF-'primed' platelets after 10 minutes of flow at low shear, in the absence (i) or presence (ii) of anti-SLC44A2. C) Graphical representation of the number of HEK293T cells transfected with SLC44A2-eGFP expression vectors binding to activated $\alpha_{IIb}\beta_3$ (captured and activated by LIBS2) after 10 mins flow at 25s^{-1}. Experiments were performed in the presence and absence of either GR144053 or anti-SLC44A2#1 antibody. Data presented are the mean number of bound cells per field of view ±SD. Data were analysed using One-Way ANOVA with multiple comparisons. ns-non-significant, ** p<0.01, *** p<0.001.*

6.2.4.4. SLC44A2 (R154Q) HEK293T cells

A SNP in *SLC44A2* has been identified by GWAS studies as being protective against deep vein thrombosis. This SNP (rs2288904-A) causes a missense mutation (R154Q) in the first extracellular loop of SLC44A2 [365,372]. I hypothesised that this mutation impairs the ability of SLC44A2 to bind to activated $\alpha_{IIb}\beta_3$ and this may represent a reason for the protective effect of this SNP.

To test this hypothesis, I performed site-directed mutagenesis to introduce this mutation (R154Q) in the vector expressing *SLC44A2*. The successful mutagenesis was verified by sequencing. Thereafter, HEK293T cells were transfected with the *SLC44A2 (R154Q)-eGFP* or the wild-type *SLC44A2-eGFP*. Transfection efficiency was observed by fluorescence microscopy (**Figure 6.10**) and confirmed by flow cytometry (data not shown). HEK293T cells were successfully transfected with both the wild-type and with the R154Q *SLC44A2* variant (**Figure 6.10**).

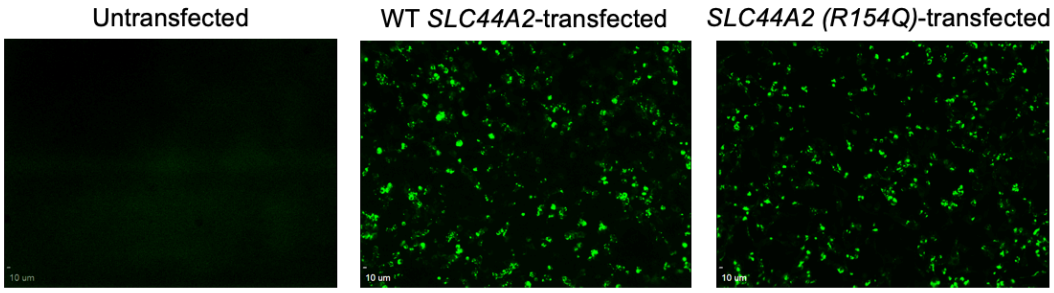

Figure 6.10 Transfection efficiency of HEK293T cells with WT SLC44A2 and SLC44A2 (R154Q).

Representative micrographs of HEK293T cells untransfected (n=6), transfected with wild-type SLC44A2-eGFP (n=6) or with the R154Q variant of SLC44A2 (n=3) after 24 hours.

In flow assays, transfected cells were first perfused over VWF-'primed' platelets at $25s^{-1}$. As shown in **Figure 6.11**, *SLC44A2*-transfected HEK293T cells bound to VWF-'primed' platelets as before, whereas *R154Q SLC44A2*-transfected HEK293T cells exhibited a significantly reduced ability to bind these platelets. As illustrated in **Figure 6.11**, the number of *SLC44A2 (R154Q)*-transfected HEK293T cells interacting with the VWF-'primed' platelets resembles the number of *SLC44A2*-transfected HEK293T cells binding when pre-incubated with anti-SLC44A2#1 or with GR144053. Perfusing transfected cells through channels coated with activated $\alpha_{IIb}\beta_3$ resulted in similar results, though the number of *SLC44A2 (R154Q)*-transfected HEK293T cells binding was only reduced by 2-fold compared to the control, similar to the results obtained when the *SLC44A2*-transfected cells were pre-incubated with anti-SLC44A2#1. Given the location of R154Q, these data further support the contention that SLC44A2 interacts with activated $\alpha_{IIb}\beta_3$ via the first extracellular loop.

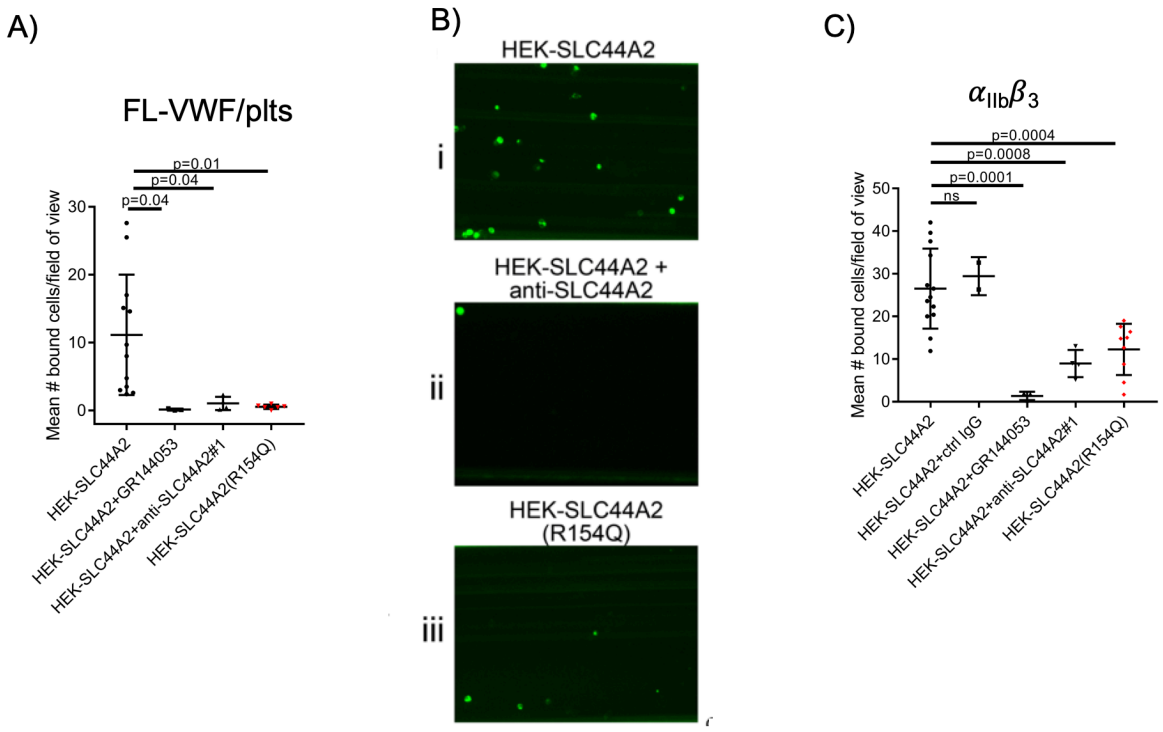

Figure 6.11 HEK293T cells transfected with SLC44A2 (R154Q) have a reduced ability to bind activated $\alpha_{IIb}\beta_3$ under flow.

A) Graphical representation of the number of HEK293T cells transfected with either SLC44A2-eGFP or SLC44A2 (R154Q)-eGFP (shown in red) expression vectors interacting with VWF-'primed' platelets. Plasma-free blood was first perfused at 1000s^{-1} for 3.5 mins to capture and 'prime' the platelets, and transfected HEK293T cells were subsequently perfused at 25s^{-1} for 10 mins, in the presence and absence of GR144053 or anti-SLC44A2#1 antibody. HEK293T cells transfected with SLC44A2-eGFP were also perfused over VWF in the absence of platelets, for 30 mins at 25s^{-1}. Data presented are the mean number of bound cells per field of view ±SD. Data were analysed using One-Way ANOVA with multiple comparisons. B) Representative micrographs of HEK293T cells transfected with i) SLC44A2-eGFP in the absence of antibody, ii) SLC44A2-eGFP in the presence of anti-SLC44A2#1 antibody and iii) SLC44A2 (R154Q)-eGFP bound to activated VWF-'primed' platelets. C) Graphical representation of the number of HEK293T cells transfected with either SLC44A2-eGFP or SLC44A2 (R154Q)-eGFP (shown in red) expression vectors binding to activated $\alpha_{IIb}\beta_3$ (captured and activated by LIBS2) after 10 mins flow at 25s^{-1}. Experiments were performed in the presence and absence of either GR144053 or anti-SLC44A2#1 antibody. Data presented are the mean number of bound cells per field of view. Data were analysed using One-Way ANOVA with multiple comparisons.

6.2.4.5. Genotyping

The polymorphism in *SLC44A2* (rs2288904-A) identified by GWAS studies to be protective against DVT has a prevalence of 22% in human population [365]. I endeavoured to genotype volunteers in an attempt to identify individuals homozygous for the risk allele (rs2288904-G/G), heterozygous individuals (rs2288904-G/A) and individuals homozygous for the protective allele (rs2288904-A/A) (**Figure 6.12**). 37 healthy volunteers who provided written informed consent were genotyped using blood collected through pin prick. As expected, the majority of individuals (31/37) were homozygous for the risk allele. 5/37 individuals were heterozygous and 1/37 was homozygous for the protective allele.

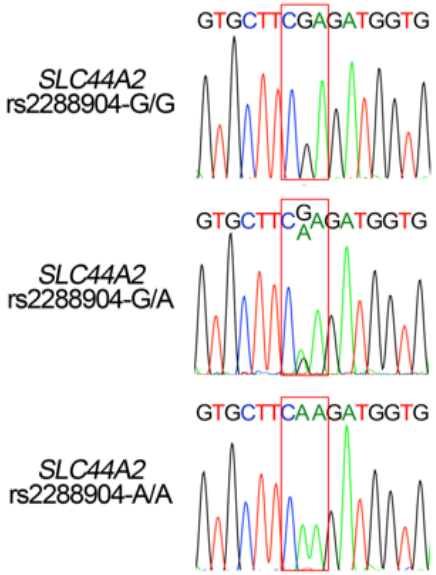

Figure 6.12 SLC44A2 (rs2288904) genotyping.

Healthy volunteers were genotyped to identify individuals homozygous for the protective rs2288904-A/A SNP in SLC44A2. Representative chromatograms for individuals with rs2288904-G/G, rs2288904-G/A, rs2288904-A/A genotypes are shown.

Flow assays were carried out to investigate whether this polymorphism has any functional consequences upon neutrophil binding to platelets. Plasma-free blood generated from individuals homozygous for the risk allele (termed R154/R154) or the protective allele (termed Q154/Q154) was perfused through channels coated with VWF at 1000s^{-1} for 3.5min, followed by 50s^{-1} for 10mins. As seen in **Figure 6.13**, neutrophils homozygous for the protective allele (Q154/Q154) exhibited markedly reduced ability to bind VWF-'primed' platelets. The observed interactions were not significantly further inhibited by the addition of the anti-SLC44A2#1 (**Figure 6.13**, **Movie 7**).

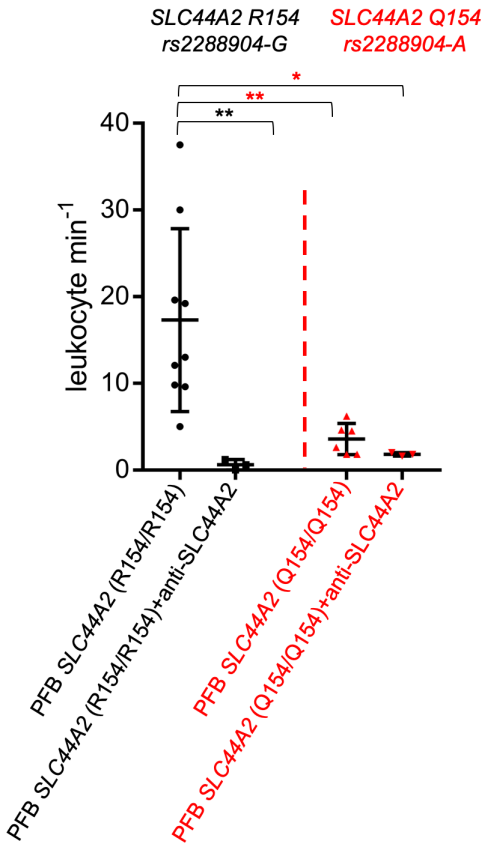

Figure 6.13 Neutrophil ability to bind to VWF-'primed' platelets is reduced in individuals homozygous for rs2288904-A SNP in SLC44A2.

*Graphical representation of the number of neutrophils rolling per minute on VWF-'primed' platelets. PFB from individuals homozygous for the R154-encoding allele of SLC44A2 (R154/R154) or the Q154-encoding allele of SLC44A2 (Q154/Q154) (shown in red) were perfused over 'primed' platelets for 10 mins at 50s^{-1}. Experiments were performed in the presence and absence of the anti-SLC44A2#1 antibody. Data plotted are mean ±SD. Data were analysed using One-Way ANOVA with multiple comparisons; * p<0.05, ** p<0.01.*

6.3. Discussion

Different lines of evidence presented in this thesis demonstrate that activated $\alpha_{IIb}\beta_3$ on VWF-'primed' platelets interacts with leukocytes via a novel receptor. This chapter aimed to identify this receptor, using various different approaches.

After confirming that platelets undergo minimal degranulation as a result of VWF A1-GPIbα dependent signalling, a role for P-selectin-PSGL-1 and CD40L-CD40 axes was excluded. The role of P-seletin-PSGL-1 was further eliminated through experiments in which P-selectin was blocked and had no impact upon the VWF-'primed' platelet-leukocyte interactions. Thereafter, I excluded the other two well-characterised counter-receptors on the leukocyte surface, Mac-1 and LFA-1 from a potential involvement in this interaction. For this purpose, I used a polyclonal antibody against β_2 integrins, which targets both Mac-1 ($\alpha_M\beta_2$) and LFA-1 ($\alpha_L\beta_2$), in flow assays. Despite the high antibody concentration, there was no effect observed on the number of platelet-leukocyte interactions or on the number of neutrophils binding to activated $\alpha_{IIb}\beta_3$. Thus, a role for Mac-1 and LFA-1 can be excluded, considering the following aspects:

1. These receptors require prior activation for ligand binding [347,396].

2. Neutrophils and T cells are the only leukocyte subsets interacting with the 'primed' platelets, whereas Mac-1 and LFA-1 are also highly expressed in monocytes, therefore these receptors could not account for the cell type specificity.

3. Leukocytes compete with fibrinogen to bind to activated $\alpha_{IIb}\beta_3$. Considering that Mac-1 binds to this integrin via fibrinogen [348], the number of platelet-leukocyte interactions would be expected to decrease in the absence of fibrinogen if the interaction was to occur through a bridging mechanism via fibrinogen.

4. Leukocytes do not bind to platelets captured by anti-PECAM-1. Mac-1 was shown to have the ability to bind to GPIbα, while LFA-1 binds to ICAM-2. Both GPIbα and ICAM-2 are

constitutively expressed on the platelet surface [141,349], thus it would be expected that anti-PECAM-1-captured platelets would also bind neutrophils and T cells under flow, if Mac-1 and LFA-1 were the receptors involved.

5. Blocking experiments using a polyclonal antibody against CD18 did not lead to a decrease in the number of VWF-'primed' platelet-leukocyte interactions.

After verifying that the interaction between VWF-'primed' platelets and neutrophils/T cells does not occur via a previously characterised mechanism, I aimed to identify the counter-receptor on neutrophils (and T cells) that binds to activated $\alpha_{IIb}\beta_3$. Assuming that neutrophils and T cells interact with activated $\alpha_{IIb}\beta_3$ via the same receptor and given the ability of activated $\alpha_{IIb}\beta_3$ to induce NETosis, I focussed on identifying the neutrophil receptor first. However, the contention that T cells interact via the same receptor needs to be validated in further experiments.

Initially, I performed pull-down assays, using different strategies. Tosylactivated magnetic beads were directly coupled to $\alpha_{IIb}\beta_3$, to LIBS2 followed by $\alpha_{IIb}\beta_3$, or to the LIBS2-$\alpha_{IIb}\beta_3$ complex pre-formed in solution. However, despite successful capture of $\alpha_{IIb}\beta_3$ on the beads, this integrin remained in an inactive state, unable to bind fibrinogen/neutrophils. To address this issue, a collaboration was established with Prof. Heyu Ni from the University of Toronto, as this group has published work using activated $\alpha_{IIb}\beta_3$-coated magnetic beads [397]. I isolated membrane proteins from purified neutrophils and confirmed the presence of the neutrophil receptor via competition flow assays. Pull-down experiments performed by Dr. Miguel Neves in Prof. Heyu Ni's lab have revealed a list of 265 proteins that bound to activated $\alpha_{IIb}\beta_3$-beads. However, most of these proteins (215) were intracellular protein contaminants, particularly cytoskeletal proteins. These experiments would need to be repeated using an improved approach to ensure the separation of the membrane protein fraction from the cytosolic proteins or aiming to pull-down purified neutrophils that have not been lysed.

Due to the issues encountered during pull-down assays, a different approach was used to identify the neutrophil (and T cell) receptor interacting with activated $\alpha_{IIb}\beta_3$. This consisted of transcriptomic analysis done in collaboration with Dr. Luigi Grassi and Dr. Mattia Frontini from the University of Cambridge, who scrutinised RNA sequencing data from the BLUEPRINT consortium [374] in an attempt to identify genes coding for transmembrane proteins mainly expressed in neutrophils (and T cells) compared to monocytes (and B cells). This strategy identified 93 potential candidates. I applied three further exclusion criteria to narrow down the list of candidates. The presence of the proteins in the plasma membrane as opposed to organelle membranes, the presence of a large (>30a.a.) extracellular domain available for binding and the preferential expression of the candidates in neutrophils compared to monocytes at a proteomic level were crucial characteristics to be fulfilled by the selected candidates. This strategy led to the identification of 30 candidates. Additional candidates could perhaps rationally be excluded based on their low expression levels across the different types of leukocytes (including neutrophils), a higher level in platelets compared to neutrophils (such as SEMA4D, CD274 and TGFBR2) or a predominantly enzymatic activity, which would make them less likely to fulfil a receptor role (i.e. RNF19A, ENTPD4, ASPRV1 and ASPRV2). Within the final list of candidates, the candidate with the highest expression in neutrophils compared to monocytes and meeting all the other criteria was SLC44A2. Moreover, when comparing the lists of candidates obtained via the transcriptomic analysis versus the pull-down assays, the only candidate identified through both approaches was SLC44A2. Based on these data, I hypothesised that SLC44A2 is the neutrophil receptor interacting with VWF-'primed' platelets via activated $\alpha_{IIb}\beta_3$.

SLC44A2 is a cell surface receptor with poorly characterised function. Its structure consists of 10 membrane-spanning domains and five extracellular loops with different lengths – 178a.a., 38a.a., 72a.a., 38a.a. and 18a.a., respectively. Based on this, its inefficient pull-down by the activated $\alpha_{IIb}\beta_3$-magnetic beads could be due to the dissolution of the neutrophil membranes, that likely affected the integrity/conformation of this multi-span membrane protein. This would

very likely have negatively impacted upon the ability of SLC44A2 to bind activated $\alpha_{IIb}\beta_3$. Further pull-down approaches would optimally be performed in the presence of intact purified neutrophils, with their lysis succeeding the binding of the neutrophil receptor to activated $\alpha_{IIb}\beta_3$. However, the issue of membrane disruption and dissociation of SLC44A2 would likely still remain.

To validate the hypothesis that neutrophils bind to activated $\alpha_{IIb}\beta_3$ via SLC44A2, I used antibodies against the first two extracellular loops of SLC44A2 in flow experiments and demonstrated that these inhibited the interaction between VWF-'primed' platelets and neutrophils, and the neutrophil binding to activated $\alpha_{IIb}\beta_3$. Of note, the antibody against the first extracellular loop of SLC44A2 (anti-SLC44A2#2) appeared to be more effective than the antibody against the second extracellular loop (anti-SLC44A2#1), providing scope to believe that SLC44A2 interacts with activated $\alpha_{IIb}\beta_3$ via the first extracellular loop. Secondly, I transfected HEK293T cells with a vector expressing *SLC44A2-eGFP* and showed that these cells developed the capacity to bind VWF-'primed' platelets and activated $\alpha_{IIb}\beta_3$ in a manner that could be inhibited by anti-SLC44A2 antibodies and $\alpha_{IIb}\beta_3$ inhibitors. HEK293T cells required a lower shear of $25s^{-1}$ in order to interact with platelets or $\alpha_{IIb}\beta_3$, likely due to their increased size compared to neutrophils (13μm diameter as opposed to 11μm), which increases the forces upon the cells and the interaction. Moreover, it may also be possible that neutrophils have an additional receptor that helps stabilise the interaction between $\alpha_{IIb}\beta_3$ and SLC44A2 and that without it they cannot withstand the forces exerted by the flowing blood. Since this may be missing from the transfected HEK293T cells, the requirement for lower shear might be explained.

Importantly, and contrary to other reports that suggest that SLC44A2 can directly bind to VWF [371], I did not observe any neutrophils binding to VWF under flow, even after prolonged perfusion (30 minutes, at $50s^{-1}$). Additionally, I did not observe any SLC44A2-transfected HEK293T cells binding to VWF after 30 minutes of flow at $25s^{-1}$ in the flow system I used.

These results confirm the dependency of transfected cell and neutrophil binding on the presence of platelets.

Another reason for our interest in SLC44A2, was its recent recognition as a risk locus for the development of DVT and stroke [365,367], two cardiovascular conditions in which platelet-neutrophil interactions were previously shown to be involved [271,272,360]. Genome-wide association studies (GWAS) on venous thromboembolism (VTE) have previously identified different risk loci with established links to the coagulation system (i.e. *F2, F5*, *F11*, *ABO*, *FGG*, *PROCR*) or well-characterised causative links (i.e. *PROS*, *PROC*, *SERPINC1*) [365-367,399]. Interestingly, a recent study further identified two genes with unknown links to the haemostatic system and no fully characterised roles – *TSPAN15* and *SLC44A2* [365]. Their involvement in the development of DVT remains unclear, although the identification of these genes provides a prospect for potential novel therapeutic targets for the treatment or prevention of DVT.

DVT is one of the leading causes of mortality worldwide [276,277]. Despite being effective, current treatment against DVT is based on anticoagulant therapy with known serious risk of bleeding as a side effect [400,401]. Moreover, although cardiovascular mortality is declining, the incidence of DVT continues to increase [277]. There is, therefore, scope for exploring novel targets to develop better treatments or prophylactic therapies for this condition.

The polymorphism in *SLC44A2* associated with protection against DVT is caused by a SNP (rs2288904-A) leading to a missense mutation (R154Q) in the region coding for the first extracellular loop of SLC44A2. The protective allele (rs2288904-A) has a prevalence of 22%, being most common in Asian populations [365]. Different studies report that this polymorphism is associated with protection against DVT [365-367,372], although the underlying mechanism is not understood. I hypothesised that *SLC44A2* rs2288904-A impairs the ability of neutrophils to bind to VWF-'primed' platelets and, therefore, to induce NETosis.

To test this, I first introduced the R154Q mutation in HEK293T cells. The number of these cells binding to VWF-'primed' platelets and activated $\alpha_{IIb}\beta_3$ was significantly lower than when

wild-type SLC44A2-transfected HEK293T cells were perfused on these channels, supporting this hypothesis. This also further supports the idea that the first extracellular loop of SLC44A2 is involved in binding activated $\alpha_{IIb}\beta_3$, as the R154Q substitution affects the first loop.

To further explore the importance of the *SLC44A2* rs2288904 polymorphism in the VWF-'primed' platelet-neutrophil interactions, I genotyped 37 healthy human volunteers who provided written informed consent and identified one individual homozygous for the protective allele – rs2288904-A/A. Neutrophils from this individual exhibited decreased ability to interact with VWF-'primed' platelets. Pilot experiments also show that fewer *SLC44A2* rs2288904-A/A neutrophils bind to activated $\alpha_{IIb}\beta_3$ compared to *SLC44A2* rs2288904-G/G neutrophils (data not shown). However, due to the donor availability, this experiment was only performed twice and was not included in the results. Neutrophils from heterozygous donors (*SLC44A2* rs2288904-G/A) do not seem to exhibit decreased binding to VWF-'primed' platelets (data not shown). Although the results suggest that the polymorphism *SLC44A2* rs2288904-A provides protection against DVT possibly due to the reduced ability of neutrophils to bind to VWF-'primed' platelets and release NETs, identifying additional individuals homozygous for the protective allele is crucial in confirming this hypothesis.

The importance of SLC44A2 in the development of DVT was also studied in mice. A recent study shows that *Slc44a2*$^{-/-}$ mice are protected against DVT, exhibiting a delayed onset of thrombus formation in the inferior vena cava stenosis model [402]. However, the mechanism behind this has not yet been explored.

Several lines of evidence presented in this chapter demonstrate that the neutrophil receptor binding to activated $\alpha_{IIb}\beta_3$ is, indeed, SLC44A2:

1. SLC44A2 is preferentially expressed in neutrophils (and T cells) compared to monocytes as revealed by proteomic and transcriptomic data.

2. Blocking either of the first two extracellular loops of SLC44A2 using two different antibodies (anti-SLC44A2#1 and anti-SLC44A2#2) significantly reduced the number of VWF-'primed' platelet-neutrophil interactions. Similarly, these blocking antibodies decreased the number of neutrophils binding to activated $\alpha_{IIb}\beta_3$-coated channels in a concentration-dependent manner.

3. HEK293T cells transfected with a vector expressing the *SLC44A2-eGFP* acquired the ability to bind to VWF-'primed' platelets and activated $\alpha_{IIb}\beta_3$ in a manner that could be inhibited by anti-SLC44A2 antibodies or by $\alpha_{IIb}\beta_3$ inhibitors (GR144053).

4. Introducing the R154Q mutation in the vector expressing the *SLC44A2-eGFP* prior to HEK293T cell transfection, resulted in an impaired ability of transfected cells to bind to VWF-'primed' platelets or activated $\alpha_{IIb}\beta_3$.

5. Neutrophils homozygous for the *SLC44A2* rs2288904-A allele, which was shown to be protective against DVT, exhibited a reduced ability to bind VWF-'primed' platelets.

Neutrophil role in DVT has been described to primarily be based on their ability to release highly pro-thrombotic NETs [272,339,340]. Based on the data presented in **Chapters 3 and 4**, I propose that the novel interaction between VWF-'primed' platelets via activated $\alpha_{IIb}\beta_3$, and neutrophils, via SLC44A2, drives NETosis under flow, being involved in the initial events leading to thrombus formation in DVT. Different lines of evidence presented both in this thesis, and in the literature, support this hypothesis. *VWF*$^{-/-}$ mice, as well as *GpIba*$^{-/-}$ mice, are protected against experimental DVT, in both stenosis and stasis models [271,403,404], confirming a role for the VWF A1-GPIbα in the development of DVT. Neutrophil and subsequent NET involvement in DVT has been confirmed by studies showing that neutrophil depletion or NET degradation protects against DVT [272,340]. Moreover, the SNP in *SLC44A2* (rs2288904-A) has recently been linked to protection against DVT [365-367,372]. Neutrophils from individuals homozygous for the *SLC44A2 rs2288904-A* allele, exhibit a reduced ability to bind to activated $\alpha_{IIb}\beta_3$, confirming a role for the $\alpha_{IIb}\beta_3$-SLC44A2 interaction in DVT. Finally, the interaction

between VWF-'primed' platelets and neutrophils appears to be augmented under disturbed flow conditions, at sites of bifurcations (**Chapter 2**) or within pockets surrounding artificial venous valves (data not shown). All these data suggest implications of this novel interaction beyond the initial scopes of this project, providing novel mechanistic insights for platelet-induced NET release and suggesting a role for activated $\alpha_{IIb}\beta_3$ and SLC44A2 in the initial events of DVT. Ultimately, this mechanism should be investigated *in vivo*. The final chapter of this thesis aims to characterise a novel knock-in mouse generated for the purpose of studying the pathophysiological importance of this project further.

7. Chapter 5 – Characterisation of VWF A1-GPIbα mediated signalling in vivo

7.1. Introduction

After characterising the VWF-dependent platelet 'priming' and subsequent platelet-leukocyte interactions *in vitro*, the final aim of my thesis was to further investigate this using an *in vivo* model. In light of my results, a novel transgenic mouse was generated, and this chapter presents its initial characterisation.

Platelet capture to sites of vessel injury is highly dependent on the VWF A1-GPIbα interaction. Although classically this interaction was thought to solely occur for the purpose of platelet recruitment, we and others have shown that this VWF-dependent tethering also induces signalling within platelets, leading to the activation of platelet integrin $\alpha_{IIb}\beta_3$ [55,405]. These signalling events are absolutely dependent on the presence of shear. VWF A1 domain binds to GPIbα via its leucine-rich repeat site and, under flow, this causes the mechano-unfolding of the juxtamembrane stalk, which likely induces a conformational change in the intracellular tail of GPIbα that modulates its signalling function [144].

The intracellular tail of GPIbα can bind to signalling molecules, such as PI3-kinase and 14-3-3 isoforms via its last 31 amino acids (a.a. 580-610 in human GPIbα and a.a. 689-718 in mouse GPIbα) [147,152,154]. Importantly, the intracellular tail of GPIbα also contains a filamin-binding site, through which GPIbα anchors the platelet actin cytoskeleton [151,406]. **Figure 7.1** illustrates the sequence alignment of the last 60 amino acids of human and mouse GPIbα. The difference in GPIbα sequence in mouse versus human is caused by the 108 amino acids longer juxtamembrane stalk in mouse GPIbα.

Figure 7.1 Intracellular tail of GPIbα.

Sequence alignment of the last 60 amino acids within the intracellular tail of GPIbα in human versus mouse. The serine residues marked in red correspond to the serine phosphorylation sites. The binding sites for filamin, PI3 kinase and 14-3-3 isoforms are indicated.

As revealed by this thesis and previously published studies, VWF A1-GPIbα signalling causes intracellular Ca^{2+} release and culminates with the activation of $\alpha_{IIb}\beta_3$ [55,405]. This has been considered redundant in the setting of normal haemostasis, due to the presence of potent platelet agonists that more robustly activate the platelets. Based on the results presented in previous chapters, I hypothesised that VWF-dependent platelet signalling with subsequent neutrophil recruitment and shear-induced NET formation is important in the initial events leading to DVT. To investigate this, a novel transgenic mouse (*GpIbα*$^{\Delta sig/\Delta sig}$) was generated using the CRISPR/Cas9 technology, to analyse the importance of VWF-mediated platelet signalling *in vivo*.

GpIbα$^{-/-}$ and *Vwf*$^{-/-}$ mice already exist [34,157]. However, in both cases, VWF-platelet recruitment is completely abolished, making it impossible to study the A1-GPIbα downstream signalling events. The presence of the extracellular domain of GPIbα, as well as VWF A1 domain are crucial for studying the role of this interaction. Moreover, it is important to preserve the filamin-binding site (a.a. 665-683 in mouse GPIbα) to prevent any cytoskeletal platelet defects that could influence platelet phenotype. Indeed, complete deletion of GPIbα in mice, as well as GPIbα deficiency in humans, known as Bernard-Soulier syndrome, is associated with the presence of giant platelets (size increase from 1-2μm to 4-10μm) within the vasculature and abnormalities in proplatelet production [155,157,407]. Previous attempts to ablate the VWF A1-GPIbα mediated signalling without affecting platelet binding to VWF or disrupting the filamin-binding site were endeavoured. Kanaji *et al.* introduced a *GpIba* transgene lacking the last 6 amino acids of the intracellular tail of GPIbα in *GpIbα*$^{-/-}$ mice. However, although the authors reported a mild phenotype, the deletion of the last 6 amino acids proved to be insufficient in completely disrupting the binding of 14-3-3 isoforms or PI3-kinase to the intracellular tail of GPIbα [408].

In light of these studies, *GpIbα*$^{\Delta sig/\Delta sig}$ mice were generated by introducing an early stop codon after Pro694 by CRISPR-Cas9 technology, leading to the deletion of the last 24 amino acids

of the intracellular tail of GPIbα (a.a. 695-718). This was hypothesised to completely (rather than partially) ablate the ability of 14-3-3 and PI3-kinase to bind and mediate signalling events within platelets, while the filamin-binding site and ability of platelets to bind to the VWF A1 domain remain intact. The aim of this chapter was to characterise these novel transgenic mice, by analysing their full blood counts, the ability of their platelets to aggregate and spread in response to various stimuli and, finally, to investigate the ability of *GpIbα*$^{\Delta sig/\Delta sig}$ to become 'primed' and recruit neutrophils under flow. We hypothesized that these mice would have normal platelets, with unaffected VWF binding, but with deficient VWF-dependent platelet 'priming'. These mice would then allow formal investigation of the importance of VWF-GPIbα mediated signalling *in vivo*.

7.2. Results

7.2.1. Evaluating full blood counts

GpIbα$^{\Delta sig/\Delta sig}$ mice were generated using the CRISPR-Cas9 technology and back-crossed to C57BL/6 background. Initial characterisation of these mice in comparison to their wild-type littermates was performed by Dr. Isabelle Salles-Crawley. *GpIbα*$^{\Delta sig/\Delta sig}$ mice were found to have normal levels of the main platelet receptors (GPIbα, GPIbβ, GPVI and $\alpha_{IIb}\beta_3$) on their platelet surface, with the truncated version of GPIbα being confirmed by Western blotting. Moreover, as predicted, these mice presented no haemostatic defect (data not shown).

The next step in characterising the *GpIbα*$^{\Delta sig/\Delta sig}$ mice was to analyse their full blood counts. Mouse blood was collected retro-orbitally in 3.8% citrate by Dr. Salles-Crawley and diluted in 1x HT buffer. Samples were analysed within the Pathology laboratory at Hammersmith Hospital London. The parameters analysed include the red blood cell, white blood cell and platelet counts, as well as haemoglobin levels and haematocrit and their values are summarised in **Figure 7.2**.

Red blood cell counts (RBC), white blood cell counts (WBC), haemoglobin levels (Hb) and haematocrit (Ht) did not appreciably vary between the two mouse genotypes - *GpIbα*$^{+/+}$ and *GpIbα*$^{\Delta sig/\Delta sig}$ (**Figure 7.2**). However, the total number of platelets (PLT) was decreased by 20% in *GpIbα*$^{\Delta sig/\Delta sig}$ mice compared to wild-type mice. Total platelet count average was 1028±187 x10^3/μl in *GpIbα*$^{+/+}$ mice, as opposed to 818±138 x10^3/μl for *GpIbα*$^{\Delta sig/\Delta sig}$ mice.

	***GPIba*$^{+/+}$**	***GPIba*$^{\Delta sig/\Delta sig}$**
RBC (10^6/μL)	8.95±0.97	8.75±0.69
WBC (10^3/μL)	5.92±1.8	6.78±1.51
Hg (g/dL)	15±1.14	14.8±1.18
Ht (%)	50.7±5.18	49.7±3.24
PLT (10^3/μL)	1028±187	818±138***

Figure 7.2 Full blood counts in GpIbα*$^{+/+}$ *and GpIbα*$^{\Delta sig/\Delta sig}$ *mice.

*Haematological markers assessed include red blood cell counts (RBC), white blood cell count (WBC), haemoglobin values (Hg), haematocrit (Ht) and platelet counts (PLT). Data displayed as mean ±SD. n=12 for each mouse genotype. Data were analysed using two-tailed, unpaired Student's t-test. *** p<0.001.*

Platelet counts were further analysed by flow cytometry (Fortessa) using precision count beads. As illustrated in **Figure 7.3**, the significant reduction in platelet count was confirmed through this approach. Moreover, the population shift on the forward scatter indicates an increase in platelet size in *GpIbα*$^{\Delta sig/\Delta sig}$ mice.

White blood cell counts including Ly6C^{high}, Ly6C^{low} monocytes, Ly6G^{high} neutrophils, CD4$^+$ T cells, CD8$^+$ T cells and CD19$^+$ B cells were also analysed using flow cytometry and revealed no differences in *GpIbα*$^{\Delta sig/\Delta sig}$ compared to *GpIbα*$^{+/+}$ mice (data not shown).

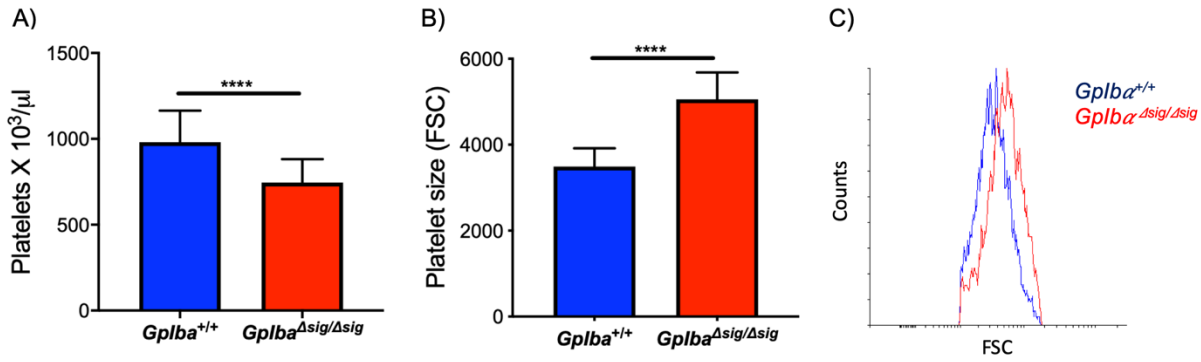

Figure 7.3 Platelet counts and size in Gplbα$^{+/+}$ and Gplbα$^{\Delta sig/\Delta sig}$ mice.

A) *Bar graph displaying the platelet counts in Gplbα$^{+/+}$ and Gplbα$^{\Delta sig/\Delta sig}$ mice as analysed by flow cytometry. n=25 (Gplbα$^{+/+}$) and n=30 (Gplbα$^{\Delta sig/\Delta sig}$).* ***B)*** *Bar graph displaying the platelet size in Gplbα$^{+/+}$ and Gplbα$^{\Delta sig/\Delta sig}$ mice as analysed by flow cytometry. n=13 (Gplbα$^{+/+}$) and n=11 (Gplbα$^{\Delta sig/\Delta sig}$). Data displayed as mean ±SD. Data were analysed using two-tailed, unpaired Student's t-test. **** p<0.0001.* ***C)*** *Representative histogram depicting the shift in the platelet population on the forward scatter (FSC) in Gplbα$^{\Delta sig/\Delta sig}$ (red) compared to Gplbα$^{+/+}$ (blue).*

7.2.2. Evaluating platelet aggregation

Platelet aggregation was analysed using the Chronolog 700 Platelet Aggregometer. Mouse platelets were washed as detailed in **Methods Section 2.10.1**, and resuspended in 1x HT buffer supplemented with 0.35% BSA. Aggregation was analysed in the presence of 1mM $CaCl_2$, 70µg/ml fibrinogen and different platelet agonists. The agonists used include thrombin, ADP and CRP, at different concentrations.

Thrombin was not expected to induce a different response in the two mouse genotypes. As predicted, using three different concentrations of thrombin (0.05U/ml, 0.02U/ml or 0.01U/ml) did not lead to any appreciable differences in platelet aggregation (**Figure 7.4**).

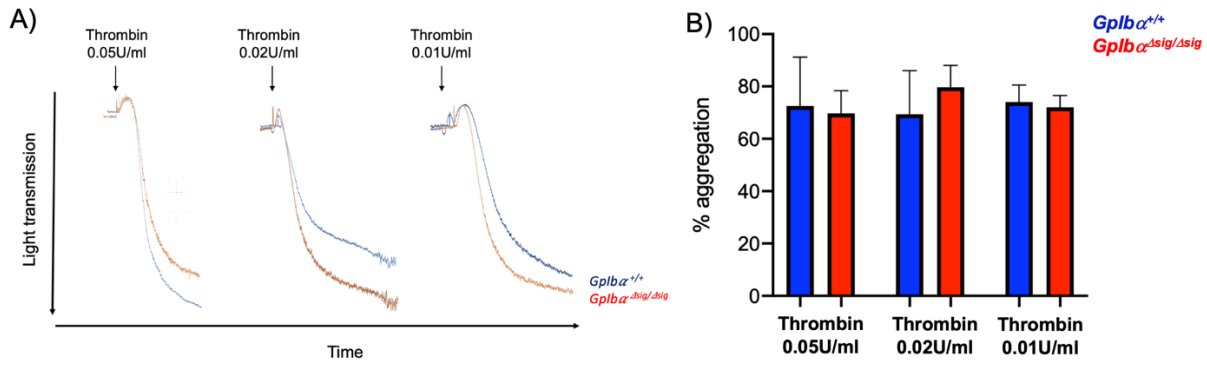

Figure 7.4 Platelet aggregation in response to thrombin.

A) *Representative aggregation traces of washed platelets isolated from GpIbα$^{+/+}$ (navy) or GpIbα$^{\Delta sig/\Delta sig}$ (red) mice and stimulated with 0.05U/ml, 0.02U/ml or 0.01U/ml thrombin. Aggregation was monitored using a Chronolog aggregometer over 6 minutes. Representative of n=3-6.* ***B)*** *Bar chart comparing the % aggregation in GpIbα$^{+/+}$ or GpIbα$^{\Delta sig/\Delta sig}$ mice using the aggregometry assay presented in* ***A)****. Data displayed as mean ±SD; n=3-6. Data were analysed using unpaired Student's t-test.*

Platelet aggregation in response to ADP (10μM, 5μM or 1μM) was also normal in *GpIbα$^{\Delta sig/\Delta sig}$* mice. The overall aggregation only reached levels of 20% in both *GpIbα$^{+/+}$* platelets and *GpIbα$^{\Delta sig/\Delta sig}$* platelets (**Figure 7.5**), due to the modest potency of this agonist that has previously been established.

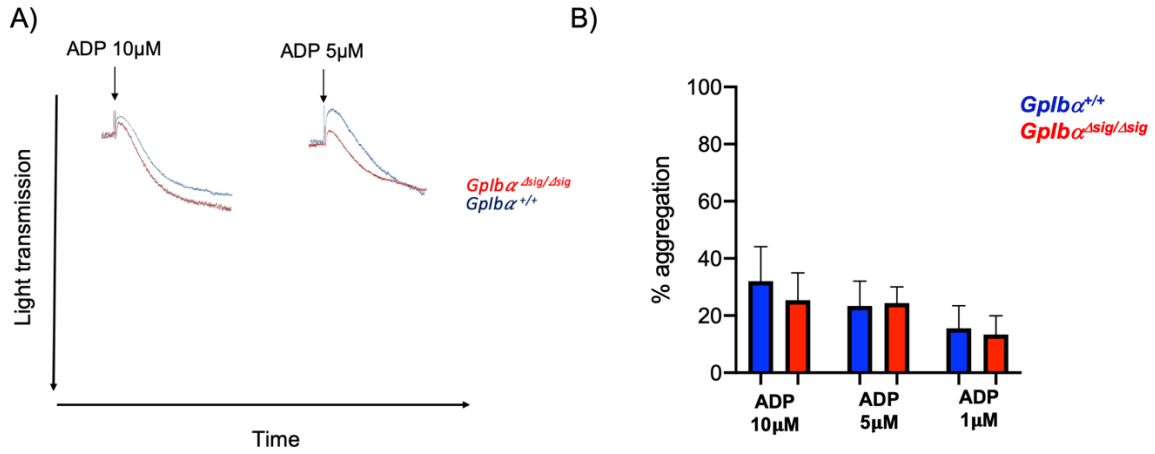

Figure 7.5 Platelet aggregation in response to ADP.

A) *Representative aggregation traces of washed platelets isolated from GpIbα$^{+/+}$ (navy) or GpIbα$^{\Delta sig/\Delta sig}$ (red) mice and stimulated with 10μM or 5μM ADP. Aggregation was monitored using a Chronolog aggregometer over 6 minutes. Representative of n=3.* ***B)*** *Bar chart comparing the % aggregation in GpIbα$^{+/+}$ or GpIbα$^{\Delta sig/\Delta sig}$ mice using the aggregometry assay presented in* ***A)****. Data displayed as mean ± SD; n=3. Data were analysed using unpaired Student's t-test.*

Finally, collagen-related peptide (CRP) (10μg/ml, 3μg/ml, 1μg/ml, 0.5μg/ml or 0.25μg/ml) was added to washed platelets immediately prior to aggregation experiments to investigate the collagen-mediated (i.e. GPVI) signalling in *GpIbα*$^{\Delta sig/\Delta sig}$ mice. Titrating the concentration of CRP from 10μg/ml to 0.25μg/ml did not result in any differences in the ability of platelets to aggregate (**Figure 7.6**).

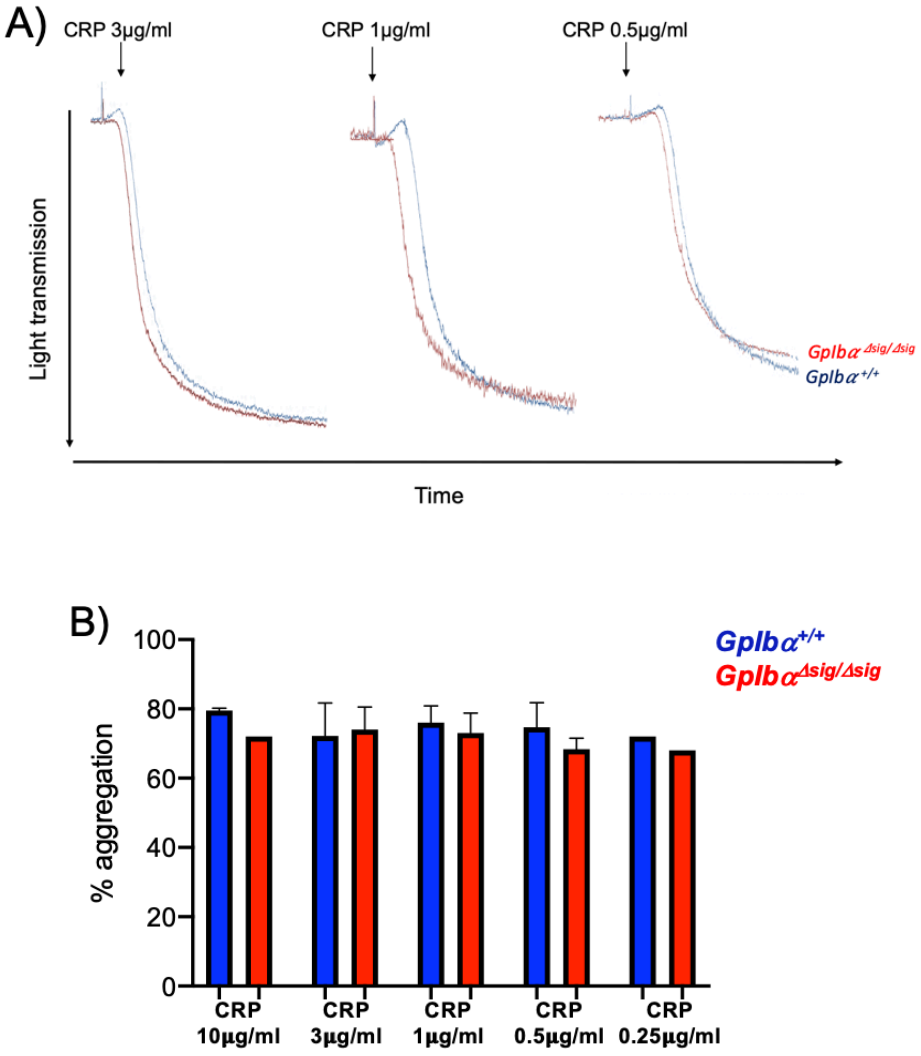

Figure 7.6 Platelet aggregation in response to CRP.

A) *Representative aggregation traces of washed platelets isolated from GpIbα*$^{+/+}$ *(navy) or GpIbα*$^{\Delta sig/\Delta sig}$ *(red) mice and stimulated with 3μg/ml, 1μg/ml or 0.5μg/ml CRP. Aggregation was monitored using a Chronolog aggregometer over 6 minutes. Representative of n=3-5.* ***B)*** *Bar chart comparing the % aggregation in GpIbα*$^{+/+}$ *or GpIbα*$^{\Delta sig/\Delta sig}$ *mice using the aggregometry assay presented in* ***A)****, alongside other concentrations of CRP (10μg/ml and 0.25μg/ml). Data displayed as mean ± SD; n=1-5. Data were analysed using unpaired Student's t-test, when n≥2.*

7.2.3. Evaluating platelet spreading

Platelet function in *GpIbα*$^{\Delta sig/\Delta sig}$ versus *GpIbα*$^{+/+}$ mice was also investigated by platelet spreading. Glass coverslips were coated with fibrinogen (200μg/ml), CRP (100μg/ml), or BSA (0.5mg/ml) and incubated with platelets under basal conditions or following thrombin-stimulation. Additional coverslips coated with fibrinogen were also treated with thrombin to generate fibrin-coated coverslips. Preliminary experiments reveal that *GpIbα*$^{\Delta sig/\Delta sig}$ and *GpIbα*$^{+/+}$ platelets exhibit similar spreading on fibrinogen under both activated and resting conditions (**Figure 7.7**).

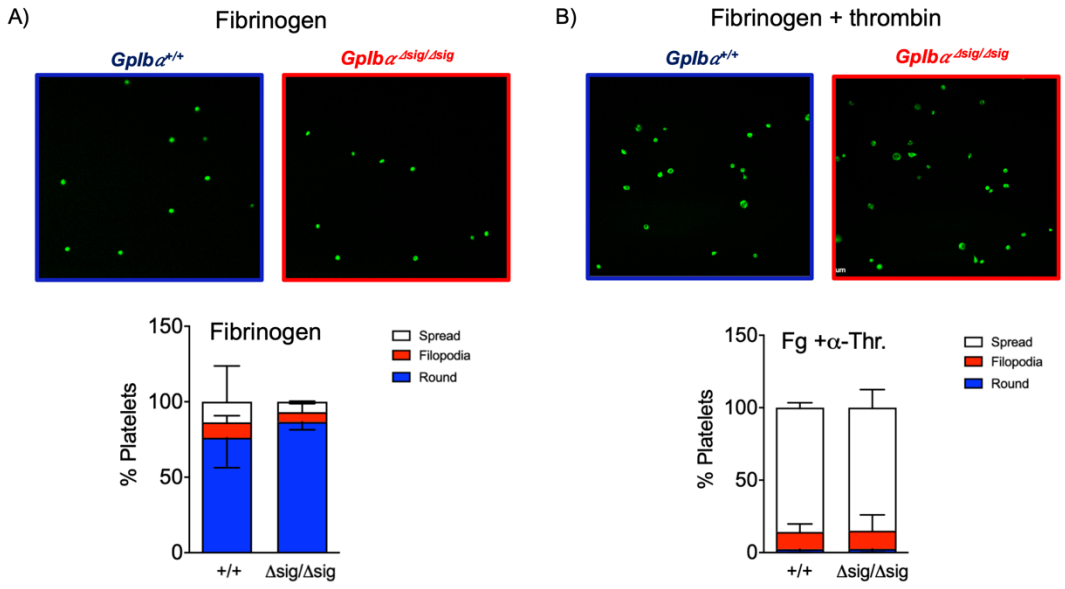

Figure 7.7 Platelet spreading on fibrinogen.

A) *Representative images and bar graph of platelets from GpIbα*$^{+/+}$ *or GpIbα*$^{\Delta sig/\Delta sig}$ *mice spread on fibrinogen under resting conditions. Bar graph presents the percentages of platelets that are round (blue), have filopodia (red) or are fully spread (white). Data are plotted as mean ±SD. n=3.* ***B)*** *Representative images and bar graph of platelets from GpIbα*$^{+/+}$ *or GpIbα*$^{\Delta sig/\Delta sig}$ *mice spread on fibrinogen after stimulation with thrombin. Bar graph presents the percentages of platelets that are round (blue), have filopodia (red) or are fully spread (white). Data are plotted as mean ±SD. n=3.*

In contrast, *GpIbα*$^{\Delta sig/\Delta sig}$ platelets appear to have a reduced ability to spread on CRP and fibrin, although these data have not been statistically analysed (**Figure 7.8**). These pilot data suggest that deleting the last 24 amino acids in the intracellular tail of GPIbα might have an effect upon GPVI-mediated platelet signalling. This contention is currently under further investigation.

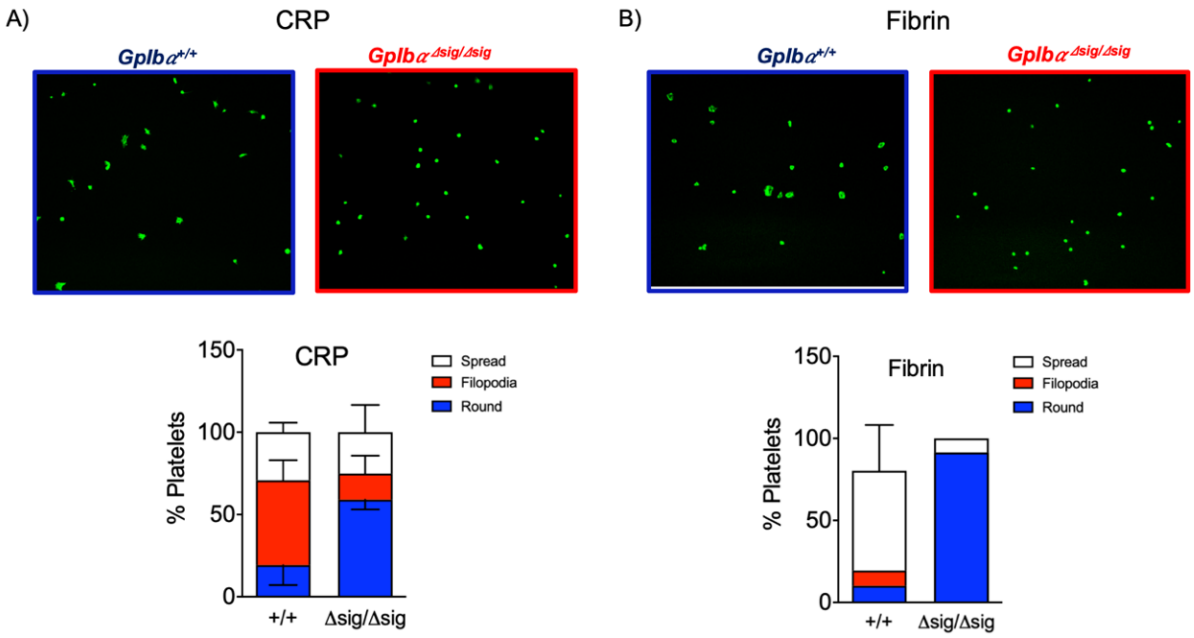

Figure 7.8 Platelet spreading on CRP and fibrin.

A) *Representative images and bar graph of platelets from GpIbα*$^{+/+}$ *or GpIbα*$^{\Delta sig/\Delta sig}$ *mice spread on CRP. Bar graph presents the percentages of platelets that are round (blue), have filopodia (red) or are fully spread (white). Data are plotted as mean ±SD. n=3.* ***B)*** *Representative images and bar graph of platelets from GpIbα*$^{+/+}$ *or GpIbα*$^{\Delta sig/\Delta sig}$ *mice spread on fibrin after stimulation with thrombin. Bar graph presents the percentages of platelets that are round (blue), have filopodia (red) or are fully spread (white). Data are plotted as mean, n=1-2.*

A pilot experiment was also performed using coverslips coated with murine VWF. Platelets from either *GpIbα*$^{+/+}$ or *GpIbα*$^{\Delta sig/\Delta sig}$ mice were pre-treated with Botrocetin in the presence or absence of GR144053 before being incubated on murine VWF-coated coverslips. Preliminary data suggests that fewer platelets from *GpIbα*$^{\Delta sig/\Delta sig}$ compared to *GpIbα*$^{+/+}$ were able to spread on murine VWF in the presence of Botrocetin and GR144053 (**Figure 7.9**), suggesting that

there is a defect in VWF-mediated platelet signalling exhibited by *GpIbα*$^{\Delta sig/\Delta sig}$ mice. The addition of GR144053 ensures that the effects observed are exclusively caused by the VWF A1-GPIbα interaction, and not by 'outside-in' signalling mediated via the VWF C4 domain binding to activated $\alpha_{IIb}\beta_3$.

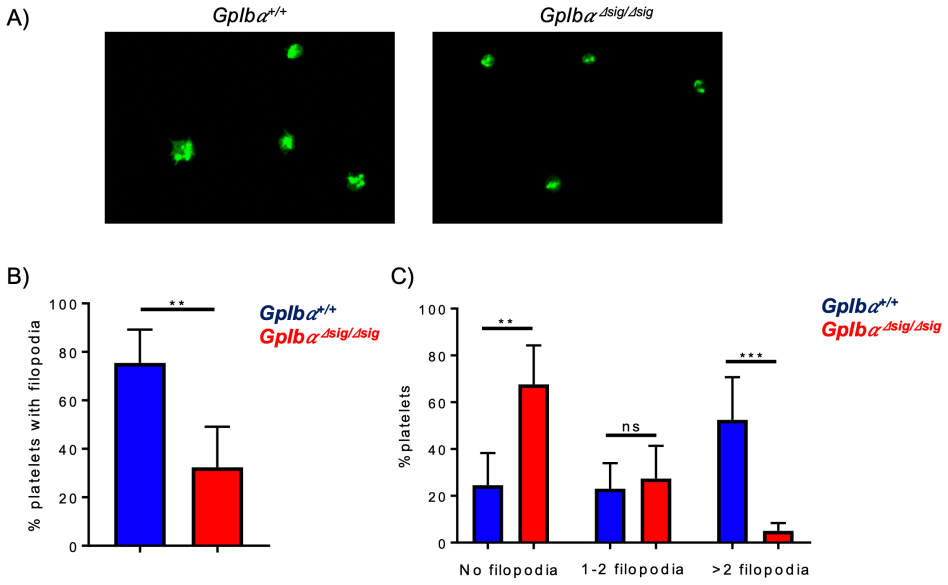

Figure 7.9 Platelet spreading on VWF.

A) *Representative images of platelets from GpIbα*$^{+/+}$ *or GpIbα*$^{\Delta sig/\Delta sig}$ *mice spread on VWF, in the presence of Botrocetin and GR144053, stained with Phalloidin.* ***B)*** *Bar graph depicting the percentage of platelets with filopodia from GpIbα*$^{+/+}$ *or GpIbα*$^{\Delta sig/\Delta sig}$ *mice.* ***C)*** *Bar graph depicting the percentages of platelets with no filopodia, 1-2 filopodia or more than 2 filopodia. Data are plotted as mean ±SD. n=4-6 fields of view from one experiment. Data were analysed using unpaired Student's t-test.*

7.2.4. Flow assays

After confirming that platelets from *GpIbα*$^{\Delta sig/\Delta sig}$ mice exhibit normal aggregation following stimulation with different agonists, we explored the implications of deleting the last 24 amino acids from the intracellular tail of GPIbα in VWF-mediated platelet capture.

Microfluidic channels were coated with murine VWF (mVWF) or the human recombinant A1*. As expected, perfusing whole blood (WB) or plasma-free blood collected from *GpIbα*$^{+/+}$ or *GpIbα*$^{\Delta sig/\Delta sig}$ mice at 1000s^{-1} through channels coated with either mVWF or recombinant A1*

resulted in normal platelet capture (**Figure 7.10**), confirming the normal expression of GPIbα extracellular domain.

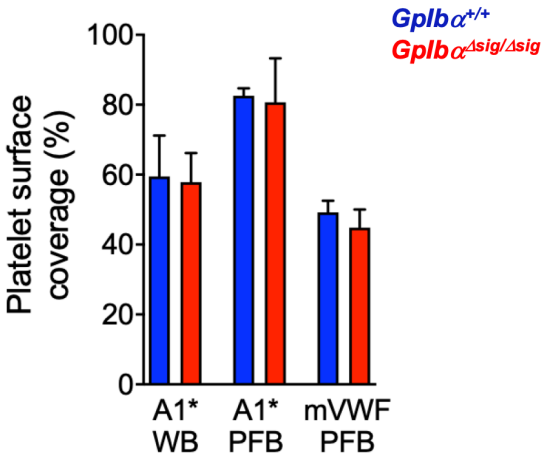

Figure 7.10 Platelet coverage on VWF A1* and murine VWF.

Bar chart depicting platelet capture on VWF A1 or murine VWF (mVWF) in whole blood (WB) or plasma-free blood (PFB) conditions from GpIbα$^{+/+}$ or GpIbα$^{Δsig/Δsig}$ mice. Platelet capture was analysed after 3 minutes of flowing WB or PFB through the channels at 1000s^{-1}. Data displayed as mean ± SEM; n=3 separate experiments for each set of conditions. Data were analysed using unpaired Student's t-test.*

The main aim of this chapter was to investigate whether platelets from *GpIbα$^{Δsig/Δsig}$* mice still retain the ability to recruit neutrophils under low shear. Neutrophils were stained with Ly6G-PE and perfused over platelets captured by VWF or A1* at low shear, for 10 minutes. Images were acquired across the channels at the end of the experiment and the number of neutrophils bound was manually counted and expressed as number of neutrophils bound per field of view. As presented by the graph in **Figure 7.11(A)**, the number of neutrophils bound was reduced by 2-fold when using *GpIbα$^{Δsig/Δsig}$* whole blood on A1*-coated channels compared to *GpIbα$^{+/+}$* whole blood.

In line with the results obtained when using human blood, there was an increase in the number of neutrophils interacting with A1*-captured platelets in plasma-free blood compared to whole blood in wild-type mice (**Figure 7.11(A)**), suggesting that neutrophils from wild-type mice compete with plasma in binding to VWF-'primed' platelets. In contrast, experiments performed

using plasma-free blood from *GpIbα*$^{\Delta sig/\Delta sig}$ mice did not exhibit an increase in the number of neutrophils binding.

Similar results were obtained when plasma-free blood was perfused through channels coated with murine VWF (mVWF). There was a 50% reduction in the number of neutrophils interacting with VWF-captured platelets from *GpIbα*$^{\Delta sig/\Delta sig}$ mice compared to their wild-type littermates. Finally, if plasma-free blood from wild-type mice was incubated with GR144053, there was a significant decrease in the number of neutrophils binding, suggesting a role for activated $\alpha_{IIb}\beta_3$ in neutrophil recruitment (**Figure 7.11(B-C)**).

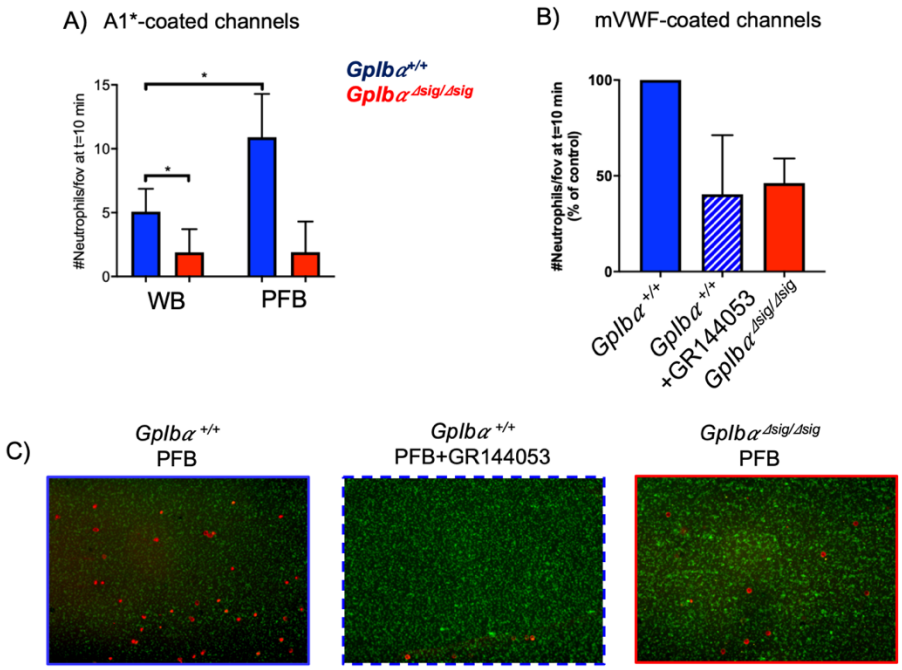

Figure 7.11 Murine VWF-'primed' platelet-neutrophil interactions.

A) *Bar chart analysing the number of neutrophils bound per field of view after 10 min of perfusion over platelets captured by A1*. Whole blood (WB) or plasma-free blood (PFB) was perfused through channels coated with A1* at 1000s*$^{-1}$ *for 3.5 min, channels were washed with 1x HT and then lysed blood labelled with Ly6G-PE was perfused through the channels for 10 min at 50s*$^{-1}$*. The number of attached neutrophils was counted across the channels after 10 minutes.* ***B)*** *Experiments were performed as described in* ***A)****, but plasma-free blood was perfused through channels coated with mVWF, in the presence or absence of GR144053. The number of neutrophils bound on the mVWF-'primed' platelets are expressed relative to the control. Data displayed as mean ±SD; n=2-4. Data were analysed using unpaired Student's t-test.* ***C)*** *Representative images of PFB platelets (green) from GpIbα*$^{+/+}$ *or GpIbα*$^{\Delta sig/\Delta sig}$ *mice, in the presence and absence of GR144053, captured by VWF and interacting with neutrophils (red). Images were captured after 10 minutes of flowing neutrophils labelled with Ly6G-APC through the channels at 50s*$^{-1}$*. Images representative of n=4.*

7.3. Discussion

The aim of this chapter was to complete the initial characterisation of a novel transgenic mouse, *GpIbα*$^{\Delta sig/\Delta sig}$, generated in light of the results presented in **Chapters 1-4**. *GpIbα*$^{\Delta sig/\Delta sig}$ were generated by CRISPR/Cas9 technology, in which an early stop codon was introduced to create a truncated version of GPIbα, lacking the last 24 amino acids of its intracellular tail. These mice are predicted to have normal capture to VWF A1 domain, as the extracellular domain of GPIbα is intact. Moreover, the filamin binding site normally represented by the sequence between a.a. 665-683, is not affected by the early stop codon, suggesting that these mice should have normal platelet numbers and size, as opposed to *GpIbα*$^{-/-}$ mice. However, despite normal capture to VWF A1 domain, *GpIbα*$^{\Delta sig/\Delta sig}$ are not expected to undergo VWF-mediated signalling, due to the deletion of the last 24 amino acids in the intracellular tail of GPIbα. This change is intended to abolish the binding of 14-3-3 isoforms and PI3-kinase, which are thought to be involved in the signalling initiation. Characterisation of *GpIbα*$^{\Delta sig/\Delta sig}$ mice was performed together with my supervisor, Dr. Isabelle Salles-Crawley.

Full blood counts in these mice and their wild-type *GpIbα*$^{+/+}$ littermates were analysed. Most parameters were within normal ranges, with no significant differences observed in red blood cell and white blood cell counts, haemoglobin levels and haematocrit. However, a reduction in platelet numbers could be observed in *GPIbα*$^{\Delta sig/\Delta sig}$ mice. Although significantly decreased, platelet numbers were only reduced by 20%, suggesting that it would be unlikely for these mice to present with a haemostatic defect, as previously shown by Morowski *et al.* [120]. In support of this, data obtained by Dr. Salles-Crawley suggests that *GpIbα*$^{\Delta sig/\Delta sig}$ mice have a normal haemostatic response following tail transection (data not shown).

Additional to the decrease in platelet counts, *GpIbα*$^{\Delta sig/\Delta sig}$ mice also present an increase in platelet size. This is unexpected given that the filamin binding site between a.a. 665-683 was preserved. However, studies suggest that there might be additional or extended filamin

binding sites within the intracellular tail of GPIbα [151] that are not fully characterised and might, therefore, have been affected by the deletion of the last 24 amino acids. Importantly, the increase in platelet size is very modest compared to the effect observed in *GpIbα*$^{-/-}$ mice (**Figure 7.12)** or in Bernard-Soulier patients (characterised by giant platelets, with a diameter of 4-10μm [155]), where the filamin binding site in GPIbα is completely disrupted [409]. The increase in platelet size might also account for the reduction in platelet numbers in *GpIbα*$^{\Delta sig/\Delta sig}$ mice.

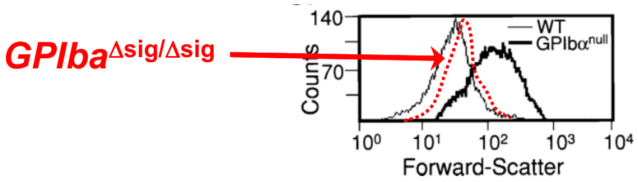

Figure 7.12 Murine platelet size

Histogram depicting the shift in the murine platelet populations from GpIbα$^{+/+}$ *(grey line), GpIbα*$^{-/-}$ *(black line) and GpIbα*$^{\Delta sig/\Delta sig}$ *mice (dotted red line), according to their size on the forward scatter. Adapted from [409] (Copyright (2000) National Academy of Sciences).*

After characterising platelet morphology and blood counts, we aimed to perform functional characterisation of the *GpIbα*$^{\Delta sig/\Delta sig}$ platelets. One of the most established ways to investigate normal platelet function is through Born-aggregometry. We did not observe a difference in either lag time or percentage of platelets aggregating in *GpIbα*$^{\Delta sig/\Delta sig}$ mice compared to their wild-type littermates, in response to either thrombin, ADP or CRP. Additional experiments using thromboxane A2 (U46619) stimulation also resulted in similar aggregation traces. This was only performed once and needs to be repeated, although deletion of GPIbα intracellular tail is not expected to have an effect upon thromboxane A2 platelet signalling. These aggregometry experiments were intended to pave the way for future experiments, which aim to study platelet aggregation in the presence of plasma and Botrocetin, or in the presence of VWF A1 domain alone, to detect a possible difference in VWF-mediated platelet aggregation between *GpIbα*$^{\Delta sig/\Delta sig}$ and *GpIbα*$^{+/+}$ platelets. It is important to note that aggregation experiments are performed in the presence of a magnetic stirrer aimed to generate shear forces within the cuvette. This will be crucial for the Botrocetin/VWF-induced platelet aggregation, given the importance of shear in VWF-mediated platelet signalling.

Platelet function was also analysed through their ability to spread on fibrinogen, CRP, fibrin and VWF. These experiments revealed that platelets from *GpIbα*$^{\Delta sig/\Delta sig}$ mice undergo normal spreading on fibrinogen, both under basal and stimulated conditions. Surprisingly, despite aggregating normally in the presence of all agonists tested, *GpIbα*$^{\Delta sig/\Delta sig}$ platelets exhibited a limited ability to spread on CRP. In line with this, data obtained by Dr. Salles-Crawley using flow cytometry also shows a decrease in activated $\alpha_{IIb}\beta_3$ and P-selectin expression on the *GpIbα*$^{\Delta sig/\Delta sig}$ platelet surface in response to CRP stimulation. These results suggest that *GpIbα*$^{\Delta sig/\Delta sig}$ mice might present a defect in GPVI-mediated signalling. GPVI is the main receptor for collagen and is also known to have the ability to bind fibrin. Indeed, *GpIbα*$^{\Delta sig/\Delta sig}$ platelets also exhibited a diminished ability to spread on fibrin, although this would need to be repeated in the future. Several studies indicate that there might be a link between GPIbα-mediated signalling and GPVI signalling [410-413]. Work is currently underway to further investigate the defect in GPVI-mediated signalling in *GpIbα*$^{\Delta sig/\Delta sig}$ mice.

Further spreading experiments confirmed the predicted effect of GPIbα truncation on VWF-mediated platelet signalling. This was demonstrated through the reduced ability of *GpIbα*$^{\Delta sig/\Delta sig}$ platelets to spread on VWF, in the presence of Botrocetin and GR144053 compared to *GpIbα*$^{+/+}$ platelets. Platelets from either genotype did not spread on VWF in the absence of Botrocetin (data not shown), as this was required to unravel VWF and promote the binding of GPIbα to the VWF A1 domain. Moreover, the addition of GR144053 was important to ensure that the effects observed solely correspond to the A1-GPIbα mediated signalling and not to any outside-in signalling induced by the VWF C4 domain binding to activated $\alpha_{IIb}\beta_3$. However, the use of Botrocetin is not physiological, therefore future experiments aim to express and purify recombinant murine VWF A1 domain.

Finally, we used whole blood and plasma-free blood from *GpIbα*$^{\Delta sig/\Delta sig}$ mice and wild-type mice in flow assays. We hypothesised that *GpIbα*$^{\Delta sig/\Delta sig}$ platelets exhibit normal binding to

VWF via its A1 domain, but that they do not subsequently express activated $\alpha_{IIb}\beta_3$ on their surface and, therefore, are unable to recruit neutrophils and induce NETosis under flow.

In support of this hypothesis, *Gp1bα*$^{\Delta sig/\Delta sig}$ platelets bound to both recombinant VWF A1* and murine full-length VWF, confirming that the extracellular domain of GPIbα is unaffected and retained the ability to bind the VWF A1 domain. However, the ability of VWF-bound mouse platelets to form aggregates was reduced compared to human platelets. We tested whether increasing the shear to 3000s^{-1} and maintaining it for longer periods of time would increase the aggregate formation under flow, but this was not the case (data not shown). Detection of murine platelet aggregates might be more technically difficult than for human platelets, due to their decreased size (approx. 0.5μm for mouse platelets compared to 1-2μm for human platelets). Interestingly, there was an apparent increase in *Gp1bα*$^{\Delta sig/\Delta sig}$ platelet velocity compared to wild-type platelets on murine VWF (data not shown). This could be due to the slightly increased platelet size in *Gp1bα*$^{\Delta sig/\Delta sig}$ mice compared to the wild-type littermates, but may also be caused by a decrease in activation of $\alpha_{IIb}\beta_3$ that, in this case, is not able to stabilise the interaction between platelets and the VWF C4 domain. The reduction in activated $\alpha_{IIb}\beta_3$ was further investigated by assessing the ability of VWF-captured platelets to bind fluorescent fibrinogen. Preliminary data suggests that there is a decrease in fibrinogen binding to platelets from *Gp1bα*$^{\Delta sig/\Delta sig}$ mice (data not shown), but this assay is technically challenging and requires further optimisation. Further experiments aim to demonstrate the activated state of $\alpha_{IIb}\beta_3$ on VWF-captured murine platelets by staining with JON/A antibody and analysing this via confocal microscopy. The ability of these platelets to degranulate and undergo Ca^{2+} signalling will also be analysed in the future.

Wild-type platelets 'primed' on VWF surfaces exhibited a similar behaviour to human platelets, as they were able to recruit neutrophils at low shear. Similar to the results obtained when using human blood, the number of murine neutrophils interacting with VWF-'primed' platelets from *Gp1bα*$^{+/+}$ mice significantly increased in the absence of plasma, suggesting that murine

neutrophils also compete with fibrinogen to bind the 'primed' platelets. In support of our hypothesis, neutrophil binding to *GpIbα*$^{+/+}$ platelets was markedly reduced in the presence of GR144053, indicating that murine VWF-'primed' platelets also interact with neutrophils via activated $\alpha_{IIb}\beta_3$. Additional experiments were performed using an anti-β_2 blocker to inhibit the Mac-1 and LFA-1 integrins on the leukocyte surface. This did not affect the number of neutrophils binding, excluding a role for β_2 integrins in binding VWF-'primed' murine platelets (data not shown, n=1). Future experiments aim to investigate whether mouse neutrophils recruited by VWF-'primed' platelets also exhibit the ability to undergo signalling leading to NET release.

As predicted, *GpIbα*$^{\Delta sig/\Delta sig}$ mice exhibited a reduced ability of VWF-'primed' platelets to recruit neutrophils under flow. A limited number of neutrophils interacted with these platelets, but this resembled the number of neutrophils interacting with *GpIbα*$^{+/+}$ platelets in the presence of GR144053. Given the manner through which blood is collected from mice (retro-orbitally) as opposed to humans (through venepuncture), it is possible that a small proportion of mouse platelets may exhibit different activation states that could account for the low number of neutrophils still interacting under these conditions. However, our results consistently show a significant reduction in the number of neutrophils interacting with VWF-'primed' platelets from *GpIbα*$^{\Delta sig/\Delta sig}$ mice as opposed to *GpIbα*$^{+/+}$ mice. Therefore, these results indirectly demonstrate the reduced presence of activated $\alpha_{IIb}\beta_3$ on *GpIbα*$^{\Delta sig/\Delta sig}$ VWF-captured platelets, confirming our original hypothesis that *GpIbα*$^{\Delta sig/\Delta sig}$ mice have reduced VWF-mediated platelet signalling and subsequent neutrophil recruitment under flow.

Work is currently underway to fully characterise *GpIbα*$^{\Delta sig/\Delta sig}$ mice. Ultimately, these mice will be used to investigate the role of the VWF-dependent platelet 'priming' in the development of various pathological conditions, particularly DVT. This will be further detailed in the Final Discussion.

8. Final discussion

8.1. Summary of background, hypothesis and aims

Despite their small size and lack of nucleus, platelet complexity is undisputed. Classically, platelets have been recognised for their essential haemostatic role, consistent with the bleeding diathesis associated with thrombocytopaenia and platelet function disorders. It is well established that, following vessel damage, platelet recruitment is crucial for the formation of a haemostatic plug that prevents excessive bleeding [107]. In most cases, this process is highly dependent on the plasma protein VWF. VWF is a multimeric protein with a complex structure consisting of a variety of different functional domains. Most of these domains are concealed under normal circumstances, as VWF circulates in a globular conformation. After vessel injury, however, subendothelial collagen is exposed that binds VWF via its A3 domain. In this immobilised form, VWF is subjected to shear forces exerted by the flowing blood and, as a result, it unravels to expose other functional domains. Among these, the A1 domain recruits platelets via their GPIbα receptor [4]. Captured platelets are exposed and respond to agonists, including collagen, thrombin and ADP, and, as a result, become activated depending on agonist identity and concentration and form a haemostatic plug (thrombus) [2,6]. Classical understanding of this process suggested that all platelets in a thrombus are equally exposed to their agonists and, as such, are, perhaps, uniformly activated, and that activation were a binary 'on and off' process. However, the question remained of what limits platelet accumulation to prevent the transition of a haemostatic plug to an occlusive thrombus from forming with each vessel injury. Recent studies have proposed a new model of thrombus architecture, hypothesising that thrombi are multi-layer structures consisting of a core and a shell region. The core is thought to consist of tightly packed platelets, exposed to a high concentration of agonists and, as a result, highly activated. Conversely, the shell is considered to contain loosely packed platelet exposed to lower concentrations of agonists and, thus, less activated. One marker distinguishing core and shell platelets is represented by P-selectin. P-selectin is stored within the α granules of the platelets and is exposed to the platelet surface as a consequence of robust platelet activation/degranulation. Core platelets are P-selectin

positive, whereas shell platelets are P-selectin negative [256-260,414,415]. Even in this simplistic model, it can be inferred that platelets have a 'tunable' response, their level of activation depending on the agonist they are exposed to, as well as the agonist concentration.

Importantly, apart from the well-characterised platelet agonists that induce signalling events within platelets, the VWF A1-GPIbα interaction not only facilitates platelet capture but also induces signalling within platelets [55,147,152,153,214,216,218,375]. Research by Zhang *et al.* isolated these events as being dependent on shear. It is thought that, upon binding to VWF A1 domain, GPIbα is subjected to rheological forces exerted by the flowing blood, which can unravel the juxtamembrane stalk of GPIbα. This acts as a mechanosensitive domain and, upon unfolding, is thought to translate the mechanical stimulus into a biochemical signal within the platelets [144]. Considering that, at sites of vessel injury, potent platelet agonists are present and can induce robust signalling events, the VWF A1-dependent signalling may appear to be redundant given the comparatively weak signal that is transduced. However, platelets have recently been shown to fulfil important roles beyond haemostasis that may be more reliant upon such signalling [122,123,262,263,265,275,282,341,416].

The platelet barrier at sites of vessel damage acts not just to limit blood loss, but to also prevent pathogens from entering the vasculature. In keeping with this, platelets have more recently been classified as immune cells [122,123,263,265,416]. Increasing evidence suggests important roles for platelets in settings of infection and inflammation. Laying the ground for the importance of platelets in immunity, work by Depperman & Kubes, and Jenne & Kubes identified crucial roles for platelets in models of infection and inflammation [122,123]. As such, it has highlighted the importance of platelets and their interaction with leukocytes in the innate immune system.

Platelet-leukocyte interactions are not only important within the setting of infection [312,346,350,352-356,358,359], but also contribute to the development of various cardiovascular diseases, such as atherosclerosis, stroke, and DVT [271,272,344,351,354,361-364]. It is clear though that resting platelets

do not interact with resting leukocytes – if this was the case they would circulate in aggregates. Previously characterised platelet-leukocyte interactions occur exclusively in the setting in which either the platelet or the leukocyte, or both cell types are robustly activated. These well-known interactions occur via P-selectin-PSGL-1, CD40L-CD40, when the platelets are activated, and activated Mac-1-GPIbα, activated Mac-1-fibrinogen-activated $\alpha_{IIb}\beta_3$ and activated LFA-1-ICAM-2, when leukocytes are activated [141,343-346,349,417]. Interestingly, a study by Zheng *et al.* has demonstrated that VWF-captured platelets are able to recruit leukocytes *in vitro* under flow, in the absence of other platelet or leukocyte agonists, so in the absence of platelet and/or leukocyte activation [85]. This finding, together with the unknown importance of VWF A1-mediated platelet signalling provided scope to believe that these mechanisms might be inter-related.

In light of these previous findings, I hypothesised that VWF A1 domain 'primes' the platelets, modulating their phenotype to allow novel platelet-leukocyte interactions to occur, which may provide new mechanistic insights into the role of platelets as immune cells.

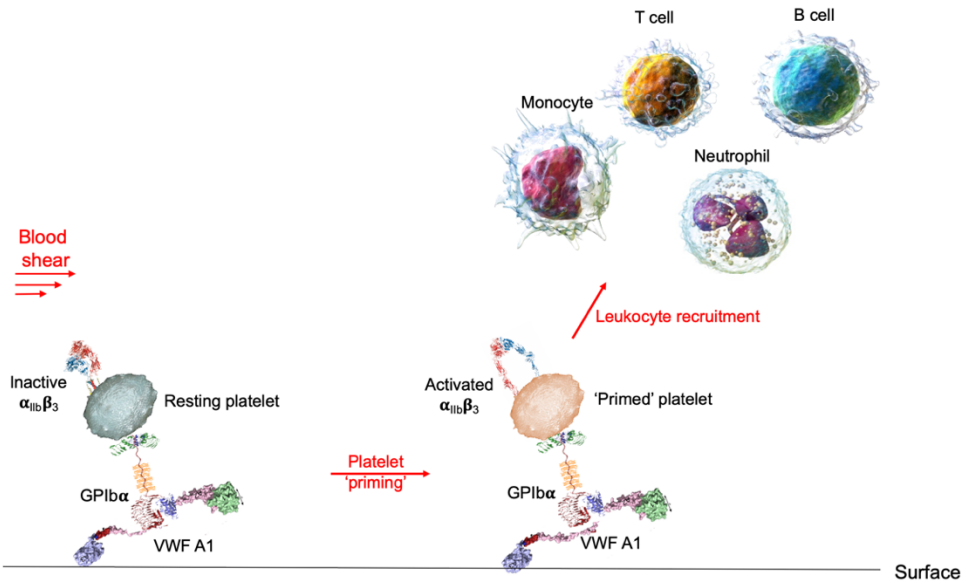

Figure 8.1 Summary of PhD hypothesis.

Globular VWF does not interact with resting platelets. However, when VWF binds to a surface or gets tangled, it can unravel and capture platelets via the A1-GPIbα interaction. I hypothesised that this can 'prime' the platelets and lead to novel interactions with leukocytes under flow.

To test this hypothesis, my PhD was designed around seven aims:

Aim 1. Express and purify recombinant VWF A1 domain and A1* (Y1271C/C1272R)

Aim 2. Characterise the VWF A1-GPIbα interaction under flow

Aim 3. Identify the platelet receptor interacting with leukocytes under flow

Aim 4. Identify the leukocyte subset interacting with the VWF-'primed' platelets

Aim 5. Analyse the impact of VWF-'primed' platelet-leukocyte interactions on leukocyte effector function

Aim 6. Identify the leukocyte receptor interacting with the VWF-'primed' platelets

Aim 7. Investigate the *in vivo* pathophysiological importance of the 'primed' platelet-leukocyte interaction

8.2. The identification of a novel platelet-leukocyte interaction

During my PhD, I established a flow system to investigate the VWF-platelet-leukocyte interactions under conditions that in some respects reflect the conditions in the vasculature *ex vivo*. Microfluidic channels were coated with FL-VWF, VWF A1 or A1*, a variant of the A1 domain with a 10-fold increased ability to bind platelets. Fluorescently labelled whole blood, plasma-free blood or isolated leukocytes were perfused through these channels at defined shear rates ($50s^{-1}$ to $1000s^{-1}$) and platelet and leukocyte capture was recorded in real-time. This approach enabled analysis and control of the platelets under flow, which cannot be mimicked under static conditions.

Using this approach, I confirmed that platelets captured by FL-VWF, VWF A1 or A1* undergo intraplatelet Ca^{2+} release and activation of integrin $\alpha_{IIb}\beta_3$ under flow. Although this finding is corroborated by other studies, these were often performed under static conditions, and/or using FL-VWF and Ristocetin/Botrocetin as non-physiological stimulants [55,220,405]. Thus, it was

essential to demonstrate that this occurs under flow, in the sole presence of VWF A1 domain. The activation of $\alpha_{IIb}\beta_3$ was determined by the ability of VWF A1-bound platelets to *1)* aggregate and *2)* bind fluorescent fibrinogen, in a manner that could be inhibited by $\alpha_{IIb}\beta_3$ blockers. Importantly, as opposed to other platelet agonists, such as thrombin or collagen, VWF A1/flow mediated signalling within platelets culminated with the activation of $\alpha_{IIb}\beta_3$ but caused minimal degranulation. Lack of α granule release was demonstrated through the minimal P-selectin exposure as detected by confocal microscopy. Conversely, dense granule release was investigated indirectly in flow assays, using Apyrase to inhibit the effect of any potential ADP released from the dense granules. As Apyrase had no effect upon platelet aggregation it was assumed that ADP was not released from the dense granules in sufficient amounts to phenotypically modify the platelets. Given the presence of activated $\alpha_{IIb}\beta_3$ but lack of degranulation on these platelets, I proposed the term **'primed' platelets** rather than activated platelets.

This finding is in line with the theory that platelets have a 'tunable' response. In fact, 'primed' platelet phenotype resembles the characteristics of the platelets in the shell region of the thrombus. These platelets are loosely packed and are known to be P-selectin negative [256-260]. VWF is important for platelet accumulation within all layers of a thrombus [418,419]. Despite the original contention that VWF-dependent platelet signalling may be redundant in the setting of haemostasis, this may play a role in the platelet recruitment and 'priming' within the shell region of the thrombus. If VWF alone could mediate full platelet activation, the presence of this defined shell region would not be observed.

After establishing the 'primed' state of VWF-bound platelets, I focussed on investigating whether this leads to subsequent leukocyte interactions. My results show that, under low shear conditions, neutrophils and T cells (and not monocytes and B cells), roll on and bind to VWF-'primed' platelets. The finding that monocytes do not interact with these platelets was initially surprising, as previously characterised platelet-leukocyte interactions mainly identify neutrophils and monocytes as the leukocyte subsets involved [272,354,363,364]. However, this cell-

specificity provided the first line of evidence to suggest that this may rely on previously uncharacterised binding partners, given that all previously characterised leukocyte receptors binding to platelets (i.e. PSGL-1, CD40, Mac-1, LFA-1) do not vary appreciably across the different leukocyte subtypes [343].

Considering that VWF-'primed' platelets present activated $\alpha_{IIb}\beta_3$ on their surface, I addressed the question of whether 'outside-in' signalling events are responsible for the subsequent leukocyte recruitment. Performing experiments in plasma-free blood though revealed a significantly higher number of leukocytes interacting with the 'primed' platelets compared to whole blood, suggesting that leukocytes compete with a plasma component to bind the 'primed' platelets. Furthermore, titrating fibrinogen back into plasma-free blood led to a concentration-dependent decrease in platelet-leukocyte interactions, indicating a competition with fibrinogen. However, it is important to note that, although present at high concentrations in whole blood (≈3mg/ml), fibrinogen does not out-compete leukocyte binding. The competition between fibrinogen and leukocytes led me to hypothesise that leukocytes directly bind to the main fibrinogen platelet receptor, activated $\alpha_{IIb}\beta_3$. Indeed, pre-incubating either whole blood or plasma-free blood with Eptifibatide or GR144053, two RGD peptide mimetics inhibiting activated $\alpha_{IIb}\beta_3$, led to a significant reduction in the number of leukocytes binding. Furthermore, both T cells and neutrophils could bind to microchannels directly coated with activated $\alpha_{IIb}\beta_3$ in a manner that could be inhibited by Eptifibatide or GR144053 and reduced by addition of fibrinogen.

As opposed to previous studies that recognise a role for activated $\alpha_{IIb}\beta_3$ in mediating leukocyte interactions via β_2 integrins, I showed that Mac-1 ($\alpha_M\beta_2$) and LFA-1 ($\alpha_L\beta_2$) are <u>not</u> involved in the experimental setup that I used via several lines of evidence: *1)* Leukocytes do not bind to platelets captured by anti-PECAM-1. Mac-1 was shown to have the ability to bind to GPIbα, while LFA-1 binds to ICAM-2. Both GPIbα and ICAM-2 are constitutively expressed on the platelet surface [141,349], thus it would be expected that anti-PECAM-1-captured platelets would

also bind neutrophils and T cells under flow, if Mac-1 and LFA-1 were the receptors involved, but this was not observed. *2)* Leukocytes compete with fibrinogen to bind to activated $\alpha_{IIb}\beta_3$. Considering that activated Mac-1 binds to this integrin via fibrinogen [348], the number of platelet-leukocyte interactions would be expected to decrease in the absence of fibrinogen, but the opposite effect was observed. *3)* Blocking experiments using a polyclonal antibody against β_2 integrins did not reduce VWF-'primed' platelet-leukocyte interactions. *4)* Neutrophils and T cells are the only leukocyte subsets interacting with the 'primed' platelets, whereas Mac-1 and LFA-1 are also highly expressed in monocytes [420,421]. Therefore, while Mac-1 may be important in certain physiological/pathological settings, it is unable to account for the recruitment of circulating leukocytes to 'primed' platelets.

I also excluded a role for P-selectin-PSGL-1 and CD40L-CD40 for the platelet-leukocyte interaction that we observe as; *1)* I detected little/no P-selectin on VWF-'primed' platelets, suggestive of minimal degranulation occurring; this also provides indirect evidence for the lack of CD40L on the platelet surface. *2)* Blocking P-selectin had no effect upon the number of leukocytes binding, and *3)* only T-cells and neutrophils bind VWF-'primed' platelets - given that all leukocytes express PSGL-1[343], and CD40, if the capture of leukocytes were entirely P-selectin or CD40L-mediated, such cell-type selectivity would not be observed. However, despite not influencing the number of platelet-leukocyte interactions, P-selectin blockade had an impact upon the rolling speed of leukocytes over VWF-primed platelets. This suggests that although low levels of P-selectin present on the platelet surface are insufficient to capture leukocytes, these may synergise with $\alpha_{IIb}\beta_3$ to slow rolling of leukocytes after their initial recruitment. It is possible that the binding of leukocytes to $\alpha_{IIb}\beta_3$ may itself cause some degranulation to occur with subsequent P-selectin exposure. However, this thesis focusses on the initial capture of leukocytes, which is independent of P-selectin. Given the recognised contribution of leukocytes to thrombus formation, it is important to speculate upon when and where leukocytes might encounter P-selectin during the normal haemostatic process. Considering the modern view of the thrombus architecture, with a core and shell region [256-260],

leucocytes that arrive at sites of thrombus formation at later stages would only be in contact with the shell region, in which platelets have been shown to be P-selectin negative [256]. As VWF is present within all layers of the thrombus, this further corroborates the contention that VWF-captured platelet can recruit leukocytes in a P-selectin-independent manner.

P-selectin and β_2 integrin-independent platelet-leukocyte interactions have been recognised by other studies. Guidotti *et al* showed that T cell interactions with platelets in models of viral hepatic infections occur independently of either P-selectin, CD40L, as well β_2 integrins. These T cells were identified to be intravascular effector CD8+ T cells that, through their interactions with platelets, can perform immunosurveillance of the liver in search for antigens [383]. Similarly, platelet-induced neutrophil recruitment and extravasation was also shown to occur through P-selectin independent pathways, supporting my results. Additionally, Petri *et al.* demonstrated that this process is highly dependent upon VWF and GPIbα [422], a finding which was corroborated by other studies investigating neutrophil recruitment in murine models of ischaemia-reperfusion injury [384,385]. All these data indicate a role for VWF and platelets beyond haemostasis and support my hypothesis that these platelets can form a previously uncharacterised interaction with T cells and neutrophils.

After demonstrating that the platelet receptor involved in this novel interaction is activated $\alpha_{IIb}\beta_3$, I endeavoured to identify the leukocyte counter-receptor. This was very challenging given the requirement for $\alpha_{IIb}\beta_3$ to be in an active conformation. The initial technique I undertook was pull-down assays. However, the different approaches I attempted proved to be ineffective in capturing and activating $\alpha_{IIb}\beta_3$ in a manner that could specifically be used to pull down the unknown receptor. To circumvent these issues, we collaborated with Prof. Heyu Ni from the University of Toronto, as his research group had an established protocol for pull-down assays using activated $\alpha_{IIb}\beta_3$-coated magnetic beads [397]. I isolated neutrophil membrane proteins and sent the sample to the University of Toronto for pull-down assays. However, despite successful capture of some membrane proteins, the majority of pulled-down

candidates were intracellular proteins, particularly cytoskeletal components. I attempted to improve the separation of membrane proteins from cytosolic proteins by biotinylating the neutrophil membranes first, but this approach used buffers incompatible with the pull-down assays. In fact, there may be limitations associated to the pull-down approach as this is based on the dissolution of the membranes, which may affect the integrity/conformation of the leukocyte receptor and, thus, its ability to efficiently bind to $\alpha_{IIb}\beta_3$.

To overcome these limitations, a different approach was used to identify the leukocyte counter-receptor, through a collaboration with Dr. Luigi Grassi and Dr. Mattia Frontini from the University of Cambridge. They performed differential expression analysis of RNA sequencing data from the Blueprint consortium [374] investigating genes encoding transmembrane proteins that are more highly expressed in neutrophils compared to monocytes and, additionally, in T cells compared to monocytes. This led to the identification of 93 potential candidates that were further scrutinised using various exclusion criteria. Interestingly, when comparing the list of candidates identified through this approach with the list of proteins pulled down by activated $\alpha_{IIb}\beta_3$ beads, only one candidate was present in both lists: SLC44A2.

Also known as choline transporter-like protein-2 (CTL-2) or human neutrophil antigen-3 (HNA-3), SLC44A2 is transmembrane protein with 10 membrane-spanning domains [368]. Both the N-terminal and C-terminal regions are present intracellularly. The N-terminal region contains several putative phosphorylation sites and, although their importance is not known, they suggest a role of SLC44A2 in downstream signalling. The transmembrane domains are interconnected via four intracellular loops and five extracellular loops of different lengths (178a.a., 38a.a., 72a.a., 38a.a. and 18a.a.). The structure of SLC44A2 is illustrated below. SLC44A2 is thought to adopt a pore-like structure within the plasma membrane, given its homology with choline-transporter protein 1 (CTL1). For this reason, SLC44A2 is speculated to have a transporter function, aiding the transport of choline, but this has not been demonstrated [369]. The multi-spanning nature of this protein could account for the low affinity of its pull-down, as its structural integrity would have been disrupted by the dissolution of the

neutrophil membrane. Of note, SLC44A2 is also expressed, at albeit lower levels, in endothelial cells and platelets. However, proteomic data suggests a >300-fold greater expression in neutrophils compared to platelets (http://immprot.org). Importantly, proteomic analysis also revealed an increased level of SLC44A2 in T cells compared to monocytes (http://immprot.org), providing scope to believe that this is the T cell receptor involved as well. This is also indicated by the efficacy of anti-SLC44A2 to reduce leukocyte binding to VWF-'primed' platelets in plasma-free blood, where both neutrophils and T cells are expected to bind. Future work aims to investigate this further and identify the T cell receptor binding to activated $\alpha_{IIb}\beta_3$.

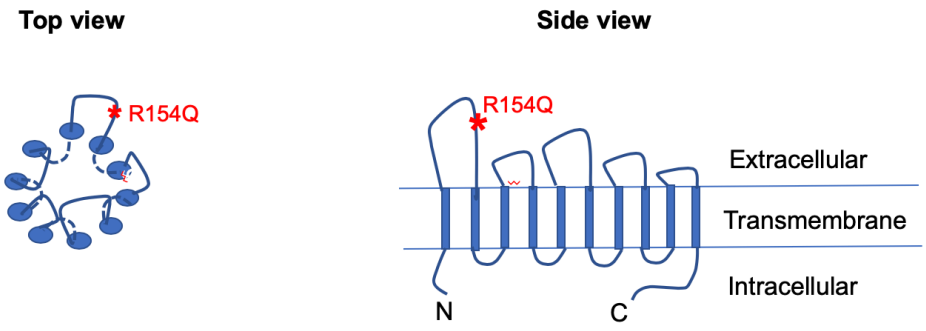

Figure 8.2 Structure of SLC44A2

Schematic representation of the structure of SLC44A2, as observed from top view or side view. It has 10 membrane-spanning domains interconnected via four intracellular loops and five extracellular loops [369]. The first extracellular loop is the largest and the polymorphism related to VTE susceptibility (rs2288904-G/A) encodes a missense mutation within this loop (R154Q) [372].

I demonstrated that SLC44A2 is the counter-receptor on neutrophils that binds to activated $\alpha_{IIb}\beta_3$ via different approaches. First, blocking SLC44A2 with two different antibodies against the first and second extracellular loops of SLC44A2 significantly reduced the interaction with both VWF-'primed' platelets and activated $\alpha_{IIb}\beta_3$. Importantly, the antibody against the first extracellular loop of SLC44A2 was more effective suggesting that this loop is directly involved in binding to activated $\alpha_{IIb}\beta_3$. The antibody against the second loop may inhibit the interaction due to steric hindrance rather than an overlap between the binding sites. Secondly,

transfecting HEK293T cells with a vector expressing *SLC44A2-eGFP* led them to acquire the ability to bind VWF-'primed' platelets and activated $\alpha_{IIb}\beta_3$ in a manner that could be inhibited by $\alpha_{IIb}\beta_3$ blockers and the anti-SLC44A2 antibodies. The affinity of SLC44A2 for activated $\alpha_{IIb}\beta_3$ may be considered to be relatively high compared to that of fibrinogen for the same ligand, considering that, even in the presence of high physiological concentrations of fibrinogen, neutrophils and T cells still interact with VWF-'primed' platelets. It can therefore be assumed that, as opposed to fibrinogen, the binding site of activated $\alpha_{IIb}\beta_3$ for SLC44A2 is not limited to the RGD-binding groove, although this needs to be investigated further.

Interestingly, other groups report that SLC44A2 can directly bind to VWF [371,423]. Bayat *et al.* suggests that HEK293T cells transfected with SLC44A2 can form a tri-molecular complex with VWF and the Mac-1 integrin under static conditions [371]. However, in the experimental setup used throughout this thesis, i.e. under flow, SLC44A2-transfected HEK293T cells did not bind to VWF in the absence of platelets, even after prolonged periods of time. This suggests that a possible interaction between SLC44A2 and VWF may only occur in the absence of flow. Similarly, results from this thesis show that perfusing isolated granulocytes over VWF-coated channels at $50s^{-1}$ does not result in any neutrophils binding. These data are in contrast with results reported in an abstract by Zirka *et al.*, which indicate that neutrophils can directly bind to VWF under flow [423]. However, more details of the experimental design would need to be analysed in order to understand this discrepancy, while comparing the numbers of neutrophils interacting with VWF as opposed to those interacting with VWF-'primed' platelets. Further studies would also need to establish whether this direct interaction is observed *in vivo* and whether this translates into any competition between platelets and neutrophils in binding VWF.

The cellular function of SLC44A2 is not well-defined. It has been associated with hair cell loss, spiral ganglion degeneration and hearing loss in mice [370], and with Meniere's disease and transfusion related acute lung injury (TRALI) in humans [368,371]. However, of interest, *SLC44A2* has recently been identified as a susceptibility locus for venous thromboembolism and stroke

[365,367,372]. Two different polymorphisms (*rs9797861-C/T* and *rs2288904-G/A*) have been associated with VTE. Of these, *rs2288904-G/A* accounts for a missense mutation within the first extracellular loop of SLC44A2 (R154Q) [365]. This has been associated with protection against DVT [372]. However, the mechanistic link between SLC44A2 and DVT is unclear.

During my PhD, I investigated this polymorphism further by transfecting HEK293T cells with *SLC44A2 (R154Q)-eGFP.* These cells had a reduced ability to bind VWF-'primed' platelets and activated $\alpha_{IIb}\beta_3$ and are in line with the contention that SLC44A2 interacts with $\alpha_{IIb}\beta_3$ via its first extracellular loop. Finally, neutrophils from an individual homozygous for the *SLC44A2 rs2288904-A* protective allele also exhibited markedly reduced ability to bind VWF-'primed' platelets. However, blood samples from additional individuals homozygous for this allele will undoubtedly strengthen this assertion.

Apart from characterising the novel interaction occurring between VWF-'primed' platelets and neutrophils via activated $\alpha_{IIb}\beta_3$-SLC44A2, I also analysed the effect of this interaction upon neutrophil phenotype. My results show that neutrophils bound to activated $\alpha_{IIb}\beta_3$ undergo Ca^{2+} signalling and are able to form neutrophil extracellular traps (NETs) in a NADPH oxidase and Ca^{2+}-dependent manner after approximately 1.5-2 hours. Notably, the process of NETosis is absolutely dependent on the presence of shear, as significantly less NETs were formed in the absence of flow. This suggests that $\alpha_{IIb}\beta_3$-induced NET formation occurs through a mechanosensitive mechanism, a theory that is supported by recent research that demonstrates the major influence of shear upon platelet-mediated NET release [394]. I hypothesise that physical pulling on the first extracellular loop of SLC44A2 is perhaps the stimulus for transducing an intracellular signal within the neutrophils.

Although platelet-mediated NETosis has been of increasing interest, previous studies assessed this in settings in which platelets were activated by thrombin or stimulated with LPS [282,325]. The mechanism uncovered during my PhD is novel, as platelets are 'primed' instead of activated and NET release is exclusively mediated by activated $\alpha_{IIb}\beta_3$ and shear, in the

absence of any other platelet receptors or platelet chemokines. The significance of this will be discussed in the next subsection.

All these results were obtained using microfluidic channels in an attempt to reflect the physiological conditions *ex vivo*. However, it is important to note a key limitation for this approach. These microchannels are rigid, linear structures, onto which proteins are immobilised directly, in a controlled purified system, with pre-determined concentrations. Human vasculature consists of intricate vessels of varying geometries, flexible and lined with endothelial cells. Moreover, in my setup, high shear was required to capture and 'prime' the platelets, followed by low shear to observe platelet-leukocyte interactions. A shear difference of such an extent ($1000s^{-1}$ to $50s^{-1}$) does not physiologically occur. To address this important issue, I performed preliminary experiments using bifurcated microchannels that perhaps slightly better reflect the vasculature. These were used in an attempt to generate disturbed/altered flow patterns and analyse platelet capture to VWF and subsequent platelet-leukocyte interactions while using low shear conditions throughout the assay. These experiments revealed that platelets could be uniformly captured and 'primed' under low shear, prior to interacting with leukocytes. Importantly, both platelet capture and leukocyte binding were augmented in regions of disturbed flow. These findings were instrumental in determining the conditions under which this VWF-'primed' platelet-leukocyte interaction may occur *in vivo*. Although classically VWF is thought to be exclusively important in platelet capture at high shear, thus playing a role in the setting of arterial thrombosis, there has been increasing evidence recently to suggest that VWF is crucial in venous thrombosis as well [271,403,404]. Although platelet binding is facilitated under high shear conditions, it still occurs under low shear [85,424,425]. My results corroborate the hypothesis that VWF-'primed' platelet-leukocyte interactions are more likely to occur under venous shear conditions. The implications of this interaction in venous thrombosis are discussed later. Work is currently underway using custom-made microchannels that mimic the venous vasculature, with venous valves and endothelial cells lining them.

8.3. Significance of this study

During my PhD, I uncovered a novel interaction between platelets and neutrophils (and T cells), together with gaining new insights into the mechanisms leading to platelet-mediated NETosis. Understanding the importance of these findings in both physiological and pathological scenarios is crucial and is the focus of future work arising from this PhD.

8.3.1. Physiological importance

Role of VWF-mediated platelet 'priming' in innate immunity

Considering that the interaction between VWF-bound platelets and leukocytes has been observed in mice and humans, this interaction may be evolutionarily preserved. Thus, it is a reasonable assumption that this interaction must have a beneficial role within the vasculature. Given the ability of VWF-'primed' platelets to mediate NETosis and the fundamental contribution of NETs to pathogen clearance, this interaction may be key to our innate immune response. The physiological role of 'primed' platelets may, therefore, be more pertinent to platelet functions beyond haemostasis. In support of this assumption are several studies that identify platelets as immune cells and recognise their crucial role in infection [122,123,265,416].

Different studies suggest that platelets contribute to infection in various ways. They were shown to be able to directly bind bacteria and viruses, through the expression of TLRs (TLR2, TLR4 and TLR7, respectively), as well as having the ability to release antimicrobial molecules, such as kinocidins, thrombocidins or defensins [262-264,282,284,285].

Platelet roles in infection have further been demonstrated by Kubes *et al*, who observed that platelets constantly scan the vascular wall, particularly within liver sinusoids [278]. Hepatic vasculature is very complex. The liver is vascularised by the hepatic artery (25-30% of the liver blood supply) and portal vein (70-75% of the hepatic blood supply), but also contains a series of small sinusoids [426], that are responsible for filtering the blood and clearing bacteria that enter the vasculature. As such, shear within these vessels is very low, averaging at around

$50s^{-1}$, which allows key interactions to take place and aid bacterial clearance. This process is highly dependent on Kupffer cells, which are defined as stationary macrophages lining the liver sinusoids. They can capture and phagocytose bacteria when they enter the vasculature, being the first line of defence once a pathogen reaches the circulation [278,427]. Importantly, platelets undergo continuous 'touch and go' interactions with Kupffer cells. Interestingly, this transient interaction is abolished in *GpIbα*$^{-/-}$ mice suggesting that this platelet 'surveillance' mechanism may be dependent upon VWF [278]. In fact, VWF staining colocalised with Kupffer cells under resting conditions. Following bacterial infection with *B. cereus* or *S. aureus*, there was an increase in the amount of VWF present on Kupffer cells and, consequently, platelets interacted with Kupffer cells in a more sustained manner. *GpIbα*$^{-/-}$ mice exhibited diminished platelet recruitment and had a significantly reduced survival rate following bacterial infection [278]. Furthermore, work by Honda & Kubes (2018) showed that these platelets can then bind neutrophils via an 'unknown' receptor and trigger NET release, in this way promoting the clearance of *E. coli* [359]. All this recent research represents an interesting platform that complements the data obtained during this PhD. The dependency on VWF and GPIbα, as well as the presence of an unknown platelet-neutrophil interaction that occurs at the same shear as in my experiments ($50s^{-1}$) provides scope to believe that the novel interaction I uncovered could perhaps occur within this system and play a role in innate immunity.

An important line of evidence acquired during my PhD that supports this hypothesis is represented by the ability of VWF-'primed' platelets to drive NETosis. NETs have been identified by Brinkmann *et al.* in 2004, as a novel pathway through which neutrophils target and kill pathogens [318]. Initially, it was thought that NETosis always results in neutrophil death, but more recent research suggests that some neutrophils undergo 'vital' NETosis and are still able to fulfil their chemotactic and phagocytic function after releasing NETs [327,328,389]. The main stimulus for NETs *in vitro* is PMA, although this is not physiological. Other studies use LPS, a component of the gram-negative bacterial wall, but results are controversial regarding the potency of LPS alone to induce NETosis [282]. Interestingly, recent studies showed that platelets

can be stimulated by LPS and promote NETosis [281,282,355]. Importantly, LPS-stimulated platelets are able to bind fibrinogen (thus have activated $\alpha_{IIb}\beta_3$ on their surface), but do not present P-selectin on their surface. The way these platelets interact with neutrophils and induce NETosis is unclear, as this was shown to be P-selectin independent [282]. The timing of NETosis is a subject of ongoing debate. *In vitro*, PMA stimulation leads to NET release after 2-4 hours, while others report NETosis after an even more prolonged stimulation time of 4-8 hours [390]. Physiologically, this response may be appropriate in the settings of extravascular NETosis, but not in the case of intravascular NETosis. Given the fast doubling time of bacteria, these would rapidly disseminate should they reach the vasculature and the formation of NETs after 2-4 hours would be futile. Interestingly, other studies suggest that platelets stimulated with thrombin can drive NETosis within minutes of interacting with neutrophils in a P-selectin-dependent manner. However, the importance of thrombin in infections is not known, thus it is unclear whether this would occur in settings of acute infections or mainly contribute to thrombotic disorders. In our system, platelets can mediate NETosis in an activated $\alpha_{IIb}\beta_3$-dependent manner, within 90 minutes of binding under flow. Therefore, my results, together with the previous observations for platelet-mediated NETosis suggest that platelets are crucial for inducing a more rapid neutrophil response. In light of this, we propose a two-hit model, in which platelets and bacteria might synergise in initiating a rapid neutrophil response and NET production.

To test this, I endeavoured to establish a system to investigate the importance of VWF platelet 'priming' and subsequent neutrophil recruitment in bacterial infections *in vitro*. Preliminary experiments are detailed in **Appendix 2** and suggest that platelets bind to bacteria via VWF and are then able to recruit leukocytes under flow. Should this be confirmed, it would provide a strong basis for the two-hit NETosis model we propose.

I propose the following mechanism for VWF-'primed' platelet-mediated NETosis in bacterial clearance *in vivo*. After a bacterial infection, Kupffer cells from hepatic sinusoids can bind VWF from the circulating blood [278]. When subjected to shear, VWF might unravel, exposing its A1 domain. The exposure of the A1 domain may capture platelets via GPIbα and cause them to become 'primed' and express activated $\alpha_{IIb}\beta_3$. These can then recruit neutrophils via SLC44A2 and trigger NET release. NETs would then entrap and clear bacteria that have entered the liver sinusoids. This proposed mechanism is visually represented below.

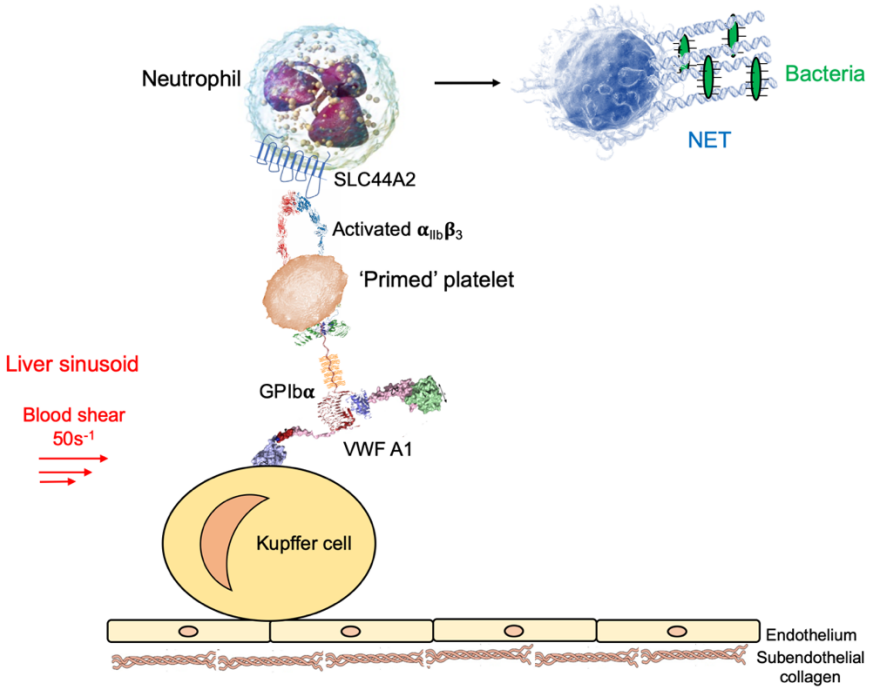

Figure 8.3 Proposed model for VWF-'primed' platelet-neutrophil interactions in innate immunity.

Kupffer cells line the hepatic sinusoid vessel wall and can become lined with VWF. Platelets can be captured by VWF and become 'primed', expressing activated $\alpha_{IIb}\beta_3$ on their surface. Subsequently, this can recruit neutrophils via SLC44A2 and drive NETosis and subsequent bacterial clearance.

8.3.2. Pathological implications

Role of VWF-mediated platelet 'priming' in DVT and other thrombotic disease

Aside from their crucial role in innate immunity, NETs are also described as highly thrombogenic structures [319,338-340]. Given NET involvement in thrombotic disorders, as well as the well-established role of VWF and platelets in thrombus formation, I hypothesised that the novel interaction between VWF-'primed' platelets and leukocytes may provide novel mechanistic insights into the pathology of various thrombotic conditions.

8.3.2.1. DVT

Despite therapeutic advances, DVT and its complications remain one of the major causes of morbidity and mortality worldwide [276]. Different risk factors have been well-characterised, including genetic predisposition, obesity, sedentarism, smoking, and surgery/trauma, however, the mechanism underlying this condition remains unclear. As the name suggests, DVT develops under venous flow, around venous valves, and seems to be favoured by turbulent/disturbed shear patterns/stasis [428]. The study of DVT development is particularly complicated as mice do not have venous valves so would not readily form thrombi within their venous vasculature. Two models have been used to study DVT in mice – the stasis model (in which flow through inferior vena cava is completely obstructed) and the stenosis model (in which the inferior vena cava is ligated but flow is only obstructed by ≈80%). The latter has been considered more reflective of the pathophysiological conditions found in humans, as thrombi from this model closely resemble the human thrombi developed in DVT [271,272]. Importantly, DVT occurs in the absence of any overt vessel damage [428], and, therefore, the main question that remains to be addressed is what drives the initiation of DVT.

VWF function has classically been described under arterial shear conditions and its contribution to arterial thrombosis is well-established. However, studies have recently demonstrated that VWF is also involved in the development of DVT, despite the absence of high shear conditions or overt vessel damage [271,272,403,404]. This was determined in experiments

performed in *Vwf*$^{-/-}$ mice, which show that these mice are protected against DVT [271]. Similarly, mice lacking the extracellular domain of GPIbα were also protected against DVT in the stenosis model [272]. These studies demonstrate the platelet-dependency of DVT development, although the precise mechanism involved is not fully understood. These previous findings provide scope to hypothesise that VWF-dependent platelet capture is crucial for the initial events in DVT. It would be interesting to investigate the effect of VWF levels upon DVT in humans by analysing whether there is a link between different types of VWD and the incidence of DVT. It could be speculated that patients with type 2A VWD would have a lower incidence of DVT given the decrease of plasma concentration of high molecular weight VWF. However, this would be difficult to ascertain, as large VWF multimers are still produced and released but are more susceptible to proteolysis by ADAMTS13. However, they might still contribute to DVT before being cleaved. Conversely, it could be hypothesised that patients with type 2B VWD may have a higher risk for developing DVT, as VWF A1 domain has an increased affinity for GPIbα. However, studies suggest that, despite higher affinity, GPIbα cannot form catch-slip bonds with type 2B VWF A1 at high shear rates [425]. Moreover, type 2B VWD also causes defects in megakaryopoiesis and is also associated with increased platelet clearance and thrombocytopaenia [99]. Finally, patients with type 3 VWD or low levels of VWF are often undergoing treatment with recombinant VWF or desmopressin (DDAVP) respectively, which stimulates endothelial cells to release VWF [429,430], and, therefore, might not exhibit a difference in the risk for DVT.

To investigate the role of VWF in venous flow using human blood, I used bifurcated microchannels and generated a pattern of disturbed flow. Under these conditions, VWF was able to recruit platelets at venous shear rates. Importantly, the ability of VWF to 'prime' platelets under low shear conditions was confirmed by the observation that these platelets are able to aggregate and recruit leukocytes, in an activated $\alpha_{IIb}\beta_3$-dependent manner. Platelet-leukocyte interactions were augmented in regions of disturbed flow where they led to the generation of microthrombi.

Indeed, the importance of platelet-leukocyte interactions has been well characterised in development of DVT. Using the stenosis model in mice, leukocytes could be observed rolling and adhering proximal to the endothelium as early as 1 hour following IVC ligation and completely lining the endothelium within 5-6 hours. Importantly, VWF deficient mice, as well as mice lacking the extracellular domain of GPIbα exhibited diminished leukocyte recruitment following stenosis of IVC [272]. These findings suggest that leukocyte capture at sites of DVT occurs in a VWF and GPIbα dependent manner. The interaction responsible for leukocyte recruitment is currently unknown, given the lack of endothelial denudation, which implies that platelets are not exposed to other agonists (i.e. collagen, thrombin, ADP) and, as such, are not activated. In line with this, studies show that endothelial P-selectin in part contributes to the development of DVT, whereas platelet P-selectin is not implicated [272]. All these data led us to believe that VWF-dependent platelet 'priming' and the subsequent leukocyte recruitment via SLC44A2 could provide novel mechanistic insights into the initiation of DVT.

In support of this contention, the leukocyte receptor SLC44A2 became a focus of haemostatic research following the discovery of its encoding gene as a susceptibility locus for venous thromboembolism (VTE). GWAS studies identified a polymorphism in *SLC44A2* (*rs2288904-G/A*), which is linked to protection against VTE. This is caused by a SNP in codon 461 of the gene, based on a substitution (G>A) that causes a missense mutation, R154Q [365,367,372]. This mutation affects the first and longest extracellular loop of SLC44A2, but its effect has not previously been investigated. My results demonstrate that this mutation in the first extracellular loop of SLC44A2 impairs its ability to bind VWF-'primed' platelets and activated $\alpha_{IIb}\beta_3$, through two lines of evidence: HEK293T cells transfected with *SLC44A2(R154Q)* have a reduced ability to bind VWF-'primed' platelets and, importantly, neutrophils homozygous for this SNP (*rs2288904-A*) also have an impaired ability to interact with VWF-'primed' platelets. These findings could, therefore, provide a causative link between the *rs2288904-G/A* polymorphism and the development of DVT. In line with this, *Slc44a2*$^{-/-}$ mice exhibit normal haemostatic

responses, but appear to be protected against DVT, suggesting a role for SLC44A2 particularly in the early development of DVT [402,431].

Additional evidence acquired during my PhD supports the involvement of the VWF-'primed' platelet-leukocyte interaction in DVT. In line with my results, the analysis of the subsets of leukocytes accumulating in the venous thrombus in the IVC stenosis model revealed that the majority of these is represented by neutrophils (~70%). A small proportion of leukocytes is represented by monocytes (~30%) [272], although the timeline of their recruitment in relation to neutrophils has not been determined, therefore they might be involved in a later step. Moreover, recent research also suggests that T cells (particularly effector memory T cells) can be recruited to sites of venous endothelial inflammation and infiltrate within the venous thrombus. The mechanism underlying their recruitment is not fully understood, but evidence suggests that this can affect the thrombus resolution process [432]. Both neutrophils and monocytes are thought to be involved in thrombus development as they provide an important source of intravascular tissue factor that can initiate the extrinsic coagulation cascade [428]. Additionally, neutrophils contribute to the development of DVT through their ability to release highly thrombotic NETs [338-340]. As a result, depleting neutrophils, administering DNase for the dissolution of NETs or inhibiting the process of NETosis by knocking out PAD4 have all been associated with DVT protection in mice [331,339].

The precise mechanism underlying the contribution of NETs to DVT is, however, not fully understood. Studies suggest that NETs are involved in thrombus growth, by entrapping red blood cells and binding additional platelets. Others indicate that NETs are able to bind coagulation factor XII and initiate the intrinsic coagulation cascade, promoting fibrin formation and aiding thrombus stability [338-340]. It is still unclear whether NETs are an initiating factor for DVT, a contributing factor to thrombus development, a key factor to thrombus stability and resistance to fibrinolysis, or if they are, in fact, the convergence point for all these different thrombogenic mechanisms. Based on my results, I propose that NETs have a defining function in the initiation events leading to DVT.

I propose that, at sites of turbulent/disturbed venous flow, such as around venous valves, VWF can unravel and tangle, becoming more resistant to cleavage by ADAMTS13. As a result, platelets are recruited by GPIbα and 'primed'. VWF-'primed' platelets can, subsequently, recruit neutrophils via activated $\alpha_{IIb}\beta_3$-SLC44A2 and trigger NETosis. This then provides a nidus for thrombus formation. In individuals with *SLC44A2 rs2288904-A* polymorphism, present in 22% of population, neutrophils have apparently diminished their ability to bind VWF-'primed' platelets. This provides mechanistic insights for understanding the link between this polymorphism and DVT protection, as well as offering important prospects for possible novel prophylactic/therapeutic strategies against DVT.

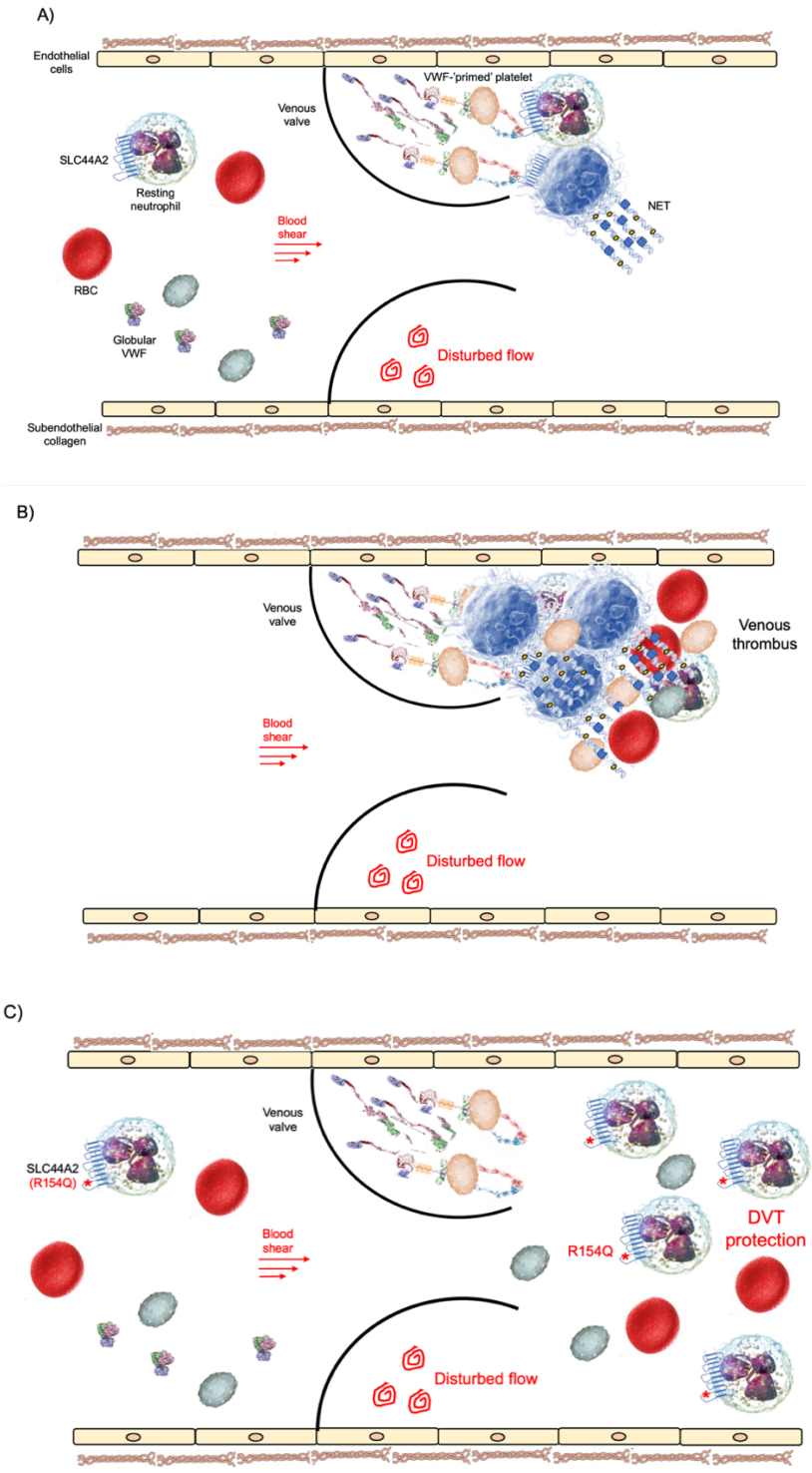

Figure 8.4 Proposed model for the initiation events leading to DVT.

A) *In venous valve pockets, disturbed flow may lead to the unravelling and tangling of plasma VWF or VWF released from endothelial cells. This can lead to platelet recruitment and 'priming' and subsequent capture of neutrophils via activated $\alpha_{IIb}\beta_3$-SLC44A2.* ***B)*** *This interaction can trigger the release of NETs, which can capture circulating red blood cells and platelets contributing to thrombus initiation. Later events might include NETs triggering the coagulation cascade by binding to FXII and inducing fibrin deposition.* ***C)*** *Neutrophils with the R154Q SLC44A2 variant (*) do not have the ability to bind activated $\alpha_{IIb}\beta_3$, offering protection against DVT.*

Therapeutic strategies for DVT

DVT is a major cause of morbidity and mortality worldwide and, despite the decrease in cardiovascular deaths, the incidence of DVT continues to increase [276,277]. Understanding the early events contributing to the development of DVT, as well as finding novel prophylactic therapies against this condition are, therefore, essential to regulate this disease. Current DVT therapy involves anticoagulant treatment. However, whereas effective, anticoagulant therapy poses an increased risk of serious bleeding in treated individuals [400,433-436]. Consequently, the identification of novel strategies to target DVT without affecting the bleeding risk is crucial. Based on the identified genetic link between *SLC44A2* and DVT and to my results which provide a mechanistic explanation for this association, we propose that targeting SLC44A2 may represent an effective adjunctive therapy for the treatment and prophylaxis of DVT.

As suggested by my data, individuals with the *rs2288904-A* polymorphism in SLC44A2 may be protected against DVT due to the impaired ability of their neutrophils to bind to activated $\alpha_{IIb}\beta_3$. It can, therefore, be assumed that disrupting the interaction between VWF-'primed' platelets and neutrophils may contribute to DVT prophylaxis. Targeting the 'primed' platelet receptor, activated $\alpha_{IIb}\beta_3$ with existing antiplatelet agents would affect platelet function and increase the risk in bleeding due to the implicit inability of platelets to aggregate. In contrast, SLC44A2 has no known haemostatic function. Thus, targeting SLC44A2 would not be expected to have an influence upon the bleeding risk in treated individuals. However, despite the predicted efficacy with minimal bleeding side effects, developing an approach to target SLC44A2 is limited by several challenges.

First of all, SLC44A2 not only has an unknown haemostatic role, but its cellular function(s) are poorly characterised. Its deficiency was associated with Meniere's disease, hearing impairment, hair loss, disorientation although the causative mechanisms underlying these phenotypic effects have not been established [370,398]. Targeting SLC44A2 before fully understanding its function would have the concomitant risk of unknown long-term side-effects.

Moreover, SLC44A2 is not expressed exclusively by neutrophils. Studies show that endothelial cells and platelets also express SLC44A2, although at appreciably lower levels (300-fold decreased expression in platelets compared to neutrophils) (http://immprot.org). Thus, to ensure minimal side effects from the associated functions in the other cell types, neutrophil SLC44A2 would have to be specifically targeted.

One possible way to target SLC44A2 would be via an antibody against its first extracellular loop, as this appears to be involved in the interaction with activated $\alpha_{IIb}\beta_3$ according to my results. However, the main limitation associated with this approach is the bivalent nature of the antibody. Due to the constitutive expression of SLC44A2 in the neutrophils, that is readily available for binding, it could be expected that a bivalent antibody might interlink neutrophils, although this was not observed in the microfluidic system I established, in the presence of anti-SLC44A2 antibodies. Circulating neutrophil aggregates could be detrimental and represent a thrombotic risk themselves. Moreover, given that my data suggests that SLC44A2-mediated NETosis occurs through a mechanosensitive mechanism, there is a risk that the antibody binding and bridging effect may trigger NET release. If this were the case, an antibody-mediated therapy would be counterintuitive as it would, instead, potentially promote thrombus formation. A way to test that is using microchannels coated with anti-SLC44A2 antibodies and monitoring bound neutrophils under flow to investigate whether they release NETs in a similar manner to activated $\alpha_{IIb}\beta_3$-captured neutrophils.

To circumvent the issues related to antibody-mediated therapy, SLC44A2 could also be targeted by Fab fragments. As opposed to antibodies, these fragments are small and monovalent, therefore would not be predicted to bridge neutrophils and induce NET release. However, due to their size and properties, Fab fragments have limitations associated to a shorter half-life.

An alternative therapeutic approach would be to target the signalling pathway leading to SLC44A2-driven NETosis. Initial results reveal the involvement of NADPH oxidase, as well as intracellular Ca^{2+} in the process of NETosis and future work aims to fully characterise the signalling downstream of the activated $\alpha_{IIb}\beta_3$-SLC44A2 interaction. However, signalling pathways are often intertwined and it is highly unlikely to find a molecule restricted to this pathway and specific to neutrophils to target.

Apart from the difficulties encountered in selecting the correct approach to target SLC44A2, challenges also exist regarding the subsequent screening process of possible candidates. This is due to the nature of the interaction that needs to be inhibited. This interaction is established between two cell types, platelets and neutrophils, and, additionally, platelets require prior VWF-dependent 'priming'. Moreover, the 'priming' of platelets and effects on neutrophil signalling are absolutely dependent on flow. Setting up a flow system to screen candidates in an efficient manner would, therefore, be very difficult.

However, despite the numerous challenges that need to be overcome to develop a therapy against SLC44A2, this remains an important and promising candidate for several reasons. First, compared to anticoagulants and antiplatelet agents, a therapy targeting SLC44A2 would not be predicted to increase the bleeding risk, which represents a major problem presently. Indeed, research is underway to develop better targets that minimise the risk of bleeding. Recent studies propose the use of PAD4 inhibitors or DNases in the treatment of DVT, to help prevent NET release or promote their dissolution, respectively [272,331,340]. However, these approaches would target all NET processes, so treated individuals might become more susceptible to infections. Therapies against SLC44A2 would potentially diminish thrombogenic NET release, while not being expected to affect other pathways driving NETosis.

8.3.2.2. Other thrombotic disorders

Although in our system we only observe the VWF-'primed' platelet-leukocyte interactions at venous shear rates, various studies identify platelet-leukocyte interactions at arterial shear rates as well. Early recruitment of leukocytes at sites of vessel damage occur in an activated endothelium-dependent manner [350], whereas leukocytes arriving at later timepoints are thought to be recruited by platelets and contribute to thrombus stability. However, considering the current understanding of the thrombus as a multi-layer structure with a core and shell regions [256], it is not fully understood how platelets recruit leukocytes at the later timepoints. According to recent literature, platelets in the shell do not present P-selectin [256,257,414,415]. Therefore, once the thrombus has formed, platelet-leukocyte interactions probably occur independently of P-selectin. The question then is – under what circumstances do leukocytes come in contact with platelet P-selectin, if these platelets are covered by the shell region? Given the presence of VWF in all layers of the thrombus, it would be interesting to speculate that, *in vivo*, the interaction uncovered in this project might occur under arterial conditions as well, although the presence of other agonists (ADP, TXA_2) would make it difficult to isolate the involvement of the VWF-mediated signalling.

As stated previously, VWF is a multimeric protein and its multimeric size directly correlates with its haemostatic potential which is regulated by ADAMTS13 [59]. It is, therefore, perhaps intuitive that the presence of larger VWF multimers or increased VWF levels within circulation constitutes a risk factor for various cardiovascular pathologies. Indeed, it has been demonstrated that the absence of ADAMTS13 in mice is related to a more thrombotic profile, both in arterial and venous vessels [437]. Studies identified high VWF and low ADAMTS13 levels as being associated with a higher risk for developing myocardial infarction [78] and ischaemic stroke [101,103]. Further evidence in mice identifies VWF as a contributing factor to the development of atherosclerosis. Studies show that *Adamts13*$^{-/-}$ mice exhibit an increased leukocyte accumulation within the carotid sinus and an accelerated plaque formation within the aortic sinus and aorta [438]. In humans, ADAMTS13 deficiency leads to thrombotic

thrombocytopenic purpura (TTP). TTP patients present with a specific clinical pentad, including fever, renal failure, thrombocytopaenia, microangiopathic haemolytic anaemia, and neurological complications. Their symptoms are caused by the presence of ultra-large VWF within their circulation, which triggers spontaneous thrombus formation within the microvasculature [106]. Despite the hereditary component of this disease, it is unclear why some patients are asymptomatic for many years and what drives the acute onset of their symptoms. Recent evidence suggests that the presence of NETs as response to unrelated infections may act as a 'second hit' in triggering the symptoms of TTP. This is in line with clinical data suggesting that minor infections often precede the onset of symptoms [439]. These data indicate that the presence of NETs promotes the formation of ultra-large VWF-dependent microthrombi within the circulation in TTP patients. It could be speculated that this process may, itself, act as a 'feedback loop' for further microthrombi development, as ultra-large VWF may 'prime' the platelets and lead to NET formation as well.

Platelet-leukocyte interactions have also been extensively described in the setting of cardiovascular disease, including stroke, atherosclerosis, atherothrombosis or heart failure [344,364]. Apart from the polymorphism linked to DVT (*rs2288904-G/A*), *SLC44A2* was identified by GWAS studies as a susceptibility locus for ischaemic stroke, through another polymorphism (*rs9797861-C/T*) [365].

Stroke is a leading cause of cardiovascular morbidity and mortality worldwide. About 80% of strokes are caused by cerebral ischaemia, resulting from a thrombus occluding cerebral blood vessels. Therefore, stroke is considered to be a thrombotic disorder. However, more recent work has re-defined stroke as a thrombo-inflammatory condition, as a link has been found between the initial thrombotic cause and the downstream inflammatory response in the severity of infarct size and ischaemia-reperfusion. Although platelet involvement in stroke has previously been well characterised as part of the underlying thrombotic cause, it recently became apparent that platelets also play a crucial role in the subsequent stroke-related inflammatory pathology. This was shown to be linked to the ability of platelets to release pro-

inflammatory chemokines, such as interleukin 1α (IL-1α) [440], but also to the platelet capacity to bind to endothelial cells and help in the recruitment of neutrophils and monocytes to the stroke site. The inflammatory involvement of platelets in stroke is thought to be mediated via GPVI, as well as the VWF A1-GPIbα axis.[441] In line with this, studies recently demonstrated the presence of VWF in thrombi from human stroke patients and the possibility of dissolving these thrombi using recombinant ADAMTS13 [442,443].

Moreover, the involvement of neutrophils in ischaemic stroke has been increasingly recognised. Studies analysing thrombi from ischaemic stroke patients reveal that these thrombi contain a high proportion of neutrophils. Additionally, staining the thrombi with an antibody against citrullinated H3 indicates that NETs are important structures within these thrombi. In light of these findings, treating these thrombi with DNase I *in vitro* seemed to be more effective than the current therapy with recombinant tissue plasminogen activator (tPA) [444]. Given the requirement for tPA to be administered within 3-5 hours from the onset of symptoms [445], finding alternative therapies to help dissolve the ischaemic thrombus would be crucial.

Given the previously demonstrated importance of VWF and GPIbα in the development of stroke, as well as the link between SLC44A2 and stroke, the interaction between VWF-'primed' platelets and leukocytes may also be involved in this condition. The SLC44A2 polymorphism related to stroke (*rs9797861-C/T*) is caused by a SNP that causes a substitution within the intronic region of *SLC44A2*. The causative link between this SNP and stroke is currently unknown. Interestingly, this polymorphism was shown to be in strong linkage disequilibrium (r^2=0.89) with *rs2288904-G/A* [367]. Future work aims to investigate whether this SNP also disrupts neutrophil binding to activated $\alpha_{IIb}\beta_3$. However, if this was the mechanism associated to protection against stroke, one would expect the *rs2288904-G/A* polymorphism to also be identified in GWAS studies of stroke. Furthermore, given the high shear conditions under which stroke thrombi form, a different mechanism might be involved.

An important contributing factor to the severity of stroke outcomes is represented by ischaemia-reperfusion injury. This occurs as a result of the reestablishment of normal flow after the dissolution or removal of the occlusive thrombus. Interestingly, recent studies recognise a role for T cells in ischaemia-reperfusion injury. Specifically, T cell-depleted mice had an improved recovery following ischaemic stroke suggesting that T cells might promote an inflammatory response that exacerbates the ischaemia-reperfusion [446,447]. The mechanism underlying T cell recruitment under these conditions is unclear. It is possible that, following ischaemic stroke, flow restriction might result in a substantially diminished shear rate downstream the occlusive thrombus. As this is an inflammatory condition and VWF is an acute phase protein, it may be assumed that endothelial cells release an increased amount of VWF under these circumstances. Upon ischaemia reperfusion, VWF might unravel, capture and 'prime' platelets. As my results show that these platelets specifically capture neutrophils and T cells, a possibility would be that this is the mechanism through which T cells are recruited and contribute to the severity of this process. However, this theory would need to be investigated in future experiments.

Another possible role for the interaction between VWF-'primed' platelets and T cells is within the setting of immune thrombocytopaenia (ITP). ITP is an autoimmune disorder manifest by defects in platelet production and low platelet counts [448]. Recent research suggests an involvement of T cells within the severity of this disease. During my PhD, I collaborated with Dr. Amna Malik and Dr. Nicola Cooper from the Haematology Department at Imperial College London and analysed blood samples from ITP patients in the flow system established. VWF-'primed' platelets from ITP patients captured a significantly higher number of CD8+ T cells under low shear conditions compared to healthy controls (data not shown). These results suggest a potential role for VWF-'primed' platelet-T cell interactions within the setting of ITP and are currently under further investigation.

8.3.1. Future directives – *In vivo* models to study the (patho)physiological role of this study

The flow setup I established during my PhD represents an attempt to mirror the physiological conditions *ex vivo*. Through this approach, I identified a novel interaction between VWF-'primed' platelets and leukocytes that might fulfil key roles in innate immunity, as well as promote the development of DVT and other thrombotic disorders. However, given the complexity of the vasculature, it is of utmost importance to study this interaction *in vivo* in order to confirm its proposed pathophysiological significance. The leading purpose of current and future work building on this project is to study the effects of specifically disrupting the interaction between activated $\alpha_{IIb}\beta_3$ and SLC44A2 in various disease models. Different mouse models could be used to inhibit this interaction, targeting either the platelet or the leukocyte.

8.3.1.1. *In vivo* model targeting VWF-dependent platelet 'priming'

In order to prevent the interaction between activated $\alpha_{IIb}\beta_3$ and SLC44A2 by targeting the platelets, VWF-dependent platelet 'priming' needs to be inhibited. *GpIba*$^{-/-}$ as well as *Vwf*$^{-/-}$ mice already exist, however, these do not only lack the VWF-dependent platelet 'priming', but also exhibit important haemostatic defects, as the VWF A1-GPIbα interaction is completely disrupted. Moreover, inhibiting this interaction by targeting $\alpha_{IIb}\beta_3$ was also not a valid approach as this would also result in lack of platelet aggregation and subsequent haemostatic problems.

To specifically ablate the VWF-mediated platelet signalling, a novel transgenic mouse, *GPIb*$\alpha^{\Delta sig/\Delta sig}$, was generated using the CRISPR/Cas9 technology. As presented in Chapter 5, this mouse lacks the last 24 amino acids within the intracellular tail of GPIbα, which should disrupt VWF-induced platelet signalling without affecting the interaction between VWF A1 domain and GPIbα. Indeed, initial characterisation of these mice revealed that they have a normal haemostatic response and normal platelet binding to VWF. As hypothesised, platelets from these mice exhibited diminished signalling following VWF A1-GPIbα interaction as

suggested by their reduced ability to spread on VWF in the presence of Botrocetin, and to bind fluorescent fibrinogen in preliminary flow assays. Consequently, as predicted, VWF-captured platelets from *GPIbα*$^{\Delta sig/\Delta sig}$ mice had a significantly lower ability to recruit neutrophils under flow. These results provide a promising platform for studying the importance of the VWF-'primed' platelet-leukocyte interaction in this mouse model.

Interestingly, additional preliminary data reveal a reduced ability of *GpIbα*$^{\Delta sig/\Delta sig}$ platelets to spread on collagen-related peptide (CRP) coated coverslips and to respond to CRP in flow cytometry experiments. These results suggest that *GpIbα*$^{\Delta sig/\Delta sig}$ mice might exhibit a defect in GPVI-mediated signalling as well and indicate a link between GPIbα and GPVI in modulating platelet phenotype. This finding is corroborated by other studies that suggest that the intracellular tail of GPIbα is important for the GPVI-FcRγ signalling pathway [410-413]. However, in aggregation assays this defect was not observed, suggesting that this may not be observed *in vivo*. This discrepancy might be due to the different sensitivities of these assays. It may be that in aggregation experiments, CRP can induce the expression of a sufficient amount of activated $\alpha_{IIb}\beta_3$ to bind fibrinogen and interlink the platelets. Moreover, the presence of shear within aggregation experiments may also account for this difference. However, under flow, *GpIbα*$^{\Delta sig/\Delta sig}$ platelets exhibited a reduced ability of forming aggregates on collagen-coated microchannels (data not shown). Work is currently underway to investigate the link between GPIbα and GPVI signalling and fully characterise these mice, before subjecting them to disease models discussed later in this section.

8.3.1.2. *In vivo* model targeting leukocytes

Another *in vivo* model to study the importance of this interaction could target leukocytes. Having identified SLC44A2 as the neutrophil receptor involved, it could be speculated that *Slc44a2*$^{-/-}$ mice would represent an appropriate model for this. *Slc44a2*$^{-/-}$ mice have been generated and recent work suggests that these mice exhibit a normal haemostatic response, and, notably, a reduced risk to developing DVT [402,431]. However, SLC44A2 is also expressed,

although at appreciably lower levels, in platelets and endothelial cells. Given the intricacy of the contributing factors to DVT, which include platelets, neutrophils and endothelial cells, it is difficult to ascertain whether *Slc44a2*$^{-/-}$ mice are protected against DVT due to the lack of neutrophil, platelet and/or endothelial cell SLC44A2. I hypothesise that the phenotype observed in *Slc44a2*$^{-/-}$ mice regarding the reduction in DVT is due to neutrophil SLC44A2, which prevents neutrophils from binding to VWF-'primed' platelets and NETose. To specifically study the effect of neutrophil SLC44A2 in DVT and other disease models, a neutrophil-specific conditional knock-out will be generated as part of future research and investigated in disease models discussed below.

Finally, considering the extensive GWAS studies showing *SLC44A2* polymorphisms being related to DVT and stroke [365,367,372], there is scope to generate mice expressing these SNPs as well. This would allow the study of the mechanisms leading to protection against DVT and stroke further. Additionally, if these mice do, as expected, have a diminished ability for neutrophils to bind VWF-'primed' platelets and subsequently form NETs, their susceptibility to infections could also be analysed.

8.3.1.3. Disease models

As discussed, we propose that the novel interaction between VWF-'primed' platelets and leukocytes provides novel mechanistic insights into the development of DVT, as well as providing new rationales for platelets seen as immune cells. Using the *in vivo* mouse models proposed above, future work aims to study the phenotype of these mice in the setting of infection, as well as in thrombotic disorders, primarily focussing on DVT and stroke.

Infection models would be based on established approaches, in which mice are injected with bacteria intra-peritoneally or via the tail vein [278,449]. Considering our hypothesis that the interaction between activated $\alpha_{IIb}\beta_3$ and SLC44A2 occurs at low shear and may play a role in bacterial clearance within hepatic vasculature, the liver sinusoids would be monitored. Mice

with impaired VWF-'primed' platelet-leukocyte interactions are expected to have an increased susceptibility to infection.

Mice do not have venous valves and, therefore, would not readily develop venous thrombi. However, previous studies established two models for venous thrombus formation in mice, the stasis and stenosis models. The stenosis model is recognised as being more reflective of the human conditions under which DVT occurs, and thrombi from these mice more closely resemble human thrombi [271,272]. In this model, the inferior vena cava (IVC) is ligated using a 30-gauge needle, which is subsequently removed, resulting in an 80-90% flow restriction. These mice develop thrombi after 6-12 hours, with fully occlusive thrombi forming after 24-48 hours [272]. Thrombi can be removed and analysed at different time-points and the different cells involved can be visualised. Thrombi can be subjected to cryosectioning and subsequent immunostaining to detect endothelial cells (anti-CD31), VWF (anti-VWF), platelets (anti-GPIbβ), neutrophils (anti-Ly6G), monocytes (anti-Ly6C), T cells (anti-CD3), B cells (anti-CD19), fibrin (anti-fibrin) and NETs (Hoechst/Sytox Green/anti-citrullinated H3).

Finally, due to the link between SLC44A2 and stroke, as well as the potential involvement of T cells, future research also aims to study ischaemic stroke and subsequent ischaemia-reperfusion injury in these mice.

9. Concluding remarks

The data presented in this thesis uncovers a novel interaction between VWF-'primed' platelets, via activated $\alpha_{IIb}\beta_3$, and neutrophils (and T cells), via SLC44A2. The results generated during my PhD are summarised in **Figure 9.1**. Under normal physiological circumstances, VWF circulates in a globular conformation and does not interact with resting platelets. However, if VWF gets arrested to a surface, be it collagen, an endothelial cell, a Kupffer cell or bacterium, or if it gets subjected to disturbed flow and tangles in venous valve pockets, VWF can unravel and capture platelets via its A1 domain, which binds GPIbα. In line with the literature, my results demonstrate that this leads to a shear-dependent, mechanosensitive transduction of a signal within platelets, that causes repeated transient intracellular Ca^{2+} release and culminates with the activation of $\alpha_{IIb}\beta_3$, 'priming' the platelets. For the first time, I demonstrated that activated $\alpha_{IIb}\beta_3$ can directly bind neutrophils (and T cells), but not monocytes and B cells, via SLC44A2. This interaction induces flow-dependent, NADPH-dependent and Ca^{2+}-dependent NET release, which could be highly beneficial and contribute to our innate immune response or, conversely, highly thrombogenic and lead to the initiation of DVT. In line with this, neutrophils homozygous for a polymorphism in *SLC44A2* (*rs2288904-A*) exhibited limited binding to VWF-'primed' platelets. Therefore, my data also provide insights into the previously unknown causative link between this polymorphism and the protection against DVT.

In conclusion, the significance of these results goes beyond the original scope of this project and provides a platform for multiple future studies, including identifying the mechanisms underlying the initiation of DVT, as well as offering new insights into platelet mediated NETosis and platelet roles in innate immunity. The ultimate purpose of this study is to develop novel, more effective, therapeutic strategies for conditions such as DVT and stroke, which would be fundamental for the field of cardiovascular research.

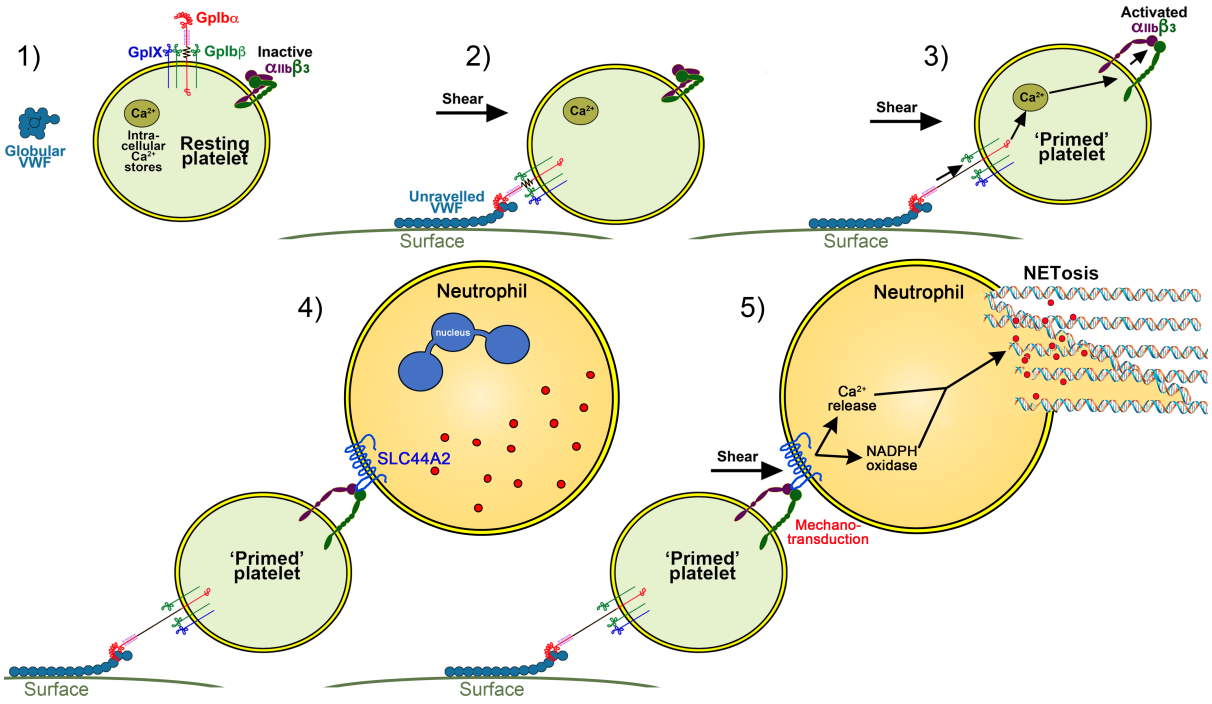

Figure 9.1 Model of platelet 'priming', neutrophil binding and NETosis.

1) *Under normal conditions, VWF circulates in plasma in a globular conformation that does not interact with platelets. Resting platelets present GPIbα on their surface - in complex with GPIbβ, GPIX and GPV - and also $\alpha_{IIb}\beta_3$ in its inactive conformation.* ***2)*** *When VWF is attached to a cell surface (e.g. activated endothelial cell/Kupffer cell or to a bacterial cell) or to an exposed collagen surface under flow, VWF unravels to expose its A1 domain enabling capture of platelets via GPIbα.* ***3)*** *Binding of platelets to VWF under flow induces mechano-unfolding of the juxtamembrane stalk of GPIbα leading to intraplatelet signalling, release of intraplatelet Ca^{2+} stores and activation of integrin $\alpha_{IIb}\beta_3$.* ***4)*** *Neutrophils can bind to activated $\alpha_{IIb}\beta_3$ under flow via an unknown receptor.* ***5)*** *Shear forces on the neutrophil induce mechanosensitive signalling into the neutrophil causing intracellular Ca^{2+} release and NADPH oxidase-dependent NETosis.*

Movie legends

Movie 1. Platelet capture on FL-VWF, VWF A1 or VWF A1*. Vena8 microchannels were coated with either full-length VWF (FL-VWF), VWF A1 or A1*. Whole blood labelled with $DiOC_6$ was perfused at $1000s^{-1}$ for 3 minutes. Note the reduced rate of platelet rolling on microchannels coated with A1* when compared to FL VWF or A1.

Movie 2. VWF A1-Gplbα interaction induces intraplatelet Ca^{2+} release under flow. Platelets were pre-loaded with Fluo-4 AM prior to perfusion through VWF A1*-coated microchannels at $1000s^{-1}$ for 5 minutes. Increases in platelet fluorescence corresponds to platelet intracellular Ca^{2+} release following attachment to VWF A1*. Note the repeated transient increases in fluorescence under flow, indicative of sustained and repeated signalling stimuli.

Movie 3. Leukocytes bind/roll on VWF-'primed' platelets. Whole blood or plasma-free blood labelled with $DiOC_6$ was perfused through channels coated with VWF A1* at high shear for 3.5 minutes to capture platelets in the presence or absence of either a blocking anti-P-selectin antibody or eptifibatide ($\alpha_{IIb}\beta_3$ blocker) prior to the acquisition of videos. The shear rate was reduced to $50s^{-1}$ to visualize leukocyte rolling or attaching (tracked in blue). Leukocytes rolled/bound on platelets in whole blood, plasma-free blood and plasma-free blood containing anti-P-selectin blocking antibody, but not in the presence of eptifibatide ($\alpha_{IIb}\beta_3$ blocker). The use of the anti-P-selectin blocking antibody did however increase the rolling velocity of leukocytes over the platelet surface.

Movie 4. Neutrophil start scanning following interaction with activated $\alpha_{IIb}\beta_3$. Following attachment of neutrophils (labelled with anti-CD16; red) to platelets (green) captured on FL-VWF (left), neutrophils start to scan the platelet surface. Similarly, neutrophils (anti-CD16-APC & Hoechst staining) bound to activated $\alpha_{IIb}\beta_3$-coated microchannels also scanned the surface and in some cases appeared to start migrating against the direction of flow. Shear rate = $50s^{-1}$.

Movie 5. Intracellular Ca^{2+} release in neutrophils following interaction with activated $\alpha_{IIb}\beta_3$ under flow. Neutrophils were pre-loaded with Fluo-4 AM and perfused over FL-VWF 'primed' platelets, $\alpha_{IIb}\beta_3$-coated or anti-CD16 coated microchannels at $50s^{-1}$. Following attachment of neutrophils to VWF-'primed' platelets or activated $\alpha_{IIb}\beta_3$ (but not anti-CD16), an increase in fluorescence corresponding to neutrophil intracellular Ca^{2+} release was observed.

Movie 6. $\alpha_{IIb}\beta_3$-induced NETosis. Isolated PMNs labelled with Hoechst (blue) and cell-impermeable Sytox Green were perfused over $\alpha_{IIb}\beta_3$-coated microchannels at $50s^{-1}$ for 10 minutes and then monitored under static conditions. Movie shown represents period from 105 to 120 minutes after attachment. Sytox Green staining appears, indicative of DNA becoming extracellular highlights the neutrophils undergoing NETosis.

Movie 7. Neutrophil binding to VWF-'primed' platelets occurs via SLC44A2 and is modified by the rs2288904 SNP. Plasma-free blood generated from individuals homozygous for the rs2288904-G/G major alleles in *SLC44A2* (SLC44A2 (R154/R154)) or rs2288904-A/A SNP (SLC44A2 (Q154/Q154)) was labelled with $DiOC_6$ and perfused through channels coated with VWF at high shear for 3.5 minutes. Shear was subsequently reduced to $50s^{-1}$. SLC44A2 (R154/R154) leukocytes (tracked in blue) were seen to roll on the VWF-'primed' platelets. The number of leukocytes interacting was severely reduced in the presence of an anti-SLC44A2 #2 antibody. Leukocytes from individuals homozygous for SLC44A2 (Q154/Q154), an allele associated with protection against DVT, exhibited reduced ability to interact with VWF-'primed' platelets.

References

1 Gale, A. J. Current understanding of hemostasis. *Toxicologic pathology* **39**, 273-280, doi:10.1177/0192623310389474 (2011).

2 Ruggeri, Z. M. Mechanisms initiating platelet thrombus formation. *Thrombosis and haemostasis* **78**, 611-616 (1997).

3 Teller, P. & White, T. K. The physiology of wound healing: injury through maturation. *The Surgical clinics of North America* **89**, 599-610, doi:10.1016/j.suc.2009.03.006 (2009).

4 Bryckaert, M., Rosa, J. P., Denis, C. V. & Lenting, P. J. Of von Willebrand factor and platelets. *Cellular and molecular life sciences : CMLS* **72**, 307-326, doi:10.1007/s00018-014-1743-8 (2015).

5 Clemetson, K. J. & Clemetson, J. M. Platelet collagen receptors. *Thrombosis and haemostasis* **86**, 189-197 (2001).

6 Dahlback, B. Blood coagulation. *Lancet (London, England)* **355**, 1627-1632, doi:10.1016/s0140-6736(00)02225-x (2000).

7 Watson, S. P., Auger, J. M., McCarty, O. J. & Pearce, A. C. GPVI and integrin alphaIIb beta3 signaling in platelets. *Journal of thrombosis and haemostasis : JTH* **3**, 1752-1762, doi:10.1111/j.1538-7836.2005.01429.x (2005).

8 Furie, B. & Furie, B. C. The molecular basis of blood coagulation. *Cell* **53**, 505-518 (1988).

9 McNicol, A. & Gerrard, J. M. Post-receptor events associated with thrombin-induced platelet activation. *Blood coagulation & fibrinolysis : an international journal in haemostasis and thrombosis* **4**, 975-991 (1993).

10 Crawley, J. T. & Lane, D. A. The haemostatic role of tissue factor pathway inhibitor. *Arteriosclerosis, thrombosis, and vascular biology* **28**, 233-242, doi:10.1161/atvbaha.107.141606 (2008).

11 Dahlback, B. The importance of the protein C system in the pathogenesis of venous thrombosis. *Hematology (Amsterdam, Netherlands)* **10 Suppl 1**, 138-139, doi:10.1080/10245330512331390195 (2005).

12 Quinsey, N. S., Greedy, A. L., Bottomley, S. P., Whisstock, J. C. & Pike, R. N. Antithrombin: in control of coagulation. *The international journal of biochemistry & cell biology* **36**, 386-389 (2004).

13 Cesarman-Maus, G. & Hajjar, K. A. Molecular mechanisms of fibrinolysis. *British journal of haematology* **129**, 307-321, doi:10.1111/j.1365-2141.2005.05444.x (2005).

14 Ginsburg, D. *et al.* Human von Willebrand factor (vWF): isolation of complementary DNA (cDNA) clones and chromosomal localization. *Science (New York, N.Y.)* **228**, 1401-1406 (1985).

15 Mancuso, D. J. *et al.* Structure of the gene for human von Willebrand factor. *The Journal of biological chemistry* **264**, 19514-19527 (1989).

16 Sadler, J. E. Biochemistry and genetics of von Willebrand factor. *Annual review of biochemistry* **67**, 395-424, doi:10.1146/annurev.biochem.67.1.395 (1998).

17 Jaffe, E. A., Hoyer, L. W. & Nachman, R. L. Synthesis of von Willebrand factor by cultured human endothelial cells. *Proceedings of the National Academy of Sciences of the United States of America* **71**, 1906-1909, doi:10.1073/pnas.71.5.1906 (1974).

18 Wagner, D. D., Olmsted, J. B. & Marder, V. J. Immunolocalization of von Willebrand protein in Weibel-Palade bodies of human endothelial cells. *The Journal of cell biology* **95**, 355-360, doi:10.1083/jcb.95.1.355 (1982).

19 Sporn, L. A., Chavin, S. I., Marder, V. J. & Wagner, D. D. Biosynthesis of von Willebrand protein by human megakaryocytes. *The Journal of clinical investigation* **76**, 1102-1106, doi:10.1172/jci112064 (1985).

20 Nachman, R., Levine, R. & Jaffe, E. A. Synthesis of factor VIII antigen by cultured guinea pig megakaryocytes. *The Journal of clinical investigation* **60**, 914-921, doi:10.1172/jci108846 (1977).
21 Wagner, D. D. Cell biology of von Willebrand factor. *Annual review of cell biology* **6**, 217-246, doi:10.1146/annurev.cb.06.110190.001245 (1990).
22 Titani, K. *et al.* Amino acid sequence of human von Willebrand factor. *Biochemistry* **25**, 3171-3184 (1986).
23 Nowak, A. A., Canis, K., Riddell, A., Laffan, M. A. & McKinnon, T. A. J. O-linked glycosylation of von Willebrand factor modulates the interaction with platelet receptor glycoprotein Ib under static and shear stress conditions. *Blood* **120**, 214-222, doi:10.1182/blood-2012-02-410050 (2012).
24 McKinnon, T. A. J. *et al.* Specific N-linked glycosylation sites modulate synthesis and secretion of von Willebrand factor. *Blood* **116**, 640-648, doi:10.1182/blood-2010-02-267450 (2010).
25 Voorberg, J. *et al.* Assembly and routing of von Willebrand factor variants: the requirements for disulfide-linked dimerization reside within the carboxy-terminal 151 amino acids. *The Journal of cell biology* **113**, 195-205, doi:10.1083/jcb.113.1.195 (1991).
26 Mayadas, T. N. & Wagner, D. D. Vicinal cysteines in the prosequence play a role in von Willebrand factor multimer assembly. *Proceedings of the National Academy of Sciences of the United States of America* **89**, 3531-3535, doi:10.1073/pnas.89.8.3531 (1992).
27 Wise, R. J., Pittman, D. D., Handin, R. I., Kaufman, R. J. & Orkin, S. H. The propeptide of von Willebrand factor independently mediates the assembly of von Willebrand multimers. *Cell* **52**, 229-236 (1988).
28 Haberichter, S. L. von Willebrand factor propeptide: biology and clinical utility. *Blood* **126**, 1753-1761, doi:10.1182/blood-2015-04-512731 (2015).
29 Lopes da Silva, M. & Cutler, D. F. von Willebrand factor multimerization and the polarity of secretory pathways in endothelial cells. *Blood* **128**, 277-285, doi:10.1182/blood-2015-10-677054 (2016).
30 Nightingale, T. & Cutler, D. The secretion of von Willebrand factor from endothelial cells; an increasingly complicated story. *Journal of thrombosis and haemostasis : JTH* **11 Suppl 1**, 192-201, doi:10.1111/jth.12225 (2013).
31 Giblin, J. P., Hewlett, L. J. & Hannah, M. J. Basal secretion of von Willebrand factor from human endothelial cells. *Blood* **112**, 957-964, doi:10.1182/blood-2007-12-130740 (2008).
32 Michaux, G. *et al.* Analysis of intracellular storage and regulated secretion of 3 von Willebrand disease–causing variants of von Willebrand factor. *Blood* **102**, 2452-2458, doi:10.1182/blood-2003-02-0599 (2003).
33 Weibel, E. R. & Palade, G. E. NEW CYTOPLASMIC COMPONENTS IN ARTERIAL ENDOTHELIA. *The Journal of cell biology* **23**, 101-112, doi:10.1083/jcb.23.1.101 (1964).
34 Denis, C. *et al.* A mouse model of severe von Willebrand disease: defects in hemostasis and thrombosis. *Proceedings of the National Academy of Sciences of the United States of America* **95**, 9524-9529, doi:10.1073/pnas.95.16.9524 (1998).
35 Cramer, E. M., Vainchenker, W., Vinci, G., Guichard, J. & Breton-Gorius, J. Gray platelet syndrome: immunoelectron microscopic localization of fibrinogen and von Willebrand factor in platelets and megakaryocytes. *Blood* **66**, 1309-1316 (1985).
36 Blann, A. D. von Willebrand factor antigen as an acute phase reactant and marker of endothelial cell injury in connective tissue diseases: a comparison with CRP, rheumatoid factor, and erythrocyte sedimentation rate. *Zeitschrift fur Rheumatologie* **50**, 320-322 (1991).
37 Pottinger, B. E., Read, R. C., Paleolog, E. M., Higgins, P. G. & Pearson, J. D. von Willebrand factor is an acute phase reactant in man. *Thrombosis research* **53**, 387-394 (1989).

38 Richardson, M. *et al.* Morphological alterations in endothelial cells associated with the release of von Willebrand factor after thrombin generation in vivo. *Arteriosclerosis and thrombosis : a journal of vascular biology* **14**, 990-999 (1994).
39 Borchiellini, A. *et al.* Quantitative analysis of von Willebrand factor propeptide release in vivo: effect of experimental endotoxemia and administration of 1-deamino-8-D-arginine vasopressin in humans. *Blood* **88**, 2951-2958 (1996).
40 Vaziri, N. D. *et al.* Coagulation and inhibitory and fibrinolytic proteins in essential hypertension. *Journal of the American Society of Nephrology : JASN* **4**, 222-228 (1993).
41 Castaman, G. & Eikenboom, J. C. J. ABO blood group also influences the von Willebrand factor (VWF) antigen level in heterozygous carriers of VWF null alleles, type 2N mutation Arg854Gln, and the missense mutation Cys2362Phe. *Blood* **100**, 1927-1928, doi:10.1182/blood-2002-04-1168 (2002).
42 Gill, J., Endres-Brooks, J., Bauer, P., Marks, W. J. & Montgomery, R. The effect of ABO blood group on the diagnosis of von Willebrand disease. *Blood* **69**, 1691-1695 (1987).
43 Sodetz, J. M., Paulson, J. C. & McKee, P. A. Carbohydrate composition and identification of blood group A, B, and H oligosaccharide structures on human Factor VIII/von Willebrand factor. *The Journal of biological chemistry* **254**, 10754-10760 (1979).
44 Fu, H. *et al.* Flow-induced elongation of von Willebrand factor precedes tension-dependent activation. *Nature communications* **8**, 324, doi:10.1038/s41467-017-00230-2 (2017).
45 Schneider, S. W. *et al.* Shear-induced unfolding triggers adhesion of von Willebrand factor fibers. *Proceedings of the National Academy of Sciences of the United States of America* **104**, 7899-7903, doi:10.1073/pnas.0608422104 (2007).
46 Siedlecki, C. A. *et al.* Shear-dependent changes in the three-dimensional structure of human von Willebrand factor. *Blood* **88**, 2939-2950 (1996).
47 Zhou, Y. F. *et al.* Sequence and structure relationships within von Willebrand factor. *Blood* **120**, 449-458, doi:10.1182/blood-2012-01-405134 (2012).
48 Emsley, J., Cruz, M., Handin, R. & Liddington, R. Crystal structure of the von Willebrand Factor A1 domain and implications for the binding of platelet glycoprotein Ib. *The Journal of biological chemistry* **273**, 10396-10401, doi:10.1074/jbc.273.17.10396 (1998).
49 Springer, T. A. Biology and physics of von Willebrand factor concatamers. *Journal of thrombosis and haemostasis : JTH* **9 Suppl 1**, 130-143, doi:10.1111/j.1538-7836.2011.04320.x (2011).
50 Jakobi, A. J., Mashaghi, A., Tans, S. J. & Huizinga, E. G. Calcium modulates force sensing by the von Willebrand factor A2 domain. *Nature communications* **2**, 385, doi:10.1038/ncomms1385 (2011).
51 Nakayama, T. *et al.* Identification of the regulatory elements of the human von Willebrand factor for binding to platelet GPIb. Importance of structural integrity of the regions flanked by the CYS1272-CYS1458 disulfide bond. *The Journal of biological chemistry* **277**, 22063-22072, doi:10.1074/jbc.M201327200 (2002).
52 Sobel, M., Soler, D. F., Kermode, J. C. & Harris, R. B. Localization and characterization of a heparin binding domain peptide of human von Willebrand factor. *The Journal of biological chemistry* **267**, 8857-8862 (1992).
53 Adachi, T. *et al.* Identification of amino acid residues essential for heparin binding by the A1 domain of human von Willebrand factor. *Biochemical and biophysical research communications* **339**, 1178-1183, doi:10.1016/j.bbrc.2005.11.126 (2006).
54 Flood, V. H. *et al.* Crucial role for the VWF A1 domain in binding to type IV collagen. *Blood* **125**, 2297-2304, doi:10.1182/blood-2014-11-610824 (2015).
55 Kasirer-Friede, A. *et al.* Signaling through GP Ib-IX-V activates alpha IIb beta 3 independently of other receptors. *Blood* **103**, 3403-3411, doi:10.1182/blood-2003-10-3664 (2004).

56 Blenner, M. A., Dong, X. & Springer, T. A. Structural basis of regulation of von Willebrand factor binding to glycoprotein Ib. *The Journal of biological chemistry* **289**, 5565-5579, doi:10.1074/jbc.M113.511220 (2014).
57 Kim, J., Zhang, C. Z., Zhang, X. & Springer, T. A. A mechanically stabilized receptor-ligand flex-bond important in the vasculature. *Nature* **466**, 992-995, doi:10.1038/nature09295 (2010).
58 Zhang, X., Halvorsen, K., Zhang, C. Z., Wong, W. P. & Springer, T. A. Mechanoenzymatic cleavage of the ultralarge vascular protein von Willebrand factor. *Science (New York, N.Y.)* **324**, 1330-1334, doi:10.1126/science.1170905 (2009).
59 Crawley, J. T., de Groot, R., Xiang, Y., Luken, B. M. & Lane, D. A. Unraveling the scissile bond: how ADAMTS13 recognizes and cleaves von Willebrand factor. *Blood* **118**, 3212-3221, doi:10.1182/blood-2011-02-306597 (2011).
60 Auton, M., Cruz, M. A. & Moake, J. Conformational stability and domain unfolding of the Von Willebrand factor A domains. *Journal of molecular biology* **366**, 986-1000, doi:10.1016/j.jmb.2006.10.067 (2007).
61 Zhang, Q. *et al.* Structural specializations of A2, a force-sensing domain in the ultralarge vascular protein von Willebrand factor. *Proceedings of the National Academy of Sciences of the United States of America* **106**, 9226-9231, doi:10.1073/pnas.0903679106 (2009).
62 Lankhof, H. *et al.* A3 domain is essential for interaction of von Willebrand factor with collagen type III. *Thrombosis and haemostasis* **75**, 950-958 (1996).
63 Mazzucato, M. *et al.* Identification of domains responsible for von Willebrand factor type VI collagen interaction mediating platelet adhesion under high flow. *The Journal of biological chemistry* **274**, 3033-3041, doi:10.1074/jbc.274.5.3033 (1999).
64 Romijn, R. A. *et al.* Identification of the collagen-binding site of the von Willebrand factor A3-domain. *The Journal of biological chemistry* **276**, 9985-9991, doi:10.1074/jbc.M006548200 (2001).
65 Santoro, S. A. Preferential binding of high molecular weight forms of von Willebrand factor to fibrillar collagen. *Biochimica et Biophysica Acta (BBA) - General Subjects* **756**, 123-126, doi:https://doi.org/10.1016/0304-4165(83)90032-6 (1983).
66 Yee, A. *et al.* A von Willebrand factor fragment containing the D'D3 domains is sufficient to stabilize coagulation factor VIII in mice. *Blood* **124**, 445-452, doi:10.1182/blood-2013-11-540534 (2014).
67 Chiu, P. L. *et al.* Mapping the interaction between factor VIII and von Willebrand factor by electron microscopy and mass spectrometry. *Blood* **126**, 935-938, doi:10.1182/blood-2015-04-641688 (2015).
68 Voorberg, J., Fontijn, R., van Mourik, J. A. & Pannekoek, H. Domains involved in multimer assembly of von willebrand factor (vWF): multimerization is independent of dimerization. *The EMBO journal* **9**, 797-803 (1990).
69 Zanardelli, S. *et al.* A novel binding site for ADAMTS13 constitutively exposed on the surface of globular VWF. *Blood* **114**, 2819-2828, doi:10.1182/blood-2009-05-224915 (2009).
70 Muia, J. *et al.* Allosteric activation of ADAMTS13 by von Willebrand factor. *Proceedings of the National Academy of Sciences* **111**, 18584-18589, doi:10.1073/pnas.1413282112 (2014).
71 Zhou, Y. F. *et al.* A pH-regulated dimeric bouquet in the structure of von Willebrand factor. *The EMBO journal* **30**, 4098-4111, doi:10.1038/emboj.2011.297 (2011).
72 Shapiro, S. E. *et al.* The von Willebrand factor predicted unpaired cysteines are essential for secretion. *Journal of thrombosis and haemostasis : JTH* **12**, 246-254, doi:10.1111/jth.12466 (2014).
73 Lankhof, H. *et al.* Role of the glycoprotein Ib-binding A1 repeat and the RGD sequence in platelet adhesion to human recombinant von Willebrand factor. *Blood* **86**, 1035-1042 (1995).
74 Katsumi, A., Tuley, E. A., Bodo, I. & Sadler, J. E. Localization of disulfide bonds in the cystine knot domain of human von Willebrand factor. *The Journal of biological chemistry* **275**, 25585-25594, doi:10.1074/jbc.M002654200 (2000).

75 Zhou, Y. F. & Springer, T. A. Highly reinforced structure of a C-terminal dimerization domain in von Willebrand factor. *Blood* **123**, 1785-1793, doi:10.1182/blood-2013-11-523639 (2014).
76 Kaufman, R. J., Dorner, A. J. & Fass, D. N. von Willebrand factor elevates plasma factor VIII without induction of factor VIII messenger RNA in the liver. *Blood* **93**, 193-197 (1999).
77 Sporn, L. A., Marder, V. J. & Wagner, D. D. Inducible secretion of large, biologically potent von Willebrand factor multimers. *Cell* **46**, 185-190 (1986).
78 Crawley, J. T., Lane, D. A., Woodward, M., Rumley, A. & Lowe, G. D. Evidence that high von Willebrand factor and low ADAMTS-13 levels independently increase the risk of a non-fatal heart attack. *Journal of thrombosis and haemostasis : JTH* **6**, 583-588, doi:10.1111/j.1538-7836.2008.02902.x (2008).
79 Ott, H. W. *et al.* Analysis of von Willebrand factor multimers by simultaneous high- and low-resolution vertical SDS-agarose gel electrophoresis and Cy5-labeled antibody high-sensitivity fluorescence detection. *American journal of clinical pathology* **133**, 322-330, doi:10.1309/ajcpzsbtd2bwomvl (2010).
80 Kumar, R. A. *et al.* Kinetics of GPIbalpha-vWF-A1 tether bond under flow: effect of GPIbalpha mutations on the association and dissociation rates. *Biophysical journal* **85**, 4099-4109, doi:10.1016/s0006-3495(03)74822-x (2003).
81 Lou, J. & Zhu, C. Flow induces loop-to-beta-hairpin transition on the beta-switch of platelet glycoprotein Ib alpha. *Proceedings of the National Academy of Sciences of the United States of America* **105**, 13847-13852, doi:10.1073/pnas.0801965105 (2008).
82 Tischer, A., Cruz, M. A. & Auton, M. The linker between the D3 and A1 domains of vWF suppresses A1-GPIbalpha catch bonds by site-specific binding to the A1 domain. *Protein science : a publication of the Protein Society* **22**, 1049-1059, doi:10.1002/pro.2294 (2013).
83 Woulfe, D., Yang, J. & Brass, L. ADP and platelets: the end of the beginning. *The Journal of clinical investigation* **107**, 1503-1505, doi:10.1172/jci13361 (2001).
84 Offermanns, S. Activation of platelet function through G protein-coupled receptors. *Circulation research* **99**, 1293-1304, doi:10.1161/01.Res.0000251742.71301.16 (2006).
85 Zheng, Y., Chen, J. & Lopez, J. A. Flow-driven assembly of VWF fibres and webs in in vitro microvessels. *Nature communications* **6**, 7858, doi:10.1038/ncomms8858 (2015).
86 Farrell, D. H., Thiagarajan, P., Chung, D. W. & Davie, E. W. Role of fibrinogen alpha and gamma chain sites in platelet aggregation. *Proceedings of the National Academy of Sciences of the United States of America* **89**, 10729-10732, doi:10.1073/pnas.89.22.10729 (1992).
87 Donadelli, R., Orje, J. N., Capoferri, C., Remuzzi, G. & Ruggeri, Z. M. Size regulation of von Willebrand factor-mediated platelet thrombi by ADAMTS13 in flowing blood. *Blood* **107**, 1943-1950, doi:10.1182/blood-2005-07-2972 (2006).
88 Koedam, J. A., Hamer, R. J., Beeser-Visser, N. H., Bouma, B. N. & Sixma, J. J. The effect of von Willebrand factor on activation of factor VIII by factor Xa. *European journal of biochemistry* **189**, 229-234 (1990).
89 Lenting, P. J., van de Loo, J. W., Donath, M. J., van Mourik, J. A. & Mertens, K. The sequence Glu1811-Lys1818 of human blood coagulation factor VIII comprises a binding site for activated factor IX. *The Journal of biological chemistry* **271**, 1935-1940, doi:10.1074/jbc.271.4.1935 (1996).
90 Nogami, K. *et al.* A novel mechanism of factor VIII protection by von Willebrand factor from activated protein C–catalyzed inactivation. *Blood* **99**, 3993-3998, doi:10.1182/blood.V99.11.3993 (2002).
91 Saenko, E. L. & Scandella, D. A mechanism for inhibition of factor VIII binding to phospholipid by von Willebrand factor. *The Journal of biological chemistry* **270**, 13826-13833, doi:10.1074/jbc.270.23.13826 (1995).
92 Bowman, M., Hopman, W. M., Rapson, D., Lillicrap, D. & James, P. The prevalence of symptomatic von Willebrand disease in primary care practice. *Journal of thrombosis and haemostasis : JTH* **8**, 213-216, doi:10.1111/j.1538-7836.2009.03661.x (2010).

93 Leebeek, F. W. & Eikenboom, J. C. Von Willebrand's Disease. *The New England journal of medicine* **375**, 2067-2080, doi:10.1056/NEJMra1601561 (2016).
94 Sadler, J. E. *et al.* Update on the pathophysiology and classification of von Willebrand disease: a report of the Subcommittee on von Willebrand Factor. *Journal of thrombosis and haemostasis : JTH* **4**, 2103-2114, doi:10.1111/j.1538-7836.2006.02146.x (2006).
95 Tiede, A., Rand, J. H., Budde, U., Ganser, A. & Federici, A. B. How I treat the acquired von Willebrand syndrome. *Blood* **117**, 6777-6785, doi:10.1182/blood-2010-11-297580 (2011).
96 Mohri, H. *et al.* Acquired von Willebrand disease associated with multiple myeloma; characterization of an inhibitor to von Willebrand factor. *Blood coagulation & fibrinolysis : an international journal in haemostasis and thrombosis* **6**, 561-566 (1995).
97 Lillicrap, D. von Willebrand disease: advances in pathogenetic understanding, diagnosis, and therapy. *Blood* **122**, 3735-3740, doi:10.1182/blood-2013-06-498303 (2013).
98 Sadler, J. E. New concepts in von Willebrand disease. *Annual review of medicine* **56**, 173-191, doi:10.1146/annurev.med.56.082103.104713 (2005).
99 Tischer, A., Madde, P., Blancas-Mejia, L. M. & Auton, M. A molten globule intermediate of the von Willebrand factor A1 domain firmly tethers platelets under shear flow. *Proteins* **82**, 867-878, doi:10.1002/prot.24464 (2014).
100 Eikenboom, J. C. Congenital von Willebrand disease type 3: clinical manifestations, pathophysiology and molecular biology. *Best practice & research. Clinical haematology* **14**, 365-379, doi:10.1053/beha.2001.0139 (2001).
101 Bongers, T. N. *et al.* High von Willebrand factor levels increase the risk of first ischemic stroke: influence of ADAMTS13, inflammation, and genetic variability. *Stroke* **37**, 2672-2677, doi:10.1161/01.STR.0000244767.39962.f7 (2006).
102 Kleinschnitz, C. *et al.* Deficiency of von Willebrand factor protects mice from ischemic stroke. *Blood* **113**, 3600-3603, doi:10.1182/blood-2008-09-180695 (2009).
103 Qizilbash, N., Duffy, S., Prentice, C. R., Boothby, M. & Warlow, C. Von Willebrand factor and risk of ischemic stroke. *Neurology* **49**, 1552-1556, doi:10.1212/wnl.49.6.1552 (1997).
104 Vischer, U. M. von Willebrand factor, endothelial dysfunction, and cardiovascular disease. *Journal of thrombosis and haemostasis : JTH* **4**, 1186-1193, doi:10.1111/j.1538-7836.2006.01949.x (2006).
105 Scully, M. *et al.* Regional UK TTP registry: correlation with laboratory ADAMTS 13 analysis and clinical features. *British journal of haematology* **142**, 819-826, doi:10.1111/j.1365-2141.2008.07276.x (2008).
106 Scully, M. *et al.* Guidelines on the diagnosis and management of thrombotic thrombocytopenic purpura and other thrombotic microangiopathies. *British journal of haematology* **158**, 323-335, doi:10.1111/j.1365-2141.2012.09167.x (2012).
107 van der Meijden, P. E. J. & Heemskerk, J. W. M. Platelet biology and functions: new concepts and clinical perspectives. *Nature reviews. Cardiology* **16**, 166-179, doi:10.1038/s41569-018-0110-0 (2019).
108 Junt, T. *et al.* Dynamic Visualization of Thrombopoiesis Within Bone Marrow. *Science (New York, N.Y.)* **317**, 1767-1770, doi:10.1126/science.1146304 (2007).
109 Lefrancais, E. *et al.* The lung is a site of platelet biogenesis and a reservoir for haematopoietic progenitors. *Nature* **544**, 105-109, doi:10.1038/nature21706 (2017).
110 McCarty, J. M., Sprugel, K. H., Fox, N. E., Sabath, D. E. & Kaushansky, K. Murine thrombopoietin mRNA levels are modulated by platelet count. *Blood* **86**, 3668-3675 (1995).
111 Kaser, A. *et al.* Interleukin-6 stimulates thrombopoiesis through thrombopoietin: role in inflammatory thrombocytosis. *Blood* **98**, 2720-2725 (2001).
112 Cohen, J. A. & Leeksma, C. H. Determination of the life span of human blood platelets using labelled diisopropylfluorophosphonate. *The Journal of clinical investigation* **35**, 964-969, doi:10.1172/jci103356 (1956).

113 Odell, T. T., Jr. & Mc, D. T. Life span of mouse blood platelets. *Proceedings of the Society for Experimental Biology and Medicine. Society for Experimental Biology and Medicine (New York, N.Y.)* **106**, 107-108 (1961).
114 Harrington, W. J., Minnich, V., Hollingsworth, J. W. & Moore, C. V. Demonstration of a thrombocytopenic factor in the blood of patients with thrombocytopenic purpura. *The Journal of laboratory and clinical medicine* **38**, 1-10 (1951).
115 Quach, M. E., Chen, W. & Li, R. Mechanisms of platelet clearance and translation to improve platelet storage. *Blood* **131**, 1512-1521, doi:10.1182/blood-2017-08-743229 (2018).
116 Radley, J. M. & Haller, C. J. Fate of senescent megakaryocytes in the bone marrow. *British journal of haematology* **53**, 277-287 (1983).
117 Grozovsky, R. *et al.* The Ashwell-Morell receptor regulates hepatic thrombopoietin production via JAK2-STAT3 signaling. *Nature medicine* **21**, 47-54, doi:10.1038/nm.3770 (2015).
118 Mitchell, W. B. & Bussel, J. B. How low can you go? *Blood* **121**, 4817-4818, doi:10.1182/blood-2013-04-497610 (2013).
119 Hanson, S. R. & Slichter, S. J. Platelet kinetics in patients with bone marrow hypoplasia: evidence for a fixed platelet requirement. *Blood* **66**, 1105-1109 (1985).
120 Morowski, M. *et al.* Only severe thrombocytopenia results in bleeding and defective thrombus formation in mice. *Blood* **121**, 4938-4947, doi:10.1182/blood-2012-10-461459 (2013).
121 Koupenova, M., Clancy, L., Corkrey, H. A. & Freedman, J. E. Circulating Platelets as Mediators of Immunity, Inflammation, and Thrombosis. *Circulation research* **122**, 337-351, doi:10.1161/circresaha.117.310795 (2018).
122 Deppermann, C. & Kubes, P. Platelets and infection. *Seminars in immunology* **28**, 536-545, doi:10.1016/j.smim.2016.10.005 (2016).
123 Jenne, C. N. & Kubes, P. Platelets in inflammation and infection. *Platelets* **26**, 286-292, doi:10.3109/09537104.2015.1010441 (2015).
124 Li, R. & Emsley, J. The organizing principle of the platelet glycoprotein Ib–IX–V complex. *Journal of Thrombosis and Haemostasis* **11**, 605-614, doi:10.1111/jth.12144 (2013).
125 Berlanga, O. *et al.* Expression of the collagen receptor glycoprotein VI during megakaryocyte differentiation. *Blood* **96**, 2740-2745 (2000).
126 Kasirer-Friede, A., Kahn, M. L. & Shattil, S. J. Platelet integrins and immunoreceptors. *Immunological reviews* **218**, 247-264, doi:10.1111/j.1600-065X.2007.00532.x (2007).
127 Piguet, P. F., Vesin, C. & Rochat, A. Beta2 integrin modulates platelet caspase activation and life span in mice. *European journal of cell biology* **80**, 171-177 (2001).
128 Zeiler, M., Moser, M. & Mann, M. Copy Number Analysis of the Murine Platelet Proteome Spanning the Complete Abundance Range. *Molecular & Cellular Proteomics* **13**, 3435-3445, doi:10.1074/mcp.M114.038513 (2014).
129 Luo, S. Z. *et al.* Glycoprotein Ibalpha forms disulfide bonds with 2 glycoprotein Ibbeta subunits in the resting platelet. *Blood* **109**, 603-609, doi:10.1182/blood-2006-05-024091 (2007).
130 Hickey, M. J., Deaven, L. L. & Roth, G. J. Human platelet glycoprotein IX. Characterization of cDNA and localization of the gene to chromosome 3. *FEBS letters* **274**, 189-192 (1990).
131 Hickey, M. J., Hagen, F. S., Yagi, M. & Roth, G. J. Human platelet glycoprotein V: characterization of the polypeptide and the related Ib-V-IX receptor system of adhesive, leucine-rich glycoproteins. *Proceedings of the National Academy of Sciences of the United States of America* **90**, 8327-8331, doi:10.1073/pnas.90.18.8327 (1993).
132 Lanza, F. *et al.* Cloning and characterization of the gene encoding the human platelet glycoprotein V. A member of the leucine-rich glycoprotein family cleaved during thrombin-induced platelet activation. *The Journal of biological chemistry* **268**, 20801-20807 (1993).

133 Wenger, R. H. *et al.* The 5' flanking region and chromosomal localization of the gene encoding human platelet membrane glycoprotein Ib alpha. *Gene* **85**, 517-524 (1989).
134 Du, X., Beutler, L., Ruan, C., Castaldi, P. & Berndt, M. Glycoprotein Ib and glycoprotein IX are fully complexed in the intact platelet membrane. *Blood* **69**, 1524-1527 (1987).
135 Modderman, P. W., Admiraal, L. G., Sonnenberg, A. & von dem Borne, A. E. Glycoproteins V and Ib-IX form a noncovalent complex in the platelet membrane. *The Journal of biological chemistry* **267**, 364-369 (1992).
136 Li, R. The Glycoprotein Ib-IX Complex. (2015).
137 Baglia, F. A., Badellino, K. O., Li, C. Q., Lopez, J. A. & Walsh, P. N. Factor XI binding to the platelet glycoprotein Ib-IX-V complex promotes factor XI activation by thrombin. *The Journal of biological chemistry* **277**, 1662-1668, doi:10.1074/jbc.M108319200 (2002).
138 Bradford, H. N., Pixley, R. A. & Colman, R. W. Human factor XII binding to the glycoprotein Ib-IX-V complex inhibits thrombin-induced platelet aggregation. *The Journal of biological chemistry* **275**, 22756-22763, doi:10.1074/jbc.M002591200 (2000).
139 Joseph, K., Nakazawa, Y., Bahou, W. F., Ghebrehiwet, B. & Kaplan, A. P. Platelet glycoprotein Ib: a zinc-dependent binding protein for the heavy chain of high-molecular-weight kininogen. *Molecular medicine (Cambridge, Mass.)* **5**, 555-563 (1999).
140 Romo, G. M. *et al.* The glycoprotein Ib-IX-V complex is a platelet counterreceptor for P-selectin. *The Journal of experimental medicine* **190**, 803-814, doi:10.1084/jem.190.6.803 (1999).
141 Simon, D. I. *et al.* Platelet glycoprotein ibalpha is a counterreceptor for the leukocyte integrin Mac-1 (CD11b/CD18). *The Journal of experimental medicine* **192**, 193-204, doi:10.1084/jem.192.2.193 (2000).
142 Huizinga, E. G. *et al.* Structures of glycoprotein Ibalpha and its complex with von Willebrand factor A1 domain. *Science (New York, N.Y.)* **297**, 1176-1179, doi:10.1126/science.107355 (2002).
143 Ju, L., Chen, Y., Xue, L., Du, X. & Zhu, C. Cooperative unfolding of distinctive mechanoreceptor domains transduces force into signals. *eLife* **5**, doi:10.7554/eLife.15447 (2016).
144 Zhang, W. *et al.* Identification of a juxtamembrane mechanosensitive domain in the platelet mechanosensor glycoprotein Ib-IX complex. *Blood* **125**, 562-569, doi:10.1182/blood-2014-07-589507 (2015).
145 Luo, S. Z. & Li, R. Specific heteromeric association of four transmembrane peptides derived from platelet glycoprotein Ib-IX complex. *Journal of molecular biology* **382**, 448-457, doi:10.1016/j.jmb.2008.07.037 (2008).
146 Bodnar, R. J., Gu, M., Li, Z., Englund, G. D. & Du, X. The cytoplasmic domain of the platelet glycoprotein Ibalpha is phosphorylated at serine 609. *The Journal of biological chemistry* **274**, 33474-33479, doi:10.1074/jbc.274.47.33474 (1999).
147 Mangin, P. *et al.* Identification of a novel 14-3-3zeta binding site within the cytoplasmic tail of platelet glycoprotein Ibalpha. *Blood* **104**, 420-427, doi:10.1182/blood-2003-08-2881 (2004).
148 Yuan, Y. *et al.* Identification of a novel 14-3-3zeta binding site within the cytoplasmic domain of platelet glycoprotein Ibalpha that plays a key role in regulating the von Willebrand factor binding function of glycoprotein Ib-IX. *Circulation research* **105**, 1177-1185, doi:10.1161/circresaha.109.204669 (2009).
149 Andrews, R. K. & Fox, J. E. Identification of a region in the cytoplasmic domain of the platelet membrane glycoprotein Ib-IX complex that binds to purified actin-binding protein. *The Journal of biological chemistry* **267**, 18605-18611 (1992).
150 Nakamura, F. *et al.* The structure of the GPIb-filamin A complex. *Blood* **107**, 1925-1932, doi:10.1182/blood-2005-10-3964 (2006).

151 Feng, S., Resendiz, J. C., Lu, X. & Kroll, M. H. Filamin A binding to the cytoplasmic tail of glycoprotein Ibalpha regulates von Willebrand factor-induced platelet activation. *Blood* **102**, 2122-2129, doi:10.1182/blood-2002-12-3805 (2003).
152 Mangin, P. *et al.* Identification of a novel 14-3-3ζ binding site within the cytoplasmic tail of platelet glycoprotein Ibα. *Blood* **104**, 420-427, doi:10.1182/blood-2003-08-2881 (2004).
153 Mangin, P. H. *et al.* Identification of five novel 14-3-3 isoforms interacting with the GPIb-IX complex in platelets. *Journal of thrombosis and haemostasis : JTH* **7**, 1550-1555, doi:10.1111/j.1538-7836.2009.03530.x (2009).
154 Mu, F. T. *et al.* A functional 14-3-3zeta-independent association of PI3-kinase with glycoprotein Ib alpha, the major ligand-binding subunit of the platelet glycoprotein Ib-IX-V complex. *Blood* **111**, 4580-4587, doi:10.1182/blood-2007-09-111096 (2008).
155 Lanza, F. Bernard-Soulier syndrome (Hemorrhagiparous thrombocytic dystrophy). *Orphanet Journal of Rare Diseases* **1**, 46, doi:10.1186/1750-1172-1-46 (2006).
156 Lopez, J. A., Andrews, R. K., Afshar-Kharghan, V. & Berndt, M. C. Bernard-Soulier syndrome. *Blood* **91**, 4397-4418 (1998).
157 Ware, J., Russell, S. & Ruggeri, Z. M. Generation and rescue of a murine model of platelet dysfunction: the Bernard-Soulier syndrome. *Proceedings of the National Academy of Sciences of the United States of America* **97**, 2803-2808, doi:10.1073/pnas.050582097 (2000).
158 Wagner, C. L. *et al.* Analysis of GPIIb/IIIa receptor number by quantification of 7E3 binding to human platelets. *Blood* **88**, 907-914 (1996).
159 Niiya, K. *et al.* Increased surface expression of the membrane glycoprotein IIb/IIIa complex induced by platelet activation. Relationship to the binding of fibrinogen and platelet aggregation. *Blood* **70**, 475-483 (1987).
160 Bennett, J. S. Structure and function of the platelet integrin alphaIIbbeta3. *The Journal of clinical investigation* **115**, 3363-3369, doi:10.1172/jci26989 (2005).
161 Hynes, R. O. Integrins: versatility, modulation, and signaling in cell adhesion. *Cell* **69**, 11-25 (1992).
162 Nurden, A. T. & Pillois, X. ITGA2B and ITGB3 gene mutations associated with Glanzmann thrombasthenia. *Platelets* **29**, 98-101, doi:10.1080/09537104.2017.1371291 (2018).
163 Duperray, A. *et al.* Biosynthesis and processing of platelet GPIIb-IIIa in human megakaryocytes. *The Journal of cell biology* **104**, 1665-1673, doi:10.1083/jcb.104.6.1665 (1987).
164 Kolodziej, M. A., Vilaire, G., Gonder, D., Poncz, M. & Bennett, J. S. Study of the endoproteolytic cleavage of platelet glycoprotein IIb using oligonucleotide-mediated mutagenesis. *The Journal of biological chemistry* **266**, 23499-23504 (1991).
165 Adair, B. D. & Yeager, M. Three-dimensional model of the human platelet integrin alpha IIbbeta 3 based on electron cryomicroscopy and x-ray crystallography. *Proceedings of the National Academy of Sciences of the United States of America* **99**, 14059-14064, doi:10.1073/pnas.212498199 (2002).
166 Carrell, N. A., Fitzgerald, L. A., Steiner, B., Erickson, H. P. & Phillips, D. R. Structure of human platelet membrane glycoproteins IIb and IIIa as determined by electron microscopy. *The Journal of biological chemistry* **260**, 1743-1749 (1985).
167 Xiong, J. P. *et al.* Crystal structure of the extracellular segment of integrin alpha Vbeta3. *Science (New York, N.Y.)* **294**, 339-345, doi:10.1126/science.1064535 (2001).
168 Xiao, T., Takagi, J., Coller, B. S., Wang, J. H. & Springer, T. A. Structural basis for allostery in integrins and binding to fibrinogen-mimetic therapeutics. *Nature* **432**, 59-67, doi:10.1038/nature02976 (2004).
169 Adair, B. D. *et al.* Three-dimensional EM structure of the ectodomain of integrin {alpha}V{beta}3 in a complex with fibronectin. *The Journal of cell biology* **168**, 1109-1118, doi:10.1083/jcb.200410068 (2005).

170 Xiong, J. P. *et al.* Crystal structure of the extracellular segment of integrin alpha Vbeta3 in complex with an Arg-Gly-Asp ligand. *Science (New York, N.Y.)* **296**, 151-155, doi:10.1126/science.1069040 (2002).
171 Takagi, J., Petre, B. M., Walz, T. & Springer, T. A. Global conformational rearrangements in integrin extracellular domains in outside-in and inside-out signaling. *Cell* **110**, 599-511, doi:10.1016/s0092-8674(02)00935-2 (2002).
172 Zhu, J. *et al.* Structure of a complete integrin ectodomain in a physiologic resting state and activation and deactivation by applied forces. *Molecular cell* **32**, 849-861, doi:10.1016/j.molcel.2008.11.018 (2008).
173 Poon, M. C., Di Minno, G., d'Oiron, R. & Zotz, R. New Insights Into the Treatment of Glanzmann Thrombasthenia. *Transfusion medicine reviews* **30**, 92-99, doi:10.1016/j.tmrv.2016.01.001 (2016).
174 Nurden, A. T. Glanzmann thrombasthenia. *Orphanet Journal of Rare Diseases* **1**, 10, doi:10.1186/1750-1172-1-10 (2006).
175 George, J. N., Caen, J. P. & Nurden, A. T. Glanzmann's thrombasthenia: the spectrum of clinical disease. *Blood* **75**, 1383-1395 (1990).
176 Hodivala-Dilke, K. M. *et al.* Beta3-integrin-deficient mice are a model for Glanzmann thrombasthenia showing placental defects and reduced survival. *The Journal of clinical investigation* **103**, 229-238, doi:10.1172/jci5487 (1999).
177 Weiss, H. J., Turitto, V. T. & Baumgartner, H. R. Further evidence that glycoprotein IIb-IIIa mediates platelet spreading on subendothelium. *Thrombosis and haemostasis* **65**, 202-205 (1991).
178 Schoenwaelder, S. M., Yuan, Y., Cooray, P., Salem, H. H. & Jackson, S. P. Calpain cleavage of focal adhesion proteins regulates the cytoskeletal attachment of integrin alphaIIbbeta3 (platelet glycoprotein IIb/IIIa) and the cellular retraction of fibrin clots. *The Journal of biological chemistry* **272**, 1694-1702, doi:10.1074/jbc.272.3.1694 (1997).
179 Bennett, J. S. & Vilaire, G. Exposure of platelet fibrinogen receptors by ADP and epinephrine. *The Journal of clinical investigation* **64**, 1393-1401, doi:10.1172/jci109597 (1979).
180 Ginsberg, M. H., Forsyth, J., Lightsey, A., Chediak, J. & Plow, E. F. Reduced surface expression and binding of fibronectin by thrombin-stimulated thrombasthenic platelets. *The Journal of clinical investigation* **71**, 619-624, doi:10.1172/JCI110808 (1983).
181 Thiagarajan, P. & Kelly, K. L. Exposure of binding sites for vitronectin on platelets following stimulation. *The Journal of biological chemistry* **263**, 3035-3038 (1988).
182 Hantgan, R. R. Fibrin protofibril and fibrinogen binding to ADP-stimulated platelets: evidence for a common mechanism. *Biochimica et biophysica acta* **968**, 24-35, doi:10.1016/0167-4889(88)90040-7 (1988).
183 Karczewski, J. *et al.* The interaction of thrombospondin with platelet glycoprotein GPIIb-IIIa. *The Journal of biological chemistry* **264**, 21322-21326 (1989).
184 Kattula, S., Byrnes, J. R. & Wolberg, A. S. Fibrinogen and Fibrin in Hemostasis and Thrombosis. *Arteriosclerosis, thrombosis, and vascular biology* **37**, e13-e21, doi:10.1161/atvbaha.117.308564 (2017).
185 Harrison, P. Platelet Alpha-granular Fibrinogen. *Platelets* **3**, 1-10, doi:10.3109/09537109209013161 (1992).
186 Durrant, T. N., van den Bosch, M. T. & Hers, I. Integrin α(IIb)β(3) outside-in signaling. *Blood* **130**, 1607-1619, doi:10.1182/blood-2017-03-773614 (2017).
187 Vinogradova, O. *et al.* A structural mechanism of integrin alpha(IIb)beta(3) "inside-out" activation as regulated by its cytoplasmic face. *Cell* **110**, 587-597 (2002).
188 Chen, Y., Yuan, Y. & Li, W. Sorting machineries: how platelet-dense granules differ from alpha-granules. *Bioscience reports* **38**, doi:10.1042/bsr20180458 (2018).
189 Thon, J. N. & Italiano, J. E. Platelets: production, morphology and ultrastructure. *Handbook of experimental pharmacology*, 3-22, doi:10.1007/978-3-642-29423-5_1 (2012).

190 Thon, J. N. *et al.* T granules in human platelets function in TLR9 organization and signaling. *The Journal of cell biology* **198**, 561-574, doi:10.1083/jcb.201111136 (2012).
191 Blair, P. & Flaumenhaft, R. Platelet alpha-granules: basic biology and clinical correlates. *Blood reviews* **23**, 177-189, doi:10.1016/j.blre.2009.04.001 (2009).
192 Heijnen, H. F. *et al.* Multivesicular bodies are an intermediate stage in the formation of platelet alpha-granules. *Blood* **91**, 2313-2325 (1998).
193 Cramer, E. M. *et al.* Uncoordinated expression of alpha-granule proteins in human megakaryocytes. *Progress in clinical and biological research* **356**, 131-142 (1990).
194 Maynard, D. M., Heijnen, H. F., Horne, M. K., White, J. G. & Gahl, W. A. Proteomic analysis of platelet alpha-granules using mass spectrometry. *Journal of thrombosis and haemostasis : JTH* **5**, 1945-1955, doi:10.1111/j.1538-7836.2007.02690.x (2007).
195 Rendu, F. & Brohard-Bohn, B. The platelet release reaction: granules' constituents, secretion and functions. *Platelets* **12**, 261-273, doi:10.1080/09537100120068170 (2001).
196 Harrison, P. & Cramer, E. M. Platelet alpha-granules. *Blood reviews* **7**, 52-62 (1993).
197 Nurden, A. T. & Nurden, P. The gray platelet syndrome: clinical spectrum of the disease. *Blood reviews* **21**, 21-36, doi:10.1016/j.blre.2005.12.003 (2007).
198 Deal, J. E., Barratt, T. M. & Dillon, M. J. Fanconi syndrome, ichthyosis, dysmorphism, jaundice and diarrhoea--a new syndrome. *Pediatric nephrology (Berlin, Germany)* **4**, 308-313 (1990).
199 Pluthero, F. G., Di Paola, J., Carcao, M. D. & Kahr, W. H. A. NBEAL2 mutations and bleeding in patients with gray platelet syndrome. *Platelets* **29**, 632-635, doi:10.1080/09537104.2018.1478405 (2018).
200 Gunay-Aygun, M. *et al.* Gray platelet syndrome: natural history of a large patient cohort and locus assignment to chromosome 3p. *Blood* **116**, 4990-5001, doi:10.1182/blood-2010-05-286534 (2010).
201 Albers, C. A. *et al.* Exome sequencing identifies NBEAL2 as the causative gene for gray platelet syndrome. *Nature Genetics* **43**, 735, doi:10.1038/ng.885

https://www.nature.com/articles/ng.885#supplementary-information (2011).
202 Gunay-Aygun, M. *et al.* NBEAL2 is mutated in gray platelet syndrome and is required for biogenesis of platelet α-granules. *Nat Genet* **43**, 732-734, doi:10.1038/ng.883 (2011).
203 Kahr, W. H. *et al.* Mutations in NBEAL2, encoding a BEACH protein, cause gray platelet syndrome. *Nat Genet* **43**, 738-740, doi:10.1038/ng.884 (2011).
204 Raccuglia, G. Gray platelet syndrome. A variety of qualitative platelet disorder. *The American journal of medicine* **51**, 818-828 (1971).
205 Youssefian, T. & Cramer, E. M. Megakaryocyte dense granule components are sorted in multivesicular bodies. *Blood* **95**, 4004-4007 (2000).
206 Leven, R. M. Isolation of primary megakaryocytes and studies of proplatelet formation. *Methods in molecular biology (Clifton, N.J.)* **272**, 281-291, doi:10.1385/1-59259-782-3:281 (2004).
207 White, J. G. The dense bodies of human platelets: inherent electron opacity of the serotonin storage particles. *Blood* **33**, 598-606 (1969).
208 Ruiz, F. A., Lea, C. R., Oldfield, E. & Docampo, R. Human platelet dense granules contain polyphosphate and are similar to acidocalcisomes of bacteria and unicellular eukaryotes. *The Journal of biological chemistry* **279**, 44250-44257, doi:10.1074/jbc.M406261200 (2004).
209 Puri, R. N. & Colman, R. W. ADP-induced platelet activation. *Critical reviews in biochemistry and molecular biology* **32**, 437-502, doi:10.3109/10409239709082000 (1997).
210 Smith, S. A. *et al.* Polyphosphate modulates blood coagulation and fibrinolysis. *Proceedings of the National Academy of Sciences of the United States of America* **103**, 903-908, doi:10.1073/pnas.0507195103 (2006).
211 Huizing, M., Malicdan, M. C. V., Gochuico, B. R. & Gahl, W. A. in *GeneReviews((R))* (eds M. P. Adam *et al.*) (University of Washington, Seattle

University of Washington, Seattle. GeneReviews is a registered trademark of the University of Washington, Seattle. All rights reserved., 1993).

212 Hermansky, F. & Pudlak, P. Albinism associated with hemorrhagic diathesis and unusual pigmented reticular cells in the bone marrow: report of two cases with histochemical studies. *Blood* **14**, 162-169 (1959).

213 Toro, C., Nicoli, E. R., Malicdan, M. C., Adams, D. R. & Introne, W. J. in *GeneReviews((R))* (eds M. P. Adam *et al.*) (University of Washington, Seattle

University of Washington, Seattle. GeneReviews is a registered trademark of the University of Washington, Seattle. All rights reserved., 1993).

214 Mazzucato, M., Pradella, P., Cozzi, M. R., De Marco, L. & Ruggeri, Z. M. Sequential cytoplasmic calcium signals in a 2-stage platelet activation process induced by the glycoprotein Ibα mechanoreceptor. *Blood* **100**, 2793-2800, doi:10.1182/blood-2002-02-0514 (2002).

215 Dai, K., Bodnar, R., Berndt, M. C. & Du, X. A critical role for 14-3-3zeta protein in regulating the VWF binding function of platelet glycoprotein Ib-IX and its therapeutic implications. *Blood* **106**, 1975-1981, doi:10.1182/blood-2005-01-0440 (2005).

216 Feng, S., Christodoulides, N., Resendiz, J. C., Berndt, M. C. & Kroll, M. H. Cytoplasmic domains of GpIbalpha and GpIbbeta regulate 14-3-3zeta binding to GpIb/IX/V. *Blood* **95**, 551-557 (2000).

217 Mu, F. T., Cranmer, S. L., Andrews, R. K. & Berndt, M. C. Functional association of phosphoinositide-3-kinase with platelet glycoprotein Ibalpha, the major ligand-binding subunit of the glycoprotein Ib-IX-V complex. *Journal of thrombosis and haemostasis : JTH* **8**, 324-330, doi:10.1111/j.1538-7836.2009.03672.x (2010).

218 McCarty, O. J., Calaminus, S. D., Berndt, M. C., Machesky, L. M. & Watson, S. P. von Willebrand factor mediates platelet spreading through glycoprotein Ib and alpha(IIb)beta3 in the presence of botrocetin and ristocetin, respectively. *Journal of thrombosis and haemostasis : JTH* **4**, 1367-1378, doi:10.1111/j.1538-7836.2006.01966.x (2006).

219 Du, X., Harris, S. J., Tetaz, T. J., Ginsberg, M. H. & Berndt, M. C. Association of a phospholipase A2 (14-3-3 protein) with the platelet glycoprotein Ib-IX complex. *The Journal of biological chemistry* **269**, 18287-18290 (1994).

220 Yin, H. *et al.* Src family tyrosine kinase Lyn mediates VWF/GPIb-IX-induced platelet activation via the cGMP signaling pathway. *Blood* **112**, 1139-1146, doi:10.1182/blood-2008-02-140970 (2008).

221 Kasirer-Friede, A. *et al.* Lateral clustering of platelet GP Ib-IX complexes leads to up-regulation of the adhesive function of integrin alpha IIbbeta 3. *The Journal of biological chemistry* **277**, 11949-11956, doi:10.1074/jbc.M108727200 (2002).

222 de Witt, S. M. *et al.* Identification of platelet function defects by multi-parameter assessment of thrombus formation. *Nature communications* **5**, 4257, doi:10.1038/ncomms5257

https://www.nature.com/articles/ncomms5257#supplementary-information (2014).

223 Deng, W. *et al.* Platelet clearance via shear-induced unfolding of a membrane mechanoreceptor. *Nature communications* **7**, 12863, doi:10.1038/ncomms12863 (2016).

224 Senis, Y. A., Mazharian, A. & Mori, J. Src family kinases: at the forefront of platelet activation. *Blood* **124**, 2013-2024, doi:10.1182/blood-2014-01-453134 (2014).

225 Li, Z., Delaney, M. K., O'Brien, K. A. & Du, X. Signaling during platelet adhesion and activation. *Arteriosclerosis, thrombosis, and vascular biology* **30**, 2341-2349, doi:10.1161/atvbaha.110.207522 (2010).

226 Tsuji, M., Ezumi, Y., Arai, M. & Takayama, H. A novel association of Fc receptor gamma-chain with glycoprotein VI and their co-expression as a collagen receptor in human platelets. *The Journal of biological chemistry* **272**, 23528-23531, doi:10.1074/jbc.272.38.23528 (1997).

227 Ezumi, Y., Shindoh, K., Tsuji, M. & Takayama, H. Physical and functional association of the Src family kinases Fyn and Lyn with the collagen receptor glycoprotein VI-Fc receptor gamma chain complex on human platelets. *The Journal of experimental medicine* **188**, 267-276, doi:10.1084/jem.188.2.267 (1998).
228 Schmaier, A. A. *et al.* Molecular priming of Lyn by GPVI enables an immune receptor to adopt a hemostatic role. *Proceedings of the National Academy of Sciences of the United States of America* **106**, 21167-21172, doi:10.1073/pnas.0906436106 (2009).
229 Alshehri, O. M. *et al.* Fibrin activates GPVI in human and mouse platelets. *Blood* **126**, 1601-1608, doi:10.1182/blood-2015-04-641654 (2015).
230 Oldham, W. M. & Hamm, H. E. Heterotrimeric G protein activation by G-protein-coupled receptors. *Nature reviews. Molecular cell biology* **9**, 60-71, doi:10.1038/nrm2299 (2008).
231 Thijs, T., Nuyttens, B. P., Deckmyn, H. & Broos, K. Platelet physiology and antiplatelet agents. *Clin Chem Lab Med* **48 Suppl 1**, S3-S13, doi:10.1515/CCLM.2010.363 (2010).
232 Smolenski, A. Novel roles of cAMP/cGMP-dependent signaling in platelets. *Journal of thrombosis and haemostasis : JTH* **10**, 167-176, doi:10.1111/j.1538-7836.2011.04576.x (2012).
233 Stalker, T. J., Newman, D. K., Ma, P., Wannemacher, K. M. & Brass, L. F. Platelet signaling. *Handbook of experimental pharmacology*, 59-85, doi:10.1007/978-3-642-29423-5_3 (2012).
234 Kahn, M. L., Nakanishi-Matsui, M., Shapiro, M. J., Ishihara, H. & Coughlin, S. R. Protease-activated receptors 1 and 4 mediate activation of human platelets by thrombin. *The Journal of clinical investigation* **103**, 879-887, doi:10.1172/jci6042 (1999).
235 Nakanishi-Matsui, M. *et al.* PAR3 is a cofactor for PAR4 activation by thrombin. *Nature* **404**, 609-613, doi:10.1038/35007085 (2000).
236 Coughlin, S. R. Protease-activated receptors in hemostasis, thrombosis and vascular biology. *Journal of thrombosis and haemostasis : JTH* **3**, 1800-1814, doi:10.1111/j.1538-7836.2005.01377.x (2005).
237 De Candia, E. *et al.* Binding of thrombin to glycoprotein Ib accelerates the hydrolysis of Par-1 on intact platelets. *The Journal of biological chemistry* **276**, 4692-4698, doi:10.1074/jbc.M008160200 (2001).
238 Estevez, B. *et al.* Signaling-mediated cooperativity between glycoprotein Ib-IX and protease-activated receptors in thrombin-induced platelet activation. *Blood* **127**, 626-636, doi:10.1182/blood-2015-04-638387 (2016).
239 Moers, A. *et al.* G13 is an essential mediator of platelet activation in hemostasis and thrombosis. *Nature medicine* **9**, 1418-1422, doi:10.1038/nm943 (2003).
240 Sah, V. P., Seasholtz, T. M., Sagi, S. A. & Brown, J. H. The role of Rho in G protein-coupled receptor signal transduction. *Annual review of pharmacology and toxicology* **40**, 459-489, doi:10.1146/annurev.pharmtox.40.1.459 (2000).
241 Stalker, T. J., Welsh, J. D. & Brass, L. F. Shaping the platelet response to vascular injury. *Current opinion in hematology* **21**, 410-417, doi:10.1097/moh.0000000000000070 (2014).
242 Cattaneo, M. & Gachet, C. ADP receptors and clinical bleeding disorders. *Arteriosclerosis, thrombosis, and vascular biology* **19**, 2281-2285 (1999).
243 Ohlmann, P. *et al.* The human platelet ADP receptor activates Gi2 proteins. *The Biochemical journal* **312 (Pt 3)**, 775-779, doi:10.1042/bj3120775 (1995).
244 Djellas, Y., Manganello, J. M., Antonakis, K. & Le Breton, G. C. Identification of Galpha13 as one of the G-proteins that couple to human platelet thromboxane A2 receptors. *The Journal of biological chemistry* **274**, 14325-14330, doi:10.1074/jbc.274.20.14325 (1999).
245 Varga-Szabo, D., Braun, A. & Nieswandt, B. Calcium signaling in platelets. *Journal of thrombosis and haemostasis : JTH* **7**, 1057-1066, doi:10.1111/j.1538-7836.2009.03455.x (2009).
246 Estevez, B. & Du, X. New Concepts and Mechanisms of Platelet Activation Signaling. *Physiology (Bethesda, Md.)* **32**, 162-177, doi:10.1152/physiol.00020.2016 (2017).

247 Moser, M., Nieswandt, B., Ussar, S., Pozgajova, M. & Fassler, R. Kindlin-3 is essential for integrin activation and platelet aggregation. *Nature medicine* **14**, 325-330, doi:10.1038/nm1722 (2008).
248 Ma, Y. Q., Qin, J., Wu, C. & Plow, E. F. Kindlin-2 (Mig-2): a co-activator of beta3 integrins. *The Journal of cell biology* **181**, 439-446, doi:10.1083/jcb.200710196 (2008).
249 Calderwood, D. A. *et al.* The Talin head domain binds to integrin beta subunit cytoplasmic tails and regulates integrin activation. *The Journal of biological chemistry* **274**, 28071-28074, doi:10.1074/jbc.274.40.28071 (1999).
250 Obergfell, A. *et al.* Coordinate interactions of Csk, Src, and Syk kinases with [alpha]IIb[beta]3 initiate integrin signaling to the cytoskeleton. *The Journal of cell biology* **157**, 265-275, doi:10.1083/jcb.200112113 (2002).
251 Arias-Salgado, E. G. *et al.* Src kinase activation by direct interaction with the integrin beta cytoplasmic domain. *Proceedings of the National Academy of Sciences of the United States of America* **100**, 13298-13302, doi:10.1073/pnas.2336149100 (2003).
252 Hitchcock, I. S. *et al.* Roles of focal adhesion kinase (FAK) in megakaryopoiesis and platelet function: studies using a megakaryocyte lineage specific FAK knockout. *Blood* **111**, 596-604, doi:10.1182/blood-2007-05-089680 (2008).
253 Obergfell, A. *et al.* The molecular adapter SLP-76 relays signals from platelet integrin alphaIIbbeta3 to the actin cytoskeleton. *The Journal of biological chemistry* **276**, 5916-5923, doi:10.1074/jbc.M010639200 (2001).
254 Wonerow, P., Pearce, A. C., Vaux, D. J. & Watson, S. P. A critical role for phospholipase Cgamma2 in alphaIIbbeta3-mediated platelet spreading. *The Journal of biological chemistry* **278**, 37520-37529, doi:10.1074/jbc.M305077200 (2003).
255 Naik, M. U., Naik, T. U., Summer, R. & Naik, U. P. Binding of CIB1 to the alphaIIb tail of alphaIIbbeta3 is required for FAK recruitment and activation in platelets. *PloS one* **12**, e0176602, doi:10.1371/journal.pone.0176602 (2017).
256 Stalker, T. J. *et al.* Hierarchical organization in the hemostatic response and its relationship to the platelet-signaling network. *Blood* **121**, 1875-1885, doi:10.1182/blood-2012-09-457739 (2013).
257 Welsh, J. D. *et al.* A systems approach to hemostasis: 1. The interdependence of thrombus architecture and agonist movements in the gaps between platelets. *Blood* **124**, 1808-1815, doi:10.1182/blood-2014-01-550335 (2014).
258 Stalker, T. J. *et al.* A systems approach to hemostasis: 3. Thrombus consolidation regulates intrathrombus solute transport and local thrombin activity. *Blood* **124**, 1824-1831, doi:10.1182/blood-2014-01-550319 (2014).
259 Tomaiuolo, M. *et al.* A systems approach to hemostasis: 2. Computational analysis of molecular transport in the thrombus microenvironment. *Blood* **124**, 1816-1823, doi:10.1182/blood-2014-01-550343 (2014).
260 Welsh, J. D. *et al.* A systems approach to hemostasis: 4. How hemostatic thrombi limit the loss of plasma-borne molecules from the microvasculature. *Blood* **127**, 1598-1605, doi:10.1182/blood-2015-09-672188 (2016).
261 Le Behot, A. *et al.* GpIbalpha-VWF blockade restores vessel patency by dissolving platelet aggregates formed under very high shear rate in mice. *Blood* **123**, 3354-3363, doi:10.1182/blood-2013-12-543074 (2014).
262 Andonegui, G. *et al.* Platelets express functional Toll-like receptor-4. *Blood* **106**, 2417-2423, doi:10.1182/blood-2005-03-0916 (2005).
263 Assinger, A. Platelets and infection - an emerging role of platelets in viral infection. *Frontiers in immunology* **5**, 649, doi:10.3389/fimmu.2014.00649 (2014).
264 Blair, P. *et al.* Stimulation of Toll-like receptor 2 in human platelets induces a thromboinflammatory response through activation of phosphoinositide 3-kinase. *Circulation research* **104**, 346-354, doi:10.1161/circresaha.108.185785 (2009).

265 Kapur, R. & Semple, J. W. Platelets as immune-sensing cells. *Blood advances* **1**, 10-14, doi:10.1182/bloodadvances.2016000067 (2016).
266 Massberg, S. *et al.* A critical role of platelet adhesion in the initiation of atherosclerotic lesion formation. *The Journal of experimental medicine* **196**, 887-896, doi:10.1084/jem.20012044 (2002).
267 Abumiya, T. *et al.* Integrin alpha(IIb)beta(3) inhibitor preserves microvascular patency in experimental acute focal cerebral ischemia. *Stroke* **31**, 1402-1409; discussion 1409-1410 (2000).
268 Boilard, E. *et al.* Platelets amplify inflammation in arthritis via collagen-dependent microparticle production. *Science (New York, N.Y.)* **327**, 580-583, doi:10.1126/science.1181928 (2010).
269 Ginsberg, M. H., Breth, G. & Skosey, J. L. Platelets in the synovial space. *Arthritis and rheumatism* **21**, 994-995 (1978).
270 Langer, H. F. *et al.* Platelets contribute to the pathogenesis of experimental autoimmune encephalomyelitis. *Circulation research* **110**, 1202-1210, doi:10.1161/circresaha.111.256370 (2012).
271 Brill, A. *et al.* von Willebrand factor-mediated platelet adhesion is critical for deep vein thrombosis in mouse models. *Blood* **117**, 1400-1407, doi:10.1182/blood-2010-05-287623 (2011).
272 von Bruhl, M. L. *et al.* Monocytes, neutrophils, and platelets cooperate to initiate and propagate venous thrombosis in mice in vivo. *The Journal of experimental medicine* **209**, 819-835, doi:10.1084/jem.20112322 (2012).
273 Burger, P. C. & Wagner, D. D. Platelet P-selectin facilitates atherosclerotic lesion development. *Blood* **101**, 2661-2666, doi:10.1182/blood-2002-07-2209 (2003).
274 Koenen, R. R. *et al.* Disrupting functional interactions between platelet chemokines inhibits atherosclerosis in hyperlipidemic mice. *Nature medicine* **15**, 97-103, doi:10.1038/nm.1898 (2009).
275 Daub, K. *et al.* Oxidized LDL-activated platelets induce vascular inflammation. *Seminars in thrombosis and hemostasis* **36**, 146-156, doi:10.1055/s-0030-1251498 (2010).
276 Wendelboe, A. M. & Raskob, G. E. Global Burden of Thrombosis: Epidemiologic Aspects. *Circulation research* **118**, 1340-1347, doi:10.1161/circresaha.115.306841 (2016).
277 Heit, J. A., Spencer, F. A. & White, R. H. The epidemiology of venous thromboembolism. *Journal of thrombosis and thrombolysis* **41**, 3-14, doi:10.1007/s11239-015-1311-6 (2016).
278 Wong, C. H., Jenne, C. N., Petri, B., Chrobok, N. L. & Kubes, P. Nucleation of platelets with blood-borne pathogens on Kupffer cells precedes other innate immunity and contributes to bacterial clearance. *Nature immunology* **14**, 785-792, doi:10.1038/ni.2631 (2013).
279 Jounai, N., Kobiyama, K., Takeshita, F. & Ishii, K. J. Recognition of damage-associated molecular patterns related to nucleic acids during inflammation and vaccination. *Frontiers in cellular and infection microbiology* **2**, 168, doi:10.3389/fcimb.2012.00168 (2012).
280 Kawai, T. & Akira, S. The role of pattern-recognition receptors in innate immunity: update on Toll-like receptors. *Nature immunology* **11**, 373-384, doi:10.1038/ni.1863 (2010).
281 Lopes Pires, M. E., Clarke, S. R., Marcondes, S. & Gibbins, J. M. Lipopolysaccharide potentiates platelet responses via toll-like receptor 4-stimulated Akt-Erk-PLA2 signalling. *PloS one* **12**, e0186981, doi:10.1371/journal.pone.0186981 (2017).
282 Clark, S. R. *et al.* Platelet TLR4 activates neutrophil extracellular traps to ensnare bacteria in septic blood. *Nature medicine* **13**, 463-469, doi:10.1038/nm1565 (2007).
283 Cole, A. M. *et al.* Cutting edge: IFN-inducible ELR- CXC chemokines display defensin-like antimicrobial activity. *Journal of immunology (Baltimore, Md. : 1950)* **167**, 623-627, doi:10.4049/jimmunol.167.2.623 (2001).
284 Yeaman, M. R. Platelets: at the nexus of antimicrobial defence. *Nature reviews. Microbiology* **12**, 426-437, doi:10.1038/nrmicro3269 (2014).

285 Yeaman, M. R., Bayer, A. S., Koo, S. P., Foss, W. & Sullam, P. M. Platelet microbicidal proteins and neutrophil defensin disrupt the Staphylococcus aureus cytoplasmic membrane by distinct mechanisms of action. *The Journal of clinical investigation* **101**, 178-187, doi:10.1172/jci562 (1998).
286 Blumenreich, M. S. in *Clinical Methods: The History, Physical, and Laboratory Examinations* (eds rd, H. K. Walker, W. D. Hall, & J. W. Hurst) (Butterworths

Butterworth Publishers, a division of Reed Publishing., 1990).
287 Jagannathan-Bogdan, M. & Zon, L. I. Hematopoiesis. *Development (Cambridge, England)* **140**, 2463-2467, doi:10.1242/dev.083147 (2013).
288 Jakubzick, C. V., Randolph, G. J. & Henson, P. M. Monocyte differentiation and antigen-presenting functions. *Nature reviews. Immunology* **17**, 349-362, doi:10.1038/nri.2017.28 (2017).
289 Coillard, A. & Segura, E. In vivo Differentiation of Human Monocytes. *Frontiers in immunology* **10**, 1907, doi:10.3389/fimmu.2019.01907 (2019).
290 Passlick, B., Flieger, D. & Ziegler-Heitbrock, H. W. Identification and characterization of a novel monocyte subpopulation in human peripheral blood. *Blood* **74**, 2527-2534 (1989).
291 Ingersoll, M. A. *et al.* Comparison of gene expression profiles between human and mouse monocyte subsets. *Blood* **115**, e10-e19, doi:10.1182/blood-2009-07-235028 (2010).
292 Mirsafian, H. *et al.* Transcriptome landscape of human primary monocytes at different sequencing depth. *Genomics* **109**, 463-470, doi:https://doi.org/10.1016/j.ygeno.2017.07.003 (2017).
293 Scott, C. L. *et al.* Bone marrow-derived monocytes give rise to self-renewing and fully differentiated Kupffer cells. *Nature communications* **7**, 10321, doi:10.1038/ncomms10321 (2016).
294 Wang, Y. *et al.* IL-34 is a tissue-restricted ligand of CSF1R required for the development of Langerhans cells and microglia. *Nature immunology* **13**, 753-760, doi:10.1038/ni.2360 (2012).
295 Cano RLE, L. H. in *Autoimmunity: From bench to bedsite* (ed Shoenfeld Y Anaya JM, Rojas-Villarraga A, et al.) Ch. 5, (2013).
296 Golubovskaya, V. & Wu, L. Different Subsets of T Cells, Memory, Effector Functions, and CAR-T Immunotherapy. *Cancers* **8**, doi:10.3390/cancers8030036 (2016).
297 Farhood, B., Najafi, M. & Mortezaee, K. CD8(+) cytotoxic T lymphocytes in cancer immunotherapy: A review. *Journal of cellular physiology* **234**, 8509-8521, doi:10.1002/jcp.27782 (2019).
298 Suzuki, I. & Fink, P. J. The dual functions of Fas ligand in the regulation of peripheral CD8⁺ and CD4⁺ T cells. *Proceedings of the National Academy of Sciences* **97**, 1707-1712, doi:10.1073/pnas.97.4.1707 (2000).
299 Hoffman, W., Lakkis, F. G. & Chalasani, G. B Cells, Antibodies, and More. *Clinical journal of the American Society of Nephrology : CJASN* **11**, 137-154, doi:10.2215/cjn.09430915 (2016).
300 Fogler, W. E. *et al.* NK cell infiltration into lung, liver, and subcutaneous B16 melanoma is mediated by VCAM-1/VLA-4 interaction. *The Journal of Immunology* **156**, 4707-4714 (1996).
301 Caligiuri, M. A. Human natural killer cells. *Blood* **112**, 461-469, doi:10.1182/blood-2007-09-077438 (2008).
302 Rezvani, K., Rouce, R., Liu, E. & Shpall, E. Engineering Natural Killer Cells for Cancer Immunotherapy. *Molecular therapy : the journal of the American Society of Gene Therapy* **25**, 1769-1781, doi:10.1016/j.ymthe.2017.06.012 (2017).
303 Karasuyama, H., Miyake, K., Yoshikawa, S. & Yamanishi, Y. Multifaceted roles of basophils in health and disease. *Journal of Allergy and Clinical Immunology* **142**, 370-380, doi:10.1016/j.jaci.2017.10.042 (2018).
304 Mayadas, T. N., Cullere, X. & Lowell, C. A. The multifaceted functions of neutrophils. *Annual review of pathology* **9**, 181-218, doi:10.1146/annurev-pathol-020712-164023 (2014).

305 Ravin, K. A. & Loy, M. The Eosinophil in Infection. *Clinical reviews in allergy & immunology* **50**, 214-227, doi:10.1007/s12016-015-8525-4 (2016).
306 Johansson, M. W. Activation states of blood eosinophils in asthma. *Clinical and experimental allergy : journal of the British Society for Allergy and Clinical Immunology* **44**, 482-498, doi:10.1111/cea.12292 (2014).
307 Basu, S., Hodgson, G., Katz, M. & Dunn, A. R. Evaluation of role of G-CSF in the production, survival, and release of neutrophils from bone marrow into circulation. *Blood* **100**, 854-861, doi:10.1182/blood.v100.3.854 (2002).
308 Mantovani, A., Cassatella, M. A., Costantini, C. & Jaillon, S. Neutrophils in the activation and regulation of innate and adaptive immunity. *Nature reviews. Immunology* **11**, 519-531, doi:10.1038/nri3024 (2011).
309 Kolaczkowska, E. & Kubes, P. Neutrophil recruitment and function in health and inflammation. *Nature reviews. Immunology* **13**, 159-175, doi:10.1038/nri3399 (2013).
310 Kostmann, R. Infantile genetic agranulocytosis; agranulocytosis infantilis hereditaria. *Acta paediatrica. Supplementum* **45**, 1-78 (1956).
311 Zeidler, C., Germeshausen, M., Klein, C. & Welte, K. Clinical implications of ELA2-, HAX1-, and G-CSF-receptor (CSF3R) mutations in severe congenital neutropenia. *British journal of haematology* **144**, 459-467, doi:10.1111/j.1365-2141.2008.07425.x (2009).
312 Sreeramkumar, V. *et al.* Neutrophils scan for activated platelets to initiate inflammation. *Science (New York, N.Y.)* **346**, 1234-1238, doi:10.1126/science.1256478 (2014).
313 Tsuboi, N., Asano, K., Lauterbach, M. & Mayadas, T. N. Human neutrophil Fcgamma receptors initiate and play specialized nonredundant roles in antibody-mediated inflammatory diseases. *Immunity* **28**, 833-846, doi:10.1016/j.immuni.2008.04.013 (2008).
314 Segal, A. W., Dorling, J. & Coade, S. Kinetics of fusion of the cytoplasmic granules with phagocytic vacuoles in human polymorphonuclear leukocytes. Biochemical and morphological studies. *The Journal of cell biology* **85**, 42-59, doi:10.1083/jcb.85.1.42 (1980).
315 Nordenfelt, P. & Tapper, H. Phagosome dynamics during phagocytosis by neutrophils. *Journal of leukocyte biology* **90**, 271-284, doi:10.1189/jlb.0810457 (2011).
316 Faurschou, M. & Borregaard, N. Neutrophil granules and secretory vesicles in inflammation. *Microbes and infection* **5**, 1317-1327 (2003).
317 Lominadze, G. *et al.* Proteomic analysis of human neutrophil granules. *Molecular & cellular proteomics : MCP* **4**, 1503-1521, doi:10.1074/mcp.M500143-MCP200 (2005).
318 Brinkmann, V. *et al.* Neutrophil extracellular traps kill bacteria. *Science (New York, N.Y.)* **303**, 1532-1535, doi:10.1126/science.1092385 (2004).
319 Kaplan, M. J. & Radic, M. Neutrophil extracellular traps: double-edged swords of innate immunity. *Journal of immunology (Baltimore, Md. : 1950)* **189**, 2689-2695, doi:10.4049/jimmunol.1201719 (2012).
320 Fuchs, T. A. *et al.* Novel cell death program leads to neutrophil extracellular traps. *The Journal of cell biology* **176**, 231-241, doi:10.1083/jcb.200606027 (2007).
321 Lin, A. M. *et al.* Mast cells and neutrophils release IL-17 through extracellular trap formation in psoriasis. *Journal of immunology (Baltimore, Md. : 1950)* **187**, 490-500, doi:10.4049/jimmunol.1100123 (2011).
322 Yousefi, S. *et al.* Catapult-like release of mitochondrial DNA by eosinophils contributes to antibacterial defense. *Nature medicine* **14**, 949-953, doi:10.1038/nm.1855 (2008).
323 Guimaraes-Costa, A. B. *et al.* Leishmania amazonensis promastigotes induce and are killed by neutrophil extracellular traps. *Proceedings of the National Academy of Sciences of the United States of America* **106**, 6748-6753, doi:10.1073/pnas.0900226106 (2009).
324 Urban, C. F., Reichard, U., Brinkmann, V. & Zychlinsky, A. Neutrophil extracellular traps capture and kill Candida albicans yeast and hyphal forms. *Cellular microbiology* **8**, 668-676, doi:10.1111/j.1462-5822.2005.00659.x (2006).

325 Etulain, J. *et al.* P-selectin promotes neutrophil extracellular trap formation in mice. *Blood* **126**, 242-246, doi:10.1182/blood-2015-01-624023 (2015).
326 Pilsczek, F. H. *et al.* A Novel Mechanism of Rapid Nuclear Neutrophil Extracellular Trap Formation in Response to Staphylococcus aureus. *The Journal of Immunology* **185**, 7413-7425, doi:10.4049/jimmunol.1000675 (2010).
327 Yipp, B. G. & Kubes, P. NETosis: how vital is it? *Blood* **122**, 2784-2794, doi:10.1182/blood-2013-04-457671 (2013).
328 Khan, M. A. & Palaniyar, N. Transcriptional firing helps to drive NETosis. *Scientific Reports* **7**, 41749, doi:10.1038/srep41749

https://www.nature.com/articles/srep41749#supplementary-information (2017).
329 Jorch, S. K. & Kubes, P. An emerging role for neutrophil extracellular traps in noninfectious disease. *Nature medicine* **23**, 279-287, doi:10.1038/nm.4294 (2017).
330 Li, P. *et al.* PAD4 is essential for antibacterial innate immunity mediated by neutrophil extracellular traps. *The Journal of experimental medicine* **207**, 1853-1862, doi:10.1084/jem.20100239 (2010).
331 Martinod, K. *et al.* Neutrophil histone modification by peptidylarginine deiminase 4 is critical for deep vein thrombosis in mice. *Proceedings of the National Academy of Sciences of the United States of America* **110**, 8674-8679, doi:10.1073/pnas.1301059110 (2013).
332 Masuda, S. *et al.* NETosis markers: Quest for specific, objective, and quantitative markers. *Clinica Chimica Acta* **459**, 89-93, doi:https://doi.org/10.1016/j.cca.2016.05.029 (2016).
333 Jimenez-Alcazar, M. *et al.* Host DNases prevent vascular occlusion by neutrophil extracellular traps. *Science (New York, N.Y.)* **358**, 1202-1206, doi:10.1126/science.aam8897 (2017).
334 Hakkim, A. *et al.* Impairment of neutrophil extracellular trap degradation is associated with lupus nephritis. *Proceedings of the National Academy of Sciences of the United States of America* **107**, 9813-9818, doi:10.1073/pnas.0909927107 (2010).
335 Kessenbrock, K. *et al.* Netting neutrophils in autoimmune small-vessel vasculitis. *Nature medicine* **15**, 623-625, doi:10.1038/nm.1959 (2009).
336 Villanueva, E. *et al.* Netting neutrophils induce endothelial damage, infiltrate tissues, and expose immunostimulatory molecules in systemic lupus erythematosus. *Journal of immunology (Baltimore, Md. : 1950)* **187**, 538-552, doi:10.4049/jimmunol.1100450 (2011).
337 Gupta, A. K., Hasler, P., Holzgreve, W., Gebhardt, S. & Hahn, S. Induction of neutrophil extracellular DNA lattices by placental microparticles and IL-8 and their presence in preeclampsia. *Human immunology* **66**, 1146-1154, doi:10.1016/j.humimm.2005.11.003 (2005).
338 Fuchs, T. A. *et al.* Extracellular DNA traps promote thrombosis. *Proceedings of the National Academy of Sciences of the United States of America* **107**, 15880-15885, doi:10.1073/pnas.1005743107 (2010).
339 Fuchs, T. A., Brill, A. & Wagner, D. D. Neutrophil extracellular trap (NET) impact on deep vein thrombosis. *Arteriosclerosis, thrombosis, and vascular biology* **32**, 1777-1783, doi:10.1161/atvbaha.111.242859 (2012).
340 Brill, A. *et al.* Neutrophil extracellular traps promote deep vein thrombosis in mice. *Journal of thrombosis and haemostasis : JTH* **10**, 136-144, doi:10.1111/j.1538-7836.2011.04544.x (2012).
341 Gaertner, F. *et al.* Migrating Platelets Are Mechano-scavengers that Collect and Bundle Bacteria. *Cell* **171**, 1368-1382.e1323, doi:10.1016/j.cell.2017.11.001 (2017).
342 Harrison-Lavoie, K. J. *et al.* P-selectin and CD63 use different mechanisms for delivery to Weibel-Palade bodies. *Traffic (Copenhagen, Denmark)* **7**, 647-662, doi:10.1111/j.1600-0854.2006.00415.x (2006).
343 Laszik, Z. *et al.* P-selectin glycoprotein ligand-1 is broadly expressed in cells of myeloid, lymphoid, and dendritic lineage and in some nonhematopoietic cells. *Blood* **88**, 3010-3021 (1996).

344 Lievens, D. *et al.* Platelet CD40L mediates thrombotic and inflammatory processes in atherosclerosis. *Blood* **116**, 4317-4327, doi:10.1182/blood-2010-01-261206 (2010).
345 Schonbeck, U. & Libby, P. The CD40/CD154 receptor/ligand dyad. *Cellular and molecular life sciences : CMLS* **58**, 4-43 (2001).
346 Vandendries, E. R., Furie, B. C. & Furie, B. Role of P-selectin and PSGL-1 in coagulation and thrombosis. *Thrombosis and haemostasis* **92**, 459-466, doi:10.1160/th04-05-0306 (2004).
347 Evangelista, V. *et al.* Platelet/polymorphonuclear leukocyte interaction: P-selectin triggers protein-tyrosine phosphorylation-dependent CD11b/CD18 adhesion: role of PSGL-1 as a signaling molecule. *Blood* **93**, 876-885 (1999).
348 Weber, C. & Springer, T. A. Neutrophil accumulation on activated, surface-adherent platelets in flow is mediated by interaction of Mac-1 with fibrinogen bound to alphaIIbbeta3 and stimulated by platelet-activating factor. *The Journal of clinical investigation* **100**, 2085-2093, doi:10.1172/jci119742 (1997).
349 Kuijper, P. H. *et al.* Platelet associated fibrinogen and ICAM-2 induce firm adhesion of neutrophils under flow conditions. *Thrombosis and haemostasis* **80**, 443-448 (1998).
350 Darbousset, R. *et al.* Tissue factor-positive neutrophils bind to injured endothelial wall and initiate thrombus formation. *Blood* **120**, 2133-2143, doi:10.1182/blood-2012-06-437772 (2012).
351 Ed Rainger, G. *et al.* The role of platelets in the recruitment of leukocytes during vascular disease. *Platelets* **26**, 507-520, doi:10.3109/09537104.2015.1064881 (2015).
352 Ribatti, D. & Crivellato, E. Giulio Bizzozero and the discovery of platelets. *Leukemia research* **31**, 1339-1341, doi:10.1016/j.leukres.2007.02.008 (2007).
353 Palabrica, T. *et al.* Leukocyte accumulation promoting fibrin deposition is mediated in vivo by P-selectin on adherent platelets. *Nature* **359**, 848-851, doi:10.1038/359848a0 (1992).
354 Goncalves, R., Zhang, X., Cohen, H., Debrabant, A. & Mosser, D. M. Platelet activation attracts a subpopulation of effector monocytes to sites of Leishmania major infection. *The Journal of experimental medicine* **208**, 1253-1265, doi:10.1084/jem.20101751 (2011).
355 McDonald, B., Urrutia, R., Yipp, B. G., Jenne, C. N. & Kubes, P. Intravascular neutrophil extracellular traps capture bacteria from the bloodstream during sepsis. *Cell host & microbe* **12**, 324-333, doi:10.1016/j.chom.2012.06.011 (2012).
356 Zuchtriegel, G. *et al.* Platelets Guide Leukocytes to Their Sites of Extravasation. *PLoS biology* **14**, e1002459, doi:10.1371/journal.pbio.1002459 (2016).
357 Carestia, A., Kaufman, T. & Schattner, M. Platelets: New Bricks in the Building of Neutrophil Extracellular Traps. *Frontiers in immunology* **7**, 271, doi:10.3389/fimmu.2016.00271 (2016).
358 Etulain, J. *et al.* P-selectin promotes neutrophil extracellular trap formation in mice. *Blood* **126**, 242-246, doi:10.1182/blood-2015-01-624023 (2015).
359 Honda, M. & Kubes, P. Neutrophils and neutrophil extracellular traps in the liver and gastrointestinal system. *Nature reviews. Gastroenterology & hepatology* **15**, 206-221, doi:10.1038/nrgastro.2017.183 (2018).
360 Nieswandt, B., Kleinschnitz, C. & Stoll, G. Ischaemic stroke: a thrombo-inflammatory disease? *The Journal of physiology* **589**, 4115-4123, doi:10.1113/jphysiol.2011.212886 (2011).
361 Gawaz, M., Fateh-Moghadam, S., Pilz, G., Gurland, H. J. & Werdan, K. Platelet activation and interaction with leucocytes in patients with sepsis or multiple organ failure. *European journal of clinical investigation* **25**, 843-851 (1995).
362 Caudrillier, A. *et al.* Platelets induce neutrophil extracellular traps in transfusion-related acute lung injury. *The Journal of clinical investigation* **122**, 2661-2671, doi:10.1172/jci61303 (2012).
363 Harding, S. A. *et al.* Increased CD40 ligand and platelet-monocyte aggregates in patients with type 1 diabetes mellitus. *Atherosclerosis* **176**, 321-325, doi:10.1016/j.atherosclerosis.2004.05.008 (2004).

364 Wrigley, B. J., Shantsila, E., Tapp, L. D. & Lip, G. Y. Increased formation of monocyte-platelet aggregates in ischemic heart failure. *Circulation. Heart failure* **6**, 127-135, doi:10.1161/circheartfailure.112.968073 (2013).
365 Germain, M. *et al.* Meta-analysis of 65,734 individuals identifies TSPAN15 and SLC44A2 as two susceptibility loci for venous thromboembolism. *American journal of human genetics* **96**, 532-542, doi:10.1016/j.ajhg.2015.01.019 (2015).
366 Germain, M. *et al.* Genetics of venous thrombosis: insights from a new genome wide association study. *PloS one* **6**, e25581, doi:10.1371/journal.pone.0025581 (2011).
367 Hinds, D. A. *et al.* Genome-wide association analysis of self-reported events in 6135 individuals and 252 827 controls identifies 8 loci associated with thrombosis. *Human molecular genetics* **25**, 1867-1874, doi:10.1093/hmg/ddw037 (2016).
368 Nair, T. S. *et al.* SLC44A2 single nucleotide polymorphisms, isoforms, and expression: Association with severity of Meniere's disease? *Genomics* **108**, 201-208, doi:10.1016/j.ygeno.2016.11.002 (2016).
369 Nair, T. S. *et al.* Identification and characterization of choline transporter-like protein 2, an inner ear glycoprotein of 68 and 72 kDa that is the target of antibody-induced hearing loss. *The Journal of neuroscience : the official journal of the Society for Neuroscience* **24**, 1772-1779, doi:10.1523/jneurosci.5063-03.2004 (2004).
370 Kommareddi, P. *et al.* Hair Cell Loss, Spiral Ganglion Degeneration, and Progressive Sensorineural Hearing Loss in Mice with Targeted Deletion of Slc44a2/Ctl2. *Journal of the Association for Research in Otolaryngology : JARO* **16**, 695-712, doi:10.1007/s10162-015-0547-3 (2015).
371 Bayat, B. *et al.* Choline Transporter-Like Protein-2: New von Willebrand Factor-Binding Partner Involved in Antibody-Mediated Neutrophil Activation and Transfusion-Related Acute Lung Injury. *Arteriosclerosis, thrombosis, and vascular biology* **35**, 1616-1622, doi:10.1161/atvbaha.115.305259 (2015).
372 Apipongrat, D., Numbenjapon, T., Prayoonwiwat, W., Arnutti, P. & Nathalang, O. Association between SLC44A2 rs2288904 polymorphism and risk of recurrent venous thromboembolism among Thai patients. *Thrombosis research* **174**, 163-165, doi:10.1016/j.thromres.2019.01.001 (2019).
373 Wegner, S. V., Schenk, F. C. & Spatz, J. P. Cobalt(III)-Mediated Permanent and Stable Immobilization of Histidine-Tagged Proteins on NTA-Functionalized Surfaces. *Chemistry – A European Journal* **22**, 3156-3162, doi:10.1002/chem.201504465 (2016).
374 Grassi, L. *et al.* Cell type specific novel lincRNAs and circRNAs in the BLUEPRINT haematopoietic transcriptomes atlas. *bioRxiv*, 764613, doi:10.1101/764613 (2019).
375 Gu, M., Xi, X., Englund, G. D., Berndt, M. C. & Du, X. Analysis of the roles of 14-3-3 in the platelet glycoprotein Ib-IX-mediated activation of integrin alpha(IIb)beta(3) using a reconstituted mammalian cell expression model. *The Journal of cell biology* **147**, 1085-1096, doi:10.1083/jcb.147.5.1085 (1999).
376 Coller, B. S. The effects of ristocetin and von Willebrand factor on platelet electrophoretic mobility. *The Journal of clinical investigation* **61**, 1168-1175, doi:10.1172/jci109032 (1978).
377 Bledzka, K., Smyth, S. S. & Plow, E. F. Integrin αIIbβ3: from discovery to efficacious therapeutic target. *Circulation research* **112**, 1189-1200, doi:10.1161/circresaha.112.300570 (2013).
378 Matsuno, H. *et al.* Effect of GR144053, a fibrinogen-receptor antagonist, on thrombus formation and vascular patency after thrombolysis by tPA in the injured carotid artery of the hamster. *Journal of cardiovascular pharmacology* **32**, 191-197, doi:10.1097/00005344-199808000-00004 (1998).
379 Honda, S. *et al.* Topography of ligand-induced binding sites, including a novel cation-sensitive epitope (AP5) at the amino terminus, of the human integrin beta 3 subunit. *The Journal of biological chemistry* **270**, 11947-11954, doi:10.1074/jbc.270.20.11947 (1995).

380 Rubak, P., Nissen, P. H., Kristensen, S. D. & Hvas, A. M. Investigation of platelet function and platelet disorders using flow cytometry. *Platelets* **27**, 66-74, doi:10.3109/09537104.2015.1032919 (2016).
381 Muller, W. A. Getting leukocytes to the site of inflammation. *Veterinary pathology* **50**, 7-22, doi:10.1177/0300985812469883 (2013).
382 Ed Rainger, G. *et al.* The role of platelets in the recruitment of leukocytes during vascular disease. *Platelets* **26**, 507-520, doi:10.3109/09537104.2015.1064881 (2015).
383 Guidotti, L. G. *et al.* Immunosurveillance of the liver by intravascular effector CD8(+) T cells. *Cell* **161**, 486-500, doi:10.1016/j.cell.2015.03.005 (2015).
384 Gandhi, C., Motto, D. G., Jensen, M., Lentz, S. R. & Chauhan, A. K. ADAMTS13 deficiency exacerbates VWF-dependent acute myocardial ischemia/reperfusion injury in mice. *Blood* **120**, 5224-5230, doi:10.1182/blood-2012-06-440255 (2012).
385 Khan, M. M., Motto, D. G., Lentz, S. R. & Chauhan, A. K. ADAMTS13 reduces VWF-mediated acute inflammation following focal cerebral ischemia in mice. *Journal of thrombosis and haemostasis : JTH* **10**, 1665-1671, doi:10.1111/j.1538-7836.2012.04822.x (2012).
386 Gupta, A. K. *et al.* Activated endothelial cells induce neutrophil extracellular traps and are susceptible to NETosis-mediated cell death. *FEBS letters* **584**, 3193-3197, doi:10.1016/j.febslet.2010.06.006 (2010).
387 Maugeri, N. *et al.* Activated platelets present high mobility group box 1 to neutrophils, inducing autophagy and promoting the extrusion of neutrophil extracellular traps. *Journal of thrombosis and haemostasis : JTH* **12**, 2074-2088, doi:10.1111/jth.12710 (2014).
388 Rossaint, J. *et al.* Synchronized integrin engagement and chemokine activation is crucial in neutrophil extracellular trap-mediated sterile inflammation. *Blood* **123**, 2573-2584, doi:10.1182/blood-2013-07-516484 (2014).
389 Carestia, A. *et al.* Mediators and molecular pathways involved in the regulation of neutrophil extracellular trap formation mediated by activated platelets. *Journal of leukocyte biology* **99**, 153-162, doi:10.1189/jlb.3A0415-161R (2016).
390 Papayannopoulos, V. Neutrophil extracellular traps in immunity and disease. *Nature reviews. Immunology* **18**, 134-147, doi:10.1038/nri.2017.105 (2018).
391 Wang, Y. *et al.* Histone hypercitrullination mediates chromatin decondensation and neutrophil extracellular trap formation. *The Journal of cell biology* **184**, 205-213, doi:10.1083/jcb.200806072 (2009).
392 Boeltz, S. *et al.* To NET or not to NET:current opinions and state of the science regarding the formation of neutrophil extracellular traps. *Cell Death & Differentiation* **26**, 395-408, doi:10.1038/s41418-018-0261-x (2019).
393 Douda, D. N., Khan, M. A., Grasemann, H. & Palaniyar, N. SK3 channel and mitochondrial ROS mediate NADPH oxidase-independent NETosis induced by calcium influx. *Proceedings of the National Academy of Sciences* **112**, 2817-2822, doi:10.1073/pnas.1414055112 (2015).
394 Yu, X., Tan, J. & Diamond, S. L. Hemodynamic force triggers rapid NETosis within sterile thrombotic occlusions. *Journal of thrombosis and haemostasis : JTH* **16**, 316-329, doi:10.1111/jth.13907 (2018).
395 Budnik, I. & Brill, A. Immune Factors in Deep Vein Thrombosis Initiation. *Trends in immunology* **39**, 610-623, doi:10.1016/j.it.2018.04.010 (2018).
396 Atarashi, K., Hirata, T., Matsumoto, M., Kanemitsu, N. & Miyasaka, M. Rolling of Th1 cells via P-selectin glycoprotein ligand-1 stimulates LFA-1-mediated cell binding to ICAM-1. *Journal of immunology (Baltimore, Md. : 1950)* **174**, 1424-1432, doi:10.4049/jimmunol.174.3.1424 (2005).
397 Xu, X. R. *et al.* Apolipoprotein A-IV binds alphaIIbbeta3 integrin and inhibits thrombosis. *Nature communications* **9**, 3608, doi:10.1038/s41467-018-05806-0 (2018).
398 Rieckmann, J. C. *et al.* Social network architecture of human immune cells unveiled by quantitative proteomics. *Nature immunology* **18**, 583-593, doi:10.1038/ni.3693 (2017).

399 Rosendaal, F. R. & Reitsma, P. H. Genetics of venous thrombosis. *Journal of thrombosis and haemostasis : JTH* **7 Suppl 1**, 301-304, doi:10.1111/j.1538-7836.2009.03394.x (2009).
400 Chan, N. C., Eikelboom, J. W. & Weitz, J. I. Evolving Treatments for Arterial and Venous Thrombosis: Role of the Direct Oral Anticoagulants. *Circulation research* **118**, 1409-1424, doi:10.1161/circresaha.116.306925 (2016).
401 Smilowitz, N. R., Mega, J. L. & Berger, J. S. Duration of anticoagulation for venous thromboembolic events. *Circulation* **130**, 2343-2348, doi:10.1161/circulationaha.114.010456 (2014).
402 Maracle, C., Tilburg, J, Zirka, G, Morange, PE, van Vijmen, BJM, Thomas, GM. *Slc44a2* deficient mice exhibit less severity of thrombus in a stenosis model of DVT. *ISTH Academy* (2019).
403 Bergmeier, W., Chauhan, A. K. & Wagner, D. D. Glycoprotein Ibalpha and von Willebrand factor in primary platelet adhesion and thrombus formation: lessons from mutant mice. *Thrombosis and haemostasis* **99**, 264-270, doi:10.1160/th07-10-0638 (2008).
404 Chauhan, A. K., Kisucka, J., Lamb, C. B., Bergmeier, W. & Wagner, D. D. von Willebrand factor and factor VIII are independently required to form stable occlusive thrombi in injured veins. *Blood* **109**, 2424-2429, doi:10.1182/blood-2006-06-028241 (2007).
405 Nesbitt, W. S. *et al.* Distinct glycoprotein Ib/V/IX and integrin alpha IIbbeta 3-dependent calcium signals cooperatively regulate platelet adhesion under flow. *The Journal of biological chemistry* **277**, 2965-2972, doi:10.1074/jbc.M110070200 (2002).
406 Feng, S., Lu, X. & Kroll, M. H. Filamin A binding stabilizes nascent glycoprotein Ibalpha trafficking and thereby enhances its surface expression. *The Journal of biological chemistry* **280**, 6709-6715, doi:10.1074/jbc.M413590200 (2005).
407 Poujol, C., Ware, J., Nieswandt, B., Nurden, A. T. & Nurden, P. Absence of GPIbalpha is responsible for aberrant membrane development during megakaryocyte maturation: ultrastructural study using a transgenic model. *Experimental hematology* **30**, 352-360 (2002).
408 Kanaji, T. *et al.* Megakaryocyte proliferation and ploidy regulated by the cytoplasmic tail of glycoprotein Ibα. *Blood* **104**, 3161-3168, doi:10.1182/blood-2004-03-0893 (2004).
409 Ware, J., Russell, S. & Ruggeri, Z. M. Generation and rescue of a murine model of platelet dysfunction: The Bernard-Soulier syndrome. *Proceedings of the National Academy of Sciences* **97**, 2803-2808, doi:10.1073/pnas.050582097 (2000).
410 Arthur, J. F. *et al.* Glycoprotein VI is associated with GPIb-IX-V on the membrane of resting and activated platelets. *Thrombosis and haemostasis* **93**, 716-723, doi:10.1160/th04-09-0584 (2005).
411 Baker, J., Griggs, R. K., Falati, S. & Poole, A. W. GPIb potentiates GPVI-induced responses in human platelets. *Platelets* **15**, 207-214, doi:10.1080/09537100410001701010 (2004).
412 Falati, S., Edmead, C. E. & Poole, A. W. Glycoprotein Ib-V-IX, a receptor for von Willebrand factor, couples physically and functionally to the Fc receptor gamma-chain, Fyn, and Lyn to activate human platelets. *Blood* **94**, 1648-1656 (1999).
413 Wu, Y. *et al.* Role of Fc receptor gamma-chain in platelet glycoprotein Ib-mediated signaling. *Blood* **97**, 3836-3845, doi:10.1182/blood.v97.12.3836 (2001).
414 de Witt, S. M. *et al.* Identification of platelet function defects by multi-parameter assessment of thrombus formation. *Nature communications* **5**, 4257, doi:10.1038/ncomms5257 (2014).
415 Shen, J. *et al.* Coordination of platelet agonist signaling during the hemostatic response in vivo. *Blood advances* **1**, 2767-2775, doi:10.1182/bloodadvances.2017009498 (2017).
416 Semple, J. W., Italiano, J. E., Jr. & Freedman, J. Platelets and the immune continuum. *Nature reviews. Immunology* **11**, 264-274, doi:10.1038/nri2956 (2011).
417 Mayadas, T. N., Johnson, R. C., Rayburn, H., Hynes, R. O. & Wagner, D. D. Leukocyte rolling and extravasation are severely compromised in P selectin-deficient mice. *Cell* **74**, 541-554 (1993).

418 Joglekar, M. V., Ware, J., Xu, J., Fitzgerald, M. E. & Gartner, T. K. Platelets, glycoprotein Ib-IX, and von Willebrand factor are required for FeCl(3)-induced occlusive thrombus formation in the inferior vena cava of mice. *Platelets* **24**, 205-212, doi:10.3109/09537104.2012.696746 (2013).
419 Verhenne, S. *et al.* Platelet-derived VWF is not essential for normal thrombosis and hemostasis but fosters ischemic stroke injury in mice. *Blood* **126**, 1715-1722, doi:10.1182/blood-2015-03-632901 (2015).
420 Shi, C., Zhang, X., Chen, Z., Robinson, M. K. & Simon, D. I. Leukocyte integrin Mac-1 recruits toll/interleukin-1 receptor superfamily signaling intermediates to modulate NF-kappaB activity. *Circulation research* **89**, 859-865, doi:10.1161/hh2201.099166 (2001).
421 Springer, T. A. Adhesion receptors of the immune system. *Nature* **346**, 425-434, doi:10.1038/346425a0 (1990).
422 Petri, B. *et al.* von Willebrand factor promotes leukocyte extravasation. *Blood* **116**, 4712-4719, doi:10.1182/blood-2010-03-276311 (2010).
423 Zirka G, R. P., Tilburg J, Maracle C, Legendre P, Alessi M, Lenting P, Morange P, Thomas G CTL-2 is a VWF receptor involved in neutrophil activation. *ECTH Abstract* (2019).
424 Miyata, S. & Ruggeri, Z. M. Distinct structural attributes regulating von Willebrand factor A1 domain interaction with platelet glycoprotein Ibalpha under flow. *The Journal of biological chemistry* **274**, 6586-6593, doi:10.1074/jbc.274.10.6586 (1999).
425 Yago, T. *et al.* Platelet glycoprotein Ibalpha forms catch bonds with human WT vWF but not with type 2B von Willebrand disease vWF. *The Journal of clinical investigation* **118**, 3195-3207, doi:10.1172/jci35754 (2008).
426 Abdel-Misih, S. R. & Bloomston, M. Liver anatomy. *The Surgical clinics of North America* **90**, 643-653, doi:10.1016/j.suc.2010.04.017 (2010).
427 Katz, S., Jimenez, M. A., Lehmkuhler, W. E. & Grosfeld, J. L. Liver bacterial clearance following hepatic artery ligation and portacaval shunt. *The Journal of surgical research* **51**, 267-270, doi:10.1016/0022-4804(91)90105-u (1991).
428 Mackman, N. New insights into the mechanisms of venous thrombosis. *The Journal of clinical investigation* **122**, 2331-2336, doi:10.1172/jci60229 (2012).
429 Ozgönenel, B., Rajpurkar, M. & Lusher, J. M. How do you treat bleeding disorders with desmopressin? *Postgraduate medical journal* **83**, 159-163, doi:10.1136/pgmj.2006.052118 (2007).
430 Federici, A. B. & James, P. Current management of patients with severe von Willebrand disease type 3: a 2012 update. *Acta haematologica* **128**, 88-99, doi:10.1159/000338208 (2012).
431 Tilburg, J. *et al.* Characterization of hemostasis in mice lacking the novel thrombosis susceptibility gene Slc44a2. *Thrombosis research* **171**, 155-159, doi:10.1016/j.thromres.2018.09.057 (2018).
432 Luther, N. *et al.* Innate Effector-Memory T-Cell Activation Regulates Post-Thrombotic Vein Wall Inflammation and Thrombus Resolution. *Circulation research* **119**, 1286-1295, doi:10.1161/circresaha.116.309301 (2016).
433 Schulman, S. Extended anticoagulation in venous thromboembolism. *The New England journal of medicine* **368**, 2329, doi:10.1056/NEJMc1304815 (2013).
434 Schulman, S. *et al.* Treatment of acute venous thromboembolism with dabigatran or warfarin and pooled analysis. *Circulation* **129**, 764-772, doi:10.1161/circulationaha.113.004450 (2014).
435 Schulman, S. *et al.* Dabigatran versus Warfarin in the Treatment of Acute Venous Thromboembolism. *New England Journal of Medicine* **361**, 2342-2352, doi:10.1056/NEJMoa0906598 (2009).
436 Wolberg, A. S. *et al.* Venous thrombosis. *Nature reviews. Disease primers* **1**, 15006, doi:10.1038/nrdp.2015.6 (2015).

437 Chauhan, A. K. *et al.* Systemic antithrombotic effects of ADAMTS13. *The Journal of experimental medicine* **203**, 767-776, doi:10.1084/jem.20051732 (2006).
438 Gandhi, C., Khan, M. M., Lentz, S. R. & Chauhan, A. K. ADAMTS13 reduces vascular inflammation and the development of early atherosclerosis in mice. *Blood* **119**, 2385-2391, doi:10.1182/blood-2011-09-376202 (2012).
439 Fuchs, T. A., Kremer Hovinga, J. A., Schatzberg, D., Wagner, D. D. & Lämmle, B. Circulating DNA and myeloperoxidase indicate disease activity in patients with thrombotic microangiopathies. *Blood* **120**, 1157-1164, doi:10.1182/blood-2012-02-412197 (2012).
440 Thornton, P. *et al.* Platelet interleukin-1alpha drives cerebrovascular inflammation. *Blood* **115**, 3632-3639, doi:10.1182/blood-2009-11-252643 (2010).
441 Kleinschnitz, C. *et al.* Targeting platelets in acute experimental stroke: impact of glycoprotein Ib, VI, and IIb/IIIa blockade on infarct size, functional outcome, and intracranial bleeding. *Circulation* **115**, 2323-2330, doi:10.1161/circulationaha.107.691279 (2007).
442 Chen, X., Cheng, X., Zhang, S. & Wu, D. ADAMTS13: An Emerging Target in Stroke Therapy. *Frontiers in neurology* **10**, 772, doi:10.3389/fneur.2019.00772 (2019).
443 Denorme, F. *et al.* ADAMTS13-mediated thrombolysis of t-PA-resistant occlusions in ischemic stroke in mice. *Blood* **127**, 2337-2345, doi:10.1182/blood-2015-08-662650 (2016).
444 Laridan, E. *et al.* Neutrophil extracellular traps in ischemic stroke thrombi. *Annals of neurology* **82**, 223-232, doi:10.1002/ana.24993 (2017).
445 Gu, L., Jian, Z., Stary, C. & Xiong, X. T Cells and Cerebral Ischemic Stroke. *Neurochemical research* **40**, 1786-1791, doi:10.1007/s11064-015-1676-0 (2015).
446 Kleinschnitz, C. *et al.* Early detrimental T-cell effects in experimental cerebral ischemia are neither related to adaptive immunity nor thrombus formation. *Blood* **115**, 3835-3842, doi:10.1182/blood-2009-10-249078 (2010).
447 Yilmaz, G., Arumugam, T. V., Stokes, K. Y. & Granger, D. N. Role of T lymphocytes and interferon-gamma in ischemic stroke. *Circulation* **113**, 2105-2112, doi:10.1161/circulationaha.105.593046 (2006).
448 Kistangari, G. & McCrae, K. R. Immune thrombocytopenia. *Hematology/oncology clinics of North America* **27**, 495-520, doi:10.1016/j.hoc.2013.03.001 (2013).
449 Kolaczkowska, E. *et al.* Molecular mechanisms of NET formation and degradation revealed by intravital imaging in the liver vasculature. *Nature communications* **6**, 6673, doi:10.1038/ncomms7673 (2015).
450 Okahashi, N. *et al.* Pili of oral Streptococcus sanguinis bind to fibronectin and contribute to cell adhesion. *Biochemical and biophysical research communications* **391**, 1192-1196, doi:10.1016/j.bbrc.2009.12.029 (2010).
451 Herzberg, M. C. *et al.* The platelet interactivity phenotype of Streptococcus sanguis influences the course of experimental endocarditis. *Infection and immunity* **60**, 4809-4818 (1992).
452 Moreillon, P. & Que, Y. A. Infective endocarditis. *Lancet (London, England)* **363**, 139-149, doi:10.1016/s0140-6736(03)15266-x (2004).

Appendix 1

Figure permission – Figure 1.7

OXFORD UNIVERSITY PRESS LICENSE TERMS AND CONDITIONS

Oct 15, 2019

This Agreement between Mrs. Adela Constantinescu-Bercu ("You") and Oxford University Press ("Oxford University Press") consists of your license details and the terms and conditions provided by Oxford University Press and Copyright Clearance Center.

License Number	4690170383462
License date	Oct 15, 2019
Licensed content publisher	Oxford University Press
Licensed content publication	American Journal of Clinical Pathology
Licensed content title	Analysis of von Willebrand Factor Multimers by Simultaneous High- and Low-Resolution Vertical SDS-Agarose Gel Electrophoresis and Cy5-Labeled Antibody High-Sensitivity Fluorescence Detection
Licensed content author	Ott, Helmut W.; Griesmacher, Andrea
Licensed content date	Jan 2, 2010
Type of Use	Thesis/Dissertation
Institution name	
Title of your work	PhD in Cardiovascular Science
Publisher of your work	Imperial College London
Expected publication date	Dec 2019
Permissions cost	0.00 GBP
Value added tax	0.00 GBP
Total	0.00 GBP
Title	PhD in Cardiovascular Science
Institution name	Imperial College London
Expected presentation date	Dec 2019
Portions	Image 1 - top agarose gel showing an example of normal plasma VWF:AG
Requestor Location	Mrs. Adela Constantinescu-Bercu Imperial College London Hammersmith Hospital Campus Du Cane Road London, W12 0NN United Kingdom Attn: Mrs. Adela Constantinescu-Bercu
Publisher Tax ID	GB125506730
Total	0.00 GBP

Terms and Conditions

STANDARD TERMS AND CONDITIONS FOR REPRODUCTION OF MATERIAL FROM AN OXFORD UNIVERSITY PRESS JOURNAL

1. Use of the material is restricted to the type of use specified in your order details.
2. This permission covers the use of the material in the English language in the following territory: world. If you have requested additional permission to translate this material, the terms and conditions of this reuse will be set out in clause 12.
3. This permission is limited to the particular use authorized in (1) above and does not allow you to sanction its use elsewhere in any other format other than specified above, nor does it apply to quotations, images, artistic works etc that have been reproduced from other sources which may be part of the material to be used.
4. No alteration, omission or addition is made to the material without our written consent. Permission must be re-cleared with Oxford University Press if/when you decide to reprint.
5. The following credit line appears wherever the material is used: author, title, journal, year, volume, issue number, pagination, by permission of Oxford University Press or the sponsoring society if the journal is a society journal. Where a journal is being published on behalf of a learned society, the details of that society must be included in the credit line.
6. For the reproduction of a full article from an Oxford University Press journal for whatever purpose, the corresponding author of the material concerned should be informed of the proposed use. Contact details for the corresponding authors of all Oxford University Press journal contact can be found alongside either the abstract or full text of the article concerned, accessible from www.oxfordjournals.org Should there be a problem clearing these rights, please contact journals.permissions@oup.com
7. If the credit line or acknowledgement in our publication indicates that any of the figures, images or photos was reproduced, drawn or modified from an earlier source it will be necessary for you to clear this permission with the original publisher as well. If this permission has not been obtained, please note that this material cannot be included in your publication/photocopies.
8. While you may exercise the rights licensed immediately upon issuance of the license at the end of the licensing process for the transaction, provided that you have disclosed complete and accurate details of your proposed use, no license is finally effective unless and until full payment is received from you (either by Oxford University Press or by Copyright Clearance Center (CCC)) as provided in CCC's Billing and Payment terms and conditions. If full payment is not received on a timely basis, then any license preliminarily granted shall be deemed automatically revoked and shall be void as if never granted. Further, in the event that you breach any of these terms and conditions or any of CCC's Billing and Payment terms and conditions, the license is automatically revoked and shall be void as if never granted. Use of materials as described in a revoked license, as well as any use of the materials beyond the scope of an unrevoked license, may constitute copyright infringement and Oxford University Press reserves the right to take any and all action to protect its copyright in the materials.
9. This license is personal to you and may not be sublicensed, assigned or transferred by you to any other person without Oxford University Press's written permission.
10. Oxford University Press reserves all rights not specifically granted in the combination of (i) the license details provided by you and accepted in the course of this licensing transaction, (ii) these terms and conditions and (iii) CCC's Billing and Payment terms and conditions.
11. You hereby indemnify and agree to hold harmless Oxford University Press and CCC, and their respective officers, directors, employs and agents, from and against any and all claims

arising out of your use of the licensed material other than as specifically authorized pursuant to this license.
12. Other Terms and Conditions:
v1.4

Questions? customercare@copyright.com or +1-855-239-3415 (toll free in the US) or +1-978-646-2777.

Appendix 2

To analyse the importance of VWF-mediated platelet 'priming' in innate immunity, I coated microchannels with bacteria overnight, at 37°C. Both gram-positive (*S. aureus*) and gram-negative bacteria (*E. coli*) were used. Bacteria were labelled with a fluorescent dye (BacLight Red) and their capture was confirmed by fluorescence microscopy. Flow assays were subsequently performed by perfusing anticoagulated whole blood labelled with $DiOC_6$ through these channels. At high shear, no platelet or leukocyte binding could be observed. In contrast, at $50s^{-1}$, platelets could be seen binding to the bacteria (**Figure 10.1**). This was followed by leukocyte recruitment, in a similar manner to the other flow experiments performed during my PhD – leukocytes first rolled over the platelets prior to stable attachment. Attached leukocytes seemed to spread within seconds of binding (data not shown), though this needs to be confirmed in future experiments. It can be assumed that these leukocytes were likely neutrophils which, once recruited by platelets, could recognise the bacteria coated on the channel and subsequently release NETs in response.

To investigate whether platelets directly bound to bacteria or whether this occurred in a VWF-dependent manner, I pre-incubated blood with an antibody against ADAMTS13. This antibody would inhibit the activity of ADAMTS13, preventing the regulation of VWF multimeric size. Thus, it would be expected that VWF would not be cleaved when it unravels and this would augment platelet recruitment. When perfusing blood in the presence of anti-ADAMTS13 through channels coated with either *S. aureus* or *E. coli* at low shear, binding of platelets was substantially augmented, suggesting that binding of platelets to bacteria in this system is dependent on VWF (**Figure 10.1**, representative of n=3).

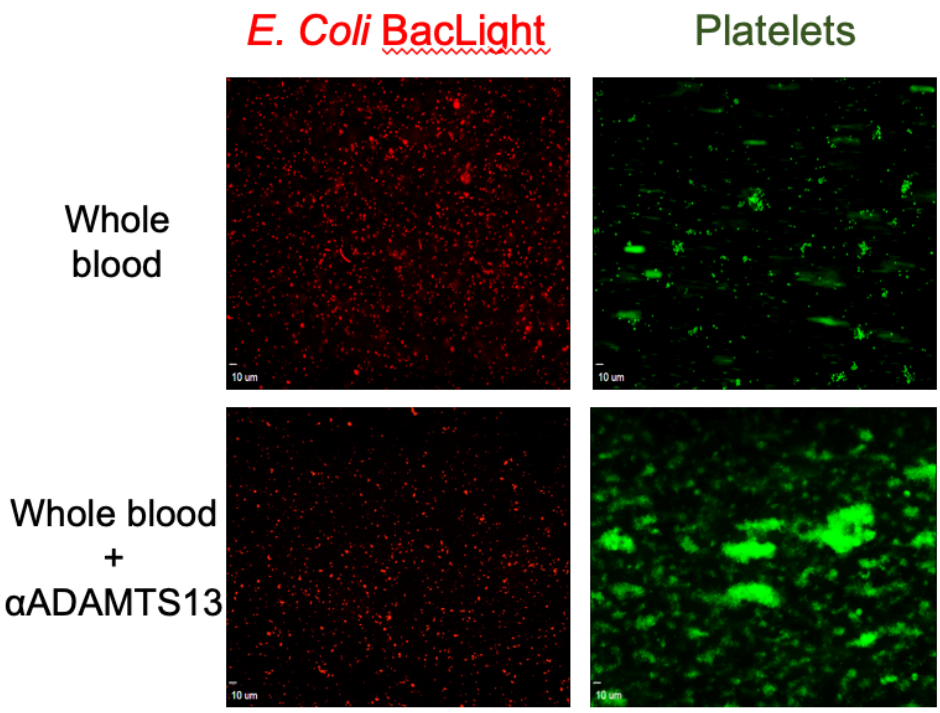

Figure 10.1 The role of VWF in platelet recruitment by E. coli.

E. coli were captured onto microfluidic channels and fluorescently labelled with BacLight (red). Whole blood was perfused at 50s^{-1} through these channels in the presence or absence of an anti-ADAMTS13 antibody and platelet capture is shown in green. Images representative of n=3.

However, it is still unclear how this system would translate physiologically and under which circumstances platelets would encounter a carpet of bacteria before this would cause a septic reaction. To overcome this, I performed experiments in which platelets were captured and 'primed' by VWF and, subsequently, fluorescently-labelled bacteria (*S. sanguinis*) was perfused over the carpet of platelets at low shear. These bacteria bound platelets (data not shown). If after the binding of bacteria, blood was perfused again through the channel, a high number of leukocytes could be seen to attach and spread (data not shown). However, it is unclear how these bacteria interacted with the 'primed' platelets.

S. sanguinis contains pilli on its surface, including PilB [450], which appears to contain an A1-like domain. I collaborated with Claire Raynaud and Dr. Vladimir Pelicic from the Centre of Molecular Bacteriology and Infection at Imperial College London and investigated the ability

of platelets to bind PilB at different shear rates. Purified recombinant PilB was coated onto Cu^{2+} microchannels via its His tag. Thereafter, labelled whole blood or plasma-free blood was perfused through these channels at different shear rates. Preliminary data suggests that platelets bind to PilB at low shear rates, providing further insights into how platelets might bind bacteria. However, these data need to be further analysed. *S. sanguinis* is recognised for its role in the pathology of infective endocarditis, being associated with sites of thrombus formation in this disease through yet unknown mechanisms [451,452]. These data might, therefore, also shed light into the pathogenesis of infective endocarditis.

24 Hills Road, **P** 01223 855346
Cambridge **W** elifesciences.org
CB2 1JP **T** @elife_sciences

FOR PEER REVIEW - CONFIDENTIAL

Activated αIIbβ3 on platelets mediates flow-dependent NETosis via SLC44A2

Tracking no: 05-11-2019-RA-eLife-53353

Impact statement: The interaction between activated αIIbβ3 on platelets and SLC44A2 on circulating neutrophils facilitates neutrophil capture and drives flow-dependent NETosis.

Competing interests: No competing interests declared

Author contributions:
Adela Constantinescu-Bercu: Data curation; Formal analysis; Validation; Investigation; Visualization; Methodology; Writing—original draft Luigi Grassi: Resources; Data curation; Formal analysis; Writing—review and editing Mattia Frontini: Resources; Data curation; Formal analysis; Writing—review and editing Isabelle Salles-Crawley: Conceptualization; Data curation; Formal analysis; Supervision; Funding acquisition; Investigation; Visualization; Methodology; Writing—original draft; Project administration Kevin Woollard: Conceptualization; Formal analysis; Supervision; Funding acquisition; Methodology; Project administration; Writing—review and editing James Crawley: Conceptualization; Formal analysis; Supervision; Funding acquisition; Methodology; Writing—original draft; Project administration

Funding:
British Heart Foundation (BHF): Isabelle I Salles-Crawley, Kevin Woollard, James TB Crawley, FS/15/65/32036; British Heart Foundation (BHF): Isabelle I Salles-Crawley, Kevin Woollard, James TB Crawley, PG/17/22/32868; British Heart Foundation (BHF): Mattia Frontini, FS/18/53/33863
The funders had no role in study design, data collection and interpretation, or the decision to submit the work for publication.

Data Availability:
All data generated or analysed during this study are included in the manuscript and supporting files. The source data underlying Figs 1c, 2b-e, 3, 4b-c, 5c-d, 6c-e, 8a, c, d and f and Supplementary Figs 1, 2, 3c-d, 4b are are provided in a separate 'Source Data' file.
N/A

Ethics:
Human Subjects: Yes Ethics Statement: Specific ethical approval was obtained from the Imperial College Research Ethics Committee (19IC5523) for drawing blood from healthy volunteers. Clinical Trial: No Animal Subjects: No

Information for reviewers (full submissions):

eLife aims to publish work of the highest scientific standards and importance in all areas of the life and biomedical sciences, from the most basic and theoretical work through to translational, applied and clinical research. Articles must be methodologically and scientifically rigorous, ethically conducted, and objectively presented according to the appropriate community standards.

You will be asked for a general assessment and a summary of any major concerns (ideally in fewer than 500 words), as well as a list of any minor comments (optional). You will also have the opportunity to comment on the statistical rigour of the work (optional).

In your general assessment, please articulate what is exciting and whether the work represents a significant contribution. Please note our guidelines about requests for additional work:

1. We will only request new work, such as experiments, analyses, or data collection, if the new data are essential to support the major conclusions. The authors must be able to do any new work in a reasonable time frame (additional work should be conducted and written up within two months); otherwise, we will usually reject the manuscript.
2. Any requests for new work must fall within the scope of the current submission and the technical expertise of the authors.

Our goal is to make peer review constructive and collaborative: after the reviews have been submitted independently, there is an online discussion between the reviewers in which each reviewer will see the identity of the other reviewers.

Activated $\alpha_{IIb}\beta_3$ on platelets mediates flow-dependent NETosis via SLC44A2

Adela Constantinescu-Bercu[1,2], Luigi Grassi[3,4,5], Mattia Frontini[3,4,6], Isabelle I. Salles-Crawley[1]*, Kevin J Woollard[2]* & James T.B. Crawley[1]*

1) Centre for Haematology, Department of Immunology and Inflammation, Imperial College London, London, UK
2) Centre for Inflammatory Disease, Department of Immunology and Inflammation, Imperial College London, London, UK
3) Department of Haematology, University of Cambridge, Cambridge Biomedical Campus, Cambridge, UK
4) National Health Service Blood and Transplant, Cambridge Biomedical Campus, Cambridge, UK
5) National Institute for Health Research BioResource, Rare Diseases, Cambridge University Hospitals, Cambridge, UK
6) British Heart Foundation Centre of Excellence, Cambridge Biomedical Campus, Cambridge, UK.

* these authors (IIS-C, KJW & JTBC) co-supervised and contributed equally to this work

Short Title: **$\alpha_{IIb}\beta_3$ and SLC44A2 in platelet-mediated NETosis**

Summary	(**40 words**)
Abstract	(**144 words**)
Main text	(**34,194 characters**) (excluding methods, references and legends)
Figures & Tables	(**9**)
Supplementary Figures	(**6**)
Movies	(**7**)

Corresponding authors:
JTBC, KJW & IIS-C
Department of Immunology and Inflammation
Imperial College London
Hammersmith Hospital Campus
London
W12 0NN
UK
Tel: +44 (0)20 8383 2297
E-mail: j.crawley@imperial.ac.uk; k.woollard@imperial.ac.uk; i.salles@imperial.ac.uk

Summary

Platelets that are primed following interaction with von Willebrand factor under flow mediated direct interactions with neutrophils via activated platelet integrin, $\alpha_{IIb}\beta_3$, and SLC44A2 on neutrophils. This interaction initiates signaling in a mechanosensitive manner that promotes neutrophil extracellular trap formation.

Abstract

Platelet-neutrophil interactions are important for innate immunity, but also contribute to the pathogenesis of deep vein thrombosis, myocardial infarction and stroke. Here we report that, under flow, von Willebrand factor/glycoprotein Ibα-dependent platelet 'priming' induces integrin $\alpha_{IIb}\beta_3$ activation that, in turn, mediates neutrophil and T-cell binding. Binding of platelet $\alpha_{IIb}\beta_3$ to SLC44A2 on neutrophils leads to mechanosensitive-dependent production of highly prothrombotic neutrophil extracellular traps. A polymorphism in *SLC44A2* (rs2288904-A) present in 22% of the population causes an R154Q substitution in an extracellular loop of SLC44A2 that is protective against venous thrombosis results in severely impaired binding to both activated $\alpha_{IIb}\beta_3$ and VWF-primed platelets. This was confirmed using neutrophils homozygous for the *SLC44A2* R154Q polymorphism. Taken together, these data reveal a previously unreported mode of platelet-neutrophil cross-talk, mechanosensitive NET production, and provide mechanistic insight into the protective effect of the *SLC44A2* rs2288904-A polymorphism in venous thrombosis.

Key words: thrombosis, platelets, neutrophils, NETs, VWF, SLC44A2, $\alpha_{IIb}\beta_3$

Introduction

To fulfil their hemostatic function, platelets must be recruited to sites of vessel damage. This process is highly dependent upon von Willebrand factor (VWF). Upon vessel injury, exposed subendothelial collagen binds plasma VWF via its A3 domain (Cruz et al., 1995). Elevated shear, or turbulent/disturbed flow, then unravels tethered VWF and exposes its A1 domain, facilitating specific capture of platelets via glycoprotein (GP)Ibα.

As well as capturing platelets under flow, the A1-GPIbα interaction also induces shear-dependent signaling events (Bryckaert et al., 2015). For this, GPIbα first binds the A1 domain of immobilized VWF (Zhang et al., 2015). Rheological forces then cause unfolding of the GPIbα mechanosensitive domain that translates the mechanical stimulus into a signal within the platelet (Ju et al., 2016; Zhang et al., 2015). This leads to release of intracellular Ca^{2+} stores and activation of the platelet integrin, $\alpha_{IIb}\beta_3$ (Gardiner et al., 2010).

VWF-mediated signaling transduces a mild signal. Consequently, these signaling events are often considered redundant within hemostasis as platelets respond more dramatically to other agonists present at sites of vessel injury (e.g. collagen, thrombin, ADP, thromboxane A2) (Jackson et al., 2003; Senis et al., 2014). Full platelet activation involves release of α- and δ-granules, presentation of new cell surface proteins, activation of cell surface integrins and alterations in the membrane phospholipid composition. The extent of platelet activation is dependent upon both the concentration, and identity, of the agonist(s) to which the platelets are exposed, which is dictated by the location of the platelets relative to the damaged vessel. For example, platelets in the core of a hemostatic plug/thrombus are exposed to higher concentrations of agonists and are more highly activated (i.e. P-selectin-positive procoagulant platelets) than those in the surrounding shell (P-selectin-negative) (de Witt et al., 2014; Shen et al., 2017; Stalker et al., 2013; Welsh et al., 2014). Thus, platelets exhibit a 'tunable' activation response determined by agonist availability.

Aside from hemostasis, platelets also have important roles as immune cells by aiding in targeting of bacteria by leukocytes (Gaertner et al., 2017; Kolaczkowska et al., 2015; Sreeramkumar et al., 2014; Wong et al., 2013). Platelet-leukocyte interactions also influence the development of inflammatory cardiovascular conditions. In deep vein thrombosis (DVT), VWF-dependent platelet recruitment, platelet-neutrophil interactions and the production of highly thrombotic neutrophil extracellular traps (NETs) all contribute to the development of a pathological thrombus (Brill et al., 2011; Brill et al., 2012; Fuchs et al., 2012a; Schulz et al., 2013; von Bruhl et al., 2012). Although the precise sequence of events still remains unclear, it appears that during the early stages of DVT, VWF-bound platelets acquire the ability to interact with leukocytes (von Bruhl et al., 2012). Exactly how this is mediated given the lack of vessel damage is unclear. It also remains to be determined precisely how platelet-tethered neutrophils undergo NETosis in DVT in the absence of an infectious agent.

Known direct platelet-leukocyte interactions involve either P-selectin or CD40L on the surface of platelets binding to P-selectin glycoligand-1 (PSGL-1) and CD40, respectively, on leukocytes (Lievens et al., 2010; Mayadas et al., 1993; Palabrica et al., 1992). As platelets must be potently activated to facilitate P-selectin/CD40L exposure, such interactions unlikely mediate the early platelet-leukocyte

interactions that occur in the murine DVT model. Consistent with this, lack of platelet P-selectin has no effect upon either leukocyte recruitment or thrombus formation in murine DVT (von Bruhl et al., 2012). Leukocytes can also indirectly interact with platelets through Mac-1 (integrin $\alpha_M\beta_2$), which can associate with activated $\alpha_{IIb}\beta_3$ via fibrinogen (Weber and Springer, 1997), or directly via GPIbα (Simon et al., 2000). Interactions are also possible through lymphocyte function-associated antigen 1 (LFA-1/integrin $\alpha_L\beta_2$) that can bind intercellular adhesion molecule 2 (ICAM-2) on platelets (Damle et al., 1992; Diacovo et al., 1994). In both instances though, leukocyte activation is necessary to activate Mac-1 or LFA-1 integrins before interactions can occur.

Although it is often assumed that only activated platelets bind leukocytes, recent studies have revealed that platelets captured under flow by VWF released from activated endothelial cells can recruit leukocytes (Doddapattar et al., 2018; Zheng et al., 2015). If VWF-GPIbα-dependent signaling is capable of promoting leukocyte binding, this may be highly relevant to the non-hemostatic platelet functions (particularly when other agonists are not available/abundant), but may also provide major mechanistic insights into the early recruitment of leukocytes during the initiation of DVT.

Genome wide association studies (GWAS) on venous thromboembolism (VTE) have identified a panel of genes (*ABO*, *F2*, *F5*, *F11*, *FGG*, *PROCR*) with well-described influences upon coagulation and thrombotic risk, as well as those with well-established causative links (e.g. *PROS*, *PROC*, *SERPINC1*) (Germain et al., 2015; Germain et al., 2011; Rosendaal and Reitsma, 2009). This is consistent with the efficacy of therapeutic targeting of coagulation to protect against DVT with anticoagulants (Chan et al., 2016). However, although the use of anticoagulants is effective, dosing and efficacy are limited by the increase in the risk of bleeding in treated individuals (Chan et al., 2016; Schulman et al., 2014; Schulman et al., 2009; Schulman et al., 2013; Wolberg et al., 2015). Therefore, alternative targets that inhibit DVT disease processes, but that do not modify bleeding risk may provide new adjunctive therapies to further protect against the development or recurrence of DVT. GWAS studies have also identified additional risk *loci* for VTE, but with no known role in coagulation (Apipongrat et al., 2019; Germain et al., 2015; Hinds et al., 2016). This provides encouragement that alternative therapeutic targets may exist with the potential to modify the disease process without affecting bleeding risk. These *loci* include *SLC44A2* and *TSPAN15* genes (Apipongrat et al., 2019; Germain et al., 2015; Hinds et al., 2016). Despite the identification of these *loci*, the function of these cell surface proteins with respect to their involvement in the pathogenesis of venous thrombosis remains unclear.

Using microfluidic flow channels to enable analysis of the phenotypic effects of VWF-GPIbα signaling under flow, we confirm the rapid activation of the platelet integrin, $\alpha_{IIb}\beta_3$. Activated $\alpha_{IIb}\beta_3$ is capable of binding directly to neutrophils via a direct interaction with SLC44A2. Under flow, this interaction transduces a signal into neutrophils capable of driving NETosis. A single nucleotide polymorphism (SNP; rs2288904-A) in *SLC44A2* (minor allele frequency 0.22) that is protective against VTE (Germain et al., 2015) encodes a R154Q substitution in the first extracellular loop of the receptor that markedly reduces neutrophil-platelet binding via activated $\alpha_{IIb}\beta_3$. These results provide a functional explanation for the protective effects of the rs2288904-A SNP and highlight the potential of SLC44A2 as an adjunctive therapeutic target in DVT.

Results

To explore the influence of platelet binding to VWF under flow upon platelet function, full length (FL-) human VWF was adsorbed directly onto microfluidic microchannel surfaces, or the isolated recombinant VWF A1 domain, or an A1 domain variant (Y1271C/C1272R, termed A1*) that exhibits a 10-fold higher affinity for GPIbα (**Fig S1**) (Blenner et al., 2014), were captured via their 6xHis tag. Fresh blood anticoagulated with D-phenylalanyl-prolyl-arginyl chloromethyl ketone (PPACK) and labelled with $DiOC_6$, was perfused through channels at $1000s^{-1}$ for 3.5 minutes. On FL-VWF, A1 or A1*, a similar time-dependent increase in platelet recruitment/surface coverage was observed (**Fig 1a** & **Fig S2**).

Platelets rolled prior to attaching more firmly on all VWF channels. However, median initial platelet rolling velocity on VWF A1 was 1.76 μms^{-1}, whereas on A1* this was significantly slower (median $0.23\mu ms^{-1}$) (**Fig 1b** & **c**), reflective of its 10-fold higher affinity for GPIbα (**Movie 1**)

Platelet binding to VWF under flow induces intraplatelet signaling and activation of $\alpha_{IIb}\beta_3$

Platelets bound to either FL-VWF, A1 or A1* formed small aggregates after about 2 minutes (**Fig 2ai**) due to activation of the platelet integrin, $\alpha_{IIb}\beta_3$, and its binding to plasma fibrinogen. Consistent with this, when plasma-free blood (i.e. RBCs, leukocytes and platelets resuspended in plasma-free buffer) was used, platelets remained as a uniform monolayer, and did not form microaggregates (**Fig 2aii**). Similarly, when activated $\alpha_{IIb}\beta_3$ was blocked in whole blood with eptifibatide or GR144053, aggregation was also inhibited (**Fig 2aiii** & **iv**). Irrespective of the surface (VWF, A1 or A1*), platelet aggregation was markedly reduced if plasma-free blood was used, or if $\alpha_{IIb}\beta_3$ was blocked (**Fig 2b-e**). These results demonstrate that the A1-GPIbα interaction leads to activation of $\alpha_{IIb}\beta_3$, which is consistent with previous reports (Goto et al., 1995; Kasirer-Friede et al.). In support of this, fluorescent fibrinogen bound to platelets tethered via FL-VWF, but not to platelets captured to channel surfaces using an anti-PECAM-1 antibody (**Fig S3a**).

To investigate the effect of A1-GPIbα-dependent signaling, platelets were preloaded with the Ca^{2+}-sensitive fluorophore, Fluo-4 AM. Platelets bound to A1* under flow exhibited repeated transient increases in fluorescence, corresponding to Ca^{2+} release from platelet intracellular stores in response to A1-GPIbα binding under flow (**Movie 2**) (Kasirer-Friede et al., 2004; Mu et al., 2010). Despite intracellular Ca^{2+} release, this did not lead to appreciable P-selectin exposure (i.e. α-granule release) (**Fig S3b**). Intraplatelet Ca^{2+} release was not detected when platelets were captured under flow using an anti-PECAM1 antibody. We therefore propose that flow-dependent VWF-GPIbα signaling 'primes', rather than activates, platelets. This priming is characterized by activation of $\alpha_{IIb}\beta_3$, but minimal α-granule release, and represents part of the tunable response of platelets.

Platelets 'primed' by VWF interact with leukocytes.

To explore the influence of platelet 'priming' upon their ability to interact with leukocytes, platelets were captured and 'primed' on VWF for 3 minutes at $1000s^{-1}$. Thereafter, leukocytes in whole blood (also labelled with $DiOC_6$) were perfused at $50s^{-1}$ and rolled on the platelet-covered surface (**Movie 3** & **Fig**

S4a). Leukocytes did not interact with platelets captured via an anti-PECAM-1 antibody (**Fig 3a**), demonstrating the dependency on prior A1-GPIbα-mediated platelet 'priming'.

As VWF-'primed' platelets present activated $\alpha_{IIb}\beta_3$, we hypothesized that 'outside-in' integrin signaling might be important for platelet-leukocyte interactions to occur (Durrant et al., 2017). Contrary to this, we observed a significant (~2-fold) increase in the number of leukocytes interacting with the VWF-bound platelets in plasma-free conditions (**Fig 3b**). Moreover, addition of purified fibrinogen to plasma-free blood to 50% normal plasma concentration significantly reduced platelet-leukocyte interactions (**Fig 3b**) suggesting that leukocytes and fibrinogen compete for binding 'primed' platelets. Blocking $\alpha_{IIb}\beta_3$ (**Fig 3a-b** & **Fig S4a**) also significantly decreased platelet-leukocyte interactions irrespective of whether platelets were captured on FL-VWF or A1*, or whether experiments were performed in whole blood or plasma-free blood (**Fig 3a-c)**.

To explore the role of activated $\alpha_{IIb}\beta_3$ in binding leukocytes, platelets were captured onto anti-PECAM-1 coated channels and an anti-β_3 antibody (ligand induced binding site – LIBS) that induces activation of $\alpha_{IIb}\beta_3$ applied (Du et al., 1993). Antibody-mediated activation of $\alpha_{IIb}\beta_3$ caused a significant increase in the number of leukocytes binding in a manner that could be blocked with GR144053 (**Fig 3d**).

The best characterized platelet-leukocyte interaction is mediated by P-selectin on activated platelets binding to PSGL-1 on leukocytes (Vandendries et al., 2004). Although we detected little/no P-selectin on the surface of VWF-'primed' platelets, this did not formally exclude a role for P-selectin in leukocyte adhesion. Therefore, we first established the efficacy of P-selectin blockade through the marked reduction of leukocyte binding to collagen captured/activated platelets (**Fig S4b-c**). However, blockade of P-selectin on FL-VWF-bound platelets from whole blood or plasma-free blood had no effect upon the number of leukocytes interacting with the platelet surface, suggesting that the recruitment of leukocytes is independent of P-selectin (**Fig 3e**). Leukocytes rolled faster over platelet surfaces after blocking P-selectin in plasma-free blood (**Fig 3f** & **Movie 3**) or whole blood (**Fig S4d**), suggesting that whereas leukocyte capture is highly dependent on activated $\alpha_{IIb}\beta_3$ (and not P-selectin), once recruited, small amounts of P-selectin on the platelet surface may slow leukocyte rolling.

Leukocytes bind directly to activated $\alpha_{IIb}\beta_3$.

To more specifically test the leukocyte interaction with activated $\alpha_{IIb}\beta_3$ (and to exclude other platelet receptors), purified $\alpha_{IIb}\beta_3$ was covalently coupled to microchannels and, thereafter, activated with Mn^{2+} (Litvinov et al., 2005). Isolated PBMCs and PMNs were perfused through $\alpha_{IIb}\beta_3$-coated channels at $50s^{-1}$. Cells from both PBMCs and PMNs (**Fig 4ai-ii** & **4b**) directly attached to the activated $\alpha_{IIb}\beta_3$ surface. This binding was significantly diminished (>70%) by adding either purified fibrinogen or eptifibatide to the PMNs (**Fig 4aiv-v** & **4b**).

We also captured purified $\alpha_{IIb}\beta_3$ to flow channel surfaces using the activating anti-β_3 (LIBS) antibody. Leukocytes were again efficiently captured to this surface in a manner that could be inhibited (~70%) by blocking $\alpha_{IIb}\beta_3$ (**Fig 4b**).

Activated (rather than resting) leukocytes can interact with platelets via Mac-1 ($\alpha_M\beta_2$) (either directly through GPIbα or via fibrinogen bridge with activated $\alpha_{IIb}\beta_3$) or LFA-1 ($\alpha_L\beta_2$) via ICAM-2 (Damle et al.,

1992; Diacovo et al., 1994; Simon et al., 2000; Weber and Springer, 1997). However, blocking β_2 suggested no role for either of these activated integrins in leukocyte binding to VWF-'primed' platelets (**Fig 4c**). In summary, we show leukocytes bind $\alpha_{IIb}\beta_3$ directly dependent upon its RGD-binding groove, but in a manner that is independent of Mac-1 or LFA-1.

T-cells and neutrophils interact with VWF-'primed' platelets via activated $\alpha_{IIb}\beta_3$.

We found no evidence of either $CD14^+$ monocytes or $CD19^+$ B-cells in PBMCs interacting with activated $\alpha_{IIb}\beta_3$. T-cells were the only cell type amongst the PBMCs capable of binding activated $\alpha_{IIb}\beta_3$ or VWF-'primed' platelets (**Fig 4d-e**).

Using isolated PMNs, we found that cells stained with anti-CD16 bound to activated $\alpha_{IIb}\beta_3$-coated channels and also to VWF-'primed' platelets (**Fig 4f** & **4g**). Based on multi-lobulated segmented nuclear morphology (**Fig 4f**), these cells were indicative of $CD16^+$ neutrophils. Neutrophils scanned the platelet- or $\alpha_{IIb}\beta_3$-coated surfaces (**Fig 4g** & **Movie 4**) suggesting that the binding of neutrophils to $\alpha_{IIb}\beta_3$ under flow may itself initiate signaling events within neutrophils. In line with this, PMNs bound to VWF-'primed' platelets (**Fig 5a**) or activated $\alpha_{IIb}\beta_3$ (**Fig 5b**) surfaces exhibited similar intracellular Ca^{2+} release (**Movie 5**) that reached a maximum after 200-300 seconds (**Fig 5c**-**d**).

Binding of neutrophils to $\alpha_{IIb}\beta_3$ under flow induces Nox- and Ca^{2+}-dependent NETosis.

Platelets assist in the targeting of intravascular bacterial pathogens through stimulation of the release of NETs (Brinkmann et al., 2004; Gaertner et al., 2017; Wong et al., 2013; Yeaman, 2014). However, the physiological agonists or mechanisms that drive NETosis are not fully resolved (Nauseef and Kubes, 2016). We therefore examined whether the binding of neutrophils to $\alpha_{IIb}\beta_3$ might induce NETosis. Isolated PMNs were perfused over either activated $\alpha_{IIb}\beta_3$ or anti-CD16 (negative control) at $50s^{-1}$ for 10 minutes and NETosis was subsequently analyzed under static conditions (**Fig 6a** & **Movie 6**). Nuclear decondensation was evident after ~60 minutes, and Sytox Green fluorescence, indicative of cell permeability that precedes NETosis, was detected from ~85 minutes. Nuclear decondensation, increased cell permeability and positive staining with a cell impermeable DNA fluorophore do not specifically identify NETosis. Therefore, anti-citrullinated histone H3 antibody was perfused through the channels after 90 minutes to more specifically identify NETs. The introduction of flow at this point caused the DNA to form extended mesh-like NETs that were stained positively by Hoechst and the anti-citrullinated histone H3 antibody (**Fig 6b**). Very similar results were obtained with PMN bound to either $\alpha_{IIb}\beta_3$ (captured by the activating anti-β_3 antibody), or to platelets 'primed' by A1* or FL-VWF. On activated $\alpha_{IIb}\beta_3$, 69% ±14% of neutrophils through the entire channel formed NETs after 2 hours, compared to minimal NETosis events (8% ±8%) when neutrophils were captured by anti-CD16 (**Fig 6c**). When neutrophils were captured on $\alpha_{IIb}\beta_3$ in the absence of flow, neutrophils attached, but NETosis was significantly reduced by 4-fold, with on 17% of neutrophils exhibiting signs of NETosis (**Fig 6c**). This suggested that the signaling mechanism from the platelet to the neutrophil is mechano-sensitive and does not require other platelet receptors or releasate components.

Neutrophils captured by an anti-CD16 antibody and stimulated with phorbol 12-myristate 13-acetate (PMA) for two hours led to 100% ±0.5% of neutrophils releasing NETs (**Fig 6d**). PMA-induced NETosis was not significantly inhibited in the presence of TMB-8 (an antagonist of intracellular Ca^{2+} release; 90% ±9%), but was effectively inhibited in by DPI (NADPH oxidase inhibitor; 16% ±13%), similar to previous reports (Gupta et al., 2014). NETosis of neutrophils captured by $\alpha_{IIb}\beta_3$ under flow was significantly inhibited by TMB-8 (17% ±9%) and DPI (25% ±10%) (**Fig 6e**). This highlights the dependency of both intracellular Ca^{2+} release and NADPH oxidase signaling pathways in NETosis in response to binding $\alpha_{IIb}\beta_3$ under flow.

'Primed' platelets interact with SLC44A2 receptor on neutrophils.

Our data point to the presence of a specific receptor on the surface of neutrophils (and T-cells) that is not present on B cells or monocytes and that is capable of binding to activated $\alpha_{IIb}\beta_3$ and transducing a signal into the cell. To identify this leukocyte counter-receptor, we analyzed RNA sequencing data from different leukocyte populations, selecting genes that are expressed at higher levels in neutrophils (or in $CD4^+$ T-cells) than in monocytes (Adams et al., 2012; Grassi et al., 2019) (**Fig 7**). We further limited the candidate search by selecting those genes that code for transmembrane proteins. Using this approach, we identified 93 candidate genes. Of these, 33 genes were excluded as they are primarily associated with intracellular membranes. An additional 16 genes were also excluded due to the presence of short extracellular regions/domains (<30 a.a.) that would unlikely be capable of facilitating interactions with an extracellular binding partner. (**Fig 7**) We then analyzed proteomic data to verify the preferential expression of the remaining candidates in neutrophils as opposed to monocytes (Rieckmann et al., 2017). These data suggested that the protein product of 14 of the remaining genes appeared to be detected in higher abundance in monocytes, which we used as a further exclusion criterion (**Fig S5a**). From the remaining 30 candidate genes, the *SLC44A2* gene was selected for validation due to its recent identification as a risk locus for both DVT and stroke (Germain et al., 2015; Hinds et al., 2016), both of which are pathologies associated with described contributions of platelet-leukocyte interactions. SLC44A2 is a cell surface receptor with 10 membrane-spanning domains and five extracellular loops of 178a.a., 38a.a., 72a.a., 38a.a. and 18a.a. in length, respectively (Nair et al., 2016). We sourced antibodies against SLC44A2 that specifically recognize amino acid sequences within the first and second extracellular loops. Published proteomic profiling confirmed the preferential expression of SLC44A2 in neutrophils (**Fig S5a**) (Rieckmann et al., 2017). Western blotting of isolated granulocyte lysates revealed two bands representing SLC44A2 (glycosylated and nascent/non-glycosylated SLC44A2) (**Fig S5b**). Perfusing human neutrophils over immobilized activated $\alpha_{IIb}\beta_3$ in the presence of the first anti-SLC44A2 antibody (anti-SLC44A2 #1) that recognizes the second extracellular loop revealed a dose-dependent blockade of neutrophil binding when compared to no antibody or control rabbit IgG (**Fig 8a-b**). A second anti-SLC44A2 antibody (anti-SLC44A2 #2) that recognizes the first extracellular loop region of SLC44A2 confirmed these findings (**Fig 8a**). The anti-SLC44A2 #2 almost completely blocked neutrophil binding to activated $\alpha_{IIb}\beta_3$ suggesting that this antibody more effectively

blocks the neutrophil binding to the integrin than anti-SLC44A2 #1. This may suggest that the first and longest extracellular loop is involved in interaction with an extracellular ligand

Based on these results, we transfected HEK293T cells with an expression vector for human SLC44A2 fused to EGFP at the intracellular C-terminus. Transfected cells were perfused through activated $\alpha_{IIb}\beta_3$ coated channels and cell binding was quantified. Transfected cells bound to these surfaces in a manner that could be blocked by GR144053 (that blocks $\alpha_{IIb}\beta_3$) or by the anti-SLC44A2 #1 antibody (**Fig 8c**).

The SNP in *SLC44A2* identified by GWAS studies that is protective against VTE and stroke (rs2288904-A) causes a missense mutation (R154Q) in the first 178a.a. extracellular loop of SLC44A2 (Germain et al., 2015). Based on this, we hypothesized that this substitution might exert a functional influence upon the ability of SLC44A2 to interact with $\alpha_{IIb}\beta_3$. Consistent with this hypothesis, HEK293T cells transfected with the SLC44A2 (R154Q)-EGFP expression vector exhibited reduced ability to interact with immobilized $\alpha_{IIb}\beta_3$ (**Fig 8c**).

To further explore the potential interaction between SLC44A2 and activated $\alpha_{IIb}\beta_3$ on platelets, we first captured and 'primed' platelets over VWF-coated surfaces and, thereafter, perfused SLC44A2-EGFP-transfected HEK293T cells. Again, these cells bound to VWF-'primed' platelets in a manner that could be blocked completely with GR144053 (to block $\alpha_{IIb}\beta_3$) or the anti-SLC44A2 #1 antibody (**Fig 8d-e**). Consistent with the previous results, HEK293T cells transfected with SLC44A2(R154Q) exhibited markedly reduced binding to VWF-'primed' platelets (**Fig 8d-e**). A previous report suggested that SLC44A2 might bind directly to VWF (Bayat et al., 2015). However, when SLC44A2-EGFP-transfected HEK293T cells were perfused of VWF surfaces, in the absence of platelets, no binding was detected (**Fig 8d**). Similarly, isolated neutrophils also failed to interact directly with VWF coated surfaces, demonstrating the absolute dependence of platelets in facilitating cell capture under flow.

Neutrophils homozygous for the rs2288904-A SNP exhibit reduced binding to activated $\alpha_{IIb}\beta_3$

The rs2288904-A SNP in *SLC44A2* has a minor allele frequency of 0.22 and is protective against VTE (Germain et al., 2015). It is therefore the common allele, rs2288904-G, that is the risk allele for VTE with an odds ratio of 1.2-1.3. The frequency of individuals homozygous for the protective rs2288904-A allele amongst VTE cases is 30%-50% lower than in healthy controls. Given its prevalence, we genotyped a group of healthy volunteers to identify individuals homozygous for the major allele (rs2288904-G/G), *SLC44A2* (R154/R154), and for the protective allele (rs2288904-A/A), SLC44A2 (Q154/Q154) (**Fig S5c**). *SLC44A2* (R154/R154) neutrophils interacted with VWF-'primed' platelets as before (**Fig 8f** & **Movie 7**). Consistent with the previous blocking experiments, this binding was partially blocked with anti-SLC44A2 #1, and almost completely blocked by anti-SLC44A2 #2 (**Fig 8f** & **Movie 7**). Furthermore, and consistent with the transfection studies, neutrophils homozygous for the protective allele, *SLC44A2* (Q154/Q154), exhibited markedly reduced (~75%) binding to VWF-'primed' platelets (**Fig 8f** & **Movie 7**) demonstrating a functional consequence of the rs2288904-A polymorphism on this neutrophil-platelet interaction.

Discussion

Although the ability of platelet GPIbα binding to VWF to mediate intraplatelet signaling events has been known for many years, the role that it fulfils remains poorly understood (Goto et al., 1995). We demonstrate that under flow GPIbα-A1 binding 'primes', rather than activates, platelets, based on the rapid activation of $\alpha_{IIb}\beta_3$, but the lack of appreciable surface P-selectin exposure (**Fig 2** & **Fig S3**). Some studies have reported that GPIbα-VWF-mediated signaling can induce modest α-granule release. However, the use of static conditions and processing of platelets may explain those observations. Despite this, when compared to other platelet agonists, degranulation and P-selectin exposure induced by VWF binding are both very low (de Witt et al., 2014; Deng et al., 2016).

That platelet binding to VWF under flow 'primes', rather than activates, platelets is consistent with *in vivo* observations. At sites of vessel damage, VWF is important for platelet accumulation through all layers of the hemostatic plug (Joglekar et al., 2013; Lei et al., 2014; Verhenne et al., 2015). All platelets within a thrombus/hemostatic plug likely form interactions with VWF. Despite this, it is only the platelets in the 'core' of the thrombus that become P-selectin-positive, procoagulant platelets, whereas the more loosely bound platelets that form the surrounding 'shell' remain essentially P-selectin-negative (Welsh et al., 2014). If VWF-binding alone were sufficient to fully activate platelets, the differential platelet characteristics of the 'core' and 'shell' would not be observed.

Although it is frequently implied that VWF is only important for platelet capture under high shear conditions, murine models of venous thrombosis with no collagen exposure have repeatedly revealed an important role for VWF-mediated platelet accumulation (Bergmeier et al., 2008; Brill et al., 2011; Chauhan et al., 2007). Platelet binding to VWF occurs most efficiently at arterial shear rates, but still occurs under lower linear venous shear (Miyata and Ruggeri, 1999; Yago et al., 2008; Zheng et al., 2015). However, linear channels do not mimic the distorted and branched paths of the vascular system that cause more disturbed flow patterns, particularly around valves. Using channels with changing geometry under lower shear conditions, we and others have noted that VWF captures platelets appreciably more efficiently in areas of disturbed flow (Zheng et al., 2015). Indeed at venous flow rates through bifurcated channels (**Fig S6a**), we detected platelet capture on FL-VWF with concomitant 'priming' and leukocyte binding (**Fig S6b**). This was appreciably augmented at bifurcation points where disturbed flow exists. Consistent with our earlier findings, leukocyte binding was almost completely inhibited when $\alpha_{IIb}\beta_3$ was blocked (**Fig S6c**). This implies that VWF can function in platelet recruitment within the venous system, particularly in areas of turbulence (e.g. branch sites, valves), which are frequently the nidus for thrombus formation in DVT.

In venous thrombosis, the thrombus generally forms over the intact endothelium, in the absence of vessel damage. This poses the question of how VWF might contribute to DVT if subendothelial collagen is not exposed. It is likely that this reflects the function of newly-secreted ultra-large VWF released from endothelial cells. Under low disturbed flow, released ultra-large VWF may tangle to form strings/cables over the surface of the endothelium. Tangled VWF strings/cables are appreciably more resistant to ADAMTS13 proteolysis than VWF that is simply unraveled. In the murine stenosis model of DVT, complete VWF-deficiency prevents platelet binding over the endothelium (Bergmeier et al., 2008; Brill et

al., 2011; Chauhan et al., 2007). Similarly, blocking GPIbα binding to VWF also completely blocks platelet accumulation and thrombus formation in the stenosis model of DVT. Thus, when platelets bind to VWF under flow in such settings, platelets may become 'primed' facilitating both aggregation and neutrophil binding through activated $\alpha_{IIb}\beta_3$, but without activating them into procoagulant platelets.

Our study reveals, that T-cells and neutrophils can bind directly to activated $\alpha_{IIb}\beta_3$ on platelets and that is coupled to microchannel surfaces (**Fig 3a-d** & **Fig 4a-b**). In both cases, the interaction was inhibited by eptifibatide and GR144053 suggesting that both cell types may share the same receptor, in a manner that is dependent upon the RGD binding groove of activated $\alpha_{IIb}\beta_3$.

Previous studies have identified roles for β_2 integrins, Mac-1 ($\alpha_M\beta_2$) and LFA-1 ($\alpha_L\beta_2$), on leukocytes in mediating interactions with platelets. It should be recognized that the interactions of these molecules are dependent upon the integrins first being activated (and therefore also the cell), which is not the case in our system and is in contrast to previous studies implicating Mac-1 and LFA-1. However, we provide evidence that Mac-1 ($\alpha_M\beta_2$) and LFA-1 ($\alpha_L\beta_2$) are not involved by: 1) Leukocytes do not bind to 'unprimed' platelets captured by anti-PECAM-1. As Mac-1 and LFA-1 bind to GPIbα and ICAM-2, respectively, both of which are constitutively presented on the platelet surface (Kuijper et al., 1998; Simon et al., 2000), if Mac-1 and LFA-1 were the receptors involved binding would have been observed in these experiments (**Fig 3a-b**). 2) Mac-1 on leukocytes can bind indirectly to activated $\alpha_{IIb}\beta_3$ via a fibrinogen bridge (Weber and Springer, 1997). However, we demonstrate that fibrinogen competes for leukocyte binding to bind to activated $\alpha_{IIb}\beta_3$ (**Fig 3b-c** & **Fig 4b**). If fibrinogen were required, removal of fibrinogen from our perfusion system would have diminished the number of leukocyte interactions with primed platelets/$\alpha_{IIb}\beta_3$ if Mac-1 were involved. 3) Antibody-mediated blocking of β_2 integrins did not reduce VWF-'primed' platelet-leukocyte interactions (**Fig 4c**). 4) Only neutrophils and T cells interact with the 'primed' platelets, whereas Mac-1 and LFA-1 are also highly expressed in monocytes which do not bind (**Fig 4d-f**).

We also excluded a role for P-selectin-PSGL-1 for the platelet-leukocyte interaction that we observe as; 1) we detected little/no P-selectin on VWF-'primed' platelets (**Fig S3**), suggestive of minimal degranulation occurring; this also provides indirect evidence for the lack of CD40L on the platelet surface. 2) P-selectin blockade had no effect upon the number of leukocytes binding (**Fig 3e**), and 3) only T-cells and neutrophils bind VWF-'primed' platelets (**Fig 4**) - given that all leukocytes express PSGL-1,(Laszik et al., 1996) and CD40, if the capture of leukocytes were entirely P-selectin or CD40L-mediated, such cell-type selectivity would not be observed. We did however measure an influence of P-selectin upon the rolling speed of leukocytes over VWF-primed platelets (**Fig 3f** & **Fig S4d**). This suggests that although low levels of P-selectin present on the platelet surface is insufficient to facilitate leukocyte capture, it may synergize to slow rolling of leukocytes that are first captured by $\alpha_{IIb}\beta_3$.

There are several studies that provide support for P-selectin-independent interactions of neutrophils and T-cells with platelets. Guidotti *et al* demonstrated the interaction of T-cells with small intrasinusoidal platelet aggregates in the liver during hepatotropic viral infections was independent of both P-selectin and CD40L in platelets (Guidotti et al., 2015). Using a murine model of peritonitis, Petri *et al* demonstrated that neutrophil recruitment and extravasation was highly dependent upon VWF, GPIbα,

and platelets, but largely independent of P-selectin (Petri et al., 2010). Two further studies also corroborate the contention that VWF/GPIbα-bound platelets are capable of promoting neutrophil recruitment/extravasation in murine models of ischemia/reperfusion via P-selectin-independent mechanisms (Gandhi et al., 2012; Khan et al., 2012). These studies support the idea that both VWF and platelets can function beyond hemostasis to fulfil a role in leukocyte recruitment at sites of inflammation.

As T-cells and neutrophils (and not B-cells or monocytes) can bind platelets via activated $\alpha_{IIb}\beta_3$, this suggests that a specific receptor exists on these cells that is absent on B-cells or monocytes. Using transcriptomic and proteomic data, we identified 30 transmembrane candidates that were preferentially expressed in neutrophils (or T-cells) over monocytes. From this list, *SLC44A2* stood out due to its recent identification as a risk locus for both VTE and stroke, but with as yet unknown functional association with these pathologies (Apipongrat et al., 2019; Germain et al., 2015; Hinds et al., 2016). As platelet-leukocyte interactions are involved in both of these thrombotic disorders, we hypothesized that SLC44A2 functions as the neutrophil counter receptor for activated $\alpha_{IIb}\beta_3$. The cellular function of SLC44A2 is not well-defined. It contains ten transmembrane domains with five extracellular loops. The intracellular N-terminal tail contains several putative phosphorylation sites of unknown functional significance. As well as neutrophils, SLC44A2 expression has also been reported in endothelial cells and platelets. However, proteomic data suggest that levels in neutrophils are >300 fold greater in neutrophils that platelets (Rieckmann et al., 2017).

We provide several lines of evidence to support the direct interaction between SLC44A2 and activated $\alpha_{IIb}\beta_3$. 1) two different anti-SLC44A2 antibodies that recognize extracellular loops of the receptor blocked the binding of neutrophils to both VWF-'primed' platelets and to activated $\alpha_{IIb}\beta_3$. 2) recombinant expression of SLC44A2 in HEK293T cells imparted the ability of these cells to bind both VWF-primed platelets and activated $\alpha_{IIb}\beta_3$ under flow in a manner that can be blocked by either GR144053 or by anti-SLC44A2 antibodies. 3) introduction of the rs2288904-A SNP in *SLC44A2* that is protective against VTE resulted in markedly reduced binding of transfected HEK293T cells to both VWF-'primed' platelets and activated $\alpha_{IIb}\beta_3$. 4) neutrophils homozygous for the rs2288904-A/A SNP exhibit significantly reduced binding to VWF-'primed' platelets.

Although NET production is an established mechanism through which neutrophils control pathogens (Brinkmann et al., 2004), many questions remain as to how NETosis is regulated (Nauseef and Kubes, 2016). Binding of platelets to Kupffer cells in the liver of mice following infection with *B. cereus* or *S. aureus* is mediated by VWF (Wong et al., 2013). This binding augments the recruitment of neutrophils, NET production and the control of infection (Kolaczkowska et al., 2015). Mice lacking VWF or GPIbα do not form these aggregates and so have diminished neutrophil recruitment and, therefore, decreased survival (Wong et al., 2013). How NETosis is initiated following platelet binding remains uncertain. Alone, lipopolysaccharide (LPS) is not a potent activator of NETosis (Clark et al., 2007). However, LPS-stimulated platelets, which bind of fibrinogen (i.e. $\alpha_{IIb}\beta_3$ is activated) and also robustly activate NETosis independent of P-selectin (Clark et al., 2007; Looney et al., 2009; Lopes Pires et al., 2017; McDonald et al., 2012).

We detected rapid release of intracellular Ca^{2+} (within minutes) in bound neutrophils (**Fig 5** & **Movie 5**) that preceded the release of NETs after 80-90 minutes (**Fig 6**). This process was dependent upon neutrophils being captured under flow, suggesting that signal transduction through binding of $\alpha_{IIb}\beta_3$ to SLC44A2 may be mechanosensitve, which is consistent with the recent report suggesting a major influence of shear upon NETosis in the presence of platelets (Yu et al., 2018). As NETosis can be induced following binding to purified $\alpha_{IIb}\beta_3$ under flow alone, this suggests that this process does not require a component of the platelet releasate (e.g. mobility group box 1, platelet factor 4, RANTES and thromboxane A2) which have been reported to be capable of driving NETosis (Carestia et al., 2016).

We propose a model in which platelets have a tunable response that can distinguish their roles in hemostasis and immune cell activation (**Fig 9**). The 'priming' of platelets by binding to VWF under flow (in the absence of other platelet agonists) may assist in the targeting of leukocytes to resolve pathogens or mediate vascular inflammatory response. The activated $\alpha_{IIb}\beta_3$ integrin can then mediate neutrophil recruitment through binding to SLC44A2 (**Fig 9**). We do not exclude a supporting role for P-selectin in maintaining T-cell/neutrophil recruitment, but this is not essential for initiating recruitment. Under flow SLC44A2 transduces a mechanical stimulus capable of promoting NETosis via a pathway involving synergy between NADPH oxidase and Ca^{2+} signaling (**Fig 9**). Homeostatically, this may be beneficial for immune responses. However, during chronic infection or vascular inflammation NET production may promote intravascular thrombosis.

This study identifies activated $\alpha_{IIb}\beta_3$ as a receptor and agonist for neutrophils through SLC44A2. This provides a previously uncharacterized mechanism of how platelet-neutrophil cross-talk is manifest in innate immunity; it also provides an explanation for how VWF and platelet-dependent neutrophil recruitment and NETosis may occur in thrombotic disorders such as DVT (Laridan et al., 2019), but also thrombotic microangiopathies like thrombotic thrombocytopenic purpura (Fuchs et al., 2012b). Identification of SLC44A2 as the counter-receptor for activated $\alpha_{IIb}\beta_3$ in conjunction with the prior identification of a protective SNP in SLC44A2 that impairs the binding of neutrophils to platelets highlights SLC44A2 as a potential therapeutic target. Recent data reveal that SLC44A2-deficient mice exhibit normal hemostatic responses (Tilburg et al., 2018), but are protected against development of venous thrombosis (Maracle et al., 2019), provide further encouragement for this strategy.

Materials and Methods

Preparation of VWF A1 domain and multimeric VWF

The coding sequence for the human VWF A1 domain (Glu1264 to Leu1469) was cloned into the pMT-puro vector, containing a C-terminal V5 and polyhistidine tag. The Y1271C/C1272R mutations were introduced by site-directed mutagenesis into A1 domain (A1*) (Blenner et al., 2014). All vectors were verified by sequencing.

Stably expressing S2 insect cells were selected using puromycin (Life Technologies). Cells were cultured under sterile conditions at 28°C in Schneider's Drosophila medium (Lonza), supplemented with 10% heat-inactivated fetal bovine serum (FBS), 50μg/ml penicillin and 50U/ml streptomycin. Cells were grown in suspension in 2L conical flasks to a density of $2x10^6$ cells/ml. Expression of VWF A1 or A1* was induced by addition of 500μM $CuSO_4$ for 5-7 days, at 28°C and 110 rpm.

Conditioned media were harvested, cleared by centrifugation, concentrated by tangential flow filtration and dialyzed against 20mM Tris (pH 7.8) 500mM NaCl. VWF A1 or A1* were purified by a two-step purification method using a Ni^{2+}-HiTrap column followed by a heparin-Sepharose column (GE Healthcare) and elution with 20mM Tris, 600mM NaCl. VWF A1 and A1* were dialyzed in phosphate-buffered saline (PBS). A1 and A1* concentrations were determined by absorbance at 280nm. Proteins were analyzed by SDS-PAGE under reducing and non-reducing, and by Western Blotting using anti-His or anti-VWF antibodies. Full length, multimeric VWF was isolated from Haemate P by gel filtration and quantified by a specific VWF ELISA, as previously described (O'Donnell et al., 2005).

Blood collection and processing

Fresh blood was collected in 40μM PPACK (for whole blood experiments), 3.13% citrate (for leukocyte isolation) or 85mM sodium citrate, 65mM citric acid, 111mM D(+) glucose, pH 4.5 (1x ACD, for plasma-free blood preparation). For reconstituted plasma-free blood, red blood cells (RBCs) and leukocytes were pelleted and washed twice. Separately, platelets were washed twice in 1x HEPES-Tyrode (HT) buffer containing 0.35% BSA, 75mU apyrase and 100nM prostaglandin E1 (Sigma). RBCs, leukocytes and platelets were resuspended in 1x HT buffer supplemented with 0.35% BSA. In some experiments, 1.3mg/ml purified fibrinogen (Haem Tech) was added. For Ca^{2+} assays, PRP was incubated with 5μM Fluo-4 AM (Thermo Fisher Scientific) for 30 minutes at 37°C prior to washing, and plasma-free blood was recalcified with 1mM $CaCl_2$ (final concentration) immediately prior to flow experiments.

Polymorphonuclear cells (PMNs) and peripheral blood mononuclear cells (PBMCs) separated using Histopaque1077 and Histopaque1119 were resuspended in 1x HT, supplemented with 1.5mM $CaCl_2$. For Ca^{2+} assays, PMNs were preloaded with 1μM Fluo-4 AM for 30 minutes at 37°C, before washing. This study was approved by the Imperial College Research Ethics Committee, and informed consent was obtained from all healthy volunteers.

Flow experiments

VenaFluoro8+ microchips (Cellix) were coated directly with 2μM VWF in PBS overnight at 4°C in a humidified chamber. Coated channels were blocked for 1 hour with 1x HEPES-Tyrode (HT) buffer containing 1% bovine serum albumin (BSA). For the isolated VWF A1 and A1* domains, NTA PEGylated

microchips (Cellix) were used to capture the A1 or A1* via their His tags (Tischer et al., 2014). Channels were stripped with EDTA before application of Co^{2+} and washing with 20mM HEPES, 150mM NaCl, pH 7.4 (HBS). To each channel, 20μl of 3.75μM VWF A1 or A1* were applied at room temperature for 20 minutes in a humidified chamber. Channels were then incubated with H_2O_2 for 30 min to oxidize Co^{2+} to Co^{3+}, which stabilizes the binding of His-tagged A1/A1* (Wegner et al., 2016).

To NHS-microchannels (Cellix), 2.6μM purified $\alpha_{IIb}\beta_3$ (ERL), 0.25mg/ml PECAM-1 (BioLegend), anti-β_3/LIBS2 antibody (Millipore), anti-CD16 (eBiosciences) or 0.25mg/ml BSA were covalently attached by amine-coupling according to manufacturer's instructions. For directly-coated $\alpha_{IIb}\beta_3$ channels, the surface was washed with HBS containing 1mM $MnCl_2$, 0.1mM $CaCl_2$ following coating. Mn^{2+} was maintained in all subsequent buffers to cause $\alpha_{IIb}\beta_3$ to favor its open, ligand binding conformation, as previously reported (Litvinov et al., 2005).

To anti-β_3/LIBS2 antibody coated channels, $\alpha_{IIb}\beta_3$ (ERL) was perfused over the surface to facilitate both capture and activation of $\alpha_{IIb}\beta_3$ on the surface.

Whole blood or plasma-free blood was perfused through channels coated with either FL-VWF, A1, A1* or anti-PECAM-1 at shear rates of 500-1500s^{-1} for 3.5 minutes, followed by 50s^{-1} for 15 minutes using a Mirus Evo Nanopump and Venaflux64 software (Cellix). In separate experiments, 2.4μM eptifibatide (Sigma), 2μM GR144053 (Tocris), or 50μg/ml anti-P-selectin blocking antibody (clone AK4; BD Biosciences) were supplemented to whole blood or plasma-free blood. $DiOC_6$ (2.5μM; Invitrogen) was used to label platelets and leukocytes. Cells were monitored in real-time using an inverted fluorescent microscope (Zeiss) or a SP5 confocal microscope (Leica). Leukocytes and platelets were distinguished by their larger size. For presentation and counting purposes, leukocytes were pseudo-colored to distinguish them. In some experiments, antibodies that recognize the second extracellular loop of SLC44A2, rabbit anti-SLC44A2 #1 (Abcam; Ab177877) or the first extracellular loop, rabbit anti-SLC44A2 #2 (LS Bio; LS-C750149) (0-20μg ml^{-1}) to block SLC44A2 were compared to non-immune rabbit IgG (Abcam; 20μg ml^{-1}) to explore the influence of SLC44A2 on neutrophils to bind to either VWF-'primed' platelets or isolated/activated $\alpha_{IIb}\beta_3$.

Isolated PMNs and PBMCs were perfused through channels coated either directly or indirectly with $\alpha_{IIb}\beta_3$, or BSA at 50s^{-1} for 15 minutes. Antibodies specific to the different types of leukocytes were added to isolated leukocytes, i.e. anti-CD16 (eBiosciences) conjugated to allophycocyanin (APC) to identify neutrophils, anti-CD14-APC for monocytes, anti-CD3-APC for T-cells and anti-CD19-APC for B-cells (BioLegend).

To visualize NETosis, neutrophils were labelled with 8μM Hoechst dye (cell permeable) and 1μM Sytox Green (cell impermeable) and monitored for 2 hours. As indicated, isolated PMNs were preincubated with 20μM TMB-8 (Ca^{2+} antagonist and protein kinase C inhibitor; Sigma), for 15 minutes, or 30μM DPI (NADPH oxidase inhibitor; Sigma) for 30 minutes at 37°C prior to NETosis assays. In some experiments, neutrophils were captured on microchannels coated with anti-CD16 and stimulated with 160nM PMA prior to analysis of NETosis in the presence and absence of inhibitors.

To confirm the presence of NETs, neutrophils that were captured by activated $\alpha_{IIb}\beta_3$ and fixed with 4% paraformaldehyde after 2 hours. Fixed neutrophils were permeabilized with 0.1% Triton X-100 in PBS for

10 minutes, blocked with 3% BSA in PBS and, thereafter, incubated with rabbit polyclonal anti-citrullinated H3 (Abcam, 10μg/ml) overnight at 4°C (Martinod et al., 2013). Neutrophils were incubated with a goat anti-rabbit secondary antibody conjugated with Alexa647 (Abcam, 1:500) and with the Hoechst dye (8μM) for 2 hours, washed and then visualised by confocal microscopy.

Quantitation of platelet rolling, aggregation and intracellular Ca^{2+} release was achieved using SlideBook 5.0 software (3i). The number of leukocytes rolling/attaching per minute at $50s^{-1}$ was derived by counting the number of cells in one field of view over a period of 13 minutes. NETosis was quantified by determining the proportion of all neutrophils in the microchannel that had undergone NETosis after 2 hours.

Transcriptomic profiling of human leukocytes

RNA sequencing data from different leukocytes were obtained from the BLUEPRINT consortium [https://www.biorxiv.org/content/10.1101/764613v1]. For this, neutrophils and monocytes were isolated from peripheral blood. PBMCs were separated by gradient centrifugation (Percoll 1.078 g/ml) whilst neutrophils were isolated by CD16 positive selection (Miltenyi) from the pellet, after red blood cell lysis. PBMCs were further separated to obtain a monocyte rich layer using a second gradient (Percoll 1.066 g/ml) and monocytes further purified by CD14 positive selection (Miltenyi) after CD16 depletion. For neutrophils and monocytes, gene expression was tested also on Illumina HT12v4 arrays (accession E-MTAB-1573 at arrayexpress). The purification of naive B lymphocytes, naive CD4 lymphocytes, naive CD8 lymphocytes used in this study has been extensively described. Regulatory CD4 lymphocytes (T regs) were isolated by flow activated cytometry using the following surface markers combinations: CD3+ CD4+ CD25+ CD127low. Cell type purity was assessed by flow cytometry and morphological analysis. RNA was extracted using TRIzol according to manufacturer's instructions, quantified using a Qubit RNA HS kit (Thermofisher) and quality controlled using a Bioanalyzer RNA pico kit (Agilent). For all cell types libraries were prepared using a TruSeq Stranded Total RNA Kit with Ribo-Zero Gold (Illumina) using 200ng of RNA. Trim Galore (v0.3.7) (http://www.bioinformatics.babraham.ac.uk/projects/trim_galore/) with parameters "-q 15 -s 3 --length 30 -e 0.05" was used to trim PCR and sequencing adapters. Trimmed reads were aligned to the Ensembl v75 human transcriptome with Bowtie 1.0.1 using the parameters "-a --best --strata -S -m 100 -X 500 --chunkmbs 256 --nofw --fr". MMSEQ (v1.0.10) was used with default parameters to quantify and normalize gene expression. Differential gene expression analyses were performed: mature neutrophils (n=7) vs monocytes (n=5) and CD4-positive/αβ T cells (n=8) vs monocytes (n=5). Regulatory T cells (T_{reg}, n=1) and native B cells (n=1), are included in the heatmap, for comparison but were not used in differential gene expression analysis due to the low number of biological replicates. We selected genes that were expressed significantly higher in neutrophils than in monocytes, and also those that were significantly higher in CD4-positive/αβ T cells than in monocytes. Their intersection identified 750 genes (598 of which protein coding). From these 598 genes, we selected the 93 genes that contained the Uniprot annotation of "INTRAMEMBRANE DOMAIN" or "TRANSMEM DOMAIN". The effective log2(FPKM+1) data were presented in the heatmap. Further selection involved discarding those transmembrane proteins that are not present on the

extracellular membrane, or primarily associated with intracellular membranes as determined by Uniprot annotation. Proteins that (where known) had extracellular regions of <30 amino acids, as determined in Uniprot, that might be less likely capable of mediating specific ligand binding were also excluded. Finally, analysis of proteomic data from the ImmProt (http://immprot.org) resource was used to verify higher levels of protein of each selected gene in neutrophils than in monocytes

Expression of SLC44A2 in HEK293T cells

The mammalian expression vector, pCMV6-Entry containing the human *SLC44A2* cDNA C-terminally fused to EGFP was purchased from OriGene. To introduce the rs2288904 SNP encoding a R154Q substitution, site-directed mutagenesis was performed using the primers; 5'-GTG GCT GAG GTG CTT CAA GAT GGT GAC TGC CCT-3', and 5'-AGG GCA GTC ACC ATC TTG AAG CAC CTC AGC CAC-3'. Successful introduction of the SNP was confirmed by sequencing.

HEK293T cells were cultured as adherent layers, in humidified incubators at 37°C, 5% CO_2, in minimum essential media (MEM; Sigma) supplemented with 10% FBS, 1U/ml Penicillin 0.1mg/ml Streptomycin, 1% non-essential amino acids (Sigma) and 2mM L-glutamine.

Cells were seeded in 6-well plates 24 hours prior to transfection and transfected using Lipofectamine 2000 (Invitrogen). Transfection efficiency was visually observed using fluorescent microscopy and quantified using flow cytometry. In all cases transfection efficiency was >75%. Cells were harvested 24 hours post-transfection with Tryplex (Life Tech) to obtain a single cell suspension. Cells were washed with complete medium and cells resuspended in serum-free OptiMEM (Life Tech) until use.

Flow assays using HEK293T cells

Microchannels were coated with FL-VWF or $\alpha_{IIb}\beta_3$ (coupled via the anti-β_3/LIBS2 antibody). Thereafter, unlabeled plasma-free blood was perfused over the FL-VWF coated channels at high shear for 3.5 minutes to capture a layer of 'primed' platelets. Platelet coverage was monitored in bright-field. Channels were subsequently washed with 1xHT buffer to remove the blood and SLC44A2-EGFP transfected HEK293T cells were perfused at low shear ($25s^{-1}$) for 10 minutes. Transfected HEK293T cells were also perfused through FL-VWF coated channels (in the absence of platelets for 30 min at $25s^{-1}$) to examine any direct interaction with VWF. Transfected HEK293T cells were also perfused through $\alpha_{IIb}\beta_3$ (coupled via the anti-β_3/LIBS2 antibody) channels at $25s^{-1}$ for 10 minutes. Binding of EGFP fluorescent HEK293T cells was quantified by counting the number of cells attached after 10 minutes across the whole channel and then expressing this as the mean number of cells/field of view. In separate experiments, the ability of GR144053 to block $\alpha_{IIb}\beta_3$, or antibodies that recognize the first extracellular loop of SLC44A2, rabbit anti-SLC44A2 #1 (Abcam; Ab177877) or rabbit anti-SLC44A2 #2 (LS Bio; LS-C750149) (0-20μg ml^{-1}) to block SLC44A2 were compared to non-immune rabbit IgG (Abcam; 20μg ml^{-1})

Genotyping

To identify individuals homozygous for the *SLC44A2* rs2288904-A SNP or for the wild type allele rs2288904-G, 25μl blood was taken by pin prick from healthy volunteers that provided written informed

consent. Genomic DNA was then extracted using PureLink® Genomic DNA kit (Invitrogen). DNA yield was quantified by NanoDrop. Genomic DNA from each volunteer was used as a template to PCR amplify a 410 base pair fragment of the *SLC44A2* gene spanning the SNP site using primers 5'-ACC TCA CGT ACC TGA ATG-3' and 5'-AGC CAT GCC CAT CCT CAT AG-3'. After amplification, samples were separated by agarose gel electrophoresis and the 410 bands excised, purified using the Gel Extraction kit (Qiagen) and sequenced using the first PCR primer. PMN isolated from genotyped individuals were subsequently used to examine their ability to bind both activated $\alpha_{IIb}\beta_3$ (captured using the LIBS2, anti-β_3 antibody) and VWF-'primed' platelets, as described above.

Statistics

Statistical analysis was performed using Prism 6.0 software (GraphPad). Differences between data/samples was analyzed using unpaired two-tailed Student's t-test or Mann-Whitney, as appropriate and as indicated in figure legends. Data are presented as mean ±standard deviation, or median ± 95% confidence interval. The number of individual experiments performed (n) is given in each legend. Values of $p<0.05$ were considered statistically significant.

Data availability

Data supporting the findings of the study are available from the corresponding author upon reasonable request. The source data underlying Figs 1c, 2b-e, 3, 4b-c, 5c-d, 6c-e, 8a, c, d and f and Supplementary Figs 1, 2, 3c-d, 4b are as a 'Source Data' file.

Acknowledgements

This work was funded through by grants from the British Heart Foundation (FS/15/65/32036 and PG/17/22/32868) awarded to J.T.B.C, K.J.W and I.I.S-C. M.F is supported by the British Heart Foundation (FS/18/53/33863). The authors declare no competing financial interests. The authors would like to thank Ying Jin and My Dang (imperial College London) for technical assistance and blood sampling. The authors would also like to thank Prof Heyu Ni and Dr Miguel Neves (University of Toronto) for helpful discussions into identification of $\alpha_{IIb}\beta_3$ binding partners.

Author contributions

A.C-B designed and performed the experiments, analyzed the data, prepared the figures and wrote the manuscript; I.I.S-C designed and performed the experiments, analyzed the data, and wrote the manuscript L.G and M.F performed leukocyte transcriptional profiling experiments. K.J.W designed experiments, analyzed the data, and wrote the manuscript; J.T.B.C designed experiments, analyzed the data, prepared the figures and wrote the manuscript.

References

Adams, D., L. Altucci, S.E. Antonarakis, J. Ballesteros, S. Beck, A. Bird, C. Bock, B. Boehm, E. Campo, A. Caricasole, F. Dahl, E.T. Dermitzakis, T. Enver, M. Esteller, X. Estivill, A. Ferguson-Smith, J. Fitzgibbon, P. Flicek, C. Giehl, T. Graf, F. Grosveld, R. Guigo, I. Gut, K. Helin, J. Jarvius, R. Kuppers, H. Lehrach, T. Lengauer, A. Lernmark, D. Leslie, M. Loeffler, E. Macintyre, A. Mai, J.H. Martens, S. Minucci, W.H. Ouwehand, P.G. Pelicci, H. Pendeville, B. Porse, V. Rakyan, W. Reik, M. Schrappe, D. Schubeler, M. Seifert, R. Siebert, D. Simmons, N. Soranzo, S. Spicuglia, M. Stratton, H.G. Stunnenberg, A. Tanay, D. Torrents, A. Valencia, E. Vellenga, M. Vingron, J. Walter, and S. Willcocks. 2012. BLUEPRINT to decode the epigenetic signature written in blood. *Nat Biotechnol* 30:224-226.

Apipongrat, D., T. Numbenjapon, W. Prayoonwiwat, P. Arnutti, and O. Nathalang. 2019. Association between SLC44A2 rs2288904 polymorphism and risk of recurrent venous thromboembolism among Thai patients. *Thromb Res* 174:163-165.

Bayat, B., Y. Tjahjono, H. Berghofer, S. Werth, H. Deckmyn, S.F. De Meyer, U.J. Sachs, and S. Santoso. 2015. Choline Transporter-Like Protein-2: New von Willebrand Factor-Binding Partner Involved in Antibody-Mediated Neutrophil Activation and Transfusion-Related Acute Lung Injury. *Arterioscler Thromb Vasc Biol* 35:1616-1622.

Bergmeier, W., A.K. Chauhan, and D.D. Wagner. 2008. Glycoprotein Ibalpha and von Willebrand factor in primary platelet adhesion and thrombus formation: lessons from mutant mice. *Thromb Haemost* 99:264-270.

Blenner, M.A., X. Dong, and T.A. Springer. 2014. Structural basis of regulation of von Willebrand factor binding to glycoprotein Ib. *J Biol Chem* 289:5565-5579.

Brill, A., T.A. Fuchs, A.K. Chauhan, J.J. Yang, S.F. De Meyer, M. Kollnberger, T.W. Wakefield, B. Lammle, S. Massberg, and D.D. Wagner. 2011. von Willebrand factor-mediated platelet adhesion is critical for deep vein thrombosis in mouse models. *Blood* 117:1400-1407.

Brill, A., T.A. Fuchs, A.S. Savchenko, G.M. Thomas, K. Martinod, S.F. De Meyer, A.A. Bhandari, and D.D. Wagner. 2012. Neutrophil extracellular traps promote deep vein thrombosis in mice. *J Thromb Haemost* 10:136-144.

Brinkmann, V., U. Reichard, C. Goosmann, B. Fauler, Y. Uhlemann, D.S. Weiss, Y. Weinrauch, and A. Zychlinsky. 2004. Neutrophil extracellular traps kill bacteria. *Science* 303:1532-1535.

Bryckaert, M., J.P. Rosa, C.V. Denis, and P.J. Lenting. 2015. Of von Willebrand factor and platelets. *Cell Mol Life Sci* 72:307-326.

Carestia, A., T. Kaufman, and M. Schattner. 2016. Platelets: New Bricks in the Building of Neutrophil Extracellular Traps. *Front Immunol* 7:271.

Chan, N.C., J.W. Eikelboom, and J.I. Weitz. 2016. Evolving Treatments for Arterial and Venous Thrombosis: Role of the Direct Oral Anticoagulants. *Circ Res* 118:1409-1424.

Chauhan, A.K., J. Kisucka, C.B. Lamb, W. Bergmeier, and D.D. Wagner. 2007. von Willebrand factor and factor VIII are independently required to form stable occlusive thrombi in injured veins. *Blood* 109:2424-2429.

Clark, S.R., A.C. Ma, S.A. Tavener, B. McDonald, Z. Goodarzi, M.M. Kelly, K.D. Patel, S. Chakrabarti, E. McAvoy, G.D. Sinclair, E.M. Keys, E. Allen-Vercoe, R. Devinney, C.J. Doig, F.H. Green, and P. Kubes. 2007. Platelet TLR4 activates neutrophil extracellular traps to ensnare bacteria in septic blood. *Nat Med* 13:463-469.

Cruz, M.A., H. Yuan, J.R. Lee, R.J. Wise, and R.I. Handin. 1995. Interaction of the von Willebrand factor (vWF) with collagen. Localization of the primary collagen-binding site by analysis of recombinant vWF a domain polypeptides. *J Biol Chem* 270:10822-10827.

Damle, N.K., K. Klussman, and A. Aruffo. 1992. Intercellular adhesion molecule-2, a second counter-receptor for CD11a/CD18 (leukocyte function-associated antigen-1), provides a costimulatory signal for T-cell receptor-initiated activation of human T cells. *Journal of immunology (Baltimore, Md. : 1950)* 148:665-671.

de Witt, S.M., F. Swieringa, R. Cavill, M.M. Lamers, R. van Kruchten, T. Mastenbroek, C. Baaten, S. Coort, N. Pugh, A. Schulz, I. Scharrer, K. Jurk, B. Zieger, K.J. Clemetson, R.W. Farndale, J.W. Heemskerk, and J.M. Cosemans. 2014. Identification of platelet function defects by multi-parameter assessment of thrombus formation. *Nat Commun* 5:4257.

Deng, W., Y. Xu, W. Chen, D.S. Paul, A.K. Syed, M.A. Dragovich, X. Liang, P. Zakas, M.C. Berndt, J. Di Paola, J. Ware, F. Lanza, C.B. Doering, W. Bergmeier, X.F. Zhang, and R. Li. 2016. Platelet clearance via shear-induced unfolding of a membrane mechanoreceptor. *Nat Commun* 7:12863.

Diacovo, T.G., A.R. deFougerolles, D.F. Bainton, and T.A. Springer. 1994. A functional integrin ligand on the surface of platelets: intercellular adhesion molecule-2. *J Clin Invest* 94:1243-1251.

Doddapattar, P., N. Dhanesha, M.R. Chorawala, C. Tinsman, M. Jain, M.K. Nayak, J.M. Staber, and A.K. Chauhan. 2018. Endothelial Cell-Derived Von Willebrand Factor, But Not Platelet-Derived, Promotes Atherosclerosis in Apolipoprotein E-Deficient Mice. *Arterioscler Thromb Vasc Biol*

Du, X., M. Gu, J.W. Weisel, C. Nagaswami, J.S. Bennett, R. Bowditch, and M.H. Ginsberg. 1993. Long range propagation of conformational changes in integrin alpha IIb beta 3. *J Biol Chem* 268:23087-23092.

Durrant, T.N., M.T. van den Bosch, and I. Hers. 2017. Integrin alphaIIbbeta3 outside-in signaling. *Blood*

Fuchs, T.A., A. Brill, and D.D. Wagner. 2012a. Neutrophil extracellular trap (NET) impact on deep vein thrombosis. *Arterioscler Thromb Vasc Biol* 32:1777-1783.

Fuchs, T.A., J.A. Kremer Hovinga, D. Schatzberg, D.D. Wagner, and B. Lammle. 2012b. Circulating DNA and myeloperoxidase indicate disease activity in patients with thrombotic microangiopathies. *Blood* 120:1157-1164.

Gaertner, F., Z. Ahmad, G. Rosenberger, S. Fan, L. Nicolai, B. Busch, G. Yavuz, M. Luckner, H. Ishikawa-Ankerhold, R. Hennel, A. Benechet, M. Lorenz, S. Chandraratne, I. Schubert, S. Helmer, B. Striednig, K. Stark, M. Janko, R.T. Bottcher, A. Verschoor, C. Leon, C. Gachet, T. Gudermann, Y.S.M. Mederos, Z. Pincus, M. Iannacone, R. Haas, G. Wanner, K. Lauber, M. Sixt, and S. Massberg. 2017. Migrating Platelets Are Mechano-scavengers that Collect and Bundle Bacteria. *Cell* 171:1368-1382 e1323.

Gandhi, C., D.G. Motto, M. Jensen, S.R. Lentz, and A.K. Chauhan. 2012. ADAMTS13 deficiency exacerbates VWF-dependent acute myocardial ischemia/reperfusion injury in mice. *Blood* 120:5224-5230.

Gardiner, E.E., J.F. Arthur, Y. Shen, D. Karunakaran, L.A. Moore, J.S. Am Esch, 2nd, R.K. Andrews, and M.C. Berndt. 2010. GPIbalpha-selective activation of platelets induces platelet signaling events comparable to GPVI activation events. *Platelets* 21:244-252.

Germain, M., D.I. Chasman, H. de Haan, W. Tang, S. Lindstrom, L.C. Weng, M. de Andrade, M.C. de Visser, K.L. Wiggins, P. Suchon, N. Saut, D.M. Smadja, G. Le Gal, A. van Hylckama Vlieg, A. Di Narzo, K. Hao, C.P. Nelson, A. Rocanin-Arjo, L. Folkersen, R. Monajemi, L.M. Rose, J.A. Brody, E. Slagboom, D. Aissi, F. Gagnon, J.F. Deleuze, P. Deloukas, C. Tzourio, J.F. Dartigues, C. Berr, K.D. Taylor, M. Civelek, P. Eriksson, C. Cardiogenics, B.M. Psaty, J. Houwing-Duitermaat, A.H. Goodall, F. Cambien, P. Kraft, P. Amouyel, N.J. Samani, S. Basu, P.M. Ridker, F.R. Rosendaal, C. Kabrhel, A.R. Folsom, J. Heit, P.H. Reitsma, D.A. Tregouet, N.L. Smith, and P.E. Morange. 2015. Meta-analysis of 65,734 individuals identifies TSPAN15 and SLC44A2 as two susceptibility loci for venous thromboembolism. *Am J Hum Genet* 96:532-542.

Germain, M., N. Saut, N. Greliche, C. Dina, J.C. Lambert, C. Perret, W. Cohen, T. Oudot-Mellakh, G. Antoni, M.C. Alessi, D. Zelenika, F. Cambien, L. Tiret, M. Bertrand, A.M. Dupuy, L. Letenneur, M. Lathrop, J. Emmerich, P. Amouyel, D.A. Tregouet, and P.E. Morange. 2011. Genetics of venous thrombosis: insights from a new genome wide association study. *PLoS One* 6:e25581.

Goto, S., D.R. Salomon, Y. Ikeda, and Z.M. Ruggeri. 1995. Characterization of the unique mechanism mediating the shear-dependent binding of soluble von Willebrand factor to platelets. *J Biol Chem* 270:23352-23361.

Grassi, L., O.G. Izuogu, N.A.N. Jorge, D. Seyres, M. Bustamante, F. Burden, S. Farrow, N. Farahi, F.J. Martin, A. Frankish, J.M. Mudge, M. Kostadima, R. Petersen, J.J. Lambourne, S. Rowlston, E. Martin-Rendon, L. Clarke, K. Downes, X. Estivill, P. Flicek, J.H.A. Martens, M.-L. Yaspo, H.G. Stunnenberg, W.H. Ouwehand, F. Passetti, E. Turro, and M. Frontini. 2019. Cell type specific novel lincRNAs and circRNAs in the BLUEPRINT haematopoietic transcriptomes atlas. *bioRxiv* 764613.

Guidotti, L.G., D. Inverso, L. Sironi, P. Di Lucia, J. Fioravanti, L. Ganzer, A. Fiocchi, M. Vacca, R. Aiolfi, S. Sammicheli, M. Mainetti, T. Cataudella, A. Raimondi, G. Gonzalez-Aseguinolaza, U. Protzer, Z.M. Ruggeri, F.V. Chisari, M. Isogawa, G. Sitia, and M. Iannacone. 2015. Immunosurveillance of the liver by intravascular effector CD8(+) T cells. *Cell* 161:486-500.

Gupta, A.K., S. Giaglis, P. Hasler, and S. Hahn. 2014. Efficient neutrophil extracellular trap induction requires mobilization of both intracellular and extracellular calcium pools and is modulated by cyclosporine A. *PLoS One* 9:e97088.

Hinds, D.A., A. Buil, D. Ziemek, A. Martinez-Perez, R. Malik, L. Folkersen, M. Germain, A. Malarstig, A. Brown, J.M. Soria, M. Dichgans, N. Bing, A. Franco-Cereceda, J.C. Souto, E.T. Dermitzakis, A. Hamsten, B.B. Worrall, J.Y. Tung, I.C. Metastroke Consortium, and M. Sabater-Lleal. 2016. Genome-wide association analysis of self-reported events in 6135 individuals and 252 827 controls identifies 8 loci associated with thrombosis. *Hum Mol Genet* 25:1867-1874.

Jackson, S.P., W.S. Nesbitt, and S. Kulkarni. 2003. Signaling events underlying thrombus formation. *J Thromb Haemost* 1:1602-1612.

789 Joglekar, M.V., J. Ware, J. Xu, M.E. Fitzgerald, and T.K. Gartner. 2013. Platelets, glycoprotein Ib-IX, and
790 von Willebrand factor are required for FeCl(3)-induced occlusive thrombus formation in the inferior
791 vena cava of mice. *Platelets* 24:205-212.
792 Ju, L., Y. Chen, L. Xue, X. Du, and C. Zhu. 2016. Cooperative unfolding of distinctive mechanoreceptor
793 domains transduces force into signals. *Elife* 5:
794 Kasirer-Friede, A., M.R. Cozzi, M. Mazzucato, L. De Marco, Z.M. Ruggeri, and S.J. Shattil. 2004.
795 Signaling through GP Ib-IX-V activates alpha IIb beta 3 independently of other receptors. *Blood*
796 103:3403-3411.
797 Khan, M.M., D.G. Motto, S.R. Lentz, and A.K. Chauhan. 2012. ADAMTS13 reduces VWF-mediated
798 acute inflammation following focal cerebral ischemia in mice. *J Thromb Haemost* 10:1665-1671.
799 Kolaczkowska, E., C.N. Jenne, B.G. Surewaard, A. Thanabalasuriar, W.Y. Lee, M.J. Sanz, K. Mowen, G.
800 Opdenakker, and P. Kubes. 2015. Molecular mechanisms of NET formation and degradation revealed
801 by intravital imaging in the liver vasculature. *Nat Commun* 6:6673.
802 Kuijper, P.H., H.I. Gallardo Tores, J.W. Lammers, J.J. Sixma, L. Koenderman, and J.J. Zwaginga. 1998.
803 Platelet associated fibrinogen and ICAM-2 induce firm adhesion of neutrophils under flow conditions.
804 *Thrombosis and haemostasis* 80:443-448.
805 Laridan, E., K. Martinod, and S.F. De Meyer. 2019. Neutrophil Extracellular Traps in Arterial and Venous
806 Thrombosis. *Semin Thromb Hemost* 45:86-93.
807 Laszik, Z., P.J. Jansen, R.D. Cummings, T.F. Tedder, R.P. McEver, and K.L. Moore. 1996. P-selectin
808 glycoprotein ligand-1 is broadly expressed in cells of myeloid, lymphoid, and dendritic lineage and in
809 some nonhematopoietic cells. *Blood* 88:3010-3021.
810 Lei, X., A. Reheman, Y. Hou, H. Zhou, Y. Wang, A.H. Marshall, C. Liang, X. Dai, B.X. Li, K.
811 Vanhoorelbeke, and H. Ni. 2014. Anfibatide, a novel GPIb complex antagonist, inhibits platelet
812 adhesion and thrombus formation in vitro and in vivo in murine models of thrombosis. *Thromb*
813 *Haemost* 111:279-289.
814 Lievens, D., A. Zernecke, T. Seijkens, O. Soehnlein, L. Beckers, I.C. Munnix, E. Wijnands, P. Goossens,
815 R. van Kruchten, L. Thevissen, L. Boon, R.A. Flavell, R.J. Noelle, N. Gerdes, E.A. Biessen, M.J.
816 Daemen, J.W. Heemskerk, C. Weber, and E. Lutgens. 2010. Platelet CD40L mediates thrombotic and
817 inflammatory processes in atherosclerosis. *Blood* 116:4317-4327.
818 Litvinov, R.I., J.S. Bennett, J.W. Weisel, and H. Shuman. 2005. Multi-step fibrinogen binding to the
819 integrin (alpha)IIb(beta)3 detected using force spectroscopy. *Biophys J* 89:2824-2834.
820 Looney, M.R., J.X. Nguyen, Y. Hu, J.A. Van Ziffle, C.A. Lowell, and M.A. Matthay. 2009. Platelet
821 depletion and aspirin treatment protect mice in a two-event model of transfusion-related acute lung
822 injury. *J Clin Invest* 119:3450-3461.
823 Lopes Pires, M.E., S.R. Clarke, S. Marcondes, and J.M. Gibbins. 2017. Lipopolysaccharide potentiates
824 platelet responses via toll-like receptor 4-stimulated Akt-Erk-PLA2 signalling. *PLoS One* 12:e0186981.
825 Maracle, C.X., J. Tilburg, G. Zirka, P.E. Morange, B.J.M. van Vlijmen, and G.M. Thomas. 2019. Slc44a2
826 Deficient Mice Exhibit Less Severity of Thrombosis in a Stenosis Model of DVT. In International
827 Society for Thrombosis and Haemostasis.
828 Martinod, K., M. Demers, T.A. Fuchs, S.L. Wong, A. Brill, M. Gallant, J. Hu, Y. Wang, and D.D. Wagner.
829 2013. Neutrophil histone modification by peptidylarginine deiminase 4 is critical for deep vein
830 thrombosis in mice. *Proc Natl Acad Sci U S A* 110:8674-8679.
831 Mayadas, T.N., R.C. Johnson, H. Rayburn, R.O. Hynes, and D.D. Wagner. 1993. Leukocyte rolling and
832 extravasation are severely compromised in P selectin-deficient mice. *Cell* 74:541-554.
833 McDonald, B., R. Urrutia, B.G. Yipp, C.N. Jenne, and P. Kubes. 2012. Intravascular neutrophil
834 extracellular traps capture bacteria from the bloodstream during sepsis. *Cell Host Microbe* 12:324-
835 333.
836 Miyata, S., and Z.M. Ruggeri. 1999. Distinct structural attributes regulating von Willebrand factor A1
837 domain interaction with platelet glycoprotein Ibalpha under flow. *J Biol Chem* 274:6586-6593.
838 Mu, F.T., S.L. Cranmer, R.K. Andrews, and M.C. Berndt. 2010. Functional association of
839 phosphoinositide-3-kinase with platelet glycoprotein Ibalpha, the major ligand-binding subunit of the
840 glycoprotein Ib-IX-V complex. *J Thromb Haemost* 8:324-330.
841 Nair, T.S., P.K. Kommareddi, M.M. Galano, D.M. Miller, B.N. Kakaraparthi, S.A. Telian, H.A. Arts, H. El-
842 Kashlan, A. Kilijanczyk, A.A. Lassig, M.P. Graham, S.G. Fisher, S.W. Stoll, R.P. Nair, J.T. Elder, and
843 T.E. Carey. 2016. SLC44A2 single nucleotide polymorphisms, isoforms, and expression: Association
844 with severity of Meniere's disease? *Genomics* 108:201-208.
845 Nauseef, W.M., and P. Kubes. 2016. Pondering neutrophil extracellular traps with healthy skepticism.
846 *Cellular microbiology* 18:1349-1357.

O'Donnell, J.S., T.A. McKinnon, J.T. Crawley, D.A. Lane, and M.A. Laffan. 2005. Bombay phenotype is associated with reduced plasma-VWF levels and an increased susceptibility to ADAMTS13 proteolysis. *Blood* 106:1988-1991.

Palabrica, T., R. Lobb, B.C. Furie, M. Aronovitz, C. Benjamin, Y.M. Hsu, S.A. Sajer, and B. Furie. 1992. Leukocyte accumulation promoting fibrin deposition is mediated in vivo by P-selectin on adherent platelets. *Nature* 359:848-851.

Petri, B., A. Broermann, H. Li, A.G. Khandoga, A. Zarbock, F. Krombach, T. Goerge, S.W. Schneider, C. Jones, B. Nieswandt, M.K. Wild, and D. Vestweber. 2010. von Willebrand factor promotes leukocyte extravasation. *Blood* 116:4712-4719.

Rieckmann, J.C., R. Geiger, D. Hornburg, T. Wolf, K. Kveler, D. Jarrossay, F. Sallusto, S.S. Shen-Orr, A. Lanzavecchia, M. Mann, and F. Meissner. 2017. Social network architecture of human immune cells unveiled by quantitative proteomics. *Nat Immunol* 18:583-593.

Rosendaal, F.R., and P.H. Reitsma. 2009. Genetics of venous thrombosis. *J Thromb Haemost* 7 Suppl 1:301-304.

Schulman, S., A.K. Kakkar, S.Z. Goldhaber, S. Schellong, H. Eriksson, P. Mismetti, A.V. Christiansen, J. Friedman, F. Le Maulf, N. Peter, C. Kearon, and R.-C.I.T. Investigators. 2014. Treatment of acute venous thromboembolism with dabigatran or warfarin and pooled analysis. *Circulation* 129:764-772.

Schulman, S., C. Kearon, A.K. Kakkar, P. Mismetti, S. Schellong, H. Eriksson, D. Baanstra, J. Schnee, S.Z. Goldhaber, and R.-C.S. Group. 2009. Dabigatran versus warfarin in the treatment of acute venous thromboembolism. *N Engl J Med* 361:2342-2352.

Schulman, S., M. Re, and R.-S.T. Investigators. 2013. Extended anticoagulation in venous thromboembolism. *N Engl J Med* 368:2329.

Schulz, C., B. Engelmann, and S. Massberg. 2013. Crossroads of coagulation and innate immunity: the case of deep vein thrombosis. *J Thromb Haemost* 11 Suppl 1:233-241.

Senis, Y.A., A. Mazharian, and J. Mori. 2014. Src family kinases: at the forefront of platelet activation. *Blood* 124:2013-2024.

Shen, J., S. Sampietro, J. Wu, J. Tang, S. Gupta, C.N. Matzko, C. Tang, Y. Yu, L.F. Brass, L. Zhu, and T.J. Stalker. 2017. Coordination of platelet agonist signaling during the hemostatic response in vivo. *Blood Adv* 1:2767-2775.

Simon, D.I., Z. Chen, H. Xu, C.Q. Li, J. Dong, L.V. McIntire, C.M. Ballantyne, L. Zhang, M.I. Furman, M.C. Berndt, and J.A. Lopez. 2000. Platelet glycoprotein ibalpha is a counterreceptor for the leukocyte integrin Mac-1 (CD11b/CD18). *J Exp Med* 192:193-204.

Sreeramkumar, V., J.M. Adrover, I. Ballesteros, M.I. Cuartero, J. Rossaint, I. Bilbao, M. Nacher, C. Pitaval, I. Radovanovic, Y. Fukui, R.P. McEver, M.D. Filippi, I. Lizasoain, J. Ruiz-Cabello, A. Zarbock, M.A. Moro, and A. Hidalgo. 2014. Neutrophils scan for activated platelets to initiate inflammation. *Science* 346:1234-1238.

Stalker, T.J., E.A. Traxler, J. Wu, K.M. Wannemacher, S.L. Cermignano, R. Voronov, S.L. Diamond, and L.F. Brass. 2013. Hierarchical organization in the hemostatic response and its relationship to the platelet-signaling network. *Blood* 121:1875-1885.

Tilburg, J., R. Adili, T.S. Nair, M.E. Hawley, D.C. Tuk, M. Jackson, H.M. Spronk, H.H. Versteeg, T.E. Carey, B.J.M. van Vlijmen, C.X. Maracle, and M. Holinstat. 2018. Characterization of hemostasis in mice lacking the novel thrombosis susceptibility gene Slc44a2. *Thromb Res* 171:155-159.

Tischer, A., P. Madde, L. Moon-Tasson, and M. Auton. 2014. Misfolding of vWF to pathologically disordered conformations impacts the severity of von Willebrand disease. *Biophys J* 107:1185-1195.

Vandendries, E.R., B.C. Furie, and B. Furie. 2004. Role of P-selectin and PSGL-1 in coagulation and thrombosis. *Thromb Haemost* 92:459-466.

Verhenne, S., F. Denorme, S. Libbrecht, A. Vandenbulcke, I. Pareyn, H. Deckmyn, A. Lambrecht, B. Nieswandt, C. Kleinschnitz, K. Vanhoorelbeke, and S.F. De Meyer. 2015. Platelet-derived VWF is not essential for normal thrombosis and hemostasis but fosters ischemic stroke injury in mice. *Blood* 126:1715-1722.

von Bruhl, M.L., K. Stark, A. Steinhart, S. Chandraratne, I. Konrad, M. Lorenz, A. Khandoga, A. Tirniceriu, R. Coletti, M. Kollnberger, R.A. Byrne, I. Laitinen, A. Walch, A. Brill, S. Pfeiler, D. Manukyan, S. Braun, P. Lange, J. Riegger, J. Ware, A. Eckart, S. Haidari, M. Rudelius, C. Schulz, K. Echtler, V. Brinkmann, M. Schwaiger, K.T. Preissner, D.D. Wagner, N. Mackman, B. Engelmann, and S. Massberg. 2012. Monocytes, neutrophils, and platelets cooperate to initiate and propagate venous thrombosis in mice in vivo. *J Exp Med* 209:819-835.

Weber, C., and T.A. Springer. 1997. Neutrophil accumulation on activated, surface-adherent platelets in flow is mediated by interaction of Mac-1 with fibrinogen bound to alphaIIbbeta3 and stimulated by platelet-activating factor. *J Clin Invest* 100:2085-2093.

Wegner, S.V., F.C. Schenk, and J.P. Spatz. 2016. Cobalt(III)-Mediated Permanent and Stable Immobilization of Histidine-Tagged Proteins on NTA-Functionalized Surfaces. *Chemistry* 22:3156-3162.

Welsh, J.D., T.J. Stalker, R. Voronov, R.W. Muthard, M. Tomaiuolo, S.L. Diamond, and L.F. Brass. 2014. A systems approach to hemostasis: 1. The interdependence of thrombus architecture and agonist movements in the gaps between platelets. *Blood* 124:1808-1815.

Wolberg, A.S., F.R. Rosendaal, J.I. Weitz, I.H. Jaffer, G. Agnelli, T. Baglin, and N. Mackman. 2015. Venous thrombosis. *Nat Rev Dis Primers* 1:15006.

Wong, C.H., C.N. Jenne, B. Petri, N.L. Chrobok, and P. Kubes. 2013. Nucleation of platelets with blood-borne pathogens on Kupffer cells precedes other innate immunity and contributes to bacterial clearance. *Nat Immunol* 14:785-792.

Yago, T., J. Lou, T. Wu, J. Yang, J.J. Miner, L. Coburn, J.A. Lopez, M.A. Cruz, J.F. Dong, L.V. McIntire, R.P. McEver, and C. Zhu. 2008. Platelet glycoprotein Ibalpha forms catch bonds with human WT vWF but not with type 2B von Willebrand disease vWF. *J Clin Invest* 118:3195-3207.

Yeaman, M.R. 2014. Platelets: at the nexus of antimicrobial defence. *Nat Rev Microbiol* 12:426-437.

Yu, X., J. Tan, and S.L. Diamond. 2018. Hemodynamic force triggers rapid NETosis within sterile thrombotic occlusions. *J Thromb Haemost* 16:316-329.

Zhang, W., W. Deng, L. Zhou, Y. Xu, W. Yang, X. Liang, Y. Wang, J.D. Kulman, X.F. Zhang, and R. Li. 2015. Identification of a juxtamembrane mechanosensitive domain in the platelet mechanosensor glycoprotein Ib-IX complex. *Blood* 125:562-569.

Zheng, Y., J. Chen, and J.A. Lopez. 2015. Flow-driven assembly of VWF fibres and webs in in vitro microvessels. *Nat Commun* 6:7858.

Figures & Legends

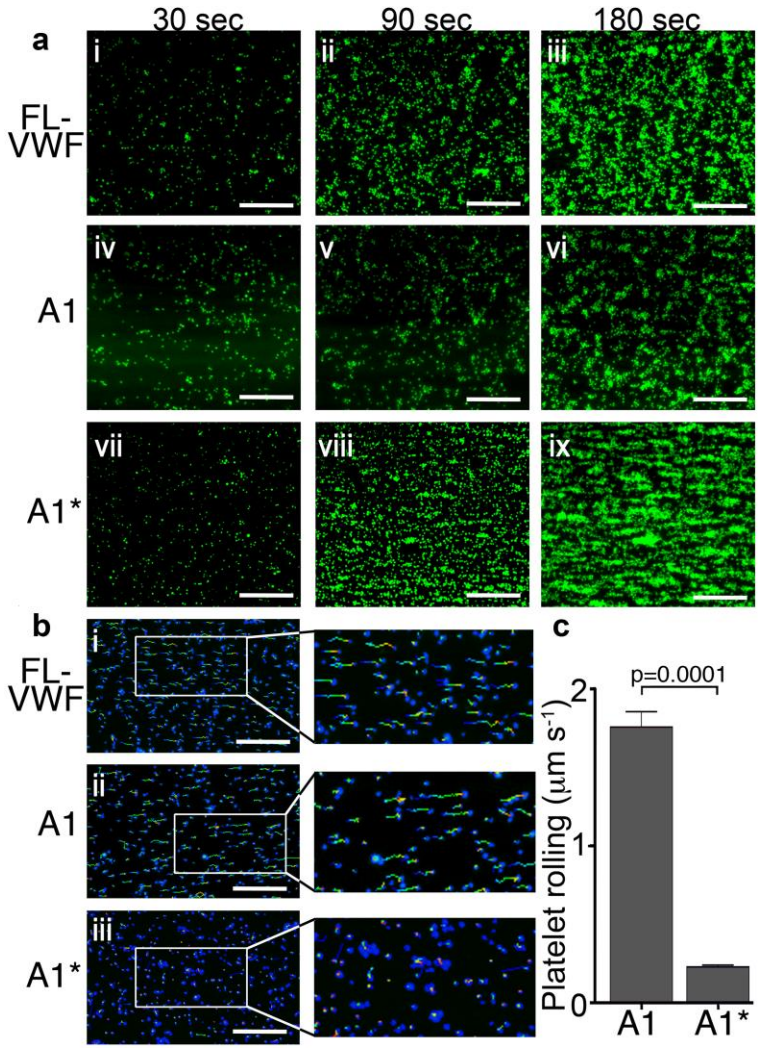

Figure 1: Platelet rolling and attachment to VWF under flow. a) Vena8 microchannels were coated with either full-length VWF (FL-VWF; i-iii), VWF A1 (iv-vi) or A1* (vii-ix). Whole blood labelled with $DiOC_6$ was perfused at $1000s^{-1}$. Representative images (n=3) of platelets (green) after 30, 90 and 180 seconds are shown. Scale; 50μm (see also **Movie 1**). **b)** Experiments performed as in a), bound platelets (blue) were tracked (depicted by multi-coloured lines) representing distance travelled in the first 30 sec of flow. Scale bar; 50μm. **c)** Platelet rolling velocity on channels coated with A1 and A1*. Data plotted are median ±95% CI. n=3562 platelets from 3 different experiments (A1) and n=4047 platelets from 3 different experiments (A1*). Data were analyzed using the Mann-Whitney test.

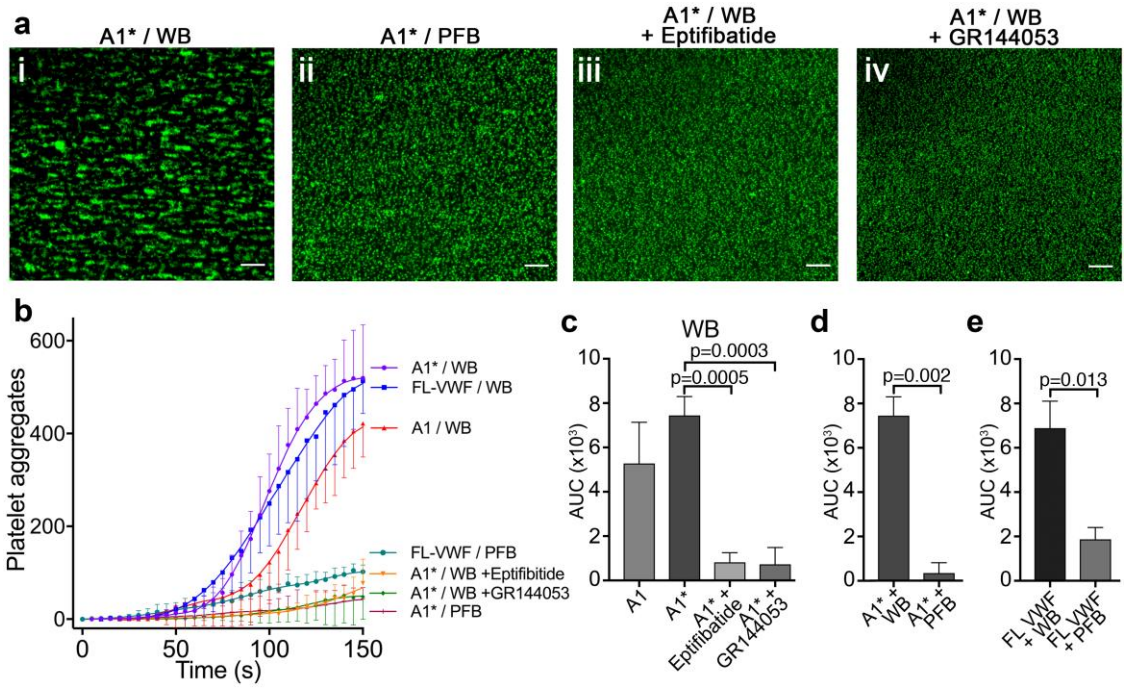

Figure 2: Platelet binding to VWF under flow induces $\alpha_{IIb}\beta_3$-dependent aggregation. a) Vena8 microchannels were coated with A1* via its 6xHis tag. i) Whole blood (WB) or ii) plasma-free blood (PFB), iii) WB containing eptifibatide or iv) WB containing GR144053 were perfused through channels at 1000s^{-1}. Representative images acquired after 3 minutes. Scale bar; 50μm. **b)** Graph measuring platelet aggregation over time in WB perfused through channels coated with A1 (red, n=3), A1* (purple, n=4) and FL-VWF (blue, n=3), WB pre-incubated with eptifibatide (orange, n=3) or GR144053 (green, n=4) over channels coated with A1* and PFB over channels coated with A1* (magenta, n=3) or FL-VWF (teal, n=3). Data plotted are mean ±SD. **c-e)** Bar charts comparing area under the curve (AUC) of the data presented in b). **c)** WB perfused over A1 or A1* with or without eptifibatide or GR144053. **d)** WB or PFB perfused over A1*. **e)** WB or PFB perfused over FL VWF. Data presented are mean ±SD, n=3 or 4 as indicated in b). Data were analyzed using the Mann-Whitney test.

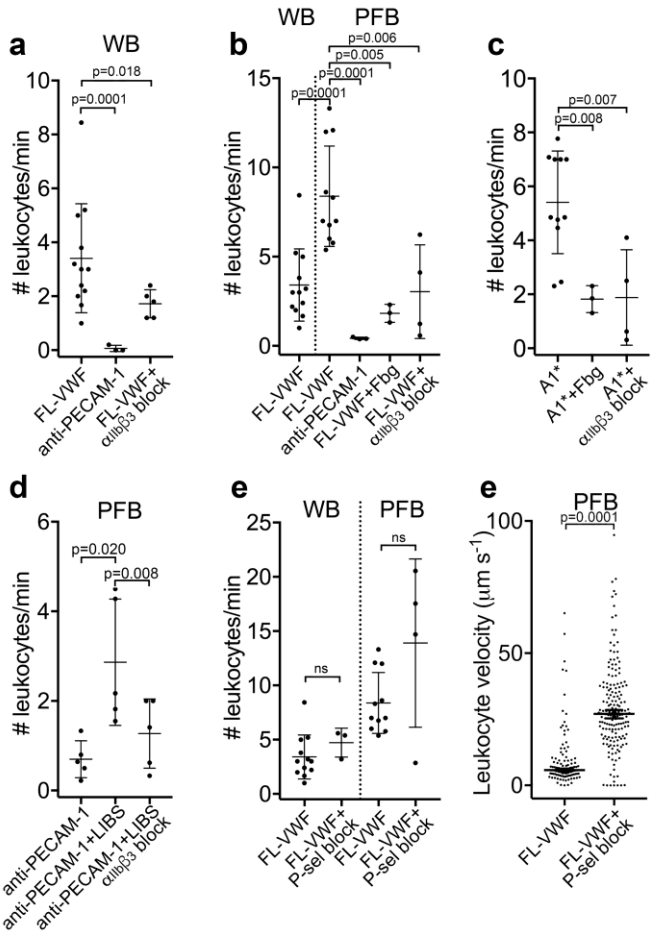

Figure 3: Leukocytes bind to VWF-bound platelets under flow (see also **Movie 3**). **a)** Graph of the number of leukocytes/minute in WB interacting with platelets bound to FL-VWF in the absence (n=12) or presence of eptifibatide/GR144053 (n=5), or binding to platelets bound to anti-PECAM-1 antibody (n=3). **b)** Graph of the number of leukocytes/minute in WB or PFB interacting with platelets bound to FL-VWF in the absence (n=12) or presence of 1.3mg/ml fibrinogen (n=3) or eptifibatide/GR144053 (n=4), or binding to platelets bound to anti-PECAM-1 antibody (n=3). **c)** Graph of the number of leukocytes/minute in PFB interacting with platelets bound to A1* in the absence (n=11) or presence of fibrinogen (n=3) or eptifibatide/GR144053 (n=4). **d)** Graph of the number of leukocytes/minute in PFB interacting with platelets bound to anti-PECAM-1 antibody in the absence (n=5) or presence of LIBS/anti-β_3 activating antibody (n=5) ± GR144053 (n=5). **e)** Graph of the number of leukocytes/minute in WB or PFB, as shown, interacting with platelets bound to FL-VWF in the absence or presence of a blocking anti-P-selectin antibody. **f)** Graph of leukocyte rolling velocity on platelets bound to FL-VWF in PFB in the absence or presence of a blocking anti-P-selectin antibody. Data shown are individual leukocyte rolling velocities (n=121 and 178, respectively) for 3 separate experiments. In all graphs, data plotted are mean ±SD. Data were analyzed using unpaired, two-tailed Student's t test; ns not significant.

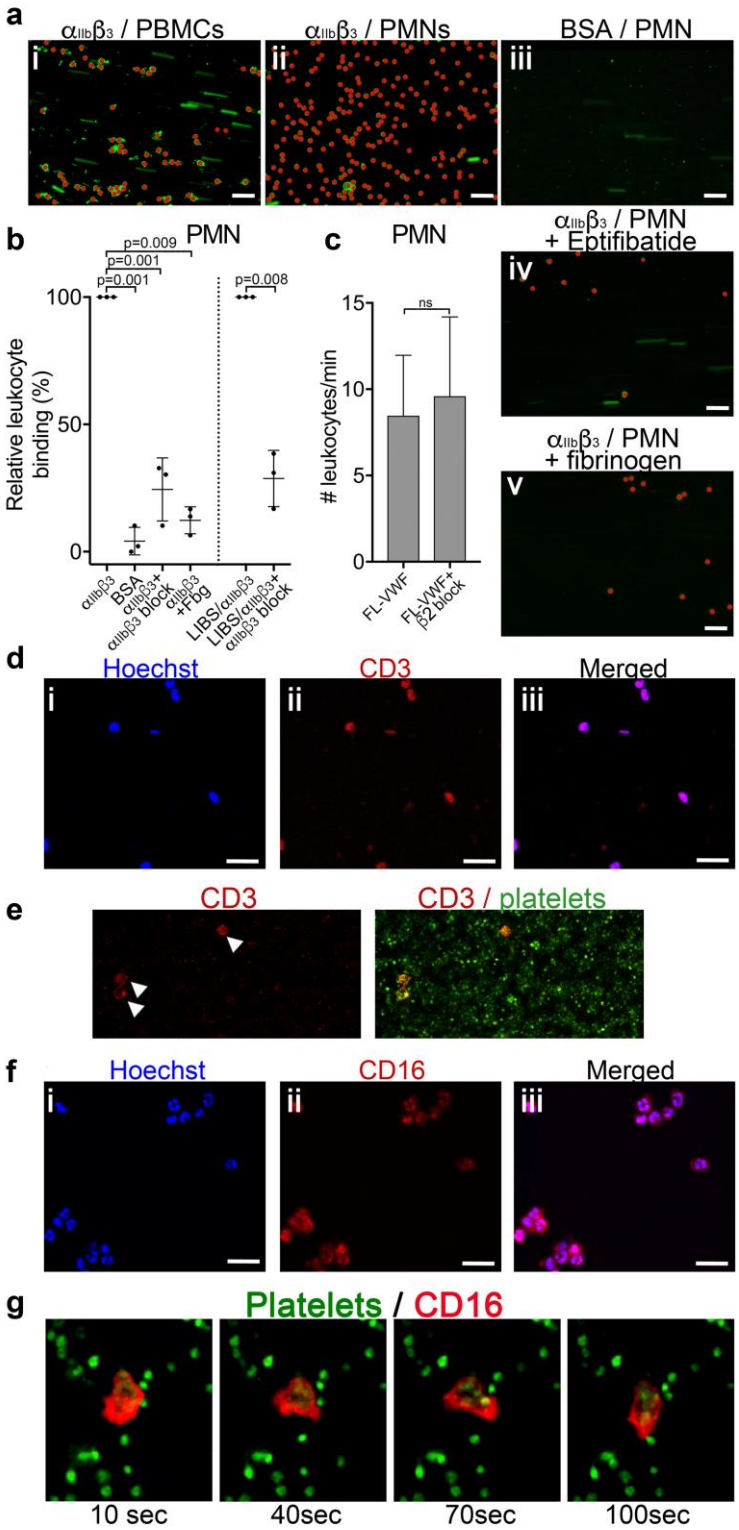

Figure 4: Leukocytes bind to activated $\alpha_{IIb}\beta_3$ under flow. a) Purified $\alpha_{IIb}\beta_3$ or BSA, as noted, were covalently coupled to microchannel surfaces by amine coupling. $\alpha_{IIb}\beta_3$ was activated using Mn^{2+} and Ca^{2+} in all buffers. PBMCs (i) or PMNs (ii-v) labelled with $DiOC_6$ were perfused through channels at $50s^{-1}$ in the presence and absence of eptifibatide (iv) or 1.3mg/ml purified fibrinogen (v). Bound leukocytes (as opposed to flowing) are pseudo-colored red to aid visualization and to distinguish from leukocytes in transit. Scale bar; 50μm. **b)** Graphical representation of relative leukocyte binding to activated $\alpha_{IIb}\beta_3$ in the presence and absence of eptifibatide or 1.3mg/ml purified fibrinogen, or to BSA after 15 minutes of PMN perfusion (n=3), or to $\alpha_{IIb}\beta_3$ captured and activated by LIBS/anti-β_3 activating antibody in the absence and presence of GR144053 (n=3). Data plotted are mean ±SD. Data were analyzed using unpaired, two-tailed Student's t test. **c)** Graph of the number of leukocytes/minute in PFB interacting with platelets bound to FL-VWF in the absence (n=12) or presence of a blocking anti-β2 integrin polyclonal antibody (n=5) capable of blocking both LFA-1 or Mac-1 on leukocytes. **d)** PBMCs stained with Hoechst dye (i - blue), anti-CD3 (ii - red) and merged (iii). Representative of n=4. Scale bar; 20μm. **e)** PFB stained with DiOC6 was perfused over FL-VWF at $1000s^{-1}$ followed by $50s^{-1}$. T-cells labelled with anti-CD3 (red - arrows) were seen to attach to 'primed' platelets **f)** PMNs stained with Hoechst dye (i - blue), anti-CD16 (ii - red) and merged (iii). Representative of n=4. Scale bar; 20μm (see also **Movie 4**). **g)** Images depicting a neutrophil stained with anti-CD16 (red) 'scanning' the 'primed' platelets stained with $DiOC_6$ (green). Images shown were taken 10, 40, 70 and 100 seconds after neutrophil attachment note the movement of the neutrophil shown - see also **Movie 4**.

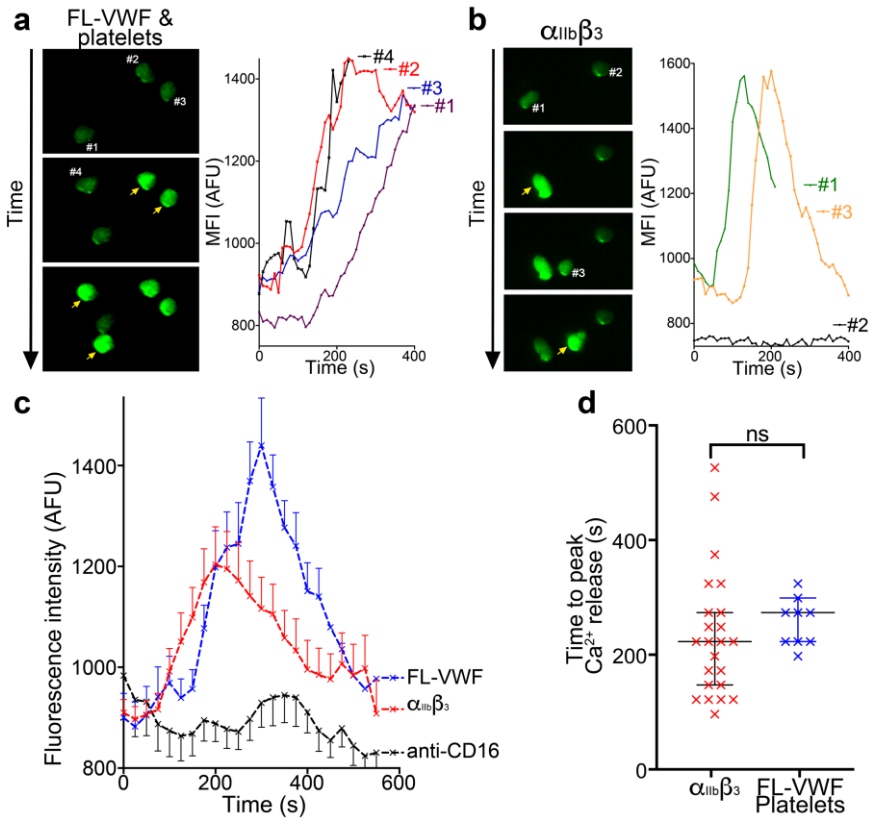

Figure 5: Binding to $\alpha_{IIb}\beta_3$ induces intracellular Ca^{2+} release in neutrophils. a) Representative images of neutrophils pre-loaded with Fluo-4 AM bound to VWF-'primed' platelets captured (**Movie 5**). Neutrophils are numbered #1-#4. The yellow arrow highlights a frame in which the fluorescence has increased in the attached neutrophil. For each neutrophil shown, intracellular Ca^{2+} release is quantified by measurement of cellular mean fluorescent intensity (MFI) over time. **b)** As in A) except neutrophils were perfused over activated $\alpha_{IIb}\beta_3$. MFI increased for neutrophils #1 and #3, but not for neutrophil #2. **c)** Graph depicting the change in MFI as a function of time after neutrophil attachment to microchannels coated with activated $\alpha_{IIb}\beta_3$ (n=24 neutrophils from 3 different experiments), VWF-'primed' platelets (n=9 neutrophils from 1 experiment) or anti-CD16 (n=13 neutrophils from 2 different experiments). Data plotted are mean ±SEM. **d)** Dot plot presenting the time between neutrophil attachment and maximum MFI of neutrophils binding to purified $\alpha_{IIb}\beta_3$ (red), or VWF-'primed' platelets (blue). Data plotted are median ±95% confidence interval. Data were analyzed using the Mann-Whitney test.

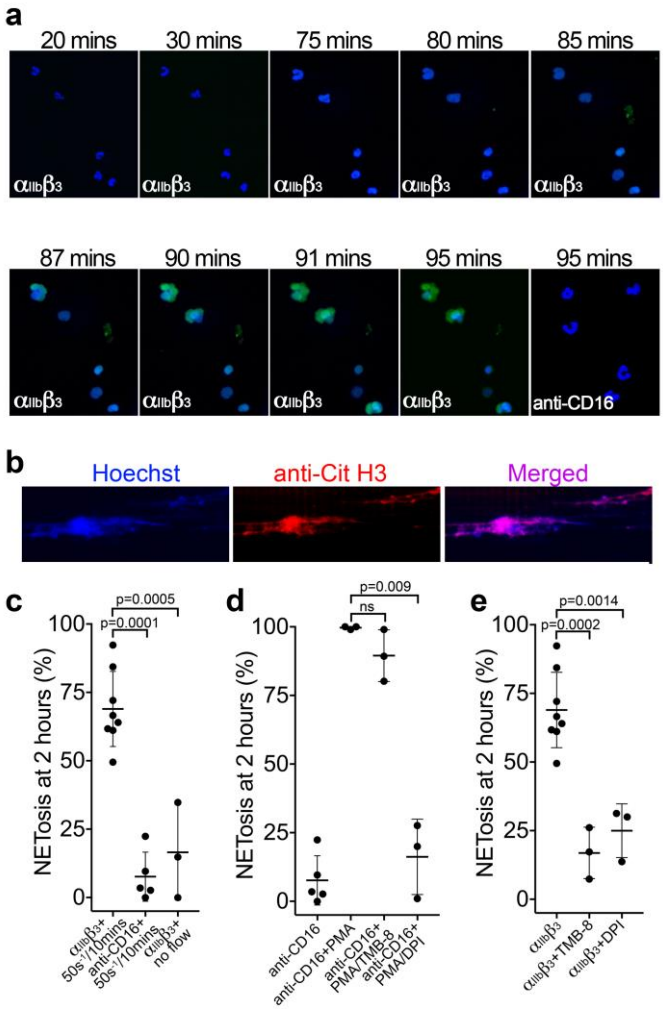

Figure 6: Binding of neutrophils to $\alpha_{IIb}\beta_3$ under flow induces NETosis. a) Isolated PMNs labelled with Hoechst (blue) and cell-impermeable Sytox Green were perfused over $\alpha_{IIb}\beta_3$-coated microchannels, or anti-CD16, (-ve ctrl) at $50s^{-1}$ for 10 minutes and then monitored under static conditions. Representative composite images after 20, 30, 75, 80, 85, 87, 90, 91 and 95 minutes of attachment. Neutrophils bound to $\alpha_{IIb}\beta_3$ exhibited nuclear decondensation and increased cell permeability that precedes NETosis after about 85 minutes, Sytox Green staining appears, indicative of DNA becoming extracellular (see **Movie 6**). Neutrophils bound to surfaces using an anti-CD16 antibody did not exhibit signs of NETosis or did so very rarely. **b)** Immunostaining of neutrophils bound to $\alpha_{IIb}\beta_3$ after 90 mins as in a). Hoechst (blue), citrullinated H3 (red) and merged images are shown. **c)** Graph showing the mean % of neutrophils ±SD in the entire microchannel that formed NETs after 2 hours of attachment on $\alpha_{IIb}\beta_3$ (n=8) or anti-CD16 (n=5), captured in the presence of flow ($50s^{-1}$/10 minutes), or captured on $\alpha_{IIb}\beta_3$ under static/no flow conditions (n=3). **d)** Graph showing the mean % of neutrophils ±SD in the entire microchannel that formed NETs after 2 hours of attachment on anti-CD16 antibody in the presence of flow ($50s^{-1}$/10 minutes) (n=5) in the presence of PMA (n=3), PMA and TMB-8 (n=3) or PMA and DPI (n=3). **e)** Graph showing the mean % of neutrophils ±SD in the entire microchannel that formed NETs after 2 hours of attachment on $\alpha_{IIb}\beta_3$ in the presence of flow ($50s^{-1}$/10 minutes) (n=8) and in the presence of TMB-8 (n=3) or DPI (n=3), as noted. Data were analyzed using unpaired, two-tailed Student's t test; ns not significant.

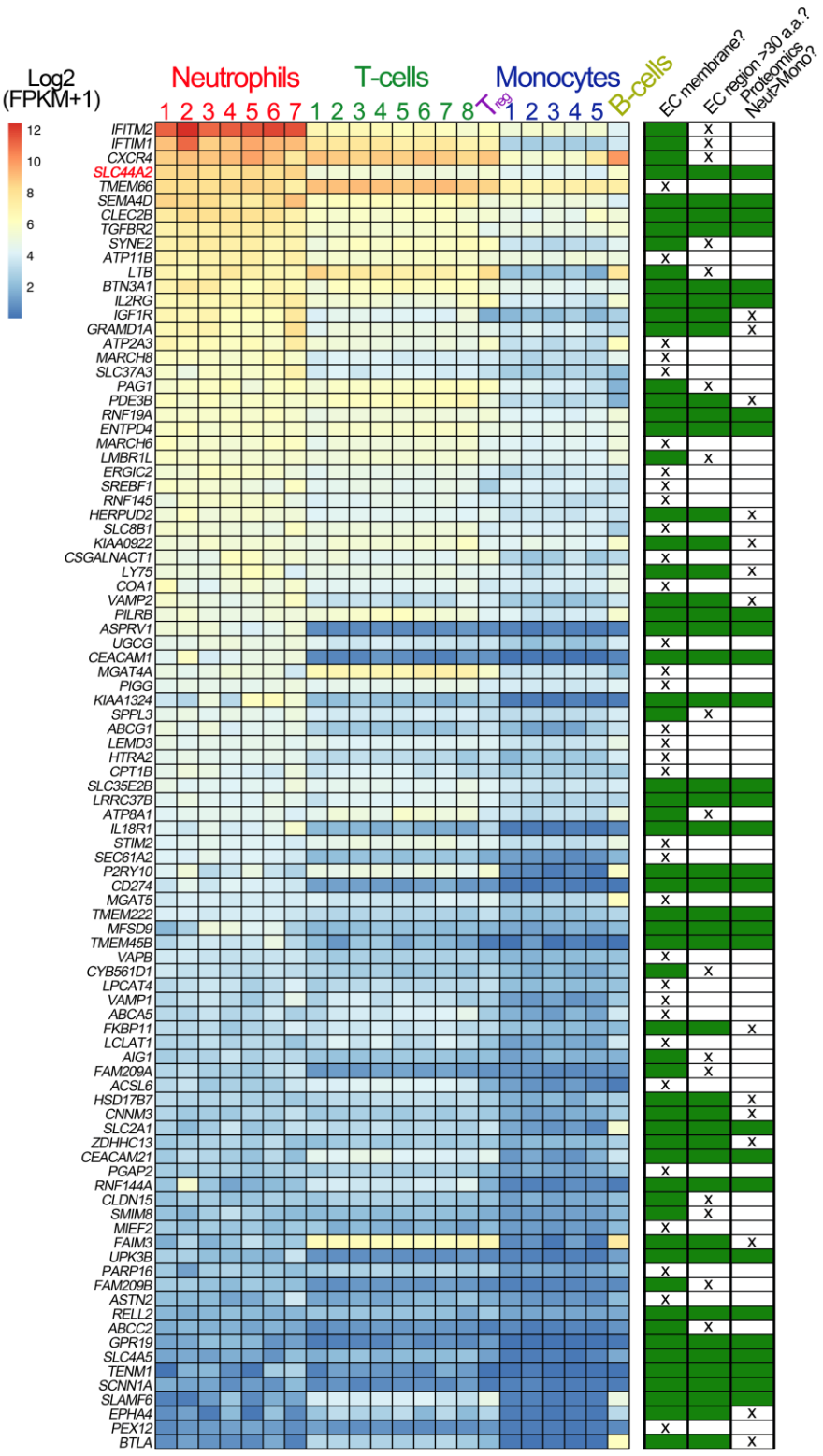

Figure 7: Transcriptomic profiling of human leukocytes. RNA sequencing data from different leukocytes were obtained from the BLUEPRINT consortium [https://www.biorxiv.org/content/10.1101/764613v1]. Differential gene expression analyses were performed: mature neutrophils (n=7) vs monocytes (n=5) and CD4-positive/$\alpha\beta$ T cells (n=8) vs monocytes (n=5). Regulatory T cells (T_{reg}, n=1) and native B cells (n=1), are included in the heatmap, for comparison but were not used in differential gene expression analysis due to the low number of biological replicates. We first selected genes that were expressed significantly higher in neutrophils than in monocytes, and also those that were significantly higher in CD4-positive/$\alpha\beta$ T cells than in monocytes. Their intersection identified 750 genes (598 of which protein coding). From these 598 genes, we selected the 93 genes that contained the Uniprot annotation of “INTRAMEMBRANE DOMAIN” or "TRANSMEM DOMAIN”. The effective log2(FPKM+1) data are presented in the heatmap of the 93 genes, with the rows ordered according to the mean neutrophil expression levels. Next to the heatmap is a table highlighting the subsequent selection criteria used to further narrow the search for candidate receptors for $\alpha_{IIb}\beta_3$. The first round of selection involved discarding those transmembrane proteins that are not present on the extracellular membrane, or primarily associated with intracellular membranes. The second selection criterion was to discard those proteins that had extracellular regions of <30 amino acids that might be less likely capable of mediating specific ligand binding. Finally, analysis of proteomic data from the ImmProt (http://immprot.org) resource was used to verify higher levels of protein of each selected gene in neutrophils than in monocytes

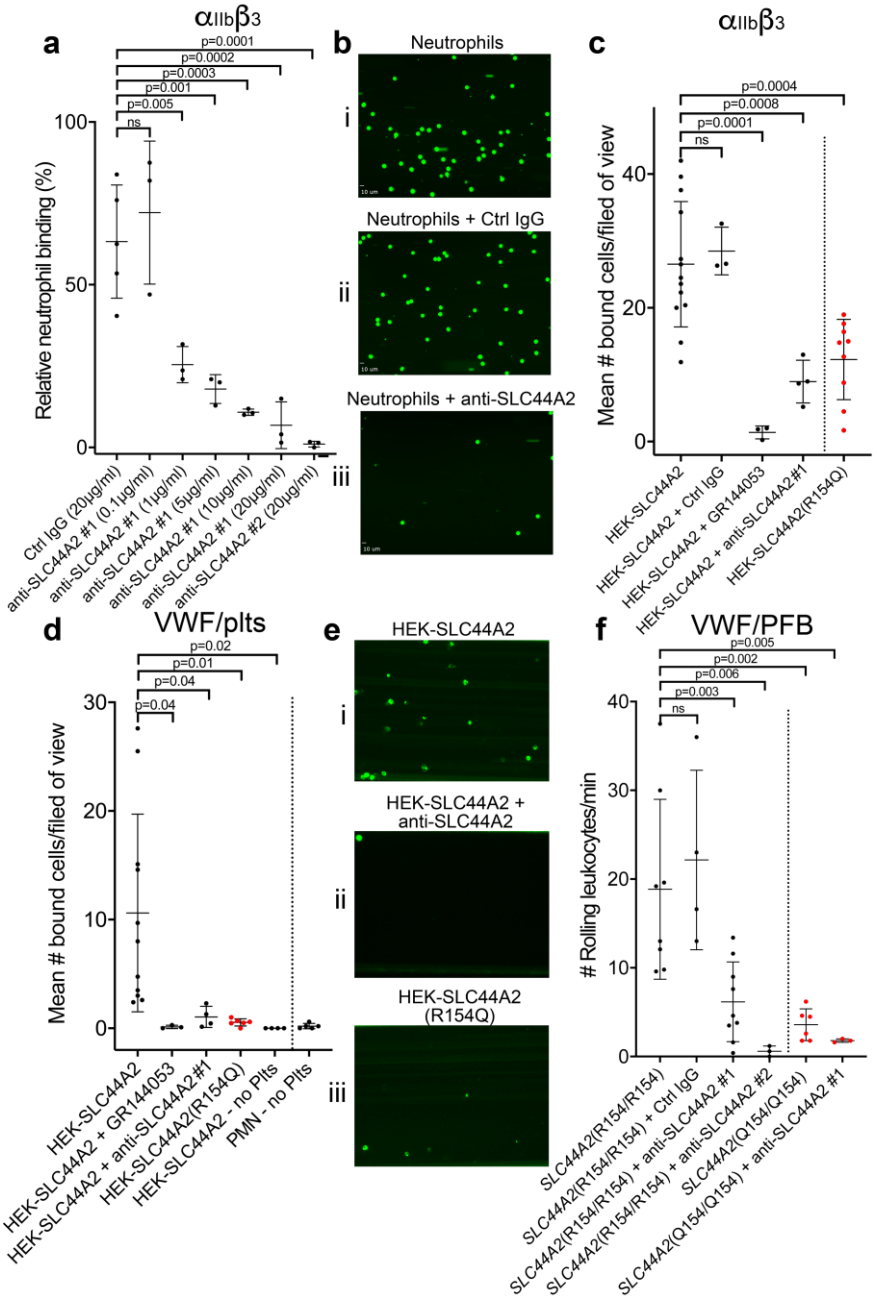

Figure 8: SLC44A2 binds activated $\alpha_{IIb}\beta_3$. a) Graphical representation of relative neutrophil binding after 15 minutes of leukocyte perfusion at $50s^{-1}$ to activated $\alpha_{IIb}\beta_3$ captured and activated by LIBS2/anti-β_3 activating antibody in the presence and absence of increasing concentrations of anti-SLC44A2#1 or #2 antibodies. Data plotted are mean ±SD. Data were analyzed using One-Way ANOVA with multiple comparisons. **b)** Representative micrographs of neutrophils bound to activated $\alpha_{IIb}\beta_3$ i) in the absence of antibody, ii) in the presence of control IgG and iii) in the presence of anti-SLC44A2#1. **c)** Graphical representation of the number of HEK293T cells transfected with either SLC44A2-EGFP or SLC44A2(R154Q)-EGFP (shown in red) expression vectors binding to activated $\alpha_{IIb}\beta_3$ (captured and activated by LIBS2/anti-β_3 activating antibody) after 10 mins flow at $25s^{-1}$. Experiments were performed in the presence and absence of either GR144053 or anti-SLC44A2#1 antibody. Data presented are the mean number of bound cells per field of view. Data were analyzed using One-Way ANOVA with multiple comparisons. **d)** Graphical representation of the number of HEK293T cells transfected with either SLC44A2-EGFP or SLC44A2(R154Q)-EGFP (shown in red) expression vectors interacting with VWF-'primed' platelets. Plasma-free blood was first perfused at $1000s^{-1}$ for 3.5 mins to capture and 'prime' the platelets, and transfected HEK293T cells were subsequently perfused at $25s^{-1}$ for 10 mins, in the presence and absence of GR144053 or anti-SLC44A2#1 antibody. HEK293T cells transfected with SLC44A2-EGFP or isolated neutrophils were also perfused over VWF in the absence of platelets, for 30 mins at $25s^{-1}$ or $50s^{-1}$ respectively. Data presented are the mean number of bound cells per field of view. Data were analyzed using One-Way ANOVA with multiple comparisons. **e)** Representative micrographs of HEK293T cells transfected with i) SLC44A2-EGFP in the absence of antibody, ii) SLC44A20EGFP in the presence of anti-SLC44A2#1 antibody and iii) SLC44A2(R154Q)-EGFP bound to activated VWF-'primed' platelets. **f)** Graphical representation of the number of neutrophils rolling per minute on VWF-'primed' platelets. PFB from individuals homozygous for the R154-encoding allele of *SLC44A2* (R154/R154) or the Q154-encoding allele of *SLC44A2* (Q154/Q154) (shown in red) were perfused over 'primed' platelets for 10 mins at $50s^{-1}$ (see **Movie 7**). Experiments were performed in the presence and absence of anti-SLC44A2#1 or anti-SLC44A2#2 antibodies. Data plotted are mean ±SD. Data were analyzed using One-Way ANOVA with multiple comparisons.

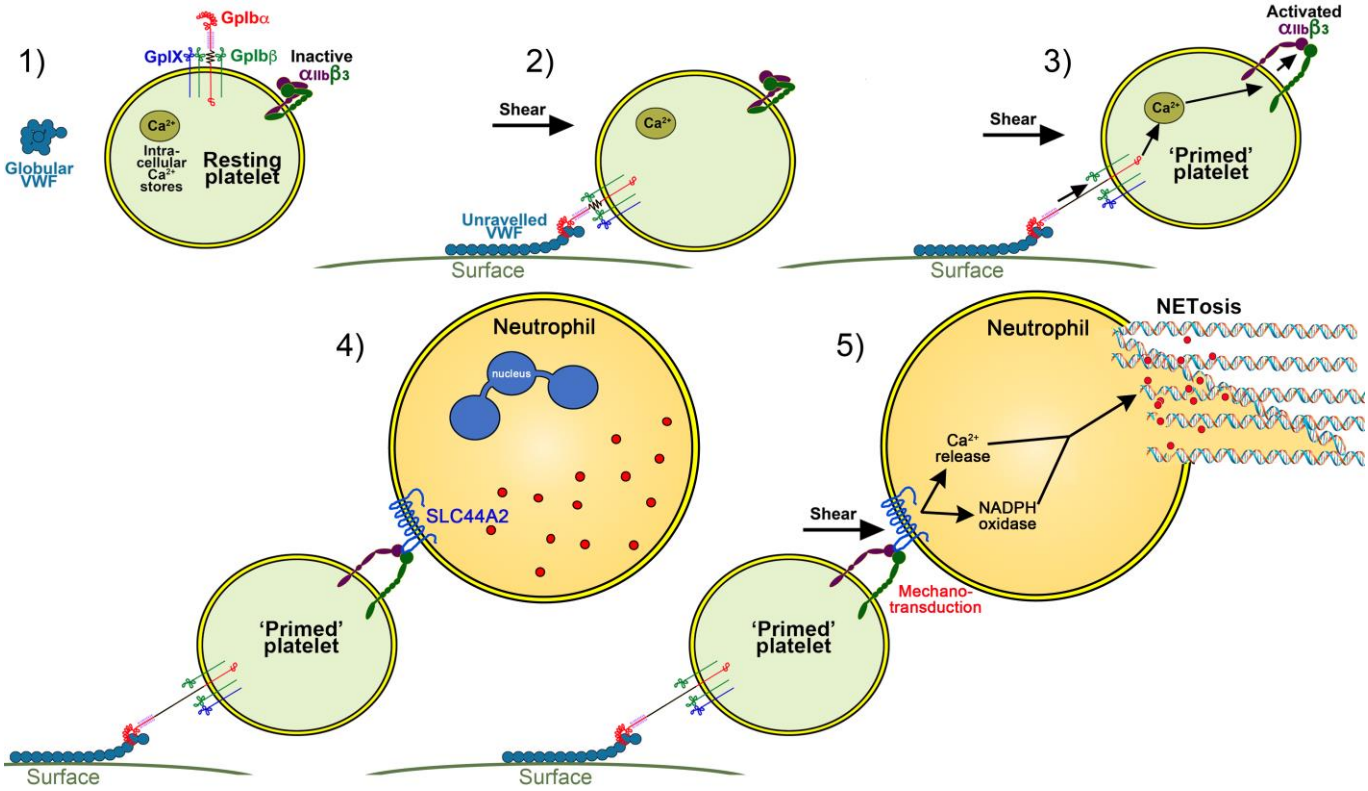

Figure 9: Model of platelet priming, neutrophil binding and NETosis. 1) Under normal conditions, VWF circulates in plasma in a globular conformation that does not interact with platelets. Resting platelets present GPIbα on their surface - in complex with GPIbβ, GPIX and GPV - and also $\alpha_{IIb}\beta_3$ in its inactive conformation. **2)** When VWF is attached to a cell surface (e.g. activated endothelial cell/Kuppfer cell or to a bacterial cell) or to an exposed collagen surface under flow, VWF unravels to expose its A1 domain enabling capture of platelets via GPIbα. **3)** Binding of platelets to VWF under flow induces mechano-unfolding of the juxtamembrane stalk of GPIbα leading to intraplatelet signaling, release of intraplatelet Ca^{2+} stores and activation of integrin $\alpha_{IIb}\beta_3$. **4)** Neutrophils can bind to activated $\alpha_{IIb}\beta_3$ under flow via SLC44A2. **5)** Shear forces on the neutrophil induce mechanosensitive signaling into the neutrophil causing intracellular Ca^{2+} release and NADPH oxidase-dependent NETosis.

Supplementary Data for

"*Activated $\alpha_{IIb}\beta_3$ on platelets mediates flow-dependent NETosis via SLC44A2*"

Adela Constantinescu-Bercu, Luigi Grassi, Mattia Frontini, Isabelle I. Salles-Crawley*, Kevin J Woollard* & James T.B. Crawley*

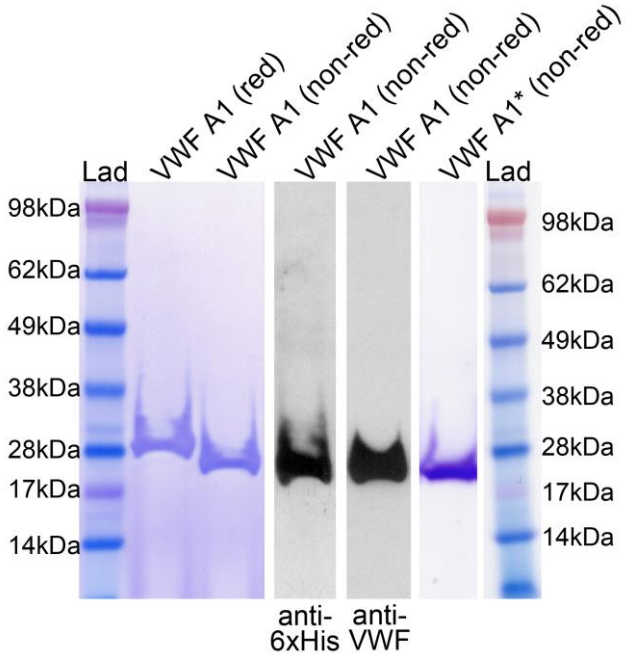

Figure S1: Analysis of purified recombinant VWF A1 and VWF A1*. VWF A1 domain with a C-terminal V5 and 6xHis tag was expressed in S2 insect cells and purified to homogeneity. Purified A1 was analyzed by SDS-PAGE and Coomassie staining under reducing and non-reducing conditions, and also by Western blotting of VWF A1 using anti-6xHis and anti-VWF antibodies. A Coomassie stain of purified VWF A1* is also shown.

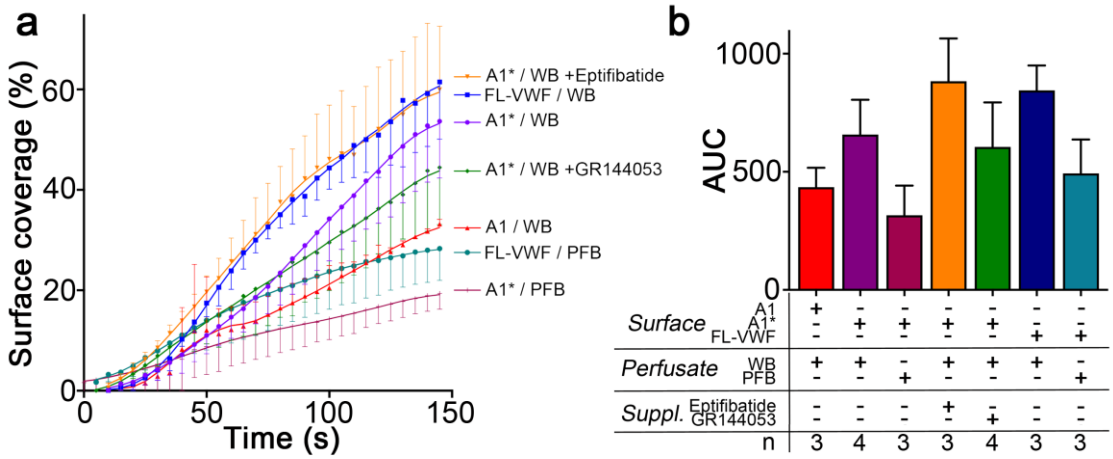

Figure S2: Platelet coverage: a) Graph showing the surface coverage over time of microchannels coated with FL-VWF, VWF A1 or VWF A1* by platelets in either whole blood (WB) or plasma-free blood (PFB) at a shear rate of $1000s^{-1}$ **b)** Graph of the area under the curve (AUC) ±SD of conditions analyzed in A) Surface coverage rates were similar on all surfaces.

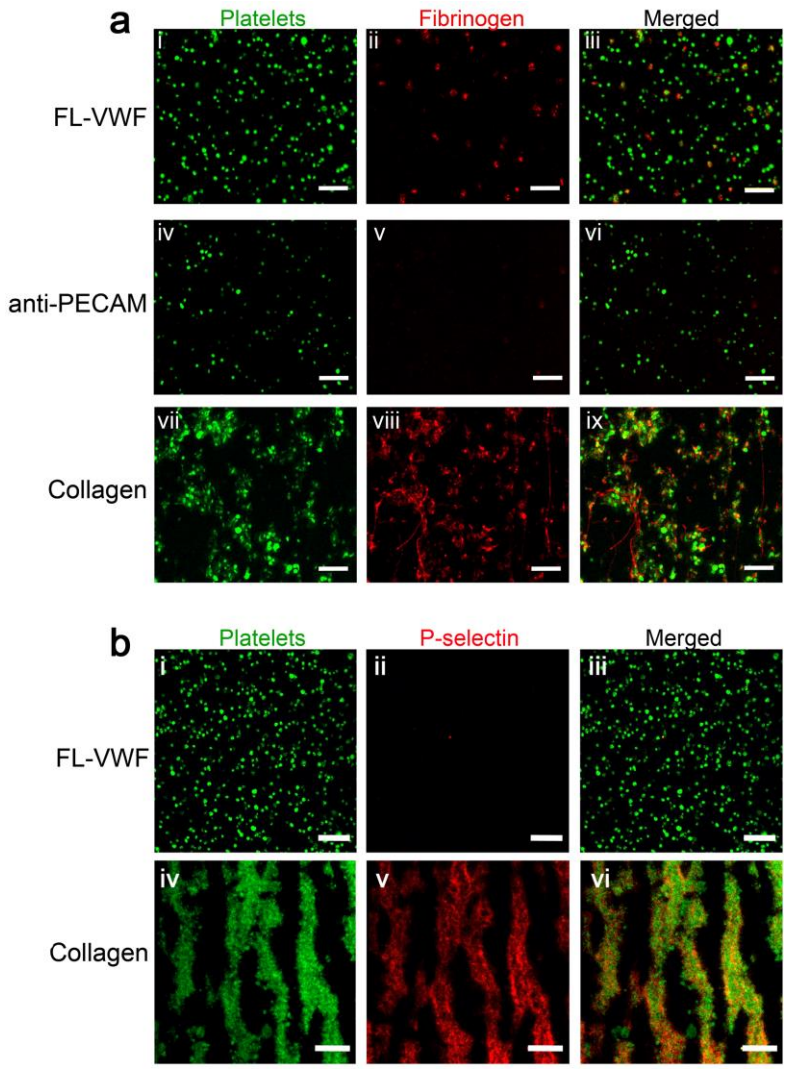

Figure S3: Platelets binding to VWF under flow are 'primed' leading to activation of $\alpha_{IIb}\beta_3$, but minimal presentation of P-selectin. a) Representative images (n=3) depicting platelets ($DiOC_6$, green) captured from plasma-free blood at $1000s^{-1}$ for 3.5 minutes onto microchannel surfaces coated with either FL-VWF (i-iii), anti-PECAM (iv-vi) or collagen (vii-ix). Plasma-free blood was supplemented with fibrinogen-Alexa647 (red). Merged images show fluorescent fibrinogen attached to the platelets captured by FL-VWF and collagen, but not by platelets captured by anti-PECAM. **b)** Representative images (n=3) depicting platelets ($DiOC_6$, green) captured from whole blood at $1000s^{-1}$ for 3.5 minutes onto microchannel surfaces coated with either FL-VWF (i-iii) or collagen (iv-vi). Blood was supplemented with anti-P-selectin-APC (red). Merged images show the presence of P-selectin on the surface of platelets captured by collagen, but very little/no P-selectin on platelets captured FL-VWF. Scale bar=20μm.

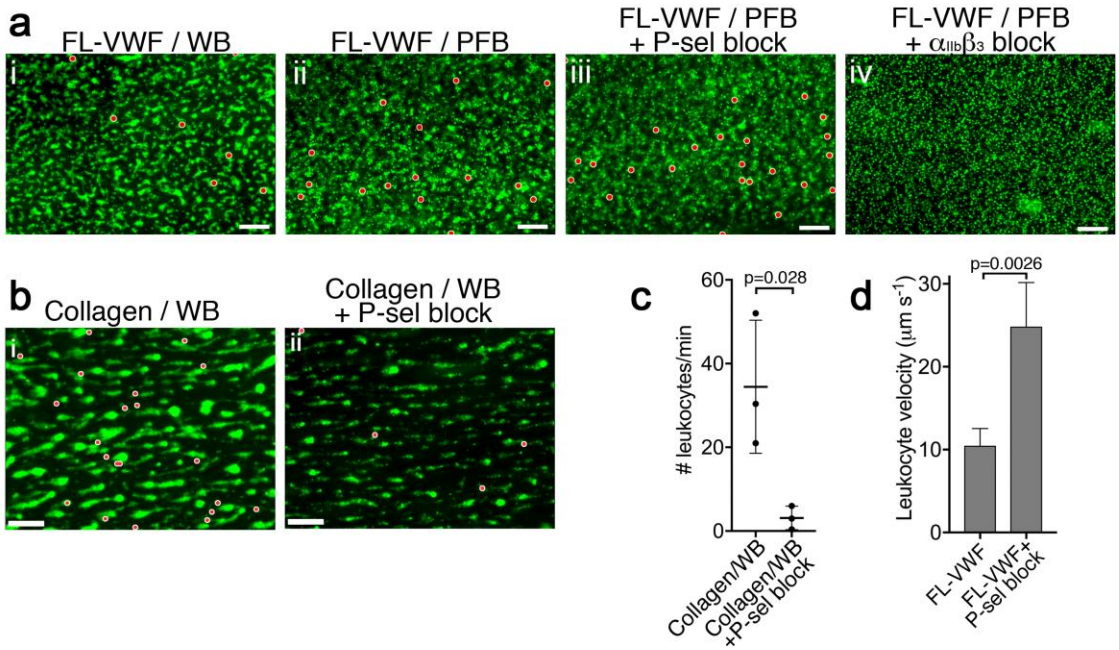

Figure S4: Antibody-mediated blockade of P-selectin diminishes leukocyte binding to collagen bound platelets. a) Vena8 microchannels were coated with FL-VWF. i) Whole blood (WB), ii) plasma-free blood (PFB), iii) WB containing anti-P-selectin blocking antibody, or iv) WB containing eptifibatide were perfused through channels at $1000s^{-1}$ for 3.5 minutes. Thereafter, the shear rate was reduced to $50s^{-1}$ for 5 minutes. Platelets and leukocytes were labelled with $DiOC_6$, platelets are shown in green, leukocytes have been pseudo-colored red to aid visualization. Scale bar; 50μm (see also **Movie EV 2**). **b)** Whole blood (WB), labelled with $DiOC_6$ was perfused over collagen microchannels at $1000s^{-1}$ for 3.5 minutes. Thereafter, the shear rate was reduced to $50s^{-1}$ to monitor leukocyte interactions. (i) Representative image (n=3) shown after 5 minutes platelets (green) and leukocytes (pseudo-colored red). (ii) as in (i) except WB was supplemented with a blocking anti-P-selectin antibody (AK-4 clone. Scale bar=50μm. **c)** The mean number of leukocytes binding per minute ±SD was calculated for each channel. There was a significant reduction in the number of leukocytes binding to collagen-bound platelets in the presence of P-selectin blocker, although leukocyte binding was not completely inhibited, suggesting that not all binding to collagen-activated platelets is P-selectin-dependent. **d)** Graph of leukocyte rolling velocity on platelets bound to FL-VWF in WB in the absence or presence of a blocking anti-P-selectin antibody. Data shown are the means of individual leukocyte rolling velocities for 3 separate experiments. Unpaired, two-tailed Student's t test.

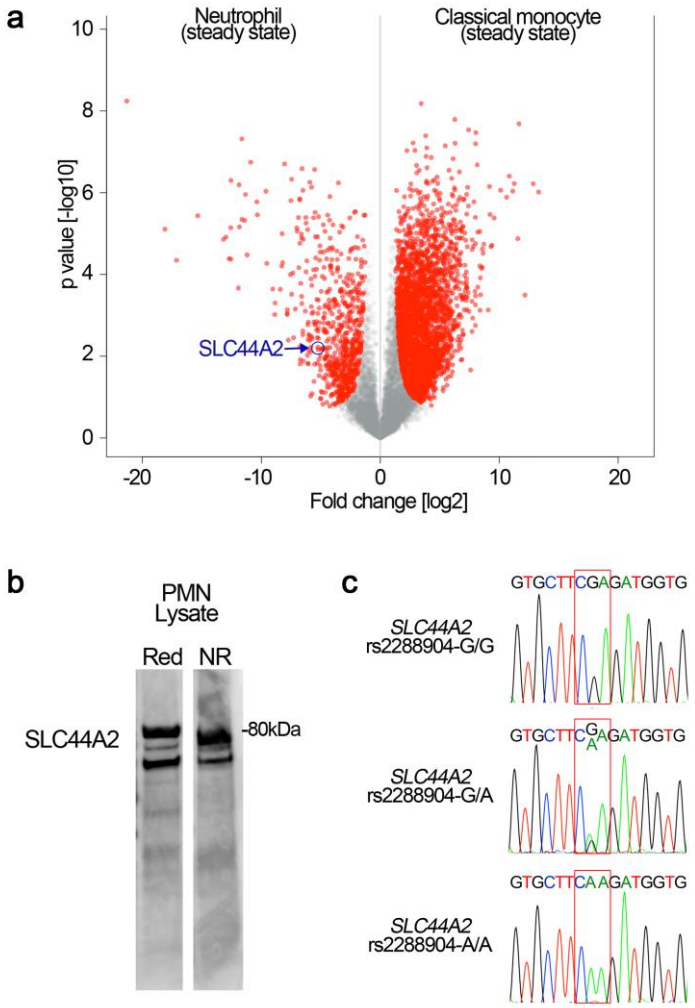

Figure S5: SLC44A2 expression in neutrophils and *SLC44A2* genotype analysis. a) Preferential expression of SLC44A2 in neutrophils over monocytes was ascertained through analysis of proteomic data from ImmProt (http://immprot.org), which is based on high-resolution mass-spectrometry proteomics performed on human hematopoietic cell populations in either steady or activated states. A pair-wise comparison between neutrophils (steady-state) and classical monocytes (steady state) is displayed as a volcano plot. Protein expression levels were compared using two-tailed Student's t-test with Welch's correction (S0=1, FDR<5%), and proteins with a significantly different expression level are shown in red on the plot. The point corresponding to SLC4A2 is highlighted revealing preferential expression in neutrophils. All 30 candidate genes identified in Fig 8 were analyzed through this comparative approach to examine preferential protein levels in neutorphils above monocytes. **b)** Isolated neutrophil lysates were analyzed by Western blotting under reducing and non-reducing conditions using anti-SLC4A2 #2 antibody. In both lanes, two bands corresponding to glycosylated (~80kDa) and nascent, non-glycosylated SLC44A2 are detected. **c)** Healthy volunteers were genotyped to identify individuals homozygous for the protective rs2288904-A/A SNP in *SLC44A2*. Representative chromatograms for individuals with rs2288904-G/G, rs2288904-G/A, rs2288904-A/A genotypes are shown.

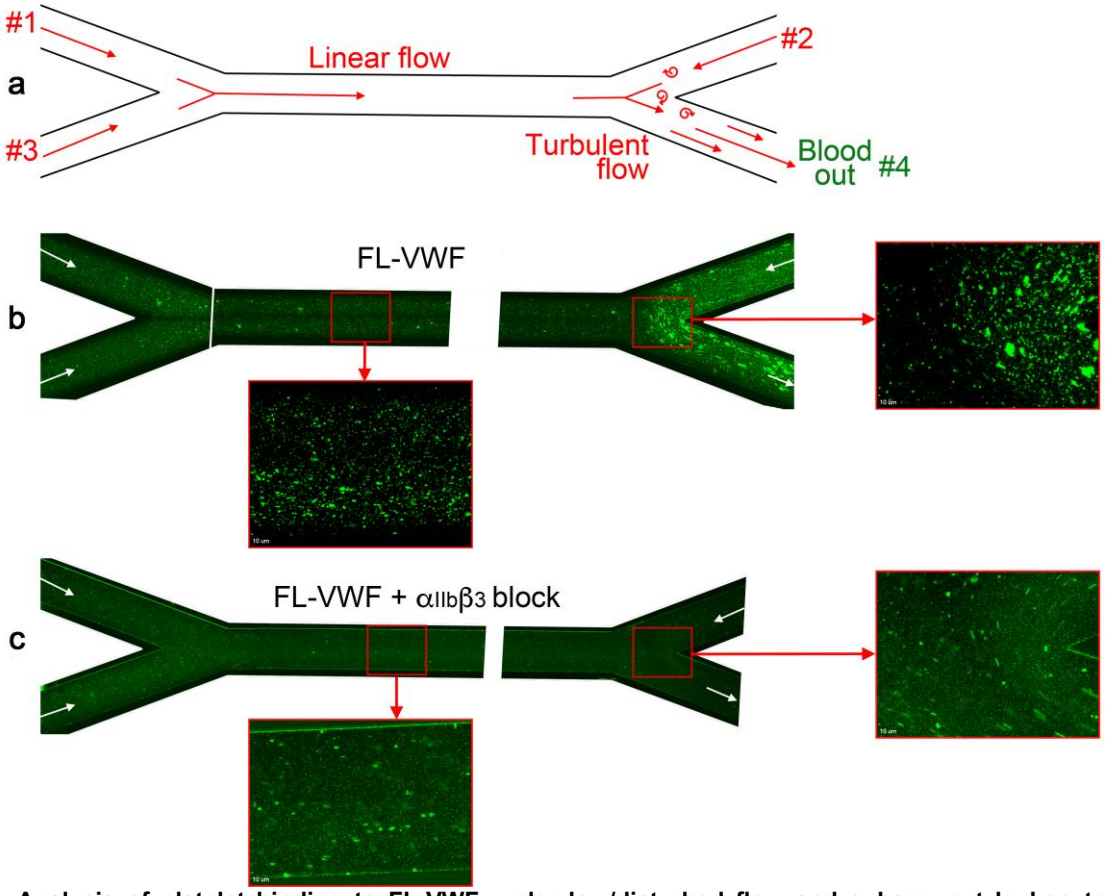

Figure S6: Analysis of platelet binding to FL-VWF under low/disturbed flow and subsequent leukocyte binding. a) Schematic representation of blood flow through bifurcated channels. Blood is drawn through inlets #1, #2 and #3, and out through outlet #4. For much of the channels, the flow is linear, with particular exception to the bifurcation site on the right where disturbed flow exists due to convergence of flows. **b)** Channels were coated with FL-VWF and whole blood labelled with DiOC6 was perfused through channels as in a), and as denoted by arrows, at an exit shear rate of $50s^{-1}$. At this low shear rate, platelets can bind to the channel surface to which leukocytes (larger cells also stained in green) also bind. Although this is evident in the linear part of the channel (inset), at the site of most turbulent flow increased platelet and leukocyte binding was observed. **c)** As in b) except GR144053 was added to block $\alpha_{IIb}\beta_3$. Blocking $\alpha_{IIb}\beta_3$ inhibited the majority of leukocyte binding to platelets (the majority of those observed are in transit). However, in the absence of leukocyte binding the binding of platelets to the VWF surface under low flow can be more clearly observed in both the linear and turbulent flow areas.

Legends to Movies (see Movie 1-7 files)

Movie 1. Platelet capture on FL-VWF, VWF A1 or VWF A1*. Vena8 microchannels were coated with either full-length VWF (FL-VWF), VWF A1 or A1*. Whole blood labelled with $DiOC_6$ was perfused at $1000s^{-1}$ for 3 minutes. Note the reduced rate of platelet rolling on microchannels coated with A1* when compared to FL VWF or A1.

Movie 2. VWF A1-Gplbα interaction induces intraplatelet Ca^{2+} release under flow. Platelets were pre-loaded with Fluo-4 AM prior to perfusion through VWF A1*-coated microchannels at $1000s^{-1}$ for 5 minutes. Increases in platelet fluorescence corresponds to platelet intracellular Ca^{2+} release following attachment to VWF A1*. Note the repeated transient increases in fluorescence under flow, indicative of sustained and repeated signaling stimuli.

Movie 3. Leukocytes bind/roll on VWF-'primed' platelets. Whole blood or plasma-free blood labelled with $DiOC_6$ was perfused through channels coated with VWF A1* at high shear for 3.5 minutes to capture platelets in the presence or absence of either a blocking anti-P-selectin antibody or eptifibatide ($\alpha_{IIb}\beta_3$ blocker) prior to the acquisition of videos. The shear rate was reduced to $50s^{-1}$ to visualize leukocyte rolling or attaching (tracked in blue). Leukocytes rolled/bound on platelets in whole blood, plasma-free blood and plasma-free blood containing anti-P-selectin blocking antibody, but not in the presence of eptifibatide ($\alpha_{IIb}\beta_3$ blocker). The use of the anti-P-selectin blocking antibody did however increase the rolling velocity of leukocytes over the platelet surface.

Movie 4. Neutrophil start scanning following interaction with activated $\alpha_{IIb}\beta_3$. Following attachment of neutrophils (labelled with anti-CD16; red) to platelets (green) captured on FL-VWF (left), neutrophils start to scan the platelet surface. Similarly, neutrophils (anti-CD16-APC & Hoechst staining) bound to activated $\alpha_{IIb}\beta_3$-coated microchannels also scanned the surface and in some cases appeared to start migrating against the direction of flow. Shear rate = $50s^{-1}$.

Movie 5. Intracellular Ca^{2+} release in neutrophils following interaction with activated $\alpha_{IIb}\beta_3$ under flow. Neutrophils were pre-loaded with Fluo-4 AM and perfused over FL-VWF 'primed' platelets, $\alpha_{IIb}\beta_3$-coated or anti-CD16 coated microchannels at $50s^{-1}$. Following attachment of neutrophils to VWF-'primed' platelets or activated $\alpha_{IIb}\beta_3$ (but not anti-CD16), an increase in fluorescence corresponding to neutrophil intracellular Ca^{2+} release was observed.

Movie 6. $\alpha_{IIb}\beta_3$-induced NETosis. Isolated PMNs labelled with Hoechst (blue) and cell-impermeable Sytox Green were perfused over $\alpha_{IIb}\beta_3$-coated microchannels at $50s^{-1}$ for 10 minutes and then monitored under static conditions. Movie shown represents period from 80 to 95 minutes after attachment. Sytox Green staining appears, indicative of DNA becoming extracellular highlights the neutrophils undergoing NETosis.

Movie 7. Neutrophil binding to VWF-'primed' platelets occurs via SLC44A2 is modified by the rs2288904 SNP. Plasma-free blood generated from individuals homozygous for the rs2288904-G major allele in *SLC44A2* (SLC44A2 (R154/R154)) or the rs2288904-A minor allele (SLC44A2 (Q154/Q154)) SNP in *SLC44A2* was labelled with $DiOC_6$ and perfused through channels coated with VWF at high shear for 3.5 minutes. Shear was subsequently reduced to $50s^{-1}$. SLC44A2 (R154/R154) leukocytes (tracked in blue) were seen to roll on the VWF-'primed' platelets. The number of leukocytes interacting was severely reduced in the presence of the anti-SLC44A2 #2 antibody. Leukocytes homozygous for the rs2288904-A minor allele, SLC44A2 (Q154/Q154), associated with protection against venous thrombosis, exhibited reduced ability to interact with VWF-'primed' platelets.